POLITECNICO DI TORINO

Tesi di Dottorato

A Mortar Element Method for the Analysis of Electromagnetic Passive Devices

Alberto **TIBALDI**

Tutore	**Coordinatore del corso di dottorato**
Prof. Renato ORTA	Prof. Ivo MONTROSSET

Gennaio 2015

List of acronyms

BI-RME Boundary Integral-Resonant Mode Expansion method

BOR Body Of Revolution

BVP Boundary Value Problem

CAD Computer-Aided Design

CMBR Cosmic Microwave Background Radiation

CMFIE Continuity of the Magnetic Field Integral Equation

CST-MS CST Microwave Studio

EFIE Electric Field Integral Equation

FBR Front to Back Ratio

FDTD Finite-Difference Time-Domain method

FEM Finite Elements Method

GNSS Global Navigation Satellite System

GSM Generalized Scattering matrix

IEIIT-CNR Istituto di Elettronica e di Ingegneria dell'Informazione e delle Tele-
comunicazioni, Consiglio Nazionale delle Ricerche

IRA-INAF Istituto di Radio Astronomia, Istituto Nazionale di AstroFisica

LG Loop Gain

MEM Mortar Element Method

MFIE Magnetic Field Integral Equation

MMT Mode-Matching Technique

MoM Method of Moments

MPIE Mixed-Potential Integral Equation

MWA Murchison Widefield Array

SAD Sardinia Array Demonstrator

SEM Spectral Element Method

SKA Square Kilometer Array

SRT Sardinia Radio Telescope

PDE Partial Differential Equation

PEC Perfect Electric Conductor

PMC Perfect Magnetic Conductor

PMCHW Poggio-Miller-Chang-Harrington-Wu

PWL Piece-Wise Linear

PO Physical Optics

RF Radio-Frequency

RFI Radio-Frequency Interference

RTPS Round-Trip Phase Shift

RWG Rao-Wilton-Glisson

SL Sturm-Liouville

SVD Singular Value Decomposition

LOFAR Low-Frequency Array

LSE Longitudinal Section Electric

LSM Longitudinal Section Magnetic

LWA Long Wavelength Array

PSW Phase-Shift Walls

TE Transverse Electric

TEM Transverse ElectroMagnetic

TM Transverse Magnetic

UAV Unmanned Aerial Vehicle

Contents

Introduction

Satellite telecommunication systems and scientific survey instruments require the design of high-performance passive waveguide components such as filters, directional couplers, power dividers, diplexers, orthomode transducers and horn antennas. Additionally to the usual specifications on matching and polarization purity, depending on the specific application, these devices need to comply with very tight constraints. As an example, nowadays a satellite is used to provide several telecommunication services; architectures based on the use of a single feed chain working in multiple bands are preferred to the ones based on multiple chains, in order to reduce mass and volume of the satellite, and its fabrication costs. Moreover, these devices have to manage high power levels, leading to the presence of additional issues, such as the multipaction phenomenon or the presence of spurious intermodulation products. On the other hand, one of the most challenging tasks in astrophysics is the construction of a polarization map of the cosmic microwave background radiation (CMBR); this map would be processed to obtain an angular power spectrum and, ultimately, cosmological parameters aimed at characterizing the thermal history of the Universe. However, this procedure is extremely complex, owing to the presence of the Bremsstrahlung or of the synchrotron radiation, that disturb the measurement. For this reason, the polarimeters used to measure the CMBR should exhibit an extreme rejection of the unpolarized background, to improve the signal-to-noise ratio.

In the majority of cases, where a synthesis technique is lacking, the design procedure is based on using electromagnetic simulators driven by optimization codes. Although general-purpose simulators can analyze almost every electromagnetic device with good precision, they are not enough efficient, in terms of computation time, to be introduced in the optimization loop. For this reason, many efforts are still invested in electromagnetic modeling, to develop fast and accurate computer-aided design (CAD) tools.

The first and main part of this Ph.D. thesis is dedicated to the application of a multi-domain spectral method to the simulation of electromagnetic passive devices.

Although spectral methods have been introduced in the mid-1940s, their first rigorous study was carried out by Gottlieb and Orszag in 1977 [1], who summarized the state of the art in their theory and application. Then, spectral domain decomposition approaches were introduced to extend spectral methods to complex domains, generating a class of schemes known as spectral element methods (SEMs) [2]. Among all the schemes that have been developed, the mortar element method (MEM) is very interesting: here, local basis functions are defined in each sub-domain; then, they are glued at the common edges of adjacent patches by enforcing continuity conditions almost everywhere. This allows to use different resolutions in different patches (*i.e.* different degrees of the basis functions), and the possibility to hybridize this numerical method, joining it with other schemes. Owing to their flexibility in the description of complex geometries, these techniques have been widely applied to models involving partial differential equations (PDEs), especially in weather modeling, in computational fluid dynamics and in structural mechanics [3], [4], [5]. Recently, these methods have been applied to electromagnetic problems in both frequency and time domains [6], [7], [8]. In [9], the authors have presented a multi-domain spectral method for the solution of the scalar Helmholtz equation relevant to the analysis of 2-D rectangular waveguide discontinuities.

The layout of the first part of the thesis is now described.

In Chapter 1, a formulation of scattering problems from electromagnetic passive structures is introduced. This is based on the decomposition of the scattering problem into two sub-problems, by applying the equivalence theorem. The electric and magnetic current densities are used to provide the excitation of the internal problem, that is described by using a system of PDEs. Then, the numerical procedure aimed at synthesizing the expansion and test functions is described. In Chapters 2, 3 and 4 the BVPs for 2-D waveguide discontinuities, periodic structures and axisymmetric devices are derived from Maxwell's equations. The formulation of Chapter 1 is applied to solve each of these scattering problems. These methods have been validated with comparisons with in-house simulators and with commercial codes. This work has been entirely carried out in the Istituto di Elettronica e di Ingegneria dell'Informazione e delle Telecomunicazioni of the Consiglio Nazionale delle Ricerche (IEIIT-CNR).

In the second part of the thesis, two different projects are described.

In Chapter 5 the development of a boundary-integral equation method aimed at analyzing dielectric lens antennas has been described. This work has been carried out in the Terahertz Sensing Group of the Delft University of Technology. This project is driven by the necessity of performing a low-frequency characterization of lens antennas, where physical optics (PO) simulators are not reliable. Nowadays,

the terahertz spectrum is almost unused; indeed, one of the most critical drawbacks of this frequency range is the absence of an efficient ultra-wide band antenna. Lens antennas have been already used in terahertz radio-astronomy, and they are among the best candidates as radiating elements for terabit wireless communication systems that will be developed in the next years. In this chapter, the formulation of the integral equations of the feeding slot is developed, as well as the one of the dielectric lens; then, the two problems are coupled and solved with the method of moments (MoM). This method has been implemented and validated with comparison with a commercial code.

In Chapter 6 the design of a cavity-backed Vivaldi antenna is described. This has been performed in the framework of the Sardinia Array Demonstrator (SAD) project, aimed at providing a test-bed for novel low-frequency radio telescopes. The antenna has been designed in cooperation with the IEIIT-CNR and with the Istituto di Radio Astronomia of the Istituto Nazionale di Astrofisica (IRA-INAF). The design is based on the improvement of an existing antenna by using physical considerations to modify its structure. Then, a benchmark of the two antennas based on a far-field model of the system noise temperature is performed. Finally, a prototype of the cavity-backed Vivaldi antenna has been characterized by means of a novel pattern measurement system.

Foundations of the mortar element method applied to electromagnetic scattering problems

1.1 Introduction

In this chapter the foundations required to properly apply the mortar element method (MEM) to the analysis of the scattering from electromagnetic passive devices are provided. Here, the formulation is referred to a generic problem, without specifying the nature of the domain or of the boundary-value problem (BVP) that has to be solved. The matrices arisen from the discretized partial differential equations (PDEs) are intended to be known; therefore, the formulae derived in this chapter are applied to the structures described in Chapters 2, 3 and 4, where the BVPs are derived from Maxwell's equations in different scenarios. The differences among the methods are mainly related to the calculation of the elements of the matrices that arise from the weak formulation of the BVP.

The formulation derived in Section 1.2 is based on the application of the equivalence theorem, which is used to separate the initial problem into two sub-problems: the internal one, which is described as a BVP solved with the MEM; the external one, where only homogeneous waveguides are involved. Then, the problems are coupled, obtaining a boundary-integral equations method, where two situations are distinguished: in one region the Green's function is approximated as an eigenfunctions expansion, whereas in the other one it is derived as the solution of the BVP.

In Section 1.3 the numerical procedure used to synthesize the MEM basis functions used to approximate the solution and to obtain the variational formulation of

the PDE.

1.2 Formulation of the scattering problem

With reference to Fig. 1.1, the equivalence theorem is applied on the two sides of each surface $\Sigma_{\mathrm{eq}}^{(k)}$ defined on the k-th access port; this leads to the definition of two couples of electric and magnetic current densities: $\widehat{\mathbf{J}}^{(k)}$, $\widehat{\mathbf{M}}^{(k)}$ on the external side of $\Sigma_{\mathrm{eq}}^{(k)}$ and $\widetilde{\mathbf{J}}^{(k)}$, $\widetilde{\mathbf{M}}^{(k)}$ on its internal side. This is used to divide the original problem into two sub-problems: in the external one, the currents $\widehat{\mathbf{J}}^{(k)}$, $\widehat{\mathbf{M}}^{(k)}$ give rise to the fields $\widehat{\mathbf{E}}^{(k)}$, $\widehat{\mathbf{H}}^{(k)}$, and to a null field inside the region Σ; in the internal one, the currents $\widetilde{\mathbf{J}}^{(k)}$, $\widetilde{\mathbf{M}}^{(k)}$ give rise to the fields $\widetilde{\mathbf{E}}^{(k)}$, $\widetilde{\mathbf{H}}^{(k)}$ inside Σ and to a null field in the external region.
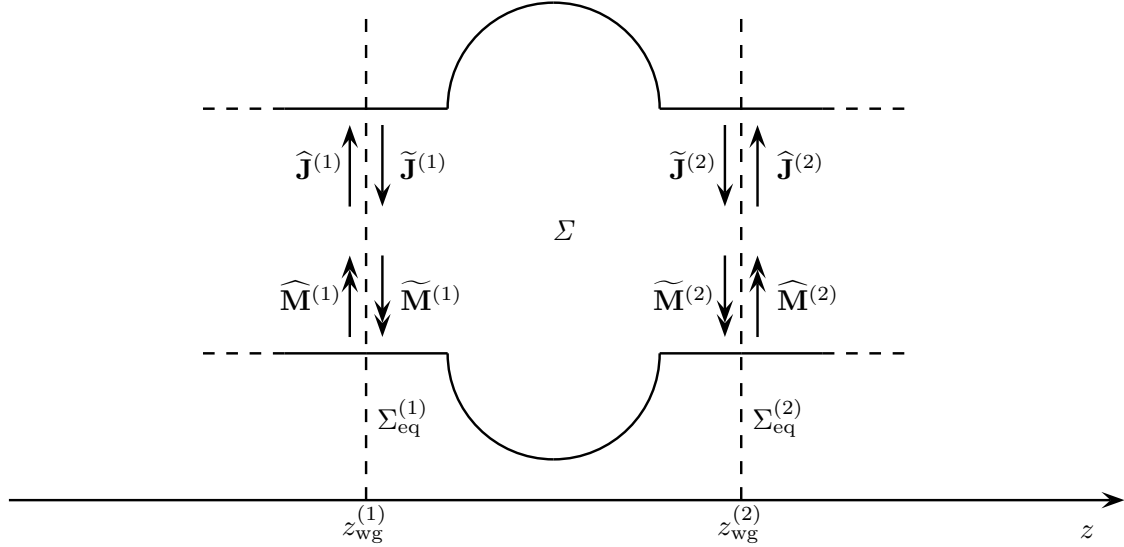
Figure 1.1: Original problem, where the electric and magnetic current densities have been defined after the application of the equivalence theorem.

Given $\mathbf{H}^{(k)}$ and $\mathbf{E}^{(k)}$ the magnetic and electric fields defined on $\Sigma_{\mathrm{eq}}^{(k)}$, the current densities are defined as:

$$
\begin{aligned}
\widehat{\mathbf{J}}^{(k)} &= -\widehat{\mathbf{n}}^{(k)} \times \widehat{\mathbf{H}}^{(k)} = -\widehat{\mathbf{n}}^{(k)} \times \widehat{\mathbf{H}}_{\mathrm{t}}^{(k)} \\
\widehat{\mathbf{M}}^{(k)} &= \widehat{\mathbf{E}}^{(k)} \times (-\widehat{\mathbf{n}}^{(k)}) = \widehat{\mathbf{E}}_{\mathrm{t}}^{(k)} \times (-\widehat{\mathbf{n}}^{(k)}) \\
\widetilde{\mathbf{J}}^{(k)} &= \widehat{\mathbf{n}}^{(k)} \times \widetilde{\mathbf{H}}^{(k)} = \widehat{\mathbf{n}}^{(k)} \times \widetilde{\mathbf{H}}_{\mathrm{t}}^{(k)} \\
\widetilde{\mathbf{M}}^{(k)} &= \widetilde{\mathbf{E}}^{(k)} \times \widehat{\mathbf{n}}^{(k)} = \widetilde{\mathbf{E}}_{\mathrm{t}}^{(k)} \times \widehat{\mathbf{n}}^{(k)},
\end{aligned}
\tag{1.1}
$$

where $\widehat{\mathbf{n}}^{(k)}$ is the unit vector normal to $\Sigma_{\mathrm{eq}}^{(k)}$ pointing towards each external region. In order to satisfy the continuity of the tangential fields at each access port, which is

$$\widehat{\mathbf{H}}_{\mathrm{t}}^{(k)} = \widetilde{\mathbf{H}}_{\mathrm{t}}^{(k)}$$
$$\widehat{\mathbf{E}}_{\mathrm{t}}^{(k)} = \widetilde{\mathbf{E}}_{\mathrm{t}}^{(k)}, \tag{1.2}$$

the currents introduced in (1.1) are chosen to be equal and opposite:

$$\mathbf{J}^{(k)} = \widehat{\mathbf{J}}^{(k)} = -\widetilde{\mathbf{J}}^{(k)}$$
$$\mathbf{M}^{(k)} = \widehat{\mathbf{M}}^{(k)} = -\widetilde{\mathbf{M}}^{(k)}. \tag{1.3}$$

These currents are conveniently represented in the modal basis:

$$\mathbf{J}^{(k)} = \sum_{n=1}^{N_{\mathrm{m}}^{(k)}} \mathring{i}_n^{(k)} \mathbf{e}_n^{(k)}$$
$$\mathbf{M}^{(k)} = \sum_{n=1}^{N_{\mathrm{m}}^{(k)}} \mathring{v}_n^{(k)} \mathbf{h}_n^{(k)}, \tag{1.4}$$

where $N_{\mathrm{m}}^{(k)}$ is the number of modes used to represent each current density. Similarly, in the external sub-problem, the field at each access port is represented by means of a modal expansion with $N_{\mathrm{m}}^{(k)}$ modes for each port:

$$\widehat{\mathbf{E}}_{\mathrm{t}}^{(k)} = \sum_{n=1}^{N_{\mathrm{m}}^{(k)}} \widehat{V}_n^{(k)} \mathbf{e}_n^{(k)}$$
$$\widehat{\mathbf{H}}_{\mathrm{t}}^{(k)} = \sum_{n=1}^{N_{\mathrm{m}}^{(k)}} \widehat{I}_n^{(k)} \mathbf{h}_n^{(k)}. \tag{1.5}$$

The internal sub-problem is formulated as a BVP solved with the MEM. The positions of the access ports are chosen by trading-off the attenuation of the evanescent modes contributions (to reduce the number of modes necessary to represent properly the field in the external sub-problem) and the number of expansion functions used to represent the solution of the internal BVP.

All the BVPs studied in this work are formulated starting from the Maxwell's equations written in absence of sources, in order to avoid problems in the representation of the source with a set of basis functions. The effect of the electric and/or magnetic current densities is accounted for by means of non-homogeneous boundary conditions, introduced in the line integrals that arise from the application of the integration by parts applied to the variational formulation of the PDE. Depending on the problem, these line integrals may contain:

- electric field components, which are related to magnetic current densities; in this case, the electric current densities should not be considered, and the correct formulation is obtained filling the zero-field region of the external sub-problem with perfect electric conductor (PEC);

- magnetic field components, which are related to electric current densities; in this case, the magnetic current densities should not be considered, and the correct formulation is obtained filling the zero-field region of the external sub-problem with perfect magnetic conductor (PMC);

- both electric and magnetic field components (vector problems); in this case, the null field region is filled with an infinitely long waveguide.

These applications of the equivalence theorem are described in the following subsections, referring to 2-ports devices.

Equivalence theorem - vector problems

Discretized vector boundary-value problem are described by the following matrix equations:

$$
(\mathbf{A}^{(\mathrm{e,e})}\mathbf{c}^{(\mathrm{e})})_r + (\mathbf{A}^{(\mathrm{e,h})}\mathbf{c}^{(\mathrm{h})})_r = \int_{\gamma_{\mathrm{wg}}^{(1)}} \mathbf{H}\, v_r^{(\mathrm{e})*}\big|_{z_{\mathrm{wg}}^{(1)}} \cdot \mathrm{d}\mathbf{s} + \int_{\gamma_{\mathrm{wg}}^{(2)}} \mathbf{H}\, v_r^{(\mathrm{e})*}\big|_{z_{\mathrm{wg}}^{(2)}} \cdot \mathrm{d}\mathbf{s},\ r = 1...N_{\mathrm{f}}
$$

$$
(\mathbf{A}^{(\mathrm{h,e})}\mathbf{c}^{(\mathrm{e})})_r + (\mathbf{A}^{(\mathrm{h,h})}\mathbf{c}^{(\mathrm{h})})_r = \int_{\gamma_{\mathrm{wg}}^{(1)}} \mathbf{E}\, v_r^{(\mathrm{h})*}\big|_{z_{\mathrm{wg}}^{(1)}} \cdot \mathrm{d}\mathbf{s} + \int_{\gamma_{\mathrm{wg}}^{(2)}} \mathbf{E}\, v_r^{(\mathrm{h})*}\big|_{z_{\mathrm{wg}}^{(2)}} \cdot \mathrm{d}\mathbf{s},\ r = 1...N_{\mathrm{f}},
$$

(1.6)

where $\gamma_{\mathrm{wg}}^{(k)}$ is the path along the k-th access port, $\mathbf{c}^{(\mathrm{e})}$ and $\mathbf{c}^{(\mathrm{h})}$ are the vectors containing the expansion coefficients of the unknown and the left-hand side matrices come from the discretization of the differential problem. Focusing on the line integrals on the right-hand side of the previous equation, for 2-D problems it can be always written that:

$$
\begin{aligned}
\mathbf{E} \cdot \mathrm{d}\mathbf{s} &= \widetilde{\mathbf{E}}_{\mathrm{t}}^{(k)} \cdot \mathrm{d}\mathbf{s} = \widetilde{E}_s^{(k)}\, \mathrm{d}s \\
\mathbf{H} \cdot \mathrm{d}\mathbf{s} &= \widetilde{\mathbf{H}}_{\mathrm{t}}^{(k)} \cdot \mathrm{d}\mathbf{s} = \widetilde{H}_s^{(k)}\, \mathrm{d}s.
\end{aligned}
$$

(1.7)

Then, by inverting (1.1) and recalling (1.3), the following expressions hold:

$$
\begin{aligned}
\widetilde{\mathbf{E}}_{\mathrm{t}}^{(k)} &= \mathbf{M}^{(k)} \times \widehat{\mathbf{n}}^{(k)} \\
\widetilde{\mathbf{H}}_{\mathrm{t}}^{(k)} &= \widehat{\mathbf{n}}^{(k)} \times \mathbf{J}^{(k)}.
\end{aligned}
$$

(1.8)

By recalling (1.4), this leads to:

$$
\widetilde{\mathbf{H}}^{(k)} \simeq \sum_{n=0}^{N_{\mathrm{m}}^{(k)}} \mathring{i}_n^{(k)}\, \mathbf{e}_n^{(k)} \times \widehat{\mathbf{n}}^{(k)} = \sum_{n=0}^{N_{\mathrm{m}}^{(k)}} \mathring{i}_n^{(k)} \mathbf{h}_n^{(k)}
$$

$$
\widetilde{\mathbf{E}}^{(k)} \simeq \sum_{n=0}^{N_{\mathrm{m}}^{(k)}} \mathring{v}_n^{(k)}\, \widehat{\mathbf{n}}^{(k)} \times \mathbf{h}_n^{(k)} = \sum_{n=0}^{N_{\mathrm{m}}^{(k)}} \mathring{v}_n^{(k)} \mathbf{e}_n^{(k)}.
$$

Therefore, the line integrals of (1.6) are re-written as:

$$
\int_{\gamma_{\mathrm{wg}}^{(k)}} \widetilde{H}_s^{(k)}\, v_r^{(\mathrm{e})*}\Big|_{z=z_{\mathrm{wg}}^{(k)}} \,\mathrm{d}s = -\sum_{n=0}^{N_{\mathrm{m}}^{(k)}} \mathring{i}_n^{(k)} \int_{\gamma_{\mathrm{wg}}^{(k)}} h_{s,n}^{(k)}\, v_r^{(\mathrm{e})*}\, \mathrm{d}s = -(\mathbf{B}^{(\mathrm{e},k)}\, \mathring{\mathbf{i}}^{(k)})_r, \quad r = 1...N_{\mathrm{f}}^{(\mathrm{e})}
$$

$$
\int_{\gamma_{\mathrm{wg}}^{(k)}} \widetilde{E}_s^{(k)}\, v_r^{(\mathrm{h})*}\Big|_{z=z_{\mathrm{wg}}^{(k)}} \,\mathrm{d}s = -\sum_{n=0}^{N_{\mathrm{m}}^{(k)}} \mathring{v}_n^{(k)} \int_{\gamma_{\mathrm{wg}}^{(k)}} e_{s,n}^{(k)}\, v_r^{(\mathrm{h})*}\, \mathrm{d}s = -(\mathbf{B}^{(\mathrm{h},k)}\, \mathring{\mathbf{v}}^{(k)})_r, \quad r = 1...N_{\mathrm{f}}^{(\mathrm{h})},
$$

where:

$$
(\mathbf{B}^{(\mathrm{e},k)})_r = \int_{\gamma_{\mathrm{wg}}^{(k)}} h_{s,n}^{(k)}\, v_r^{(\mathrm{e})*}\Big|_{z=z_{\mathrm{wg}}^{(k)}} \,\mathrm{d}s
$$

$$
(\mathbf{B}^{(\mathrm{h},k)})_r = \int_{\gamma_{\mathrm{wg}}^{(k)}} e_{s,n}^{(k)}\, v_r^{(\mathrm{h})*}\Big|_{z=z_{\mathrm{wg}}^{(k)}} \,\mathrm{d}s.
$$

So, (1.6) are written as:

$$
\mathbf{A}^{(\mathrm{e},\mathrm{e})}\, \mathbf{c}^{(\mathrm{e})} + \mathbf{A}^{(\mathrm{e},\mathrm{h})}\, \mathbf{c}^{(\mathrm{h})} = -\mathbf{B}^{(\mathrm{e},1)}\, \mathring{\mathbf{i}}^{(1)} + \mathbf{B}^{(\mathrm{e},2)}\, \mathring{\mathbf{i}}^{(2)}
$$

$$
\mathbf{A}^{(\mathrm{h},\mathrm{e})}\, \mathbf{c}^{(\mathrm{e})} + \mathbf{A}^{(\mathrm{h},\mathrm{h})}\, \mathbf{c}^{(\mathrm{h})} = -\mathbf{B}^{(\mathrm{h},1)}\, \mathring{\mathbf{v}}^{(1)} + \mathbf{B}^{(\mathrm{h},2)}\, \mathring{\mathbf{v}}^{(2)},
$$

where the negative sign is used to keep into account the direction of the integration path. Then, these equations are grouped as follows:

$$
\underbrace{\begin{bmatrix} \mathbf{A}^{(\mathrm{e},\mathrm{e})} & \mathbf{A}^{(\mathrm{e},\mathrm{h})} \\ \mathbf{A}^{(\mathrm{h},\mathrm{e})} & \mathbf{A}^{(\mathrm{h},\mathrm{h})} \end{bmatrix}}_{\mathbf{A}} \underbrace{\begin{bmatrix} \mathbf{c}^{(\mathrm{e})} \\ \mathbf{c}^{(\mathrm{h})} \end{bmatrix}}_{\mathbf{c}} = \underbrace{\begin{bmatrix} -\mathbf{B}^{(\mathrm{e},1)} & \mathbf{0} & \mathbf{B}^{(\mathrm{e},2)} & \mathbf{0} \\ \mathbf{0} & -\mathbf{B}^{(\mathrm{h},1)} & \mathbf{0} & \mathbf{B}^{(\mathrm{h},2)} \end{bmatrix}}_{\mathbf{B}} \underbrace{\begin{bmatrix} \mathring{\mathbf{i}}^{(1)} \\ \mathring{\mathbf{v}}^{(1)} \\ \mathring{\mathbf{i}}^{(2)} \\ \mathring{\mathbf{v}}^{(2)} \end{bmatrix}}_{\mathbf{x}}, \quad (1.9)
$$

which is compactly written as:

$$
\mathbf{A}\,\mathbf{c} = \mathbf{B}\,\mathbf{x}.
$$

This equation establishes a relationship between the coefficients equivalent currents defined on each waveguide port, $\mathbf{x}$, and the expansion coefficients $\mathbf{c}$ of the unknowns of the internal problem. Hence, by solving it with respect to $\mathbf{x}$,

$$
\mathbf{c} = \mathbf{G}\,\mathbf{x} = \mathbf{A}^{-1}\mathbf{B}\,\mathbf{x}, \quad (1.10)
$$

a representation of the Green's function of the region Σ is obtained. Focusing on the external problem, the hybrid circuit of Fig. 1.2, valid for each n-th mode, is associated to the waveguide device, where the electromagnetic problem in each access waveguide is presented by an equivalent multi-modal circuit. Here, the coefficients $\mathring{i}_n^{(k)}$ and $\mathring{v}_n^{(k)}$ of (1.4) have the circuit interpretation of current and voltage generators on the modal lines, whereas the coefficients $\widehat{V}_n^{(k)}$ and $\widehat{I}_n^{(k)}$ are the voltages and currents on the modal lines. The term $Z_{\infty,n}^{(k)}$ is the modal characteristic impedance and $V_n^{(\mathrm{inc},k)}$ is the modal projection of the incident field at the k-th waveguide port. The sources $\mathring{v}_n^{(k)}$ and $\mathring{i}_n^{(k)}$ are found by projecting the magnetic and electric current
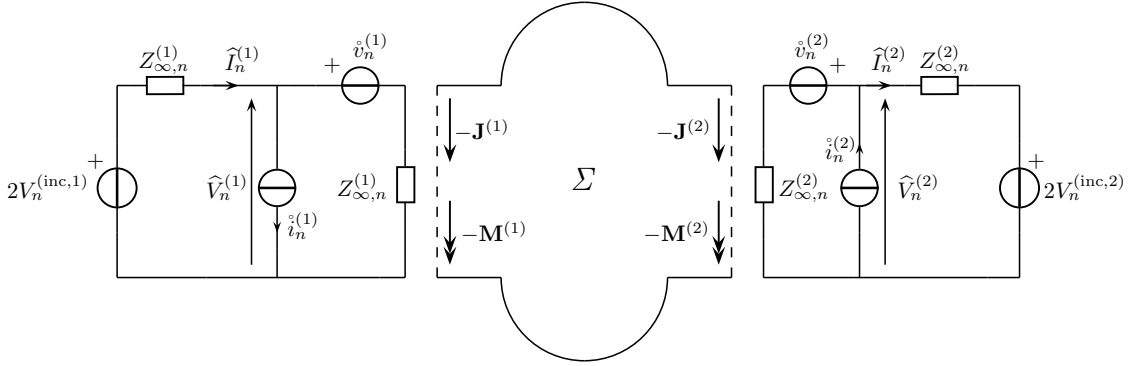
Figure 1.2: Equivalent modal circuit relative to the n-th waveguide mode; $Z_{\infty,n}^{(k)}$ is the characteristic impedance at the k-th access port; the sources are related to the equivalent current densities; $V_n^{(\mathrm{inc},k)}$ is the incidence voltage of the n-th mode.

densities on the waveguide modes[1]:

$$
\begin{aligned}
\mathring{v}_n^{(k)} &= \langle \mathbf{M}^{(k)}, \mathbf{h}_n^{(k)} \rangle \\
\mathring{i}_n^{(k)} &= \langle \mathbf{J}^{(k)}, \mathbf{e}_n^{(k)} \rangle.
\end{aligned}
\tag{1.11}
$$

Then, the solution of the hybrid equivalent circuit yields the expression of the modal voltage and current vectors $\widehat{\mathbf{V}}^{(k)}$ and $\widehat{\mathbf{I}}^{(k)}$ in terms of the modal generators $\mathring{\mathbf{i}}^{(k)}$ and $\mathring{\mathbf{v}}^{(k)}$ and of the modal incidence vector $\mathbf{V}^{(\mathrm{inc},k)}$ that collect the respective coefficients [10, Chap. 2]

---

[1]All the problems that have been studied with this technique are self-adjoint, therefore the modes constitute an orthonormal set.

$$\widehat{\mathbf{V}}^{(1)} = \mathbf{V}^{(\text{inc},1)} - \frac{1}{2}\mathbf{Z}_\infty^{(1)}\, \mathring{\mathbf{i}}^{(1)} + \frac{1}{2}\mathring{\mathbf{v}}^{(1)}$$

$$\widehat{\mathbf{I}}^{(1)} = \mathbf{Y}_\infty^{(1)}\, \mathbf{V}^{(\text{inc},1)} + \frac{1}{2}\mathring{\mathbf{i}}^{(1)} - \frac{1}{2}\mathbf{Y}_\infty^{(1)}\, \mathring{\mathbf{v}}^{(1)}$$

$$\widehat{\mathbf{V}}^{(2)} = \mathbf{V}^{(\text{inc},2)} + \frac{1}{2}\mathbf{Z}_\infty^{(2)}\, \mathring{\mathbf{i}}^{(2)} + \frac{1}{2}\mathring{\mathbf{v}}^{(2)}$$

$$\widehat{\mathbf{I}}^{(2)} = -\mathbf{Y}_\infty^{(2)}\, \mathbf{V}^{(\text{inc},2)} + \frac{1}{2}\mathring{\mathbf{i}}^{(2)} + \frac{1}{2}\mathbf{Y}_\infty^{(2)}\, \mathring{\mathbf{v}}^{(2)}.$$

$$(1.12)$$

The formulation of the scattering problem is completed by coupling the internal and external sub-problems by enforcing the continuity conditions of the tangential electric and the magnetic fields at the access ports (1.2):

$$\widehat{\mathbf{E}}_{\text{t}}^{(k)} = \widetilde{\mathbf{E}}_{\text{t}}^{(k)}$$
$$\widehat{\mathbf{H}}_{\text{t}}^{(k)} = \widetilde{\mathbf{H}}_{\text{t}}^{(k)}.$$

These conditions are written in weak form by projecting them on the modal basis:

$$\langle\widehat{\mathbf{E}}_{\text{t}}^{(k)}, \mathbf{e}_q^{(k)}\rangle = \langle\widetilde{\mathbf{E}}_{\text{t}}^{(k)}, \mathbf{e}_q^{(k)}\rangle$$
$$\langle\widehat{\mathbf{H}}_{\text{t}}^{(k)}, \mathbf{h}_q^{(k)}\rangle = \langle\widetilde{\mathbf{H}}_{\text{t}}^{(k)}, \mathbf{h}_q^{(k)}\rangle.$$

For what concerns the access port terms, it can be noted that, according to (1.5):

$$\langle\widehat{\mathbf{E}}_{\text{t}}^{(k)}, \mathbf{e}_q^{(k)}\rangle = \widehat{V}_q^{(k)}$$
$$\langle\widehat{\mathbf{H}}_{\text{t}}^{(k)}, \mathbf{h}_q^{(k)}\rangle = \widehat{I}_q^{(k)}.$$

Instead, for what concerns the k-th port of the internal problem, these terms can be written as:

$$\langle\widetilde{\mathbf{E}}_{\text{t}}^{(k)}, \mathbf{e}_q^{(k)}\rangle = (\mathbf{T}_k^{(\text{e},\text{e})}\mathbf{c}^{(\text{e})} + \mathbf{T}_k^{(\text{e},\text{h})}\mathbf{c}^{(\text{h})})_q$$
$$\langle\widetilde{\mathbf{H}}_{\text{t}}^{(k)}, \mathbf{h}_q^{(k)}\rangle = (\mathbf{T}_k^{(\text{h},\text{e})}\mathbf{c}^{(\text{e})} + \mathbf{T}_k^{(\text{h},\text{h})}\mathbf{c}^{(\text{h})})_q,$$

where the expressions of the matrix elements depend on the specific differential problem. Then, by recalling (1.12) and by grouping the two projections, it can be found:

$$\underbrace{\begin{bmatrix} \mathbf{T}_1^{(\text{e},\text{e})} & \mathbf{T}_1^{(\text{e},\text{h})} \\[6pt] \mathbf{T}_1^{(\text{h},\text{e})} & \mathbf{T}_1^{(\text{h},\text{h})} \\[6pt] \mathbf{T}_2^{(\text{e},\text{e})} & \mathbf{T}_2^{(\text{e},\text{h})} \\[6pt] \mathbf{T}_2^{(\text{h},\text{e})} & \mathbf{T}_2^{(\text{h},\text{h})} \end{bmatrix}}_{\mathbf{T}} \mathbf{c} = \frac{1}{2}\underbrace{\begin{bmatrix} -\mathbf{Z}_\infty^{(1)} & \mathbf{I} & \mathbf{0} & \mathbf{0} \\[6pt] \mathbf{I} & -\mathbf{Y}_\infty^{(1)} & \mathbf{0} & \mathbf{0} \\[6pt] \mathbf{0} & \mathbf{0} & \mathbf{Z}_\infty^{(2)} & \mathbf{I} \\[6pt] \mathbf{0} & \mathbf{0} & \mathbf{I} & \mathbf{Y}_\infty^{(2)} \end{bmatrix}}_{\mathbf{D}} \mathbf{x} + \underbrace{\begin{bmatrix} \mathbf{I} & \mathbf{0} \\[6pt] \mathbf{Y}_\infty^{(1)} & \mathbf{0} \\[6pt] \mathbf{0} & \mathbf{I} \\[6pt] \mathbf{0} & -\mathbf{Y}_\infty^{(2)} \end{bmatrix}}_{\mathbf{K}} \underbrace{\begin{bmatrix} \mathbf{V}^{(\text{inc},1)} \\[6pt] \mathbf{V}^{(\text{inc},2)} \end{bmatrix}}_{\mathbf{V}^{(\text{inc})}},$$

$$(1.13)$$

that is:

$$\mathbf{T}\,\mathbf{c} = \mathbf{D}\,\mathbf{x} + \mathbf{K}\,\mathbf{V}^{(\mathrm{inc})}.$$

Then, by substituting (1.9):

$$\mathbf{T}\,\mathbf{G}\,\mathbf{x} = \mathbf{D}\,\mathbf{x} + \mathbf{K}\,\mathbf{V}^{(\mathrm{inc})},$$

so,

$$[\mathbf{T}\,\mathbf{G} - \mathbf{D}]\,\mathbf{x} = \mathbf{K}\,\mathbf{V}^{(\mathrm{inc})},$$

and, finally:

$$\mathbf{x} = [\mathbf{T}\,\mathbf{G} - \mathbf{D}]^{-1}\,\mathbf{K}\,\mathbf{V}^{(\mathrm{inc})}.$$

The generalized scattering matrix (GSM) of the device is evaluated from $\mathbf{x}$. The electromagnetic field at the access ports has an incident and a scattered components:

$$\widehat{\mathbf{V}}^{(1)} = \mathbf{V}^{(\mathrm{inc},1)} + \mathbf{V}^{(\mathrm{scat},1)} = (\mathbf{Z}_\infty^{(1)})^{\frac{1}{2}}\left[\mathbf{a}^{(1)} + \mathbf{b}^{(1)}\right]$$
$$\widehat{\mathbf{V}}^{(2)} = \mathbf{V}^{(\mathrm{inc},2)} + \mathbf{V}^{(\mathrm{scat},2)} = (\mathbf{Z}_\infty^{(2)})^{\frac{1}{2}}\left[\mathbf{a}^{(2)} + \mathbf{b}^{(2)}\right];$$

on the other hand, by recalling (1.12),

$$\widehat{\mathbf{V}}^{(1)} = \mathbf{V}^{(\mathrm{inc},1)} - \frac{1}{2}\mathbf{Z}_\infty^{(1)}\,\mathring{\mathbf{i}}^{(1)} + \frac{1}{2}\mathring{\mathbf{v}}^{(1)}$$
$$\widehat{\mathbf{V}}^{(2)} = \mathbf{V}^{(\mathrm{inc},2)} + \frac{1}{2}\mathbf{Z}_\infty^{(2)}\,\mathring{\mathbf{i}}^{(2)} + \frac{1}{2}\mathring{\mathbf{v}}^{(2)}.$$

Then, the following equations are obtained:

$$\mathbf{b}^{(1)} = -\frac{1}{2}(\mathbf{Z}_\infty^{(1)})^{\frac{1}{2}}\,\mathring{\mathbf{i}}^{(1)} + \frac{1}{2}(\mathbf{Y}_\infty^{(1)})^{\frac{1}{2}}\,\mathring{\mathbf{v}}^{(1)}$$
$$\mathbf{b}^{(2)} = +\frac{1}{2}(\mathbf{Z}_\infty^{(2)})^{\frac{1}{2}}\,\mathring{\mathbf{i}}^{(2)} + \frac{1}{2}(\mathbf{Y}_\infty^{(2)})^{\frac{1}{2}}\,\mathring{\mathbf{v}}^{(2)}.$$

These equations are written in matrix form as:

$$\underbrace{\begin{bmatrix}\mathbf{b}^{(1)}\\[1ex]\mathbf{b}^{(2)}\end{bmatrix}}_{\mathbf{b}} = \frac{1}{2}\underbrace{\begin{bmatrix}-(\mathbf{Z}_\infty^{(1)})^{\frac{1}{2}} & (\mathbf{Y}_\infty^{(1)})^{\frac{1}{2}} & \mathbf{0} & \mathbf{0}\\[1ex] \mathbf{0} & \mathbf{0} & (\mathbf{Z}_\infty^{(2)})^{\frac{1}{2}} & (\mathbf{Y}_\infty^{(2)})^{\frac{1}{2}}\end{bmatrix}}_{\mathbf{P}}\mathbf{x},$$

but:

$$\mathbf{x} = [\mathbf{T}\,\mathbf{G} - \mathbf{D}]^{-1}\,\mathbf{K}\,\mathbf{V}^{(\mathrm{inc})} = [\mathbf{T}\,\mathbf{G} - \mathbf{D}]^{-1}\,\mathbf{K}\underbrace{\begin{bmatrix} (\mathbf{Z}^{(1)}_{\infty})^{\frac{1}{2}} & \mathbf{0} \\ \mathbf{0} & (\mathbf{Z}^{(2)}_{\infty})^{\frac{1}{2}} \end{bmatrix}}_{\mathbf{Q}}\underbrace{\begin{bmatrix} \mathbf{a}^{(1)} \\ \\ \mathbf{a}^{(2)} \end{bmatrix}}_{\mathbf{a}}.$$

So:

$$\mathbf{b} = \frac{1}{2}\mathbf{P}\,[\mathbf{T}\,\mathbf{G} - \mathbf{D}]^{-1}\,\mathbf{K}\mathbf{Q}\mathbf{a};$$

therefore, the GSM, $\mathbf{S}$, is:

$$\mathbf{S} = \frac{1}{2}\mathbf{P}\,[\mathbf{T}\,\mathbf{G} - \mathbf{D}]^{-1}\,\mathbf{K}\mathbf{Q}. \tag{1.14}$$

Equivalence theorem - PMC formulation

The case where the discretized BVP is written in form

$$(\mathbf{A}^{(\mathrm{e,e})}\mathbf{c}^{(\mathrm{e})})_r = \int_{\gamma^{(1)}_{\mathrm{wg}}} \mathbf{H}\,v_r^{(\mathrm{e})*}\big|_{z^{(1)}_{\mathrm{wg}}} \cdot \mathrm{d}\mathbf{s} + \int_{\gamma^{(2)}_{\mathrm{wg}}} \mathbf{H}\,v_r^{(\mathrm{e})*}\big|_{z^{(2)}_{\mathrm{wg}}} \cdot \mathrm{d}\mathbf{s}, \ \ r = 1...N^{(\mathrm{e})}_{\mathrm{f}} \tag{1.15}$$

is now considered. By recalling (1.7), (1.8) and (1.4) it can be written, just like in the previous case:

$$\mathbf{A}^{(\mathrm{e,e})}\mathbf{c}^{(\mathrm{e})} = -\mathbf{B}^{(\mathrm{e,1})}\,\mathring{\mathbf{i}}^{(1)} + \mathbf{B}^{(\mathrm{e,2})}\,\mathring{\mathbf{i}}^{(2)},$$

where:

$$(\mathbf{B}^{(\mathrm{e},k)})_r = \int_{\gamma^{(k)}_{\mathrm{wg}}} h^{(k)}_{s,n}\,v_r^{(\mathrm{e})*}\big|_{z=z^{(k)}_{\mathrm{wg}}} \, \mathrm{d}s.$$

This can be grouped as:

$$\mathbf{A}^{(\mathrm{e,e})}\,\mathbf{c}^{(\mathrm{e})} = \underbrace{\begin{bmatrix} -\mathbf{B}^{(\mathrm{e,1})} & \mathbf{B}^{(\mathrm{e,2})} \end{bmatrix}}_{\mathbf{B}^{(\mathrm{e})}}\underbrace{\begin{bmatrix} \mathring{\mathbf{i}}^{(1)} \\ \\ \mathring{\mathbf{i}}^{(2)} \end{bmatrix}}_{\mathring{\mathbf{i}}}, \tag{1.16}$$

or, compactly:

$$\mathbf{A}^{(\mathrm{e,e})}\,\mathbf{c}^{(\mathrm{e})} = \mathbf{B}^{(\mathrm{e})}\,\mathring{\mathbf{i}}.$$

No electric field is present in the right-hand side integrals, therefore the magnetic current densities do not provide any contribution to (1.15). For this reason, it

is convenient to complete the equivalent external problem by filling the zero-field region with PMC, to eliminate their radiation contribution in the scattering problem. Focusing on the external problem, the hybrid multi-modal circuit of Fig. 1.3 is associated to the waveguide device. The expansion coefficients in this circuit have the same meaning of the ones of Fig. 1.2. This leads to the equivalent circuit of

Figure 1.3: Equivalent modal circuit relative to the n-th waveguide mode. $Z_{\infty,n}$ is the characteristic impedance at the access port; the sources are related to the equivalent current densities; $V_n^{(\text{inc})}$ is the incidence voltage of the n-th mode.

Fig. 1.3; its solution is:

$$
\begin{aligned}
\widehat{\mathbf{V}}^{(1)} &= 2\mathbf{V}^{(\text{inc},1)} - \mathbf{Z}_\infty^{(1)}\,\mathring{\mathbf{i}}^{(1)} \\
\widehat{\mathbf{I}}^{(1)} &= \mathring{\mathbf{i}}^{(1)} \\
\widehat{\mathbf{V}}^{(2)} &= 2\mathbf{V}^{(\text{inc},2)} + \mathbf{Z}_\infty^{(2)}\,\mathring{\mathbf{i}}^{(2)} \\
\widehat{\mathbf{I}}^{(2)} &= \mathring{\mathbf{i}}^{(2)}.
\end{aligned}
\tag{1.17}
$$

The formulation is completed by enforcing the continuity of the electric field at the access ports. Indeed, the unknown of the differential problem is an electric field, whereas the magnetic field is proportional to its derivative; moreover, the magnetic field continuity is guaranteed by the choice of the electric current density of Fig. 1.1. Since

$$
\langle \widetilde{\mathbf{E}}_{\text{t}}^{(k)}, \mathbf{e}_q^{(k)} \rangle = (\mathbf{T}_k^{(\text{e,e})}\,\mathbf{c}^{(\text{e})})_q,
$$

the continuity equations at the access ports are:

$$
\begin{aligned}
-\mathbf{Z}_\infty^{(1)}\,\mathring{\mathbf{i}}^{(1)} + 2\mathbf{V}^{(\text{inc},1)} &= \mathbf{T}_1^{(\text{e,e})}\,\mathbf{c}^{(\text{e})} \\
\mathbf{Z}_\infty^{(2)}\,\mathring{\mathbf{i}}^{(2)} + 2\mathbf{V}^{(\text{inc},2)} &= \mathbf{T}_2^{(\text{e,e})}\,\mathbf{c}^{(\text{e})},
\end{aligned}
$$

which are grouped as:

$$\underbrace{\begin{bmatrix} \mathbf{T}_1^{(\mathrm{e,e})} \\ \\ \mathbf{T}_2^{(\mathrm{e,e})} \end{bmatrix}}_{\mathbf{T}^{(\mathrm{e,e})}} \mathbf{c}^{(\mathrm{e})} = \underbrace{\begin{bmatrix} -\mathbf{Z}_\infty^{(1)} & \mathbf{0} \\ \\ \mathbf{0} & \mathbf{Z}_\infty^{(2)} \end{bmatrix}}_{\mathbf{D}^{(\mathrm{e})}} \mathring{\mathbf{i}} + 2 \underbrace{\begin{bmatrix} \mathbf{V}^{(\mathrm{inc},1)} \\ \\ \mathbf{V}^{(\mathrm{inc},2)} \end{bmatrix}}_{\mathbf{V}^{(\mathrm{inc})}},$$

or, more compactly:

$$\mathbf{T}^{(\mathrm{e,e})}\, \mathbf{c}^{(\mathrm{e})} = \mathbf{D}^{(\mathrm{e})}\, \mathring{\mathbf{i}} + 2\mathbf{V}^{(\mathrm{inc})}.$$

By inverting (1.16) and substituting it in the last equation, the following expression is obtained:

$$\mathbf{T}^{(\mathrm{e,e})}(\mathbf{A}^{(\mathrm{e,e})})^{-1}\mathbf{B}^{(\mathrm{e})}\mathring{\mathbf{i}} = \mathbf{D}^{(\mathrm{e})}\, \mathring{\mathbf{i}} + 2\mathbf{V}^{(\mathrm{inc})},$$

from where:

$$\mathring{\mathbf{i}} = 2 \left[\mathbf{T}^{(\mathrm{e,e})}(\mathbf{A}^{(\mathrm{e,e})})^{-1}\mathbf{B}^{(\mathrm{e})} - \mathbf{D}^{(\mathrm{e})} \right]^{-1} \mathbf{V}^{(\mathrm{inc})}.$$

Then, from (1.17), it known that $\widehat{\mathbf{I}}^{(k)} = \mathring{\mathbf{i}}^{(k)}$, therefore:

$$\widehat{\mathbf{I}}^{(1)} = \mathbf{I}^{(\mathrm{inc},1)} + \mathbf{I}^{(\mathrm{scat},1)} = (\mathbf{Y}_\infty^{(1)})^{\frac{1}{2}} \left[\mathbf{a}^{(1)} - \mathbf{b}^{(1)} \right]$$
$$\widehat{\mathbf{I}}^{(2)} = \mathbf{I}^{(\mathrm{inc},2)} + \mathbf{I}^{(\mathrm{scat},2)} = (\mathbf{Y}_\infty^{(2)})^{\frac{1}{2}} \left[-\mathbf{a}^{(2)} + \mathbf{b}^{(2)} \right],$$

that are compactly written as:

$$\mathring{\mathbf{i}} = \underbrace{\begin{bmatrix} (\mathbf{Y}_\infty^{(1)})^{\frac{1}{2}} & \mathbf{0} \\ \\ \mathbf{0} & -(\mathbf{Y}_\infty^{(2)})^{\frac{1}{2}} \end{bmatrix}}_{\mathbf{P}^{(\mathrm{e})}} \begin{bmatrix} \mathbf{a}^{(1)} \\ \\ \mathbf{a}^{(2)} \end{bmatrix} - \underbrace{\begin{bmatrix} (\mathbf{Y}_\infty^{(1)})^{\frac{1}{2}} & \mathbf{0} \\ \\ \mathbf{0} & -(\mathbf{Y}_\infty^{(2)})^{\frac{1}{2}} \end{bmatrix}}_{\mathbf{P}^{(\mathrm{e})}} \begin{bmatrix} \mathbf{b}^{(1)} \\ \\ \mathbf{b}^{(2)} \end{bmatrix}.$$

Instead, from the solution of the scattering problem:

$$\mathring{\mathbf{i}} = 2 \left[\mathbf{T}^{(\mathrm{e,e})}(\mathbf{A}^{(\mathrm{e,e})})^{-1}\mathbf{B}^{(\mathrm{e})} - \mathbf{D}^{(\mathrm{e})} \right]^{-1} \underbrace{\begin{bmatrix} (\mathbf{Z}_\infty^{(1)})^{\frac{1}{2}} & \mathbf{0} \\ \\ \mathbf{0} & (\mathbf{Z}_\infty^{(2)})^{\frac{1}{2}} \end{bmatrix}}_{(\mathbf{Q}^{(\mathrm{e})})} \begin{bmatrix} \mathbf{a}^{(1)} \\ \\ \mathbf{a}^{(2)} \end{bmatrix}.$$

Then:

$$\begin{bmatrix} \mathbf{b}^{(1)} \\ \\ \mathbf{b}^{(2)} \end{bmatrix} = \left[\mathbf{I} - 2(\mathbf{P}^{(\mathrm{e})})^{-1} \left[\mathbf{T}^{(\mathrm{e,e})}(\mathbf{A}^{(\mathrm{e,e})})^{-1}\mathbf{B}^{(\mathrm{e})} - \mathbf{D}^{(\mathrm{e})} \right]^{-1} \mathbf{Q}^{(\mathrm{e})} \right] \begin{bmatrix} \mathbf{a}^{(1)} \\ \\ \mathbf{a}^{(2)} \end{bmatrix}.$$

To sum up, the expression of the GSM is:

$$\mathbf{S} = \mathbf{I} - 2(\mathbf{P}^{(e)})^{-1} \left[\mathbf{T}^{(e,e)}(\mathbf{A}^{(e,e)})^{-1}\mathbf{B}^{(e)} - \mathbf{D}^{(e)}\right]^{-1} \mathbf{Q}^{(e)}.$$

Equivalence theorem - PEC formulation

The situation where the discretized BVP is written in form

$$(\mathbf{A}^{(h,h)}\mathbf{c}^{(h)})_r = \int_{\gamma_{\mathrm{wg}}^{(1)}} \mathbf{E}\, v_r^{(h)*}\big|_{z_{\mathrm{wg}}^{(1)}} \cdot \mathrm{d}\mathbf{s} + \int_{\gamma_{\mathrm{wg}}^{(2)}} \mathbf{E}\, v_r^{(h)*}\big|_{z_{\mathrm{wg}}^{(2)}} \cdot \mathrm{d}\mathbf{s}, \ \ r = 1...N_{\mathrm{f}}^{(h)}. \qquad (1.18)$$

is now considered. By recalling (1.7), (1.8) and (1.4) it can be written, just like in the previous case:

$$\mathbf{A}^{(h,h)}\mathbf{c}^{(h)} = -\mathbf{B}^{(h,1)}\,\mathring{\mathbf{v}}^{(1)} + \mathbf{B}^{(h,2)}\,\mathring{\mathbf{v}}^{(2)},$$

where:

$$(\mathbf{B}^{(h,k)})_r = \int_{\gamma_{\mathrm{wg}}^{(k)}} e_{s,n}^{(k)}\, v_r^{(h)*}\big|_{z=z_{\mathrm{wg}}^{(k)}} \,\mathrm{d}s.$$

This can be grouped as:

$$\mathbf{A}^{(h,h)}\,\mathbf{c}^{(h)} = \underbrace{\begin{bmatrix}-\mathbf{B}^{(h,1)} & \mathbf{B}^{(h,2)}\end{bmatrix}}_{\mathbf{B}^{(h)}} \underbrace{\begin{bmatrix}\mathring{\mathbf{v}}^{(1)} \\ \mathring{\mathbf{v}}^{(2)}\end{bmatrix}}_{\mathring{\mathbf{v}}}, \qquad (1.19)$$

or, compactly:

$$\mathbf{A}^{(h,h)}\,\mathbf{c}^{(h)} = \mathbf{B}^{(h)}\,\mathring{\mathbf{v}}.$$

No magnetic field is present in the right-hand side integrals, therefore the electric current densities are not present in (1.18). For this reason, it is convenient to complete the equivalent external problem by filling the zero-field region with PEC, to eliminate their radiation contribution in the scattering problem.

Focusing on the external problem, the hybrid multi-modal circuit of Fig. 1.4 is associated to the waveguide device. The quantities in this circuit have the same meaning of the ones of Fig. 1.2. This leads to the equivalent circuit of Fig. 1.3; its solution is:
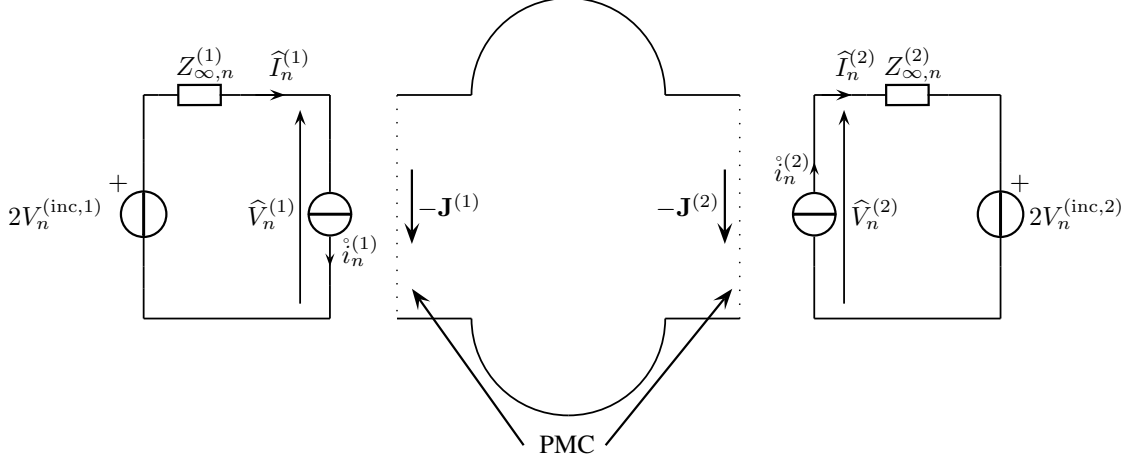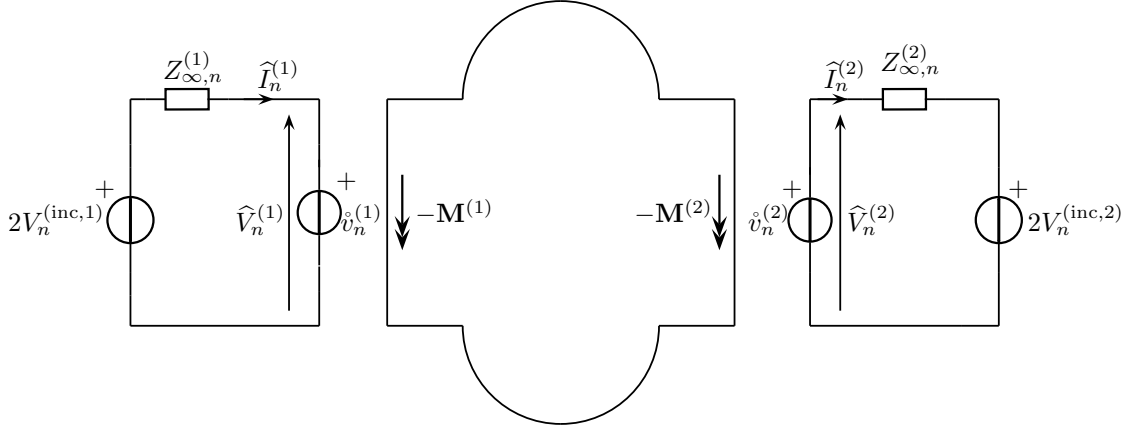
Figure 1.4: Equivalent modal circuit relative to the n-th waveguide mode. $Z_{\infty,n}$ is the characteristic impedance at the access port; the sources are related to the equivalent current densities; $V_n^{(\mathrm{inc})}$ is the incidence voltage of the n-th mode.

$$
\begin{aligned}
\widehat{\mathbf{V}}^{(1)} &= \mathring{\mathbf{v}}^{(1)} \\
\widehat{\mathbf{I}}^{(1)} &= 2\mathbf{Y}_\infty^{(1)}\,\mathbf{V}^{(\mathrm{inc},1)} - \mathbf{Y}_\infty^{(1)}\,\mathring{\mathbf{v}}^{(1)} \\
\widehat{\mathbf{V}}^{(2)} &= \mathring{\mathbf{v}}^{(2)} \\
\widehat{\mathbf{I}}^{(2)} &= -2\mathbf{Y}_\infty^{(2)}\mathbf{V}^{(\mathrm{inc},2)} + \mathbf{Y}_\infty^{(2)}\,\mathring{\mathbf{v}}^{(2)}.
\end{aligned}
\tag{1.20}
$$

The formulation is completed by enforcing the continuity of the magnetic field at the access ports. Indeed, the unknown of the differential problem is a magnetic field, whereas the electric field is proportional to its derivative; moreover, the electric field continuity is guaranteed by the choice of the magnetic current density of Fig. 1.1. Since

$$
\langle \widetilde{\mathbf{H}}_{\mathrm{t}}^{(k)}, \mathbf{h}_q^{(k)} \rangle = (\mathbf{T}_k^{(\mathrm{h,h})}\,\mathbf{c}^{(\mathrm{h})})_q,
$$

the continuity equations at the access ports are:

$$
\begin{aligned}
2\mathbf{Y}_\infty^{(1)}\,\mathbf{V}^{(\mathrm{inc},1)} - \mathbf{Y}_\infty^{(1)}\,\mathring{\mathbf{v}}^{(1)} &= \mathbf{T}_1^{(\mathrm{h,h})}\,\mathbf{c}^{(\mathrm{h})} \\
-2\mathbf{Y}_\infty^{(2)}\mathbf{V}^{(\mathrm{inc},2)} + \mathbf{Y}_\infty^{(2)}\,\mathring{\mathbf{v}}^{(2)} &= \mathbf{T}_2^{(\mathrm{h,h})}\,\mathbf{c}^{(\mathrm{h})},
\end{aligned}
$$

that are grouped as:

$$
\underbrace{\begin{bmatrix} \mathbf{T}_1^{(\mathrm{h,h})} \\[2mm] \mathbf{T}_2^{(\mathrm{h,h})} \end{bmatrix}}_{\mathbf{T}^{(\mathrm{h})}} \mathbf{c}^{(\mathrm{h})} = \underbrace{\begin{bmatrix} -\mathbf{Y}_\infty^{(1)} & \mathbf{0} \\[2mm] \mathbf{0} & \mathbf{Y}_\infty^{(2)} \end{bmatrix}}_{\mathbf{D}^{(\mathrm{h})}} \mathring{\mathbf{v}} - 2\underbrace{\begin{bmatrix} -\mathbf{Y}_\infty^{(1)} & \mathbf{0} \\[2mm] \mathbf{0} & \mathbf{Y}_\infty^{(2)} \end{bmatrix}}_{\mathbf{D}^{(\mathrm{h})}} \underbrace{\begin{bmatrix} \mathbf{V}^{(\mathrm{inc},1)} \\[2mm] \mathbf{V}^{(\mathrm{inc},2)} \end{bmatrix}}_{\mathbf{V}^{(\mathrm{inc})}},
$$

or, more compactly:

$$\mathbf{T}^{(\mathrm{h,h})}\,\mathbf{c}^{(\mathrm{h})} = \mathbf{D}^{(\mathrm{h})}\,\mathring{\mathbf{v}} - 2\mathbf{D}^{(\mathrm{h})}\,\mathbf{V}^{(\mathrm{inc})}.$$

and, by inverting (1.19) and substituting it in the last equation,

$$\mathbf{T}^{(\mathrm{h,h})}(\mathbf{A}^{(\mathrm{h,h})})^{-1}\mathbf{B}^{(\mathrm{h})}\mathring{\mathbf{v}} = \mathbf{D}^{(\mathrm{h})}\,\mathring{\mathbf{v}} - 2\mathbf{D}^{(\mathrm{h})}\,\mathbf{V}^{(\mathrm{inc})},$$

from where:

$$\mathring{\mathbf{v}} = -2\left[\mathbf{T}^{(\mathrm{h,h})}(\mathbf{A}^{(\mathrm{h,h})})^{-1}\mathbf{B}^{(\mathrm{h})} - \mathbf{D}^{(\mathrm{h})}\right]^{-1}\mathbf{D}^{(\mathrm{h})}\,\mathbf{V}^{(\mathrm{inc})}.$$

Then, from (1.20), it known that $\widehat{\mathbf{V}}^{(k)} = \mathring{\mathbf{v}}^{(k)}$, therefore:

$$\widehat{\mathbf{V}}^{(1)} = \mathbf{V}^{(\mathrm{inc},1)} + \mathbf{V}^{(\mathrm{scat},1)} = (\mathbf{Z}_{\infty}^{(1)})^{\frac{1}{2}}\left[\mathbf{a}^{(1)} + \mathbf{b}^{(1)}\right]$$
$$\widehat{\mathbf{V}}^{(2)} = \mathbf{V}^{(\mathrm{inc},2)} + \mathbf{V}^{(\mathrm{scat},2)} = (\mathbf{Z}_{\infty}^{(2)})^{\frac{1}{2}}\left[\mathbf{a}^{(2)} + \mathbf{b}^{(2)}\right],$$

which are compactly written as:

$$\mathring{\mathbf{v}} = \underbrace{\begin{bmatrix}(\mathbf{Z}_{\infty}^{(1)})^{\frac{1}{2}} & \mathbf{0} \\ \mathbf{0} & (\mathbf{Z}_{\infty}^{(2)})^{\frac{1}{2}}\end{bmatrix}}_{\mathbf{P}^{(\mathrm{h})}}\begin{bmatrix}\mathbf{a}^{(1)} \\ \mathbf{a}^{(2)}\end{bmatrix} + \underbrace{\begin{bmatrix}(\mathbf{Z}_{\infty}^{(1)})^{\frac{1}{2}} & \mathbf{0} \\ \mathbf{0} & (\mathbf{Z}_{\infty}^{(2)})^{\frac{1}{2}}\end{bmatrix}}_{\mathbf{P}^{(\mathrm{h})}}\begin{bmatrix}\mathbf{b}^{(1)} \\ \mathbf{b}^{(2)}\end{bmatrix}.$$

Instead, from the solution of the scattering problem:

$$\mathring{\mathbf{v}} = -2\left[\mathbf{T}^{(\mathrm{h,h})}(\mathbf{A}^{(\mathrm{h,h})})^{-1}\mathbf{B}^{(\mathrm{h})} - \mathbf{D}^{(\mathrm{h})}\right]^{-1}\mathbf{D}^{(\mathrm{h})}\underbrace{\begin{bmatrix}(\mathbf{Z}_{\infty}^{(1)})^{\frac{1}{2}} & \mathbf{0} \\ \mathbf{0} & (\mathbf{Z}_{\infty}^{(2)})^{\frac{1}{2}}\end{bmatrix}}_{(\mathbf{Q}^{(\mathrm{h})})}\begin{bmatrix}\mathbf{a}^{(1)} \\ \mathbf{a}^{(2)}\end{bmatrix}.$$

Then:

$$\begin{bmatrix}\mathbf{b}^{(1)} \\ \mathbf{b}^{(2)}\end{bmatrix} = -\left[\mathbf{I} + 2(\mathbf{P}^{(\mathrm{h})})^{-1}\left[\mathbf{T}^{(\mathrm{h,h})}(\mathbf{A}^{(\mathrm{h,h})})^{-1}\mathbf{B}^{(\mathrm{h})} - \mathbf{D}^{(\mathrm{h})}\right]^{-1}\mathbf{D}^{(\mathrm{h})}\mathbf{Q}^{(\mathrm{h})}\right]\begin{bmatrix}\mathbf{a}^{(1)} \\ \mathbf{a}^{(2)}\end{bmatrix}.$$

So, the expression of the GSM is:

$$\mathbf{S} = -\left[\mathbf{I} + 2(\mathbf{P}^{(\mathrm{h})})^{-1}\left[\mathbf{T}^{(\mathrm{h,h})}(\mathbf{A}^{(\mathrm{h,h})})^{-1}\mathbf{B}^{(\mathrm{h})} - \mathbf{D}^{(\mathrm{h})}\right]^{-1}\mathbf{D}^{(\mathrm{h})}\mathbf{Q}^{(\mathrm{h})}\right].$$

1.3 Synthesis of the MEM basis functions

Multi-domain spectral methods in two dimensions are based on the decomposition of the domain Σ of the BVP in a small number of quadrilateral sub-domains (or patches) $\Sigma^{(j)}$ as exemplified in Fig. 1.5, where five patches are defined. Local basis functions are defined for each patch in a reference (or parent) domain that can be transformed into the j-th patch through an analytical blending mapping. The key point of multi-domain spectral methods is the definition of a set of entire-domain basis functions starting from the local sets; in the mortar element method, this is obtained by enforcing the continuity of the basis functions in weak form, according to the mortar-matching technique.

In this section the procedure aimed at synthesizing numerically the MEM basis functions is described. Starting from an initial set of local basis functions, this is augmented with singular weights to account for the presence of sharp edges, where some field components diverge. Then, several basis recombination procedures are applied to obtain a set of orthonormal entire-domain basis functions satisfying the boundary conditions of the problem.
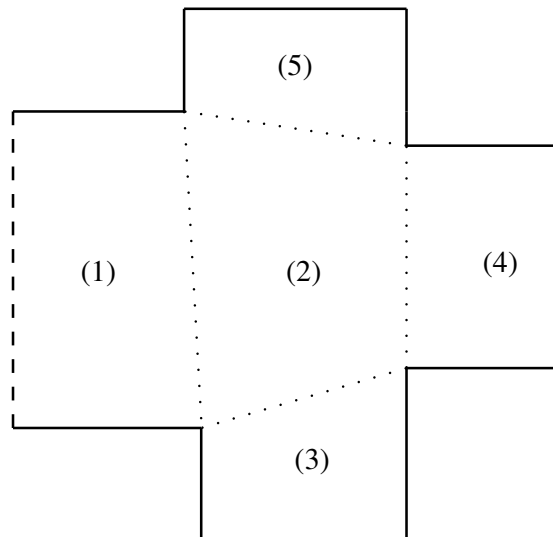
Figure 1.5: Example of domain that can not be mapped into a single reference domain; the solid lines identify the sides where PEC boundary conditions have to be enforced; the dashed lines are the access ports; the dotted lines are the common edges between different patches. In this example, each patch can be mapped to the parent domain through a bilinear mapping.

1.3.1 Synthesis of non-specialized basis functions

The tensor product of the solution of Sturm-Liouville (SL) problems defined in the parent domain is typically used to synthesize spectral methods basis functions. Indeed, the spectral approximation of the solution of a differential problem is usually regarded as a finite expansion of eigenfunctions of a SL problem; in spectral methods, the most appealing problems are the ones such that the expansion of an infinitely smooth function in terms of their eigenfunctions guarantees spectral accuracy. In particular, spectral accuracy is ensured if the SL problem is singular [3]. Among these issues, particular importance rests with those problems whose eigenfunctions are algebraic polynomials, because of the efficiency with they can be evaluated and differentiated numerically. In this work, Chebyshev polynomials have been used as generating functions; these polynomials are properly defined in the interval $[-1, 1]$. Therefore, it is possible to define the functions $P_{\iota\kappa}(\boldsymbol{\sigma})$ as:

$$P_{\iota\kappa}(\boldsymbol{\sigma}) = P_{\iota\kappa}(\xi, \eta) = T_{\iota}(\xi)T_{\kappa}(\eta), \qquad \xi, \eta \in [-1, 1],$$

where $\boldsymbol{\sigma} = (\xi, \eta)$ is the variable of the domain where the basis functions are defined. The non-specialized basis functions on the spatial domain are defined as:

$$\phi_{\tau}^{(j)}(\mathbf{r}) = P_{\iota\kappa}(\mathbf{r}(\boldsymbol{\sigma})), \qquad \mathbf{r} \in \Sigma^{(j)},$$

where $\tau = (\iota, \kappa)$ is a double index. The expressions of the mapping $\mathbf{r}(\boldsymbol{\sigma})$ are reported in the Appendix A for two cases: the bilinear case, which is used to map the reference domain to a generic quadrilateral with straight edges, and the analytical blending mapping, based on the Gordon-Hall formula.

1.3.2 Introduction of singular weights

One of the most appealing properties of spectral methods is their exponential convergence; however, this can be deteriorated by the presence of sharp edges, since they introduce a singular behavior in some field components. To restore the convergence rate, the set of basis functions can be augmented with weights that model the asymptotic behavior of the electromagnetic field in the proximity of each corner [11].

The spatial domain Σ is mapped into the companion domain, which is obtained rectifying each curved edge with the straight line tangent at the corner. In the case of structures composed only of straight lines, the two domains are coincident. Let $\boldsymbol{\chi} = F_{\chi\sigma}^{(j)}(\boldsymbol{\sigma})$ be the mapping from the $\boldsymbol{\sigma}$ domain to the companion domain; according to Fig. 1.6, let ρ_e and ϑ_e be the distance and the angular coordinates of

a cylindrical system centered in the e-th corner; let δ_e be the angular dimension of the corner; then, the following expressions have been derived in Appendix A:
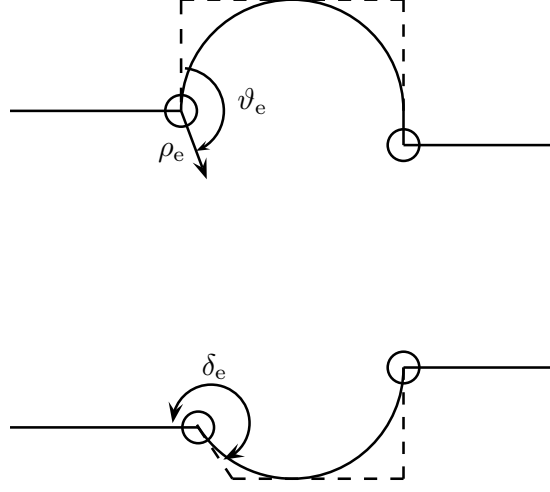
Figure 1.6: Example of domain where the companion domain is not coincident to the natural domain. The dashed lines identify the sides used to define the corner; the circles identify the sharp edges that require to be described with proper basis functions; δ_e is the angle of the edge; ρ_e, ϑ_e are the radial and azimuthal coordinates defined on the e-th corner.

- the i-th singular function aimed at describing the electric field component parallel to the edge is:

$$\psi_{p_i}^{(\mathrm{h})} = \rho_e^{\frac{p_i \pi}{\delta_e}} \sin\left(\frac{p_i \pi}{\delta_e} \vartheta_e\right), \quad p_i = 1, 2... \tag{1.21}$$

- the i-th singular function aimed at describing the magnetic field component parallel to the edge is:

$$\psi_{p_i}^{(\mathrm{h})} = \rho_e^{\frac{p_i \pi}{\delta_e}} \cos\left(\frac{p_i \pi}{\delta_e} \vartheta_e\right), \quad p_i = 1, 2... \tag{1.22}$$

Now the set of non-specialized basis functions $\{\phi_\tau^{(j)}(\mathbf{r})\}$ is augmented by using (1.21) or (1.22) as weights, defining:

$$f_\alpha^{(j)}(\mathbf{r}) = \bigcup_{p=p_1}^{p_s} \psi_p^{(\mathrm{e|h})}(\boldsymbol{\chi}) \phi_\tau^{(j)}(\mathbf{r}).$$

The non-specialized functions $f_\alpha^{(j)}(\mathbf{r})$ are the union of the sets of functions $\phi_\tau^{(j)}(\mathbf{r})$ multiplied times the singular weighting functions ψ_p for every considered p; in other

words, $\{f_\alpha^{(j)}(\mathbf{r})\} = \{\{\phi_\tau^{(j)}(\mathbf{r})\}, \{\psi_{p_1}^{(e|h)}(\boldsymbol{\chi})\phi_\tau^{(j)}(\mathbf{r})\}, \{\psi_{p_2}^{(e|h)}(\boldsymbol{\chi})\phi_\tau^{(j)}(\mathbf{r})\}, ...\}$. Usually, $p = \{0, 1\}$. The resulting multi-index α is three-dimensional: $\alpha = (\iota, \kappa, p)$, since it can assume, for each p, the values of the index τ.

1.3.3 Essential boundary conditions and orthonormalization

It is necessary to distinguish two classes of boundary conditions: essential and natural [12].

- Essential boundary conditions have to be enforced explicitly; this is done by synthesizing basis functions that individually satisfy these conditions. Dirichlet boundary conditions are an example of essential boundary conditions.

- Natural boundary conditions can be either enforced explicitly just like essential conditions, or by modifying the weak formulation of the problem. Neumann or Robin boundary conditions can be enforced naturally. This is commonly done through the boundary contribution that arise from the application of integration by parts in the weak formulation of the problem.

The naif application of the essential boundary condition can be applied in both cases, but it may damage the convergence of the method, since it would produce basis functions that are too specialized. This is shown, with an example, in Section 2.3.
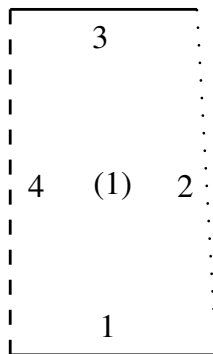
Figure 1.7: Detail of Fig. 1.5 where the patch (1) is reported. The numbers not included in parentheses identify the edges of the patch. The solid line identify the PEC boundary conditions; the dashed line identifies an access port; the dotted line identifies an edge where continuity conditions have to be enforced.

The enforcement of natural boundary conditions regards the formulation of the differential problem, and therefore it is discussed in the next chapters. So, if no

essential boundary condition should be enforced, it is possible to skip these steps, by defining:

$$g_\beta^{(j)}(\mathbf{r}) = f_\beta^{(j)}(\mathbf{r}).$$

Otherwise, let γ be the boundary of the domain Σ, and let $\gamma_{(\text{BC})}$ be the union of the segments of γ where Dirichlet boundary conditions should be enforced. Then, let $\gamma_{(\text{BC})}^{(j)}$ be the part of boundary of the j-th patch where the condition is required. In Fig. 1.7 an example of patch is reported; for this example, $\gamma_{(\text{BC})}^{(j)}$ consists of the edges 1 and 3.

In this section a set of functions $\{g_\beta^{(j)}(\mathbf{r})\}$ that satisfy a Dirichlet boundary condition on $\gamma_{(\text{BC})}^{(j)}$ is defined by applying a basis recombination approach to the set of functions $\{f_\alpha^{(j)}(\mathbf{r})\}$. This means that each β-th function is defined as:

$$g_\beta^{(j)}(\mathbf{r}) = \sum_\alpha y_\alpha^{(j,\beta)} f_\alpha^{(j)}(\mathbf{r}),$$

where $\{y_\alpha^{(j,\beta)}\}$ are chosen in such a way that:

$$g_\beta^{(j)}(\mathbf{r}) = 0, \quad \mathbf{r} \in \gamma_{(\text{BC})}^{(j)}, \quad \forall \beta.$$

This condition is required in weak form, by projecting this equation on a set of test function $\{v_\upsilon(\mathbf{r})\}$ defined on $\gamma_{(\text{BC})}^{(j)}$:

$$\langle g_\beta^{(j)}(\mathbf{r}), v_\upsilon(\mathbf{r}) \rangle = 0, \quad \forall \beta, \upsilon;$$

then, by substituting the previous expression:

$$\sum_\alpha y_\alpha^{(j,\beta)} \langle f_\alpha^{(j)}(\mathbf{r}), v_\upsilon(\mathbf{r}) \rangle = 0, \quad \forall \beta, \upsilon.$$

Let the matrix element $\mathbf{L}_{\upsilon\alpha}^{(j)}$ be defined as:

$$\mathbf{L}_{\upsilon\alpha}^{(j)} = \langle f_\alpha^{(j)}(\mathbf{r}), v_\upsilon(\mathbf{r}) \rangle = \int_{\gamma_{(\text{BC})}^{(j)}} f_\alpha^{(j)} v_\upsilon^* \, \mathrm{d}s,$$

then, the previous condition are written in matrix form as:

$$\mathbf{L}^{(j)} \mathbf{Y}^{(j)} = \mathbf{0},$$

where $\mathbf{Y}^{(j)}$ is the matrix having as columns the vectors $\mathbf{y}^{(j,\beta)}$; the β-th vector corresponds to the function $g_\beta^{(j)}(\mathbf{r})$. In other words, since the previous system is homogeneous, the matrix $\mathbf{Y}^{(j)}$ is built using as columns the elements of the kernel of the

matrix $\mathbf{L}^{(j)}$. An orthonormal basis of the kernel of a matrix can be found by means of the singular value decomposition (SVD); by considering the SVD of $\mathbf{L}^{(j)}$:

$$\mathbf{L}^{(j)} = \mathbf{U}^{(j,\mathrm{g})} \, \mathbf{S}^{(j,\mathrm{g})} \, (\mathbf{V}^{(j,\mathrm{g})})^{\mathrm{H}}.$$

The basis of the kernel of $\mathbf{L}^{(j)}$ is given by the columns of the matrix $\mathbf{V}^{(j,\mathrm{g})}$ corresponding to the null singular values, *i.e.*, below a threshold ε_{g}. The number of columns of $\mathbf{G}^{(j)}$ equals the dimension of the set $\{f_\alpha^{(j)}(\mathbf{r})\}$, whereas its number of rows equals the dimension of $\{g_\beta^{(j)}(\mathbf{r})\}$. So, by defining two column vectors of functions $\mathbf{f}^{(j)}(\mathbf{r})$ and $\mathbf{g}^{(j)}(\mathbf{r})$, it is possible to relate them as:

$$\mathbf{g}^{(j)}(\mathbf{r}) = (\mathbf{G}^{(j)})^{\mathrm{T}} \mathbf{f}^{(j)}(\mathbf{r}).$$

Orthonormalization

The functions belonging to the set $\{g_\beta^{(j)}(\mathbf{r})\}$ are not linearly independent, due to the introduction of the effect of the sharp edges. Indeed, far from the edges the weighted functions become almost proportional to the non-weighted ones, leading to the generation of redundancies in the field representation. For this reason, a basis recombination approach aimed at providing local sets of orthonormal functions is applied:

$$h_t^{(j)}(\mathbf{r}) = \sum_\beta H_{t\beta}^{(j)} g_\beta^{(j)}(\mathbf{r}).$$

The procedure aimed at obtaining the coefficients $H_{t\beta}^{(j)}$ is now described. Let $(\mathbf{M})_{\beta_1 \beta_2}$ be the generic element of the Gram matrix of the functions $\{g_\beta^{(j)}(\mathbf{r})\}$:

$$(\mathbf{M}^{(j)})_{\beta_1 \beta_2} = \langle g_{\beta_2}^{(j)}(\mathbf{r}), g_{\beta_1}^{(j)}(\mathbf{r}) \rangle = \int_{\Sigma^{(j)}} g_{\beta_2}^{(j)}(\mathbf{r}) g_{\beta_1}^{(j)*}(\mathbf{r}) \, \mathrm{d}\mathbf{r}.$$

The coefficients $H_{t\beta}^{(j)}$ are found as a basis of the range of the matrix $\mathbf{M}^{(j)}$; this can be evaluated with the SVD:

$$\mathbf{M}^{(j)} = \mathbf{U}^{(j,\mathrm{h})} \, \mathbf{S}^{(j,\mathrm{h})} \, (\mathbf{V}^{(j,\mathrm{h})})^{\mathrm{H}}.$$

Indeed, the columns of the matrix $\mathbf{U}^{(j,\mathrm{h})}$ corresponding to the most significant singular values of $\mathbf{S}^{(j,\mathrm{h})}$, *i.e.*, above a threshold ε_{h}, are an orthonormal basis of the range of the matrix $\mathbf{M}^{(j)}$. The length of each column of $\mathbf{U}^{(j,\mathrm{h})}$ equals the number of functions belonging to $\{g_\beta^{(j)}(\mathbf{r})\}$. The t-th column of the matrix $\mathbf{H}^{(j)}$ gives the recombination coefficients used to obtain the function $h_t^{(j)}(\mathbf{r})$. Therefore, it is possible to find the vector of functions $\mathbf{h}^{(j)}(\mathbf{r})$ as:

$$\mathbf{h}^{(j)}(\mathbf{r}) = (\mathbf{H}^{(j)})^{\mathrm{T}}\mathbf{g}^{(j)}(\mathbf{r}).$$

1.3.4 Continuity conditions

In the previous section a set of orthonormal boundary-adapted functions $\{h_t^{(j)}(\mathbf{r})\}$ has been defined in each j-th patch. In this section, a procedure for the synthesis of entire-domain basis functions $\{u_c(\mathbf{r})\}$ based on the mortar-matching method is described. Firstly, a unique set of basis functions is defined as the union of the N_{p} sets and by forcing their continuity. Let $\{h_l(\mathbf{r})\}$ be the union of the sets of basis functions in different patches:

$$\{h_l(\mathbf{r})\} = \bigcup_{j=1}^{N_{\mathrm{p}}} \left\{ h_t^{(j)}(\mathbf{r}) \right\}.$$

Here, the multi-index $l = (t, j)$, where t another multi-index, is used to indicate the elements of the new set. Then, the following basis recombination approach is applied to obtain the entire-domain basis functions:

$$u_c(\mathbf{r}) = \sum_l d_l^{(c)} h_l(\mathbf{r}).$$

The functions $u_c(\mathbf{r})$ have to be continuous on the entire domain Σ; this means that, given i and j two adjacent patches and γ_{ij} the common edge between them, they have to satisfy the following condition:

$$u_c|_{\gamma_{ij}^{(i)}} = u_c|_{\gamma_{ij}^{(j)}},$$

where the left-hand side and the right-hand side contain the restrictions of the basis functions u_c on the patches i and j. A set of 1-D functions μ_ν is defined on γ_{ij}. The continuity condition is cast in weak form by using μ_ν as test functions; for this reason, μ_ν are usually called "mortar functions", since they act as mortar between bricks, to join them:

$$\int_{\gamma_{ij}} \left[u_c|_{\gamma_{ij}^{(i)}} - u_c|_{\gamma_{ij}^{(j)}} \right] \mu_\nu \, \mathrm{d}s = 0, \quad \forall \nu.$$

The definition of the basis functions u_c is then substituted:

$$\sum_l d_l^{(c)} \int_{\gamma_{ij}} \left[h_l(\mathbf{r})|_{\gamma_{ij}^{(i)}} - h_l(\mathbf{r})|_{\gamma_{ij}^{(j)}} \right] \mu_\nu \, \mathrm{d}s = 0, \quad \forall \nu.$$

A matrix $\mathbf{N}$ is now defined:

$$(\mathbf{N})_{\nu l} = \int_{\gamma_{ij}} \left[h_l(\mathbf{r})|_{\gamma_{ij}^{(i)}} - h_l(\mathbf{r})|_{\gamma_{ij}^{(j)}} \right] \mu_\nu \, \mathrm{d}s.$$

Then, the problem is reduced to a homogeneous algebraic system:

$$\mathbf{N}\,\mathbf{O} = \mathbf{0},$$

where $\mathbf{O}$ is the matrix built using the vectors $\mathbf{d}^{(c)}$ as columns. Just like in the essential boundary conditions case, the columns of $\mathbf{D}$ are the elements of a basis of the kernel of $\mathbf{N}$, which is evaluated with the SVD:

$$\mathbf{N} = \mathbf{U}^{(\mathrm{u})}\,\mathbf{S}^{(\mathrm{u})}\,(\mathbf{V}^{(\mathrm{u})})^{\mathrm{H}},$$

where $\mathbf{O}$ is built with the columns of $\mathbf{V}$ corresponding to the singular values that are smaller than a threshold ε_{u}. Finally, given $\mathbf{h}(\mathbf{r})$ the vector of functions $h_l(\mathbf{r})$, the vector $\mathbf{u}(\mathbf{r})$ of entire-domain continuous functions $u_c(\mathbf{r})$ is obtained:

$$\mathbf{u}(\mathbf{r}) = \mathbf{O}^{\mathrm{T}}\mathbf{h}(\mathbf{r}).$$

These are the functions used to expand the unknown of the differential problem, synthesized according to the mortar element method.

1.4   Conclusions

In this chapter the foundations of the application of the mortar element method to electromagnetic guided problems have been produced. In the first section the formulation of three different scattering problems has been described; these formulations will be applied to the boundary-value problems described in the next chapters, relatively to different structures. In the last section the procedure aimed at synthesizing the MEM expansion and test functions is described.

Mortar element analysis of 2-D waveguide discontinuities

2.1   Introduction

Although a general waveguide device is three-dimensional, a significant sub-class is given by two-dimensional waveguide junctions, where the dimension of the problem is reduced by 1 by exploiting the translational symmetry of the components. There are two main categories of these components: E-plane and H-plane ones; two examples of step waveguide junctions are reported in Fig. 2.1. Since both discontinuities lie on the yz plane, the categorization of E-plane and H-plane devices depends on the incident field: assuming to excite the structure with the fundamental mode of its access waveguide, in the E-plane structure the electric field is polarized along y (TE$_{10}$ mode), whereas in the H-plane one the magnetic field is polarized along y (TE$_{01}$ mode). A multi-domain spectral method aimed at analyzing homogeneous
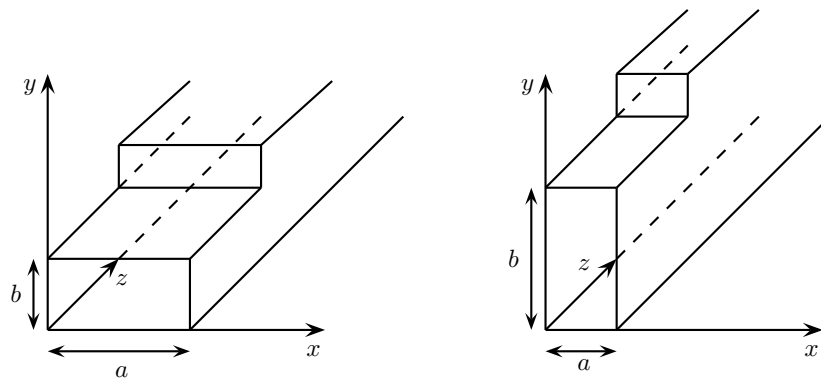
Figure 2.1: Left: sketch of a E-plane waveguide step. Right: sketch of a H-plane waveguide step.

E-plane and H-plane junctions has been recently developed [9]. Here, the symmetry is exploited by transversalizing the equations with respect to the invariance direction x. Then, the incident fields are represented as a LSE$^{(x)}$ and LSM$^{(x)}$ mode expansions. The unknown fields in the device are described using entire-domain basis functions that keep into account the boundary conditions and the field behavior in the proximity of sharp corners.

In Section 2.2 the formulation described in [9] is revised and extended to the case of non-homogeneous dielectrics. Since in the H-plane case the electromagnetic field is constant along x, no hybrid modes are excited; on the other hand, E-plane devices with inhomogeneous dielectric are described by a vector differential problem, since both the electric and magnetic field components along the invariance direction are present. In Section 2.3 the effect of the enforcement of the boundary conditions on the convergence of the method is discussed.

2.2 Theory

2.2.1 Description of the reference scattering problem

The present method is applicable to structures that exhibit translational symmetry and it is used to compute the GSM of the device. For the sake of clarity and without any loss of generality the method is here described by considering the reference structure shown in Fig. 2.2, consisting of a waveguide stub. The vertical dashed lines identify the separation section $\Sigma_{\text{eq}}^{(k)}$ between the internal (gray) and external sub-problems, where the access ports are defined. The incident field is given by a combination of LSE$^{(x)}$ (E-plane devices) or LSM$^{(x)}$ modes (H-plane devices); the x dependence of the field components is maintained in each point of Σ, owing to the translational symmetry of the structure; this is:

$$\mathbf{H}(x, y, z) = \mathbf{H}_{\text{t}}^{(x)} \cos\left(\frac{m\pi}{a}x\right) + \widehat{\mathbf{x}}\, H_x \sin\left(\frac{m\pi}{a}x\right)$$
$$\mathbf{E}(x, y, z) = \mathbf{E}_{\text{t}}^{(x)} \sin\left(\frac{m\pi}{a}x\right) + \widehat{\mathbf{x}}\, E_x \cos\left(\frac{m\pi}{a}x\right),$$

where a is the dimension of the waveguide device along x. Let k_x be defined as:

$$k_x \triangleq \frac{m\pi}{a}.$$

The BVP defined in Σ is derived from the curl Maxwell's equations in absence of sources that keep into account this dependence, which are
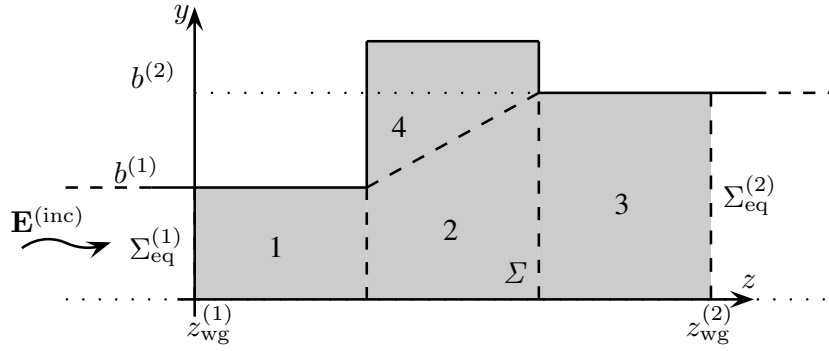
Figure 2.2: Section in the zy plane of an asymmetric waveguide stub. The gray internal region Σ is divided in four patches separated by the dashed lines to apply the multi-domain strategy. Each access port is located at $z = z_{\mathrm{wg}}^{(k)}$ and its height is $b^{(k)}$.

$$\frac{\partial E_z}{\partial y} - \frac{\partial E_y}{\partial z} = -\mathrm{j}kZH_x \tag{2.1}$$

$$\frac{\partial E_x}{\partial z} - k_x E_z = -\mathrm{j}kZH_y \tag{2.2}$$

$$k_x E_y - \frac{\partial E_x}{\partial y} = -\mathrm{j}kZH_z \tag{2.3}$$

$$\frac{\partial H_z}{\partial y} - \frac{\partial H_y}{\partial z} = \mathrm{j}kYE_x \tag{2.4}$$

$$\frac{\partial H_x}{\partial z} + k_x H_z = \mathrm{j}kYE_y \tag{2.5}$$

$$-k_x H_y - \frac{\partial H_x}{\partial y} = \mathrm{j}kYE_z, \tag{2.6}$$

where:

$$Z = \sqrt{\frac{\mu}{\varepsilon}} \qquad k = \omega\sqrt{\mu\varepsilon}.$$

The electromagnetic problem is now conveniently formulated in terms of the E_x and H_x components. Hence, by manipulating (2.2), (2.3), (2.5), (2.6), the following equations are obtained:

$$E_y = \frac{1}{k^2 - k_x^2}\left[-k_x\frac{\partial E_x}{\partial y} - \mathrm{j}kZ\frac{\partial H_x}{\partial z}\right] \tag{2.7}$$

$$E_z = \frac{1}{k^2 - k_x^2}\left[\mathrm{j}kZ\frac{\partial H_x}{\partial y} - k_x\frac{\partial E_x}{\partial z}\right] \tag{2.8}$$

$$H_y = \frac{1}{k^2 - k_x^2}\left[\mathrm{j}kY\frac{\partial E_x}{\partial z} + k_x\frac{\partial H_x}{\partial y}\right] \tag{2.9}$$

$$H_z = \frac{1}{k^2 - k_x^2}\left[k_x\frac{\partial H_x}{\partial z} - \mathrm{j}kY\frac{\partial E_x}{\partial y}\right]. \tag{2.10}$$

The derivation of these expressions is reported in Appendix B.3. The remaining components of the Maxwell's curl equations (2.1) and (2.4) are used to formulate the internal BVP; these equations are supplemented with the PEC boundary conditions on the segment $\gamma_{\mathrm{PEC}} \subset \gamma$, being γ the boundary of Σ:

$$\begin{cases} E_x = 0, & (z, y) \in \gamma_{\mathrm{PEC}} \\ \mathbf{E}_{\mathrm{t}}^{(x)} \cdot \widehat{\mathbf{s}} = 0, & (z, y) \in \gamma_{\mathrm{PEC}}, \end{cases} \tag{2.11}$$

where $\mathbf{E}_{\mathrm{t}}^{(x)}$ is the electric field in the (z, y) plane and $\widehat{\mathbf{s}}$ is the tangent unit vector on γ. The unknowns E_x and H_x are then represented as linear combinations of entire-domain basis functions defined on Σ:

$$E_x = \sum_{c=1}^{N_{\mathrm{fun}}^{(e)}} c_c^{(e)} u_c^{(e)}(z, y) \tag{2.12}$$

$$H_x = \sum_{c=1}^{N_{\mathrm{fun}}^{(h)}} c_c^{(h)} u_c^{(h)}(z, y). \tag{2.13}$$

The basis functions $u_c^{(h)}$ belong to the space $V^{(h)}$ of continuous functions with integrable derivatives, whereas $u_c^{(e)}$ belong to $V^{(e)} \subset V^{(h)}$, including only functions vanishing on γ_{PEC}. Indeed, the Dirichlet condition on E_x is essential, and it has to be included in the basis functions. On the contrary, the condition on $\mathbf{E}_{\mathrm{t}}^{(x)}$ is natural and it may be enforced in the weak formulation without further specializing the functions used to represent H_x [12, Chap. 3]. These functions are synthesized numerically, as described in Section 1.3.

2.2.2 Formulation of the internal BVP: E-plane devices

In the generic E-plane device case, where inhomogeneous dielectrics may be present, it is convenient to represent the field at the access ports in terms of TE_z and TM_z

modes in place of LSE$^{(x)}$ and LSM$^{(x)}$ ones, since the latter ones are not orthogonal. The x components of the Maxwell's curl equations (2.1) and (2.4) are cast in weak form by projecting them onto a set of functions $v_r^{(h)} = u_r^{(h)}$ and $v_r^{(e)} = u_r^{(e)}$ respectively; then, the Stokes theorem is applied to perform integration by parts, leading to:

$$
jkZ \iint_\Sigma H_x v_r^{(h)*} \, dz \, dx - \iint_\Sigma \left[E_z \frac{\partial v_r^{(h)*}}{\partial y} - E_y \frac{\partial v_r^{(h)*}}{\partial z} \right] dz \, dx = \oint_\gamma (\mathbf{E}_t^{(x)} v_r^{(h)*}) \cdot d\mathbf{s}
$$

$$(2.14)$$

$$
-jkY \iint_\Sigma E_x v_r^{(e)*} \, dz \, dx - \iint_\Sigma \left[H_z \frac{\partial v_r^{(e)*}}{\partial y} - H_y \frac{\partial v_r^{(e)*}}{\partial z} \right] dz \, dx = \oint_\gamma (\mathbf{H}_t^{(x)} v_r^{(e)*}) \cdot d\mathbf{s}.
$$

$$(2.15)$$

The proper decomposition approach is described in Fig. 2.3, where the equivalence

Figure 2.3: Hybrid equivalent multi-modal circuit of the waveguide structure shown in Fig. 2.2, where only one equivalent modal circuit is shown for each access waveguide.

theorem is applied by introducing a couple of oppositely directed electric and magnetic current densities on the two sides of $\Sigma_{eq}^{(k)}$. The γ_{PEC} contributions to the line integrals of (2.15) are zero since the test functions $v_r^{(e)}$ are vanishing; on the other hand, the γ_{PEC} contributions to the line integrals of (2.14) are set to zero to enforce the second condition of (2.11) as a natural boundary condition; therefore, the only non-vanishing contributions to the line integrals come from the equivalent currents

defined ont he access ports. Noting that, at the access ports, $\mathbf{E}_{\mathrm{t}}^{(x)} \cdot \mathrm{d}\mathbf{s} = \widetilde{\mathbf{E}}_{\mathrm{t}}^{(k)} \cdot \mathrm{d}\mathbf{s}$ and $\mathbf{H}_{\mathrm{t}}^{(x)} \cdot \mathrm{d}\mathbf{s} = \widetilde{\mathbf{H}}_{\mathrm{t}}^{(k)} \cdot \mathrm{d}\mathbf{s}$, according to Section 1.2:

$$
\oint_\gamma (\mathbf{H}_{\mathrm{t}}^{(x)} v_r^{(\mathrm{e})*}) \cdot \mathrm{d}\mathbf{s} = -\sum_{n=1}^{N_{\mathrm{m}}} \mathring{i}_n^{(1)} \int_0^{b^{(1)}} h_{y,n}^{(1)} v_r^{(\mathrm{e})*} \bigg|_{z=z_{\mathrm{wg}}^{(1)}} \mathrm{d}y + \sum_{n=1}^{N_{\mathrm{m}}} \mathring{i}_n^{(2)} \int_0^{b^{(2)}} h_{y,n}^{(2)} v_r^{(\mathrm{e})*} \bigg|_{z=z_{\mathrm{wg}}^{(2)}} \mathrm{d}y
$$

$$
\oint_\gamma (\mathbf{E}_{\mathrm{t}}^{(x)} v_r^{(\mathrm{h})*}) \cdot \mathrm{d}\mathbf{s} = -\sum_{n=1}^{N_{\mathrm{m}}} \mathring{v}_n^{(1)} \int_0^{b^{(1)}} e_{y,n}^{(1)} v_r^{(\mathrm{h})*} \bigg|_{z=z_{\mathrm{wg}}^{(1)}} \mathrm{d}y + \sum_{n=1}^{N_{\mathrm{m}}} \mathring{v}_n^{(2)} \int_0^{b^{(2)}} e_{y,n}^{(2)} v_r^{(\mathrm{h})*} \bigg|_{z=z_{\mathrm{wg}}^{(2)}} \mathrm{d}y.
$$

The following matrix elements are then defined:

$$
\begin{aligned}
(\mathbf{B}^{(\mathrm{e},k)})_{rn} &= \int_0^{b^{(k)}} h_{y,n}^{(k)} v_r^{(\mathrm{e}),k} \bigg|_{z=z_{\mathrm{wg}}^{(k)}} \mathrm{d}y \\
(\mathbf{B}^{(\mathrm{h},k)})_{rn} &= \int_0^{b^{(k)}} e_{y,n}^{(k)} v_r^{(\mathrm{h}),k} \bigg|_{z=z_{\mathrm{wg}}^{(k)}} \mathrm{d}y.
\end{aligned}
\tag{2.16}
$$

Then, by substituting (2.7) $\div$ (2.9) and (2.12)-(2.13) in (2.14) and (2.15), the following system of matrix equations is obtained:

$$
\begin{cases}
\mathbf{A}^{(\mathrm{e},\mathrm{e})} \mathbf{c}^{(\mathrm{e})} + \mathbf{A}^{(\mathrm{e},\mathrm{h})} \mathbf{c}^{(\mathrm{h})} = \mathbf{B}^{(\mathrm{e},2)} \mathring{\mathbf{i}}^{(2)} - \mathbf{B}^{(\mathrm{e},1)} \mathring{\mathbf{i}}^{(1)} \\
\mathbf{A}^{(\mathrm{h},\mathrm{e})} \mathbf{c}^{(\mathrm{e})} + \mathbf{A}^{(\mathrm{h},\mathrm{h})} \mathbf{c}^{(\mathrm{h})} = \mathbf{B}^{(\mathrm{h},2)} \mathring{\mathbf{v}}^{(2)} - \mathbf{B}^{(\mathrm{h},1)} \mathring{\mathbf{v}}^{(1)},
\end{cases}
\tag{2.17}
$$

where:

$$
\begin{aligned}
\mathbf{A}^{(\mathrm{e},\mathrm{e})} &= -\frac{\mathrm{j}kY}{k^2 - k_x^2} \left[(k^2 - k_x^2)\mathbf{M}^{(\mathrm{e})} - \mathbf{K}^{(\mathrm{e})} \right] \\
\mathbf{A}^{(\mathrm{e},\mathrm{h})} &= \frac{k_x}{k^2 - k_x^2} \mathbf{L}^{(\mathrm{e})} \\
\mathbf{A}^{(\mathrm{h},\mathrm{e})} &= -\frac{k_x}{k^2 - k_x^2} \mathbf{L}^{(\mathrm{h})} \\
\mathbf{A}^{(\mathrm{h},\mathrm{h})} &= \frac{\mathrm{j}kZ}{k^2 - k_x^2} \left[(k^2 - k_x^2)\mathbf{M}^{(\mathrm{h})} - \mathbf{K}^{(\mathrm{h})} \right],
\end{aligned}
$$

and

$$(\mathbf{M}^{(\mathrm{e})})_{rc} = \iint_{\Sigma} u_c^{(\mathrm{e})} v_r^{(\mathrm{e})*} \, \mathrm{d}z \, \mathrm{d}x$$

$$(\mathbf{K}^{(\mathrm{e})})_{rc} = \iint_{\Sigma} \left[\frac{\partial u_c^{(\mathrm{e})}}{\partial y} \frac{\partial v_r^{(\mathrm{e})*}}{\partial y} + \frac{\partial u_c^{(\mathrm{e})}}{\partial z} \frac{\partial v_r^{(\mathrm{e})*}}{\partial z} \right] \, \mathrm{d}z \, \mathrm{d}x$$

$$(\mathbf{L}^{(\mathrm{e})})_{rc} = \iint_{\Sigma} \left[\frac{\partial u_c^{(\mathrm{h})}}{\partial y} \frac{\partial v_r^{(\mathrm{e})*}}{\partial z} - \frac{\partial u_c^{(\mathrm{h})}}{\partial z} \frac{\partial v_r^{(\mathrm{e})*}}{\partial y} \right] \, \mathrm{d}z \, \mathrm{d}x$$

$$(\mathbf{M}^{(\mathrm{h})})_{rc} = \iint_{\Sigma} u_c^{(\mathrm{h})} v_r^{(\mathrm{h})*} \, \mathrm{d}z \, \mathrm{d}x$$

$$(\mathbf{K}^{(\mathrm{h})})_{rc} = \iint_{\Sigma} \left[\frac{\partial u_c^{(\mathrm{h})}}{\partial y} \frac{\partial v_r^{(\mathrm{h})*}}{\partial y} + \frac{\partial u_c^{(\mathrm{h})}}{\partial z} \frac{\partial v_r^{(\mathrm{h})*}}{\partial z} \right] \, \mathrm{d}z \, \mathrm{d}x$$

$$(\mathbf{L}^{(\mathrm{h})})_{rc} = \iint_{\Sigma} \left[\frac{\partial u_c^{(\mathrm{e})}}{\partial y} \frac{\partial v_r^{(\mathrm{h})*}}{\partial z} - \frac{\partial u_c^{(\mathrm{e})}}{\partial z} \frac{\partial v_r^{(\mathrm{h})*}}{\partial y} \right] \, \mathrm{d}z \, \mathrm{d}x.$$

2.2.3 Formulation of the internal BVP: homogeneous E-plane devices

In the case of E-plane devices filled with homogeneous dielectric, $E_x = 0$ in every point of the structure, as it is proved in [13]. In this case, the incident field is a $\mathrm{LSE}_{1n}^{(x)}$ mode, no $\mathrm{LSM}^{(x)}$ mode is coupled, and the BVP describing these components is scalar. This is obtained by considering (2.1), (2.7) and (2.8) with $E_x = 0$:

$$\frac{\partial E_z}{\partial y} - \frac{\partial E_y}{\partial z} = -\mathrm{j}kZH_x$$

$$E_y = \frac{-\mathrm{j}kZ}{k^2 - k_x^2} \frac{\partial H_x}{\partial z}$$

$$E_z = \frac{\mathrm{j}kZ}{k^2 - k_x^2} \frac{\partial H_x}{\partial y}.$$

The first equation is cast in weak form by projecting it on the test functions $v_r^{(\mathrm{h})}$; then, integration by parts is applied to the resulting equation, leading to:

$$\mathrm{j}kZ \iint_{\Sigma} H_x v_r^{(\mathrm{h})*} \, \mathrm{d}z \, \mathrm{d}x - \iint_{\Sigma} \left[E_z \frac{\partial v_r^{(\mathrm{h})*}}{\partial y} - E_y \frac{\partial v_r^{(\mathrm{h})*}}{\partial z} \right] \, \mathrm{d}z \, \mathrm{d}x = \oint_{\gamma} (\mathbf{E}_{\mathrm{t}}^{(x)} v_r^{(\mathrm{h})*}) \cdot \mathrm{d}\mathbf{s}.$$

Since no magnetic field excitation is appearing in the line integrals, the proper version of the equivalence theorem is the one where PEC is used to fill the zero-field regions, to eliminate the contributions of the electric current densities. This is described in Fig. 2.4, where the equivalent problems are reported together with

their hybrid circuits. The following matrix equation is obtained by applying the same considerations of the previous case:
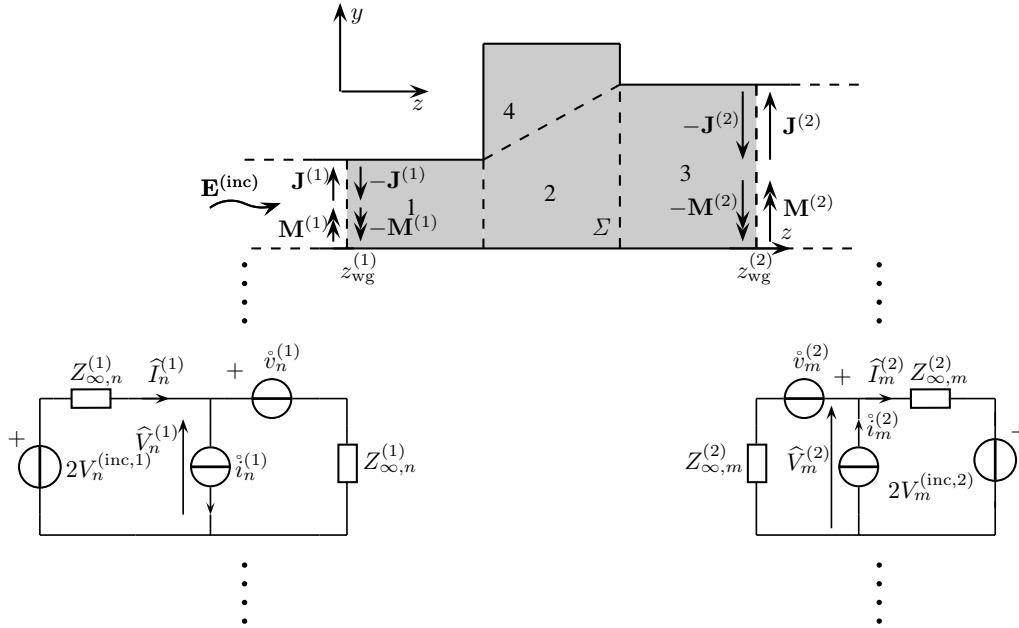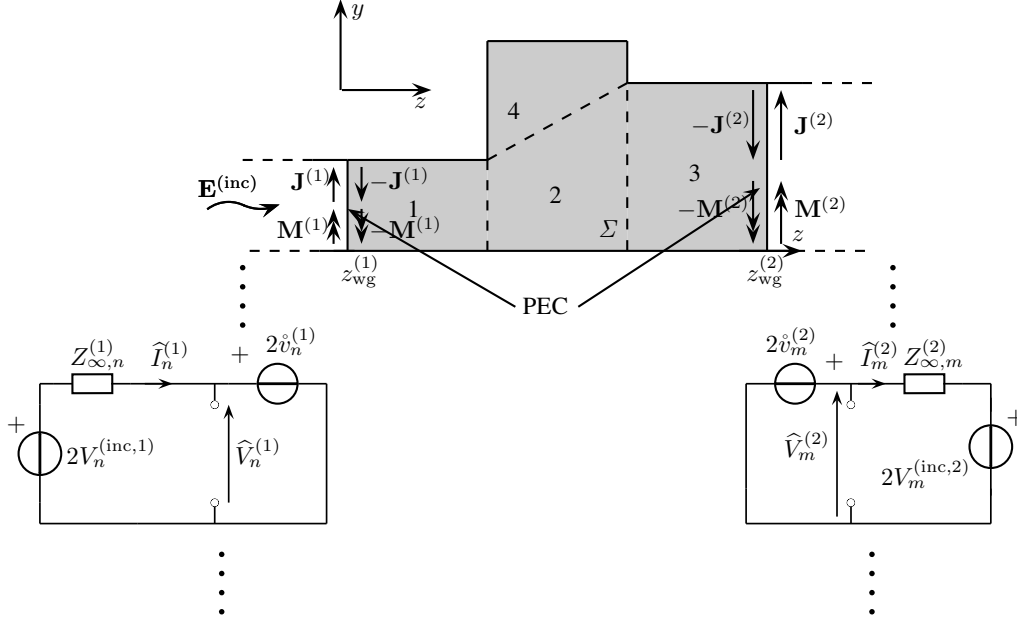

Figure 2.4: Hybrid equivalent multi-modal circuit of the waveguide structure shown in Fig. 2.2, where only one equivalent modal circuit is shown for each access waveguide.

$$\mathbf{A}^{(\mathrm{h,h})}\,\mathbf{c}^{(\mathrm{h})} = \mathbf{B}^{(\mathrm{h},2)}\mathring{\mathbf{v}}^{(2)} - \mathbf{B}^{(\mathrm{h},1)}\mathring{\mathbf{v}}^{(1)},$$

where the line integrals are defined as in (2.16). The matrix on the left-hand side is defined as:

$$\mathbf{A}^{(\mathrm{h,h})} = \mathrm{j}kZ\left[\mathbf{M}^{(\mathrm{h})} - \frac{1}{k^2 - k_x^2}\mathbf{K}^{(\mathrm{h})}\right],$$

where

$$\mathbf{M}^{(\mathrm{h})} = \iint_{\Sigma} u_c^{(\mathrm{h})} v_r^{(\mathrm{h})*}\,\mathrm{d}z\,\mathrm{d}x$$

$$\mathbf{K}^{(\mathrm{h})} = \iint_{\Sigma}\left[\frac{\partial u_c^{(\mathrm{h})}}{\partial y}\frac{\partial v_r^{(\mathrm{h})*}}{\partial y} + \frac{\partial u_c^{(\mathrm{h})}}{\partial z}\frac{\partial v_r^{(\mathrm{h})*}}{\partial z}\right]\,\mathrm{d}z\,\mathrm{d}x$$

2.2.4 Formulation of the internal BVP: H-plane devices

In the H-plane device case, the incident field is a $\mathrm{LSM}_{0n}^{(x)}$ mode, meaning that the electromagnetic field is constant along the invariance direction of the structure. For

this reason, even if the device has non-homogeneous dielectric, no $\mathrm{LSE}_{mn}^{(x)}$ mode is coupled, and the BVP describing these components is scalar. This is obtained by considering (2.4), (2.9) and (2.10) with $k_x = 0$:

$$\frac{\partial H_z}{\partial y} - \frac{\partial H_y}{\partial z} = \mathrm{j}kYE_x$$
$$H_y = -\frac{1}{\mathrm{j}kZ}\frac{\partial E_x}{\partial z}$$
$$H_z = \frac{1}{\mathrm{j}kZ}\frac{\partial E_x}{\partial y}.$$

The first equation is cast in weak form by projecting it on the test functions $v_r^{(e)}$ satisfying the PEC boundary conditions on γ_{PEC}; then, integration by parts is applied to the resulting equation, leading to:

$$-\mathrm{j}kY\iint_{\Sigma} E_x v_r^{(e)*} \,\mathrm{d}z\,\mathrm{d}x - \iint_{\Sigma}\left[H_z\frac{\partial v_r^{(e)*}}{\partial y} - H_y\frac{\partial v_r^{(e)*}}{\partial z}\right]\mathrm{d}z\,\mathrm{d}x = \oint_{\gamma}(\mathbf{H}_{\mathrm{t}}^{(x)} v_r^{(e)*}) \cdot \mathrm{d}\mathbf{s}.$$

Since no electric field excitation is appearing in the line integrals, the proper version of the equivalence theorem is the one where perfect magnetic conductor (PMC) is used to fill the zero-field regions, to eliminate the contributions of the magnetic current densities. This is described in Fig. 2.5, where the equivalent problems are reported together with their hybrid circuits. The following matrix equation is obtained by applying the same considerations of the previous case:

$$\mathbf{A}^{(e,e)}\,\mathbf{c}^{(e)} = \mathbf{B}^{(e,2)}\overset{\circ}{\mathbf{i}}{}^{(2)} - \mathbf{B}^{(e,1)}\overset{\circ}{\mathbf{i}}{}^{(1)},$$

where the line integrals are defined as in (2.16). The matrix on the left-hand side is defined as:

$$\mathbf{A}^{(e,e)} = -\mathrm{j}kY\left[\mathbf{M}^{(e)} - \frac{1}{k^2}\mathbf{K}^{(e)}\right],$$

where

$$\mathbf{M}^{(e)} = \iint_{\Sigma} u_c^{(e)} v_r^{(e)*} \,\mathrm{d}z\,\mathrm{d}x$$
$$\mathbf{K}^{(e)} = \iint_{\Sigma}\left[\frac{\partial u_c^{(e)}}{\partial y}\frac{\partial v_r^{(e)*}}{\partial y} + \frac{\partial u_c^{(e)}}{\partial z}\frac{\partial v_r^{(e)*}}{\partial z}\right]\mathrm{d}z\,\mathrm{d}x.$$
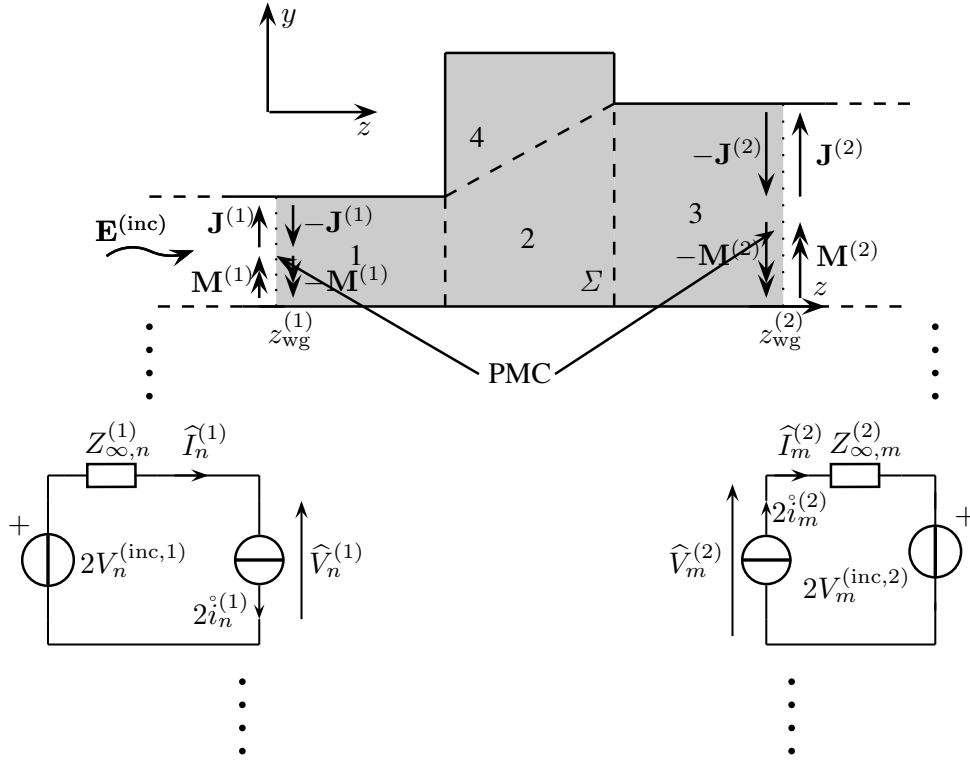
Figure 2.5: Hybrid equivalent multi-modal circuit of the waveguide structure shown in Fig. 2.2, where only one equivalent modal circuit is shown for each access waveguide.

2.3 Results - convergence analysis

This method has been applied to the analysis and design of several E-plane and H-plane devices presented in [9] and not reported here. In this section a convergence study of the method with respect to the number of expansion and test functions used to represent the solution of the internal problem is presented for two different implementations of the method. As discussed in the Section 2.2, it is not mandatory to specialize the basis functions $u_c^{(\mathrm{h})}$ used to expand H_x, since the related boundary condition can be enforced naturally, acting on the line integrals that arise from the integration by parts. However, in the original implementation of the method, the procedure described in Appendix A.1 was used to enforce the condition

$$\left.\frac{\partial u_c}{\partial n}\right|_{\gamma_{\mathrm{PEC}}} = 0,$$

being n the normal direction to γ. A convergence study is performed on the waveguide stub reported in Fig. 2.6, where $w = 6$ mm, $R_1 = R_2 = 9.525$ mm, $L_1 = L_2 = 4$ mm, $h = 5$ mm, to understand which is the most convenient procedure to be applied in these situations. It is remarked that this problem affects only E-plane devices,
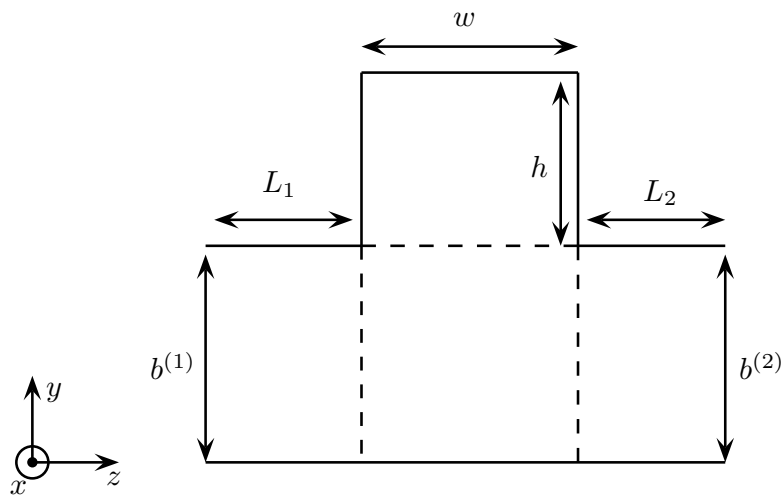
Figure 2.6: Sketch of a waveguide stub
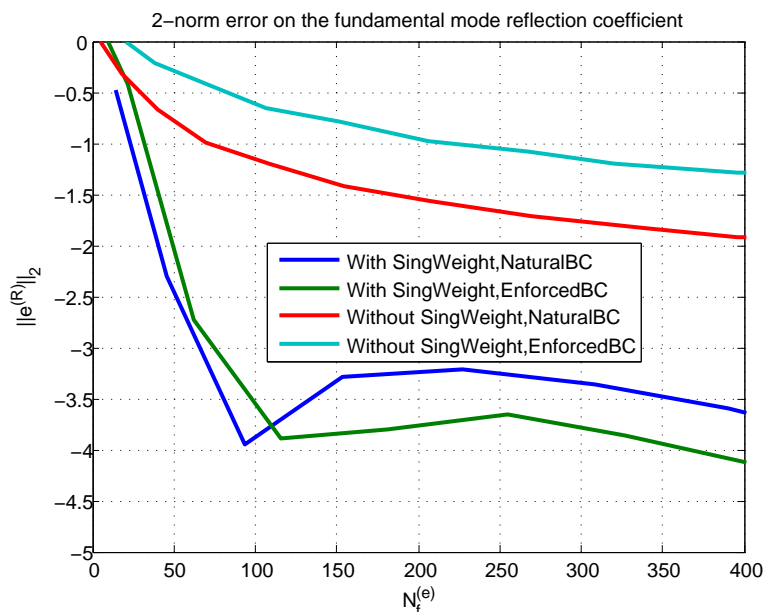
Figure 2.7: Convergence study applied to the waveguide stub of Fig. 2.6.

since $H_x = 0$ in H-plane discontinuities. In Fig. 2.7 it is observed that, for poly-nomial basis functions, the convergence of the method is much slower in the case of explicitly enforced boundary conditions. On the other hand, if the set of polynomial basis functions is augmented with the asymptotic behaviors of the electromagnetic field in the proximity of sharp edges, the convergence properties are independent of the method of enforcing the boundary condition. This is related to the fact that, if each basis function satisfies the Neumann boundary condition, it isn't capable of properly representing a divergent field behavior; on the other hand, this is restored

by introducing the singular weight.

Chapter 3

Mortar element analysis of 2-D periodic structures

3.1 Introduction

Periodic structures are widely used as models in optics and electromagnetics. For this reason, in recent years many efforts have been made aiming at developing fast and accurate electromagnetic simulators for several problems that involve periodicity. The characterization of reflection gratings has been performed by introducing problem-matched basis functions used to approximate the solution of an integral equation with the method of moments (MoM) [14]. The frequency response of photonic crystals has been evaluated with a hybrid finite element method (FEM) exploiting a Floquet mode representation of the electromagnetic field [15] [16]. The two-dimensional scattering of a plane wave from a periodic array of composite dielectric cylinders has been studied with the MoM accelerated by means of a multi-grid method [17], or with the aggregate T-matrix method for cylindrical structures [18]. Frequency-selective surfaces have been analyzed by determining numerically the Green's function of a screen perforated by multiply connected apertures [19]. Dielectric frequency-selective surfaces have been analyzed using a vectorial modal method [20]. The boundary integral-resonant mode expansion method (BI-RME) has been used to study electromagnetic band-gap structures [21], [22]. The finite-difference time-domain method (FDTD) has been used to analyze the guided-wave characteristics of substrate integrated nonradiative dielectric waveguides [23].

In this chapter the development of a simulator of 2-D dielectric periodic structures based on the MEM is described. This work has been formerly developed for the E-polarization and H-polarization cases [24], then for the skew incidence case [25], [26]. The domain decomposition strategy is based on defining patches filled

with homogeneous dielectric; by this way, a proper representation of the electromagnetic field in the internal problem can be obtained using a small number of basis functions. The flexibility in the description of the geometry is exploited in order to analyze structures with rounded corners; by this way, it is possible to model the non-idealities caused by manufacturing processes. The weak formulation of the internal BVP is derived starting from Maxwell's equations; this leads to the definition of the matrices used in Chapter 1. Then, a validation of the numerical scheme is performed by comparison with a MoM code and with the CST Microwave Studio code (CST-MS) [27].

3.2 Theory

3.2.1 Description of the reference scattering problem

The present technique can be applied to the analysis of 2-D periodic structures excited by a plane wave with arbitrary incidence. This is used to compute the
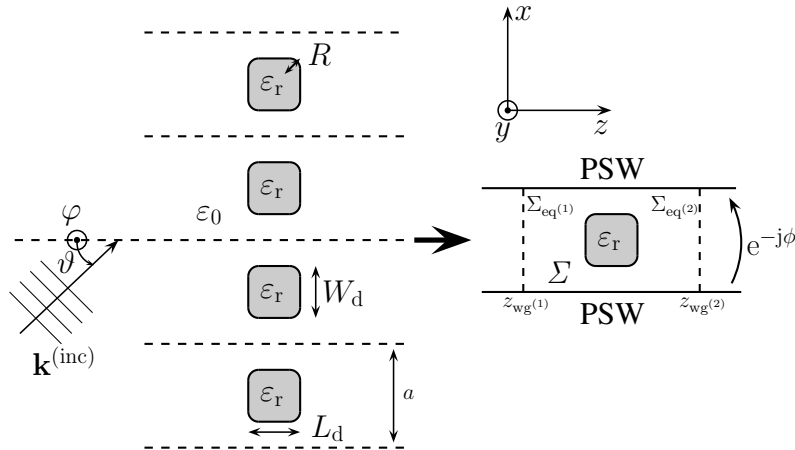
Figure 3.1: Left: sketch of the geometry of the structure; right: unit cell. The horizontal solid lines are phase-shift walls PSW with phase shift $\phi = k_x^{(\text{inc})}a$; the vertical dashed lines define the access ports; the parameter a is the period; L_d and W_d are the length and width of the dielectric rod respectively; R is the radius of curvature of the rounded corners.

generalized scattering matrix in the Floquet modes basis. The geometry sketched in Fig. 3.1 is used as reference for the description of the formulation; the structure consists of a periodic array of infinitely long dielectric rods with refractive index $n = \sqrt{\varepsilon_\text{r}}$ surrounded by vacuum. The effect of dielectric losses can be accounted for, therefore the dielectric constant ε_r is intended to be a complex number. The array direction is x and each rod is placed along y. The period of the structure is a, each
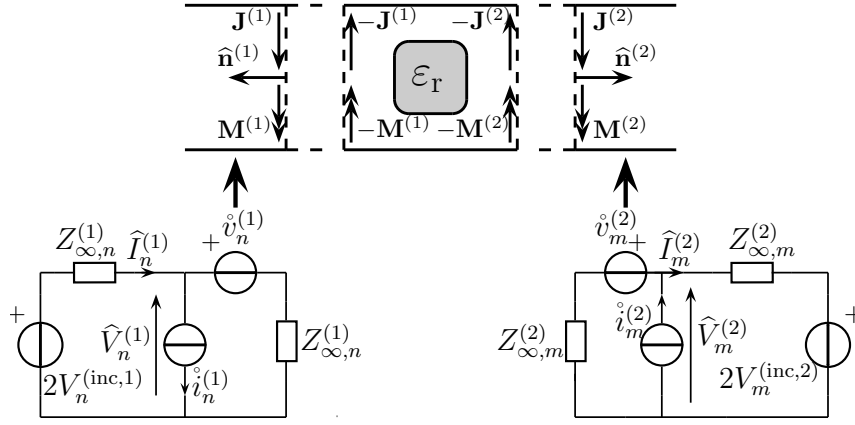
Figure 3.2: Top: definition of the two sub-problems; bottom: equivalent multi-modal circuit of the external sub-problem, where only the n-th mode contribution is shown.

bar has length L_d, width W_d and the corners are rounded with radius of curvature R. The wavevector of the incident plane wave is

$$\mathbf{k}^{(\mathrm{inc})} = k_0 \left(\sin\vartheta\cos\varphi, \sin\vartheta\sin\varphi, \cos\vartheta\right) =$$
$$= (k_x^{(\mathrm{inc})}, k_y^{(\mathrm{inc})}, k_z^{(\mathrm{inc})}),$$

where k_0 is the free-space wave number. The unit cell consists of a phase-shift wall waveguide with a dielectric obstacle; the pseudo-periodicity boundary conditions for the electric and magnetic fields $\mathbf{E}$ and $\mathbf{H}$ are

$$\begin{cases} \mathbf{E}(z, a) = \mathbf{E}(z, 0)\, \mathrm{e}^{-\mathrm{j}\phi} \\ \mathbf{H}(z, a) = \mathbf{H}(z, 0)\, \mathrm{e}^{-\mathrm{j}\phi}, \end{cases}$$

where $\phi = k_x^{(\mathrm{inc})} a$ is the phase shift originated by the incident wave and indicated in Fig. 3.1.

The decomposition of the problem according to Section 1.2 and the relative modal circuit are sketched in Fig. 3.2, where the access ports are located at $z = z_\mathrm{wg}^{(k)}$; the current densities and the fields on the surfaces $\Sigma_\mathrm{eq}^{(k)}$ where the equivalence theorem is applied are represented using a Floquet modes expansion, and the formulation of the external problem is completed by matching the PSW waveguides. The expressions of the Floquet modes are reported in Appendix C.1.

3.2.2 Formulation of the internal boundary-value problem

The boundary-value problem defined in the internal region Σ is derived from the Maxwell's curl equations, written in cartesian coordinates and in absence of sources.

Since the structure is invariant with respect to y, each field component has the same $e^{-jk_y y}$ dependence of the incident field; therefore, the y derivatives in the Maxwell's equations are replaced with "$-jk_y$":

$$-jk_y E_z - \frac{\partial E_y}{\partial z} = -jkZH_x \tag{3.1}$$

$$\frac{\partial E_x}{\partial z} - \frac{\partial E_z}{\partial x} = -jkZH_y \tag{3.2}$$

$$\frac{\partial E_y}{\partial x} + jk_y E_x = -jkZH_z \tag{3.3}$$

$$-jk_y H_z - \frac{\partial H_y}{\partial z} = jkYE_x \tag{3.4}$$

$$\frac{\partial H_x}{\partial z} - \frac{\partial H_z}{\partial x} = jkYE_y \tag{3.5}$$

$$\frac{\partial H_y}{\partial x} + jk_y H_x = jkYE_z, \tag{3.6}$$

where:

$$k = k_0 n \qquad Z = \sqrt{\frac{\mu}{\varepsilon}} = \frac{Z_0}{n}.$$

Hence, it is possible to use E_y, H_y as Hertz potentials from which the remaining components are obtained, by manipulating (3.1), (3.3), (3.4), (3.6):

$$E_x = -\frac{j}{k^2 - k_y^2}\left(k_y\frac{\partial E_y}{\partial x} - kZ\frac{\partial H_y}{\partial z}\right) \tag{3.7}$$

$$E_z = -\frac{j}{k^2 - k_y^2}\left(k_y\frac{\partial E_y}{\partial z} + kZ\frac{\partial H_y}{\partial x}\right) \tag{3.8}$$

$$H_x = -\frac{j}{k^2 - k_y^2}\left(k_y\frac{\partial H_y}{\partial x} + kY\frac{\partial E_y}{\partial z}\right) \tag{3.9}$$

$$H_z = -\frac{j}{k^2 - k_y^2}\left(k_y\frac{\partial H_y}{\partial z} - kY\frac{\partial E_y}{\partial x}\right). \tag{3.10}$$

The derivation of these expressions is reported in Appendix C.3.

If the plane wave is incident in the zx plane (*i.e.*, $\varphi = 0$), the problem splits up into the independent E-polarization and H-polarization scalar ones. The unknowns of the problem are expanded as

$$E_y \simeq \sum_{c=1}^{N_f} c_c^{(e)} u_c(z, x)$$

$$H_y \simeq \sum_{c=1}^{N_f} c_c^{(h)} u_c(z, x), \tag{3.11}$$
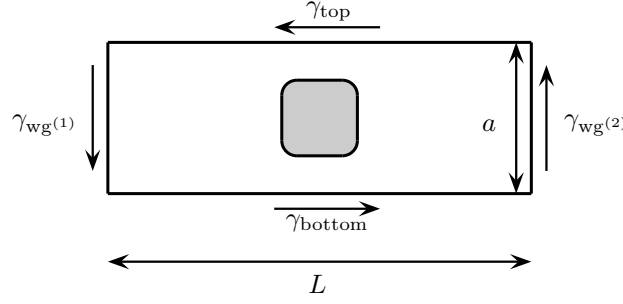
Figure 3.3: Sketch of the internal sub-problem, where the boundary contributions are emphasized.

where $\{u_c(z, x)\}$ belong to the function space V of continuous functions with integrable derivatives satisfying the pseudo-periodicity condition

$$u_c(z, a) = u_c(z, 0)e^{-\mathrm{j}\phi} \quad z \in [0, L] \quad \forall c = 1...N_{\mathrm{f}}. \tag{3.12}$$

The synthesis of these functions is performed according to the MEM, as described in Section 1.3 and in Appendix C.2. A set of local basis functions is defined on the parent domain for each patch, and then these functions are specialized to satisfy the pseudo-periodicity essential boundary conditions.

Equations (3.7) ÷ (3.10) are obtained from the x and z components of the curl Maxwell's equations; the y components (3.2) and (3.5) are cast in weak form by projecting them onto a set of test functions $v_r = u_r$, chosen accordingly to the Galerkin version of the method of weighted residuals:

$$-\mathrm{j}kZ \iint_{\Sigma} H_y v_r^* \, \mathrm{d}x \, \mathrm{d}z = \iint_{\Sigma} \left[\frac{\partial E_x}{\partial z} - \frac{\partial E_z}{\partial x} \right] v_r^* \, \mathrm{d}x \, \mathrm{d}z$$

$$\mathrm{j} \iint_{\Sigma} kY E_y v_r^* \, \mathrm{d}x \, \mathrm{d}z = \iint_{\Sigma} \left[\frac{\partial H_x}{\partial z} - \frac{\partial H_z}{\partial x} \right] v_r^* \, \mathrm{d}x \, \mathrm{d}z.$$

Then, integration by parts by means of Stokes theorem is performed, and the following equations are obtained:

$$\mathrm{j} \iint_{\Sigma} kY E_y v_r^* \, \mathrm{d}x \, \mathrm{d}z + \iint_{\Sigma} \left[H_x \frac{\partial v_r^*}{\partial z} - H_z \frac{\partial v_r^*}{\partial x} \right] \mathrm{d}x \, \mathrm{d}z = \oint_{\gamma} (\mathbf{H}_{\mathrm{t}}^{(y)} v_r^*) \cdot \mathrm{d}\mathbf{s} \tag{3.13}$$

$$-\mathrm{j}kZ \iint_{\Sigma} H_y v_r^* \, \mathrm{d}x \, \mathrm{d}z + \iint_{\Sigma} \left[E_x \frac{\partial v_r^*}{\partial z} - E_z \frac{\partial v_r^*}{\partial x} \right] \mathrm{d}x \, \mathrm{d}z = \oint_{\gamma} (\mathbf{E}_{\mathrm{t}}^{(y)} v_r^*) \cdot \mathrm{d}\mathbf{s}, \tag{3.14}$$

where $\gamma = \gamma_{\mathrm{top}} \cup \gamma_{\mathrm{bottom}} \cup \gamma_{\mathrm{wg}}^{(1)} \cup \gamma_{\mathrm{wg}}^{(2)}$ is the boundary of Σ and $\mathbf{E}_{\mathrm{t}}^{(y)}$ and $\mathbf{H}_{\mathrm{t}}^{(y)}$ are the electric and magnetic fields transverse to y, as shown in Fig. 3.3. The top and bottom contributions to the right-hand side integrals are set equal to zero to

enforce the pseudo-periodicity of E_x, E_z, H_x, H_z as natural boundary conditions [12, Chap. 3]. Working on the right-hand side of (3.13), the following expressions are written:

$$
\oint_\gamma (\mathbf{H}_t^{(y)} v_r^*) \cdot d\mathbf{s} = \int_{\gamma_{\text{bottom}}} H_z v_r^*|_{x=0} \, dz + \int_{\gamma_{\text{wg}}^{(2)}} H_x v_r^*|_{z=z_{\text{wg}}^{(2)}} \, dx + \int_{\gamma_{\text{top}}} H_z v_r^*|_{x=a} \, dz +
$$
$$
+ \int_{\gamma_{\text{wg}}^{(1)}} H_x v_r^*|_{z=z_{\text{wg}}^{(1)}} \, dx =
$$
$$
= \int_0^L H_z v_r^*|_{x=0} \, dz + \int_0^a H_x v_r^*|_{z=z_{\text{wg}}^{(2)}} \, dx - \int_0^L H_z v_r^*|_{x=a} \, dz +
$$
$$
- \int_0^a H_x v_r^*|_{z=z_{\text{wg}}^{(1)}} \, dx,
$$

where the signs are chosen accordingly to the path orientation. The pseudo-periodicity boundary condition on H_z is:

$$
H_z|_{x=a} = H_z|_{x=0} \, e^{-j\phi}.
$$

This condition is written in weak form, by testing it on 1-D basis functions $f_r(z)$:

$$
\int_0^L H_z|_{x=a} f_r^*(z) \, dz = \int_0^L H_z|_{x=0} f_r^*(z) e^{-j\phi} \, dz.
$$

Since ϕ is independent of z, it is written:

$$
\int_0^L H_z|_{x=a} f_r^*(z) e^{+j\phi} \, dz = \int_0^L H_z|_{x=0} f_r^*(z) \, dz,
$$

which is:

$$
\int_0^L H_z|_{x=a} (f_r(z) e^{-j\phi})^* \, dz = \int_0^L H_z|_{x=0} f_r^*(z) \, dz.
$$

Then, according to (3.12):

$$
v_r(z, x)|_{x=0} = f_r(z)
$$

$$
v_r(z, x)|_{x=a} = f_r(z) e^{-j\phi}.
$$

Indeed, the two restrictions are equal, less than the pseudo-periodicity condition. Therefore, the equation is written as:

$$
\int_0^L H_z v_r^*|_{x=a} \, dz = \int_0^L H_z v_r^*|_{x=0} \, dz.
$$

For this reason, these two integrals should be removed from the formulation, to satisfy in a natural way the pseudo-periodicity condition on H_z. The same calculations hold for E_z. Then, since both the φ and the z components of the electromagnetic field satisfy the pseudo-periodicity conditions, the x components automatically satisfy them as well.

Since $(3.1) \div (3.6)$ are written in absence of sources, the effect of the current densities is accounted for as a non-homogeneous boundary condition. Then, by observing that, at the access ports, $\mathbf{E}_{\mathrm{t}}^{(y)} \cdot \mathrm{d}\mathbf{s} = \widetilde{\mathbf{E}}_{\mathrm{t}}^{(k)} \cdot \mathrm{d}\mathbf{s}$ and $\mathbf{H}_{\mathrm{t}}^{(y)} \cdot \mathrm{d}\mathbf{s} = \widetilde{\mathbf{H}}_{\mathrm{t}}^{(k)} \cdot \mathrm{d}\mathbf{s}$, according to Section 1.2:

$$\oint_{\gamma} (\mathbf{H}_{\mathrm{t}}^{(y)} v_r^*) \cdot \mathrm{d}\mathbf{s} = -\sum_{n=1}^{N_{\mathrm{m}}} \mathring{i}_n^{(1)} \int_0^a h_{x,n}^{(1)} v_r^* \bigg|_{z=z_{\mathrm{wg}}^{(1)}} \mathrm{d}x + \sum_{n=1}^{N_{\mathrm{m}}} \mathring{i}_n^{(2)} \int_0^a h_{x,n}^{(2)} v_r^* \bigg|_{z=z_{\mathrm{wg}}^{(2)}} \mathrm{d}x$$

$$\oint_{\gamma} (\mathbf{E}_{\mathrm{t}}^{(y)} v_r^*) \cdot \mathrm{d}\mathbf{s} = -\sum_{n=1}^{N_{\mathrm{m}}} \mathring{v}_n^{(1)} \int_0^a e_{x,n}^{(1)} v_r^* \bigg|_{z=z_{\mathrm{wg}}^{(1)}} \mathrm{d}x + \sum_{n=1}^{N_{\mathrm{m}}} \mathring{v}_n^{(2)} \int_0^a e_{x,n}^{(2)} v_r^* \bigg|_{z=z_{\mathrm{wg}}^{(2)}} \mathrm{d}x.$$

Therefore:

$$(\mathbf{B}^{(\mathrm{e},k)})_{rn} = \int_0^a h_{x,n}^{(k)} v_r^* \bigg|_{z=z_{\mathrm{wg}}^{(k)}} \mathrm{d}x$$

$$(\mathbf{B}^{(\mathrm{h},k)})_{rn} = \int_0^a e_{x,n}^{(k)} v_r^* \bigg|_{z=z_{\mathrm{wg}}^{(k)}} \mathrm{d}x.$$

For what concerns the left-hand sides, by substituting $(3.7) \div (3.11)$ in (3.13) and (3.14), the following system of matrix equations is obtained:

$$\begin{cases} \mathbf{A}^{(\mathrm{e,e})}\mathbf{c}^{(\mathrm{e})} + \mathbf{A}^{(\mathrm{e,h})}\mathbf{c}^{(\mathrm{h})} = \mathbf{B}^{(\mathrm{e},2)}\mathring{\mathbf{i}}^{(2)} - \mathbf{B}^{(\mathrm{e},1)}\mathring{\mathbf{i}}^{(1)} \\ \mathbf{A}^{(\mathrm{h,e})}\mathbf{c}^{(\mathrm{e})} + \mathbf{A}^{(\mathrm{h,h})}\mathbf{c}^{(\mathrm{h})} = \mathbf{B}^{(\mathrm{h},2)}\mathring{\mathbf{v}}^{(2)} - \mathbf{B}^{(\mathrm{h},1)}\mathring{\mathbf{v}}^{(1)}, \end{cases} \tag{3.15}$$

where:

$$\mathbf{A}^{(\mathrm{e,e})} = \mathrm{j}\left[\mathbf{M} - \mathbf{K}\right]$$
$$\mathbf{A}^{(\mathrm{e,h})} = \mathrm{j}\mathbf{L}$$
$$\mathbf{A}^{(\mathrm{h,h})} = \mathrm{j}\mathbf{L}$$
$$\mathbf{A}^{(\mathrm{h,e})} = \mathrm{j}\left[\mathbf{M} - \mathbf{K}\right],$$

and:

$$(\mathbf{M})_{rc} = \iint_{\Sigma} kY u_c^{(e)} v_r^* \, dz dx$$

$$(\mathbf{K})_{rc} = \iint_{\Sigma} \frac{kY}{k^2 - k_y^2} \left[\frac{\partial u_c^{(e)}}{\partial z} \frac{\partial v_r^*}{\partial z} + \frac{\partial u_c^{(e)}}{\partial x} \frac{\partial v_r^*}{\partial x} \right] \, dx \, dz$$

$$(\mathbf{L})_{rc} = \iint_{\Sigma} \frac{k_y}{k^2 - k_y^2} \left[\frac{\partial u_c^{(h)}}{\partial z} \frac{\partial v_r^*}{\partial x} - \frac{\partial u_c^{(h)}}{\partial x} \frac{\partial v_r^*}{\partial z} \right] \, dx \, dz.$$

3.2.3 Continuity equations at the access ports

The formulation of the method is completed by coupling the internal and external sub-problems through the continuity conditions of the transverse fields at the access ports, as in Chapter 1. The matrix $\mathbf{T}$ containing the projections of the restrictions of the basis functions at the access ports is now reported:

$$\mathbf{T} = \begin{bmatrix} \mathbf{T}_1^{(e,e)} & \mathbf{T}_1^{(e,h)} \\[1em] \mathbf{T}_1^{(h,e)} & \mathbf{T}_1^{(h,h)} \\[1em] \mathbf{T}_2^{(e,e)} & \mathbf{T}_2^{(e,h)} \\[1em] \mathbf{T}_2^{(h,e)} & \mathbf{T}_2^{(h,h)} \end{bmatrix},$$

where:

$$(\mathbf{T}_k^{(e,e)})_{rc} = \int_0^a \left[u_c e_{y,r}^* - \frac{jk_y}{k^2 - k_y^2} \frac{\partial u_c}{\partial x} e_{x,r}^* \right] \Bigg|_{z_{wg}^{(k)}} \, dx$$

$$(\mathbf{T}_k^{(e,h)})_{rc} = \int_0^a \frac{jkZ}{k^2 - k_y^2} \frac{\partial u_c}{\partial z} e_{x,r}^* \Bigg|_{z_{wg}^{(k)}} \, dx$$

$$(\mathbf{T}_k^{(h,e)})_{rc} = -\int_0^a \frac{jkY}{k^2 - k_y^2} \frac{\partial u_c}{\partial z} h_{x,r}^* \Bigg|_{z_{wg}^{(k)}} \, dx$$

$$(\mathbf{T}_k^{(h,h)})_{rc} = \int_0^a \left[u_c h_{y,r}^* - \frac{jk_y}{k^2 - k_y^2} \frac{\partial u_c}{\partial x} h_{x,r}^* \right] \Bigg|_{z_{wg}^{(k)}} \, dx.$$

3.3 Results

In this section the mortar element method is validated through a comparison with results obtained with a MoM code and with the CST-MS frequency domain solver. The integrals involved in the evaluation of the matrix elements are calculated with a

Gauss-Legendre quadrature rule with $N_{quad} = 32$ nodes. It is remarked that, at the interfaces between different dielectrics, some field derivatives are discontinuous; for this reason, it is convenient to divide the domain Σ in patches where the dielectric is homogeneous, to avoid Gibbs phenomena.

3.3.1 Array of rectangular dielectric rods with H-polarized and E-polarized plane waves

The first benchmark case is an array of rectangular dielectric rods. The unit cell of the problem and the patching used for the domain decomposition are reported in Fig. 3.4. The geometry of the structure is defined by: $a = 400$ µm; the length of the dielectric L_d is 120 µm; the width of the dielectric W_d is 100 µm; the access ports are placed at $L_1 = 100$ µm from the left part of the dielectric and at $L_2 = 300$ µm from its right part. The refraction coefficient n is 2.25.
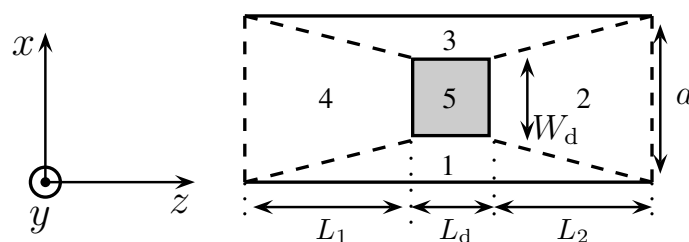
Figure 3.4: Domain decomposition approach applied to the array of rectangular dielectric rods; the dashed lines and the numbers identify the patches. The distance from the access ports are L_1 and L_2; the patch 5 is filled with dielectric $\varepsilon_r = n^2$.

Figures 3.5 and 3.6 show the reflection coefficient response for the fundamental Floquet TE_z and TM_z modes, for an incidence angle of $\vartheta = 80°$. These results are compared with the ones obtained by means of an in-house mode-matching code where 51 modes have been used to guarantee the convergence of the method [30], [31]. The MEM code was used with $N_f = 48$. There is a remarkable agreement between the curves relative to the TE_z polarization even in presence of the Wood's anomaly that occur in the proximity of the frequency where the -1 order mode starts propagating in the grazing direction. On the other hand, the solution of the TM_z problem is not very accurate, owing to the singularity of the electromagnetic field in the proximity of the dielectric edge. Indeed, even if the domain decomposition approach solves the Gibbs phenomena issues, the number of functions should be increased to obtain a better representation of the singular field components. This is proved in Fig. 3.5, where, with $N_f = 186$, a good agreement is achieved. Figure 3.7 shows a comparison of the convergence curves for the TE_z and TM_z incidence
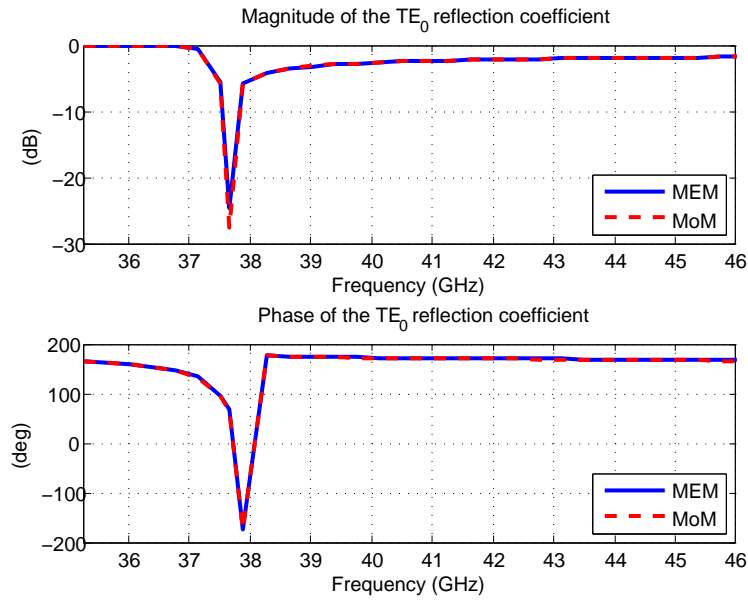
Figure 3.5: Magnitude and phase of the TE_0 reflection coefficient for the structure in Fig. 3.4.
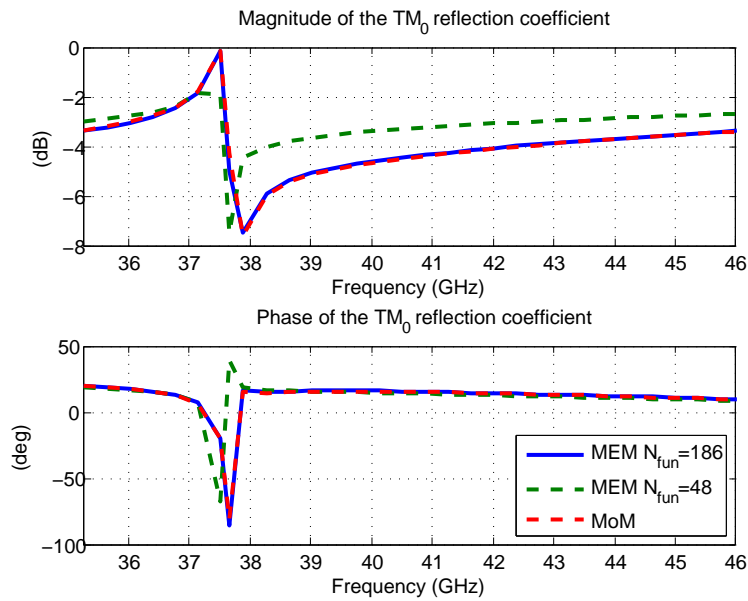
Figure 3.6: Magnitude and phase of the TM_0 reflection coefficient for the structure in Fig. 3.4.

cases; the difference in the convergence rates for the two polarizations is apparent.
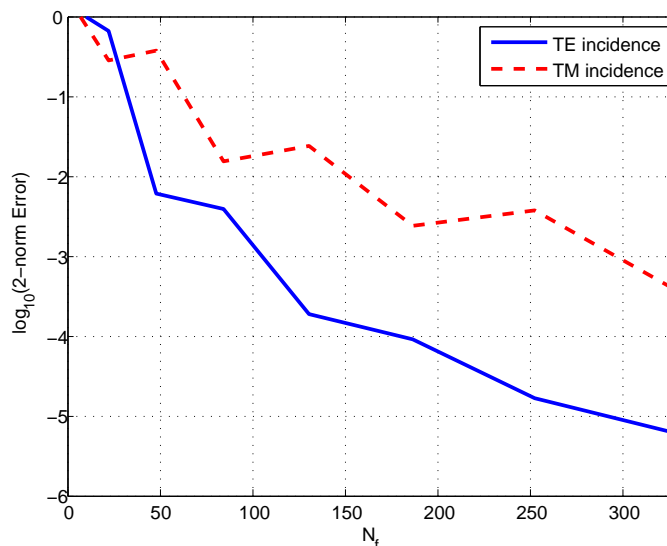
Figure 3.7: Convergence study of the infinity norm error of the TE_0 (solid curve) and TM_0 (dashed curve) reflection coefficients.

3.3.2 Array of dielectric cylinders with skew incident plane waves

As second benchmark case the array of circular cylinders analyzed by Yokota and Sesay is considered [17]. Each cylinder has radius $0.3a$, where a is the period of the structure, as reported in Fig. 3.8. Figure 3.9 shows the adopted patching. Figure
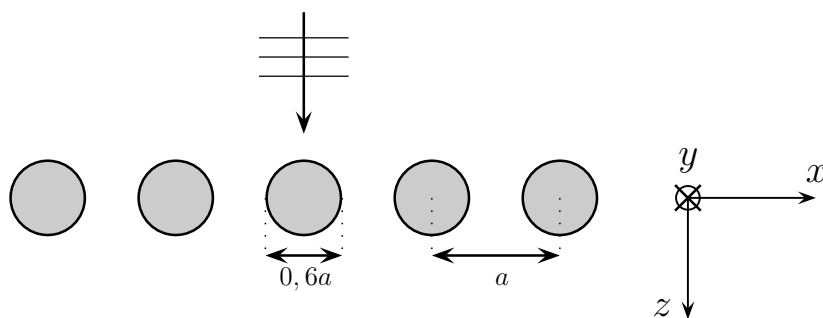
Figure 3.8: Array of cylindrical rods excited by an incident plane wave.

3.10 shows the TE_0 mode power reflection coefficient $|R_0|^2$ for different permittivities; a plane wave with $\varphi = \vartheta = 0°$ is incident on the structure. It is observed that the peak of the power reflectance moves to higher frequencies as the permettivity decreases; also, the sideband of the power reflectance decreases with decreasing permittivity of the cylinder. Good agreement is obtained with the reference, obtained using frequency domain solver of CST-MS, for every analyzed case.
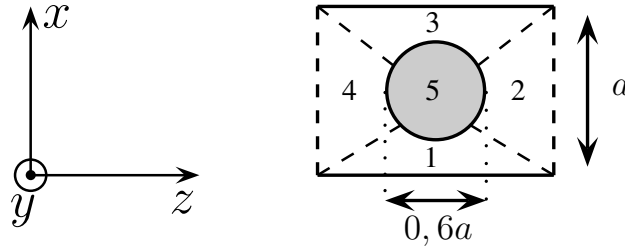
Figure 3.9: Domain decomposition approach applied to the array of cylinders described in Fig. 3.8; the dashed lines and the numbers identify the patches. The patch 5 is filled with dielectric ε_{r}.

3.3.3 Array of dielectric rods with skew incident plane waves

The third analyzed structure is the array of dielectric rods used as reference for the formulation, presented in Fig. 3.1. The domain decomposition approach applied to this structure is described in Fig. 3.11, where five patches have been adopted.

The geometry of the structure is defined by: $a = 100$ µm, $L_{\mathrm{d}} = 40$ µm, $W_{\mathrm{d}} = 30$ µm. The access ports are located $L_{\mathrm{ref}} = 55$ µm from each vertical dielectric interface, the refractive index in the patch 1 is $n = 2.21$, the incidence angles of the plane wave are $\vartheta = 55°$ and $\varphi = 20°$.

In Fig. 3.12 the TE_0-TE_0 reflection coefficient is reported; $N_{\mathrm{m}} = 8$ modes have been used to represent the electromagnetic field at each access port and $N_{\mathrm{f}} = 84$ entire-domain basis functions (that are generated by means of fifth-degree polynomials) are used to represent E_y and H_y. The reference solution has been obtained by an in-house MoM code where $N_{\mathrm{m,MoM}} = 50$ modes are used to approximate the Green's function [30], [31]. This choice ensures the convergence of the scattering parameter. Good agreement between the two curves can be observed even if in the available MoM code the corners are assumed to be sharp, whereas in the MEM code they are rounded with $R = L_{\mathrm{d}}/40$. In Fig. 3.14 the magnitude and phase of the TE_0 mode reflection coefficient obtained with the MEM (solid lines) and with the MoM (dashed lines) are reported for $f = 1.2$ THz as a function of the incidence angles. In Fig. 3.15 the simulations of the frequency responses of the TE_0-TE_0 mode reflection coefficients obtained with the MEM using different radii of curvature R is reported; it is observed that the presence of rounded corners causes a shift of the frequency of the reflection zero.

In Fig. 3.13 a comparison between the TE_0-TE_0 reflection coefficient simulated with the MEM code and with CST-MS is shown for the same structure with radii of curvature of the corners changed to $R = L_{\mathrm{d}}/4$; a remarkable agreement is achieved also in this case.
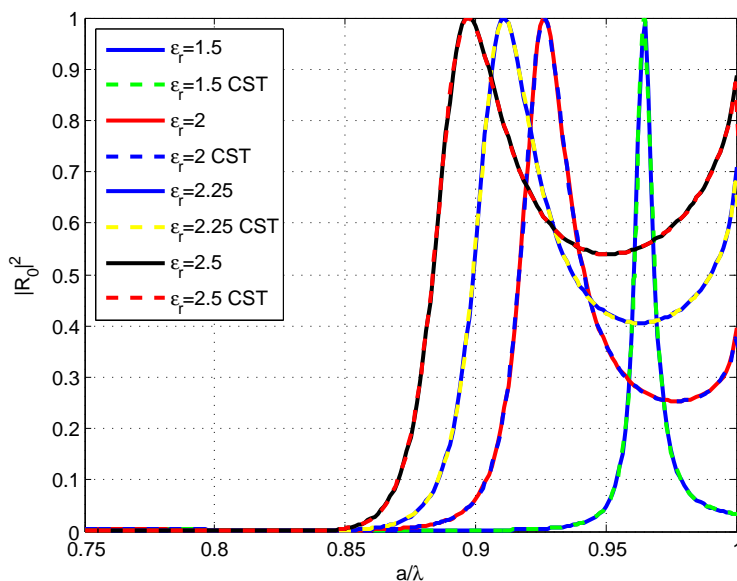
Figure 3.10: Power reflection coefficient $|R_0|^2$ of the fundamental space harmonics for different relative permittivities as a function of the normalized frequency a/λ.
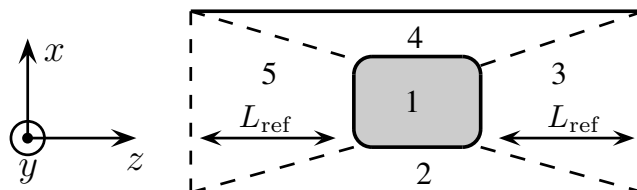
Figure 3.11: Domain decomposition approach applied to the structure of Fig. 3.1; the dashed lines and the numbers identify the patches. The distance from the access ports if L_{ref}. The patch 1 is filled with dielectric $\varepsilon_{\mathrm{r}} = n^2$.

3.3.4 Surface-relief diffraction grating

The MEM has been used to analyze a silicon surface-relief diffraction grating, where the rounded corners take into account the non-idealities that occur during the manufacturing process. A typical fabrication cycle has four steps: spin photoresist, expose and develop, etch, and clean. The first cause of rounding is the thickness nonuniformity of the applied mask, particularly with photoresist masks. Secondly, etching may not be as anisotropic as desired, leading to the rounding of sharp corners [28]. The geometry of this structure and its patching are reported in Fig. 3.16. The period is $a = 2$ μm, the dielectric tooth dimensions are $L_{\mathrm{d}} = 700$ nm and $W_{\mathrm{d}} = 800$ nm, the distance of the left port from the dielecric is $L_1 = 1$ μm, the height of the dielectric substrate is $L_{\mathrm{s}} = 500$ nm, the distance of the right port from
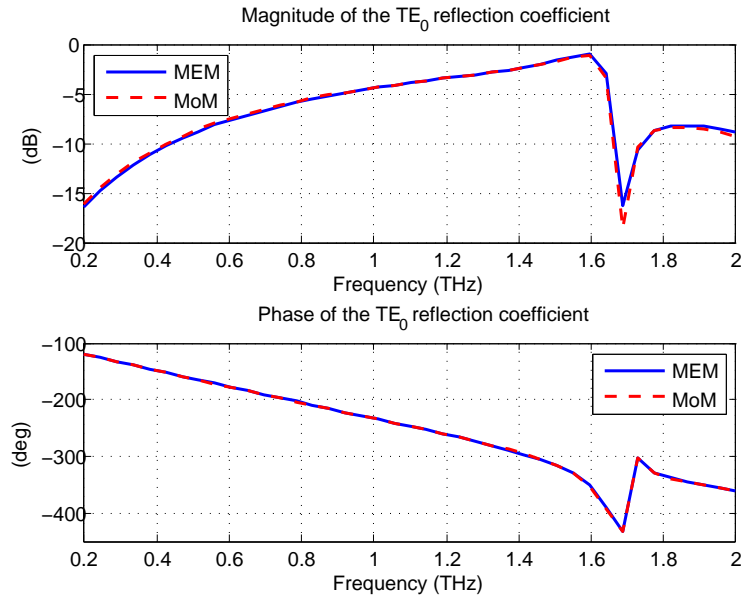
Figure 3.12: Magnitude and phase of the TE_0 mode reflection coefficient of the array of dielectric rods of Fig. 3.11, with $R = L_d/40$. The solid and dotted curves refer to the MEM and with MoM simulations.
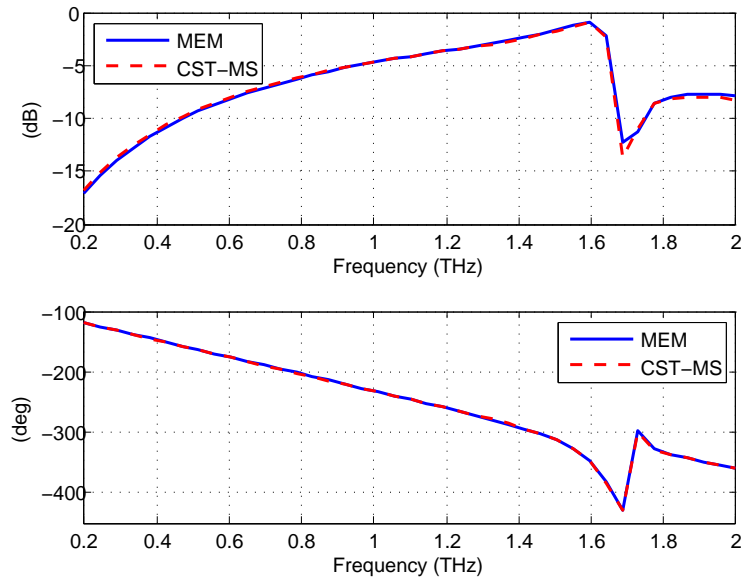
Figure 3.13: Magnitude and phase of the TE_0-TE_0 mode reflection coefficient for the array of dielectric rods of Fig. 3.11, with $R = L_d/4$. The solid and dotted curves refer to results obtained with the MEM technique and with CST-MS, respectively.
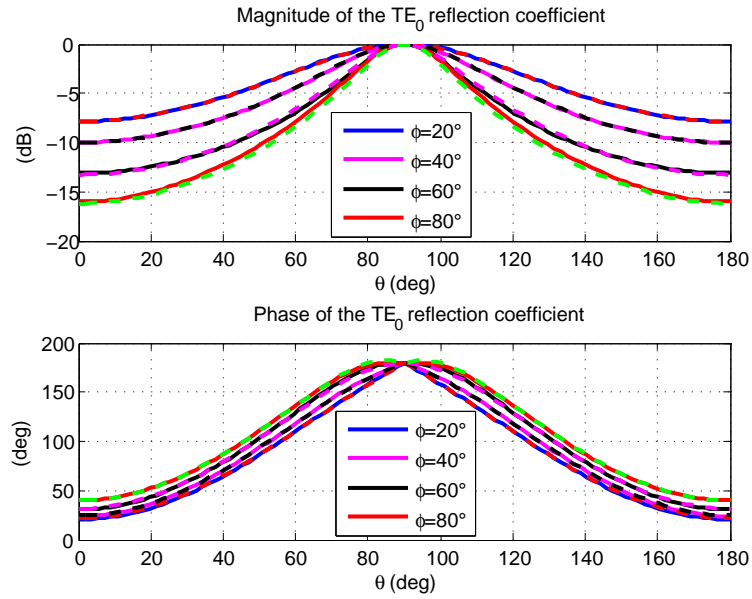
Figure 3.14: Magnitude and phase of the TE_0 mode reflection coefficient versus ϑ of the array of dielectric rods of Fig. 3.11, with $R = L_d/40$, for $f = 1.2$ THz, for some φ angles.
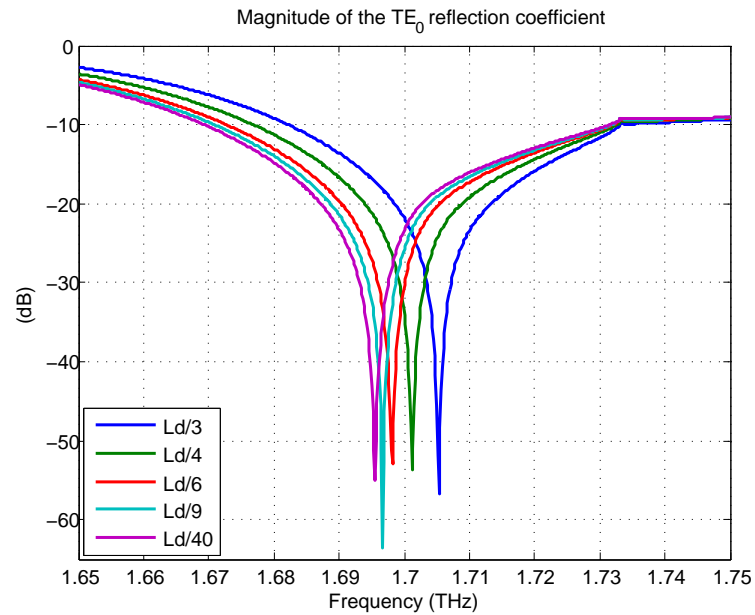
Figure 3.15: Magnitude of the TE_0 mode reflection coefficient of the array of dielectric rods of Fig. 3.11, with $\vartheta = 55°$, $\varphi = 20°$, for different values of the curvature radius R.
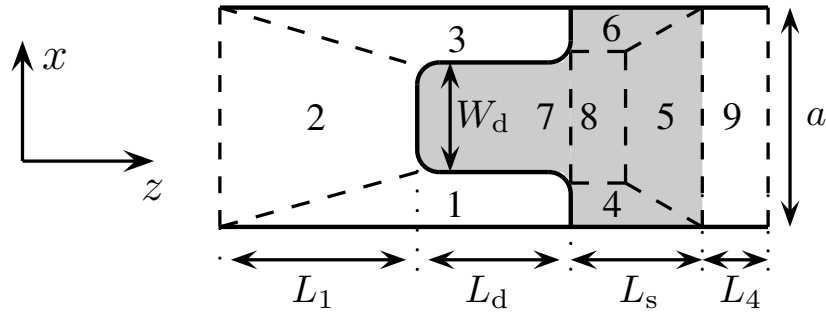
Figure 3.16: Domain decomposition approach applied to the realistic model of a surface-relief diffraction grating. The patches 4 to 8 are filled with dielectric $\varepsilon_r = n^2$, the remaining ones with vacuum; all the corners are rounded, with radius of curvature R.

the substrate is $L_2 = 500$ nm, $R = L_d/4$, the incidence direction is $\vartheta = 43°$, $\varphi = 30°$. The silicon dispersion model (Edwards and Ochoa, 1980) is reported in Fig. 3.17 for the relevant frequency range [29]:

$$n = 3.41983 + \frac{0.159906}{\lambda^2 - 0.028} - 0.123109 \left(\frac{1}{\lambda^2 - 0.028} \right)^2 +$$
$$+ 1.26878 \times 10^{-6} \lambda^2 - 1.95104 \times 10^{-9} \lambda^4$$

In Figs. 3.18, 3.19 and 3.20 the comparisons of the TE_0-TE_0, TM_0-TM_0 and TM_0-TE_0, reflection coefficients simulated with the MEM code and with CST-MS are reported. $N_f = 148$ entire domain basis functions (generated by polynomials of degree 5) and $N_m = 4$ modes have been used in the MEM simulations. A remarkable agreement has been achieved also for very low levels of reflection coefficient.

3.4 Conclusions

The formulation of the plane wave scattering problem from a dielectric periodic structure has been presented; the unit cell problem has been solved by means of the mortar element method. The results of this technique have been compared to reference solutions obtained with a MoM code and with a commercial code. This procedure validated the numerical method.
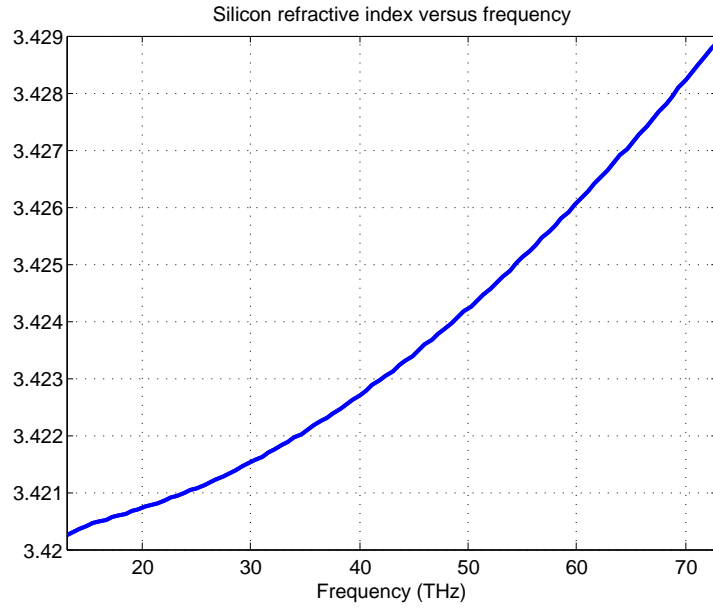
Figure 3.17: Refractive index of silicon versus frequency.
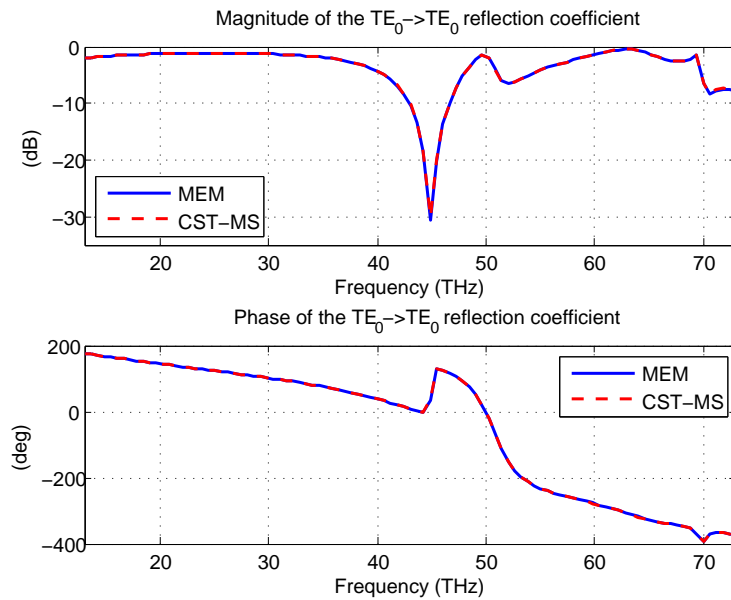
Figure 3.18: Magnitude and phase of the TE_0-TE_0 reflection coefficient for the surface-relief diffraction grating of Fig. 3.16, with $R = L_d/4$. The solid and dotted curves refer to results obtained with the MEM technique and with CST-MS, respectively.
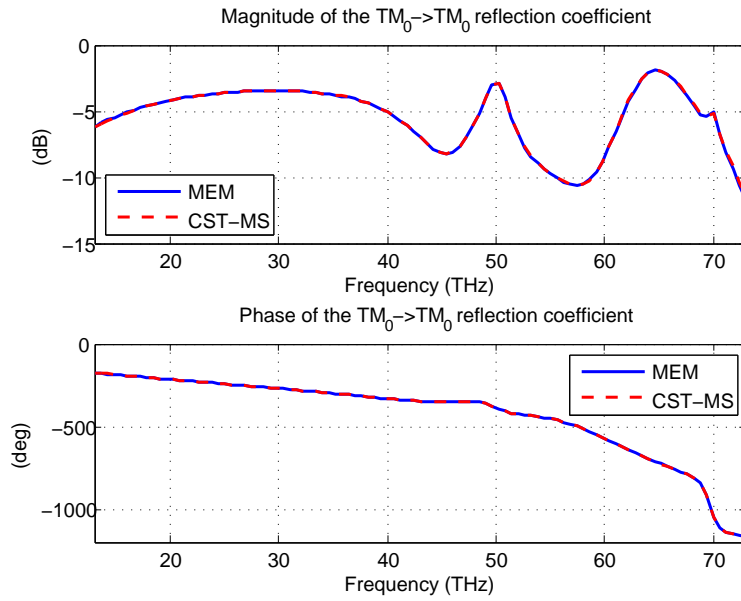
Figure 3.19: Magnitude and phase of the TM_0-TM_0 reflection coefficient for the surface-relief diffraction grating of Fig. 3.16, with $R = L_d/4$. The solid and dotted curves refer to results obtained with the MEM technique and with CST-MS, respectively.
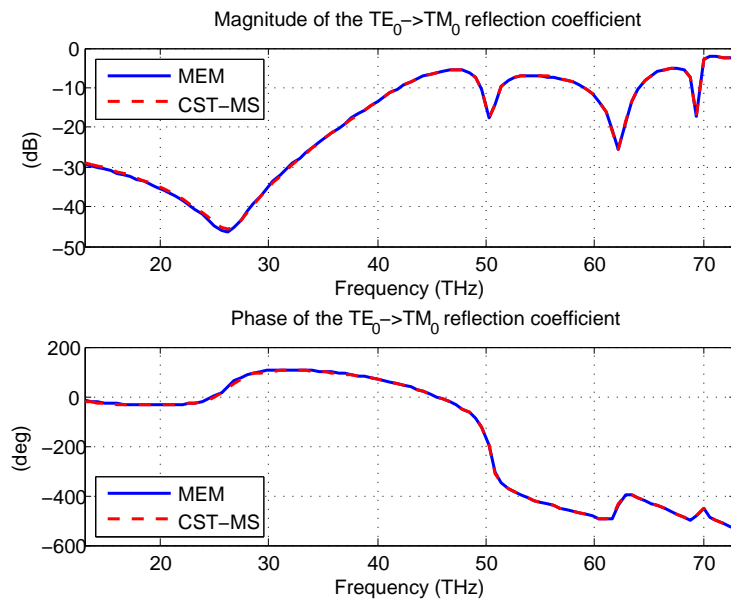
Figure 3.20: Magnitude and phase of the TM_0-TE_0 (TE_0 incident) reflection coefficient for the surface-relief diffraction grating of Fig. 3.16, with $R = L_d/4$. The solid and dotted curves refer to results obtained with the MEM technique and with CST-MS.

Chapter 4

Mortar element analysis of axisymmetric guiding structures

4.1 Introduction

Axisymmetric waveguide components are widely used as building blocks for complex radio-frequency systems, especially in high-frequency and high-power applications, such as satellite telecommunication payloads. As an example, multi-beam antennas are systems with very demanding design specifications that are widely used to cover a well-defined geographical region with several beams generated by an array of radiators that feed a reflecting surface [32]. Thanks to their potential characteristics in terms of matching, low cross-polarization levels and high efficiency, smooth-walls circular horn antennas are optimal candidates as array elements. These devices are composed by a cascade of slope discontinuities such as the one reported in Fig. 4.1, which are designed to excite the desired field configuration. Although in regions 1 and 3 the electromagnetic field can be represented by means of circular and conical waveguide modes respectively, no modal representation of the field in region 2 is available [33]. Hence, the application of the mode-matching technique (MMT) to this discontinuity is not straightforward. A classical analysis procedure adopted to overcome this problem is based on the introduction of a staircase approximation of the tapered profile. The discretized geometry is, then, analyzed as a cascade of waveguide steps, where each step is characterized by its generalized scattering matrix (GSM). Each GSM is obtained by applying either the MMT or the method of moments (MoM) [34], [35], [36]. However, this strategy is not particularly suitable for the analysis of complex-shape structures, *e.g.*, choked mode converters used in compact corrugated horn antennas [37], [38], [39]. An alternative approach involves the use of the finite-element method (FEM) of scattering problems involving pene-
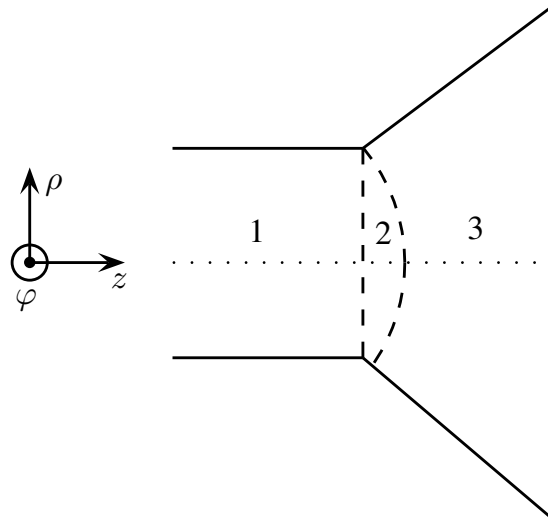
Figure 4.1: Longitudinal section of a junction between a circular and a conical waveguide. The dotted line is the longitudinal axis, whereas the dashed lines denote the waveguide ports for the regions 1 and 3.

trable bodies of revolution has been introduced in the late '70s [40]; more recently, another FEM-based formulation has been applied to the development of a CAD tool for radiating structures [41].

In this chapter a novel technique aimed at analyzing axisymmetric waveguide structures is described [42]. The decomposition approach described in Section 1.2 is applied to this method: the external sub-problem refers to the canonical access waveguides for which the modal basis representation is available, whereas the internal one is defined on the complex-shape region inside the device, where the boundary value problem (BVP) is solved by means of a multi-domain spectral method, *i.e.*, the mortar element method (MEM). In Section 4.2 the formulations of the internal BVP and of the continuity conditions of the tangential fields at the access ports are described. Section 4.3 reports the validation of the present method by comparison with other numerical techniques for some devices.

4.2 Theory

4.2.1 Description of the reference scattering problem

The present method is applicable to structures that exhibit axial symmetry and it is used to compute the GSM of the device in the circular waveguide mode basis. For the sake of clarity and without any loss of generality, the method is here described by considering the reference structure shown in Fig. 4.2 consisting of a slope transition

between two circular waveguides. The vertical dashed lines identify the separation section $\Sigma_{\mathrm{eq}}^{(k)}$ between the internal (gray) and external sub-problems, where the access ports are defined. The incident field $\mathbf{E}^{(\mathrm{inc})}$ is circularly polarized, meaning that a $\mathrm{e}^{\mathrm{j}m\varphi}$ azimuthal dependence of each field component is assumed. The BVP defined
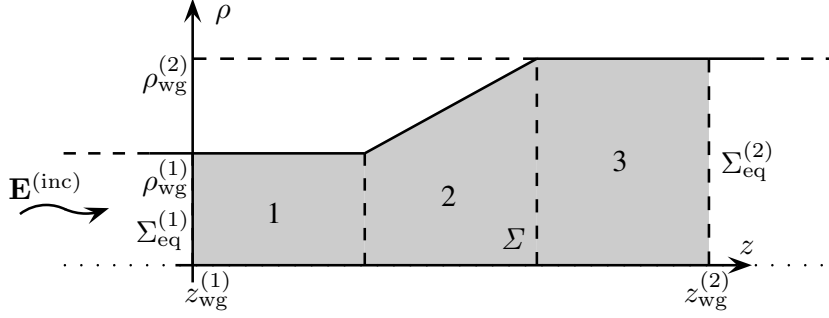
Figure 4.2: Section in the (z, ρ) plane of a slope discontinuity. The gray internal region Σ is divided in three patches separated by the dashed lines to apply the multi-domain strategy. Each access port is located at $z = z_{\mathrm{wg}}^{(k)}$ and its radius is $\rho = \rho_{\mathrm{wg}}^{(k)}$.

in the internal region Σ is derived from the curl Maxwell's equations in absence of sources, written in cylindrical coordinates; the angular derivatives are replaced by "$\mathrm{j}m$", being m the index of the cylindrical harmonic index, owing to the harmonic azimuthal field dependence and to the axial symmetry of the structure:

$$\frac{1}{\rho}\mathrm{j}mE_z - \frac{\partial E_\varphi}{\partial z} = -\mathrm{j}\omega\mu H_\rho \tag{4.1}$$

$$\frac{\partial E_\rho}{\partial z} - \frac{\partial E_z}{\partial \rho} = -\mathrm{j}\omega\mu H_\varphi \tag{4.2}$$

$$\frac{1}{\rho}\left(\frac{\partial(\rho E_\varphi)}{\partial \rho} - \mathrm{j}mE_\rho\right) = -\mathrm{j}\omega\mu H_z \tag{4.3}$$

$$\frac{1}{\rho}\mathrm{j}mH_z - \frac{\partial H_\varphi}{\partial z} = \mathrm{j}\omega\epsilon E_\rho \tag{4.4}$$

$$\frac{\partial H_\rho}{\partial z} - \frac{\partial H_z}{\partial \rho} = \mathrm{j}\omega\epsilon E_\varphi \tag{4.5}$$

$$\frac{1}{\rho}\left(\frac{\partial(\rho H_\varphi)}{\partial \rho} - \mathrm{j}mH_\rho\right) = \mathrm{j}\omega\epsilon E_z. \tag{4.6}$$

Here, ε and μ are intended to be complex quantities. As in the 2-D analysis of E/H-plane components [9], the electromagnetic problem in axisymmetric devices is conveniently formulated in terms of the field components directed along the invariance direction of the structure, which in this case are E_φ and H_φ. Hence, the

remaining components are obtained as a function of the angular ones, by manipulating (4.1), (4.3), (4.4), (4.6):

$$E_\rho = -\frac{j}{m^2 - k^2\rho^2}\left(m\frac{\partial(\rho E_\varphi)}{\partial\rho} + kZ\rho^2\frac{\partial H_\varphi}{\partial z}\right) \tag{4.7}$$

$$H_\rho = -\frac{j}{m^2 - k^2\rho^2}\left(m\frac{\partial(\rho H_\varphi)}{\partial\rho} - kY\rho^2\frac{\partial E_\varphi}{\partial z}\right) \tag{4.8}$$

$$E_z = -\frac{j}{m^2 - k^2\rho^2}\left(m\rho\frac{\partial E_\varphi}{\partial z} - kZ\rho\frac{\partial(\rho H_\varphi)}{\partial\rho}\right) \tag{4.9}$$

$$H_z = -\frac{j}{m^2 - k^2\rho^2}\left(kY\rho\frac{\partial(\rho E_\varphi)}{\partial\rho} + m\rho\frac{\partial H_\varphi}{\partial z}\right), \tag{4.10}$$

where:

$$k = \omega\sqrt{\mu\varepsilon}, \qquad Z = \sqrt{\frac{\mu}{\varepsilon}}.$$

The derivation of these expressions is reported in Appendix D.2. Unless $m = 0$, these components depend on both E_φ and H_φ and, hence, the boundary value problem is vectorial. On the other hand, if $m = 0$, the problem splits up into the independent TE_z (involving the E_φ, H_ρ, H_z components) and TM_z (involving the H_φ, E_ρ, E_z components) problems; these cases are studied separately from the general one. It has to be noted that, up to this point, the singularity in $\rho = m/k$ appearing in the right-hand sides of (4.7) ÷ (4.10) is removable, since these expressions represent regular functions and no approximation has been introduced.

The remaining components of the Maxwell's curl equations (4.2) and (4.5) are used with (4.7) ÷ (4.10) to formulate the internal BVP; these equations are supplemented with the PEC boundary conditions on the segment γ_{PEC} where they are required:

$$\begin{cases} E_\varphi = 0 & (z,\rho) \in \gamma_{\text{PEC}} \\ \mathbf{E}_{\text{t}}^{(\varphi)} \cdot \widehat{\mathbf{s}} = 0 & (z,\rho) \in \gamma_{\text{PEC}}, \end{cases} \tag{4.11}$$

where $\mathbf{E}_{\text{t}}^{(\varphi)}$ is the electric field in the (z,ρ) plane and $\widehat{\mathbf{s}}$ is the tangent unit vector of γ_{PEC}. The unknowns E_φ and H_φ are then represented as linear combinations of entire-domain basis functions defined on the region Σ:

$$E_\varphi = \sum_{c=1}^{N_{\text{fun}}^{(\text{e})}} c_c^{(\text{e})} u_c^{(\text{e})}(z,\rho)$$

$$\tag{4.12}$$

$$H_\varphi = \sum_{c=1}^{N_{\text{fun}}^{(\text{h})}} c_c^{(\text{h})} u_c^{(\text{h})}(z,\rho).$$

The basis functions $u_c^{(h)}$ belong to the space $V^{(h)}$ of continuous functions with integrable derivatives, whereas $u_c^{(e)}$ belong to the sub-space $V^{(e)} \subset V^{(h)}$, which includes only functions vanishing on γ_{PEC}. Indeed, the Dirichlet condition on E_φ is an essential boundary condition and it has to be explicitly enforced. On the contrary, the condition on $\mathbf{E}_\mathrm{t}^{(\varphi)}$ is of natural type and, consequently, it is enforced in the weak formulation without further specializing the functions used to represent H_φ [12, Chap. 3]. These sets of entire-domain basis functions are numerically synthesized as described in Section 1.3.

4.2.2 Formulation of the internal BVP : $m \neq 0$ case

The φ components of the Maxwell's curl equations (4.2) and (4.5) are cast in weak form by projecting them onto a set of functions $v_r^{(h)} = u_r^{(h)}$ and $v_r^{(e)} = u_r^{(e)}$ respectively:

$$-\mathrm{j}kZ \iint_\Sigma H_\varphi v_r^{(h)*}\,\mathrm{d}z\,\mathrm{d}\rho = \iint_\Sigma \left[\frac{\partial E_\rho}{\partial z} - \frac{\partial E_z}{\partial \rho} \right] v_r^{(h)*}\,\mathrm{d}z\,\mathrm{d}\rho$$

$$\mathrm{j}kY \iint_\Sigma E_\varphi v_r^{(e)*}\,\mathrm{d}z\,\mathrm{d}\rho = \iint_\Sigma \left[\frac{\partial H_\rho}{\partial z} - \frac{\partial H_z}{\partial \rho} \right] v_r^{(e)*}\,\mathrm{d}z\,\mathrm{d}\rho.$$

Then, integration by parts by means of the Stokes theorem is performed, and the following equations are obtained:

$$-\mathrm{j}kZ \iint_\Sigma H_\varphi v_r^{(h)*}\,\mathrm{d}z\,\mathrm{d}\rho + \iint_\Sigma \left[E_\rho \frac{\partial v_r^{(h)*}}{\partial z} - E_z \frac{\partial v_r^{(h)*}}{\partial \rho} \right]\mathrm{d}z\,\mathrm{d}\rho = \oint_\gamma (\mathbf{E}_\mathrm{t}^{(\varphi)} v_r^{(h)*}) \cdot \mathrm{d}\mathbf{s}$$

(4.13)

$$\mathrm{j}kY \iint_\Sigma E_\varphi v_r^{(e)*}\,\mathrm{d}z\,\mathrm{d}\rho + \iint_\Sigma \left[H_\rho \frac{\partial v_r^{(e)*}}{\partial z} - H_z \frac{\partial v_r^{(e)*}}{\partial \rho} \right]\mathrm{d}z\,\mathrm{d}\rho = \oint_\gamma (\mathbf{H}_\mathrm{t}^{(\varphi)} v_r^{(e)*}) \cdot \mathrm{d}\mathbf{s},$$

(4.14)

where $\gamma = \gamma_{\mathrm{PEC}} \cup \gamma_{\mathrm{axis}} \cup \gamma_{\mathrm{wg}}^{(1)} \cup \gamma_{\mathrm{wg}}^{(2)}$ is the boundary of Σ as shown in Fig. 4.4 and $\mathbf{E}_\mathrm{t}^{(\varphi)}$ and $\mathbf{H}_\mathrm{t}^{(\varphi)}$ are the electric and magnetic fields transverse to φ.

Since the general $m \neq 0$ case gives rise to a vector differential problem, the decomposition approach applied to the structure is described in the top part of Fig. 4.3, where the equivalence theorem is applied by introducing a couple of oppositely directed electric and magnetic current densities on the two sides of $\Sigma_{\mathrm{eq}}^{(k)}$; these currents are conveniently represented with the modes of the k-th access port waveguide, accordingly to Section 1.2. The bottom part of Fig. 4.3 reports the hybrid circuit associated to the access waveguide, where only one equivalent modal circuit is shown for each access port.

Figure 4.3: Hybrid equivalent multi-modal circuit of the waveguide structure shown in Fig. 4.2, where only one equivalent modal circuit is shown for each access waveguide.
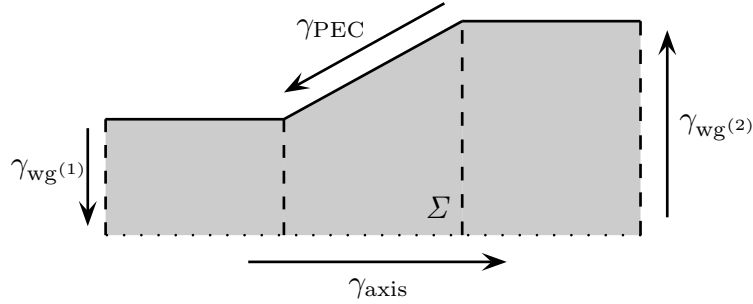
Figure 4.4: Sketch of the internal sub-problem, where the boundary contributions are emphasized.

As it can be inferred from (4.7) $\div$ (4.10), the contribution of the axis $\rho = 0$ to the line integrals in the right-hand sides of (4.13) and (4.14) is zero. Moreover, the contribution of γ_{PEC} to the line integrals of (4.14) is zero since the test functions $v_r^{(\mathrm{e})}$ are vanishing on it; this is equivalent to requiring no condition from $\mathbf{H}_{\mathrm{t}}^{(\varphi)}$. Finally, the contribution of γ_{PEC} to the line integral of (4.13) is set to zero to enforce the second condition of (4.11) as a natural boundary condition; therefore, the only non-vanishing contributions to the line integrals come from the equivalent currents defined on the access ports. Noting that, at the access ports, $\mathbf{E}_{\mathrm{t}}^{(\varphi)} \cdot \mathrm{d}\mathbf{s} = \widetilde{\mathbf{E}}_{\mathrm{t}}^{(k)} \cdot \mathrm{d}\mathbf{s}$

and $\mathbf{H}_\mathrm{t}^{(\varphi)} \cdot \mathrm{d}\mathbf{s} = \widetilde{\mathbf{H}}_\mathrm{t}^{(k)} \cdot \mathrm{d}\mathbf{s}$, according to Section 1.2:

$$
\oint_\gamma (\mathbf{H}_\mathrm{t}^{(\varphi)} v_r^{(\mathrm{e})*}) \cdot \mathrm{d}\mathbf{s} = -\sum_{n=1}^{N_\mathrm{m}} \mathring{i}_n^{(1)} \int_0^{\rho_\mathrm{wg}^{(1)}} h_{\rho,n}^{(1)} v_r^{(\mathrm{e})*} \bigg|_{z=z_\mathrm{wg}^{(1)}} \mathrm{d}\rho + \sum_{n=1}^{N_\mathrm{m}} \mathring{i}_n^{(2)} \int_0^{\rho_\mathrm{wg}^{(2)}} h_{\rho,n}^{(2)} v_r^{(\mathrm{e})*} \bigg|_{z=z_\mathrm{wg}^{(2)}} \mathrm{d}\rho
$$

$$
\oint_\gamma (\mathbf{E}_\mathrm{t}^{(\varphi)} v_r^{(\mathrm{h})*}) \cdot \mathrm{d}\mathbf{s} = -\sum_{n=1}^{N_\mathrm{m}} \mathring{v}_n^{(1)} \int_0^{\rho_\mathrm{wg}^{(1)}} e_{\rho,n}^{(1)} v_r^{(\mathrm{h})*} \bigg|_{z=z_\mathrm{wg}^{(1)}} \mathrm{d}\rho + \sum_{n=1}^{N_\mathrm{m}} \mathring{v}_n^{(2)} \int_0^{\rho_\mathrm{wg}^{(2)}} e_{\rho,n}^{(2)} v_r^{(\mathrm{h})*} \bigg|_{z=z_\mathrm{wg}^{(2)}} \mathrm{d}\rho.
$$

The following matrix elements are then defined:

$$
(\mathbf{B}^{(\mathrm{e},k)})_{rn} = \int_0^{\rho_\mathrm{wg}^{(k)}} h_{\rho,n}^{(k)} v_r^{(\mathrm{e})} \bigg|_{z=z_\mathrm{wg}^{(k)}} \mathrm{d}\rho
$$

$$
(\mathbf{B}^{(\mathrm{h},k)})_{rn} = \int_0^{\rho_\mathrm{wg}^{(k)}} e_{\rho,n}^{(k)} v_r^{(\mathrm{h})} \bigg|_{z=z_\mathrm{wg}^{(k)}} \mathrm{d}\rho.
$$

(4.15)

Then, by substituting (4.7) ÷ (4.10) and (4.12) in (4.13) and (4.14), the following system of matrix equations is obtained:

$$
\begin{cases} \mathbf{A}^{(\mathrm{e},\mathrm{e})}\mathbf{c}^{(\mathrm{e})} + \mathbf{A}^{(\mathrm{e},\mathrm{h})}\mathbf{c}^{(\mathrm{h})} = \mathbf{B}^{(\mathrm{e},2)}\mathring{\mathbf{i}}^{(2)} - \mathbf{B}^{(\mathrm{e},1)}\mathring{\mathbf{i}}^{(1)} \\ \mathbf{A}^{(\mathrm{h},\mathrm{e})}\mathbf{c}^{(\mathrm{e})} + \mathbf{A}^{(\mathrm{h},\mathrm{h})}\mathbf{c}^{(\mathrm{h})} = \mathbf{B}^{(\mathrm{h},2)}\mathring{\mathbf{v}}^{(2)} - \mathbf{B}^{(\mathrm{h},1)}\mathring{\mathbf{v}}^{(1)}, \end{cases}
$$

(4.16)

where:

$$
\mathbf{A}^{(\mathrm{e},\mathrm{e})} = \mathrm{j}kY \left[\mathbf{M}^{(\mathrm{e})} + \mathbf{K}^{(\mathrm{e})} \right]
$$

$$
\mathbf{A}^{(\mathrm{e},\mathrm{h})} = \mathrm{j}m\mathbf{L}^{(\mathrm{e})}
$$

$$
\mathbf{A}^{(\mathrm{h},\mathrm{e})} = \mathrm{j}m\mathbf{L}^{(\mathrm{h})}
$$

$$
\mathbf{A}^{(\mathrm{h},\mathrm{h})} = -\mathrm{j}kZ \left[\mathbf{M}^{(\mathrm{h})} + \mathbf{K}^{(\mathrm{h})} \right],
$$

and

$$(\mathbf{M}^{(e)})_{rc} = \iint_{\Sigma} u_c^{(e)} v_r^{(e)*} \mathrm{d}\rho \mathrm{d}z$$

$$(\mathbf{K}^{(e)})_{rc} = \iint_{\Sigma} \left\{ \frac{1}{m^2 - k^2\rho^2} \rho \left[\rho \frac{\partial u_c^{(e)}}{\partial z} \frac{\partial v_r^{(e)*}}{\partial z} + \frac{\partial(\rho u_c^{(e)})}{\partial \rho} \frac{\partial v_r^{(e)*}}{\partial \rho} \right] \right\} \mathrm{d}\rho \mathrm{d}z$$

$$(\mathbf{L}^{(e)})_{rc} = \iint_{\Sigma} \left\{ \frac{1}{m^2 - k^2\rho^2} \left[\frac{\partial(\rho u_c^{(h)})}{\partial \rho} \frac{\partial v_r^{(e)*}}{\partial z} - \rho \frac{\partial u_c^{(h)}}{\partial z} \frac{\partial v_r^{(e)*}}{\partial \rho} \right] \right\} \mathrm{d}\rho \mathrm{d}z$$

$$(\mathbf{M}^{(h)})_{rc} = \iint_{\Sigma} u_c^{(h)} v_r^{(h)*} \mathrm{d}\rho \mathrm{d}z$$

$$(\mathbf{K}^{(h)})_{rc} = \iint_{\Sigma} \left\{ \frac{1}{m^2 - k^2\rho^2} \rho \left[\rho \frac{\partial u_c^{(h)}}{\partial z} \frac{\partial v_r^{(h)*}}{\partial z} + \frac{\partial(\rho u_c^{(h)})}{\partial \rho} \frac{\partial v_r^{(h)*}}{\partial \rho} \right] \right\} \mathrm{d}\rho \mathrm{d}z$$

$$(\mathbf{L}^{(h)})_{rc} = \iint_{\Sigma} \left\{ \frac{1}{m^2 - k^2\rho^2} \left[\frac{\partial(\rho u_c^{(e)})}{\partial \rho} \frac{\partial v_r^{(h)*}}{\partial z} - \rho \frac{\partial u_c^{(e)}}{\partial z} \frac{\partial v_r^{(h)*}}{\partial \rho} \right] \right\} \mathrm{d}\rho \mathrm{d}z.$$

Since these integrals are obtained substituting a combination of the basis/test functions and of their derivatives, the singularity in $\rho = m/k$ is no longer removable, therefore the integral has to be evaluated with an ad-hoc quadrature scheme, introduced in Appendix D.3.

4.2.3 Formulation of the internal BVP: $m = 0$, TM$_z$ case

In the TM$_z$ problem of the $m = 0$ case, (4.7) and (4.9) simplify as:

$$
\begin{aligned}
E_\rho &= \frac{\mathrm{j}}{kY} \frac{\partial H_\varphi}{\partial z} \\
E_z &= -\frac{\mathrm{j}}{kY\rho} \frac{\partial(\rho H_\varphi)}{\partial \rho} = -\frac{\mathrm{j}}{kY\rho} H_\varphi - \frac{\mathrm{j}}{kY} \frac{\partial H_\varphi}{\partial \rho}.
\end{aligned}
\tag{4.17}
$$

Then, (4.2) is cast in weak form by projecting it on test functions defined as $w_r^{(h)} = \rho^2 v_r^{(h)}$, where $v_r^{(h)} = u_r^{(h)}$ as in the previous section; this eliminates the singularity of the field components (4.17) in $\rho = 0$. Then, the Stokes theorem is applied to obtain the resulting equation:

$$-\mathrm{j}kZ \iint_{\Sigma} H_\varphi w_r^{(h)*} \, \mathrm{d}z \, \mathrm{d}\rho + \iint_{\Sigma} \left[E_\rho \frac{\partial w_r^{(h)*}}{\partial z} - E_z \frac{\partial w_r^{(h)*}}{\partial \rho} \right] \mathrm{d}z \, \mathrm{d}\rho = \oint_{\gamma} (\mathbf{E}_t^{(\varphi)} w_r^{(h)*}) \cdot \mathrm{d}\mathbf{s}.$$

Since no magnetic field excitation is appearing in the line integrals, the proper version of the equivalence theorem is the one where PEC is used to fill the zero-field regions, to eliminate the contributions of the electric current densities. This is described in Fig. 4.5, where the equivalent problems are reported with their hybrid
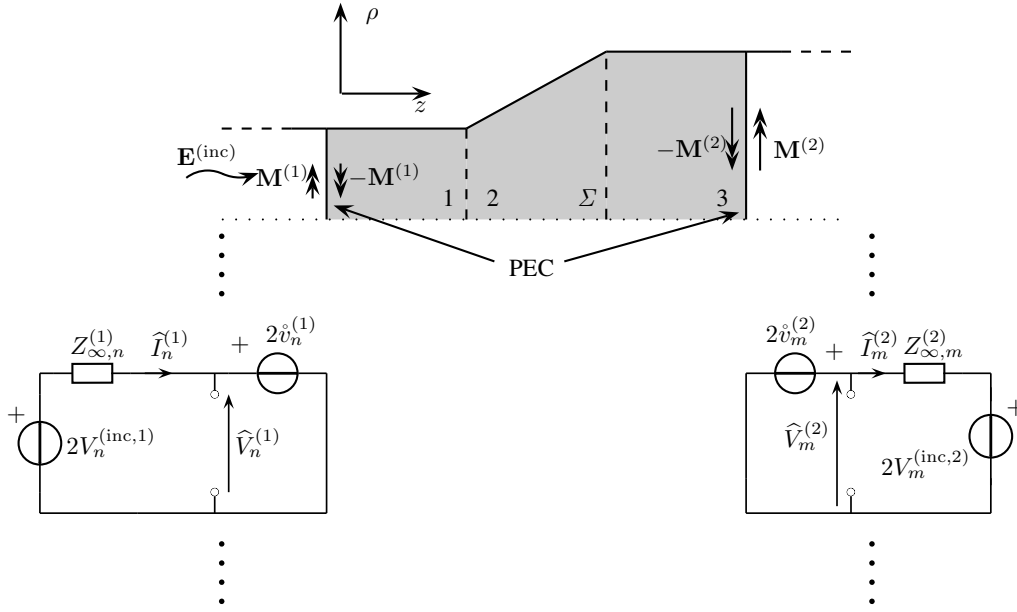
Figure 4.5: Hybrid equivalent multi-modal circuit of the waveguide structure shown in Fig. 4.2, where only one equivalent modal circuit is shown for each access waveguide.

circuits. By applying the same considerations of the previous case, the following matrix equation is obtained:

$$\mathbf{A}^{(\mathrm{h,h})}\,\mathbf{c}^{(\mathrm{h})} = \mathbf{B}^{(\mathrm{h},2)}\mathring{\mathbf{v}}^{(2)} - \mathbf{B}^{(\mathrm{h},1)}\mathring{\mathbf{v}}^{(1)}, \tag{4.18}$$

where the line integrals are defined as:

$$(\mathbf{B}^{(\mathrm{h},k)})_{rn} = \int_{0}^{\rho_{\mathrm{wg}}^{(k)}} e_{\rho,n}^{(k)} v_{r}^{(\mathrm{h})}\bigg|_{z=z_{\mathrm{wg}}^{(k)}} \rho^2\,\mathrm{d}\rho,$$

whereas the left-hand side is written as:

$$\mathbf{A}^{(\mathrm{h,h})} = -\mathrm{j}kZ\mathbf{M}^{(\mathrm{h},0)} - \frac{1}{\mathrm{j}kY}\mathbf{K}^{(\mathrm{h},0)},$$

where:

$$\mathbf{M}^{(\mathrm{h},0)} = \iint_{\varSigma} u_c^{(\mathrm{h})} v_r^{(\mathrm{h})*}\rho^2\,\mathrm{d}z\,\mathrm{d}\rho$$

$$\mathbf{K}^{(\mathrm{h},0)} = \iint_{\varSigma} \frac{\partial u_c^{(\mathrm{h})}}{\partial z}\frac{\partial v_r^{(\mathrm{h})*}}{\partial z}\rho^2\,\mathrm{d}z\,\mathrm{d}\rho + \iint_{\varSigma}\left[u_c^{(\mathrm{h})} + \rho\frac{\partial u_c^{(\mathrm{h})}}{\partial \rho}\right]\left[\rho\frac{\partial v_r^{(\mathrm{h})*}}{\partial \rho} + 2v_r^{(\mathrm{h})*}\right]\mathrm{d}z\,\mathrm{d}\rho.$$

4.2.4 Formulation of the internal BVP: $m = 0$, $\mathbf{TE}_z$ case

In the TE_z problem of the $m = 0$ case, (4.8) and (4.10) simplify as:

$$H_\rho = -\frac{\mathrm{j}}{kZ}\frac{\partial E_\varphi}{\partial z}$$
$$H_z = \frac{\mathrm{j}}{kZ\rho}\frac{\partial(\rho E_\varphi)}{\partial \rho} = \frac{\mathrm{j}}{kZ\rho}E_\varphi + \frac{\mathrm{j}}{kZ}\frac{\partial E_\varphi}{\partial \rho}.$$

(4.19)

Then, (4.2) is cast in weak form by projecting it on test functions defined as $w_r^{(e)} = \rho^2 v_r^{(e)}$, where $v_r^{(e)} = u_r^{(e)}$ as in the previous section; this eliminates the singularity of the field components (4.19) in $\rho = 0$. Then, the Stokes theorem is applied as follows:

$$\mathrm{j}kY \iint_\Sigma E_\varphi w_r^{(e)*}\,\mathrm{d}z\,\mathrm{d}\rho + \iint_\Sigma \left[H_\rho \frac{\partial w_r^{(e)*}}{\partial z} - H_z \frac{\partial w_r^{(e)*}}{\partial \rho}\right]\mathrm{d}z\,\mathrm{d}\rho = \oint_\gamma (\mathbf{H}_{\mathrm{t}}^{(\varphi)} w_r^{(e)*}) \cdot \mathrm{d}\mathbf{s}.$$

Since no electric field excitation is appearing in the line integrals, the proper version of the equivalence theorem is the one where PMC is used to fill the zero-field regions, to eliminate the contributions of the magnetic current densities. This is described in Fig. 4.6, where the equivalent problems are reported together with their hybrid circuits. By applying the same considerations of the previous case, the following matrix equation is obtained:

$$\mathbf{A}^{(e,e)}\,\mathbf{c}^{(e)} = \mathbf{B}^{(e,2)}\mathring{\mathbf{i}}^{(2)} - \mathbf{B}^{(e,1)}\mathring{\mathbf{i}}^{(1)},$$

(4.20)

where the line integrals are defined as:

$$(\mathbf{B}^{(e,k)})_{rn} = \int_0^{\rho_{\mathrm{wg}}^{(k)}} h_{\rho,n}^{(k)} v_r^{(e)}\bigg|_{z=z_{\mathrm{wg}}^{(k)}} \rho^2\,\mathrm{d}\rho,$$

whereas the left-hand side is written as:

$$\mathbf{A}^{(e,e)} = \mathrm{j}kY\mathbf{M}^{(e,0)} + \frac{1}{\mathrm{j}kZ}\mathbf{K}^{(e,0)},$$

where:

$$\mathbf{M}^{(e,0)} = \iint_\Sigma u_c^{(e)} v_r^{(e)*}\rho^2\,\mathrm{d}z\,\mathrm{d}\rho$$

$$\mathbf{K}^{(e,0)} = \iint_\Sigma \frac{\partial u_c^{(e)}}{\partial z}\frac{\partial v_r^{(e)*}}{\partial z}\rho^2\,\mathrm{d}z\,\mathrm{d}\rho + \iint_\Sigma \left[u_c^{(e)} + \rho\frac{\partial u_c^{(e)}}{\partial \rho}\right]\left[\rho\frac{\partial v_r^{(e)*}}{\partial \rho} + 2v_r^{(e)*}\right]\mathrm{d}z\,\mathrm{d}\rho.$$
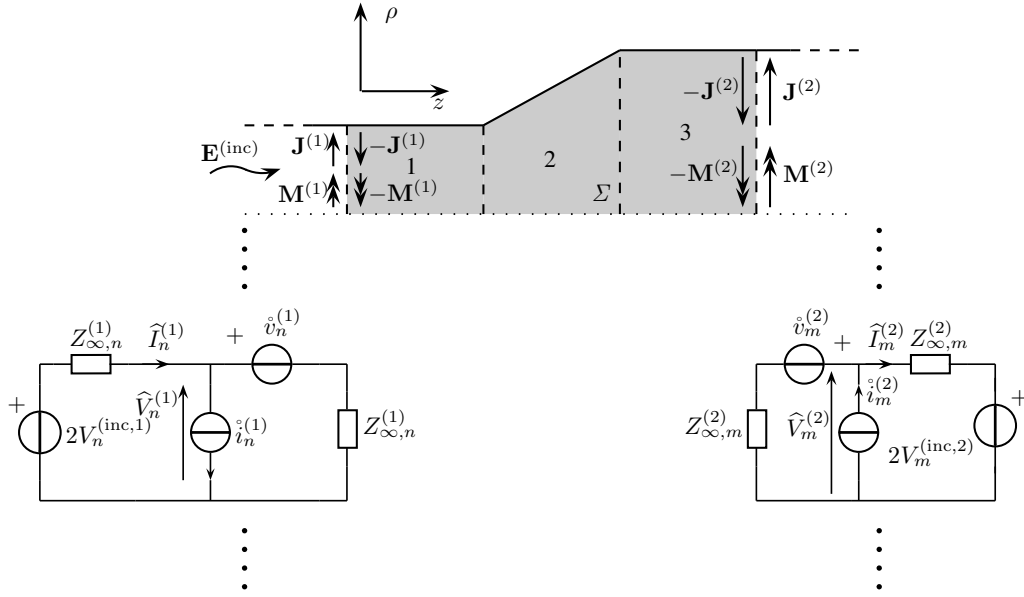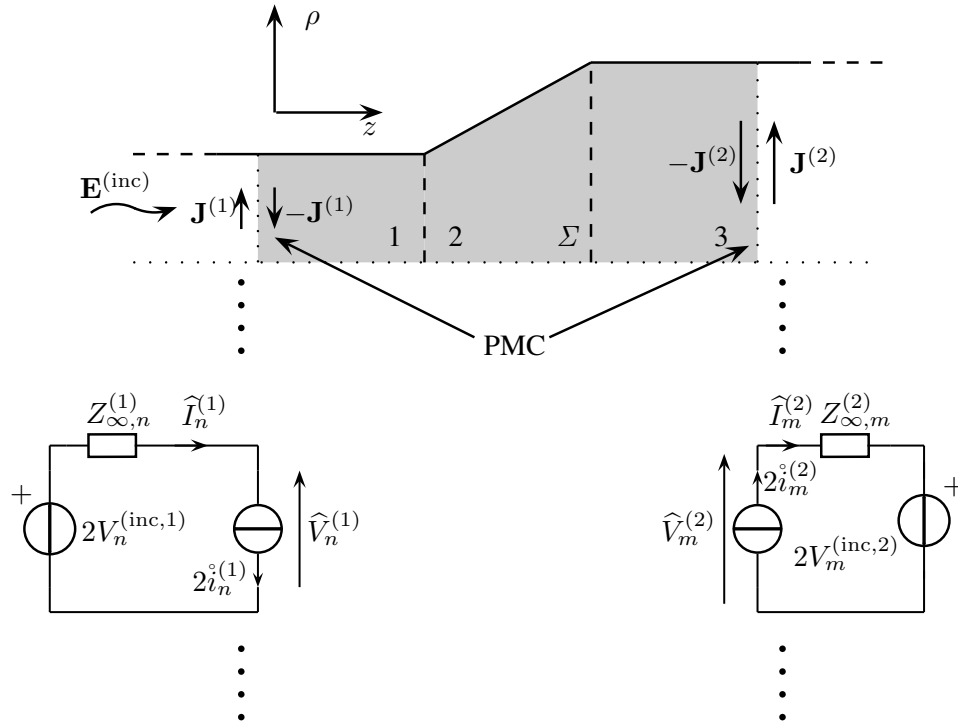
Figure 4.6: Hybrid equivalent multi-modal circuit of the waveguide structure shown in Fig. 4.2, where only one equivalent modal circuit is shown for each access waveguide.

4.3 Results

In this section a validation of the MEM is presented by considering two benchmark cases and a more complex axisymmetric waveguide structure, *i.e.*, a choked mode converter.

4.3.1 Circular waveguide stub

As a first benchmark case, the Ku-band circular waveguide stub shown in Fig. 4.7 is considered. The input and output waveguides radii are $R_1 = R_2 = 9.525$ mm, the stub width is $w = 6$ mm, the stub length is $h = 5$ mm and the lengths of the input lines are $L_1 = L_2 = 4$ mm. The electromagnetic field at the access ports is represented by using $N_{\mathrm{m}} = N_{\mathrm{m}}^{(\mathrm{MEM})} = 10$ modes, whereas the unknowns E_φ and H_φ are expanded with $N_{\mathrm{fun}}^{(\mathrm{e})} = 32$ and $N_{\mathrm{fun}}^{(\mathrm{h})} = 46$ global basis functions, respectively. Although the polynomial degree of the basis functions $\{u_c^{(\mathrm{e})}\}$ and $\{u_c^{(\mathrm{h})}\}$ is the same, $N_{\mathrm{fun}}^{(\mathrm{e})}$ is smaller due to the enforcement of the essential boundary condition. The reference solution is obtained by a mode-matching code, where $N_{\mathrm{m}}^{(\mathrm{MMT})} = 20$ modes are used at the step aperture to ensure the convergence of the scattering parameters.
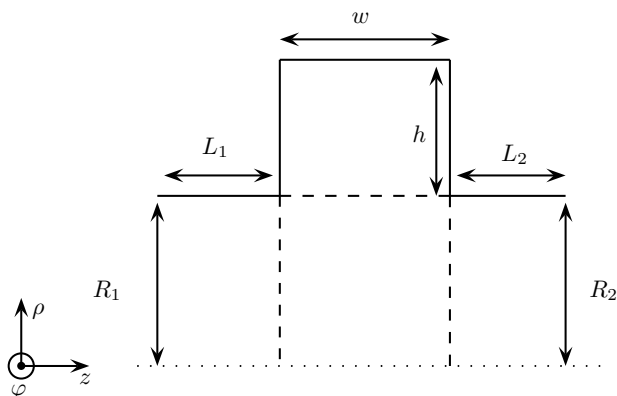
Figure 4.7: Longitudinal section of the smooth waveguide transition considered as a second benchmark case. This structure is described with a single patch. The dashed lines denote the access waveguide ports with input waveguide radii R_1 and R_2; L is the length of the structure.

Fig. 4.8 reports the comparison between the MEM and MMT curves relative to the TE_{11} mode transmission coefficient. A remarkable agreement is achieved between the two curves, with particular reference to the frequency of the transmission zero. A convergence study of the numerical method with respect to the number of basis
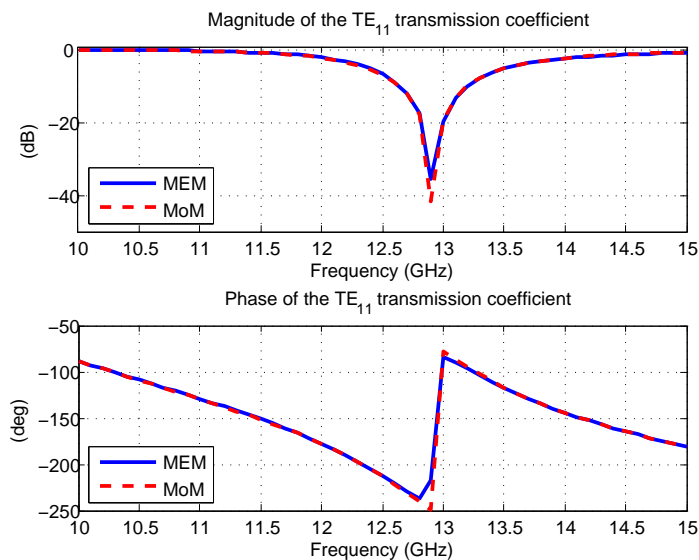
Figure 4.8: Magnitude and phase of the TE_{11} mode transmission coefficient of the circular waveguide stub shown in Fig. 4.7 ($R_1 = R_2 = 9.525$ mm, $h = 5$ mm, $w = 6$ mm, $L_1 = L_2 = 4$ mm). The dotted curve (reference) refers to the MMT simulation. The solid and dashed curves are obtained by the MEM, using singular and polynomial basis functions, respectively.

functions used to represent E_φ and H_φ has been carried out for this structure. Three types of basis functions have been investigated: polynomials, polynomials weighted by functions that keep into account the radial asymptotic behavior of the field in the proximity of the edges, and polynomials weighted by functions keeping into account both the radial and the azimuthal asymptotic behaviors at the edges. The expressions of the asymptotic field behaviours at sharp edges can be found in Appendix A.2. Figure 4.9 shows the 2-norm relative error $||e^{(T)}||_2$ in the transmission coefficient versus the total number of entire domain basis functions $n = N_{\mathrm{fun}}^{(e)} + N_{\mathrm{fun}}^{(h)}$. The reference solution is obtained using $n > 1000$. The dot refers to the MEM simulation
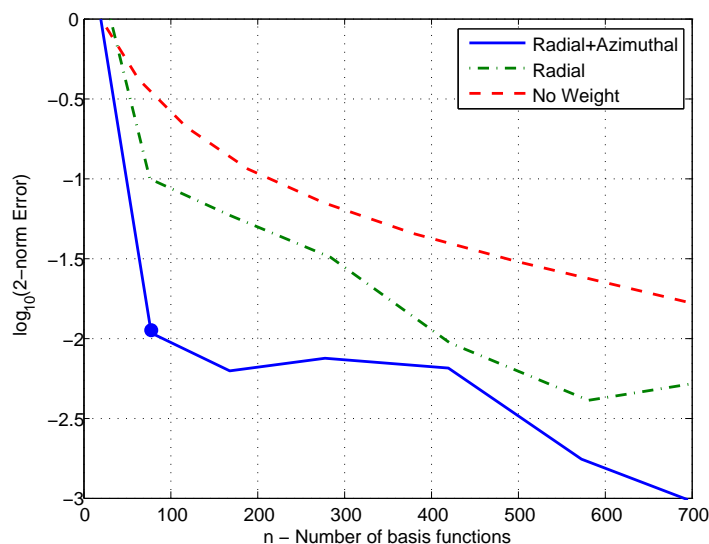
Figure 4.9: Convergence analysis of the MEM applied to the circular waveguide stub shown in Fig. 4.7 ($R_1 = R_2 = 9.525$ mm, $h = 5$ mm, $w = 6$ mm, $L_1 = L_2 = 4$ mm). The curves report the 2-norm relative error $||e^{(T)}||_2$ of the transmission coefficient versus the total number of entire domain basis functions $n = N_{\mathrm{fun}}^{(e)} + N_{\mathrm{fun}}^{(h)}$. The basis functions used in the convergence analysis are non-weighted polynomials (dashed line), polynomials weighted by radial singular functions (dash-dotted line), and polynomials weighted by singular functions with radial and azimuthal behavior (solid line). The dot refers to the MEM simulation shown in Fig. 4.8.

shown in Fig. 4.8 for which an accuracy level of 10^{-2} is achieved. It has to be noted that at this value of accuracy, which is of interest in the design of high-performance waveguide components, the use of singular weighting functions with both radial and azimuthal behavior reduces the required number of basis functions by approximately one order of magnitude as compared to the case of simple polynomials.
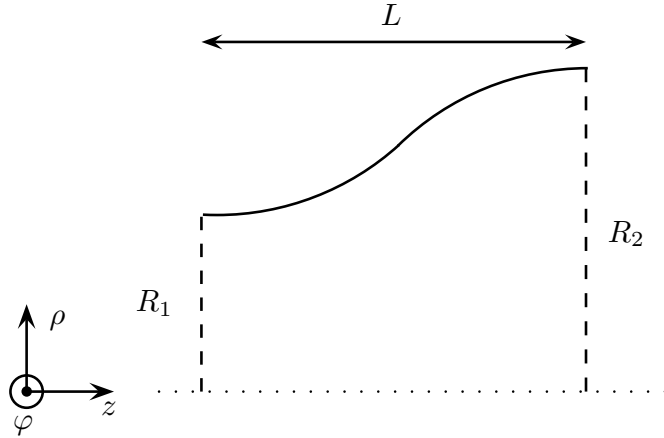
Figure 4.10: Longitudinal section of the smooth waveguide transition considered as a second benchmark case. This structure is described with a single patch. The dashed lines denote the access waveguide ports with input waveguide radii R_1 and R_2; L is the length of the structure.

4.3.2 Smooth waveguide transition

The Ka-band smooth waveguide transition shown in Fig. 4.10 is considered as a second benchmark case. This structure is relevant to assess the capability of the method to describe structures with curved sides by using a single patch. The input and output waveguides radii are $R_1 = 3.4$ mm and $R_2 = 5$ mm, and the length of the junction is $L = 4$ mm. The electromagnetic fields at the access ports are represented by using $N_{\mathrm{m}}^{(\mathrm{MEM})} = 10$ modes, whereas E_φ and H_φ are expanded with $N_{\mathrm{fun}}^{(\mathrm{e})} = 56$ and $N_{\mathrm{fun}}^{(\mathrm{h})} = 64$ global basis functions, respectively.

The reference solution is obtained by a staircase approximation of the profile that is analyzed as a cascade of circular waveguide steps, each one simulated by the MMT. To assess the MMT accuracy, two discretizations are considered, *i.e.*, $\lambda_{\min}/20$ (8 steps) and $\lambda_{\min}/100$ (40 steps) [36]. $N_{\mathrm{m}}^{(\mathrm{MMT})} = 20$ modes are used in the computation of the GSM of each step. The comparison between the reflection coefficient at port 1 for the TE$_{11}$ mode computed by the MEM and MMT is reported in Fig. 4.11. In addition to a good agreement between the MEM and MMT results, it can be noticed that the MMT provides high accuracy in the phase of the reflection coefficient only when a very small discretization distance $d_{\min} = \lambda_{\min}/100$ is used.

A convergence study of the MEM with respect to the number of basis functions used to represent E_φ and H_φ has been carried out for this structure. In this case, owing to the absence of sharp edges, polynomials can properly represent the electromagnetic field and, hence, the use of polynomials with weighting functions is not investigated. Figure 4.12 shows the 2-norm relative error $||e^{(R)}||_2$ in the reflection
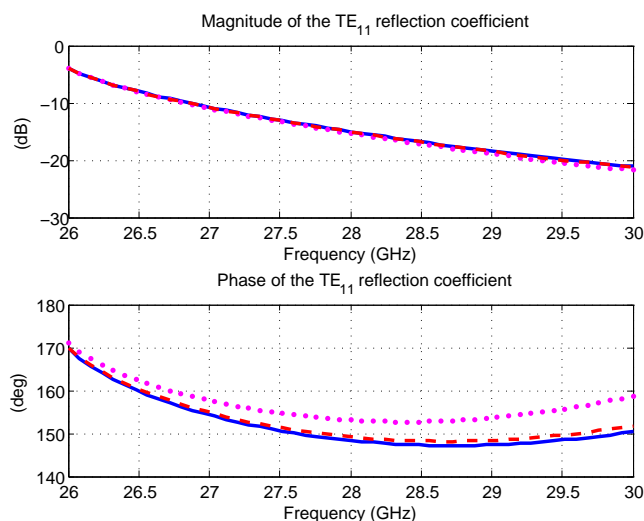
Figure 4.11: TE_{11} mode reflection coefficient of the smooth waveguide transition shown in Fig. 4.10 ($R_1 = 3.4$ mm, $R_2 = 5$ mm, $L = 4$ mm). The solid curve refers to the MEM simulations, whereas the dotted and dashed lines indicate the MMT results for the discretizations $\lambda_{\min}/20$ and $\lambda_{\min}/100$, respectively.

coefficient versus the total number of entire domain basis functions $n = N_{\mathrm{fun}}^{(\mathrm{e})} + N_{\mathrm{fun}}^{(\mathrm{h})}$. The dot refers to the MEM simulation shown in Fig. 4.11 for which an accuracy better than 1% is achieved. An exponentially-convergent behavior $\propto n^r$, typical of spectral methods, is observed with an exponential index of convergence r of about 0.8 (dashed line in Fig. 4.12).

4.3.3 Choked mode converter

The MEM has been applied also to the analysis of a choked mode converter [37]. This device is used as the input section of corrugated horn antennas [38], [39], in order to transform the TE_{11} mode into the balanced hybrid HE_{11} mode in a compact space; this field configuration is very interesting for its radiation properties, such as the extremely low cross-polarization [43]; further details concerning the evaluation of the modal conversion efficiency are resumed in Appendix D.4. Along with very low values of side-lobe level and cross-polarization, this mode converter provides significant advantages in terms of manufacturing. A 3-D cut of the device described in [39] operating in the X-band is drawn in Fig. 4.13. Figure 4.14 show the comparisons between the magnitude of the TE_{11}-TE_{11} reflection coefficient, and of the mode conversion efficiency evaluated on 4 modes; the fifth and sixth higher-order modes have an attenuation greater than 30 dB and they are considered negligible. The results have been computed with the MEM and the frequency domain solver of
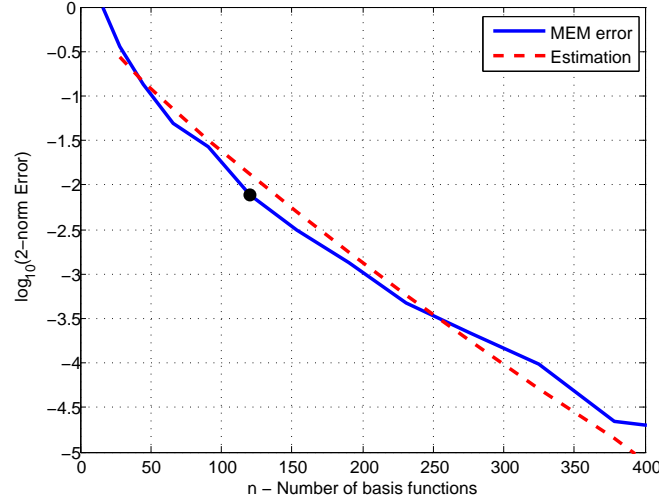
Figure 4.12: Convergence analysis of the MEM applied to the smooth waveguide transition shown in Fig. 4.10 ($R_1 = 3.4$ mm, $R_2 = 5$ mm, $L = 4$ mm). The solid curve report the 2-norm relative error $||e^{(R)}||_2$ in the reflection coefficient versus the total number of entire domain basis functions $n = N_{\text{fun}}^{(e)} + N_{\text{fun}}^{(h)}$ (non-weighted polynomials). The dot refers to the MEM simulation shown in Fig. 4.11, whereas the dashed line indicates the exponential behaviour $\propto n^{0.8}$

CST-MS [27]. In the MEM analysis, the structure has been decomposed into the four blocks shown in the longitudinal section displayed in Fig. 4.13. For each of them, the GSM has been evaluated by using $N_{\text{m}}^{(\text{MEM})} = 15$, $N_{\text{fun}}^{(e)} = 181$ and $N_{\text{fun}}^{(h)} = 216$. Finally, the GSM of the entire structure has been computed as the cascade of the four blocks. A remarkable agreement between the two methods has been achieved, thus validating the applicability of the MEM to the analysis of complex axisymmetric waveguide devices.

4.4 Conclusions

In this chapter a novel analysis technique of axisymmetric guiding structures has been presented. The main advantage of the present method is its capability of efficiently analyzing any structure, including tapered transitions without profile approximation, with any type of waveguides at the access ports, *e.g.*, circular, coaxial or conical waveguides. The results obtained with the code implementing this scheme have been compared to reference solutions for two benchmark cases and for a choked mode converter, finding a very good agreement.
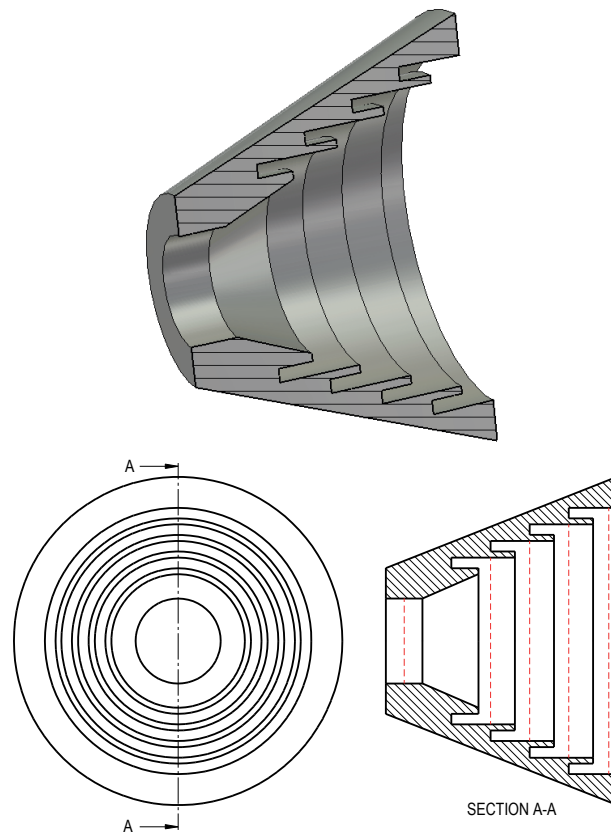
Figure 4.13: Choked mode converter described in [39]. In the longitudinal section, the dashed lines indicate the reference planes of the building blocks analyzed in the MEM simulation.
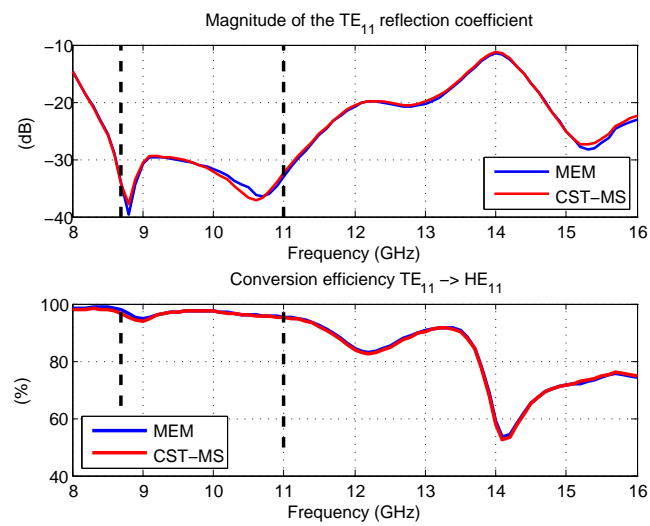
Figure 4.14: Top: magnitude of the reflection coefficient for the TE_{11} mode of the choked mode converter shown in Fig. 4.13. Bottom: modal conversion efficiency. The blue and red curves refer to results obtained with the MEM and the frequency domain solver of CST-MS, respectively.

Chapter 5

A boundary-integral equation method for lens antennas

5.1 Introduction

In the last years many efforts have been spent on the development of terahertz electromagnetic systems, in particular for astrophysics or security broad-band imaging. Moreover, since the terahertz electromagnetic spectrum is almost unoccupied compared to the microwaves one, it could be exploited for terabit communications, to obtain wireless networks with a bitrate comparable to the fiber optics one. The hardest obstacles in this direction are the poor sensitivity of the devices and the absence of high-power sources. For what concerns the first issue, sensitivity could be improved by designing ad-hoc broad-band terahertz antennas.

One of the key features of a broad-band antenna is its radiation dispersion, *i.e.*, the position of its phase center, which, usually, has a strong frequency dependence. On the other hand, if the antenna is used to couple the field from a reflector, the phase center should remain fixed in the focus in the entire operative band. Considering the canonical case of an infinitely long slot printed on a ground plane located between hemi-spaces filled with different dielectric media, it is known that it radiates in the denser dielectric with two cones, with vertex coincident to the feeding point and with aperture angle independent of frequency [44], [45]. In other words, this would be an almost non-dispersive antenna, since its phase center would be fixed in a huge frequency range. This slot could be used as feeding element of a lens antenna, which is a frequency-independent structure [46], to focus the two cones into a single beam. The leaky-lens antenna has been obtained by merging these ideas [47], [48], [49]; this is an ultra wide-band leaky antenna with fixed beam. This structure has been already used in several terahertz applications, such as the realization of kinetic
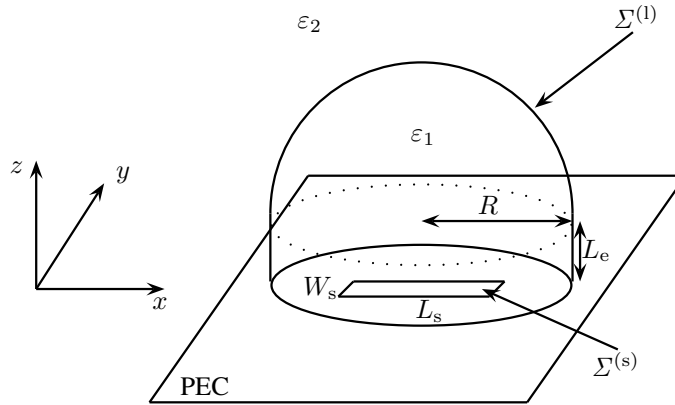
Figure 5.1: Sketch of a lens antenna fed by a slot on a ground plane.

inductance detectors [50].

Although the characterization of these antennas at high frequencies can be effectively performed by using physical optics simulators (PO), small lenses can not be analyzed with this method, due to the multiple reflections inside the dielectric that are not kept into account by the PO.

In this chapter the development of a full-wave simulator aimed at studying lens antennas is described; both the slot antenna and the dielectric lens are modeled, to keep into account mutual coupling effects. In Sections 5.2 and 5.3 the formulations of the slot and lens problems are developed; these formulations refer to the simplified case of a structure with no air-gap between the slot and the lens. In Section 5.4 the two problems are coupled and the integral equations described in these sections are solved by means of the method of moments (MoM). In Section 5.5 some implementation notes are described. In Section 5.6 some preliminary results obtained comparing, when possible, the MoM code with a commercial code are presented.

5.2 Formulation of the slot problem

5.2.1 Continuity of the magnetic field integral equation

The technique described in this chapter is applied to the structure sketched in Fig. 5.1: a lens antenna given by a dielectric hemisphere placed on a dielectric cylinder is excited by a slot on a ground plane; the relative dielectric constant of the lens is ε_1. The slot has length L_s, width W_s, the cylinder has height L_e and radius R. Assuming that the slot is radiating in two uniform half-spaces filled with dielectric ε_1 (top) and ε_0 (bottom), the equivalence theorem is applied leading to the two de-coupled problems sketched in Fig. 5.2: the slot area $\Sigma^{(\mathrm{s})}$ in the ground plane is filled with PEC, and a couple of oppositely directed magnetic current densities
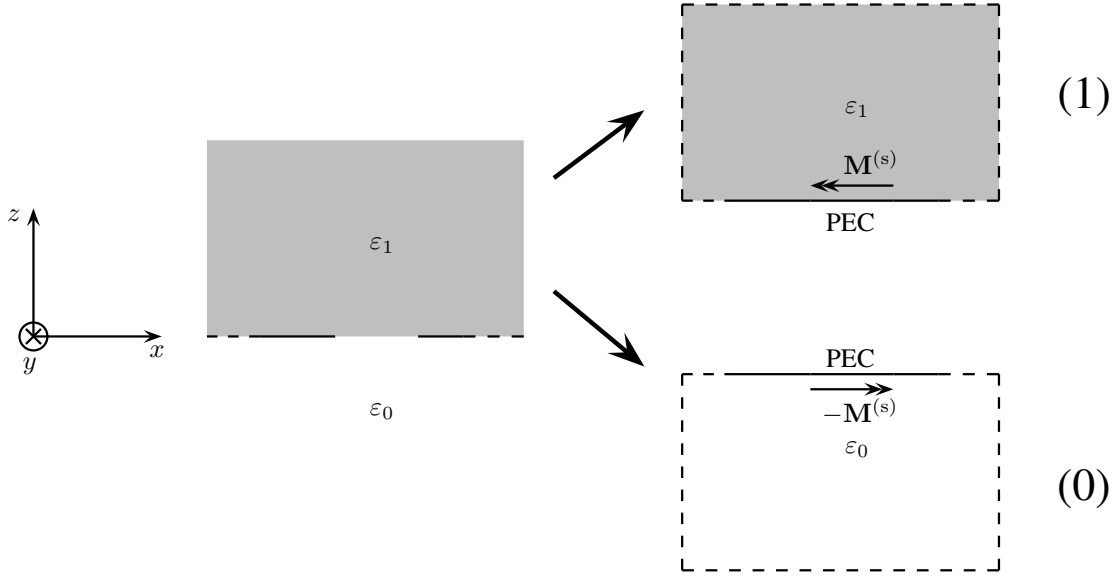
Figure 5.2: Slot radiating on two homogeneous half-spaces (left), and equivalent sub-problems.

are introduced to restore the slot field. Then, the continuity of the magnetic field integral equation (CMFIE) is formulated to complete the slot problem [51]. Let $\mathbf{H}_1$ and $\mathbf{H}_0$ be the magnetic field in the top and bottom regions; then, the CMFIE is:

$$\mathbf{H}_1 = \mathbf{H}_0.$$

Both these fields are then written as the sum of the incident and the scattered contributions:

$$\mathbf{H}_1 = \mathbf{H}_1^{(\text{inc})} + \mathbf{H}_1^{(\text{scat})} \tag{5.1}$$

$$\mathbf{H}_0 = \mathbf{H}_0^{(\text{inc})} + \mathbf{H}_0^{(\text{scat})}. \tag{5.2}$$

Therefore, by substituting and re-arranging, the following expression is obtained:

$$\mathbf{H}_1^{(\text{scat})} - \mathbf{H}_0^{(\text{scat})} = \mathbf{H}_0^{(\text{inc})} - \mathbf{H}_1^{(\text{inc})}.$$

Then, let $\mathbf{H}^{(\text{inc})}$ equal the right-hand side term; then, the CMFIE is written using the integral representation of the magnetic field in each equivalent sub-problem:

$$\iint_{\Sigma^{(s)}} \mathbf{G}^{(1)} \cdot \mathbf{M}^{(s)}\, \mathrm{d}x'\mathrm{d}y' - \iint_{\Sigma^{(s)}} \mathbf{G}^{(0)} \cdot (-\mathbf{M}^{(s)})\, \mathrm{d}x'\mathrm{d}y' = \mathbf{H}^{(\mathrm{inc})},$$

where $\mathbf{M}^{(s)} = \mathbf{M}^{(s)}(x', y')$; $\mathbf{G}^{(k)} = \mathbf{G}^{(k)}(x, x', y, y')$ is the Green's function of the k-th region. The primed variables represent the source points, whereas the unprimed ones the points of the spatial domain. The integral equation becomes:

$$\iint_{\Sigma^{(s)}} \left[\mathbf{G}^{(1)}(x, x', y, y') + \mathbf{G}^{(0)}(x, x', y, y')\right] \cdot \mathbf{M}^{(s)}(x', y')\, \mathrm{d}x'\mathrm{d}y' = \mathbf{H}^{(\mathrm{inc})}. \qquad (5.3)$$

5.2.2 Method of moments - slot problem

The unknown of the integral equation is $\mathbf{M}^{(s)}$; therefore, it is represented as a sum of known functions defined on $\Sigma_n^{(s)} \subset \Sigma^{(s)}$, weighted by unknown coefficients:

$$\mathbf{M}^{(s)}(x, y) = \sum_{c=1}^{N_{\mathrm{fun}}^{(s)}} x_c^{(s)} \mathbf{M}_c(x, y); \qquad (5.4)$$

additional details concerning the chosen basis functions are found in Appendix E.3.1. By substituting this expression in (5.3) and by applying the Galerkin version of the method of weighted residuals, $i.e.$, using as test functions the expansion functions, the following equation is written:

$$\mathbf{A}^{(\mathrm{s,s})}\, \mathbf{x}^{(s)} = \iint_{\Sigma_r^{(s)}} \mathbf{M}_r(x, y) \cdot \mathbf{H}^{(\mathrm{inc})}\, \mathrm{d}x\, \mathrm{d}y, \quad \forall r = 1...N_{\mathrm{fun}}^{(s)}, \qquad (5.5)$$

where:

$$(\mathbf{A}^{(\mathrm{s,s})})_{rc} = \iint_{\mathbb{R}^2} \widetilde{\mathbf{M}}_r^{(s)}(-k_x, -k_y) \cdot \widetilde{\mathbf{G}}(k_x, k_y) \cdot \widetilde{\mathbf{M}}_c^{(s)}(k_x, k_y)\, \mathrm{d}k_x\, \mathrm{d}k_y,$$

and:

$$\mathbf{G}(x, x', y, y') = \frac{1}{4\pi^2} \iint_{\mathbb{R}^2} \widetilde{\mathbf{G}}(k_x, k_y) \mathrm{e}^{-\mathrm{j}k_x(x-x')} \mathrm{e}^{-\mathrm{j}k_y(y-y')}\, \mathrm{d}k_x\, \mathrm{d}k_y$$

$$\widetilde{\mathbf{M}}_r^{(s)}(-k_x, -k_y) = \iint_{\Sigma_r^{(s)}} \mathbf{M}_m(x, y) \mathrm{e}^{-\mathrm{j}k_x x} \mathrm{e}^{-\mathrm{j}k_y y} \mathrm{d}x \mathrm{d}y$$

$$\widetilde{\mathbf{M}}_c^{(s)}(k_x, k_y) = \iint_{\Sigma_c^{(s)}} \mathbf{M}_n(x', y') \mathrm{e}^{\mathrm{j}k_x x} \mathrm{e}^{\mathrm{j}k_y y} \mathrm{d}x \mathrm{d}y,$$

where $\widetilde{\mathbf{G}}(k_x, k_y)$, $\widetilde{\mathbf{M}}_r^{(s)}(-k_x, -k_y)$ and $\widetilde{\mathbf{M}}_c^{(s)}(k_x, k_y)$ are the Fourier transforms of the Green's function $\mathbf{G}$ and of the basis functions used to approximate the slot magnetic current density. Additional details are reported in Appendices E.3 and E.2, where the derivation of these expressions of the MoM matrices and of the spectral domain dyadic Green's functions are reported.
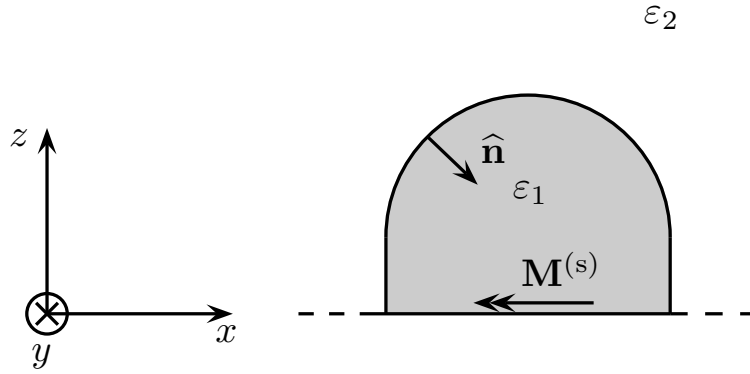
Figure 5.3: Sketch of the lens antenna, fed by the equivalent slot magnetic current density $\mathbf{M}^{(\mathrm{s})}$.

5.3   Formulation of the lens problem

The integral equations describing the lens antenna are now deduced, for the problem sketched in Fig. 5.3; here, the slot magnetic current densities $\mathbf{M}^{(\mathrm{s})}$ are the sources of the problem. Let $\Sigma^{(\mathrm{l})}$ be the separation surface between the dielectric volume ($\varepsilon_{\mathrm{r}} = \varepsilon_1$) and the vacuum ($\varepsilon_{\mathrm{r}} = \varepsilon_2$). Let $(\mathbf{E}_1, \mathbf{H}_1)$ be the electromagnetic field defined inside $\Sigma^{(\mathrm{l})}$. The external region with fields $(\mathbf{E}_2, \mathbf{H}_2)$ is unbounded and no current densities are present. This problem is divided in two homogeneous sub-problems by means of the equivalence theorem by introducing current densities on $\Sigma^{(\mathrm{l})}$. Since all sources are defined in the internal region (1), the electromagnetic field is written as the sum of the incident and the scattered contributions:

$$\begin{cases} \mathbf{E}_1 = \mathbf{E}_1^{(\mathrm{inc})} + \mathbf{E}_1^{(\mathrm{scat})} \\ \mathbf{H}_1 = \mathbf{H}_1^{(\mathrm{inc})} + \mathbf{H}_1^{(\mathrm{scat})}. \end{cases} \tag{5.6}$$

For what concerns the external region (2), there is only the scattered contribution, owing to the absence of sources:

$$\begin{cases} \mathbf{E}_2 = \mathbf{E}_2^{(\mathrm{scat})} \\ \mathbf{H}_2 = \mathbf{H}_2^{(\mathrm{scat})}. \end{cases} \tag{5.7}$$

The continuity equations of the tangent fields on $\Sigma^{(\mathrm{l})}$ are now written:

$$\begin{cases} \widehat{\mathbf{n}} \times \mathbf{E}_1 = \widehat{\mathbf{n}} \times \mathbf{E}_2 \\ \widehat{\mathbf{n}} \times \mathbf{H}_1 = \widehat{\mathbf{n}} \times \mathbf{H}_2 \end{cases} \tag{5.8}$$

Starting from these equations, the two equivalent sub-problems are now formulated.

79
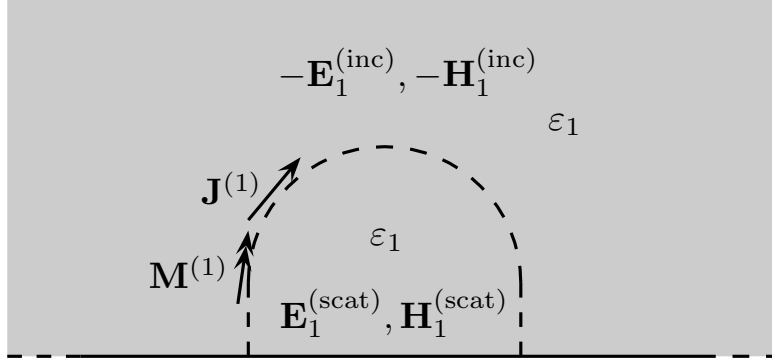
Figure 5.4: No-scatterer equivalent sub-problem.

5.3.1 Equivalent problem 1: *no-scatterer* problem

The first equivalent problem is the no-scatterer one, described in Fig. 5.4. Here, the space is filled with dielectric ε_1; then, inside $\Sigma^{(\mathrm{l})}$, $(\mathbf{E}, \mathbf{H}) = (\mathbf{E}_1^{(\mathrm{scat})}, \mathbf{H}_1^{(\mathrm{scat})})$, whereas outside of $\Sigma^{(\mathrm{l})}$, $(\mathbf{E}, \mathbf{H}) = (-\mathbf{E}_1^{(\mathrm{inc})}, -\mathbf{H}_1^{(\mathrm{inc})})$. The equivalence of this sub-problem with the original one is guaranteed by defining the electric and magnetic current densities $\mathbf{J}^{(1)}$ and $\mathbf{M}^{(1)}$ on $\Sigma^{(\mathrm{l})}$. Equations (5.6) and (5.7) are now substituted in the first equation of (5.8):

$$\widehat{\mathbf{n}} \times (\mathbf{E}_1^{(\mathrm{inc})} + \mathbf{E}_1^{(\mathrm{scat})}) = \widehat{\mathbf{n}} \times \mathbf{E}_2^{(\mathrm{scat})}.$$

By bringing the incident term of the left-hand side to the right-hand side, this equation becomes:

$$\widehat{\mathbf{n}} \times \mathbf{E}_1^{(\mathrm{scat})} = -\widehat{\mathbf{n}} \times \mathbf{E}_1^{(\mathrm{inc})} + \widehat{\mathbf{n}} \times \mathbf{E}_2^{(\mathrm{scat})},$$

so, by defining:

$$\mathbf{M}^{(1)} = \widehat{\mathbf{n}} \times \mathbf{E}_2^{(\mathrm{scat})} = -\mathbf{E}_2^{(\mathrm{scat})} \times \widehat{\mathbf{n}}, \tag{5.9}$$

the following expression is written:

$$\widehat{\mathbf{n}} \times \mathbf{E}_1^{(\mathrm{scat})} = -\widehat{\mathbf{n}} \times \mathbf{E}_1^{(\mathrm{inc})} + \mathbf{M}^{(1)}.$$

This equation represents the scenario of Figure 5.4. Similar considerations are then applied to the magnetic field, leading to:

$$\widehat{\mathbf{n}} \times (\mathbf{H}_1^{(\mathrm{inc})} + \mathbf{H}_1^{(\mathrm{scat})}) = \widehat{\mathbf{n}} \times \mathbf{H}_2^{(\mathrm{scat})}.$$

This becomes:

$$\widehat{\mathbf{n}} \times \mathbf{H}_1^{(\mathrm{scat})} = -\widehat{\mathbf{n}} \times \mathbf{H}_1^{(\mathrm{inc})} + \widehat{\mathbf{n}} \times \mathbf{H}_2^{(\mathrm{scat})}.$$
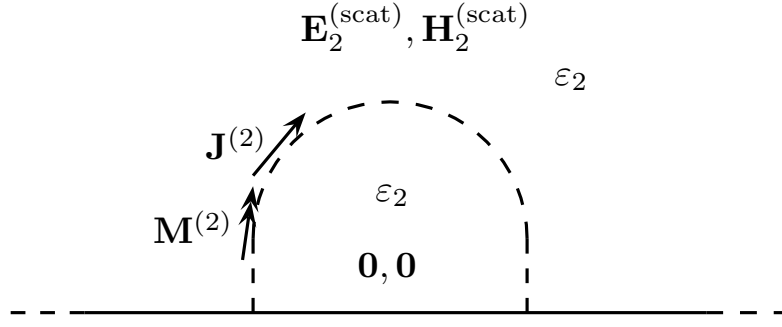
Figure 5.5: No field in the source region equivalent sub-problem.

Then, by defining:

$$\mathbf{J}^{(1)} = \widehat{\mathbf{n}} \times \mathbf{H}_2^{(\text{scat})}, \tag{5.10}$$

this becomes:

$$\widehat{\mathbf{n}} \times \mathbf{H}_1^{(\text{scat})} = -\widehat{\mathbf{n}} \times \mathbf{H}_1^{(\text{inc})} + \mathbf{J}^{(1)}. \tag{5.11}$$

In both terms we have only current densities or field components defined on the medium 1; therefore, in this problem, the entire space is filled with homogeneous medium characterized by a dielectric constant equal to ε_1.

5.3.2 Equivalent problem 2: *no field in the source region problem*

In the second equivalent problem, which is described in Figure 5.5, there is no field in the source region. The space is filled with dielectric ε_2. Inside the surface $\Sigma^{(l)}$ the electromagnetic field is null, whereas, outside of it, it equals the initial problems' one: $(\mathbf{E}_2^{(\text{scat})}, \mathbf{H}_2^{(\text{scat})})$. To guarantee the equivalence of this sub-problem with the original one, the electric and magnetic current densities $\mathbf{J}^{(2)}$ and $\mathbf{M}^{(2)}$ are defined on $\Sigma^{(l)}$. So, by working on (5.6), (5.7) and (5.8), the following equations are written:

$$\widehat{\mathbf{n}} \times (\mathbf{E}_1^{(\text{inc})} + \mathbf{E}_1^{(\text{scat})}) = \widehat{\mathbf{n}} \times \mathbf{E}_2^{(\text{scat})}$$
$$\widehat{\mathbf{n}} \times (\mathbf{H}_1^{(\text{inc})} + \mathbf{H}_1^{(\text{scat})}) = \widehat{\mathbf{n}} \times \mathbf{H}_2^{(\text{scat})}.$$

Then, it is necessary to bring to the right-hand side all the terms in the left-hand side:

$$\mathbf{0} = \widehat{\mathbf{n}} \times \mathbf{E}_2^{(\text{scat})} - \widehat{\mathbf{n}} \times (\mathbf{E}_1^{(\text{inc})} + \mathbf{E}_1^{(\text{scat})})$$
$$\mathbf{0} = \widehat{\mathbf{n}} \times \mathbf{H}_2^{(\text{scat})} - \widehat{\mathbf{n}} \times (\mathbf{H}_1^{(\text{inc})} + \mathbf{H}_1^{(\text{scat})}).$$

Then, by defining:

$$\mathbf{M}^{(2)} = (\mathbf{E}_1^{(\text{inc})} + \mathbf{E}_1^{(\text{scat})}) \times \widehat{\mathbf{n}} = -\widehat{\mathbf{n}} \times (\mathbf{E}_1^{(\text{inc})} + \mathbf{E}_1^{(\text{scat})}) \tag{5.12}$$

$$\mathbf{J}^{(2)} = -\widehat{\mathbf{n}} \times (\mathbf{H}_1^{(\text{inc})} + \mathbf{H}_1^{(\text{scat})}), \tag{5.13}$$

these equations become:

$$\mathbf{0} = \widehat{\mathbf{n}} \times \mathbf{E}_2^{(\text{scat})} + \mathbf{M}^{(2)} \tag{5.14}$$

$$\mathbf{0} = \widehat{\mathbf{n}} \times \mathbf{H}_2^{(\text{scat})} + \mathbf{J}^{(2)} \tag{5.15}$$

There are no field contributions from the internal region, since they are included in the magnetic current densities; moreover, inside $\Sigma^{(1)}$ there is no field, so it is possible to fill this volume with dielectric ε_2.

5.3.3 PMCHW formulation

In this section the previous results are merged to obtain the integral equation according to the Poggio-Miller-Chang-Harrington-Wu formulation (PMCHW) [52]. From (5.9) and (5.14), since (5.8) holds, the following equation is obtained:

$$\widehat{\mathbf{n}} \times (\mathbf{E}_1^{(\text{inc})} + \mathbf{E}_1^{(\text{scat})}) = \widehat{\mathbf{n}} \times \mathbf{E}_2^{(\text{scat})}.$$

Similar results hold for the magnetic field:

$$\mathbf{M} = \mathbf{M}^{(1)} = -\mathbf{M}^{(2)} \tag{5.16}$$

$$\mathbf{J} = \mathbf{J}^{(1)} = -\mathbf{J}^{(2)}. \tag{5.17}$$

Let $\Sigma^{(1)-}$ and $\Sigma^{(1)+}$ indicate a neighborhood of $\Sigma^{(1)}$ inside and outside the volume delimited by the surface; then, the following fields are defined:

- $\mathbf{E}_1^+, \mathbf{H}_1^+$ are the electric and magnetic field radiated by the currents $\mathbf{J}, \mathbf{M}$ relatively to the problem 1 (no-scatterer problem) on $\Sigma^{(1)+}$, therefore in a homogeneous medium characterized by ε_1;

- $\mathbf{E}_2^-, \mathbf{H}_2^-$ are the electric and magnetic field radiated by the currents $\mathbf{J}, \mathbf{M}$ relatively to the problem 2 (no field in source region problem) on $\Sigma^{(1)-}$, therefore in a homogeneous medium characterized by ε_1.

The following continuity equations are now written:

$$\begin{cases} \widehat{\mathbf{n}} \times \mathbf{E}_1^+ = -\widehat{\mathbf{n}} \times \mathbf{E}_1^{(\text{inc})} \\ \widehat{\mathbf{n}} \times \mathbf{H}_1^+ = -\widehat{\mathbf{n}} \times \mathbf{H}_1^{(\text{inc})} \\ \widehat{\mathbf{n}} \times \mathbf{E}_2^- = \mathbf{0} \\ \widehat{\mathbf{n}} \times \mathbf{H}_2^- = \mathbf{0}. \end{cases} \tag{5.18}$$

Now, let us consider two coefficients $\alpha, \beta \in \mathbb{C}$; then, these four equations are combined by taking the first and third one, multiplying them times α and β, and adding them to the second and fourth ones. This leads to the following set of equations:

$$\begin{cases} -\widehat{\mathbf{n}} \times \left(\alpha \mathbf{E}_1^+ + \mathbf{E}_2^- \right) = \widehat{\mathbf{n}} \times \left(\alpha \mathbf{E}_1^{(\text{inc})} \right) \\ -\widehat{\mathbf{n}} \times \left(\beta \mathbf{H}_1^+ + \mathbf{H}_2^- \right) = \widehat{\mathbf{n}} \times \left(\beta \mathbf{H}_1^{(\text{inc})} \right). \end{cases} \tag{5.19}$$

If $\alpha = \beta = 1$, this is the PMCHW formulation:

$$\begin{cases} -\widehat{\mathbf{n}} \times \left(\mathbf{E}_1^+ + \mathbf{E}_2^- \right) = \widehat{\mathbf{n}} \times \left(\mathbf{E}_1^{(\text{inc})} \right) \\ -\widehat{\mathbf{n}} \times \left(\mathbf{H}_1^+ + \mathbf{H}_2^- \right) = \widehat{\mathbf{n}} \times \left(\mathbf{H}_1^{(\text{inc})} \right). \end{cases} \tag{5.20}$$

It is possible to write (5.20) in a more compact and useful way; first, these equations are projected on the unit vector $\widehat{\mathbf{t}}$ tangent to $\Sigma^{(\text{l})}$; then, the superscripts are removed, leading to:

$$\begin{cases} -\left(\mathbf{E}_{\text{t}}^{(1)} + \mathbf{E}_{\text{t}}^{(2)} \right) = \mathbf{E}_1^{(\text{inc})} \\ -\left(\mathbf{H}_{\text{t}}^{(1)} + \mathbf{H}_{\text{t}}^{(2)} \right) = \mathbf{H}_1^{(\text{inc})}. \end{cases} \tag{5.21}$$

5.3.4 Method of moments - lens problem

Equations (5.21) are now modified and discretized according to the method of moments. The electric and magnetic fields in these equations are represented using the mixed-potential integral equation (MPIE) formulation described in Appendix E.1.2; here, the differential operators are shifted on the current densities, obtaining more regular integrand functions. Since the structure is backed by a ground plane, the proper Green's function is used to calculate the electromagnetic field; this is derived in Appendix E.1.6. The unknowns of the problem are the electric and magnetic current densities $\mathbf{J}$ and $\mathbf{M}$ defined on the dielectric discontinuity; both these quantities are represented using the Rao-Wilton-Glisson basis functions (RWG) [53]:

$$
\mathbf{f}_n(\mathbf{r}) =
\begin{cases}
\dfrac{l_n}{2A_n^+}\boldsymbol{\rho}_n^+, & \text{if } \mathbf{r} \in T_n^+ \\[2mm]
\dfrac{l_n}{2A_n^-}\boldsymbol{\rho}_n^-, & \text{if } \mathbf{r} \in T_n^- \\[2mm]
\underline{0} & \text{otherwise.}
\end{cases}
\tag{5.22}
$$

So:

$$
\mathbf{J}(\mathbf{r}) \simeq \sum_{c=1}^{N_{\text{fun}}} x_c^{(\mathrm{j})}\, \mathbf{f}_c(\mathbf{r})
$$

$$
\mathbf{M}(\mathbf{r}) \simeq \sum_{c=1}^{N_{\text{fun}}} x_c^{(\mathrm{m})}\, \mathbf{f}_c(\mathbf{r}).
\tag{5.23}
$$

The weak-form MPIE representation of the electric field is:

$$
\left\langle \mathbf{E}_{\mathrm{t}}^{(\mathrm{j})}, \mathbf{f}_r(\mathbf{r}) \right\rangle = \sum_{c=1}^{N_{\text{fun}}} x_c^{(\mathrm{j})}(\mathbf{D}^{(j)})_{rc} - \sum_{c=1}^{N_{\text{fun}}} x_c^{(\mathrm{m})}(\mathbf{K}^{(j)})_{rc},
$$

where,

$$
(\mathbf{D}^{(j)})_{rc} = \mathrm{j}\omega\mu_0 \int_{\mathcal{D}_r} \mathbf{f}_r(\mathbf{r}) \cdot \int_{\mathcal{D}_c'} g_j(\mathbf{r} - \mathbf{r}')\mathbf{f}_c(\mathbf{r}')\, \mathrm{d}\mathbf{r}'\, \mathrm{d}\mathbf{r}+
$$

$$
+ \frac{1}{\mathrm{j}\omega\varepsilon_0\varepsilon_j} \int_{\mathcal{D}_r} \nabla \cdot \mathbf{f}_r(\mathbf{r}) \int_{\mathcal{D}_c'} g_j(\mathbf{r} - \mathbf{r}')\nabla \cdot \mathbf{f}_c(\mathbf{r}')\, \mathrm{d}\mathbf{r}'\mathrm{d}\mathbf{r}
\tag{5.24}
$$

$$
(\mathbf{K}^{(j)})_{rc} = \int_{\mathcal{D}_r} \mathbf{f}_r(\mathbf{r}) \cdot \int_{\mathcal{D}_c'} [\nabla g_j(\mathbf{r} - \mathbf{r}')] \times \mathbf{f}_c(\mathbf{r}')\, \mathrm{d}\mathbf{r}'\, \mathrm{d}\mathbf{r}.
\tag{5.25}
$$

Similar results hold for the magnetic field:

$$
\left\langle \mathbf{H}_{\mathrm{t}}^{(j)}, \mathbf{f}_r(\mathbf{r}) \right\rangle = \frac{1}{Z_j^2} \sum_{c=1}^{N_{\text{fun}}} x_c^{(\mathrm{m})}(\mathbf{D}^{(j)})_{rc} + \sum_{c=1}^{N_{\text{fun}}} x_c^{(\mathrm{j})}(\mathbf{K}^{(j)})_{mn},
$$

where:

$$
Z_j = \sqrt{\frac{\mu_0}{\varepsilon_0\varepsilon_j}}.
$$

All the calculations aimed at obtaining these results are reported in Appendix E.4. Finally the matrix versions of the PMCHW equations are:

$$
\begin{cases}
-(\mathbf{D}^{(1)} + \mathbf{D}^{(2)})\mathbf{x}^{(\mathrm{j})} + (\mathbf{K}^{(1)} + \mathbf{K}^{(2)})\mathbf{x}^{(\mathrm{m})} = \left\langle \mathbf{E}_1^{(\mathrm{inc})}, \mathbf{f}_r(\mathbf{r}) \right\rangle, & \forall r = 1...N_{\text{fun}} \\[3mm]
-\dfrac{1}{Z_j^2}(\mathbf{K}^{(1)} + \mathbf{K}^{(2)})\mathbf{x}^{(\mathrm{j})} - (\mathbf{D}^{(1)} + \mathbf{D}^{(2)})\mathbf{x}^{(\mathrm{m})} = \left\langle \mathbf{H}_1^{(\mathrm{inc})}, \mathbf{f}_r(\mathbf{r}) \right\rangle, & \forall r = 1...N_{\text{fun}},
\end{cases}
$$

which is compactly written as:

$$\begin{bmatrix} \mathbf{A}^{(e,j)} & \mathbf{A}^{(e,m)} \\ \mathbf{A}^{(h,j)} & \mathbf{A}^{(h,m)} \end{bmatrix} \begin{bmatrix} \mathbf{x}^{(j)} \\ \mathbf{x}^{(m)} \end{bmatrix} = \begin{bmatrix} \mathbf{b}^{(e)} \\ \mathbf{b}^{(h)} \end{bmatrix}, \tag{5.26}$$

where:

$$\mathbf{A}^{(e,j)} = -(\mathbf{D}^{(1)} + \mathbf{D}^{(2)})$$
$$\mathbf{A}^{(e,m)} = \mathbf{K}^{(1)} + \mathbf{K}^{(2)}$$
$$\mathbf{A}^{(h,j)} = -(\mathbf{K}^{(1)} + \mathbf{K}^{(2)})$$
$$\mathbf{A}^{(h,m)} = -\frac{1}{Z_j^2}(\mathbf{D}^{(1)} + \mathbf{D}^{(2)}).$$

5.4   Coupling of lens and slot problems

Equations (5.5) and (5.27) are now coupled using their right-hand side terms as coupling terms. Indeed, the incident field on the lens is generated by the slot; on the other hand, the field scattered by the dielectric interface causes a variation of $\mathbf{M}^{(s)}$ with respect to the current present when the slot is radiating in the homogeneous space. For this reason, the following expression is written relatively to the slot:

$$\mathbf{H}^{(inc)} = \underbrace{\mathbf{H}^{(inc,s)}}_{\text{source}} + \underbrace{\mathbf{H}^{(j)} + \mathbf{H}^{(m)}}_{\text{lens}} =$$
$$= \hat{\mathbf{x}}\delta(x)\delta(y)\delta(z) + \mathbf{G}^{(h,j)} \overset{*}{:} \mathbf{J} + \mathbf{G}^{(h,m)} \overset{*}{:} \mathbf{M}.$$

The incident magnetic field on the slot has three contributions: the source one, which is the known term of the problem (the spatial Dirac delta) plus the contributions coming from the electric and magnetic current densities defined on the slot. For what concerns the lens, the only source term is $\mathbf{M}^{(s)}$, therefore:

$$\mathbf{E}_1^{(inc)} = \mathbf{E}^{(s)} = \mathbf{G}^{(e,s)} \overset{*}{:} \mathbf{M}^{(s)}$$
$$\mathbf{H}_1^{(inc)} = \mathbf{H}^{(s)} = \mathbf{G}^{(h,s)} \overset{*}{:} \mathbf{M}^{(s)}.$$

Since the slot and the lens are spatially separated, the MoM integrals do not contain any singularity, the Green's function field representation is used in place of the MPIE; in these cases, the dyadic Green's function is derived in Appendices E.1.5 and E.1.6. Then, by recalling (5.4) and (5.22):

$$\mathbf{H}^{(\mathrm{inc})} = \widehat{\mathbf{x}}\delta(x)\delta(y)\delta(z) + \sum_{c=1}^{N_{\mathrm{fun}}} x_c^{(\mathrm{j})} \iint_{\mathcal{D}_c'} \mathbf{G}^{(\mathrm{h,j})}(\mathbf{r},\mathbf{r}') \cdot \mathbf{f}_c(\mathbf{r}') \, \mathrm{d}\mathbf{r}' +$$

$$+ \sum_{c=1}^{N_{\mathrm{fun}}} x_c^{(\mathrm{m})} \iint_{\mathcal{D}_c'} \mathbf{G}^{(\mathrm{h,m})}(\mathbf{r},\mathbf{r}') \cdot \mathbf{f}_c(\mathbf{r}') \, \mathrm{d}\mathbf{r}'$$

$$\mathbf{E}_1^{(\mathrm{inc})} = \sum_{c=1}^{N_{\mathrm{fun}}^{(\mathrm{s})}} x_c^{(\mathrm{s})} \iint_{\mathcal{D}_c'} \mathbf{G}^{(\mathrm{e,s})}(\mathbf{r},\mathbf{r}') \cdot \mathbf{M}_c^{(\mathrm{s})}(\mathbf{r}') \, \mathrm{d}\mathbf{r}'$$

$$\mathbf{H}_1^{(\mathrm{inc})} = \sum_{c=1}^{N_{\mathrm{fun}}^{(\mathrm{s})}} x_c^{(\mathrm{s})} \iint_{\mathcal{D}_c'} \mathbf{G}^{(\mathrm{h,s})}(\mathbf{r},\mathbf{r}') \cdot \mathbf{M}_c^{(\mathrm{s})}(\mathbf{r}') \, \mathrm{d}\mathbf{r}'.$$

Therefore, the matrix equation of the coupled problems, after substituting these terms in (5.4) and (5.22), is:

$$\begin{bmatrix} \mathbf{A}^{(\mathrm{e,j})} & \mathbf{A}^{(\mathrm{e,m})} & \mathbf{A}^{(\mathrm{e,s})} \\ \\ \mathbf{A}^{(\mathrm{h,j})} & \mathbf{A}^{(\mathrm{h,m})} & \mathbf{A}^{(\mathrm{h,s})} \\ \\ \mathbf{A}^{(\mathrm{s,j})} & \mathbf{A}^{(\mathrm{s,m})} & \mathbf{A}^{(\mathrm{s,s})} \end{bmatrix} \begin{bmatrix} \mathbf{x}^{(\mathrm{j})} \\ \\ \mathbf{x}^{(\mathrm{m})} \\ \\ \mathbf{x}^{(\mathrm{s})} \end{bmatrix} = \mathbf{b}, \tag{5.27}$$

where $\mathbf{b}$ comes from the projection of the source $\widehat{\mathbf{x}}\delta(x)\delta(y)\delta(z)$ on the test functions, and:

$$(\mathbf{A}^{(\mathrm{s,j})})_{rc} = -(\mathbf{A}^{(\mathrm{e,s})})_{rc} = \iint_{\mathcal{D}_r} \mathbf{f}_r(\mathbf{r}) \cdot \iint_{\mathcal{D}_c'} \mathbf{G}^{(\mathrm{e,s})}(\mathbf{r},\mathbf{r}') \cdot \mathbf{M}_c^{(\mathrm{s})}(\mathbf{r}') \, \mathrm{d}\mathbf{r}'$$

$$(\mathbf{A}^{(\mathrm{s,m})})_{rc} = (\mathbf{A}^{(\mathrm{h,s})})_{rc} = \iint_{\mathcal{D}_r} \mathbf{f}_r(\mathbf{r}) \cdot \iint_{\mathcal{D}_c'} \mathbf{G}^{(\mathrm{h,s})}(\mathbf{r},\mathbf{r}') \cdot \mathbf{M}_c^{(\mathrm{s})}(\mathbf{r}') \, \mathrm{d}\mathbf{r}'.$$

5.5 Implementation notes

5.5.1 Calculation of singular integrals

The integrand functions of (5.24) and (5.25) are singular if the cell where the field is generated (source cell) has common points with the one where the field is observed (observation cell). This occurs for $r = c$, which is the self-term case, but also if the source cell has a common edge with the observation cell, which is the near-term case. This problem is very known in literature and it has been tackled in several ways.

The classical approach for the calculation of these integrals is the singularity subtraction scheme: the Taylor expansion of the scalar Green's function is subtracted from the Green's function itself, to obtain continuous integrand functions;

this integral can be calculated numerically by means of an ad-hoc Gauss-Legendre quadrature rule [56], [12]. The integral involving the Taylor expansion can be calculated analytically [54], [55].

In the method described in this chapter the zero-order Taylor expansion is subtracted and re-added to the scalar Green's function; the self terms of (5.25) are zero, as proved in Appendix E.4; the self terms of (5.24) are calculated with the closed-form formulas introduced in [57]. The near terms are calculated with the algorithm described in [58], which summarizes the singularity-subtraction schemes proposed in literature.

5.5.2   Introduction of symmetries in the MoM matrix

Although the shape of the lens suggests to use a BOR formulation, this problem is 3-dimensional owing to the presence of the feeding slot, therefore the field in the lens cannot be expanded using cylindrical harmonics as suggested in [52]. However, the complexity of the problem has been reduced by developing an ad-hoc meshing tool, which is used to discretize the lens as a set of slices, as depicted in Fig. 5.6. This tool provides a proper numeration of the RWG basis functions, transforming the symmetry of the lens into a symmetry of the MoM matrix. The result is a block-Toeplitz MoM matrix, where only the integrals belonging to few blocks should be calculated. Then, the matrix is assembled *a posteriori*; moreover, this division in blocks suggests to apply a parallel approach to the calculation of the integrals. Figure 5.7 shows a plot of the phase of the MoM matrix elements; several patterns can be observed.

5.6   Results

The method described in the previous sections has has been validated through a comparison with the time-domain solver of CST Microwave Studio (CST-MS). In Fig. 5.8 the E-plane and H-plane radiation patterns of a lens antenna with $\varepsilon_1 = 11.9$, $L_s = 50$ mm, $W_s = 1$ mm, $L_e = 30$ mm, $R = 95$ mm are reported for $f = 3.5$ GHz. In Fig. 5.9 the E-plane and H-plane radiation patterns of a lens antenna with $\varepsilon_1 = 11.9$, $L_s = 100$ mm, $W_s = 1$ mm, $L_e = 30$ mm, $R = 95$ mm are reported for $f = 2.25$ GHz. Since in both the figures a good agreement can be observed, the formulation of the method and the implemented code is validated.

Hemisphere + Extension length mesh
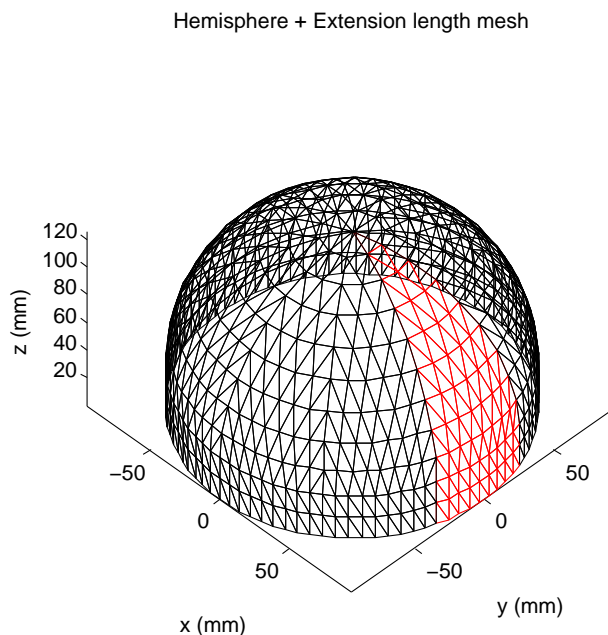
Figure 5.6: Example of mesh of a lens antenna with $R = 90$ mm, $L_e = 30$ mm, $f = 1.5$ GHz; the mesh consists of 10 slices.

5.7 Conclusions

In this chapter the development of a boundary-integral equation method aimed at analyzing dielectric lens antennas has been described. The method can be used to evaluate the mutual effects between lens and slot. The slot problem is described by using the CMFIE, which is solved by means of a method of moments defined in the spectral domain. The lens problem by using the PMCHW formulation, where the fields are described by using a MPIE formulation. The method has been validated by comparing the radiation patterns obtained with the present method and with a commercial simulator.
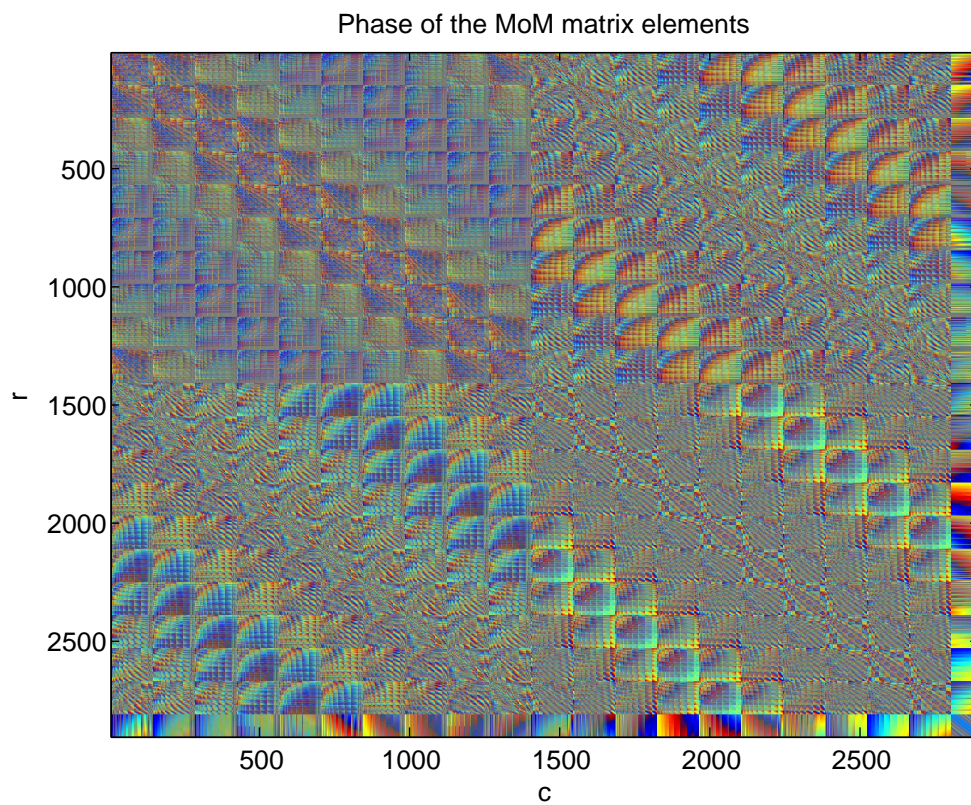
Figure 5.7: Phase of the MoM matrix elements for a lens antenna with $R = 90$ mm, $L_{\mathrm{e}} = 30$ mm, $f = 1.5$ GHz; the presence of symmetries in the matrix can be observed; r and c are the matrix element indexes.
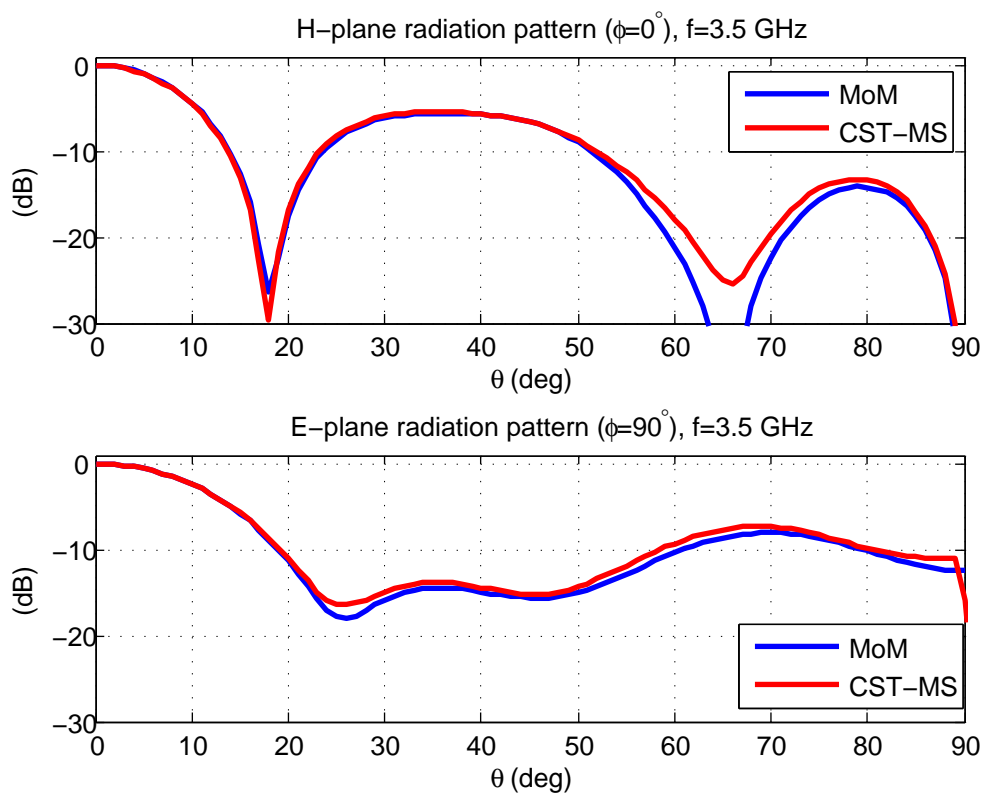
Figure 5.8: Radiation pattern for the lens antenna with $\varepsilon_1 = 11.9$, $L_s = 50$ mm, $W_s = 1$ mm, $L_e = 30$ mm, $R = 95$, at $f = 3.5$ GHz.
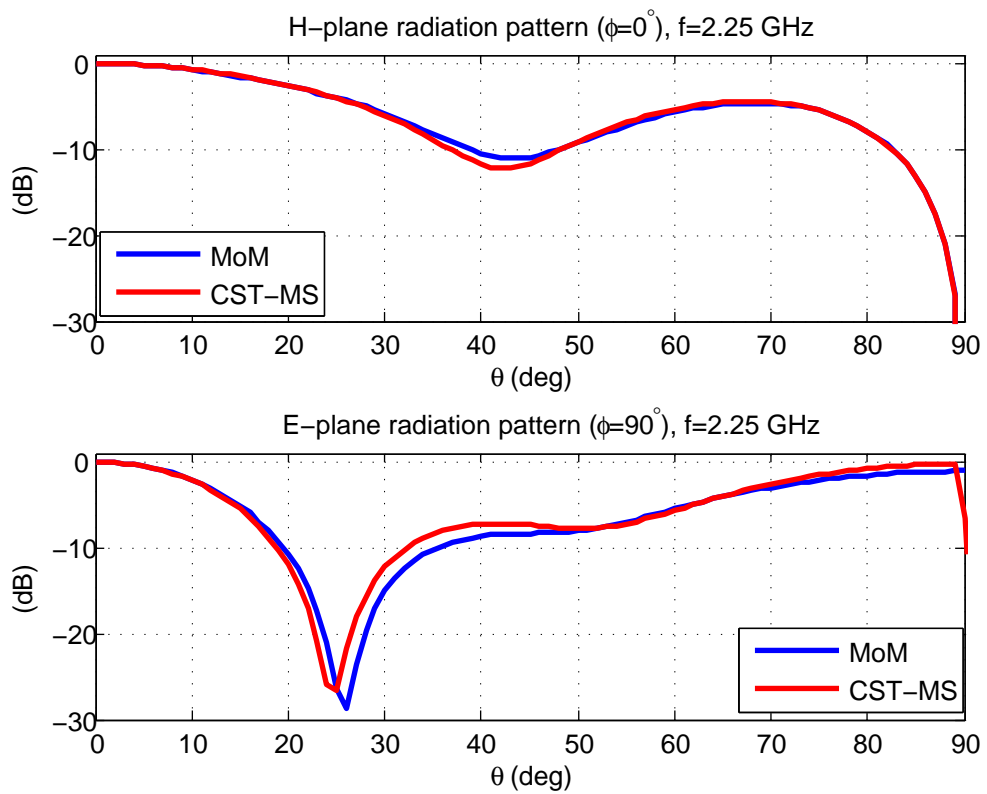
Figure 5.9: Radiation pattern for the lens antenna with $\varepsilon_1 = 11.9$, $L_s = 50$ mm, $W_s = 1$ mm, $L_e = 30$ mm, $R = 95$, at $f = 3.5$ GHz.

Design of a dual-polarization Vivaldi antenna

6.1 Introduction

Modern low frequency radio telescopes are based on the use of large aperture arrays, where imaging is performed by using state-of-the art digital back-ends and signal processing software. The Low-Frequency Array (LOFAR), the Long Wavelength Array (LWA), the Murchison Widefield Array (MWA) and the Square Kilometer Array (SKA) are among the most famous examples of a new generation of either existing or planned radio telescopes based on this concept [59], [60], [61], [62], [63].

In Italy, the Sardinia Array Demonstrator (SAD) is currently under development. This project is founded by the Sardinia Regional Government and by the Italian National Institute for Astrophysics (IRA-INAF), and it is motivated by the intention to offer a technological and scientific test-bed to gain experiences and prove crucial concepts, algorithms and techniques for digital beam forming, data acquisition/transmission, calibration, imaging, and RFI mitigation. The project started in march 2013 and it is expected to be concluded in march 2016. SAD will consist of the installation of an aperture array constituted by dual-polarized low-frequency antennas [64]. The SAD antennas will be deployed within the perimeter of the Sardinia Radio Telescope (SRT) site, which is located in the proximity of the town of San Basilio, 35 km north of the city of Cagliari. The aperture array will be composed of 128 antennas distributed in a 64 m diameter core and in four 15 m diameter satellite stations, as depicted in Fig. 6.1. Furthermore, given the closeness of the SRT, it will be possible to attempt join experiments correlating aperture array and single-dish data.

In this chapter the design of the SAD array element is described. This comes from
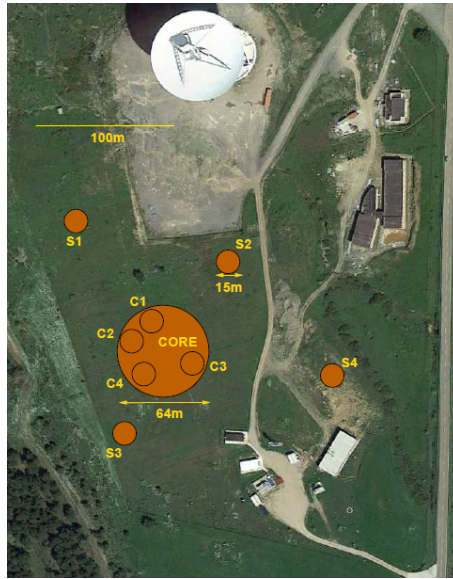
Figure 6.1: Aerial view of the SRT site showing the locations for the 64 m core and the four 15 m satellite stations of SAD.

the optimization of the italian Vivaldi antenna prototype v2.0 built by IRA-INAF in cooperation with the IEIIT-CNR of Torino, which has been developed in the framework of the Aperture Array Verification Program in the pathway to the SKA [65], [66]. Although the features of the Vivaldi v2.0 were already close to the goals required by the SAD project, by studying the RFI environment at the SRT site it has been discovered that the portion of the radio spectrum best suited for low-frequency observations is from 250 to 450 MHz, therefore the Vivaldi v3.1, which is a new prototype optimized for this frequency range, has been developed [67] [68].

In Section 6.2 the cavity-backed Vivaldi antenna concept is introduced starting from the Vivaldi v2.0. In Section 6.3 the evaluation of the sensitivity is described, and a comparison of the Vivaldi v2.0 and v3.1 antennas is presented. In Section 6.4 the characterization of the prototype of the Vivaldi v3.1 is presented, discussing the measured reflection coefficients and radiation patterns.

6.2 Cavity-backed Vivaldi antenna

The Vivaldi v2.0, which is a dual linear polarization Vivaldi antenna backed by a circular stub, was designed to operate in the $[70, 450]$ MHz frequency range; the prototype of this antenna is shown in Fig. 6.2. The main characteristics of this antenna are: unbalanced 50 Ω coaxial cable excitation, -10 dB matching, low cross polarization on the principal axes, absence of bulky dielectric parts or ground planes, small size, easiness of installation, robustness and affordability in the manufactur-
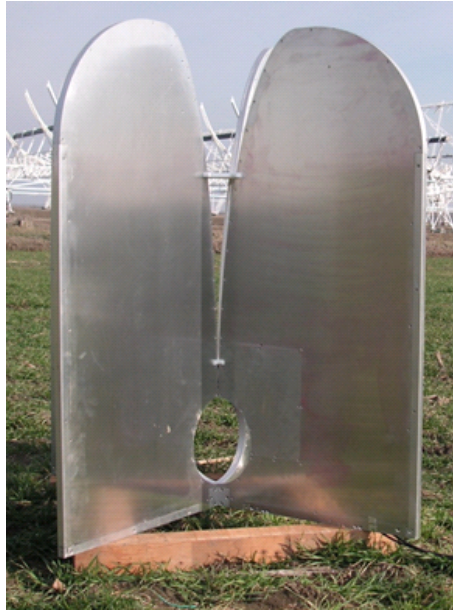
Figure 6.2: Prototype of the Vivaldi v2.0 antenna realized by IRA-INAF.

ing process. Although this antenna exhibits several interesting features, a significant amount of power is radiated in the back direction, causing a reduction of the sensitivity.

The Vivaldi v2.0 can be seen as an open-boundary quad-ridge horn, where the four ridges are the wings of the Vivaldi. For this reason, the back lobes issue has been tackled by introducing a field confinement in its rear part, transforming the open-boundary horn into a TEM horn, as sketched in Fig. 6.3. This requires the design of a ridge waveguide operating in the required frequency range and of a back cavity aimed at minimizing the reflection coefficient seen from the coaxial cable that provides the excitation. Then, the Vivaldi section is joined to the waveguide end. The final structure consists of a ridge waveguide, a backing cavity, of the radiating section and of the waveguide to free-space transition.

Although this strategy is very effective, the resulting structure is quite expensive, due to its manufacturing complexity. To reduce these complications, the cavity-backed Vivaldi antenna sketched in the right part of Fig. 6.4 has been conceived, removing the ridge waveguide part: this is a dual-polarization Vivaldi section, where the four wings are placed on a metal cavity. A comparison of the front-to-back ratios (FBRs) of the three antennas with different backing structures sketched in Fig. 6.4 is reported in Fig. 6.5; here, the dashed line is related to the stub-backed Vivaldi (Fig. 6.4, left), the dash-dotted line to the Vivaldi backed by a ground plane (Fig. 6.4, center) and the solid line to the cavity-backed Vivaldi (Fig. 6.4, right). It is observed that the FBR can not be improved simply by introducing a ground plane,
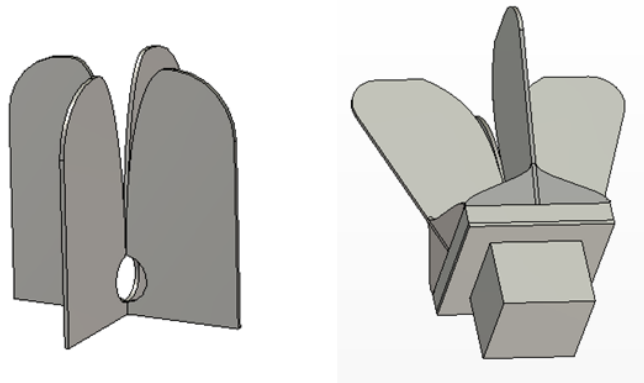
Figure 6.3: Left: sketch of the Vivaldi v2.0 (open boundary horn). Right: sketch of a TEM horn.
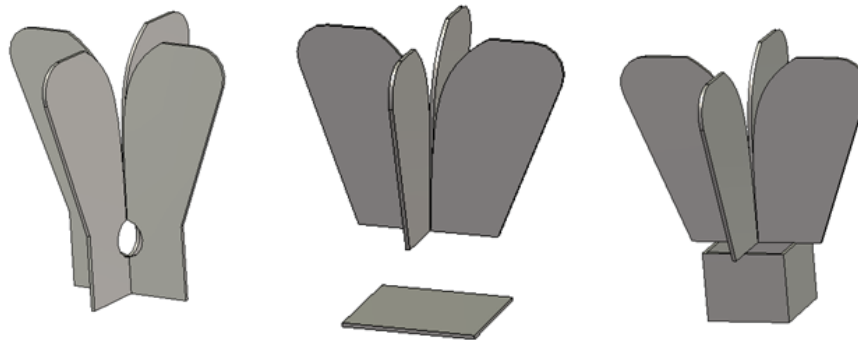
Figure 6.4: Three Vivaldi sections with different backing structures. Left: stub-backed Vivaldi antenna; center: ground-plane backed Vivaldi antenna; right: cavity-backed Vivaldi antenna.

since the ripple is increased without any significant improvement. Instead, the FBR curve of the cavity-backed Vivaldi is almost monotone, with improved values at higher frequencies. It is known that a Vivaldi antenna behaves as a dipole for low frequencies, whereas it works as a tapered slot, where the surface currents are mainly concentrated in the aperture part, for higher frequencies; to clarify this point in Fig. 6.6 the surface currents on the cavity-backed Vivaldi antenna are shown at 70 MHz, where the dipole mode is dominant, and at 450 MHz, where the tapered slot is dominant. The presence of the cavity excites the tapered slot operation mode more than the dipole one, also at lower frequencies. This is interesting because the tapered slot is more directive, leading to higher FBR; furthermore, since the ripple arises from the competition between the two operation modes, if the tapered slot is dominant, the ripple is reduced.
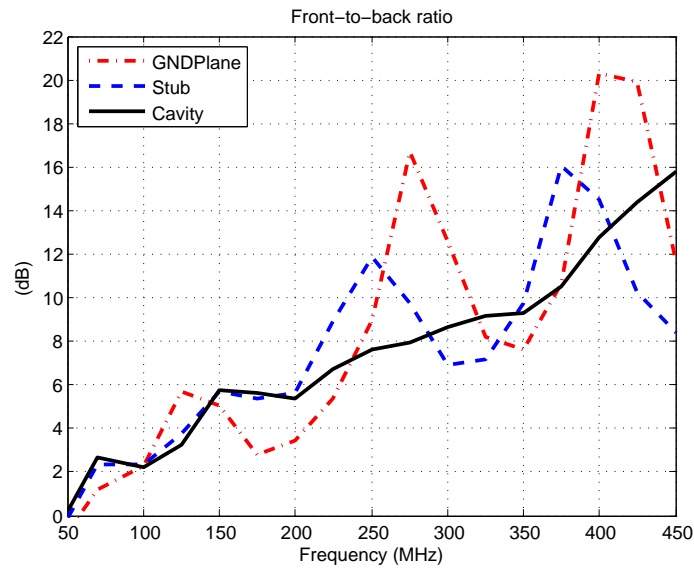
Figure 6.5: Front-to-back ratio of Vivaldi antennas with three backing structures.
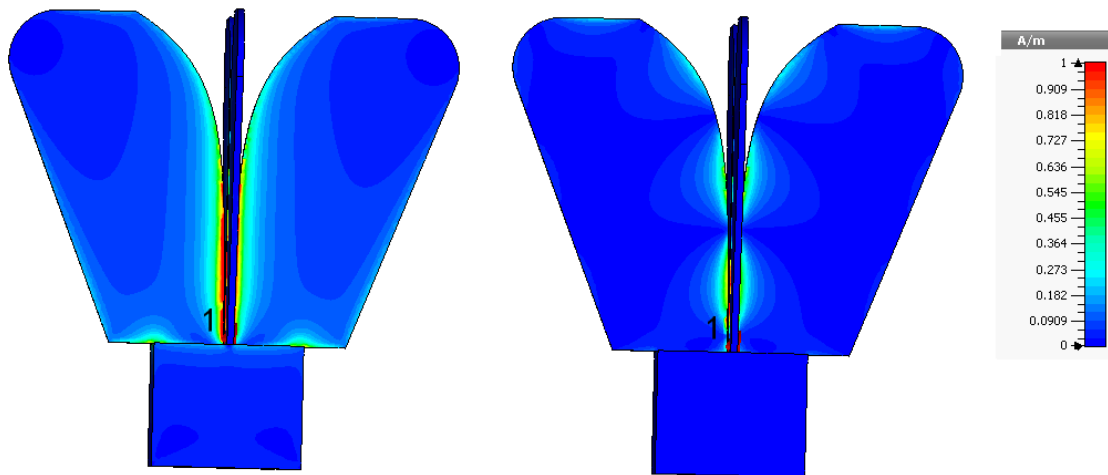
Figure 6.6: Simulation of the surface currents on the cavity-backed Vivaldi antenna at 70 MHz (left) and at 450 MHz (right). At higher frequencies, the tapered-slot operation mode is apparently excited, whereas at low frequencies currents are spread on the entire structure.

6.3 Performance characterization

The characterization of the antenna performance is based on the sensitivity parameter S, which is defined as the ratio of the element effective area A_{eff} to its noise temperature T_{sys}:

$$S(\widehat{\mathbf{r}}, f) \triangleq \frac{A_{\mathrm{eff}}(\widehat{\mathbf{r}}, f)}{T_{\mathrm{sys}}(f)} \quad \left(\frac{\mathrm{m}^2}{\mathrm{K}}\right),$$

where $\widehat{\mathbf{r}}$ indicates the observation direction and f is the frequency. The effective area A_{eff} is calculated from the radiation patterns, which are obtained using a full-wave simulator. The system noise temperature can be calculated as the sum of three contributions:

$$T_{\mathrm{sys}}(f) = T_{\mathrm{ant,sky}}(f) + T_{\mathrm{ant,gnd}}(f) + T_{\mathrm{rec}}(f),$$

where $T_{\mathrm{ant,sky}}(f)$ and $T_{\mathrm{ant,gnd}}(f)$ quantify the noise contributions coming from the sky and from the ground; the latter contribution is strictly related to the FBR of the antenna, and it keeps into account the contributions directly coming from ground and the ones coming from the sky and reflected on the ground. These two quantities are evaluated by means of the Cortes model, which is a far-field noise model [69]; A_{eff} is one of the inputs of the model. The measured receiver noise temperature $T_{\mathrm{rec}}(f)$ is approximately equal to 30 K in the entire band.
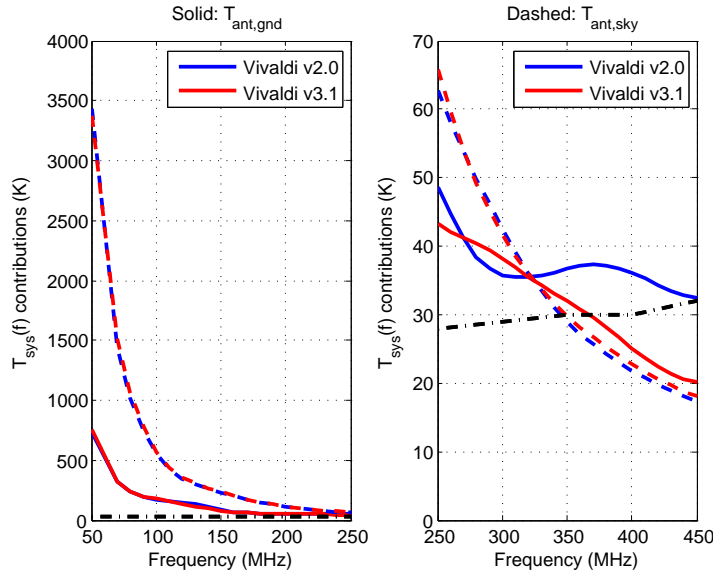
Figure 6.7: Noise temperature contributions of the Vivaldi v2.0 and v3.1, for the bands B_1 and B_2; the solid and dashed curves are the ground-noise and sky-noise contributions respectively, whereas the black dash-dotted curve is the measured receiver noise contribution.

In Fig. 6.7 the three noise contributions are reported, for the Vivaldi v2.0 and v3.1, in two sub-bands: $B_1 = [50, 250]$ MHz and $B_2 = [250, 450]$ MHz, where B_2 is the operative band of the design. The blue curves are associated to the Vivaldi v2.0, whereas the red ones to the Vivaldi v3.1; the solid and dashed curves are the

ground-noise and sky-noise contributions, whereas the black dash-dotted curve is the measured receiver noise contribution. It can be seen that the lower band is sky-noise dominated, therefore it is understood that an optimization procedure on this band would be almost ineffective, since the curves associated to the two antennas are very similar. On the contrary B_2 contains a transition between the sky-noise and the receiver-noise domination; in this band the three contributions are of the same order of magnitude, and a geometry optimization can be performed; the Vivaldi v3.1 is the result of this procedure. It is observed from Fig. 6.7 that the ground-noise contribution of this antenna, which is strictly related to the FBR, is reduced of almost 10 K at high frequencies. The sensitivity plots of the Vivaldi v2.0 and v3.1 antennas are compared in Fig. 6.8 for $\vartheta = 0°$ and $\vartheta = 45°$, where the performance improvement of the new antenna is apparent, in particular for low angles.
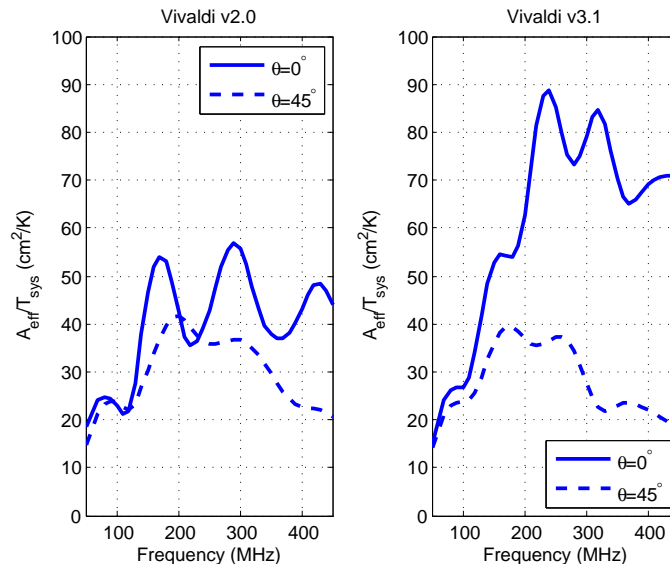
Figure 6.8: Sensitivity versus frequency for the Vivaldi v2.0 (left) and v3.1 (right).

6.4 Prototype of the Vivaldi v3.1

In Fig. 6.9 the prototype of the Vivaldi v3.1 is shown; the main dimensions of the antenna are 1.2×1.2 m^2 footprint and 1.5 m height. Although this prototype is useful to perform an electromagnetic characterization, it is not completely optimized under the mechanical point of view; the Vivaldi v3.1 version for the mass production is currently under development.

In Fig. 6.10 the simulated reflection coefficient (black curve) is compared to the measured reflection coefficients at the two antenna ports; a good agreement has been

Figure 6.9: Prototype of the Vivaldi v3.1 on the IEIIT-CNR roof, for the reflection coefficient measurement.

achieved in the whole band.

The measurement of the radiation pattern of the antenna is not straightforward, owing to the low operating frequency range (leading to large far-field distance) and to the dimensions and weight of the antenna. Therefore, it has been performed by using a novel technique based on an unmanned aerial vehicle (UAV). This consists of a GNSS-controlled hexacopter capable of flying autonomously for 15 minutes. This has been equipped with a continuous-wave RF signal generator based on a phase-locked loop synthesizer, with a dipole antenna. The signal received by the antenna under test is measured by a spectrum analyzer, and the radiation pattern is obtained by post-processing the GNSS signals and the acquired RF data. This system allows the analysis of either the single antenna or of the entire array, simulating the actual scenario (*i.e.*, the aperture array directed towards the sky) [70], [71].

In Figs. 6.11 and 6.12 the H-plane co-polar and cross-polar measured and simulated patterns are compared for $f = 50$ MHz and $f = 450$ MHz; in Fig. 6.13 the E-plane co-polar and cross-polar patterns are reported for $f = 300$ MHz. There is a reasonable agreement between the simulated and measured co-polar patterns, but the comparison on the cross-polar is poor. These measurements have been performed with an early-stage version of the measurement system, where the GNSS measurements of the hexacopter position were not accurate enough; currently, a differential GNSS receiver has been introduced in the system, leading to much more accurate position. Moreover, a correction strategy for the orientation angles has been developed to reduce the errors on both the co-polar pattern symmetry and the cross-pol levels.
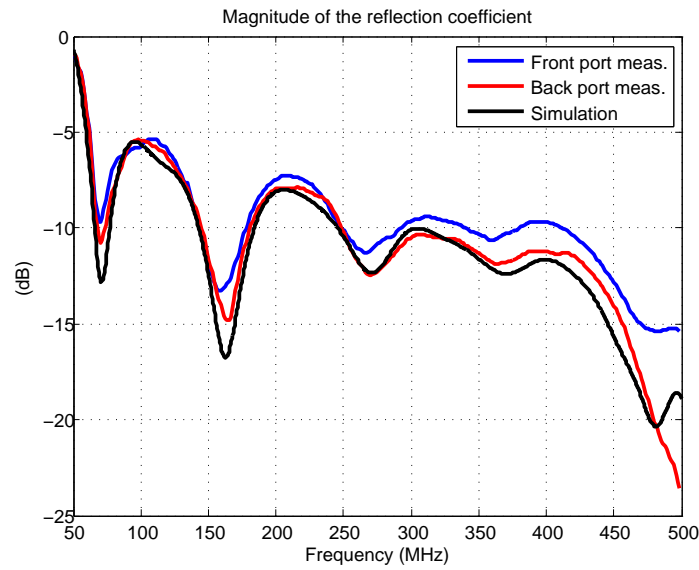
Figure 6.10: Measured and simulated reflection coefficient of the Vivaldi v3.1.
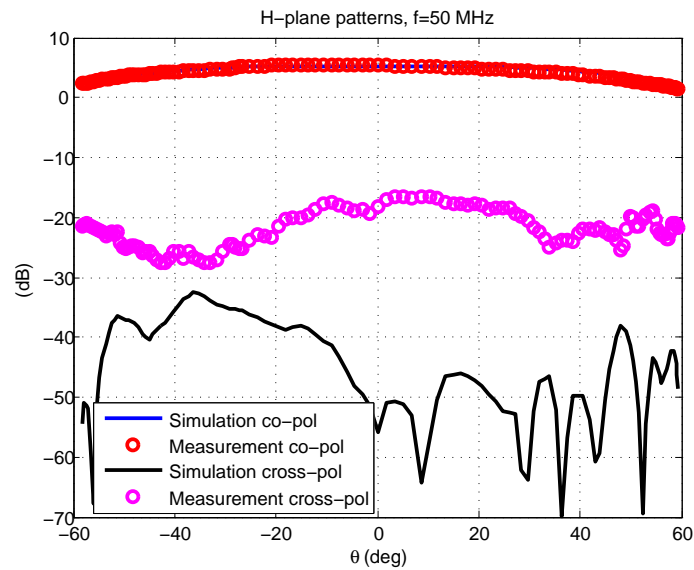
Figure 6.11: Measured and simulated H-plane co-polar and cross-polar radiation patterns of the Vivaldi v3.1, at $f = 50$ MHz.

6.5   Conclusions

In this chapter the design of the radiating element that will be used in the SAD project has been described. This is a cavity-backed Vivaldi antenna, whose concept has been produced starting from an existing design. A benchmark of the sensitivity of the old and new designs has been performed. A prototype of the antenna has been built and characterized, leading to satisfying results.
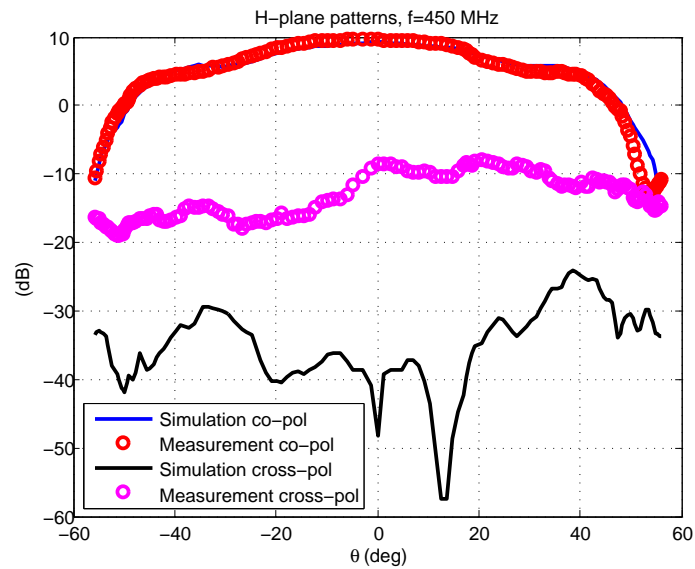
Figure 6.12: Measured and simulated H-plane co-polar and cross-polar radiation patterns of the Vivaldi v3.1, at $f = 450$ MHz.
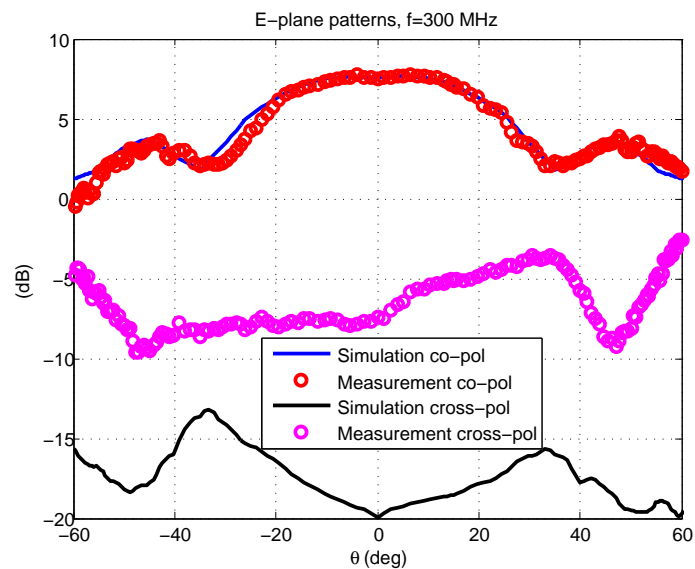
Figure 6.13: Measured and simulated E-plane co-polar and cross-polar radiation patterns of the Vivaldi v3.1, at $f = 300$ MHz.

Appendix of "Foundations of the mortar element method applied electromagnetic scattering problems"

A.1 Non-specialized basis functions

The non-specialized basis functions are defined on the parent domain $\boldsymbol{\sigma} \in [-1, 1] \times [-1, 1]$; in this work, Chebyshev polynomials have been adopted as generating functions:

$$\phi_\tau^{(j)}(\mathbf{r}) = P_{\iota\kappa}(\mathbf{r}(\boldsymbol{\sigma})) = P_{\iota\kappa}(\xi, \eta) = T_\iota(\xi)T_\kappa(\eta),$$

where:

$$T_n(t) = \cos(n \arccos t).$$

Depending on the application, the spatial domain variable $\mathbf{r}$ may span the (z, x) plane for the periodic structures case, the (z, ρ) plane for the axisymmetric structures case, or other possibilities. In the following, $\mathbf{r} = (x, y)$.

It is useful to derive the expressions of the derivatives of the basis functions in the natural domain; this is done by applying the chain rule:

$$\frac{\partial \phi_\tau^{(j)}}{\partial x} = \frac{\partial \phi_\tau^{(j)}}{\partial \xi}\frac{\partial \xi}{\partial x} + \frac{\partial \phi_\tau^{(j)}}{\partial \eta}\frac{\partial \eta}{\partial x}$$
$$\frac{\partial \phi_\tau^{(j)}}{\partial y} = \frac{\partial \phi_\tau^{(j)}}{\partial \xi}\frac{\partial \xi}{\partial y} + \frac{\partial \phi_\tau^{(j)}}{\partial \eta}\frac{\partial \eta}{\partial y},$$

where:

$$\frac{\partial \phi_\tau^{(j)}}{\partial \xi} = \frac{\mathrm{d}T_\iota(\xi)}{\mathrm{d}\xi} T_\kappa(\eta) \qquad \frac{\partial \phi_\tau^{(j)}}{\partial \eta} = T_\iota(\xi) \frac{\mathrm{d}T_\kappa(\eta)}{\mathrm{d}\eta}$$

where:

$$\frac{\mathrm{d}T_n(t)}{\mathrm{d}t} = nU_{n-1}(t), n = 1, ...$$

and:

$$U_n(t) = \frac{\sin((n+1)\arccos(t))}{\sin(\arccos(t))}.$$

The remaining terms, related to the mappings, are discussed in the following sections.

A.1.1 Bilinear mapping

The bilinear mapping is used to transform the square parent domain into a generic trapezoid; this can be applied for example to the structure reported in Fig. A.1. Given (u, v) spanning in the unit square $[0, 1] \times [0, 1]$, the bilinear mapping expression is:

$$\begin{aligned}
x(u, v) &= (au + b)(cv + D) = acuv + adu + bcv + bd = \\
&= A + Bu + Cv + Duv \\
y(u, v) &= (eu + f)(gv + h) = eguv + ehu + fgv + fh = \\
&= E + Fu + Gv + Huv.
\end{aligned} \tag{A.1}$$

Let P_1, P_2, P_3, P_4 be the four points of the trapezoid in the spatial domain; then, $P_1 = (x_1, y_1)$; $P_2 = (x_2, y_2)$; $P_3 = (x_3, y_3)$; $P_4 = (x_4, y_4)$. Then:

- the point $(0, 0)$ in the parent domain is mapped to P_1;

- the point $(0, 1)$ in the parent domain is mapped to P_2;

- the point $(1, 0)$ in the parent domain is mapped to P_3;

- the point $(1, 1)$ in the parent domain is mapped to P_4.

By using these four conditions in the first equation of (A.1) the following systems of equations is derived:

$$\begin{cases}
x_1 = A \\
x_2 = A + B \\
x_3 = A + B + C + D \\
x_4 = A + C
\end{cases}$$
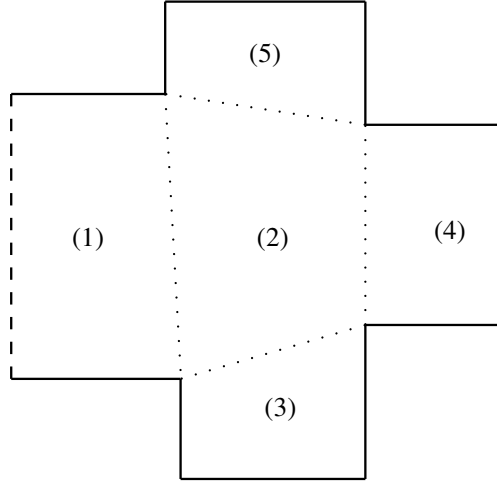
Figure A.1: Example of domain that can not be mapped into a single reference domain; the solid lines identify the sides where PEC boundary conditions have to be enforced; the dashed lines are the access ports; the dotted lines are the common edges between different patches. In this example, each patch can be mapped to the parent domain through a bilinear mapping.

$$
\begin{cases}
y_1 = E \\
y_2 = E + F \\
y_3 = E + F + G + H \\
y_4 = E + G.
\end{cases}
$$

By solving these systems, the following expressions are found:

$$
\begin{aligned}
A &= x_1 & E &= y_1 \\
B &= x_2 - x_1 & F &= y_2 - y_1 \\
C &= x_4 - x_1 & G &= y_4 - y_1 \\
D &= (x_3 - x_4) + (x_1 - x_2) & H &= (y_3 - y_4) + (y_1 - y_2).
\end{aligned}
$$

Once that the mapping is known, it is useful to know its derivatives:

$$
\frac{\partial x}{\partial u} = B + Dv \qquad \frac{\partial x}{\partial v} = C + Du
$$

$$
\frac{\partial y}{\partial u} = F + Hv \qquad \frac{\partial y}{\partial v} = G + Hu.
$$

The derivatives of the inverse mapping can be found, starting from these last expressions, by inverting the jacobian matrix, defined as:

$$\mathbf{J} = \begin{bmatrix} \dfrac{\partial x}{\partial u} & \dfrac{\partial x}{\partial v} \\[2ex] \dfrac{\partial y}{\partial u} & \dfrac{\partial y}{\partial v} \end{bmatrix}$$

So:

$$\mathbf{J}^{-1} = \begin{bmatrix} \dfrac{\partial u}{\partial x} & \dfrac{\partial u}{\partial y} \\[2ex] \dfrac{\partial v}{\partial x} & \dfrac{\partial v}{\partial y} \end{bmatrix} = \dfrac{1}{\dfrac{\partial x}{\partial u}\dfrac{\partial y}{\partial v} - \dfrac{\partial x}{\partial v}\dfrac{\partial y}{\partial u}} \begin{bmatrix} \dfrac{\partial y}{\partial v} & -\dfrac{\partial x}{\partial v} \\[2ex] -\dfrac{\partial y}{\partial u} & \dfrac{\partial x}{\partial u} \end{bmatrix}.$$

The bilinear mapping transforms the (u,v) unit square into a generic quadrilateral with straight edges; since all the formulas are referred to the (ξ, η) square with side 2, the following additional mapping is introduced:

$$u = \frac{1}{2}\xi + \frac{1}{2} \quad \Longleftrightarrow \quad \xi = 2u - 1$$
$$v = \frac{1}{2}\eta + \frac{1}{2} \quad \Longleftrightarrow \quad \eta = 2v - 1.$$

So:

$$\frac{\partial \xi}{\partial u} = \frac{\partial \eta}{\partial v} = 2$$

A.1.2 Gordon-Hall formula

It is possible to map each point of the reference domain $\boldsymbol{\sigma} = (\xi, \eta)$, where $(\xi, \eta) \in [-1,1] \times [-1,1]$, in a generic quadrilateral in the natural domain $\mathbf{r}$ with either straight or curved edges by using the Gordon-Hall formula [2] [9]:

$$\begin{aligned}
\mathbf{r}(\boldsymbol{\sigma}) = & \frac{1-\eta}{2}\boldsymbol{\pi}_1(\xi) + \frac{1+\eta}{2}\boldsymbol{\pi}_3(\xi) + \\
& + \frac{1-\xi}{2}\left(\boldsymbol{\pi}_4(\eta) - \frac{1+\eta}{2}\boldsymbol{\pi}_4(1) - \frac{1-\eta}{2}\boldsymbol{\pi}_4(-1)\right) + \\
& + \frac{1+\xi}{2}\left(\boldsymbol{\pi}_2(\eta) - \frac{1+\eta}{2}\boldsymbol{\pi}_2(1) - \frac{1-\eta}{2}\boldsymbol{\pi}_2(-1)\right),
\end{aligned}$$

where $\boldsymbol{\pi}_i$ is the mapping from the $[-1,1]$ interval to the curve representing the i-th edge. If $i = 1,3$, the parameterization is defined such that, for increasing ξ, the curve goes from left to right in the natural domain while, for $i = 2,4$, to increasing η corresponds a mapping from bottom to top; this is sketched in Fig. A.2. This procedure is applied to find the mapping for each j-th patch.

parent domain   natural domain
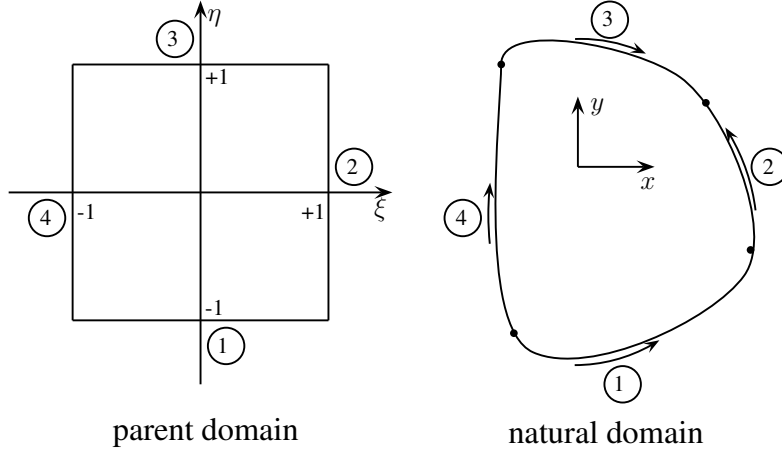
Figure A.2: Left: reference domain $\boldsymbol{\sigma}$; right: example of natural domain in the plane (z, x); each encircled number identifies the i-th edge in the parent and natural domains; the arrows indicate the direction of the parametric curves of the edges for increasing ξ or η.

The Gordon-Hall formula can be written in an expanded fashion:

$$
\begin{bmatrix} x(\xi, \eta) \\ y(\xi, \eta) \end{bmatrix} = \frac{1-\eta}{2} \begin{bmatrix} x_1(\xi) \\ y_1(\xi) \end{bmatrix} + \frac{1+\eta}{2} \begin{bmatrix} x_3(\xi) \\ y_3(\xi) \end{bmatrix} +
$$

$$
+ \frac{1-\xi}{2} \left(\underbrace{\begin{bmatrix} x_4(\eta) \\ y_4(\eta) \end{bmatrix} - \frac{1+\eta}{2} \begin{bmatrix} x_4(1) \\ y_4(1) \end{bmatrix} - \frac{1-\eta}{2} \begin{bmatrix} x_4(-1) \\ y_4(-1) \end{bmatrix}}_{\mathbf{A}(\eta)} \right) +
$$

$$
+ \frac{1+\xi}{2} \left(\underbrace{\begin{bmatrix} x_2(\eta) \\ y_2(\eta) \end{bmatrix} - \frac{1+\eta}{2} \begin{bmatrix} x_2(1) \\ y_2(1) \end{bmatrix} - \frac{1-\eta}{2} \begin{bmatrix} x_2(-1) \\ y_2(-1) \end{bmatrix}}_{\mathbf{B}(\eta)} \right) =
$$

$$
= \frac{1-\eta}{2} \begin{bmatrix} x_1(\xi) \\ y_1(\xi) \end{bmatrix} + \frac{1+\eta}{2} \begin{bmatrix} x_3(\xi) \\ y_3(\xi) \end{bmatrix} + \frac{1-\xi}{2} \begin{bmatrix} A_x(\eta) \\ A_y(\eta) \end{bmatrix} + \frac{1+\xi}{2} \begin{bmatrix} B_x(\eta) \\ B_y(\eta) \end{bmatrix} .
$$

The derivatives with respect to the reference domain variables are now calculated:

$$
\frac{\partial \mathbf{r}}{\partial \xi} = \frac{1-\eta}{2} \frac{\partial \boldsymbol{\pi}_1}{\partial \xi} + \frac{1+\eta}{2} \frac{\partial \boldsymbol{\pi}_3}{\partial \xi} - \frac{1}{2} \mathbf{A}(\eta) + \frac{1}{2} \mathbf{B}(\eta)
$$

$$
\frac{\partial \mathbf{r}}{\partial \eta} = -\frac{1}{2} \boldsymbol{\pi}_1(\xi) + \frac{1}{2} \boldsymbol{\pi}_3(\xi) + \frac{1-\xi}{2} \frac{\partial \mathbf{A}}{\partial \eta} + \frac{1+\xi}{2} \frac{\partial \mathbf{B}}{\partial \eta},
$$

where:

$$\frac{\partial \mathbf{A}}{\partial \eta} = \frac{\partial \boldsymbol{\pi}_4}{\partial \eta} - \frac{1}{2}\boldsymbol{\pi}_4(1) + \frac{1}{2}\boldsymbol{\pi}_4(-1)$$

$$\frac{\partial \mathbf{B}}{\partial \eta} = \frac{\partial \boldsymbol{\pi}_2}{\partial \eta} - \frac{1}{2}\boldsymbol{\pi}_2(1) + \frac{1}{2}\boldsymbol{\pi}_2(-1)$$

and:

$$\frac{\partial \boldsymbol{\pi}_i}{\partial \xi} = \begin{bmatrix} \dfrac{\partial x_i}{\partial \xi} \\[2ex] \dfrac{\partial y_i}{\partial \xi} \end{bmatrix} \qquad\qquad \frac{\partial \boldsymbol{\pi}_i}{\partial \eta} = \begin{bmatrix} \dfrac{\partial x_i}{\partial \eta} \\[2ex] \dfrac{\partial y_i}{\partial \eta} \end{bmatrix}.$$

Then, the derivatives of the mapping in the natural domain are computed as:

$$\begin{bmatrix} \dfrac{\partial \mathbf{r}}{\partial x} \\[2ex] \dfrac{\partial \mathbf{r}}{\partial y} \end{bmatrix} = \frac{1}{\dfrac{\partial x}{\partial \xi}\dfrac{\partial y}{\partial \eta} - \dfrac{\partial x}{\partial \eta}\dfrac{\partial y}{\partial \xi}} \begin{bmatrix} \dfrac{\partial y}{\partial \eta} & -\dfrac{\partial y}{\partial \xi} \\[2ex] -\dfrac{\partial x}{\partial \eta} & \dfrac{\partial x}{\partial \xi} \end{bmatrix} \begin{bmatrix} \dfrac{\partial \mathbf{r}}{\partial \xi} \\[2ex] \dfrac{\partial \mathbf{r}}{\partial \eta} \end{bmatrix}.$$

Parameterization of a curved edge

In this section the parameterization shown in Fig. A.3, that is used to model an edge with starting and ending curved parts with central straight part, is described.
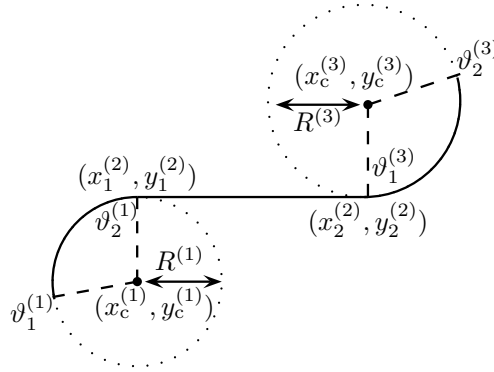
Figure A.3: Example of curved-straight-curved edge. The numbers in the superscripts identify the k-th part of the edge; $R^{(k)}$ is the radius of curvature of the i-th edge; $(x_c^{(k)}, y_c^{(k)})$ are the centers of the circles modeling the edges; $\vartheta_{1,2}^{(k)}$ are the starting and ending angles of the k-th circle; $(x_{1,2}^{(2)}, y_{1,2}^{(2)})$ are the starting and ending points of the straight part.

Let t be the parameter of the curve; then, the lengths of each part of the edge are:

$$L^{(1)} = \left| R^{(1)}(\vartheta_2^{(1)} - \vartheta_1^{(1)}) \right|$$
$$L^{(2)} = \sqrt{(x_2^{(2)} - x_1^{(2)})^2 + (y_2^{(2)} - y_1^{(2)})^2}$$
$$L^{(3)} = \left| R^{(3)}(\vartheta_2^{(3)} - \vartheta_1^{(3)}) \right|.$$

Then, it is possible to find the extremes, in t, of each sub-interval depending on its length, according to the following criterium:

$$t_1^{(1)} = -1$$
$$t_2^{(1)} = -1 + 2\frac{L^{(1)}}{L^{(1)} + L^{(2)} + L^{(3)}}$$
$$t_1^{(2)} = -1 + 2\frac{L^{(1)}}{L^{(1)} + L^{(2)} + L^{(3)}}$$
$$t_2^{(2)} = -1 + 2\frac{L^{(1)} + L^{(2)}}{L^{(1)} + L^{(2)} + L^{(3)}}$$
$$t_1^{(3)} = -1 + 2\frac{L^{(1)} + L^{(2)}}{L^{(1)} + L^{(2)} + L^{(3)}}$$
$$t_2^{(3)} = +1.$$

The expression of the parametric curve is:

$$x(t) = \begin{cases} x_c^{(1)} + R^{(1)} \cos \vartheta^{(1)} & t_1^{(1)} \le t < t_2^{(1)} \\ m(t, t_1^{(2)}, t_2^{(2)}, x_1^{(2)}, x_2^{(2)}) & t_1^{(2)} \le t \le t_2^{(2)} \\ x_c^{(3)} + R^{(3)} \cos \vartheta^{(3)} & t_1^{(3)} < t \le t_2^{(3)} \end{cases}$$

$$y(t) = \begin{cases} y_c^{(1)} + R^{(1)} \sin \vartheta^{(1)} & t_1^{(1)} \le t < t_2^{(1)} \\ m(t, t_1^{(2)}, t_2^{(2)}, y_1^{(2)}, y_2^{(2)}) & t_1^{(2)} \le t \le t_2^{(2)} \\ y_c^{(3)} + R^{(3)} \sin \vartheta^{(3)} & t_1^{(3)} < t \le t_2^{(3)} \end{cases},$$

where:

$$m(t, \alpha, \beta, a, b) = \frac{b - a}{\beta - \alpha}(t - \alpha) + a$$

$$\vartheta^{(1)} = m(t, t_1^{(1)}, t_2^{(1)}, \vartheta_1^{(1)}, \vartheta_2^{(1)})$$

$$\vartheta^{(3)} = m(t, t_1^{(3)}, t_2^{(3)}, \vartheta_1^{(3)}, \vartheta_2^{(3)}).$$

The derivatives of this mapping can be immediately computed; given m_t the derivative of the function m, that is:

$$m_t = m_t(\alpha, \beta, a, b) = \frac{b - a}{\beta - \alpha}.$$

So, the following expressions are written:

$$\frac{\mathrm{d}x(t)}{\mathrm{d}t} = \begin{cases} -R^{(1)} \sin \vartheta^{(1)} \dfrac{\mathrm{d}\vartheta^{(1)}}{\mathrm{d}t} & t_1^{(1)} \leq t < t_2^{(1)} \\ m_t(t_1^{(2)}, t_2^{(2)}, x_1^{(2)}, x_2^{(2)}) & t_1^{(2)} \leq t \leq t_2^{(2)} \\ -R^{(3)} \sin \vartheta^{(3)} \dfrac{\mathrm{d}\vartheta^{(3)}}{\mathrm{d}t} & t_1^{(3)} < t \leq t_2^{(3)} \end{cases}$$

$$\frac{\mathrm{d}y(t)}{\mathrm{d}t} = \begin{cases} R^{(1)} \cos \vartheta^{(1)} \dfrac{\mathrm{d}\vartheta^{(1)}}{\mathrm{d}t} & t_1^{(1)} \leq t < t_2^{(1)} \\ m_t(t_1^{(2)}, t_2^{(2)}, y_1^{(2)}, y_2^{(2)}) & t_1^{(2)} \leq t \leq t_2^{(2)} \\ R^{(3)} \cos \vartheta^{(3)} \dfrac{\mathrm{d}\vartheta^{(3)}}{\mathrm{d}t} & t_1^{(3)} < t \leq t_2^{(3)} \end{cases},$$

where:

$$\frac{\mathrm{d}\vartheta^{(1)}}{\mathrm{d}t} = m_t(t_1^{(1)}, t_2^{(1)}, \vartheta_1^{(1)}, \vartheta_2^{(1)})$$

$$\frac{\mathrm{d}\vartheta^{(3)}}{\mathrm{d}t} = m_t(t_1^{(3)}, t_2^{(3)}, \vartheta_1^{(3)}, \vartheta_2^{(3)}).$$

A.2 Asymptotic behavior of the electromagnetic field at sharp edges

In this appendix a formulation for the numerical determination of the singularity rate of the electromagnetic field in the proximity of sharp metallic edges based on azimuthal transmission lines is introduced. The space is divided in several regions, and the medium that fills the i-th region is characterized by its relative dielectric constant ε_i and by its relative magnetic permeability μ_i.

The most suitable coordinate system for the description of this problem is the cylindrical one: (ρ, φ, z). The starting point of the formulation are the Maxwell's curl equations:

$$\begin{cases} \nabla \times \mathbf{E} = -\mathrm{j}\omega\mu_i \mathbf{H} \\ \nabla \times \mathbf{H} = \mathrm{j}\omega\varepsilon_i \mathbf{E}. \end{cases}$$

In this formulation, no variation along the z direction is assumed; in other words:
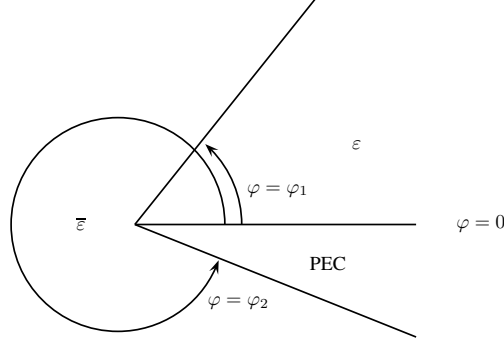
Figure A.4: Geometry of the problem.

$$\frac{\partial}{\partial z}[] = 0,$$

therefore, these two vector equations are written as six scalar equations, as follows:

$$\frac{1}{\rho}\frac{\partial H_z^{(i)}}{\partial \varphi} = \mathrm{j}\omega\varepsilon_i E_\rho^{(i)} \tag{A.2}$$

$$-\frac{\partial H_z^{(i)}}{\partial \rho} = \mathrm{j}\omega\varepsilon_i E_\varphi^{(i)} \tag{A.3}$$

$$\frac{1}{\rho}\frac{\partial(\rho H_\varphi^{(i)})}{\partial \rho} - \frac{1}{\rho}\frac{\partial H_\rho^{(i)}}{\partial \varphi} = \mathrm{j}\omega\varepsilon_i E_z^{(i)} \tag{A.4}$$

$$\frac{1}{\rho}\frac{\partial E_z^{(i)}}{\partial \varphi} = -\mathrm{j}\omega\mu_i H_\rho^{(i)} \tag{A.5}$$

$$-\frac{\partial E_z^{(i)}}{\partial \rho} = -\mathrm{j}\omega\mu_i H_\varphi^{(i)} \tag{A.6}$$

$$\frac{1}{\rho}\frac{\partial(\rho E_\varphi^{(i)})}{\partial \rho} - \frac{1}{\rho}\frac{\partial E_\rho^{(i)}}{\partial \varphi} = -\mathrm{j}\omega\mu_i H_z^{(i)}. \tag{A.7}$$

The components $E_z^{(i)}$ and $H_z^{(i)}$ satisfy the Helmholtz equations:

$$(\nabla_{\mathrm{t}}^2 + k_i^2)E_z^{(i)} = 0 \tag{A.8}$$

$$(\nabla_{\mathrm{t}}^2 + k_i^2)H_z^{(i)} = 0, \tag{A.9}$$

where:

$$k_i^2 = \omega^2\varepsilon_i\mu_i. \tag{A.10}$$

Since in this formulation the electromagnetic field has no variation along the z direction, the two differential problems are not coupled; this means that the problem

in $E_z^{(i)}$ and the one in $H_z^{(i)}$ can be solved separately; then, two proper expansions for the unknowns of the problem $E_z^{(i)}$ and $H_z^{(i)}$ are defined:

$$E_z^{(i)} = \sum_{k=1}^{\infty} \sum_{j=1}^{\infty} \left[\rho^{t_j} V_{ij}^{'(k)}(\varphi, t_j) \right]$$

$$H_z^{(i)} = \sum_{k=1}^{\infty} \sum_{j=1}^{\infty} \left[\rho^{t_j} I_{ij}^{''(k)}(\varphi, t_j) \right],$$

where t_j is the j-th eigenvalue of the problem and the functions $V_{ij}^{'(k)}(\varphi, t_j)$ and $I_{ij}^{''(k)}(\varphi, t_j)$ are the k-th coefficients of the radial expansion. In the first expression the coefficient has the physical meaning of a voltage (since an electric field component is expanded), while in the second case it has the physical meaning of a current (since a magnetic field component is expanded); the prime apex is related to the fact that E_z is non-vanishing only with TM_z modes, while the second apex for I identifies TE_z modes; no coupling between TE_z and TM_z modes occurs.

The transverse Laplace operator in cylindrical coordinates for a scalar function ϕ can be written as:

$$\nabla_{\mathrm{t}}^2 \phi = \frac{\partial^2 \phi}{\partial \rho^2} + \frac{1}{\rho} \frac{\partial \phi}{\partial \rho} + \frac{1}{\partial \rho^2} \frac{\partial^2 \phi}{\partial \varphi^2}.$$

Since the objective is the determination of the singular asymptotic behavior, for $k > 1$ the field expansions are regular; moreover, the lowest value of t_j is the singularity rate. So, by writing the transverse Laplace operator of $E_z^{(i)}$, the following equations are obtained:

$$\nabla_{\mathrm{t}}^2 E_z^{(i)} = (t_j)(t_j - 1)\rho^{t_j-2} V_{ij}'(\varphi, t_j) + t_j \rho^{t_j-2} V_{ij}'(\varphi, t_j) + \rho^{t_j-2} \frac{\partial^2 V_{ij}'(\varphi, t_j)}{\partial \varphi^2} =$$

$$= \rho^{t_j-2} \left(\frac{\partial^2 V_{ij}'}{\partial \varphi^2} + t_j^2 V_{ij}' \right).$$

This is substituted in the Helmholtz equation (A.8), obtaining

$$\rho^{t_j-2} \left(\frac{\partial^2 V_{ij}'}{\partial \varphi^2} + t_j^2 V_{ij}' \right) + \rho^{t_j} V_{ij}' + ... = 0.$$

The equation above is not complete, because the contributions to the ρ^{t_j} coefficient have not been written. However, the only coefficient of ρ^{t_j-2} is the written one; therefore, to satisfy the Helmholtz equation, the coefficient of ρ^{t_j-2} has to equal zero; this means that the following equation holds:

$$\frac{\partial^2 V_{ij}'}{\partial \varphi^2} + t_j^2 V_{ij}' = 0. \tag{A.11}$$

Then, by applying the same ideas on the second Helmholtz equation:

$$\frac{\partial^2 I_{ij}''}{\partial \varphi^2} + t_j^2 I_{ij}'' = 0. \tag{A.12}$$

Since the problems related to the TE_z modes and to the TM_z modes can be solved separately, from now on the two formulations will be developed in two different subsections.

A.2.1 TE$_z$ modes

In this section the singularity rate of the electromagnetic field will be evaluated by solving an eigenvalue problem. From now on, let $t \triangleq t_1$, and $I_i'' = I_{i1}''$; therefore, (A.12) can be written as:

$$\frac{\mathrm{d}^2 I_i''}{\mathrm{d}\varphi^2} + t^2 I_i'' = 0.$$

This is a current wave equation, exactly as the one that can be derived from the telegraphers' equations eliminating the voltage V_i''. It should be remarked that I_i'' comes from the first term of the radial expansion of $H_z^{(i)}$, therefore:

$$H_z^{(i)} \simeq \rho^t I_i''(\varphi, t).$$

The solution of the wave equations can be written as the superposition of a progressive and a regressive azimuthal waves:

$$I_i''(\varphi, t) = I_{i,0}''^+ \mathrm{e}^{-\mathrm{j}t\varphi} + I_{i,0}''^- \mathrm{e}^{+\mathrm{j}t\varphi} = I_i''^+(\varphi) + I_i''^-(\varphi).$$

This expression can also be used to evaluate the radial component of the electric field, $E_\rho^{(i)}$; in fact, by inverting (A.2), the following expression is obtained:

$$E_\rho^{(i)} = \frac{1}{\rho}\frac{1}{\mathrm{j}\omega\varepsilon_i}\frac{\partial H_z^{(i)}}{\partial\varphi} = \frac{1}{\rho}\frac{1}{\mathrm{j}\omega\varepsilon_i}\frac{\partial}{\partial\varphi}\left[\rho^t I_i''(\varphi,t)\right] = \rho^{t-1}\frac{1}{\mathrm{j}\omega\varepsilon_i}\frac{\partial I_i''(\varphi,t)}{\partial\varphi}.$$

This is now written explicitly, using the $I_i''(\varphi, t)$ defined above:

$$E_\rho^{(i)} = \rho^{t-1}\frac{1}{\mathrm{j}\omega\varepsilon_i}\frac{\partial I_i''(\varphi,t)}{\partial\varphi} = \rho^{t-1}\frac{1}{\mathrm{j}\omega\varepsilon_i}\left[-\mathrm{j}t I_{i,0}''^+ \mathrm{e}^{-\mathrm{j}t\varphi} + \mathrm{j}t I_{i,0}''^- \mathrm{e}^{+\mathrm{j}t\varphi}\right] =$$

$$= -\rho^{t-1}\frac{\mathrm{j}t}{\mathrm{j}\omega\varepsilon_i}\left[I_{i,0}''^+ \mathrm{e}^{-\mathrm{j}t\varphi} - I_{i,0}''^- \mathrm{e}^{+\mathrm{j}t\varphi}\right].$$

Now, let us define $Z_{\infty,i}''$ as:

$$Z_{\infty,i}'' = \frac{t}{\omega\varepsilon_i},$$

then, the azimuthal voltage V_i'' is defined as:

$$V_i''(\varphi, t) = Z_{\infty,i}'' \left[I_{i,0}''^{+} \mathrm{e}^{-\mathrm{j}t\varphi} - I_{i,0}''^{-} \mathrm{e}^{+\mathrm{j}t\varphi} \right] = V_i''^{+}(\varphi) + V_i''^{-}(\varphi),$$

so, from here, the following expressions are obtained:

$$E_\rho^{(i)} = \rho^{t-1} V_i''(\varphi, t),$$

where V_i'', I_i'' satisfy the following azimuthal telegraphers' equations:

$$\begin{cases} -\dfrac{\mathrm{d}V_i''}{\mathrm{d}\varphi} = \mathrm{j}t Z_{\infty,i}'' I_i'' \\ -\dfrac{\mathrm{d}I_i''}{\mathrm{d}\varphi} = \mathrm{j}t Y_{\infty,i}'' V_i''. \end{cases}$$

The parameter t is found as the solution of an eigenvalue problem; therefore, the reflection coefficient $\Gamma''(\varphi)$ is defined as:

$$\Gamma''(\varphi) = \frac{V''^{-}(\varphi)}{V''^{+}(\varphi)}.$$

Now some formulas for the computations on Γ are recalled; all these formulas are valid for both TE and TM modes, therefore the apexes will be omitted. It is known that the formula for the propagation of the reflection coefficient is:

$$\Gamma(\varphi_1) = \Gamma(\varphi_2) \mathrm{e}^{-\mathrm{j}2t(\varphi_2 - \varphi_1)}.$$

Let us assume that in $\varphi = B$ there is a dielectric discontinuity; in $\varphi = B^+$, there is the medium identified by $i = 3$; in $\varphi = B^-$, the one identified by $i = 2$; let F_B be the Fresnel reflection coefficient of the interface; this can be written as:

$$F_B = \frac{Z_{\infty,3} - Z_{\infty,2}}{Z_{\infty,3} + Z_{\infty,2}} = -\frac{\varepsilon_3 - \varepsilon_2}{\varepsilon_3 + \varepsilon_2},$$

then:

$$\Gamma_{B^-} = \frac{F_B + \Gamma_{B^+}}{1 + F_B \Gamma_{B^+}}.$$

All these formulas are applied to calculate the loop gain (LG) of the transmission line; this can be used in order to set the eigenvalue problem and find the values of t related to the free oscillations of the system defined above. The free oscillations are the ones for which the loop gain has absolute value equal to 1, and round-trip phase shift RTPS (that is the phase of the LG) multiple of 2π.

The problem of the determination of t can be defined as the transmission lines problem of Figure A.5; in $\varphi = A$, looking towards left, it is possible to see a short
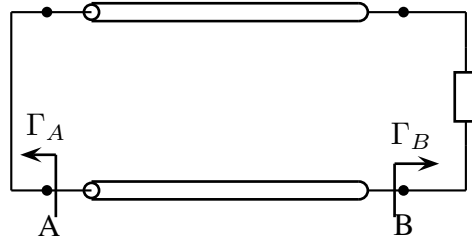
Figure A.5: Transmission line where the loop gain is calculated.

circuit; for the TE_z case, where the primary quantity is the current, the boundary condition that has to be enforced is:

$$\frac{\mathrm{d}I(\varphi, t)}{\mathrm{d}\varphi}\bigg|_{\varphi=A} = 0.$$

This means that:

$$\overleftarrow{\Gamma}_A = 1.$$

Instead, the reflection coefficient towards right is calculated as:

$$\vec{\Gamma}_A = \vec{\Gamma}_{B^-} \mathrm{e}^{-2\mathrm{j}tl_{AB}}.$$

It is known that the loop gain LG equals:

$$\mathrm{LG} = \vec{\Gamma}_A \overleftarrow{\Gamma}_A.$$

The absolute value of LG equals 1, since there are no losses; for what concerns the RTPS:

$$\mathrm{RTPS} = \angle \mathrm{LG} = \angle \overleftarrow{\Gamma}_A + \angle \vec{\Gamma}_{B^-} - 2tl_{AB}.$$

The term t is the number that identifies the free oscillations of this system; therefore, it is necessary to find the solutions of the equation

$$\mathrm{RTPS} = j2\pi,$$

so, of the equation:

$$\angle \overleftarrow{\Gamma}_A + \angle \vec{\Gamma}_{B^-} - 2tl_{AB} = j2\pi.$$

In this equation, $\overleftarrow{\Gamma}_A$ is known (defined by PEC boundary condition); $\angle \vec{\Gamma}_{B^-}$ is known (it can be found by standard transmission line theory, considering at the right end of the structure a PEC boundary condition); l_{AB} is known; therefore, t is the only unknown; fixed $j = 1$, t can be derived from this equation, as:

$$t = \frac{1}{2l_{AB}} \left[\angle \overleftarrow{\Gamma}_A + \angle \vec{\Gamma}_{B^-} - 2j\pi \right].$$

Once that t is known, and each reflection coefficient at each dielectric interface is known from the standard transmission line theory, it is possible to apply the formulas written above using the t that has been found and so determining also the azimuthal dependence of the electromagnetic field in the proximity of the sharp edge.

The solution to this problem can be fould by means of a numerical method, solving $\text{RTPS}(t) = j2\pi$, for $j = 1$. The case of a PEC wedge in homogeneous dielectric is interesting and it can be solved analytically; in this case, $\overleftarrow{\Gamma}_A = \vec{\Gamma}_{B^-} = -1$; the first eigenvalue is for $j = 0$; therefore, from the loop gain equation, the following relationship is derived:

$$\pi + \pi - 2tl_{AB} = 0 \Longrightarrow t = \frac{\pi}{l_{AB}}.$$

For instance, if $l_{AB} = \frac{3\pi}{2}$,

$$t = \frac{\pi}{3\frac{\pi}{2}} = \frac{2}{3},$$

this result is known and it confirms the validity of this theory. For what concerns the azimutal behavior, let us consider a PEC block defined from $\varphi = \frac{3\pi}{2}$ to 2π; then, since $\Gamma(\varphi) = -1$ (voltage reflection coefficient)

$$I_{i,0}''^+ = I_{i,0}''^-,$$

so:

$$I_i''(\varphi) = I_{i,0}''^+ \left[e^{-jt\varphi} + e^{+jt\varphi} \right] \propto \cos(t\varphi).$$

Therefore, the field component satisfies the following property:

$$H_z'' \propto \rho^{t-1} \cos(t\varphi).$$

A.2.2 TM$_z$ modes

Now the problem relative to the TM$_z$ modes will be solved by following a procedure similar to the previous one. In this case, (A.11) can be written as:

$$\frac{\partial^2 V_i'}{\partial \varphi^2} + t^2 V_i' = 0.$$

The following expression can be written:

$$E_z^{(i)} \simeq \rho^t V_i'(\varphi, t).$$

So:

$$V_i'(\varphi, t) = V_{i,0}'^{+} \mathrm{e}^{-\mathrm{j}t\varphi} + V_{i,0}'^{-} \mathrm{e}^{+\mathrm{j}t\varphi} = V_i'^{+}(\varphi) + V_i'^{-}(\varphi).$$

By inverting (A.5) the following expression is found:

$$H_\rho^{(i)} = -\frac{1}{\rho \mathrm{j}\omega\mu_i} \frac{\partial E_z^{(i)}}{\partial \varphi} = -\frac{1}{\rho} \frac{1}{\mathrm{j}\omega\mu_i} \frac{\partial}{\partial \varphi} \left[\rho^t V_i'(\varphi, t) \right] = -\rho^{t-1} \frac{1}{\mathrm{j}\omega\mu_i} \frac{\partial V_i'(\varphi, t)}{\partial \varphi},$$

and then this can be written explicitly, obtaining:

$$H_\rho^{(i)} = -\rho^{t-1} \frac{1}{\mathrm{j}\omega\mu_i} \left[-\mathrm{j}t V_{i,0}'^{+} \mathrm{e}^{-\mathrm{j}t\varphi} + \mathrm{j}t V_{i,0}'^{-} \mathrm{e}^{+\mathrm{j}t\varphi} \right] =$$

$$= \rho^{t-1} \frac{\mathrm{j}t}{\mathrm{j}\omega\mu_i} \left[V_{i,0}'^{+} \mathrm{e}^{-\mathrm{j}t\varphi} - V_{i,0}'^{-} \mathrm{e}^{+\mathrm{j}t\varphi} \right].$$

Now, let us define $Y_{\infty,i}'$ as:

$$Y_{\infty,i}' = \frac{t}{\omega\mu_i},$$

and the following expression is written:

$$Y_{\infty,i}' \left[V_{i,0}'^{+} \mathrm{e}^{-\mathrm{j}t\varphi} - V_{i,0}'^{-} \mathrm{e}^{+\mathrm{j}t\varphi} \right] = I_i'^{+}(\varphi) + I_i'^{-}(\varphi),$$

leading to:

$$H_\rho^{(i)} = \rho^{t-1} I_i'(\varphi, t),$$

where V_i', I_i' satisfy the following azimuthal telegraphers equations:

$$\begin{cases} -\dfrac{\mathrm{d}V_i'}{\mathrm{d}\varphi} = \mathrm{j}t Z_{\infty,i}' I_i' \\ -\dfrac{\mathrm{d}I_i'}{\mathrm{d}\varphi} = \mathrm{j}t Y_{\infty,i}' V_i'. \end{cases}$$

For the TM_z modes formulation the reflection coefficient $\Gamma'(\varphi)$ is defined as:

$$\Gamma'(\varphi) = \frac{V_i'^{-}(\varphi)}{V_i'^{+}(\varphi)}.$$

The same considerations can be applied, and then:

$$t = \frac{1}{2l_{AB}} \left[\angle \overleftarrow{\Gamma}_A + \angle \overrightarrow{\Gamma}_{B^-} - 2j\pi \right]$$

is the solution of the eigenvalue problem. Let us consider a PEC block defined from $\varphi = \frac{3\pi}{2}$ to 2π; then, since $\Gamma(\varphi) = -1$ (voltage reflection coefficient)

$$V_{i,0}'^{+} = -V_{i,0}'^{-},$$

so:

$$V_i'(\varphi) = V_{i,0}'^{+} \left[e^{-jt\varphi} - e^{+jt\varphi} \right] \propto \cos(t\varphi).$$

So:

$$E_z' \propto \rho^{t-1} \sin(t\varphi).$$

A.2.3   Implementation notes

Once that the azimuthal behavior is known, it is necessary to implement it correctly, in a carthesian reference system. Since all these results are in a cylindrical coordinate system, the polar-carthesian transformations are now reviewed and applied to the case study.

Carthesian to cylindrical

Let us define the following mapping:

$$\begin{cases} u = \rho \cos \varphi \\ v = \rho \sin \varphi, \end{cases}$$

and the inverse mapping:

$$\begin{cases} \rho = \sqrt{u^2 + v^2} \\ \varphi = \tan^{-1}\left(\dfrac{v}{u}\right). \end{cases}$$

Let f be a function of u and v; then, by applying the chain rule:

$$\rho \frac{\partial f}{\partial \rho} = \rho \left[\frac{\partial f}{\partial u}\frac{\partial u}{\partial \rho} + \frac{\partial f}{\partial v}\frac{\partial v}{\partial \rho} \right] = \rho \frac{\partial f}{\partial u} \cos \varphi + \rho \frac{\partial f}{\partial v} \sin \varphi = u \frac{\partial f}{\partial u} + v \frac{\partial f}{\partial v},$$

and

$$\frac{\partial f}{\partial \varphi} = \frac{\partial f}{\partial u}\frac{\partial u}{\partial \varphi} + \frac{\partial f}{\partial v}\frac{\partial v}{\partial \varphi} = -\rho \frac{\partial f}{\partial u} \sin \varphi + \rho \frac{\partial f}{\partial v} \cos \varphi = -v \frac{\partial f}{\partial u} + u \frac{\partial f}{\partial v},$$

therefore:

$$\begin{cases} \rho \dfrac{\partial}{\partial \rho} = u \dfrac{\partial}{\partial u} + v \dfrac{\partial}{\partial v} \\[2mm] \dfrac{\partial}{\partial \varphi} = -v \dfrac{\partial}{\partial u} + u \dfrac{\partial}{\partial v}. \end{cases}$$

Cylindrical to carthesian

Now, let us start from $f = f(\rho, \varphi)$; the objective is the determination of the derivatives in the (u, v) plane. Once again, it is possible to start from the chain rule:

$$\frac{\partial f}{\partial u} = \frac{\partial f}{\partial \rho}\frac{\partial \rho}{\partial u} + \frac{\partial f}{\partial \varphi}\frac{\partial \varphi}{\partial u}$$

$$\frac{\partial f}{\partial v} = \frac{\partial f}{\partial \rho}\frac{\partial \rho}{\partial v} + \frac{\partial f}{\partial \varphi}\frac{\partial \varphi}{\partial v}.$$

Now, it is necessary to evaluate all these derivatives. The first two terms are found differentiating $\rho = \rho(u, v)$:

$$\frac{\partial \rho}{\partial u} = \frac{u}{\sqrt{u^2 + v^2}},$$

and

$$\frac{\partial \rho}{\partial v} = \frac{v}{\sqrt{u^2 + v^2}},$$

then:

$$\frac{\partial \varphi}{\partial u} = \frac{1}{1 + \frac{v^2}{u^2}}\frac{\partial}{\partial u}\left(\frac{v}{u}\right) = \frac{-\frac{v}{u^2}}{1 + \frac{v^2}{u^2}} = -\frac{v}{u^2 + v^2},$$

and, similarly:

$$\frac{\partial \varphi}{\partial v} = \frac{\frac{1}{u}}{1 + \frac{v^2}{u^2}} = \frac{u}{u^2 + v^2}.$$

Now, it is possible to substitute these formulas in the chain rules:

$$\frac{\partial f}{\partial u} = \frac{\partial f}{\partial \rho}\frac{u}{\sqrt{u^2 + v^2}} - \frac{\partial f}{\partial \varphi}\frac{v}{u^2 + v^2},$$

and:

$$\frac{\partial f}{\partial v} = \frac{\partial f}{\partial \rho}\frac{v}{\sqrt{u^2 + v^2}} + \frac{\partial f}{\partial \varphi}\frac{u}{u^2 + v^2},$$

but it is observed that:

$$\frac{u}{\sqrt{u^2 + v^2}} = \frac{u}{\rho} = \cos \varphi,$$

and

$$\frac{v}{u^2 + v^2} = \frac{v}{\sqrt{u^2 + v^2}}\frac{1}{\sqrt{u^2 + v^2}} = \frac{v}{\rho}\frac{1}{\rho} = \frac{1}{\rho}\sin\varphi,$$

and, similarly:

$$\frac{v}{\sqrt{u^2 + v^2}} = \sin\varphi \quad \frac{u}{u^2 + v^2} = \frac{1}{\rho}\cos\varphi,$$

so, after a substitution in the chain rule expressions, the following equations are found:

$$\begin{cases} \dfrac{\partial f}{\partial u} = \cos\varphi\dfrac{\partial f}{\partial \rho} - \sin\varphi\dfrac{1}{\rho}\dfrac{\partial f}{\partial \varphi} \\ \dfrac{\partial f}{\partial v} = \sin\varphi\dfrac{\partial f}{\partial \rho} + \cos\varphi\dfrac{1}{\rho}\dfrac{\partial f}{\partial \varphi}. \end{cases}$$

A.2.4   Derivation of the non-azimuthal weight function

The first case study is the following one:

$$f(\rho, \varphi) = \rho^t,$$

so:

$$\begin{cases} \dfrac{\partial f}{\partial u} = t\rho^{t-1}\cos\varphi \\ \dfrac{\partial f}{\partial v} = t\rho^{t-1}\sin\varphi. \end{cases}$$

A.2.5   Derivation of the azimuthal weight function for the TE$_z$ case

If the weighting functions has into account the presence of the azimuthal behavior, it can be written as:

$$f(\rho, \varphi) = \rho^t\cos(t\varphi).$$

So:

$$\begin{aligned} \frac{\partial f}{\partial u} &= t\rho^{t-1}\cos\varphi\cos(t\varphi) + t\rho^{t-1}\sin(t\varphi)\sin(\varphi) = \\ &= t\rho^{t-1}\left(\cos(t\varphi)\cos(\varphi) + \sin(\varphi)\sin(t\varphi)\right) = \\ &= t\rho^{t-1}\cos\left[(t-1)\varphi\right] \end{aligned}$$

$$\frac{\partial f}{\partial v} = t\rho^{t-1} \sin\varphi \cos(t\varphi) - t\rho^{t-1} \cos\varphi \sin(t\varphi) =$$
$$= t\rho^{t-1} \left(\sin(\varphi) \cos(t\varphi) + \cos(\varphi) \sin(t\varphi) \right) =$$
$$= t\rho^{t-1} \sin\left[(t-1)\varphi \right].$$

A.2.6 Derivation of the azimuthal weight function for the TM$_z$ case

If the weighting functions has into account the presence of the azimuthal behavior, it can be written as:

$$f(\rho, \varphi) = \rho^t \sin(t\varphi),$$

So:

$$\frac{\partial f}{\partial u} = t\rho^{t-1} \cos\varphi \sin(t\varphi) - t\rho^{t-1} \cos(t\varphi) =$$
$$= t\rho^{t-1} \left(\sin(t\varphi) \cos(\varphi) - \sin(\varphi) \cos(t\varphi) \right) =$$
$$= t\rho^{t-1} \sin\left[(t-1)\varphi \right]$$

$$\frac{\partial f}{\partial v} = t\rho^{t-1} \sin\varphi \sin(t\varphi) + t\rho^{t-1} \cos\varphi \cos(t\varphi) =$$
$$= t\rho^{t-1} \left(\cos(\varphi) \cos(t\varphi) + \sin(\varphi) \sin(t\varphi) \right) =$$
$$= t\rho^{t-1} \cos\left[(t-1)\varphi \right].$$

Appendix of "Mortar element analysis of 2-D waveguide discontinuities"

B.1   TE$_z$ and TM$_z$ modes

In this section the expressions of the TE$_z$ and TM$_z$ modes of a rectangular waveguide are reported from [72]. These expressions are used to derive the LSE$^{(x)}$ and LSM$^{(x)}$ modes, and to expand the field at the access ports in inhomogeneous E-plane discontinuities.

- TM$_z$ modes; given m and n different from zero:

$$
\begin{aligned}
e'_x &= -\frac{2}{a}\frac{m}{C_{mn}}\cos\left(\frac{m\pi}{a}x\right)\sin\left(\frac{n\pi}{b}y\right) \\
e'_y &= -\frac{2}{b}\frac{n}{C_{mn}}\sin\left(\frac{m\pi}{a}x\right)\cos\left(\frac{n\pi}{b}y\right) \\
h'_x &= \frac{2}{b}\frac{n}{C_{mn}}\sin\left(\frac{m\pi}{a}x\right)\cos\left(\frac{n\pi}{b}y\right) \\
h'_y &= -\frac{2}{a}\frac{m}{C_{mn}}\cos\left(\frac{m\pi}{a}x\right)\sin\left(\frac{n\pi}{b}y\right).
\end{aligned}
$$

- TE$_z$ modes; excluding the case $m = n = 0$:

$$e''_x = \frac{\sqrt{\epsilon_m \epsilon_n}}{b} \frac{n}{C_{mn}} \cos\left(\frac{m\pi}{a}x\right) \sin\left(\frac{n\pi}{b}y\right)$$

$$e''_y = -\frac{\sqrt{\epsilon_m \epsilon_n}}{a} \frac{m}{C_{mn}} \sin\left(\frac{m\pi}{a}x\right) \cos\left(\frac{n\pi}{b}y\right)$$

$$h''_x = \frac{\sqrt{\epsilon_m \epsilon_n}}{a} \frac{m}{C_{mn}} \sin\left(\frac{m\pi}{a}x\right) \cos\left(\frac{n\pi}{b}y\right)$$

$$h''_y = \frac{\sqrt{\epsilon_m \epsilon_n}}{b} \frac{n}{C_{mn}} \cos\left(\frac{m\pi}{a}x\right) \sin\left(\frac{n\pi}{b}y\right).$$

Here, a and b are the dimensions of the waveguide on the x and y axes, then

$$C_{mn} = \sqrt{m^2 \frac{b}{a} + n^2 \frac{a}{b}},$$

and

$$\epsilon_n = \begin{cases} 1, & n = 0 \\ 2, & n \neq 0 \end{cases}.$$

B.2 $\quad$ LSE$^{(x)}$ and LSM$^{(x)}$ modes

B.2.1 $\quad$ Derivation of LSE$^{(x)}$ modes

In this section the expressions of the LSE$^{(x)}$ modes are derived by combining the TE$_z$ and TM$_z$ ones. From now on, the z subscript is omitted. LSE$^{(x)}$ modes have no x component of the electric field, meaning that:

$$E_x = 0.$$

The component E_x is written as a combination of TE and TM modes:

$$E_x = E'_x + E''_x = V'e'_x + V''e''_x =$$
$$= \left[-V'\frac{2}{a}\frac{m}{C_{mn}} + V''\frac{\sqrt{\epsilon_m \epsilon_n}}{b}\frac{n}{C_{mn}}\right]\cos(k_x x)\sin(k_x x),$$

where:

$$k_x = \frac{m\pi}{a} \qquad k_y = \frac{n\pi}{b} \qquad C_{mn} = \sqrt{m^2\frac{b}{a} + n^2\frac{a}{b}}, \qquad \text{(B.1)}$$

and V', V'' are the TM and TE modal voltages. The condition on E_x is translated in the following relationship between the modal voltages:

$$-V'\frac{2}{a}\frac{m}{C_{mn}} + V''\frac{\sqrt{\epsilon_m\epsilon_n}}{b}\frac{n}{C_{mn}} = 0,$$

which means

$$\frac{V'}{V''} = \frac{\sqrt{\epsilon_m\epsilon_n}}{2}\frac{na}{mb}.$$

Then, according to (B.1),

$$\frac{na}{mb} = \frac{k_y}{k_x},$$

therefore:

$$\frac{V'}{V''} = \frac{\sqrt{\epsilon_m\epsilon_n}}{2}\frac{k_y}{k_x}. \tag{B.2}$$

From here on, the progressive wave case is considered, meaning that:

$$V'' \propto \mathrm{e}^{-\mathrm{j}k_z z},$$

where:

$$k_0^2 = k_x^2 + k_y^2 + k_z^2.$$

So:

$$
\begin{aligned}
I'' &= Y_\infty'' V'' = Y_0\frac{k_z}{k_0}V'' \\
I' &= Y_\infty' V' = Y_0\frac{k_0}{k_z}V'.
\end{aligned}
\tag{B.3}
$$

To calculate the proper current combination aimed at obtaining LSE$^{(x)}$ modes, (B.3) are used with (B.2) to calculate:

$$
\begin{aligned}
\frac{I'}{I''} &= Y_0\frac{k_0}{k_z}\frac{V'}{I''} = Y_0\frac{k_0}{k_z}\frac{V'}{Y_0\frac{k_z}{k_0}V''} = \frac{k_0^2}{k_z^2}\frac{V'}{V''} = \\
&= \frac{k_0^2}{k_z^2}\frac{\sqrt{\epsilon_m\epsilon_n}}{2}\frac{k_y}{k_x}.
\end{aligned}
\tag{B.4}
$$

Equations (B.2) and (B.4) provide the correct combination of TE and TM modes to obtain LSE$^{(x)}$ modes. These expressions are now used to calculate the LSE$^{(x)}$ mode fields.

Derivation of E_y

The component E_y is now written as:

$$E_y = E_y' + E_y'' = V'e_y' + V''e_y'' = V'' \left[\frac{V'}{V''} e_y' + e_y'' \right] =$$

$$= V'' \left[-\frac{2}{b} \frac{n}{C_{mn}} \frac{V'}{V''} - \frac{\sqrt{\epsilon_m \epsilon_n}}{a} \frac{m}{C_{mn}} \right] \sin(k_x x) \cos(k_y y) =$$

$$= -V'' \left[\frac{2}{b} \frac{n}{C_{mn}} \frac{\sqrt{\epsilon_m \epsilon_n}}{2} \frac{k_y}{k_x} + \frac{\sqrt{\epsilon_m \epsilon_n}}{a} \frac{m}{C_{mn}} \right] \sin(k_x x) \cos(k_y y) =$$

$$= -V'' \frac{\sqrt{\epsilon_m \epsilon_n}}{\pi C_{mn}} \frac{k_x^2 + k_y^2}{k_x} \sin(k_x x) \cos(k_y y), \tag{B.5}$$

where for the last step (B.1) was used.

Derivation of H_x

The component H_x is now written as:

$$H_x = H_x' + H_x'' = I'h_x' + I''h_x'' = I'' \left[\frac{I'}{I''} h_x' + h_x'' \right] =$$

$$= I'' \left[\frac{2n}{bC_{mn}} \frac{I'}{I''} + \frac{\sqrt{\epsilon_m \epsilon_n}}{a} \frac{m}{C_{mn}} \right] \sin(k_x x) \cos(k_y y) =$$

$$= I'' \left[\frac{2n}{bC_{mn}} \frac{k_0^2}{k_z^2} \frac{\sqrt{\epsilon_m \epsilon_n}}{2} \frac{k_y}{k_x} + \frac{\sqrt{\epsilon_m \epsilon_n}}{a} \frac{m}{C_{mn}} \right] \sin(k_x x) \cos(k_y y) =$$

$$= I'' \frac{\sqrt{\epsilon_m \epsilon_n}}{\pi C_{mn}} \frac{k_0^2 k_y^2 + k_x^2 k_z^2}{k_x k_z^2} \sin(k_x x) \cos(k_y y). \tag{B.6}$$

Derivation of H_y

The component H_y is now written as:

$$H_y = H_y' + H_y'' = I'h_y' + I''h_y'' = I'' \left[\frac{I'}{I''} h_y' + h_y'' \right] =$$

$$= I'' \left[-\frac{2m}{aC_{mn}} \frac{k_0^2}{k_z^2} \frac{\sqrt{\epsilon_m \epsilon_n}}{2} \frac{k_y}{k_x} + \frac{\sqrt{\epsilon_m \epsilon_n}}{b} \frac{n}{C_{mn}} \right] \cos(k_x x) \sin(k_y y) =$$

$$= I'' \frac{\sqrt{\epsilon_m \epsilon_n}}{\pi C_{mn}} \left[-\frac{k_0^2}{k_z^2} k_y + k_y \right] \cos(k_x x) \sin(k_y y) =$$

$$= I'' \frac{\sqrt{\epsilon_m \epsilon_n}}{\pi C_{mn}} k_y \frac{k_z^2 - k_0^2}{k_z^2} \cos(k_x x) \sin(k_y y). \tag{B.7}$$

Derivation of E_z

The field component E_z may be written as:

$$E_z = I'Z'_\infty e'_z,$$

where:

$$e'_z = -\mathrm{j}\frac{\sqrt{k_x^2 + k_y^2}}{k_z}\Phi(x,y),$$

and

$$\Phi(x,y) = \frac{2}{\sqrt{ab}}\sin(k_x x)\cos(k_y y).$$

Therefore, by using (B.3) and (B.4):

$$
\begin{aligned}
E_z &= -\mathrm{j}I''\frac{I'}{I''}\frac{\sqrt{k_x^2+k_y^2}}{k_z}\Phi = \\
&= -\mathrm{j}I''\frac{k_0^2}{k_z^2}\frac{\sqrt{\epsilon_m\epsilon_n}}{2}\frac{k_y}{k_x}\frac{\sqrt{k_x^2+k_y^2}}{k_z}\frac{k_z}{k_0}Z_0\Phi = \\
&= -\mathrm{j}I''\frac{k_0^2}{k_z^2}\frac{k_y}{k_x}\frac{\sqrt{k_x^2+k_y^2}}{k_0}Z_0\frac{\sqrt{\epsilon_m\epsilon_n}}{2}\frac{2}{\sqrt{ab}}\sin(k_x x)\sin(k_y y) = \\
&= -\mathrm{j}I''k_0 Z_0\frac{k_y}{k_x}\frac{\sqrt{k_x^2+k_y^2}}{k_z^2}\sqrt{\frac{\epsilon_m\epsilon_n}{ab}}\sin(k_x x)\sin(k_y y).
\end{aligned}
\tag{B.8}
$$

Derivation of H_z

The field component H_z is now written as:

$$H_z = V''Y''_\infty h''_z,$$

where:

$$h''_z = -\mathrm{j}\frac{\sqrt{k_x^2 + k_y^2}}{k_z}\Psi(x,y),$$

and:

$$\Psi(x,y) = \sqrt{\frac{\epsilon_m\epsilon_n}{ab}}\cos(k_x x)\cos(k_y y).$$

Therefore:

$$H_z = -\mathrm{j}V''\frac{\sqrt{k_x^2 + k_y^2}}{k_z}Y_0\frac{k_z}{k_0}\sqrt{\frac{\epsilon_m\epsilon_n}{ab}}\cos(k_x x)\cos(k_y y) =$$

$$= -\mathrm{j}Y_0 V''\frac{\sqrt{k_x^2 + k_y^2}}{k_0}\sqrt{\frac{\epsilon_m\epsilon_n}{ab}}\cos(k_x x)\cos(k_y y). \tag{B.9}$$

B.2.2   Normalization

In the previous section the expressions of the non-vanishing field components have been derived. Now, a procedure aimed at normalizing these quantities is described. The field power is calculated as the flux of the Poynting vector:

$$P = \int_0^b\int_0^a (\mathbf{E}\times\mathbf{H}^*)\cdot\widehat{\mathbf{z}}\,\mathrm{d}x\,\mathrm{d}y.$$

Indeed, $\mathbf{E}$ and $\mathbf{H}$ are transverse fields, since we are working on mode functions. In this situation, since $E_x = 0$, we have:

$$\mathbf{E} = E_y\widehat{\mathbf{y}} + E_z\widehat{\mathbf{z}}$$
$$\mathbf{H} = H_x\widehat{\mathbf{x}} + H_y\widehat{\mathbf{y}} + H_z\widehat{\mathbf{z}}.$$

So:

$$(\mathbf{E}\times\mathbf{H}^*)\cdot\widehat{\mathbf{z}} = [(E_y\widehat{\mathbf{y}} + E_z\widehat{\mathbf{z}})\times(H_x\widehat{\mathbf{x}} + H_y\widehat{\mathbf{y}} + H_z\widehat{\mathbf{z}})^*]\cdot\widehat{\mathbf{z}} =$$
$$= -E_y H_x^*;$$

therefore:

$$P = \int_0^b\int_0^a (-E_y H_x^*)\,\mathrm{d}x\,\mathrm{d}y.$$

Since power depends only on E_y and H_x, the normalized functions e^E and h^E are defined starting from these components, as follows:

$$E_y = V^E e^E \tag{B.10}$$
$$H_x = I^E h^E, \tag{B.11}$$

where:

$$-\int_0^b\int_0^a e^E h^{E*}\,\mathrm{d}x\,\mathrm{d}y = 1, \tag{B.12}$$

and

$$e^E = -h^E. \tag{B.13}$$

If these two normalization criteria are applied, the flux is only related tot he normalized modal voltage and current, since:

$$P = \int_0^b \int_0^a (-E_y H_x^*)\, \mathrm{d}x\, \mathrm{d}y = -V^E I^{E*} \int_0^b \int_0^a e^E h^{E*}\, \mathrm{d}x\, \mathrm{d}y =$$
$$= V^E I^E \int_0^b \int_0^a \left| e^E \right|^2\, \mathrm{d}x\, \mathrm{d}y = V^E I^E, \tag{B.14}$$

and

$$Z_\infty^E = -\frac{E_y}{H_x} = \frac{V^E}{I^E}. \tag{B.15}$$

From the previous section it has been shown that:

$$E_y = -A_y \sin(k_x x) \cos(k_y y) V''$$
$$H_x = A_x \sin(k_x x) \cos(k_y y) I'',$$

where:

$$A_y = \frac{\sqrt{\epsilon_m \epsilon_n}}{\pi C_{mn}} \frac{k_y^2 + k_x^2}{k_x} \tag{B.16}$$
$$A_x = \frac{\sqrt{\epsilon_m \epsilon_n}}{\pi C_{mn}} \frac{k_0^2 k_y^2 + k_x^2 k_z^2}{k_x k_z^2}. \tag{B.17}$$

Normalization is performed by defining two constants α_x and α_y such that:

$$E_y = \underbrace{(-A_y \alpha_y \sin(k_x x) \cos(k_y y))}_{e^E} \underbrace{\frac{V''}{\alpha_y}}_{V^E}$$
$$H_x = \underbrace{(A_x \alpha_x \sin(k_x x) \cos(k_y y))}_{h^E} \underbrace{\frac{I''}{\alpha_x}}_{I^E}.$$

These constants are now calculated using conditions (B.12) and (B.13). First:

$$P = \int_0^b \int_0^a E_y H_x^*\, \mathrm{d}x\, \mathrm{d}y = V^E I^{E*} A_x A_y \alpha_x \alpha_y \int_0^b \int_0^a \sin^2(k_x x) \cos^2(k_y y)\, \mathrm{d}x\, \mathrm{d}y = 1.$$

Focusing on the integral,

$$\int_0^b \int_0^a \sin^2(k_x x) \cos^2(k_y y) \, dx \, dy = \int_0^a \sin^2(k_x x) \, dx \int_0^b \cos^2(k_y y) \, dy = \frac{ab}{2\epsilon_n}.$$

Indeed, this integral is non-zero only if $m \geq 1$. So, according to (B.12),

$$A_x A_y \alpha_x \alpha_y \frac{ab}{2\epsilon_n} = 1,$$

meaning that:

$$\alpha_x \alpha_y \frac{2\epsilon_n}{A_x A_y ab}. \tag{B.18}$$

Then, from (B.13),

$$\left| e^E \right| = \left| h^E \right|,$$

meaning that:

$$A_y \alpha_y = A_x \alpha_x,$$

or:

$$\frac{\alpha_x}{\alpha_y} = \frac{A_y}{A_x}. \tag{B.19}$$

Equations (B.18) and (B.19) are solved together, obtaining:

$$\alpha_x^2 \frac{A_x}{A_y} = \frac{2\epsilon_n}{A_x A_y ab},$$

which is:

$$\alpha_x = \frac{1}{A_x} \sqrt{\frac{2\epsilon_n}{ab}}. \tag{B.20}$$

Similarly,

$$\alpha_y = \frac{1}{A_y} \sqrt{\frac{2\epsilon_n}{ab}}. \tag{B.21}$$

Calculation of the LSE$^{(x)}$ characteristic impedance

According to (B.15), the characteristic impedance for LSE$^{(x)}$ modes is defined as:

$$Z_\infty^E = \frac{V^E}{I^E}.$$

Now its explicit expression is derived.

$$Z_\infty^E = \frac{V^E}{I^E} = \frac{\frac{V''}{\alpha_y}}{\frac{I''}{\alpha_x}} = \frac{\alpha_x}{\alpha_y}\frac{V''}{I''} = \frac{\alpha_x}{\alpha_y}Z_\infty'' =$$

$$= \frac{\frac{1}{A_x}\sqrt{\frac{2\epsilon_n}{ab}}}{\frac{1}{A_y}\sqrt{\frac{2\epsilon_n}{ab}}}Z_\infty'' = \frac{A_y}{A_x}Z_\infty'' = \frac{A_y}{A_x}Z_0\frac{k_0}{k_z} =$$

$$= \frac{\frac{k_x^2+k_y^2}{k_x}}{\frac{k_0^2k_y^2+k_x^2k_z^2}{k_xk_z^2}} = \frac{k_z^2(k_x^2+k_y^2)}{(k_0^2-k_x^2)(k_x^2+k_y^2)} =$$

$$= \frac{k_z^2}{k_y^2+k_z^2}Z_0\frac{k_0}{k_z} = \frac{k_0k_z}{k_y^2+k_z^2}Z_0. \tag{B.22}$$

Calculation of the normalized E_y and H_x components

From (B.10) the expression of E_y is.

$$E_y = V^E e^E = -A_y\alpha_y\sin(k_xx)\cos(k_yy)V^E =$$

$$= \underbrace{-\sqrt{\frac{2\epsilon_n}{ab}}\sin(k_xx)\cos(k_yy)}_{e^E}V^E. \tag{B.23}$$

Similarly:

$$H_x = I^E h^E = A_x\alpha_x\sin(k_xx)\cos(k_yy)I^E =$$

$$= \underbrace{\sqrt{\frac{2\epsilon_n}{ab}}\sin(k_xx)\cos(k_yy)}_{h^E}I^E. \tag{B.24}$$

Calculation of the normalized H_y component

From (B.7), for $m \geq 1$, H_y is obtained as:

$$H_y = I'' \frac{\sqrt{2\epsilon_n}}{\pi C_{mn}} \frac{k_y k_z^2 - k_y k_0^2}{k_z^2} \cos(k_x x) \sin(k_y y) =$$

$$= -\frac{I''}{\alpha_x''} \frac{\sqrt{2\epsilon_n}}{\pi C_{mn}} k_y \frac{k_x^2 + k_y^2}{k_z^2} \cos(k_x x) \sin(k_y y) =$$

$$= -I^E \sqrt{\frac{2\epsilon_n}{ab}} \frac{\pi C_{mn}}{\sqrt{2\epsilon_n}} \frac{k_z^2 k_x k_y (k_x^2 + k_y^2)}{k_z^2 (k_0^2 k_y^2 + k_x^2 k_z^2)} \frac{\sqrt{2\epsilon_n}}{\pi C_{mn}} \cos(k_x x) \sin(k_y y) =$$

$$= -I^E \sqrt{\frac{2\epsilon_n}{ab}} \frac{k_x k_y (k_x^2 + k_y^2)}{k_x^2 (k_0^2 - k_x^2 - k_y^2) + k_0^2 k_y^2} \cos(k_x x) \sin(k_y y) =$$

$$= -I^E \sqrt{\frac{2\epsilon_n}{ab}} \frac{k_x k_y}{k_0^2 - k_x^2} \cos(k_x x) \sin(k_y y) =$$

$$= -I^E \sqrt{\frac{2\epsilon_n}{ab}} \frac{k_x k_y}{k_y^2 + k_z^2} \cos(k_x x) \sin(k_y y). \tag{B.25}$$

It is remarked that, if $n = 0$, $H_y = 0$; indeed,

$$k_y = \frac{n\pi}{b}.$$

Calculation of the normalized E_z component

From (B.8), for $m \geq 1$, E_z is obtained as:

$$E_z = -\mathrm{j}I'' k_0 Z_0 \frac{k_y}{k_x} \frac{\sqrt{k_x^2 + k_y^2}}{k_z^2} \sqrt{\frac{2\epsilon_n}{ab}} \sin(k_x x) \sin(k_y y) =$$

$$= -\mathrm{j}I^E k_0 Z_0 \alpha_x \frac{k_y}{k_x} \frac{\sqrt{k_x^2 + k_y^2}}{k_z^2} \sqrt{\frac{2\epsilon_n}{ab}} \sin(k_x x) \sin(k_y y) =$$

$$= -\mathrm{j}I^E k_0 Z_0 \sqrt{\frac{2\epsilon_n}{ab}} \frac{\pi C_{mn}}{\sqrt{2\epsilon_n}} \frac{k_y k_z^2}{(k_0^2 - k_x^2)(k_x^2 + k_y^2)} \frac{\sqrt{k_x^2 + k_y^2}}{k_z^2} \sqrt{\frac{2\epsilon_n}{ab}} \sin(k_x x) \sin(k_x x) =$$

$$= -\mathrm{j}k_0 Z_0 I^E \pi C_{mn} \frac{\sqrt{2\epsilon_n}}{ab} \frac{k_y}{(k_0^2 - k_x^2)\sqrt{k_x^2 + k_y^2}} \sin(k_x x) \sin(k_y y).$$

Recalling (B.1),

$$\frac{\pi C_{mn}}{ab} = \sqrt{\frac{m^2 \pi^2}{a^3 b} + \frac{n^2 \pi^2}{ab^3}} = \frac{1}{\sqrt{ab}} \sqrt{k_x^2 + k_y^2}.$$

This is substituted in the previous expression, obtaining:

$$E_z = -\mathrm{j}k_0 Z_0 I^E \sqrt{\frac{2\epsilon_n}{ab}} \frac{k_y}{k_z^2 + k_y^2} \sin(k_x x) \sin(k_y y). \tag{B.26}$$

Now, recalling (B.22), this can be re-written multiplying and dividing times k_z:

$$E_z = -j\frac{k_y}{k_z}I^E\sqrt{\frac{2\epsilon_n}{ab}}\frac{k_0 k_z Z_0}{k_z^2 + k_y^2}\sin(k_x x)\sin(k_y y) =$$

$$= -jZ_\infty^E I^E \underbrace{\frac{k_y}{k_z}\sqrt{\frac{2\epsilon_n}{ab}}\sin(k_x x)\sin(k_y y)}_{e_z^E}\,. \tag{B.27}$$

Calculation of the normalized H_z component

From (B.9) H_z is obtained, for $m \geq 1$, as:

$$H_z = -jY_0 V'' \frac{\sqrt{k_x^2 + k_y^2}}{k_0}\sqrt{\frac{2\epsilon_n}{ab}}\cos(k_x x)\cos(k_y y) =$$

$$= -jY_0 V^E \alpha_y \frac{\sqrt{k_x^2 + k_y^2}}{k_0}\sqrt{\frac{2\epsilon_n}{ab}}\cos(k_x x)\cos(k_y y) =$$

$$= -jY_0 \sqrt{\frac{2\epsilon_n}{ab}}\frac{k_x}{k_x^2 + k_y^2}\frac{\pi C_{mn}}{\sqrt{2\epsilon_n}}\sqrt{\frac{2\epsilon_n}{ab}}\frac{\sqrt{k_x^2 + k_y^2}}{k_0}\cos(k_x x)\cos(k_y y) =$$

$$= -jV^E Y_0 \sqrt{\frac{2\epsilon_n}{ab}}\frac{k_x}{k_0}\cos(k_x x)\cos(k_y y).$$

This equation is now multiplied and divided times $\frac{k_y^2 + k_z^2}{k_z}$ to make the LSE$^{(x)}$ modal admittance appear:

$$H_z = -jV^E Y_0 \sqrt{\frac{2\epsilon_n}{ab}}\frac{k_x}{k_0}\frac{k_y^2 + k_z^2}{k_z}\frac{k_z}{k_y^2 + k_z^2}\cos(k_x x)\cos(k_y y) =$$

$$= -jV^E Y_\infty^E \frac{k_x k_z}{k_y^2 + k_z^2}\underbrace{\sqrt{\frac{2\epsilon_n}{ab}}\cos(k_x x)\cos(k_y y)}_{h_z^E}\,. \tag{B.28}$$

B.2.3 Summary of LSE$^{(x)}$ mode functions

In the previous sections, the following LSE$^{(x)}$ mode functions have been derived:

$$e_y^E = e^E = -\sqrt{\frac{2\epsilon_n}{ab}} \sin(k_x x) \cos(k_y y)$$

$$h_x^E = h^E = \sqrt{\frac{2\epsilon_n}{ab}} \sin(k_x x) \cos(k_y y)$$

$$h_y^E = -\sqrt{\frac{2\epsilon_n}{ab}} \frac{k_x k_y}{k_y^2 + k_z^2} \cos(k_x x) \sin(k_y y)$$

$$e_z^E = \frac{k_y}{k_z} \sqrt{\frac{2\epsilon_n}{ab}} \sin(k_x x) \sin(k_y y)$$

$$h_z^E = \frac{k_x k_z}{k_y^2 + k_z^2} \sqrt{\frac{2\epsilon_n}{ab}} \cos(k_x x) \cos(k_y y).$$

B.2.4 Derivation of LSM$^{(x)}$ modes

In this section the expressions of the LSM$^{(x)}$ modes are derived. In this case, the combination of TM and TE modes should satisfy the following relationship:

$$H_x = 0,$$

where:

$$H_x = H_x' + H_x'' = I' h_x' + I'' h_x'' =$$
$$= \left[I' \frac{2n}{bC_{mn}} + I'' \frac{\sqrt{\epsilon_m \epsilon_n}}{a} \frac{m}{C_{mn}} \right] \sin(k_x x) \cos(k_y y) = 0.$$

This is satisfied if:

$$I' \frac{2n}{bC_{mn}} + I'' \frac{\sqrt{\epsilon_m \epsilon_n}}{a} \frac{m}{C_{mn}} = 0,$$

so:

$$\frac{I'}{I''} = -\frac{\sqrt{\epsilon_m \epsilon_n}}{a} \frac{mb}{2n}.$$

Since:

$$\frac{mb}{na} = \frac{k_x}{k_y},$$

$$\frac{I'}{I''} = -\frac{\sqrt{\epsilon_m \epsilon_n}}{2} \frac{k_x}{k_y}. \tag{B.29}$$

From now on, a progressive wave is considered, and (B.3) still holds. This is used with (B.29) to calculate the proper voltage combination aimed at obtaining LSM$^{(x)}$ modes:

$$\frac{V'}{V''} = Z_0 \frac{k_z}{k_0} \frac{I'}{I''} = Z_0 \frac{k_z}{k_0} \frac{I'}{I'' Z_0 \frac{k_0}{k_z}} = \frac{k_z^2}{k_0^2} \frac{I'}{I''} =$$
$$= -\frac{k_z^2}{k_0^2} \frac{k_x}{k_y} \frac{\sqrt{\epsilon_m \epsilon_n}}{2}. \tag{B.30}$$

Equations (B.29) and (B.30) provide the correct combination of TE and TM modes to obtain LSM$^{(x)}$ modes. Now these expressions are used to calculate the non-vanishing LSM$^{(x)}$ mode fields.

Derivation of E_y

The component E_y is now written as:

$$E_y = E'_y + E''_y = V'e'_y + V''e''_y = V'' \left[\frac{V'}{V''} e'_y + e''_y \right] =$$
$$= V'' \left[\frac{k_z^2}{k_0^2} \frac{k_x}{k_y} \frac{\sqrt{\epsilon_m \epsilon_n}}{2} \frac{2}{b} \frac{n}{C_{mn}} - \frac{\sqrt{\epsilon_m \epsilon_n}}{a} \frac{m}{C_{mn}} \right] \sin(k_x x) \cos(k_y y) =$$
$$= V'' \frac{\sqrt{\epsilon_m \epsilon_n}}{\pi C_{mn}} \left[\frac{k_z^2}{k_0^2} k_x - k_x \right] \sin(k_x x) \cos(k_y y) =$$
$$= V'' \frac{\sqrt{\epsilon_m \epsilon_n}}{\pi C_{mn}} k_x \frac{k_z^2 - k_0^2}{k_0^2} \sin(k_x x) \cos(k_y y). \tag{B.31}$$

Derivation of H_y

The component H_y is now written as:

$$H_y = H'_y + H''_y = I'h'_y + I''h''_y = I'' \left[\frac{I'}{I''} h'_y + h''_y \right] =$$
$$= I'' \left[\frac{\sqrt{\epsilon_m \epsilon_n}}{2} \frac{k_x}{k_y} \frac{2m}{aC_{mn}} + \frac{\sqrt{\epsilon_m \epsilon_n}}{b} \frac{b}{C_{mn}} \right] \cos(k_x x) \sin(k_y y) =$$
$$= I'' \frac{\sqrt{\epsilon_m \epsilon_n}}{\pi C_{mn}} \left[\frac{k_x^2}{k_y} + k_y \right] \cos(k_x x) \sin(k_y y) =$$
$$= I'' \frac{\sqrt{\epsilon_m \epsilon_n}}{\pi C_{mn}} \frac{k_x^2 + k_y^2}{k_y} \cos(k_x x) \sin(k_y y). \tag{B.32}$$

Derivation of E_x

The component E_x is now written as:

$$E_x = E_x' + E_x'' = V'e_x' + V''e_x'' = V'' \left[\frac{V'}{V''} e_x' + e_x'' \right] =$$

$$= V'' \left[\frac{k_z^2}{k_0^2} \frac{k_x}{k_y} \frac{\sqrt{\epsilon_m \epsilon_n}}{2} \frac{2}{a} \frac{m}{C_{mn}} + \frac{\sqrt{\epsilon_m \epsilon_n}}{b} \frac{n}{C_{mn}} \right] \cos(k_x x) \sin(k_y y) =$$

$$= V'' \frac{\sqrt{\epsilon_m \epsilon_n}}{\pi C_{mn}} \left[\frac{k_z^2}{k_0^2} \frac{k_x^2}{k_y} + k_y \right] \cos(k_x x) \sin(k_y y) =$$

$$= V'' \frac{\sqrt{\epsilon_m \epsilon_n}}{\pi C_{mn}} \frac{k_z^2 k_x^2 + k_y^2 k_0^2}{k_y k_0^2} \cos(k_x x) \sin(k_y y). \tag{B.33}$$

Derivation of E_z

The component E_z is now written as:

$$E_z = I' Z_\infty' e_z',$$

where:

$$e_z' = -\mathrm{j} \frac{\sqrt{k_x^2 + k_y^2}}{k_z} \Phi(x, y),$$

and

$$\Phi(x, y) = \frac{2}{\sqrt{ab}} \sin(k_x x) \sin(k_y y).$$

Therefore:

$$E_z = -\mathrm{j} I'' \frac{I'}{I''} \frac{\sqrt{k_x^2 + k_y^2}}{k_z} \frac{2}{\sqrt{ab}} \sin(k_x x) \sin(k_y y) =$$

$$= \mathrm{j} Z_\infty' \frac{k_x}{k_y} \frac{\sqrt{\epsilon_m \epsilon_n}}{2} I'' \frac{\sqrt{k_x^2 + k_y^2}}{k_z} \frac{2}{\sqrt{ab}} \sin(k_x x) \sin(k_y y) =$$

$$= \mathrm{j} \sqrt{\frac{\epsilon_m \epsilon_n}{ab}} \frac{\sqrt{k_x^2 + k_y^2}}{k_z} Z_0 \frac{k_z}{k_0} \frac{k_x}{k_y} \sin(k_x x) \sin(k_y y) =$$

$$= \mathrm{j} Z_0 I'' \sqrt{\frac{\epsilon_m \epsilon_n}{ab}} \frac{\sqrt{k_x^2 + k_y^2}}{k_0} \frac{k_x}{k_y} \sin(k_x x) \sin(k_y y). \tag{B.34}$$

Derivation of H_z

The component H_z is now written as:

$$H_z = V'' Y_\infty'' h_z'',$$

where:

$$h_z'' = -j\frac{\sqrt{k_x^2 + k_y^2}}{k_z}\Psi(x,y),$$

and

$$\Psi(x,y) = \sqrt{\frac{\epsilon_m \epsilon_n}{ab}}\cos(k_x x)\cos(k_y y).$$

Therefore:

$$H_z = -jY_0 V''\frac{\sqrt{k_x^2 + k_y^2}}{k_0}\sqrt{\frac{\epsilon_m \epsilon_n}{ab}}\cos(k_x x)\cos(k_y y). \tag{B.35}$$

B.2.5 Normalization

Just like in the previous case,

$$P = \int_0^b \int_0^a (\mathbf{E}\times\mathbf{H}^*)\cdot\widehat{\mathbf{z}}\,dx\,dy,$$

where, in this case,

$$\mathbf{E} = E_x\widehat{\mathbf{x}} + E_y\widehat{\mathbf{y}} + E_z\widehat{\mathbf{z}}, \qquad \mathbf{H} = H_y\widehat{\mathbf{y}} + H_z\widehat{\mathbf{z}}.$$

So:

$$(\mathbf{E}\times\mathbf{H}^*)\cdot\widehat{\mathbf{z}} = [(E_x\widehat{\mathbf{x}} + E_y\widehat{\mathbf{y}} + E_z\widehat{\mathbf{z}})\times(H_y\widehat{\mathbf{y}} + H_z\widehat{\mathbf{z}})^*] =$$
$$= E_x H_y^*.$$

Since power depends only on E_x and H_y, the normalized functions e^H and h^H are defined starting from these components:

$$E_x = V^H e^H$$
$$H_y = I^H h^H,$$

where:

$$\int_0^b \int_0^a e^H h^{H*}\,dx\,dy = 1,$$

and

$$e^H = h^H.$$

By this way,

$$P = V^H I^{H*},$$

and;

$$Z_\infty^H = \frac{E_x}{H_y} = \frac{V^H}{I^H}. \tag{B.36}$$

From the previous section, it has been shown that:

$$E_x = A_x \cos(k_x x) \sin(k_y y) V''$$
$$H_y = A_y \cos(k_x x) \sin(k_y y) I'',$$

where:

$$A_x = \frac{\sqrt{\epsilon_m \epsilon_n}}{\pi C_{mn}} \frac{k_z^2 k_x^2 + k_y^2 k_0^2}{k_y k_0^2} \tag{B.37}$$

$$A_y = \frac{\sqrt{\epsilon_m \epsilon_n}}{\pi C_{mn}} \frac{k_x^2 + k_y^2}{k_y}. \tag{B.38}$$

Normalization is performed by defining the two constants α_x and α_y such that:

$$E_x = \underbrace{A_x \alpha_x \cos(k_x x) \sin(k_y y)}_{e^H} \underbrace{\frac{V''}{\alpha_x}}_{V^H}$$

$$H_y = \underbrace{A_y \alpha_y \cos(k_x x) \sin(k_y y)}_{h^H} \underbrace{\frac{I''}{\alpha_y}}_{I^H}.$$

Using similar steps to the LSE$^{(x)}$ case, for $m \geq 1$,

$$\alpha_x = \frac{1}{A_x} \sqrt{\frac{2\epsilon_n}{ab}}$$

$$\alpha_y = \frac{1}{A_y} \sqrt{\frac{2\epsilon_n}{ab}}.$$

Calculation of the LSM$^{(x)}$ characteristic impedance

From (B.36),

$$Z_\infty^H = \frac{V^H}{I^H},$$

therefore:

$$
Z_\infty^H = \frac{\frac{V''}{\alpha_x}}{\frac{I''}{\alpha_y}} = \frac{\alpha_y}{\alpha_x}\frac{V''}{I''} = \frac{A_x}{A_y}\frac{V''}{I''} =
$$

$$
= \frac{A_x}{A_y}Z_\infty'' = Z_0\frac{k_0}{k_z}\frac{A_x}{A_y} = Z_0\frac{k_0}{k_z}\frac{\frac{k_z^2 k_x^2 + k_y^2 k_0^2}{k_y k_0^2}}{\frac{k_x^2+k_y^2}{k_y}} = Z_0\frac{k_0}{k_z}\frac{k_z^2 k_x^2 + k_y^2 k_x^2 + k_y^4 + k_y^2 k_z^2}{k_0^2(k_x^2+k_y^2)} =
$$

$$
= \frac{k_y^2 + k_z^2}{k_0 k_z}Z_0. \tag{B.39}
$$

Calculation of the normalized E_x and H_y components

From (B.33), the following expression is written:

$$
E_x = A_x\alpha_x\cos(k_x x)\sin(k_y y)V^H =
$$

$$
= \underbrace{\sqrt{\frac{2\epsilon_n}{ab}}\cos(k_x x)\sin(k_y y)}_{e^H}\, V^H. \tag{B.40}
$$

Similarly, from (B.32):

$$
H_y = A_y\alpha_y\cos(k_x x)\sin(k_y y)I^H =
$$

$$
= \underbrace{\sqrt{\frac{2\epsilon_n}{ab}}\cos(k_x x)\sin(k_y y)}_{h^H}\, I^H. \tag{B.41}
$$

Calculation of the normalized E_y component

From (B.31), for $m \geq 1$, the following expression is written:

$$
E_y = \frac{\sqrt{2\epsilon_n}}{\pi C_{mn}}k_x\frac{k_z^2 - k_0^2}{k_0^2}\sin(k_x x)\cos(k_y y) =
$$

$$
= -V^H\alpha_x\frac{\sqrt{2\epsilon_n}}{\pi C_{mn}}k_x\frac{k_x^2 + k_y^2}{k_0^2}\sin(k_x x)\cos(k_y y) =
$$

$$
= -V^H\sqrt{\frac{2\epsilon_n}{ab}}\frac{\pi C_{mn}}{\sqrt{2\epsilon_n}}\frac{k_x k_y k_0^2}{(k_x^2+k_y^2)(k_y^2+k_z^2)}\frac{k_x^2+k_y^2}{k_0^2}\frac{\sqrt{2\epsilon_n}}{\pi C_{mn}}\sin(k_x x)\cos(k_y y) =
$$

$$
= -V^H\sqrt{\frac{2\epsilon_n}{ab}}\frac{k_x k_y}{k_y^2 + k_z^2}\sin(k_x x)\cos(k_y y). \tag{B.42}
$$

Calculation of the normalized E_z component

From (B.34), the following expression is written:

$$
\begin{aligned}
E_z &= \mathrm{j}Z_0 I'' \sqrt{\frac{2\epsilon_n}{ab}} \frac{\sqrt{k_x^2 + k_y^2}}{k_0} \frac{k_x}{k_y} \sin(k_x x)\sin(k_y y) = \\
&= \mathrm{j}Z_0 I^H \alpha_y \sqrt{\frac{2\epsilon_n}{ab}} \frac{\sqrt{k_x^2 + k_y^2}}{k_0} \frac{k_x}{k_y} \sin(k_x x)\sin(k_y y) = \\
&= \mathrm{j}Z_0 I^H \frac{\pi C_{mn}}{ab} \sqrt{2\epsilon_n} \frac{k_y}{k_x^2 + k_y^2} \frac{k_x}{k_y} \frac{\sqrt{k_x^2 + k_y^2}}{k_0} \sin(k_x x)\sin(k_y y) = \\
&= \mathrm{j}Z_0 I^H \sqrt{\frac{2\epsilon_n}{ab}} \frac{k_x}{k_0} \sin(k_x x)\sin(k_y y) = \\
&= \mathrm{j}I^H Z_0 \frac{k_y^2 + k_z^2}{k_z k_0} \frac{k_z k_x}{k_y^2 + k_z^2} \sin(k_x x)\sin(k_y y) = \\
&= -\mathrm{j}Z_\infty^H I^H \underbrace{\left(-\frac{k_x k_z}{k_y^2 + k_z^2} \sin(k_x x)\sin(k_y y)\right)}_{e_z^H}.
\end{aligned}
\tag{B.43}
$$

Calculation of the normalized H_z component

From (B.35), the following expression is written:

$$
\begin{aligned}
H_z &= -\mathrm{j}Y_0 V'' \frac{\sqrt{k_x^2 + k_y^2}}{k_0} \sqrt{\frac{2\epsilon_n}{ab}} \cos(k_x x)\cos(k_y y) = \\
&= -\mathrm{j}Y_0 V^H \alpha_x \frac{\sqrt{k_x^2 + k_y^2}}{k_0} \sqrt{\frac{2\epsilon_n}{ab}} \cos(k_x x)\cos(k_y y) = \\
&= -\mathrm{j}Y_0 V^H \sqrt{2\epsilon_n} \frac{\pi C_{mn}}{ab} \frac{k_y k_0^2}{(k_x^2 + k_y^2)(k_y^2 + k_z^2)} \frac{\sqrt{k_x^2 + k_y^2}}{k_0} \cos(k_x x)\cos(k_y y) = \\
&= -\mathrm{j}Y_0 V^H \sqrt{\frac{2\epsilon_n}{ab}} \frac{k_y k_0}{k_y^2 + k_z^2} \cos(k_x x)\cos(k_y y) = \\
&= -\mathrm{j}Y_\infty^H V^H \underbrace{\sqrt{\frac{2\epsilon_n}{ab}} \frac{k_y}{k_z} \cos(k_x x)\cos(k_y y)}_{h_z^H}.
\end{aligned}
\tag{B.44}
$$

B.2.6 Summary of LSM$^{(x)}$ mode functions

$$e_x^H = e^H = \sqrt{\frac{2\epsilon_n}{ab}} \cos(k_x x) \sin(k_y y)$$

$$h_y^H = h^H = \sqrt{\frac{2\epsilon_n}{ab}} \cos(k_x x) \sin(k_y y)$$

$$e_y^H = -\sqrt{\frac{2\epsilon_n}{ab}} \frac{k_x k_y}{k_y^2 + k_z^2} \sin(k_x x) \cos(k_y y)$$

$$e_z^H = -\frac{k_x k_z}{k_y^2 + k_z^2} \sin(k_x x) \sin(k_y y)$$

$$h_z^H = \sqrt{\frac{2\epsilon_n}{ab}} \frac{k_y}{k_z} \cos(k_x x) \cos(k_y y).$$

B.3 Field representation for E-plane and H-plane waveguide discontinuities

In this section the equations used to describe the electromagnetic behavior of 2-D waveguide discontinuities are derived starting from the space-frequency Maxwell's curl equations:

$$\begin{cases} \nabla \times \mathbf{E}(\mathbf{r}, \omega) = -\mathrm{j}\omega\mu\mathbf{H}(\mathbf{r}, \omega) \\ \nabla \times \mathbf{H}(\mathbf{r}, \omega) = \mathrm{j}\omega\varepsilon\mathbf{E}(\mathbf{r}, \omega). \end{cases}$$

These equations are now written in cartesian coordinates; for the sake of compactness, from here on the dependence on space and frequency is omitted:

$$\frac{\partial E_z}{\partial y} - \frac{\partial E_y}{\partial z} = -\mathrm{j}\omega\mu H_x$$

$$\frac{\partial E_x}{\partial z} - \frac{\partial E_z}{\partial x} = -\mathrm{j}\omega\mu H_y$$

$$\frac{\partial E_y}{\partial x} - \frac{\partial E_x}{\partial y} = -\mathrm{j}\omega\mu H_z$$

$$\frac{\partial H_z}{\partial y} - \frac{\partial H_y}{\partial z} = \mathrm{j}\omega\varepsilon E_x$$

$$\frac{\partial H_x}{\partial z} - \frac{\partial H_z}{\partial x} = \mathrm{j}\omega\varepsilon E_y$$

$$\frac{\partial H_y}{\partial x} - \frac{\partial H_x}{\partial y} = \mathrm{j}\omega\varepsilon E_z.$$

The structures that are analyzed in this chapter are translationally symmetric along x; for this reason, the x dependence of the field in the junction is the same as the incident field one, that is assumed to be a LSE$^{(x)}$ or LSM$^{(x)}$ mode. Therefore:

$$\mathbf{H}(x, y, z) = \mathbf{H}_\mathrm{t}^{(x)} \cos\left(\frac{m\pi}{a}x\right) + \widehat{\mathbf{x}}\, H_x \sin\left(\frac{m\pi}{a}x\right)$$

$$\mathbf{E}(x, y, z) = \mathbf{E}_\mathrm{t}^{(x)} \sin\left(\frac{m\pi}{a}x\right) + \widehat{\mathbf{x}}\, E_x \cos\left(\frac{m\pi}{a}x\right),$$

where a is the dimension of the device along x. Let k_x be defined as:

$$k_x \triangleq \frac{m\pi}{a}.$$

Maxwell's equations are now re-written keeping into account this field dependence, obtaining:

$$\frac{\partial E_z}{\partial y} \sin k_x x - \frac{\partial E_y}{\partial z} \sin k_x x = -\mathrm{j}kZH_x \sin k_x x$$

$$\frac{\partial E_x}{\partial z} \cos k_x x - k_x E_z \cos k_x x = -\mathrm{j}kZH_y \cos k_x x$$

$$k_x E_y \cos k_x x - \frac{\partial E_x}{\partial y} \cos k_x x = -\mathrm{j}kZH_z \cos k_x x$$

$$\frac{\partial H_z}{\partial y} \cos k_x x - \frac{\partial H_y}{\partial z} \cos k_x x = \mathrm{j}kY E_x \cos k_x x$$

$$\frac{\partial H_x}{\partial z} \sin k_x x + k_x H_z \sin k_x x = \mathrm{j}kY E_y \sin k_x x$$

$$- k_x H_y \sin k_x x - \frac{\partial H_x}{\partial y} \sin k_x x = \mathrm{j}kY E_z \sin k_x x,$$

where:

$$Z = \sqrt{\frac{\mu}{\varepsilon}} \qquad k = \omega\sqrt{\mu\varepsilon}.$$

Then, all the x dependences simplify, leading to:

$$\frac{\partial E_z}{\partial y} - \frac{\partial E_y}{\partial z} = -\mathrm{j}kZH_x \tag{B.45}$$

$$\frac{\partial E_x}{\partial z} - k_x E_z = -\mathrm{j}kZH_y \tag{B.46}$$

$$k_x E_y - \frac{\partial E_x}{\partial y} = -\mathrm{j}kZH_z \tag{B.47}$$

$$\frac{\partial H_z}{\partial y} - \frac{\partial H_y}{\partial z} = \mathrm{j}kY E_x \tag{B.48}$$

$$\frac{\partial H_x}{\partial z} + k_x H_z = \mathrm{j}kY E_y \tag{B.49}$$

$$- k_x H_y - \frac{\partial H_x}{\partial y} = \mathrm{j}kY E_z. \tag{B.50}$$

In the following subsections, the field components E_y, H_y, E_z, H_z will be expressed as functions of the derivatives of the E_x and H_x components, which are used as Hertz potentials of this formulation.

Derivation of E_z

From (B.46) and (B.50), the following expression is derived:

$$H_y = -\frac{1}{k_x}\left[\mathrm{j}kY E_z + \frac{\partial H_x}{\partial y}\right]$$

$$H_y = -\frac{1}{\mathrm{j}kZ}\left[\frac{\partial E_x}{\partial z} - k_x E_z\right].$$

So, by equating these two expressions, the following equation leads:

$$-k_x\frac{\partial E_x}{\partial z} + k_x^2 E_z = k^2 E_z - \mathrm{j}kZ\frac{\partial H_x}{\partial y},$$

which becomes:

$$E_z = \frac{1}{k^2 - k_x^2}\left[\mathrm{j}kZ\frac{\partial H_x}{\partial y} - k_x\frac{\partial E_x}{\partial z}\right].$$

Derivation of H_z

The expressions of E_y are derived from (B.47) and (B.49):

$$E_y = \frac{1}{\mathrm{j}kY}\left[\frac{\partial H_x}{\partial z} + k_x H_z\right]$$

$$E_y = \frac{1}{k_x}\left[-\mathrm{j}kZ H_z + \frac{\partial E_x}{\partial y}\right].$$

These two expressions are equated, leading to

$$\mathrm{j}kY\frac{\partial E_x}{\partial y} + k^2 H_z = k_x\frac{\partial H_x}{\partial z} + k_x^2 H_z,$$

which becomes:

$$H_z = \frac{1}{k^2 - k_x^2}\left[k_x\frac{\partial H_x}{\partial z} - \mathrm{j}kY\frac{\partial E_x}{\partial y}\right].$$

Derivation of E_y

The expressions of H_z are derived from (B.47) and (B.49):

$$H_z = -\frac{1}{\mathrm{j}kZ}\left[k_x E_y - \frac{\partial E_x}{\partial y}\right]$$

$$H_z = \frac{1}{k_x}\left[\mathrm{j}kY E_y - \frac{\partial H_x}{\partial z}\right].$$

These two expressions are equated, leading to

$$k^2 E_y + \mathrm{j}kZ\frac{\partial H_x}{\partial z} = k_x^2 E_y - k_x\frac{\partial E_x}{\partial y},$$

which becomes:

$$E_y = \frac{1}{k^2 - k_x^2}\left[-k_x\frac{\partial E_x}{\partial y} - \mathrm{j}kZ\frac{\partial H_x}{\partial z}\right].$$

Derivation of H_y

The expressions of E_z are derived from (B.46) and (B.50):

$$E_z = \frac{1}{k_x}\left[\mathrm{j}kZH_y + \frac{\partial E_x}{\partial z}\right]$$

$$E_z = \frac{1}{\mathrm{j}kY}\left[-k_x H_y - \frac{\partial H_x}{\partial y}\right].$$

These two expressions are equated, leading to

$$\mathrm{j}kY\frac{\partial E_x}{\partial z} - k^2 H_y = -k_x^2 H_y - k_x\frac{\partial H_x}{\partial y},$$

which leads to:

$$H_y = \frac{1}{k^2 - k_x^2}\left[\mathrm{j}kY\frac{\partial E_x}{\partial z} + k_x\frac{\partial H_x}{\partial y}\right].$$

Resume of the expressions of the field components

The expressions derived in the previous subsections are now summarized:

$$E_y = \frac{1}{k^2 - k_x^2}\left[-k_x\frac{\partial E_x}{\partial y} - \mathrm{j}kZ\frac{\partial H_x}{\partial z}\right] \tag{B.51}$$

$$E_z = \frac{1}{k^2 - k_x^2}\left[\mathrm{j}kZ\frac{\partial H_x}{\partial y} - k_x\frac{\partial E_x}{\partial z}\right] \tag{B.52}$$

$$H_y = \frac{1}{k^2 - k_x^2}\left[\mathrm{j}kY\frac{\partial E_x}{\partial z} + k_x\frac{\partial H_x}{\partial y}\right] \tag{B.53}$$

$$H_z = \frac{1}{k^2 - k_x^2}\left[k_x\frac{\partial H_x}{\partial z} - \mathrm{j}kY\frac{\partial E_x}{\partial y}\right]. \tag{B.54}$$

B.3.1 Formulation of the internal BVP: E-plane devices

Considering (B.45) and (B.48), the weak formulation is now built as it follows:

$$\iint_{\Sigma} \left[\frac{\partial E_z}{\partial y} - \frac{\partial E_y}{\partial z} \right] v_r^{(\mathrm{h})*} \, \mathrm{d}z \, \mathrm{d}x = -\mathrm{j}kZ \iint_{\Sigma} H_x v_r^{(\mathrm{h})*} \, \mathrm{d}z \, \mathrm{d}x$$

$$\iint_{\Sigma} \left[\frac{\partial H_z}{\partial y} - \frac{\partial H_y}{\partial z} \right] v_r^{(\mathrm{e})*} \, \mathrm{d}z \, \mathrm{d}x = \mathrm{j}kY \iint_{\Sigma} E_x v_r^{(\mathrm{e})*} \, \mathrm{d}z \, \mathrm{d}x$$

where the test functions $v_r^{(\mathrm{h})}$ and $v_r^{(\mathrm{e})}$ belong to the following function spaces:

$$V^{(\mathrm{h})} \triangleq \left\{ v_r^{(\mathrm{h})} \; : r \in \mathbb{N}, \; v_r^{(\mathrm{h})} \in \mathrm{C}^{(0)}(\Sigma), \frac{\partial v_r^{(\mathrm{h})}}{\partial x}, \frac{\partial v_r^{(\mathrm{h})}}{\partial z} \in L^2(\Sigma \setminus \partial \Sigma) \right\},$$

$$V^{(\mathrm{e})} \triangleq \left\{ v_r^{(\mathrm{e})} \; : r \in \mathbb{N}, \; v_r^{(\mathrm{e})} \in \mathrm{C}^{(0)}(\Sigma), \frac{\partial v_r^{(\mathrm{e})}}{\partial x}, \frac{\partial v_r^{(\mathrm{e})}}{\partial z} \in L^2(\Sigma \setminus \partial \Sigma), v_r^{(\mathrm{e})}\big|_{\gamma_{\mathrm{PEC}}} = 0 \right\}.$$

Both $V^{(\mathrm{h})}$ and $V^{(\mathrm{e})}$ contain continuous functions with square-integrable derivatives; additionally, the functions in $V^{(\mathrm{e})}$ are further specialized to satisfy the homogeneous Dirichlet boundary condition on γ_{PEC}. Then, the following vector theorem is applied to the weak-formulated equations:

$$\iint_{\Sigma} \left[\frac{\partial A_y}{\partial z} - \frac{\partial A_z}{\partial y} \right] f \, \mathrm{d}z \, \mathrm{d}y = -\iint_{\Sigma} \left[A_y \frac{\partial f}{\partial z} - A_z \frac{\partial f}{\partial y} \right] \mathrm{d}z \, \mathrm{d}y + \oint_{\gamma} (f \mathbf{A}) \cdot \mathrm{d}\mathbf{s}.$$

Focusing on the first equation, the following expression is obtained:

$$\mathrm{j}kZ \iint_{\Sigma} H_x v_r^{(\mathrm{h})*} \, \mathrm{d}z \, \mathrm{d}x - \iint_{\Sigma} \left[E_z \frac{\partial v_r^{(\mathrm{h})*}}{\partial y} - E_y \frac{\partial v_r^{(\mathrm{h})*}}{\partial z} \right] \mathrm{d}z \, \mathrm{d}x = \oint_{\gamma} (\mathbf{E}_{\mathrm{t}}^{(x)} v_r^{(\mathrm{h})*}) \cdot \mathrm{d}\mathbf{s}$$

$$(\mathrm{LHS})_r^{(\mathrm{h})} = (\mathrm{RHS})_r^{(\mathrm{h})}. \qquad (\mathrm{B}.55)$$

The unknowns E_x, H_x are represented using the following expansions:

$$H_x(z,y) = \sum_{c=1}^{N_{\mathrm{f}}^{(\mathrm{h})}} c_c^{(\mathrm{h})} u_c^{(\mathrm{h})}(z,y) \qquad (\mathrm{B}.56)$$

$$E_x(z,y) = \sum_{c=1}^{N_{\mathrm{f}}^{(\mathrm{e})}} c_c^{(\mathrm{e})} u_c^{(\mathrm{e})}(z,y), \qquad (\mathrm{B}.57)$$

where $u_c^{(e)} = v_c^{(e)}, u_c^{(h)} = v_c^{(h)}$. Equations (B.51), (B.52) are then substituted in (B.55), leading to:

$$
\begin{aligned}
(\text{LHS})_r^{(h)} = {} & jkZ \sum_{c=1}^{N_f^{(h)}} c_c^{(h)} \iint_{\Sigma} u_c^{(h)} v_r^{(h)*} \,\mathrm{d}z\,\mathrm{d}x + \\
& - \frac{jkZ}{k^2 - k_x^2} \sum_{c=1}^{N_f^{(h)}} c_c^{(h)} \iint_{\Sigma} \frac{\partial u_c^{(h)}}{\partial y} \frac{\partial v_r^{(h)*}}{\partial y} \,\mathrm{d}z\,\mathrm{d}x + \\
& + \frac{k_x}{k^2 - k_x^2} \sum_{c=1}^{N_f^{(e)}} c_c^{(e)} \iint_{\Sigma} \frac{\partial u_c^{(e)}}{\partial z} \frac{\partial v_r^{(h)*}}{\partial y} \,\mathrm{d}z\,\mathrm{d}x + \\
& - \frac{k_x}{k^2 - k_x^2} \sum_{c=1}^{N_f^{(e)}} c_c^{(e)} \iint_{\Sigma} \frac{\partial u_c^{(e)}}{\partial y} \frac{\partial v_r^{(h)*}}{\partial z} \,\mathrm{d}z\,\mathrm{d}x + \\
& - \frac{jkZ}{k^2 - k_x^2} \sum_{c=1}^{N_f^{(h)}} c_c^{(h)} \iint_{\Sigma} \frac{\partial u_c^{(h)}}{\partial z} \frac{\partial v_r^{(h)*}}{\partial z} \,\mathrm{d}z\,\mathrm{d}x.
\end{aligned}
$$

Then, after some arrangement, the following expression is obtained.

$$
\begin{aligned}
(\text{LHS})_r^{(h)} = {} & jkZ \sum_{c=1}^{N_f^{(h)}} c_c^{(h)} \iint_{\Sigma} u_c^{(h)} v_r^{(h)*} \,\mathrm{d}z\,\mathrm{d}x + \\
& - \frac{jkZ}{k^2 - k_x^2} \sum_{c=1}^{N_f^{(h)}} c_c^{(h)} \iint_{\Sigma} \left[\frac{\partial u_c^{(h)}}{\partial y} \frac{\partial v_r^{(h)*}}{\partial y} + \frac{\partial u_c^{(h)}}{\partial z} \frac{\partial v_r^{(h)*}}{\partial z} \right] \,\mathrm{d}z\,\mathrm{d}x + \\
& + \frac{k_x}{k^2 - k_x^2} \sum_{c=1}^{N_f^{(e)}} c_c^{(e)} \iint_{\Sigma} \left[\frac{\partial u_c^{(e)}}{\partial y} \frac{\partial v_r^{(h)*}}{\partial z} - \frac{\partial u_c^{(e)}}{\partial z} \frac{\partial v_r^{(h)*}}{\partial y} \right] \,\mathrm{d}z\,\mathrm{d}x.
\end{aligned}
$$

By defining:

$$
\begin{aligned}
(\mathbf{M}^{(h)})_{rc} &= \iint_{\Sigma} u_c^{(h)} v_r^{(h)*} \,\mathrm{d}z\,\mathrm{d}x \\
(\mathbf{K}^{(h)})_{rc} &= \iint_{\Sigma} \left[\frac{\partial u_c^{(h)}}{\partial y} \frac{\partial v_r^{(h)*}}{\partial y} + \frac{\partial u_c^{(h)}}{\partial z} \frac{\partial v_r^{(h)*}}{\partial z} \right] \,\mathrm{d}z\,\mathrm{d}x \\
(\mathbf{L}^{(h)})_{rc} &= \iint_{\Sigma} \left[\frac{\partial u_c^{(e)}}{\partial y} \frac{\partial v_r^{(h)*}}{\partial z} - \frac{\partial u_c^{(e)}}{\partial z} \frac{\partial v_r^{(h)*}}{\partial y} \right] \,\mathrm{d}z\,\mathrm{d}x,
\end{aligned}
$$

it is possible to write compactly the equation as:

$$(\text{LHS})_r^{(\text{h})} = -\frac{k_x}{k^2 - k_x^2}\mathbf{L}^{(\text{h})}\,\mathbf{c}^{(\text{e})} + \frac{\mathrm{j}kZ}{k^2 - k_x^2}\left[(k^2 - k_x^2)\mathbf{M}^{(\text{h})} - \mathbf{K}^{(\text{h})}\right]\mathbf{c}^{(\text{h})} =$$
$$= \mathbf{A}^{(\text{h,e})}\,\mathbf{c}^{(\text{e})} + \mathbf{A}^{(\text{h,h})}\,\mathbf{c}^{(\text{h})}.$$

With similar steps, by defining the following matrices:

$$(\mathbf{M}^{(\text{e})})_{rc} = \iint_\Sigma u_c^{(\text{e})} v_r^{(\text{e})*}\,\mathrm{d}z\,\mathrm{d}x$$

$$(\mathbf{K}^{(\text{e})})_{rc} = \iint_\Sigma \left[\frac{\partial u_c^{(\text{e})}}{\partial y}\frac{\partial v_r^{(\text{e})*}}{\partial y} + \frac{\partial u_c^{(\text{e})}}{\partial z}\frac{\partial v_r^{(\text{e})*}}{\partial z}\right]\mathrm{d}z\,\mathrm{d}x$$

$$(\mathbf{L}^{(\text{e})})_{rc} = \iint_\Sigma \left[\frac{\partial u_c^{(\text{h})}}{\partial y}\frac{\partial v_r^{(\text{e})*}}{\partial z} - \frac{\partial u_c^{(\text{h})}}{\partial z}\frac{\partial v_r^{(\text{e})*}}{\partial y}\right]\mathrm{d}z\,\mathrm{d}x,$$

the remaining equation is written as:

$$(\text{LHS})_r^{(\text{e})} = -\frac{\mathrm{j}kY}{k^2 - k_x^2}\left[(k^2 - k_x^2)\mathbf{M}^{(\text{e})} - \mathbf{K}^{(\text{e})}\right]\mathbf{c}^{(\text{e})} + \frac{k_x}{k^2 - k_x^2}\mathbf{L}^{(\text{e})}\,\mathbf{c}^{(\text{h})} =$$
$$= \mathbf{A}^{(\text{e,e})}\,\mathbf{c}^{(\text{e})} + \mathbf{A}^{(\text{e,h})}\,\mathbf{c}^{(\text{h})}.$$

Formulation of the continuity equations

In this section the guidelines for the derivation of the projection matrix elements related to the continuity equations at the access ports are reported, to complete the formulation of the scattering problem. The scalar products used in this context are defined, at the k-th access port, as:

$$\langle \mathbf{a}, \mathbf{b}\rangle = \frac{a}{2}\int_0^{b^{(k)}} \mathbf{a}(z, y)\cdot\mathbf{b}^*(z, y)\,\mathrm{d}y.$$

Continuity of the electric field

The electric field continuity equation at the k-th access port is:

$$\left\langle \widehat{\mathbf{E}}_{\text{t}}^{(k)}, \mathbf{e}_q^{(k)}\right\rangle = \left\langle \widetilde{\mathbf{E}}_{\text{t}}^{(k)}, \mathbf{e}_q^{(k)}\right\rangle,$$

where:

$$\left\langle \widetilde{\mathbf{E}}_{\text{t}}^{(k)}, \mathbf{e}_q^{(k)}\right\rangle = \left\langle \widetilde{E}_y^{(k)}, e_{y,q}^{(k)}\right\rangle + \left\langle \widetilde{E}_x^{(k)}, e_{x,q}^{(k)}\right\rangle.$$

Then, recalling (B.51):

$$\left\langle \widetilde{E}_y^{(k)}, e_{y,q}^{(k)} \right\rangle = -\frac{k_x}{k^2 - k_x^2} \sum_{c=1}^{N_{\mathrm{f}}^{(\mathrm{e})}} c_c^{(\mathrm{e})} \left\langle \left.\frac{\partial u_c^{(\mathrm{e})}}{\partial y}\right|_{z=z_{\mathrm{wg}}^{(k)}}, e_{y,q}^{(k)} \right\rangle +$$

$$-\frac{\mathrm{j}kZ}{k^2 - k_x^2} \sum_{c=1}^{N_{\mathrm{f}}^{(\mathrm{h})}} c_c^{(\mathrm{h})} \left\langle \left.\frac{\partial u_c^{(\mathrm{h})}}{\partial z}\right|_{z=z_{\mathrm{wg}}^{(k)}}, e_{y,q}^{(k)} \right\rangle$$

$$\left\langle \widetilde{E}_x^{(k)}, e_{x,q}^{(k)} \right\rangle = \sum_{c=1}^{N_{\mathrm{f}}^{(\mathrm{e})}} c_c^{(\mathrm{e})} \left\langle \left.u_c^{(\mathrm{e})}\right|_{z=z_{\mathrm{wg}}^{(k)}}, e_{x,q}^{(k)} \right\rangle .$$

So, the following matrix elements are defined:

$$\begin{cases} (\mathbf{C}^{(\mathrm{e},k)})_{qc} = \left\langle \left.u_c^{(\mathrm{e})}\right|_{z=z_{\mathrm{wg}}^{(k)}}, e_{x,q}^{(k)} \right\rangle \\[2ex] (\mathbf{H}^{(\mathrm{e},k)})_{qc} = \left\langle \left.\dfrac{\partial u_c^{(\mathrm{e})}}{\partial y}\right|_{z=z_{\mathrm{wg}}^{(k)}}, e_{y,q}^{(k)} \right\rangle \\[3ex] (\mathbf{K}^{(\mathrm{h},k)})_{qc} = \left\langle \left.\dfrac{\partial u_c^{(\mathrm{h})}}{\partial z}\right|_{z=z_{\mathrm{wg}}^{(k)}}, e_{y,q}^{(k)} \right\rangle , \end{cases} \tag{B.58}$$

and it is possible to write the projection term of the equation in matrix form as:

$$\left[\mathbf{C}^{(\mathrm{e},k)} - \frac{k_x}{k^2 - k_x^2}\mathbf{H}^{(\mathrm{e},k)}\right]\mathbf{c}^{(\mathrm{e})} - \frac{\mathrm{j}kZ}{k^2 - k_x^2}\mathbf{K}^{(\mathrm{h},k)}\mathbf{c}^{(\mathrm{h})}$$
$$\mathbf{T}_k^{(\mathrm{e},\mathrm{e})}\mathbf{c}^{(\mathrm{e})} + \mathbf{T}_k^{(\mathrm{e},\mathrm{h})}\mathbf{c}^{(\mathrm{h})} . \tag{B.59}$$

Continuity of the magnetic field

The magnetic field continuity equation at the k-th access port is:

$$\left\langle \widehat{\mathbf{H}}_{\mathrm{t}}^{(k)}, \mathbf{h}_q^{(k)} \right\rangle = \left\langle \widetilde{\mathbf{H}}_{\mathrm{t}}^{(k)}, \mathbf{h}_q^{(k)} \right\rangle ,$$

where:

$$\left\langle \widetilde{\mathbf{H}}_{\mathrm{t}}^{(k)}, \mathbf{h}_q^{(k)} \right\rangle = \left\langle \widetilde{H}_y^{(k)}, h_{y,q}^{(k)} \right\rangle + \left\langle \widetilde{H}_x^{(k)}, h_{x,q}^{(k)} \right\rangle .$$

Then, recalling (B.53):

$$\left\langle \widetilde{H}_y^{(k)}, h_{y,q}^{(k)} \right\rangle = \frac{k_x}{k^2 - k_x^2} \sum_{c=1}^{N_{\mathrm{f}}^{(\mathrm{h})}} c_c^{(\mathrm{h})} \left\langle \left. \frac{\partial u_c^{(\mathrm{h})}}{\partial y} \right|_{z=z_{\mathrm{wg}}^{(k)}}, h_{y,q}^{(k)} \right\rangle +$$

$$\frac{\mathrm{j}kY}{k^2 - k_x^2} \sum_{c=1}^{N_{\mathrm{f}}^{(\mathrm{e})}} c_c^{(\mathrm{e})} \left\langle \left. \frac{\partial u_c^{(\mathrm{e})}}{\partial z} \right|_{z=z_{\mathrm{wg}}^{(k)}}, h_{y,q}^{(k)} \right\rangle$$

$$\left\langle \widetilde{H}_x^{(k)}, h_{x,q}^{(k)} \right\rangle = \sum_{c=1}^{N_{\mathrm{f}}^{(\mathrm{h})}} c_c^{(\mathrm{h})} \left\langle \left. u_c^{(\mathrm{h})} \right|_{z=z_{\mathrm{wg}}^{(k)}}, h_{x,q}^{(k)} \right\rangle.$$

So, the following matrix elements are defined:

$$\begin{cases} (\mathbf{C}^{(\mathrm{h},k)})_{qc} = \left\langle \left. u_c^{(\mathrm{h})} \right|_{z=z_{\mathrm{wg}}^{(k)}}, h_{x,q}^{(k)} \right\rangle \\[2mm] (\mathbf{H}^{(\mathrm{h},k)})_{qc} = \left\langle \left. \frac{\partial u_c^{(\mathrm{h})}}{\partial y} \right|_{z=z_{\mathrm{wg}}^{(k)}}, h_{y,q}^{(k)} \right\rangle \\[2mm] (\mathbf{K}^{(\mathrm{e},k)})_{qc} = \left\langle \left. \frac{\partial u_c^{(\mathrm{h})}}{\partial z} \right|_{z=z_{\mathrm{wg}}^{(k)}}, h_{y,q}^{(k)} \right\rangle, \end{cases} \tag{B.60}$$

and it is possible to write the projection term of the equation in matrix form as:

$$\frac{\mathrm{j}kY}{k^2 - k_x^2} \mathbf{K}^{(\mathrm{e},k)} \mathbf{c}^{(\mathrm{e})} + \left[\mathbf{C}^{(\mathrm{h},k)} + \frac{k_x}{k^2 - k_x^2} \mathbf{H}^{(\mathrm{h},k)} \right] \mathbf{c}^{(\mathrm{h})}$$
$$\mathbf{T}_k^{(\mathrm{h},\mathrm{e})} \mathbf{c}^{(\mathrm{e})} + \mathbf{T}_k^{(\mathrm{h},\mathrm{h})} \mathbf{c}^{(\mathrm{h})}. \tag{B.61}$$

B.3.2 Formulation of the internal BVP: homogeneous E-plane devices

In this section the formulation of the differential problem for E-plane devices filled with homogeneous dielectric is reported. Assuming that the exciting field of the structure is given by a combination of $\mathrm{LSE}_{1n}^{(x)}$ modes and that the zy section of the structure is filled with homogeneous dielectric, $E_x = 0$ in every point of the structure. In this case, the vector problem is reduced to a scalar one characterized by (B.45), (B.51), (B.52), here reported with $E_x = 0$:

$$\frac{\partial E_z}{\partial y} - \frac{\partial E_y}{\partial z} = -\mathrm{j}kZH_x$$
$$E_y = \frac{-\mathrm{j}kZ}{k^2 - k_x^2} \frac{\partial H_x}{\partial z}$$
$$E_z = \frac{\mathrm{j}kZ}{k^2 - k_x^2} \frac{\partial H_x}{\partial y}.$$

A weak differential problem is now built by testing the first equation on functions $\{v_r^{(\mathrm{h})}\}$ defined in the previous section:

$$\iint_{\Sigma} \left[\frac{\partial E_z}{\partial y} - \frac{\partial E_y}{\partial z} \right] v_r^{(\mathrm{h})*} \, \mathrm{d}z \, \mathrm{d}x = -\mathrm{j}kZ \iint_{\Sigma} H_x v_r^{(\mathrm{h})*} \, \mathrm{d}z \, \mathrm{d}x.$$

The Stokes theorem is now appled to integrate by parts this equation, leading to:

$$\mathrm{j}kZ \iint_{\Sigma} H_x v_r^{(\mathrm{h})*} \, \mathrm{d}z \, \mathrm{d}x - \iint_{\Sigma} \left[E_z \frac{\partial v_r^{(\mathrm{h})*}}{\partial y} - E_y \frac{\partial v_r^{(\mathrm{h})*}}{\partial z} \right] \mathrm{d}z \, \mathrm{d}x = \oint_{\gamma} (\mathbf{E}_{\mathrm{t}}^{(x)} v_r^{(\mathrm{h})*}) \cdot \mathrm{d}\mathbf{s}$$

$$(\mathrm{LHS})_r^{(\mathrm{h})} = (\mathrm{RHS})_r^{(\mathrm{h})}.$$

By substituting the expressions of the components in this equation, the left-hand side term is written as:

$$(\mathrm{LHS})_r^{(\mathrm{h})} = \mathrm{j}kZ \left\{ \iint_{\Sigma} H_x v_r^{(\mathrm{h})*} \, \mathrm{d}z \, \mathrm{d}x + \right.$$
$$\left. - \iint_{\Sigma} \frac{1}{k^2 - k_x^2} \left[\frac{\partial H_x}{\partial y} \frac{\partial v_r^{(\mathrm{h})*}}{\partial y} + \frac{\partial H_x}{\partial z} \frac{\partial v_r^{(\mathrm{h})*}}{\partial z} \right] \mathrm{d}z \, \mathrm{d}x \right\}.$$

The unknown H_x is represented as in (B.56):

$$H_x(z, y) = \sum_{c=1}^{N_{\mathrm{f}}^{(\mathrm{h})}} c_c^{(\mathrm{h})} u_c^{(\mathrm{h})}(z, y),$$

therefore,

$$\mathrm{j}kZ \sum_{c=1}^{N_{\mathrm{f}}^{(\mathrm{h})}} c_c^{(\mathrm{h})} \left\{ \iint_{\Sigma} u_c^{(\mathrm{h})} v_r^{(\mathrm{h})*} \, \mathrm{d}z \, \mathrm{d}x + \right.$$
$$\left. - \frac{1}{k^2 - k_x^2} \iint_{\Sigma} \left[\frac{\partial u_c^{(\mathrm{h})}}{\partial y} \frac{\partial v_r^{(\mathrm{h})*}}{\partial y} + \frac{\partial u_c^{(\mathrm{h})}}{\partial z} \frac{\partial v_r^{(\mathrm{h})*}}{\partial z} \right] \mathrm{d}z \, \mathrm{d}x \right\}.$$

For what concerns the right-hand side line integrals, they are treated as described in Section 1.2, where PEC is used to fill the zero-field regions, to eliminate the contributions of the electric current densities. According to this formulation, the line integrals are written in matrix form as follows:

$$(\mathbf{B}^{(\mathrm{h},k)})_{rn} = \int_0^{b^{(k)}} e_{y,n}^{(k)} v_r^{(\mathrm{h})*} \bigg|_{z=z_{\mathrm{wg}}^{(k)}} \mathrm{d}y$$

So, the discretized equation is compactly written in matrix form as:

$$\mathbf{A}^{(\mathrm{h,h})}\,\mathbf{c}^{(\mathrm{h})} = \mathbf{B}^{(\mathrm{h},2)}\mathring{\mathbf{v}}^{(2)} - \mathbf{B}^{(\mathrm{h},1)}\mathring{\mathbf{v}}^{(1)},$$

where:

$$\mathbf{A}^{(\mathrm{h,h})} = \mathrm{j}kZ\left[\mathbf{M}^{(\mathrm{h})} - \frac{1}{k^2 - k_x^2}\mathbf{K}^{(\mathrm{h})}\right],$$

and:

$$\mathbf{M}^{(\mathrm{h})} = \iint_{\Sigma} u_c^{(\mathrm{h})}v_r^{(\mathrm{h})*}\,\mathrm{d}z\,\mathrm{d}x$$

$$\mathbf{K}^{(\mathrm{h})} = \iint_{\Sigma}\left[\frac{\partial u_c^{(\mathrm{h})}}{\partial y}\frac{\partial v_r^{(\mathrm{h})*}}{\partial y} + \frac{\partial u_c^{(\mathrm{h})}}{\partial z}\frac{\partial v_r^{(\mathrm{h})*}}{\partial z}\right]\,\mathrm{d}z\,\mathrm{d}x$$

Formulation of the continuity equations

The electric field continuity is automatically satisfied by the choice of the magnetic current densities at the access ports, as discussed in Chapter 1; therefore, to complete the formulation of the problem the continuity of the tangent magnetic field continuity has to be enforced. Since $\mathbf{H}_{\mathrm{t}} = \widehat{\mathbf{x}}H_x$, the continuity condition that should be enforced is:

$$\left\langle \widehat{H}_x^{(k)}, h_{x,q}^{(k)}\right\rangle = \left\langle \widetilde{H}_x^{(k)}, h_{x,q}^{(k)}\right\rangle,$$

which is written explicitly as:

$$\frac{a}{2}\int_0^{b^{(k)}} \widehat{H}_x^{(k)}h_{x,q}^{(k)*}\mathrm{d}y = \frac{a}{2}\sum_{c=0}^{N_{\mathrm{f}}^{(\mathrm{h})}} c_c^{(\mathrm{h})}\int_0^{b^{(k)}} \widetilde{H}_x^{(k)}h_{x,q}^{(k)*}\mathrm{d}y,$$

so, the right-hand side of this condition is written as:

$$\frac{a}{2}\sum_{c=0}^{N_{\mathrm{f}}^{(\mathrm{h})}} c_c^{(\mathrm{h})}\int_0^{b^{(k)}} u_c^{(\mathrm{h})}h_{x,q}^{(k)*}\,\mathrm{d}y = \mathbf{C}^{(\mathrm{h},k)}\,\mathbf{c}^{(\mathrm{h})},$$

and so:

$$\mathbf{T}_k^{(\mathrm{h})} = \mathbf{C}^{(\mathrm{h},k)},$$

where:

$$(\mathbf{C}^{(\mathrm{h},k)})_{qc} = \frac{a}{2}\int_0^{b^{(k)}} u_c^{(\mathrm{h})}h_{x,q}^{(k)*}\mathrm{d}y.$$

B.3.3 Formulation of the internal BVP: H-plane devices

Assuming that the incident field is a combination of $\text{LSM}_{0n}^{(x)}$ modes, $H_x = 0$ in every point of the structure, independently on the presence of non-homogeneous dielectrics; indeed, the field does not have any variation along x, therefore no mode coupling may occur. In this case, the problem is scalar, and it is characterized by (B.48), (B.53), (B.54), here reported for $\xi_0 = 0$:

$$
\frac{\partial H_z}{\partial y} - \frac{\partial H_y}{\partial z} = \mathrm{j}kY E_x
$$

$$
H_y = -\frac{1}{\mathrm{j}kZ}\frac{\partial E_x}{\partial z}
$$

$$
H_z = \frac{1}{\mathrm{j}kZ}\frac{\partial E_x}{\partial y}
$$

A weak differential problem is now built by projecting the first equation on functions $\{v_r^{(\mathrm{e})}\}$ belonging to the function space $V^{(\mathrm{e})}$ defined as in the previous section:

$$
-\mathrm{j}kY \iint_{\Sigma} E_x v_r^{(\mathrm{e})*}\,\mathrm{d}z\,\mathrm{d}x - \iint_{\Sigma}\left[H_z\frac{\partial v_r^{(\mathrm{e})*}}{\partial y} - H_y\frac{\partial v_r^{(\mathrm{e})*}}{\partial z}\right]\mathrm{d}z\,\mathrm{d}x = \oint_{\gamma}(\mathbf{H}_{\mathrm{t}}^{(x)}v_r^{(\mathrm{e})*})\cdot\mathrm{d}\mathbf{s}
$$

$$
(\mathrm{LHS})_r^{(\mathrm{e})} = (\mathrm{RHS})_r^{(\mathrm{e})}.
$$

So, by substituting the expressions of the components in this equation, the left-hand side term is written as:

$$
(\mathrm{LHS})_r^{(\mathrm{e})} = -\mathrm{j}kY\left\{\iint_{\Sigma}E_x v_r^{(\mathrm{e})*}\,\mathrm{d}z\,\mathrm{d}x + \right.
$$
$$
\left. -\iint_{\Sigma}\frac{1}{k^2}\left[\frac{\partial E_x}{\partial y}\frac{\partial v_r^{(\mathrm{e})*}}{\partial y} + \frac{\partial E_x}{\partial z}\frac{\partial v_r^{(\mathrm{e})*}}{\partial z}\right]\mathrm{d}z\,\mathrm{d}x\right\}.
$$

The unknown E_x is represented as in (B.56); therefore,

$$
-\mathrm{j}kY\sum_{c=1}^{N_{\mathrm{f}}^{(\mathrm{e})}} c_c^{(\mathrm{e})}\left\{\iint_{\Sigma}u_c^{(\mathrm{e})}v_r^{(\mathrm{e})*}\,\mathrm{d}z\,\mathrm{d}x + \right.
$$
$$
\left. -\frac{1}{k^2}\iint_{\Sigma}\left[\frac{\partial u_c^{(\mathrm{e})}}{\partial y}\frac{\partial v_r^{(\mathrm{e})*}}{\partial y} + \frac{\partial u_c^{(\mathrm{e})}}{\partial z}\frac{\partial v_r^{(\mathrm{e})*}}{\partial z}\right]\mathrm{d}z\,\mathrm{d}x\right\}.
$$

For what concerns the right-hand side line integrals, they are treated as described in Section 1.2, where PMC is used to fill the zero-field regions, to eliminate the

contributions of the magnetic current densities. According to this formulation, the line integrals are written in matrix form as follows:

$$(\mathbf{B}^{(\mathrm{e},k)})_{rn} = \int_0^{b^{(k)}} h_{y,n}^{(k)} v_r^{(\mathrm{e})*} \bigg|_{z=z_{\mathrm{wg}}^{(k)}} \mathrm{d}y$$

So, the discretized equation is compactly written in matrix form as:

$$\mathbf{A}^{(\mathrm{e},\mathrm{e})}\, \mathbf{c}^{(\mathrm{e})} = \mathbf{B}^{(\mathrm{e},2)}\mathring{\mathbf{i}}^{(2)} - \mathbf{B}^{(\mathrm{e},1)}\mathring{\mathbf{i}}^{(1)},$$

where:

$$\mathbf{A}^{(\mathrm{e},\mathrm{e})} = -\mathrm{j}kY\left[\mathbf{M}^{(\mathrm{e})} - \frac{1}{k^2}\mathbf{K}^{(\mathrm{e})}\right],$$

and:

$$\mathbf{M}^{(\mathrm{e})} = \iint_\Sigma u_c^{(\mathrm{e})} v_r^{(\mathrm{e})*}\, \mathrm{d}z\, \mathrm{d}x$$

$$\mathbf{K}^{(\mathrm{e})} = \iint_\Sigma \left[\frac{\partial u_c^{(\mathrm{e})}}{\partial y}\frac{\partial v_r^{(\mathrm{e})*}}{\partial y} + \frac{\partial u_c^{(\mathrm{e})}}{\partial z}\frac{\partial v_r^{(\mathrm{e})*}}{\partial z}\right]\, \mathrm{d}z\, \mathrm{d}x$$

Formulation of the continuity equations

The continuity of the magnetic field is automatically satisfied by the choice of the electric current densities at the access ports, as discussed in Chapter 1; therefore, to complete the formulation of the problem the continuity of the tangent magnetic field has to be enforced. Since $\mathbf{E}_\mathrm{t} = \widehat{\mathbf{x}}E_x$, the continuity condition that should be enforced is:

$$\left\langle \widehat{E}_x^{(k)}, e_{x,q}^{(k)}\right\rangle = \left\langle \widetilde{E}_x^{(k)}, e_{x,q}^{(k)}\right\rangle,$$

which is written explicitly as:

$$\frac{a}{2}\int_0^{b^{(k)}} \widehat{E}_x^{(k)} e_{x,q}^{(k)*}\, \mathrm{d}y = \frac{a}{2}\sum_{c=0}^{N_\mathrm{f}^{(\mathrm{e})}} c_c^{(\mathrm{e})}\int_0^{b^{(k)}} \widetilde{E}_x^{(k)} e_{x,q}^{(k)*}\, \mathrm{d}y,$$

so, the right-hand side of this condition is written as:

$$\frac{a}{2}\sum_{c=0}^{N_\mathrm{f}^{(\mathrm{e})}} c_c^{(\mathrm{e})}\int_0^{b^{(k)}} u_c^{(\mathrm{e})} e_{x,q}^{(k)*}\, \mathrm{d}y = \mathbf{C}^{(\mathrm{e},k)}\, \mathbf{c}^{(\mathrm{e})},$$

and so:

$$\mathbf{T}_k^{(\mathrm{e})} = \mathbf{C}^{(\mathrm{e},k)},$$

where:

$$(\mathbf{C}^{(\mathrm{e},k)})_{qc} = \frac{a}{2} \int_0^{b^{(k)}} u_c^{(\mathrm{e})} e_{x,q}^{(k)*} \, \mathrm{d}y.$$

Appendix of "Mortar element analysis of 2-D periodic structures"

C.1 Floquet mode functions

In this section the expressions of the Floquet modes used to represent the electromagnetic field in a phase-shift wall waveguide are derived. The potential functions $\Phi(x, y)$ and $\Psi(x, y)$ relative to TM and TE modes satisfy the Helmholtz equation:

$$\nabla_t \Phi(x, y) + k_t' \Phi(x, y) = 0$$
$$\nabla_t \Psi(x, y) + k_t' \Psi(x, y) = 0.$$

The free-space solutions of these equations are [10, Chap. 3]:

$$\Psi(x, y) = A\,\mathrm{e}^{-\mathrm{j}k_x x}\mathrm{e}^{-\mathrm{j}k_y y}$$
$$\Phi(x, y) = B\,\mathrm{e}^{-\mathrm{j}k_x x}\mathrm{e}^{-\mathrm{j}k_y y},$$

where $k_x, k_y \in \mathbb{R}$. Now, the free space is divided in sections parallel to y and distant a; then:

$$\Psi(x + a, y) = \Psi(x, y)\mathrm{e}^{-\mathrm{j}\phi} = A\,\mathrm{e}^{-\mathrm{j}k_x x}\mathrm{e}^{-\mathrm{j}k_y y}\mathrm{e}^{-\mathrm{j}\phi}$$
$$\Phi(x + a, y) = \Phi(x, y)\mathrm{e}^{-\mathrm{j}\phi} = B\,\mathrm{e}^{-\mathrm{j}k_x x}\mathrm{e}^{-\mathrm{j}k_y y}\mathrm{e}^{-\mathrm{j}\phi}.$$

This is a pseudo-periodicity condition with a phase shift ϕ. On the other hand:

$$\Psi(x + a, y) = A\,\mathrm{e}^{-\mathrm{j}k_x(x+a)}\mathrm{e}^{-\mathrm{j}k_y y}\mathrm{e}^{-\mathrm{j}\phi}$$
$$\Phi(x + a, y) = B\,\mathrm{e}^{-\mathrm{j}k_x(x+a)}\mathrm{e}^{-\mathrm{j}k_y y}\mathrm{e}^{-\mathrm{j}\phi}.$$

So, by equating the two last expressions, the following expressions are obtained:

$$A\,e^{-jk_x x}e^{-jk_y y}e^{-j\phi} = A\,e^{-jk_x(x+a)}e^{-jk_y y}e^{-j\phi}$$
$$B\,e^{-jk_x x}e^{-jk_y y}e^{-j\phi} = B\,e^{-jk_x(x+a)}e^{-jk_y y}e^{-j\phi}.$$

From here, the following phase equation is found:

$$k_x x + k_x a = k_x x + \phi + 2m\pi,$$

meaning that:

$$k_x = k_{x,m} = m\frac{2\pi}{a} + \frac{\phi}{a}, \quad m = 0, \pm1, \pm2...$$

In other words, k_x belongs to a discrete set. The potential functions Φ are now normalized:

$$||\Phi(x,y)||_2 = 1 \implies \int_0^a |\Phi|^2 \,\mathrm{d}x = A^2 \int_0^a \mathrm{d}x = A^2 a = 1,$$

leading to:

$$A = \frac{1}{\sqrt{a}};$$

so, the potential functions can be written as:

$$\Phi_m(x,y) = \Psi_m(x,y) = \frac{1}{\sqrt{a}}e^{-jk_{x,m}x}e^{-jk_y y}.$$

The expression of the phase-shift ϕ introduced by the unit cell is now derived. By assuming that the structure is excited by a plane wave identified by its wavevector $\mathbf{k}^{(\mathrm{inc})} = (k_x^{(\mathrm{inc})}, k_y^{(\mathrm{inc})}, k_z^{(\mathrm{inc})})$, where:

$$(k_x^{(\mathrm{inc})}, k_y^{(\mathrm{inc})}, k_z^{(\mathrm{inc})}) = k_0(\sin\vartheta\cos\varphi, \sin\vartheta\sin\varphi, \cos\vartheta).$$

So, $k_x^{(\mathrm{inc})}$ is found as

$$k_x^{(\mathrm{inc})} = k_0\sin\vartheta\cos\varphi,$$

where ϑ and φ are the zenith and azimuth incidence angles of the plane wave. Therefore, since the components of $\mathbf{k}^{(\mathrm{inc})}$ transverse to the propagation direction z have to be continuous,

$$\begin{cases} k_x = k_x^{(\mathrm{inc})} \\ k_y = k_y^{(\mathrm{inc})}; \end{cases}$$

so:

$$\mathrm{e}^{-\mathrm{j}k_x a} = \mathrm{e}^{-\mathrm{j}k_x^{(\mathrm{inc})}a} = \mathrm{e}^{-\mathrm{j}k_0 a \sin\vartheta \cos\varphi} = \mathrm{e}^{-\mathrm{j}\phi}.$$

Therefore:

$$\phi = k_0 a \sin\vartheta \cos\varphi.$$

C.1.1 Expressions of the Floquet mode functions

The eigenvalues of the Helmholtz equations are:

$$k'_{\mathrm{t},m} = k''_{\mathrm{t},m} = \sqrt{k_{x,m}^2 + k_y^2}.$$

So, from the definition of the potential functions,

$$\mathbf{e}'_m = -\frac{\nabla_{\mathrm{t}}\Phi_m(x,y)}{k'_{\mathrm{t},m}}, \quad \mathbf{h}'_m = \widehat{\mathbf{z}} \times \mathbf{e}'_m$$

$$\mathbf{h}''_m = -\frac{\nabla_{\mathrm{t}}\Psi_m(x,y)}{k''_{\mathrm{t},m}}, \quad \mathbf{e}''_m = \mathbf{h}''_m \times \widehat{\mathbf{z}}.$$

Then:

$$\mathbf{e}'_m = -\frac{1}{k'_{\mathrm{t},m}} \left[\widehat{\mathbf{x}}\frac{\partial\Phi_m}{\partial x} + \widehat{\mathbf{y}}\frac{\partial\Phi_m}{\partial y} \right] = \frac{\mathrm{j}}{\sqrt{a}} \left[\frac{k_{x,m}}{k'_{\mathrm{t},m}}\widehat{\mathbf{x}} + \frac{k_y}{k'_{\mathrm{t},m}}\widehat{\mathbf{y}} \right] \mathrm{e}^{-\mathrm{j}k_{x,m}x}\mathrm{e}^{-\mathrm{j}k_y y}$$

$$\mathbf{h}''_m = -\frac{1}{k'_{\mathrm{t},m}} \left[\widehat{\mathbf{x}}\frac{\partial\Psi_m}{\partial x} + \widehat{\mathbf{y}}\frac{\partial\Psi_m}{\partial y} \right] = \frac{\mathrm{j}}{\sqrt{a}} \left[\frac{k_{x,m}}{k''_{\mathrm{t},m}}\widehat{\mathbf{x}} + \frac{k_y}{k''_{\mathrm{t},m}}\widehat{\mathbf{y}} \right] \mathrm{e}^{-\mathrm{j}k_{x,m}x}\mathrm{e}^{-\mathrm{j}k_y y},$$

and:

$$\mathbf{h}'_m = \widehat{\mathbf{z}} \times \widetilde{\mathbf{e}}'_m = \frac{\mathrm{j}}{\sqrt{a}} \left[\frac{k_{x,m}}{k'_{\mathrm{t},m}}\widehat{\mathbf{y}} - \frac{k_y}{k'_{\mathrm{t},m}}\widehat{\mathbf{x}} \right] \mathrm{e}^{-\mathrm{j}k_{x,m}x}\mathrm{e}^{-\mathrm{j}k_y y}$$

$$\mathbf{e}''_m = \widehat{\mathbf{h}}''_m \times \widehat{\mathbf{z}} = \frac{\mathrm{j}}{\sqrt{a}} \left[-\frac{k_{x,m}}{k''_{\mathrm{t},m}}\widehat{\mathbf{y}} + \frac{k_y}{k''_{\mathrm{t},m}}\widehat{\mathbf{x}} \right] \mathrm{e}^{-\mathrm{j}k_{x,m}x}\mathrm{e}^{-\mathrm{j}k_y y}.$$

Resume of Floquet modes expressions

The expressions of the Floquet modes are now resumed:

$$e'_{x,m} = \frac{\mathrm{j}}{\sqrt{a}} \frac{k_{x,m}}{k'_{\mathrm{t},m}} \mathrm{e}^{-\mathrm{j}k_{x,m}x} \mathrm{e}^{-\mathrm{j}k_y y}$$

$$e'_{y,m} = \frac{\mathrm{j}}{\sqrt{a}} \frac{k_y}{k'_{\mathrm{t},m}} \mathrm{e}^{-\mathrm{j}k_{x,m}x} \mathrm{e}^{-\mathrm{j}k_y y}$$

$$h'_{x,m} = -\frac{\mathrm{j}}{\sqrt{a}} \frac{k_y}{k'_{\mathrm{t},m}} \mathrm{e}^{-\mathrm{j}k_{x,m}x} \mathrm{e}^{-\mathrm{j}k_y y}$$

$$h'_{y,m} = \frac{\mathrm{j}}{\sqrt{a}} \frac{k_{x,m}}{k'_{\mathrm{t},m}} \mathrm{e}^{-\mathrm{j}k_{x,m}x} \mathrm{e}^{-\mathrm{j}k_y y}$$

$$e''_{x,m} = \frac{\mathrm{j}}{\sqrt{a}} \frac{k_{x,m}}{k''_{\mathrm{t},m}} \mathrm{e}^{-\mathrm{j}k_{x,m}x} \mathrm{e}^{-\mathrm{j}k_y y}$$

$$e''_{y,m} = \frac{\mathrm{j}}{\sqrt{a}} \frac{k_y}{k''_{\mathrm{t},m}} \mathrm{e}^{-\mathrm{j}k_{x,m}x} \mathrm{e}^{-\mathrm{j}k_y y}$$

$$h''_{x,m} = \frac{\mathrm{j}}{\sqrt{a}} \frac{k_y}{k''_{\mathrm{t},m}} \mathrm{e}^{-\mathrm{j}k_{x,m}x} \mathrm{e}^{-\mathrm{j}k_y y}$$

$$h''_{y,m} = -\frac{\mathrm{j}}{\sqrt{a}} \frac{k_{x,m}}{k''_{\mathrm{t},m}} \mathrm{e}^{-\mathrm{j}k_{x,m}x} \mathrm{e}^{-\mathrm{j}k_y y}.$$

C.2 Synthesis of the basis functions

The synthesis procedure of the basis functions follows the one of Section 1.3. These functions should satisfy the pseudo-periodicity boundary condition:

$$u_c(z, a) = u_c(z, 0)\mathrm{e}^{-\mathrm{j}\phi}. \tag{C.1}$$

Let $f_\alpha(z, x)$ be the α-th entire domain basis function used to represent the solution of the boundary value problem. Then, it is possible to write the c-th basis function satisfying (C.1) as:

$$u_c(z, x) = \sum_\alpha y_\alpha^{(c)} f_\alpha(z, x);$$

then, both sides are tested on 1-D functions $T_\nu(z)$:

$$\langle u_c(z, x), T_\nu(z) \rangle = \sum_\alpha y_\alpha^{(c)} \langle f_\alpha(z, x), T_\nu(z) \rangle.$$

Therefore, given the following definitions:

$$(\mathbf{b}^{(c)}(x))_\nu = \langle u_c(z, x), T_\nu(z) \rangle,$$

and:

$$(\mathbf{L}^{(c)}(x))_{\nu\alpha} = \langle f_\alpha(z, x), T_\nu(z) \rangle,$$

the boundary condition (C.1) is written as:

$$\mathbf{b}^{(c)}(a) - \mathbf{b}^{(c)}(0)\mathrm{e}^{-\mathrm{j}\phi} = \mathbf{0}.$$

This can be re-written as:

$$\mathbf{L}^{(c)}(a)\mathbf{y}^{(c)} - \mathrm{e}^{-\mathrm{j}\phi}\mathbf{L}^{(c)}(0)\mathbf{y}^{(c)} = \mathbf{0},$$

which becomes:

$$\left[\mathbf{L}^{(c)}(a) - \mathrm{e}^{-\mathrm{j}\phi}\mathbf{L}^{(c)}(0)\right]\mathbf{y}^{(c)} = \mathbf{0}.$$

The recombination coefficients $\mathbf{y}^{(c)}$ are found by finding a basis of the kernel of the matrix $\left[\mathbf{L}^{(c)}(a) - \mathrm{e}^{-\mathrm{j}\phi}\mathbf{L}^{(c)}(0)\right]$. This can be found by following the procedure described in Section 1.3.

C.3 Field representation for 2-D periodic structures

C.3.1 Derivation of the relationships between the field components

In this section the equations used to describe the electromagnetic behavior of 2-D periodic structures excited by means of a plane wave are derived starting from the space-frequency Maxwell's curl equations (C.2):

$$\begin{cases} \nabla \times \mathbf{E}(\mathbf{r}, \omega) = -\mathrm{j}\omega\mu\mathbf{H}(\mathbf{r}, \omega) \\ \nabla \times \mathbf{H}(\mathbf{r}, \omega) = \mathrm{j}\omega\varepsilon\mathbf{E}(\mathbf{r}, \omega). \end{cases} \tag{C.2}$$

These equations are now written in cartesian coordinates; for the sake of compactness, from here on the dependence on space and frequency is omitted:

$$\frac{\partial E_z}{\partial y} - \frac{\partial E_y}{\partial z} = -\mathrm{j}\omega\mu H_x$$

$$\frac{\partial E_x}{\partial z} - \frac{\partial E_z}{\partial x} = -\mathrm{j}\omega\mu H_y$$

$$\frac{\partial E_y}{\partial x} - \frac{\partial E_x}{\partial y} = -\mathrm{j}\omega\mu H_z$$

$$\frac{\partial H_z}{\partial y} - \frac{\partial H_y}{\partial z} = \mathrm{j}\omega\varepsilon E_x$$

$$\frac{\partial H_x}{\partial z} - \frac{\partial H_z}{\partial x} = \mathrm{j}\omega\varepsilon E_y$$

$$\frac{\partial H_y}{\partial x} - \frac{\partial H_x}{\partial y} = \mathrm{j}\omega\varepsilon E_z.$$

The coordinate system is chosen in such a way that the invariance direction is parallel y. The wave vector $\mathbf{k}^{(\mathrm{inc})}$ characterizing the incident plane wave is:

$$\mathbf{k}^{(\mathrm{inc})} = \omega\sqrt{\mu\varepsilon}\left(\sin\vartheta\cos\varphi, \sin\vartheta\sin\varphi, \cos\vartheta\right) =$$
$$= \omega\sqrt{\mu\varepsilon}\left(k_x, k_y, k_z\right).$$

Therefore, owing to the translational invariance of the structure, each component of the electromagnetic field has the same y dependence of the incident field:

$$\begin{matrix}\mathbf{E}(x,y,z,\omega)\\\mathbf{H}(x,y,z,\omega)\end{matrix} \propto \mathrm{e}^{-\mathrm{j}k_y y}, \quad k_y \in \mathbb{R}.$$

Now, by substituting this in the curl equations the following expressions are found:

$$-\mathrm{j}k_y E_z - \frac{\partial E_y}{\partial z} = -\mathrm{j}kZH_x \tag{C.3}$$

$$\frac{\partial E_x}{\partial z} - \frac{\partial E_z}{\partial x} = -\mathrm{j}kZH_y \tag{C.4}$$

$$\frac{\partial E_y}{\partial x} + \mathrm{j}k_y E_x = -\mathrm{j}kZH_z \tag{C.5}$$

$$-\mathrm{j}k_y H_z - \frac{\partial H_y}{\partial z} = \mathrm{j}kYE_x \tag{C.6}$$

$$\frac{\partial H_x}{\partial z} - \frac{\partial H_z}{\partial x} = \mathrm{j}kYE_y \tag{C.7}$$

$$\frac{\partial H_y}{\partial x} + \mathrm{j}k_y H_x = \mathrm{j}kYE_z, \tag{C.8}$$

where:

$$kZ = \omega\sqrt{\mu\varepsilon}\sqrt{\frac{\mu}{\varepsilon}} = \omega\mu,$$

and

$$kY = \omega\sqrt{\mu\varepsilon}\sqrt{\frac{\varepsilon}{\mu}} = \omega\varepsilon.$$

In the following subsections, the field components E_x, H_x, E_z, H_z will be expressed as functions of the derivatives of the components parallel to the invariance direction: E_y and H_y.

Derivation of H_x

E_z is found inverting (C.3) and (C.8):

$$E_z = -\frac{1}{\mathrm{j}k_y}\left(-\mathrm{j}kZH_x + \frac{\partial E_y}{\partial z}\right),$$

$$E_z = \frac{1}{\mathrm{j}kY}\left(\frac{\partial H_y}{\partial x} + \mathrm{j}k_yH_x\right).$$

Then, these two expressions are equated:

$$-\frac{1}{\mathrm{j}k_y}\left(-\mathrm{j}kZH_x + \frac{\partial E_y}{\partial z}\right) = \frac{1}{\mathrm{j}kY}\left(\frac{\partial H_y}{\partial x} + \mathrm{j}k_yH_x\right).$$

From here, by means of some manipulations:

$$\mathrm{j}k^2H_x - kY\frac{\partial E_y}{\partial z} = k_y\frac{\partial H_y}{\partial x} + \mathrm{j}k_y^2H_x,$$

so:

$$\mathrm{j}(k^2 - k_y^2)H_x = kY\frac{\partial E_y}{\partial z} + k_y\frac{\partial H_y}{\partial x}.$$

Finally:

$$H_x = -\frac{\mathrm{j}}{k^2 - k_y^2}\left(k_y\frac{\partial H_y}{\partial x} + kY\frac{\partial E_y}{\partial z}\right).$$

Derivation of E_z

H_x is found inverting (C.3) and (C.8):

$$H_x = -\frac{1}{\mathrm{j}kZ}\left(-\mathrm{j}k_yE_z - \frac{\partial E_y}{\partial z}\right),$$

$$H_x = \frac{1}{\mathrm{j}k_y}\left(\mathrm{j}kYE_z - \frac{\partial H_y}{\partial x}\right).$$

Then, these two expressions are equated:

$$-\frac{1}{\mathrm{j}kZ}\left(-\mathrm{j}k_y E_z - \frac{\partial E_y}{\partial z}\right) = \frac{1}{\mathrm{j}k_y}\left(\mathrm{j}kY E_z - \frac{\partial H_y}{\partial x}\right).$$

So, after some manipulations:

$$\mathrm{j}k_y^2 E_z + k_y \frac{\partial E_y}{\partial z} = -kZ\frac{\partial H_y}{\partial x} + \mathrm{j}k^2 E_z,$$

so:

$$\mathrm{j}(k^2 - k_y^2)E_z = kZ\frac{\partial H_y}{\partial x} + k_y\frac{\partial E_y}{\partial z},$$

which leads to:

$$E_z = -\frac{\mathrm{j}}{k^2 - k_y^2}\left(k_y\frac{\partial E_y}{\partial z} + kZ\frac{\partial H_y}{\partial x}\right).$$

Derivation of E_x

H_z is found inverting (C.5) and (C.6):

$$H_z = -\frac{1}{\mathrm{j}kZ}\left(\frac{\partial E_y}{\partial x} + \mathrm{j}k_y E_x\right),$$

$$H_z = -\frac{1}{\mathrm{j}k_y}\left(\frac{\partial H_y}{\partial z} + \mathrm{j}kY E_x\right).$$

These two expressions are equated:

$$-\frac{1}{\mathrm{j}kZ}\left(\frac{\partial E_y}{\partial x} + \mathrm{j}k_y E_x\right) = -\frac{1}{\mathrm{j}k_y}\left(\frac{\partial H_y}{\partial z} + \mathrm{j}kY E_x\right).$$

From here, with some algebra:

$$k_y\frac{\partial E_y}{\partial x} + \mathrm{j}k_y^2 E_x = kZ\frac{\partial H_y}{\partial x} + \mathrm{j}k^2 E_x;$$

then:

$$\mathrm{j}(k^2 - k_y^2)E_x = k_y\frac{\partial E_y}{\partial x} - kZ\frac{\partial H_y}{\partial z}.$$

So, finally:

$$E_x = -\frac{\mathrm{j}}{k^2 - k_y^2}\left(k_y\frac{\partial E_y}{\partial x} - kZ\frac{\partial H_y}{\partial z}\right).$$

Derivation of H_z

E_x is found inverting (C.5) and (C.6):

$$E_x = -\frac{1}{\mathrm{j}k_y}\left(\frac{\partial E_y}{\partial x} + \mathrm{j}kZH_z\right),$$

$$E_x = -\frac{1}{\mathrm{j}kY}\left(\mathrm{j}k_yH_z + \frac{\partial H_y}{\partial z}\right).$$

Then, these two are equated:

$$-\frac{1}{\mathrm{j}kY}\left(\mathrm{j}k_yH_z + \frac{\partial H_y}{\partial z}\right) = -\frac{1}{\mathrm{j}k_y}\left(\frac{\partial E_y}{\partial x} + \mathrm{j}kZH_z\right).$$

So, with some algebra:

$$\mathrm{j}k_y^2 H_z + k_y\frac{\partial H_y}{\partial z} = kY\frac{\partial E_y}{\partial x} + \mathrm{j}k^2 H_z.$$

Then:

$$\mathrm{j}(k^2 - k_y^2)H_z = k_y\frac{\partial H_y}{\partial z} - kY\frac{\partial E_y}{\partial x},$$

so:

$$H_z = -\frac{\mathrm{j}}{k^2 - k_y^2}\left(k_y\frac{\partial H_y}{\partial z} - kY\frac{\partial E_y}{\partial x}\right).$$

Resume of the expressions of the field components

The expressions derived in the previous subsections are now summarized:

$$E_x = -\frac{\mathrm{j}}{k^2 - k_y^2}\left(k_y\frac{\partial E_y}{\partial x} - kZ\frac{\partial H_y}{\partial z}\right), \tag{C.9}$$

$$E_z = -\frac{\mathrm{j}}{k^2 - k_y^2}\left(k_y\frac{\partial E_y}{\partial z} + kZ\frac{\partial H_y}{\partial x}\right), \tag{C.10}$$

$$H_x = -\frac{\mathrm{j}}{k^2 - k_y^2}\left(k_y\frac{\partial H_y}{\partial x} + kY\frac{\partial E_y}{\partial z}\right), \tag{C.11}$$

$$H_z = -\frac{\mathrm{j}}{k^2 - k_y^2}\left(k_y\frac{\partial H_y}{\partial z} - kY\frac{\partial E_y}{\partial x}\right). \tag{C.12}$$

C.3.2 Weak formulation of the problem

Differential problem

In this section the weak formulation of the 2-D periodic structures problem is derived starting from (C.4) and (C.7) and (C.9)-(C.12). The results of this procedure are

the expressions of the matrix elements of the matrices introduced in the scattering formulation of Chapter 1. The unused curl equations are:

$$\frac{\partial E_x}{\partial z} - \frac{\partial E_z}{\partial x} = -\mathrm{j}kZH_y$$
$$\frac{\partial H_x}{\partial z} - \frac{\partial H_z}{\partial x} = \mathrm{j}kYE_y.$$

Let $\mathbf{A} = A_z\widehat{\mathbf{z}} + A_x\widehat{\mathbf{x}}$ and f be a vector field and a scalar function; then, the following vector theorem holds:

$$\iint_\Omega \left[\frac{\partial A_x}{\partial z} - \frac{\partial A_z}{\partial x}\right] f\,\mathrm{d}z\mathrm{d}x = -\iint_\Omega \left[A_x\frac{\partial f}{\partial z} - A_z\frac{\partial f}{\partial x}\right]\mathrm{d}z\mathrm{d}x + \oint_{\gamma_\Omega} (\mathbf{A}f)\cdot\mathrm{d}\mathbf{s}. \tag{C.13}$$

To apply this theorem it is necessary to choose test functions $v_r \in V$:

$$V \triangleq \left\{v_r\ :r \in \mathbb{N},\ v_r \in \mathrm{C}^{(0)}(\Sigma), \frac{\partial v_r}{\partial x}, \frac{\partial v_r}{\partial z} \in L^2(\Sigma \setminus \partial\Sigma)\right\}.$$

The functions in V are continuous with square-integrable derivatives. Moreover, these functions are further specialized to satisfy the pseudo-periodicity boundary conditions:

$$v_r(z, a) = v_r(z, 0)\mathrm{e}^{-\mathrm{j}\phi}, \quad \forall z \in [0, L],$$

where L is the maximum z dimension of Σ. The weak formulation of (C.7) is then obtained by applying the vector theorem (C.13):

$$\mathrm{j}\iint_\Sigma kYE_yv_r^*\,\mathrm{d}z\mathrm{d}x + \iint_\Sigma \left[H_x\frac{\partial v_r^*}{\partial z} - H_z\frac{\partial v_r^*}{\partial x}\right]\mathrm{d}z\mathrm{d}x = \oint_{\gamma_\Sigma} (\mathbf{H}v_r^*)\cdot\mathrm{d}\mathbf{s}$$
$$(\mathrm{LHS})_r^{(\mathrm{e})} = (\mathrm{RHS})_r^{(\mathrm{e})}, \tag{C.14}$$

where $(\mathrm{LHS})_r^{(\mathrm{e})}$ and $(\mathrm{RHS})_r^{(\mathrm{e})}$ are defined as the left-hand side and as the right-hand side members of the equation. Now, let us recall (C.11) and (C.12):

$$H_x = -\frac{\mathrm{j}}{k^2 - k_y^2}\left(k_y\frac{\partial H_y}{\partial x} + kY\frac{\partial E_y}{\partial z}\right),$$
$$H_z = -\frac{\mathrm{j}}{k^2 - k_y^2}\left(k_y\frac{\partial H_y}{\partial z} - kY\frac{\partial E_y}{\partial x}\right).$$

These equations are now substituted in $(\mathrm{LHS})_r^{(\mathrm{e},j)}$, leading to:

$$(\text{LHS})_r^{(\text{e})} = \text{j} \iint_\Sigma kY E_y v_r^* \, \mathrm{d}z\mathrm{d}x +$$

$$- \iint_\Sigma \frac{\text{j}k_y}{k^2 - k_y^2} \frac{\partial H_y}{\partial x} \frac{\partial v_r^*}{\partial z} \, \mathrm{d}z\mathrm{d}x - \iint_\Sigma \frac{\text{j}kY}{k^2 - k_y^2} \frac{\partial E_y}{\partial z} \frac{\partial v_r^*}{\partial z} \, \mathrm{d}z\mathrm{d}x +$$

$$+ \iint_\Sigma \frac{\text{j}k_y}{k^2 - k_y^2} \frac{\partial H_y}{\partial z} \frac{\partial v_r^*}{\partial x} \, \mathrm{d}z\mathrm{d}x - \iint_\Sigma \frac{\partial E_y}{\partial x} \frac{\partial v_r^*}{\partial x} \, \mathrm{d}z\mathrm{d}x =$$

$$= \text{j} \iint_\Sigma kY E_y v_r^* \, \mathrm{d}z\mathrm{d}x +$$

$$- \iint_\Sigma \frac{\text{j}kY}{k^2 - k_y^2} \left[\frac{\partial E_y}{\partial z} \frac{\partial v_r^*}{\partial z} + \frac{\partial E_y}{\partial x} \frac{\partial v_r^*}{\partial x} \right] \, \mathrm{d}z\mathrm{d}x +$$

$$+ \iint_\Sigma \frac{\text{j}k_y}{k^2 - k_y^2} \left[\frac{\partial H_y}{\partial z} \frac{\partial v_r^*}{\partial x} - \frac{\partial H_y}{\partial x} \frac{\partial v_r^*}{\partial z} \right] \, \mathrm{d}z\mathrm{d}x.$$

Now, the unknowns E_y and H_y, are represented as a linear combination of basis functions u_r:

$$E_y = \sum_{c=1}^{N_\text{f}} c_c^{(\text{e})} u_c$$

$$H_y = \sum_{c=1}^{N_\text{f}} c_c^{(\text{h})} u_c, \tag{C.15}$$

where $u_c = v_c$. Then, by substituting these expressions, $(\text{LHS})_r^{(\text{e})}$ is:

$$(\text{LHS})_r^{(\text{e})} = \text{j} \sum_{c=1}^{N_\text{f}} c_c^{(\text{e})} \iint_\Sigma kY u_c^{(\text{e})} v_r^* \, \mathrm{d}z\mathrm{d}x +$$

$$- \text{j} \sum_{c=1}^{N_\text{f}} c_c^{(\text{e})} \iint_\Sigma \frac{kY}{k^2 - k_y^2} \left[\frac{\partial u_c^{(\text{e})}}{\partial z} \frac{\partial v_r^*}{\partial z} + \frac{\partial u_c^{(\text{e})}}{\partial x} \frac{\partial v_r^*}{\partial x} \right] \, \mathrm{d}z\mathrm{d}x +$$

$$+ \text{j} \sum_{c=1}^{N_\text{f}} c_c^{(\text{h})} \iint_\Sigma \frac{k_y}{k^2 - k_y^2} \left[\frac{\partial u_c^{(\text{h})}}{\partial z} \frac{\partial v_r^*}{\partial x} - \frac{\partial u_c^{(\text{h})}}{\partial x} \frac{\partial v_r^*}{\partial z} \right] \, \mathrm{d}z\mathrm{d}x.$$

The following matrices are defined:

$$(\mathbf{M})_{rc} = \iint_\Sigma kY u_c^{(\text{e})} v_r^* \, \mathrm{d}z\mathrm{d}x$$

$$(\mathbf{K})_{rc} = \iint_\Sigma \frac{kY}{k^2 - k_y^2} \left[\frac{\partial u_c^{(\text{e})}}{\partial z} \frac{\partial v_r^*}{\partial z} + \frac{\partial u_c^{(\text{e})}}{\partial x} \frac{\partial v_r^*}{\partial x} \right] \, \mathrm{d}x \, \mathrm{d}z$$

$$(\mathbf{L})_{rc} = \iint_\Sigma \frac{k_y}{k^2 - k_y^2} \left[\frac{\partial u_c^{(\text{h})}}{\partial z} \frac{\partial v_r^*}{\partial x} - \frac{\partial u_c^{(\text{h})}}{\partial x} \frac{\partial v_r^*}{\partial z} \right] \, \mathrm{d}x \, \mathrm{d}z.$$

Then, $(\text{LHS})^{(\text{e})}$ becomes:

$$(\text{LHS})^{(\text{e})} = \text{j}\left[\mathbf{M} - \mathbf{K}\right]\mathbf{c}^{(\text{e})} + \text{j}\mathbf{L}\,\mathbf{c}^{(\text{h})} =$$
$$= \mathbf{A}^{(\text{e,e})}\,\mathbf{c}^{(\text{e})} + \mathbf{A}^{(\text{e,h})}\,\mathbf{c}^{(\text{h})}.$$

It is possible to obtain similar results either by applying the same steps on the remaining Maxwell's equation or by duality. By this way:

$$(\text{LHS})^{(\text{h})} = \text{j}\mathbf{L}\,\mathbf{c}^{(\text{e})} + \text{j}\left[\mathbf{M} - \mathbf{K}\right]\mathbf{c}^{(\text{h})} =$$
$$= \mathbf{A}^{(\text{h,e})}\,\mathbf{c}^{(\text{e})} + \mathbf{A}^{(\text{h,h})}\,\mathbf{c}^{(\text{h})}.$$

C.3.3 Formulation of the continuity equations

In this section the projection matrix elements related to the continuity equations at the access ports are derived, to complete the formulation of the scattering problem. The scalar products used in this context are defined as:

$$\langle \mathbf{a}, \mathbf{b} \rangle = \int_0^a \mathbf{a} \cdot \mathbf{b}^* \, \mathrm{d}x$$

Continuity of the electric field at port 1

The first continuity condition is:

$$\left\langle \widehat{\mathbf{E}}_{\text{t}}^{(1)}, \mathbf{e}_q^{(1)} \right\rangle = \left\langle \widetilde{\mathbf{E}}_{\text{t}}^{(1)}, \mathbf{e}_q^{(1)} \right\rangle.$$

So:

$$\left\langle \widetilde{\mathbf{E}}_{\text{t}}^{(1)}, \mathbf{e}_q^{(1)} \right\rangle = \left\langle \widetilde{E}_x^{(1)}, e_{x,q}^{(1)} \right\rangle + \left\langle \widetilde{E}_y^{(1)}, e_{y,q}^{(1)} \right\rangle.$$

Recalling (C.9), the first term can be re-written as:

$$\left\langle \widetilde{E}_x^{(1)}, e_{x,q}^{(1)} \right\rangle = -\frac{\text{j}k_y}{k^2 - k_y^2}\sum_{c=1}^{N_{\text{f}}} c_c^{(\text{e})} \left\langle \left.\frac{\partial u_c}{\partial x}\right|_{z_{\text{wg}}^{(1)}}, e_{x,q}^{(1)} \right\rangle + \frac{\text{j}kZ}{k^2 - k_y^2}\sum_{c=1}^{N_{\text{f}}} c_c^{(\text{h})} \left\langle \left.\frac{\partial u_c}{\partial z}\right|_{z_{\text{wg}}^{(1)}}, e_{x,q}^{(1)} \right\rangle,$$

and

$$\left\langle \widetilde{E}_y^{(1)}, e_{y,q}^{(1)} \right\rangle = \sum_{r=1}^{N_{\text{f}}} c_c^{(\text{e})} \left\langle \left.u_c\right|_{z_{\text{wg}}^{(1)}}, e_{y,q}^{(1)} \right\rangle.$$

So, the following matrix elements are defined:

$$\left(\mathbf{C}^{(\mathrm{e},1)}\right)_{qc} = \left\langle \left. u_c \right|_{z_{\mathrm{wg}}^{(1)}} , e_{y,q}^{(1)} \right\rangle$$

$$\left(\mathbf{H}^{(\mathrm{e},1)}\right)_{qc} = \left\langle \left. \frac{\partial u_c}{\partial x} \right|_{z_{\mathrm{wg}}^{(1)}} , e_{x,q}^{(1)} \right\rangle$$

$$\left(\mathbf{K}^{(\mathrm{h},1)}\right)_{qc} = \left\langle \left. \frac{\partial u_c}{\partial z} \right|_{z_{\mathrm{wg}}^{(1)}} , e_{x,q}^{(1)} \right\rangle .$$

Then, this side of the equation is written in matrix form as

$$\left(\mathbf{C}^{(\mathrm{e},1)} - \frac{\mathrm{j}k_y}{k^2 - k_y^2} \mathbf{H}^{(\mathrm{e},1)} \right) \mathbf{c}^{(\mathrm{e})} + \frac{\mathrm{j}kZ}{k^2 - k_y^2} \mathbf{K}^{(\mathrm{h},1)} \mathbf{c}^{(\mathrm{h})} .$$

Continuity of the electric field at port 2

The second continuity condition is:

$$\left\langle \widehat{\mathbf{E}}_{\mathrm{t}}^{(2)} , \mathbf{e}_q^{(2)} \right\rangle = \left\langle \widetilde{\mathbf{E}}_{\mathrm{t}}^{(2)} , \mathbf{e}_q^{(2)} \right\rangle ,$$

where:

$$\left\langle \widehat{\mathbf{E}}_{\mathrm{t}}^{(2)} , \mathbf{e}_q^{(2)} \right\rangle = \left\langle \widehat{E}_x^{(2)} , e_{x,q}^{(2)} \right\rangle + \left\langle .\widehat{E}_y^{(2)} , e_{y,q}^{(2)} \right\rangle$$

Recalling (C.9), the first term can be re-written as:

$$\left\langle \widehat{E}_x^{(2)} , e_{x,q}^{(2)} \right\rangle = -\frac{\mathrm{j}k_y}{k^2 - k_y^2} \sum_{c=1}^{N_{\mathrm{f}}} c_c^{(\mathrm{e})} \left\langle \left. \frac{\partial u_c}{\partial x} \right|_{z_{\mathrm{wg}}^{(2)}} , e_{x,q}^{(2)} \right\rangle + \frac{\mathrm{j}kZ}{k^2 - k_y^2} \sum_{c=1}^{N_{\mathrm{f}}} c_c^{(\mathrm{h})} \left\langle \left. \frac{\partial u_c}{\partial z} \right|_{z_{\mathrm{wg}}^{(2)}} , e_{x,q}^{(2)} \right\rangle ,$$

and

$$\left\langle \widehat{E}_y^{(2)} , e_{y,q}^{(2)} \right\rangle = \sum_{c=1}^{N_{\mathrm{f}}} c_c^{(\mathrm{e})} \left\langle \left. u_c \right|_{z_{\mathrm{wg}}^{(2)}} , e_{y,q}^{(2)} \right\rangle .$$

So, the following matrix elements are defined:

$$\left(\mathbf{C}^{(\mathrm{e},2)}\right)_{qc} = \left\langle \left. u_c \right|_{z_{\mathrm{wg}}^{(2)}} , e_{y,q}^{(2)} \right\rangle$$

$$\left(\mathbf{H}^{(\mathrm{e},2)}\right)_{qc} = \left\langle \left. \frac{\partial u_c}{\partial x} \right|_{z_{\mathrm{wg}}^{(2)}} , e_{x,q}^{(2)} \right\rangle$$

$$\left(\mathbf{K}^{(\mathrm{h},2)}\right)_{qc} = \left\langle \left. \frac{\partial u_c}{\partial z} \right|_{z_{\mathrm{wg}}^{(2)}} , e_{x,q}^{(2)} \right\rangle .$$

Then, this side of the equation is written in matrix form as:

$$\left(\mathbf{C}^{(e,2)} - \frac{jk_y}{k^2 - k_y^2} \mathbf{H}^{(e,2)} \right) \mathbf{c}^{(e)} + \frac{jkZ}{k^2 - k_y^2} \mathbf{K}^{(h,2)} \mathbf{c}^{(h)}.$$

Continuity of the magnetic field at port 1

The third continuity condition is:

$$\left\langle \widehat{\mathbf{H}}_t^{(1)}, \mathbf{h}_q^{(1)} \right\rangle = \left\langle \widetilde{\mathbf{H}}_t^{(1)}, \mathbf{h}_q^{(1)} \right\rangle,$$

where:

$$\left\langle \widetilde{\mathbf{H}}_t^{(1)}, \mathbf{h}_q^{(1)} \right\rangle = \left\langle \widetilde{H}_x^{(1)}, h_{x,q}^{(1)} \right\rangle + \left\langle \widetilde{H}_y^{(1)}, h_{y,q}^{(1)} \right\rangle.$$

Recalling (C.11), the first term can be re-written as:

$$\left\langle \widetilde{H}_x^{(1)}, h_{x,q}^{(1)} \right\rangle = -\frac{jk_y}{k^2 - k_y^2} \sum_{c=1}^{N_f} c_c^{(h)} \left\langle \left. \frac{\partial u_c}{\partial x} \right|_{z_{wg}^{(1)}}, h_{x,q}^{(1)} \right\rangle - \frac{jkY}{k^2 - k_y^2} \sum_{c=1}^{N_f} c_c^{(e)} \left\langle \left. \frac{\partial u_c^{(e)}}{\partial z} \right|_{z_{wg}^{(1)}}, h_{x,q}^{(1)} \right\rangle,$$

and

$$\left\langle \widetilde{H}_y^{(1)}, h_{y,q}^{(1)} \right\rangle = \sum_{c=1}^{N_f} c_c^{(h)} \left\langle \left. u_c^{(h)} \right|_{z_{wg}^{(1)}}, h_{y,q}^{(1)} \right\rangle.$$

So, the following matrix elements are defined:

$$(\mathbf{C}^{(h,1)})_{qc} = \left\langle \left. u_c^{(h)} \right|_{z_{wg}^{(1)}}, h_{y,q}^{(1)} \right\rangle$$

$$(\mathbf{H}^{(h,1)})_{qc} = \left\langle \left. \frac{\partial u_c^{(h)}}{\partial x} \right|_{z_{wg}^{(1)}}, h_{x,q}^{(1)} \right\rangle$$

$$(\mathbf{K}^{(e,1)})_{qc} = \left\langle \left. \frac{\partial u_c^{(e)}}{\partial z} \right|_{z_{wg}^{(1)}}, h_{x,q}^{(1)} \right\rangle.$$

Then, this side of the equation is written in matrix form as:

$$\left(\mathbf{C}^{(h,1)} - \frac{jk_y}{k^2 - k_y^2} \mathbf{H}^{(h,1)} \right) \mathbf{c}^{(h)} - \frac{jkY}{k^2 - k_y^2} \mathbf{K}^{(e,1)} \mathbf{c}^{(e)}.$$

Continuity of the magnetic field at port 2

The last continuity condition is:

$$\left\langle \widehat{\mathbf{H}}_{\text{t}}^{(2)}, \mathbf{h}_q^{(2)} \right\rangle = \left\langle \widetilde{\mathbf{H}}_{\text{t}}^{(2)}, \mathbf{h}_q^{(2)} \right\rangle,$$

where:

$$\left\langle \widehat{\mathbf{H}}_{\text{t}}^{(2)}, \mathbf{h}_q^{(2)} \right\rangle = \left\langle \widehat{H}_x^{(2)}, h_{x,q}^{(2)} \right\rangle + \left\langle \widehat{H}_y^{(2)}, h_{y,q}^{(2)} \right\rangle.$$

Recalling (C.11), the first term can be re-written as:

$$\left\langle \widehat{H}_x^{(2)}, h_{x,q}^{(2)} \right\rangle = -\frac{\mathrm{j}k_y}{k^2 - k_y^2} \sum_{c=1}^{N_{\text{f}}} c_c^{(\text{h})} \left\langle \left. \frac{\partial u_c}{\partial x} \right|_{z_{\text{wg}}^{(2)}}, h_{x,q}^{(2)} \right\rangle - \frac{\mathrm{j}kY}{k^2 - k_y^2} \sum_{c=1}^{N_{\text{f}}} c_c^{(\text{e})} \left\langle \left. \frac{\partial u_c^{(\text{e})}}{\partial z} \right|_{z_{\text{wg}}^{(2)}}, h_{x,q}^{(2)} \right\rangle,$$

and

$$\left\langle \widehat{H}_y^{(2)}, h_{y,t}^{(2)} \right\rangle = \sum_{c=1}^{N_{\text{f}}} c_c^{(\text{h})} \left\langle \left. u_c^{(\text{h})} \right|_{z_{\text{wg}}^{(2)}}, h_{y,q}^{(2)} \right\rangle.$$

So, the following matrix elements are defined:

$$(\mathbf{C}^{(\text{h},1)})_{qc} = \left\langle \left. u_c^{(\text{h})} \right|_{z_{\text{wg}}^{(2)}}, h_{y,q}^{(2)} \right\rangle$$

$$(\mathbf{H}^{(\text{h},1)})_{qc} = \left\langle \left. \frac{\partial u_c^{(\text{h})}}{\partial x} \right|_{z_{\text{wg}}^{(2)}}, h_{x,q}^{(2)} \right\rangle$$

$$(\mathbf{K}^{(\text{e},1)})_{qc} = \left\langle \left. \frac{\partial u_c^{(\text{e})}}{\partial z} \right|_{z_{\text{wg}}^{(2)}}, h_{x,q}^{(2)} \right\rangle.$$

Then, this side of the equation is written in matrix form as:

$$\left(\mathbf{C}^{(\text{h},1)} - \frac{\mathrm{j}k_y}{k^2 - k_y^2} \mathbf{H}^{(\text{h},1)} \right) \mathbf{c}^{(\text{h})} - \frac{\mathrm{j}kY}{k^2 - k_y^2} \mathbf{K}^{(\text{e},1)} \mathbf{c}^{(\text{e})}.$$

Definition of the projection matrix

The matrix $\mathbf{T}$ is defined as:

$$\mathbf{T} = \begin{bmatrix} \mathbf{C}^{(\mathrm{e},1)} - \dfrac{\mathrm{j}k_y}{k^2 - k_y^2}\mathbf{H}^{(\mathrm{e},1)} & \dfrac{\mathrm{j}kZ}{k^2 - k_y^2}\mathbf{K}^{(\mathrm{h},1)} \\[2em] -\dfrac{\mathrm{j}kY}{k^2 - k_y^2}\mathbf{K}^{(\mathrm{e},1)} & \mathbf{C}^{(\mathrm{h},1)} - \dfrac{\mathrm{j}k_y}{k^2 - k_y^2}\mathbf{H}^{(\mathrm{h},1)} \\[2em] \mathbf{C}^{(\mathrm{e},2)} - \dfrac{\mathrm{j}k_y}{k^2 - k_y^2}\mathbf{H}^{(\mathrm{e},2)} & \dfrac{\mathrm{j}kZ}{k^2 - k_y^2}\mathbf{K}^{(\mathrm{h},2)} \\[2em] -\dfrac{\mathrm{j}kY}{k^2 - k_y^2}\mathbf{K}^{(\mathrm{e},2)} & \mathbf{C}^{(\mathrm{h},2)} - \dfrac{\mathrm{j}k_y}{k^2 - k_y^2}\mathbf{H}^{(\mathrm{h},2)} \end{bmatrix}.$$

Appendix D

Appendix of "Mortar element analysis of axisymmetric guiding structures"

D.1 Circular waveguide modes

The technique described in Chapter 4 is applicable to axisymmetric structures excited by circularly polarized incident fields, with angular dependence is $e^{+jm\varphi}$. Therefore, the generating functions of the TM_{mn} and TE_{mn} mode functions are:

$$\Phi_{mn} = A_{mn}\, J_m(k'_{t,i}\rho)\, e^{+jm\varphi}$$

$$\Psi_{mn} = B_{mn}\, J_m(k''_{t,i}\rho)\, e^{+jm\varphi},$$

where $k'_{t,i} = \chi_{mn}/a$, $k''_{t,i} = \chi'_{mn}/2$, a is the waveguide radius, $i = (m_i, n_i)$ and $j = (m_j, n_j)$ are multiple indexes, χ_{mn} and χ'_{mn} are the n-th zeros of the Bessel function of first kind and order m, and of its derivative, respectively. The normalization constants A_{mn} and B_{mn} are now calculated. Starting from Φ_{mn}:

$$\langle\Phi_i, \Phi_j\rangle = \int_0^{2\pi}\int_0^a \Phi_i\Phi_j^*\, \rho\, d\rho\, d\varphi = \delta_{ij}\int_0^{2\pi}\int_0^a A_{mn}^2 J_m^2(k'_{t,i}\rho)\, e^{+jm\varphi}e^{-jm\varphi}\, \rho\, d\rho\, d\varphi$$

$$= A_{mn}^2\delta_{ij}\int_0^{2\pi} d\varphi \int_0^a \rho\, J_m^2(k'_{t,i}\rho)d\rho = 2\pi\, \delta_{ij}A_{mn}^2\int_0^a \rho\, J_m^2(k'_{t,i}\rho)d\rho.$$

The indefinite integral is calculated by means of the Lommel integral formula:

$$\int^x J_m^2(\alpha t)\, t\, dt = \frac{x^2}{2}\left[J_m'(\alpha x) + \left(1 - \frac{m^2}{\alpha^2 x^2}\right)J_m^2(\alpha x)\right].$$

It is apparent that one contribution equals zero in the relevant interval; therefore:

$$\langle\Phi_i, \Phi_j\rangle = \pi A_{mn}^2 a^2\left[J_{m+1}(k'_{t,i}a)\right]^2;$$

so:

$$A_{mn} = \frac{1}{\sqrt{\pi}} \frac{1}{a\, \mathrm{J}_{m+1}(k'_{\mathrm{t},i}a)}.$$

Similarly, for TE_{mn} modes, the normalization constant is

$$B_{mn} = \frac{1}{\sqrt{\pi}} \frac{\chi'_{mn}}{\sqrt{\chi'^2_{mn} - m^2}} \frac{1}{a\, \mathrm{J}_m(k''_{\mathrm{t},i}a)}.$$

To summarize:

$$\Phi_{mn} = \frac{1}{\sqrt{\pi}} \frac{\mathrm{J}_m(k'_{\mathrm{t},i}\rho)}{a\, \mathrm{J}_{m+1}(k'_{\mathrm{t},i}a)} \mathrm{e}^{+\mathrm{j}m\varphi}$$

$$\Psi_{mn} = \frac{1}{\sqrt{\pi}} \frac{\chi'_{mn}}{\sqrt{\chi'^2_{mn} - m^2}} \frac{\mathrm{J}_m(k''_{\mathrm{t},i}\rho)}{a\, \mathrm{J}_m(k''_{\mathrm{t},i}a)} \mathrm{e}^{+\mathrm{j}m\varphi}.$$

The expressions of the mode functions $\mathbf{e}'_i(\boldsymbol{\rho})$, $\mathbf{h}'_i(\boldsymbol{\rho})$, $\mathbf{h}''_i(\boldsymbol{\rho})$, $\mathbf{e}''_i(\boldsymbol{\rho})$ are now calculated. The following relationships hold:

$$\mathbf{e}'_i(\boldsymbol{\rho}) = -\frac{\nabla_{\mathrm{t}}\Phi_i(\boldsymbol{\rho})}{k'_{\mathrm{t},i}}$$

$$\mathbf{h}''_i(\boldsymbol{\rho}) = -\frac{\nabla_{\mathrm{t}}\Psi_i(\boldsymbol{\rho})}{k''_{\mathrm{t},i}},$$

as well as the following impedance relationships:

$$\mathbf{h}'_i(\boldsymbol{\rho}) = \widehat{\mathbf{z}} \times \mathbf{e}'_i(\boldsymbol{\rho})$$

$$\mathbf{e}''_i(\boldsymbol{\rho}) = \mathbf{h}''(\boldsymbol{\rho}) \times \widehat{\mathbf{z}}.$$

Finally, it is useful to recall the expression of the transverse gradient in cylindrical coordinates:

$$\nabla_{\mathrm{t}}f = \frac{\partial f}{\partial\rho}\widehat{\boldsymbol{\rho}} + \frac{1}{\rho}\frac{\partial f}{\partial\varphi}\widehat{\boldsymbol{\varphi}}.$$

TM modes

$$\mathbf{e}'_i(\boldsymbol{\rho}) = -\frac{1}{k'_{\mathrm{t},i}} \left[\frac{1}{\sqrt{\pi}} k'_{\mathrm{t},i} \frac{\mathrm{J}'_m(k'_{\mathrm{t},i}\rho)}{a\, \mathrm{J}_{m+1}(k'_{\mathrm{t},i}a)} \mathrm{e}^{+\mathrm{j}m\varphi}, \quad \frac{1}{\rho}\frac{\mathrm{j}m}{\sqrt{\pi}} \frac{\mathrm{J}_m(k'_{\mathrm{t},i}\rho)}{a\, \mathrm{J}_{m+1}(k'_{\mathrm{t},i}a)} \mathrm{e}^{+\mathrm{j}m\varphi} \right] =$$

$$= \left[-\frac{1}{\sqrt{\pi}} \frac{\mathrm{J}'_m(k'_{\mathrm{t},i}\rho)}{a\mathrm{J}_{m+1}(k'_{\mathrm{t},i}a)} \mathrm{e}^{+\mathrm{j}m\varphi}, \quad \frac{-\mathrm{j}m}{\sqrt{\pi}k'_{\mathrm{t},i}a} \frac{\mathrm{J}_m(k'_{\mathrm{t},i}\rho)}{\rho\, \mathrm{J}_{m+1}(k'_{\mathrm{t},i}a)} \mathrm{e}^{+\mathrm{j}m\varphi} \right].$$

Then, since

$$\mathbf{h}'_i = \widehat{\mathbf{z}} \times \mathbf{e}'_i = \widehat{\boldsymbol{\rho}}\left(-e'_\varphi\right) - \widehat{\boldsymbol{\varphi}}\left(-e'_\rho\right),$$

the following expressions are obtained:

$$\begin{cases} h'_\rho = -e'_\varphi \\ h'_\varphi = e'_\rho. \end{cases}$$

TE modes

$$\mathbf{h}''_i(\boldsymbol{\rho}) = -\frac{1}{k''_{\mathrm{t},i}} \left[\frac{k''_{\mathrm{t},i}}{\sqrt{\pi}} \frac{\chi'_{mn}}{\sqrt{\chi'^2_{mn} - m^2}} \frac{\mathrm{J}'_m(k''_{\mathrm{t},i}\rho)}{a \, \mathrm{J}_m(k''_{\mathrm{t},i}a)} \mathrm{e}^{+\mathrm{j}m\varphi}, \quad \frac{1}{\rho} \frac{\mathrm{j}m}{\sqrt{\pi}} \frac{\chi'_{mn}}{\sqrt{\chi'^2_{mn} - m^2}} \frac{\mathrm{J}_m(k''_{\mathrm{t},i}\rho)}{a \, \mathrm{J}_m(k''_{\mathrm{t},i}a)} \mathrm{e}^{+\mathrm{j}m\varphi} \right] =$$

$$= \left[-\frac{k''_{\mathrm{t},i}}{\sqrt{\pi}} \frac{1}{\sqrt{(k''_{\mathrm{t},i}a)^2 - m^2}} \frac{\mathrm{J}'_m(k''_{\mathrm{t},i}\rho)}{\mathrm{J}_m(k''_{\mathrm{t},i}a)} \mathrm{e}^{+\mathrm{j}m\varphi}, \quad \frac{-\mathrm{j}m}{\sqrt{\pi}} \frac{1}{\sqrt{(k''_{\mathrm{t},i}a)^2 - m^2}} \frac{\mathrm{J}_m(k''_{\mathrm{t},i}\rho)}{\rho \, \mathrm{J}_m(k''_{\mathrm{t},i}a)} \mathrm{e}^{+\mathrm{j}m\varphi} \right].$$

Then, since

$$\mathbf{h}''_i = \begin{bmatrix} h''_\rho, & h''_\varphi, & 0 \end{bmatrix},$$

and

$$\mathbf{e}''_i = \mathbf{h}''_i \times \widehat{\mathbf{z}} = \widehat{\boldsymbol{\rho}} \left(h''_\varphi \right) - \widehat{\boldsymbol{\varphi}} \left(-h''_\rho \right),$$

the following expressions are written:

$$\begin{cases} e''_\rho = h''_\varphi \\ e''_\varphi = -h''_\rho. \end{cases}$$

Summary of circular waveguide modes

Considering the $\mathrm{e}^{+\mathrm{j}m\varphi}$ polarization, modal eigenfunctions are, for TM modes:

$$e'_\rho = -\frac{1}{\sqrt{\pi}} \frac{\mathrm{J}'_m(k'_{\mathrm{t},i}\rho)}{a \mathrm{J}_{m+1}(k'_{\mathrm{t},i}a)} \mathrm{e}^{+\mathrm{j}m\varphi}$$

$$e'_\varphi = \frac{-\mathrm{j}m}{\sqrt{\pi}k'_{\mathrm{t},i}a} \frac{\mathrm{J}_m(k'_{\mathrm{t},i}\rho)}{\rho \, \mathrm{J}_{m+1}(k'_{\mathrm{t},i}a)} \mathrm{e}^{+\mathrm{j}m\varphi}$$

$$h'_\rho = \frac{\mathrm{j}m}{\sqrt{\pi}k'_{\mathrm{t},i}a} \frac{\mathrm{J}_m(k'_{\mathrm{t},i}\rho)}{\rho \, \mathrm{J}_{m+1}(k'_{\mathrm{t},i}a)} \mathrm{e}^{+\mathrm{j}m\varphi}$$

$$h'_\varphi = -\frac{1}{\sqrt{\pi}} \frac{\mathrm{J}'_m(k'_{\mathrm{t},i}\rho)}{a \mathrm{J}_{m+1}(k'_{\mathrm{t},i}a)} \mathrm{e}^{+\mathrm{j}m\varphi},$$

and, for TE modes:

$$e''_\rho = \frac{-\mathrm{j}m}{\sqrt{\pi}} \frac{1}{\sqrt{(k''_{\mathrm{t},i}a)^2 - m^2}} \frac{\mathrm{J}_m(k''_{\mathrm{t},i}\rho)}{\rho\, \mathrm{J}_m(k''_{\mathrm{t},i}a)} \mathrm{e}^{+\mathrm{j}m\varphi}$$

$$e''_\varphi = \frac{k''_{\mathrm{t},i}}{\sqrt{\pi}} \frac{1}{\sqrt{(k''_{\mathrm{t},i}a)^2 - m^2}} \frac{\mathrm{J}'_m(k''_{\mathrm{t},i}\rho)}{\mathrm{J}_m(k''_{\mathrm{t},i}a)} \mathrm{e}^{+\mathrm{j}m\varphi}$$

$$h''_\rho = -\frac{k''_{\mathrm{t},i}}{\sqrt{\pi}} \frac{1}{\sqrt{(k''_{\mathrm{t},i}a)^2 - m^2}} \frac{\mathrm{J}'_m(k''_{\mathrm{t},i}\rho)}{\mathrm{J}_m(k''_{\mathrm{t},i}a)} \mathrm{e}^{+\mathrm{j}m\varphi}$$

$$h''_\varphi = \frac{-\mathrm{j}m}{\sqrt{\pi}} \frac{1}{\sqrt{(k''_{\mathrm{t},i}a)^2 - m^2}} \frac{\mathrm{J}_m(k''_{\mathrm{t},i}\rho)}{\rho\, \mathrm{J}_m(k''_{\mathrm{t},i}a)} \mathrm{e}^{+\mathrm{j}m\varphi}.$$

For $\mathrm{e}^{-\mathrm{j}m\varphi}$ field dependence, with similar steps the following expressions are obtained:

$$e'_\rho = -\frac{1}{\sqrt{\pi}} \frac{\mathrm{J}'_m(k'_{\mathrm{t},i}\rho)}{a\mathrm{J}_{m+1}(k'_{\mathrm{t},i}a)} \mathrm{e}^{-\mathrm{j}m\varphi}$$

$$e'_\varphi = \frac{\mathrm{j}m}{\sqrt{\pi}k'_{\mathrm{t},i}a} \frac{\mathrm{J}_m(k'_{\mathrm{t},i}\rho)}{\rho\, \mathrm{J}_{m+1}(k'_{\mathrm{t},i}a)} \mathrm{e}^{-\mathrm{j}m\varphi}$$

$$h'_\rho = -\frac{\mathrm{j}m}{\sqrt{\pi}k'_{\mathrm{t},i}a} \frac{\mathrm{J}_m(k'_{\mathrm{t},i}\rho)}{\rho\, \mathrm{J}_{m+1}(k'_{\mathrm{t},i}a)} \mathrm{e}^{-\mathrm{j}m\varphi}$$

$$h'_\varphi = -\frac{1}{\sqrt{\pi}} \frac{\mathrm{J}'_m(k'_{\mathrm{t},i}\rho)}{a\mathrm{J}_{m+1}(k'_{\mathrm{t},i}a)} \mathrm{e}^{-\mathrm{j}m\varphi},$$

whereas, for TE modes:

$$e''_\rho = \frac{\mathrm{j}m}{\sqrt{\pi}} \frac{1}{\sqrt{(k''_{\mathrm{t},i}a)^2 - m^2}} \frac{\mathrm{J}_m(k''_{\mathrm{t},i}\rho)}{\rho\, \mathrm{J}_m(k''_{\mathrm{t},i}a)} \mathrm{e}^{-\mathrm{j}m\varphi}$$

$$e''_\varphi = \frac{k''_{\mathrm{t},i}}{\sqrt{\pi}} \frac{1}{\sqrt{(k''_{\mathrm{t},i}a)^2 - m^2}} \frac{\mathrm{J}'_m(k''_{\mathrm{t},i}\rho)}{\mathrm{J}_m(k''_{\mathrm{t},i}a)} \mathrm{e}^{-\mathrm{j}m\varphi}$$

$$h''_\rho = -\frac{k''_{\mathrm{t},i}}{\sqrt{\pi}} \frac{1}{\sqrt{(k''_{\mathrm{t},i}a)^2 - m^2}} \frac{\mathrm{J}'_m(k''_{\mathrm{t},i}\rho)}{\mathrm{J}_m(k''_{\mathrm{t},i}a)} \mathrm{e}^{-\mathrm{j}m\varphi}$$

$$h''_\varphi = \frac{\mathrm{j}m}{\sqrt{\pi}} \frac{1}{\sqrt{(k''_{\mathrm{t},i}a)^2 - m^2}} \frac{\mathrm{J}_m(k''_{\mathrm{t},i}\rho)}{\rho\, \mathrm{J}_m(k''_{\mathrm{t},i}a)} \mathrm{e}^{-\mathrm{j}m\varphi}.$$

D.2 Field representation for axisymmetric structures

D.2.1 Derivation of the relationships between the field components

In this section the equations used to describe the electromagnetic behavior of axisymmetric structures are derived starting from the space-frequency Maxwell's curl equations:

$$
\begin{cases}
\nabla \times \mathbf{E}(\mathbf{r}, \omega) = -\mathrm{j}\omega\mu\mathbf{H}(\mathbf{r}, \omega) \\
\nabla \times \mathbf{H}(\mathbf{r}, \omega) = \mathrm{j}\omega\epsilon\mathbf{E}(\mathbf{r}, \omega).
\end{cases}
\tag{D.1}
$$

These equations are written in cylindrical coordinates, where z is chosen to be coincident with the axis of the device:

$$
\frac{1}{\rho}\frac{\partial E_z}{\partial \varphi} - \frac{\partial E_\varphi}{\partial z} = -\mathrm{j}\omega\mu H_\rho
$$

$$
\frac{\partial E_\rho}{\partial z} - \frac{\partial E_z}{\partial \rho} = -\mathrm{j}\omega\mu H_\varphi
$$

$$
\frac{1}{\rho}\left(\frac{\partial(\rho E_\varphi)}{\partial \rho} - \frac{\partial E_\rho}{\partial \varphi}\right) = -\mathrm{j}\omega\mu H_z
$$

$$
\frac{1}{\rho}\frac{\partial H_z}{\partial \varphi} - \frac{\partial H_\varphi}{\partial z} = \mathrm{j}\omega\epsilon E_\rho
$$

$$
\frac{\partial H_\rho}{\partial z} - \frac{\partial H_z}{\partial \rho} = \mathrm{j}\omega\epsilon E_\varphi
$$

$$
\frac{1}{\rho}\left(\frac{\partial(\rho H_\varphi)}{\partial \rho} - \frac{\partial H_\rho}{\partial \varphi}\right) = \mathrm{j}\omega\epsilon E_z.
$$

Since the incident field has a $\mathrm{e}^{\mathrm{j}m\varphi}$ angular dependence and the structure exhibits axial symmetry, its angular dependence is preserved in the device; this means that it is possible to apply the spatial Fourier transform on the φ variable, substituting the angular derivatives with $\mathrm{j}m$:

$$
\frac{\mathrm{d}}{\mathrm{d}\varphi}\mathrm{e}^{\mathrm{j}m\varphi} = \mathrm{j}m\,\mathrm{e}^{\mathrm{j}m\varphi} \implies \frac{\mathrm{d}}{\mathrm{d}\varphi} \longleftrightarrow \mathrm{j}m.
$$

Then,

$$\frac{1}{\rho}\mathrm{j}mE_z - \frac{\partial E_\varphi}{\partial z} = -\mathrm{j}\omega\mu H_\rho \tag{D.2}$$

$$\frac{\partial E_\rho}{\partial z} - \frac{\partial E_z}{\partial \rho} = -\mathrm{j}\omega\mu H_\varphi \tag{D.3}$$

$$\frac{1}{\rho}\left(\frac{\partial(\rho E_\varphi)}{\partial \rho} - \mathrm{j}mE_\rho\right) = -\mathrm{j}\omega\mu H_z \tag{D.4}$$

$$\frac{1}{\rho}\mathrm{j}mH_z - \frac{\partial H_\varphi}{\partial z} = \mathrm{j}\omega\epsilon E_\rho \tag{D.5}$$

$$\frac{\partial H_\rho}{\partial z} - \frac{\partial H_z}{\partial \rho} = \mathrm{j}\omega\epsilon E_\varphi \tag{D.6}$$

$$\frac{1}{\rho}\left(\frac{\partial(\rho H_\varphi)}{\partial \rho} - \mathrm{j}mH_\rho\right) = \mathrm{j}\omega\epsilon E_z. \tag{D.7}$$

The expressions of the E_ρ, E_z, H_ρ, H_z components as functions of the angular ones are now derived.

Derivation of E_ρ

The expressions of H_z are now derived from (D.4), (D.5):

$$H_z = -\frac{1}{\mathrm{j}kZ\rho}\left(\frac{\partial(\rho E_\varphi)}{\partial \rho} - \mathrm{j}mE_\rho\right)$$

$$H_z = \frac{\rho}{\mathrm{j}m}\left(\mathrm{j}kY E_\rho + \frac{\partial H_\varphi}{\partial z}\right).$$

Then, these two expressions are equated, leading to:

$$-\mathrm{j}m\frac{\partial(\rho E_\varphi)}{\partial \rho} - m^2 E_\rho = -k^2\rho^2 E_\rho + \mathrm{j}kZ\rho^2\frac{\partial H_\varphi}{\partial z},$$

so:

$$(m^2 - k^2\rho^2)E_\rho = -\mathrm{j}m\frac{\partial(\rho E_\varphi)}{\partial \rho} - \mathrm{j}kZ\rho^2\frac{\partial H_\varphi}{\partial z},$$

and then, finally:

$$E_\rho = -\frac{\mathrm{j}}{m^2 - k^2\rho^2}\left(m\frac{\partial(\rho E_\varphi)}{\partial \rho} + kZ\rho^2\frac{\partial H_\varphi}{\partial z}\right).$$

Derivation of E_z

Now H_ρ is derived from (D.2), (D.7):

$$H_\rho = -\frac{1}{\mathrm{j}kZ}\left(\frac{\mathrm{j}m}{\rho}E_z - \frac{\partial E_\varphi}{\partial z}\right)$$

$$H_\rho = -\frac{1}{\mathrm{j}m}\left(\mathrm{j}kY\rho E_z - \frac{\partial(\rho H_\varphi)}{\partial\rho}\right).$$

Then, these two expressions are equated:

$$-\frac{m^2}{\rho}E_z - \mathrm{j}m\frac{\partial E_\varphi}{\partial z} = -k^2\rho E_z - \mathrm{j}kZ\frac{\partial(\rho H_\varphi)}{\partial\rho},$$

so:

$$E_z(m^2 - k^2\rho^2) = -\mathrm{j}m\rho\frac{\partial E_\varphi}{\partial z} + \mathrm{j}kZ\rho\frac{\partial(\rho H_\varphi)}{\partial\rho},$$

and then:

$$E_z = -\frac{\mathrm{j}}{m^2 - k^2\rho^2}\left(m\rho\frac{\partial E_\varphi}{\partial z} - kZ\rho\frac{\partial(\rho H_\varphi)}{\partial\rho}\right).$$

Derivation of H_ρ

The component E_z is now derived from (D.2), (D.7):

$$E_z = \frac{\rho}{\mathrm{j}m}\left(\frac{\partial E_\varphi}{\partial z} - \mathrm{j}kZH_\rho\right)$$

$$E_z = \frac{1}{\mathrm{j}kY\rho}\left(\frac{\partial(\rho H_\varphi)}{\partial\rho} - \mathrm{j}mH_\rho\right).$$

Then, these two expressions are equated:

$$\mathrm{j}kY\rho^2\frac{\partial E_\varphi}{\partial z} + k^2\rho^2 H_\rho = \mathrm{j}m\frac{\partial(\rho H_\varphi)}{\partial\rho} + m^2 H_\rho,$$

leading to:

$$H_\rho(m^2 - k^2\rho^2) = \mathrm{j}kY\rho^2\frac{\partial E_\varphi}{\partial z} - \mathrm{j}m\frac{\partial(\rho H_\varphi)}{\partial\rho},$$

and, finally:

$$H_\rho = -\frac{\mathrm{j}}{m^2 - k^2\rho^2}\left(m\frac{\partial(\rho H_\varphi)}{\partial\rho} - kY\rho^2\frac{\partial E_\varphi}{\partial z}\right).$$

Derivation of H_z

The expressions of E_ρ are now derived from (D.4), (D.5):

$$E_\rho = -\frac{1}{\mathrm{j}m}\left(-\mathrm{j}kZ\rho H_z - \frac{\partial(\rho E_\varphi)}{\partial\rho}\right)$$

$$E_\rho = \frac{1}{\mathrm{j}kY} \left(\frac{\mathrm{j}m}{\rho} H_z - \frac{\partial H_\varphi}{\partial z} \right).$$

Then, these two expressions are equated:

$$k^2 \rho H_z - \mathrm{j}kY \frac{\partial(\rho E_\varphi)}{\partial \rho} = \frac{m^2}{\rho} H_z + \mathrm{j}m \frac{\partial H_\varphi}{\partial z},$$

so:

$$H_z(m^2 - k^2\rho^2) = -\mathrm{j}kY\rho \frac{\partial(\rho E_\varphi)}{\partial \rho} - \mathrm{j}m\rho \frac{\partial H_\varphi}{\partial z},$$

and, finally:

$$H_z = -\frac{\mathrm{j}}{m^2 - k^2\rho^2} \left(m\rho \frac{\partial H_\varphi}{\partial z} + kY \frac{\partial(\rho E_\varphi)}{\partial \rho} \right).$$

Resume of electromagnetic field components

The expressions obtained in the previous section are now summarized:

$$E_\rho = -\frac{\mathrm{j}}{m^2 - k^2\rho^2} \left(m \frac{\partial(\rho E_\varphi)}{\partial \rho} + kZ\rho^2 \frac{\partial H_\varphi}{\partial z} \right) \tag{D.8}$$

$$H_\rho = -\frac{\mathrm{j}}{m^2 - k^2\rho^2} \left(m \frac{\partial(\rho H_\varphi)}{\partial \rho} - kY\rho^2 \frac{\partial E_\varphi}{\partial z} \right) \tag{D.9}$$

$$E_z = -\frac{\mathrm{j}}{m^2 - k^2\rho^2} \left(m\rho \frac{\partial E_\varphi}{\partial z} - kZ\rho \frac{\partial(\rho H_\varphi)}{\partial \rho} \right) \tag{D.10}$$

$$H_z = -\frac{\mathrm{j}}{m^2 - k^2\rho^2} \left(kY\rho \frac{\partial(\rho E_\varphi)}{\partial \rho} + m\rho \frac{\partial H_\varphi}{\partial z} \right). \tag{D.11}$$

D.2.2 Formulation of the internal BVP: $m \neq 0$ case

Differential problem

Even if the two second-order equations in E_φ and H_φ can be easily derived by inserting (D.8) $\div$ (D.11) in (D.3) and (D.6), it is convenient to shift the differential operators from the field components to the test functions by using the following vector theorem:

$$\iint_\Sigma \left[\frac{\partial A_\rho}{\partial z} - \frac{\partial A_z}{\partial \rho} \right] f \, \mathrm{d}z \, \mathrm{d}\rho = -\iint_\Sigma \left[A_\rho \frac{\partial f}{\partial z} - A_z \frac{\partial f}{\partial \rho} \right] \mathrm{d}z \, \mathrm{d}\rho + \oint_\gamma (f\mathbf{A}) \cdot \mathrm{d}\mathbf{s},$$

where Σ is the domain where the BVP has to be solved, and γ is its boundary. The first step is to cast (D.3) and (D.6) in weak form, by projecting them on functions $v_r^{(\mathrm{e})}$ and $v_r^{(\mathrm{h})}$ belonging to the following function spaces:

$$V^{(e)} \triangleq \left\{ v_r^{(e)} : r \in \mathbb{N},\ v_r^{(e)} \in C^{(0)}(\varSigma), \frac{\partial v_r^{(e)}}{\partial x}, \frac{\partial v_r^{(e)}}{\partial z} \in L^2(\varSigma \setminus \partial\varSigma), v_r^{(e)}\big|_{\gamma_{\mathrm{PEC}}} = 0 \right\}$$

$$V^{(h)} \triangleq \left\{ v_r^{(h)} : r \in \mathbb{N},\ v_r^{(h)} \in C^{(0)}(\varSigma), \frac{\partial v_r^{(h)}}{\partial x}, \frac{\partial v_r^{(h)}}{\partial z} \in L^2(\varSigma \setminus \partial\varSigma) \right\},$$

where γ_{PEC} is the PEC part of boundary of $\varSigma$. The functions belonging to both spaces are continuous with square-integrable derivatives; moreover, the ones belonging to $V^{(e)}$ are further specialized to satisfy the Dirichlet boundary condition. Focusing on (D.6), its weak form is:

$$jkY \iint_{\varSigma} E_\varphi v_r^{(e)*} \mathrm{d}\rho\,\mathrm{d}z + \iint_{\varSigma} \left[H_\rho \frac{\partial v_r^{(e)*}}{\partial z} - H_z \frac{\partial v_r^{(e)*}}{\partial \rho} \right] \mathrm{d}\rho\,\mathrm{d}z = \oint_{\gamma} \left[\mathbf{H}_{\mathrm{t}}^{(\varphi)} v_r^{(e)*} \right] \cdot \mathrm{d}\mathbf{s}$$

$$(\mathrm{LHS})_r^{(e)} = (\mathrm{RHS})_r^{(e)}. \qquad (\mathrm{D}.12)$$

According to the method of weighted residuals, the φ components of the electromagnetic field are written as series expansions, using functions $u_c^{(e)} \in V^{(e)}$ and $u_c^{(h)} \in V^{(h)}$, as follows;

$$E_\varphi = \sum_{c=1}^{N_{\mathrm{f}}^{(e)}} c_c^{(e)} u_c^{(e)} \qquad (\mathrm{D}.13)$$

$$H_\varphi = \sum_{c=1}^{N_{\mathrm{f}}^{(h)}} c_c^{(h)} u_c^{(h)}, \qquad (\mathrm{D}.14)$$

where $u_c^{(e)} = v_c^{(e)}, u_c^{(h)} = v_c^{(h)}$. The left-hand side of (D.12) is now written using these expansions for the φ components

$$(\text{LHS})_r^{(e)} = \mathrm{j}kY \sum_{c=0}^{N_{\mathrm{f}}^{(e)}} c_c^{(e)} \iint_{\Sigma} u_c^{(e)} v_r^{(e)*} \mathrm{d}\rho \mathrm{d}z +$$

$$- \sum_{c=0}^{N_{\mathrm{f}}^{(h)}} c_c^{(h)} \iint_{\Sigma} \frac{\mathrm{j}m}{m^2 - k^2\rho^2} \frac{\partial(\rho u_c^{(h)})}{\partial\rho} \frac{\partial v_r^{(e)*}}{\partial z} \mathrm{d}\rho \mathrm{d}z +$$

$$+ \sum_{c=0}^{N_{\mathrm{f}}^{(e)}} c_c^{(e)} \iint_{\Sigma} \frac{\mathrm{j}kY\rho^2}{m^2 - k^2\rho^2} \frac{\partial u_c^{(e)}}{\partial z} \frac{\partial v_r^{(e)*}}{\partial z} \mathrm{d}\rho \mathrm{d}z +$$

$$+ \sum_{c=0}^{N_{\mathrm{f}}^{(e)}} c_c^{(e)} \iint_{\Sigma} \frac{\mathrm{j}kY\rho}{m^2 - k^2\rho^2} \frac{\partial(\rho u_c^{(e)})}{\partial\rho} \frac{\partial v_r^{(e)*}}{\partial\rho} \mathrm{d}\rho \mathrm{d}z +$$

$$- \sum_{c=0}^{N_{\mathrm{f}}^{(h)}} c_c^{(h)} \iint_{\Sigma} \frac{\mathrm{j}m\rho}{m^2 - k^2\rho^2} \frac{\partial u_c^{(h)}}{\partial z} \frac{\partial v_r^{(e)*}}{\partial\rho} \mathrm{d}\rho \mathrm{d}z$$

Then, after some arrangement:

$$(\text{LHS})_r^{(e)} = \mathrm{j}kY \sum_{c=0}^{N_{\mathrm{f}}^{(e)}} c_c^{(e)} \iint_{\Sigma} u_c^{(e)} v_r^{(e)*} \mathrm{d}\rho \mathrm{d}z +$$

$$+ \sum_{c=0}^{N_{\mathrm{f}}^{(h)}} c_c^{(h)} \iint_{\Sigma} \left\{ \frac{\mathrm{j}m}{m^2 - k^2\rho^2} \left[\frac{\partial(\rho u_c^{(h)})}{\partial\rho} \frac{\partial v_r^{(e)*}}{\partial z} - \rho \frac{\partial u_c^{(h)}}{\partial z} \frac{\partial v_r^{(e)*}}{\partial\rho} \right] \right\} \mathrm{d}\rho \mathrm{d}z +$$

$$+ \sum_{c=0}^{N_{\mathrm{f}}^{(e)}} c_c^{(e)} \iint_{\Sigma} \left\{ \frac{\mathrm{j}kY}{m^2 - k^2\rho^2} \rho \left[\rho \frac{\partial u_c^{(e)}}{\partial z} \frac{\partial v_r^{(e)*}}{\partial z} + \frac{\partial(\rho u_c^{(e)})}{\partial\rho} \frac{\partial v_r^{(e)*}}{\partial\rho} \right] \right\} \mathrm{d}\rho \mathrm{d}z.$$

By defining:

$$(\mathbf{M}^{(e)})_{rc} = \iint_{\Sigma} u_c^{(e)} v_r^{(e)*} \mathrm{d}\rho \mathrm{d}z$$

$$(\mathbf{K}^{(e)})_{rc} = \iint_{\Sigma} \left\{ \frac{1}{m^2 - k^2\rho^2} \rho \left[\rho \frac{\partial u_c^{(e)}}{\partial z} \frac{\partial v_r^{(e)*}}{\partial z} + \frac{\partial(\rho u_c^{(e)})}{\partial\rho} \frac{\partial v_r^{(e)*}}{\partial\rho} \right] \right\} \mathrm{d}\rho \mathrm{d}z$$

$$(\mathbf{L}^{(e)})_{rc} = \iint_{\Sigma} \left\{ \frac{1}{m^2 - k^2\rho^2} \left[\frac{\partial(\rho u_c^{(h)})}{\partial\rho} \frac{\partial v_r^{(e)*}}{\partial z} - \rho \frac{\partial u_c^{(h)}}{\partial z} \frac{\partial v_r^{(e)*}}{\partial\rho} \right] \right\} \mathrm{d}\rho \mathrm{d}z,$$

it is possible to write compactly the equation as:

$$(\text{LSE})^{(e)} = \mathrm{j}kY \left[\mathbf{M}^{(e)} + \mathbf{K}^{(e)} \right] \mathbf{c}^{(e)} + \mathrm{j}m\mathbf{L}^{(e)} \mathbf{c}^{(h)} =$$
$$= \mathbf{A}^{(e,e)} \mathbf{c}^{(e)} + \mathbf{A}^{(e,h)} \mathbf{c}^{(h)}.$$

The following duality theorem is then applied:

$$c_c^{(e)} \longleftrightarrow c_c^{(h)}$$
$$u_c^{(e)} \longleftrightarrow u_c^{(h)}$$
$$v_r^{(e)} \longleftrightarrow v_r^{(h)}$$
$$Z \longleftrightarrow -Y,$$

the following matrices are defined,

$$(\mathbf{M}^{(h)})_{rc} = \iint_{\Sigma} u_c^{(h)} v_r^{(h)*} \mathrm{d}\rho \mathrm{d}z$$

$$(\mathbf{K}^{(h)})_{rc} = \iint_{\Sigma} \left\{ \frac{1}{m^2 - k^2 \rho^2} \rho \left[\rho \frac{\partial u_c^{(h)}}{\partial z} \frac{\partial v_r^{(h)*}}{\partial z} + \frac{\partial(\rho u_c^{(h)})}{\partial \rho} \frac{\partial v_r^{(h)*}}{\partial \rho} \right] \right\} \mathrm{d}\rho \mathrm{d}z$$

$$(\mathbf{L}^{(h)})_{rc} = \iint_{\Sigma} \left\{ \frac{1}{m^2 - k^2 \rho^2} \left[\frac{\partial(\rho u_c^{(e)})}{\partial \rho} \frac{\partial v_r^{(h)*}}{\partial z} - \rho \frac{\partial u_c^{(e)}}{\partial z} \frac{\partial v_r^{(h)*}}{\partial \rho} \right] \right\} \mathrm{d}\rho \mathrm{d}z,$$

and the dual equation is written as:

$$(\mathrm{LSE})^{(h)} = \mathrm{j}m\mathbf{L}^{(h)} \mathbf{c}^{(e)} - \mathrm{j}kZ \left[\mathbf{M}^{(h)} + \mathbf{K}^{(h)} \right] \mathbf{c}^{(h)} =$$
$$= \mathbf{A}^{(h,e)} \mathbf{c}^{(e)} + \mathbf{A}^{(h,h)} \mathbf{c}^{(h)}.$$

Formulation of the continuity equations

In this section the projection matrix elements related to the continuity equations at the access ports are derived, to complete the formulation of the scattering problem. The scalar products used in this context are defined, at the k-th access port, as:

$$\langle \mathbf{a}, \mathbf{b} \rangle = 2\pi \int_0^{\rho_{\mathrm{wg}}^{(k)}} \mathbf{a}(\rho, \varphi) \cdot \mathbf{b}^*(\rho, \varphi) \rho \, \mathrm{d}\rho.$$

Continuity of the electric field at port 1

The first continuity equation is:

$$\left\langle \widehat{\mathbf{E}}_{\mathrm{t}}^{(1)}, \mathbf{e}_q^{(1)} \right\rangle = \left\langle \widetilde{\mathbf{E}}_{\mathrm{t}}^{(1)}, \mathbf{e}_q^{(1)} \right\rangle,$$

where:

$$\left\langle \widetilde{\mathbf{E}}_{\mathrm{t}}^{(1)}, \mathbf{e}_q^{(1)} \right\rangle = \left\langle \widetilde{E}_{\rho}^{(1)}, e_{\rho,q}^{(1)} \right\rangle + \left\langle \widetilde{E}_{\varphi}^{(1)}, e_{\varphi,q}^{(1)} \right\rangle.$$

Then, recalling (D.8):

$$\left\langle \widetilde{E}_\rho^{(1)}, e_{\rho,q}^{(1)} \right\rangle = \sum_{c=1}^{N_{\mathrm{f}}^{(\mathrm{e})}} c_c^{(\mathrm{e})} \left\langle -\frac{\mathrm{j}m}{m^2 - k^2\rho^2} \left(\rho\frac{\partial u_c^{(\mathrm{e})}}{\partial\rho} + u_c^{(\mathrm{e})} \right)\bigg|_{z=z_{\mathrm{wg}}^{(1)}}, e_{\rho,q}^{(1)} \right\rangle +$$

$$+ \sum_{c=1}^{N_{\mathrm{f}}^{(\mathrm{h})}} c_c^{(\mathrm{h})} \left\langle -\frac{\mathrm{j}kZ\rho^2}{m^2 - k^2\rho^2} \frac{\partial u_c^{(\mathrm{h})}}{\partial z}\bigg|_{z=z_{\mathrm{wg}}^{(1)}}, e_{\rho,q}^{(1)} \right\rangle$$

$$\left\langle \widetilde{E}_\varphi^{(1)}, e_{\varphi,q}^{(1)} \right\rangle = \sum_{c=1}^{N_{\mathrm{f}}^{(\mathrm{e})}} c_c^{(\mathrm{e})} \left\langle u_c^{(\mathrm{e})}\big|_{z=z_{\mathrm{wg}}^{(1)}}, e_{\varphi,q}^{(1)} \right\rangle.$$

So, the following matrix elements are defined:

$$\begin{cases} (\mathbf{C}^{(\mathrm{e},1)})_{qc} = \left\langle u_c^{(\mathrm{e})}\big|_{z=z_{\mathrm{wg}}^{(1)}}, e_{\varphi,q}^{(1)} \right\rangle \\[2mm] (\mathbf{H}^{(\mathrm{e},1)})_{qc} = \left\langle \frac{1}{m^2 - k^2\rho^2} \left(\rho\frac{\partial u_c^{(\mathrm{e})}}{\partial\rho} + u_c^{(\mathrm{e})} \right)\bigg|_{z=z_{\mathrm{wg}}^{(1)}}, e_{\rho,q}^{(1)} \right\rangle \\[2mm] (\mathbf{K}^{(\mathrm{h},1)})_{qc} = \left\langle \frac{\rho^2}{m^2 - k^2\rho^2} \frac{\partial u_c^{(\mathrm{h})}}{\partial z}\bigg|_{z=z_{\mathrm{wg}}^{(1)}}, e_{\rho,q}^{(1)} \right\rangle, \end{cases}$$

and then it is possible to write the projection term of the equation in matrix form as:

$$\left[\mathbf{C}^{(\mathrm{e},1)} - \mathrm{j}m\mathbf{H}^{(\mathrm{e},1)} \right] \mathbf{c}^{(\mathrm{e})} - \mathrm{j}kZ\mathbf{K}^{(\mathrm{h},1)}\mathbf{c}^{(\mathrm{h})}.$$

Continuity of the magnetic field at port 1

The second continuity equation is:

$$\left\langle \widehat{\mathbf{H}}_{\mathrm{t}}^{(1)}, \mathbf{h}_q^{(1)} \right\rangle = \left\langle \widetilde{\mathbf{H}}_{\mathrm{t}}^{(1)}, \mathbf{h}_q^{(1)} \right\rangle,$$

where:

$$\left\langle \widetilde{\mathbf{H}}_{\mathrm{t}}^{(1)}, \mathbf{h}_q^{(1)} \right\rangle = \left\langle \widetilde{H}_\rho^{(1)}, h_{\rho,q}^{(1)} \right\rangle + \left\langle \widetilde{H}_\varphi^{(1)}, h_{\varphi,q}^{(1)} \right\rangle.$$

By recalling (D.9) the following equations are obtained:

$$\left\langle \widetilde{H}_\rho^{(1)}, h_{\rho,q}^{(1)} \right\rangle = \sum_{c=1}^{N_f^{(e)}} c_c^{(e)} \left\langle \left. \frac{jkY\rho^2}{m^2 - k^2\rho^2} \frac{\partial u_c^{(e)}}{\partial z} \right|_{z=z_{wg}^{(1)}}, h_{\rho,q}^{(1)} \right\rangle +$$

$$+ \sum_{c=1}^{N_f^{(h)}} c_c^{(h)} \left\langle -\frac{jm}{m^2 - k^2\rho^2} \left(\left. \frac{\partial u_c^{(h)}}{\partial \rho} \right|_{z=z_{wg}^{(1)}} + u_c^{(h)} \right), h_{\rho,q}^{(1)} \right\rangle$$

$$\left\langle \widetilde{H}_\varphi^{(1)}, h_{\varphi,q}^{(1)} \right\rangle = \sum_{c=1}^{N_f^{(h)}} c_c^{(h)} \left\langle \left. u_c^{(h)} \right|_{z=z_{wg}^{(1)}}, h_{\varphi,q}^{(1)} \right\rangle .$$

So, the following matrix elements are defined:

$$\begin{cases} (\mathbf{C}^{(h,1)})_{qc} = \left\langle \left. u_c^{(h)} \right|_{z=z_{wg}^{(1)}}, h_{\varphi,q}^{(1)} \right\rangle \\[2em] (\mathbf{H}^{(h,1)})_{qc} = \left\langle \left. \frac{1}{m^2 - k^2\rho^2} \left(\frac{\partial u_c^{(h)}}{\partial \rho} + u_c^{(h)} \right) \right|_{z=z_{wg}^{(1)}}, h_{\rho,q}^{(1)} \right\rangle \\[2em] (\mathbf{K}^{(e,1)})_{qc} = \left\langle \left. \frac{\rho^2}{m^2 - k^2\rho^2} \frac{\partial u_c^{(e)}}{\partial z} \right|_{z=z_{wg}^{(1)}}, h_{\rho,q}^{(1)} \right\rangle , \end{cases}$$

so, it is possible to write this side of the equation as:

$$\left[\mathbf{C}^{(h,1)} - jm\mathbf{H}^{(h,1)} \right] \mathbf{c}^{(h)} + jkY\mathbf{K}^{(e,1)}\mathbf{c}^{(e)}.$$

Continuity of the electric field at port 2

The third continuity equation is:

$$\left\langle \widehat{\mathbf{E}}_t^{(2)}, \mathbf{e}_q^{(2)} \right\rangle = \left\langle \widetilde{\mathbf{E}}_t^{(2)}, \mathbf{e}_q^{(2)} \right\rangle ,$$

where:

$$\left\langle \widehat{\mathbf{E}}_t^{(2)}, \mathbf{e}_q^{(2)} \right\rangle = \left\langle \widehat{E}_\rho^{(2)}, e_{\rho,q}^{(2)} \right\rangle + \left\langle \widehat{E}_\varphi^{(2)}, e_{\varphi,q}^{(2)} \right\rangle .$$

Then, recalling (D.8):

$$\left\langle \widehat{E}_\rho^{(2)}, e_{\rho,q}^{(2)} \right\rangle = \sum_{c=1}^{N_{\mathrm{f}}^{(\mathrm{e})}} c_c^{(\mathrm{e})} \left\langle -\frac{\mathrm{j}m}{m^2 - k^2\rho^2} \left(\rho\frac{\partial u_c^{(\mathrm{e})}}{\partial\rho} + u_c^{(\mathrm{e})} \right)\bigg|_{z=z_{\mathrm{wg}}^{(2)}}, e_{\rho,q}^{(2)} \right\rangle +$$

$$+ \sum_{c=1}^{N_{\mathrm{f}}^{(\mathrm{h})}} c_c^{(\mathrm{h})} \left\langle -\frac{\mathrm{j}kZ\rho^2}{m^2 - k^2\rho^2} \frac{\partial u_c^{(\mathrm{h})}}{\partial z}\bigg|_{z=z_{\mathrm{wg}}^{(2)}}, e_{\rho,q}^{(2)} \right\rangle$$

$$\left\langle \widehat{E}_\varphi^{(2)}, e_{\varphi,q}^{(2)} \right\rangle = \sum_{c=1}^{N_{\mathrm{f}}^{(\mathrm{e})}} c_c^{(\mathrm{e})} \left\langle u_c^{(\mathrm{e})}\big|_{z=z_{\mathrm{wg}}^{(2)}}, e_{\varphi,q}^{(2)} \right\rangle.$$

So, the following matrix elements are defined:

$$\begin{cases} (\mathbf{C}^{(\mathrm{e},2)})_{qc} = \left\langle u_r^{(\mathrm{e})}\big|_{z=z_{\mathrm{wg}}^{(2)}}, e_{\varphi,t}^{(2)} \right\rangle \\[2ex] (\mathbf{H}^{(\mathrm{e},2)})_{qc} = \left\langle \frac{1}{m^2 - k^2\rho^2} \left(\rho\frac{\partial u_r^{(\mathrm{e})}}{\partial\rho} + u_r^{(\mathrm{e})} \right)\bigg|_{z=z_{\mathrm{wg}}^{(2)}}, e_{\rho,t}^{(2)} \right\rangle \\[2ex] (\mathbf{K}^{(\mathrm{h},2)})_{qc} = \left\langle \frac{\rho^2}{m^2 - k^2\rho^2} \frac{\partial u_r^{(\mathrm{h})}}{\partial z}\bigg|_{z=z_{\mathrm{wg}}^{(2)}}, e_{\rho,t}^{(2)} \right\rangle, \end{cases}$$

and then it is possible to write the projection term of the equation in matrix form as:

$$\left[\mathbf{C}^{(\mathrm{e},2)} - \mathrm{j}m\mathbf{H}^{(\mathrm{e},2)} \right] \mathbf{c}^{(\mathrm{e})} - \mathrm{j}kZ\mathbf{K}^{(\mathrm{h},2)}\mathbf{c}^{(\mathrm{h})}.$$

Continuity of the magnetic field at port 2

The last continuity equation is:

$$\left\langle \widehat{\mathbf{H}}_{\mathrm{t}}^{(2)}, \mathbf{h}_q^{(2)} \right\rangle = \left\langle \widetilde{\mathbf{H}}_{\mathrm{t}}^{(2)}, \mathbf{h}_q^{(2)} \right\rangle,$$

where:

$$\left\langle \widehat{\mathbf{H}}_{\mathrm{t}}^{(2)}, \mathbf{h}_q^{(2)} \right\rangle = \left\langle \widehat{H}_\rho^{(2)}, h_{\rho,q}^{(2)} \right\rangle + \left\langle \widehat{H}_\varphi^{(2)}, h_{\varphi,q}^{(2)} \right\rangle.$$

Then, by recalling (D.9):

$$\left\langle \widehat{H}_\rho^{(2)}, h_{\rho,q}^{(2)} \right\rangle = \sum_{c=1}^{N_f^{(e)}} c_c^{(e)} \left\langle \left. \frac{jkY\rho^2}{m^2 - k^2\rho^2} \frac{\partial u_c^{(e)}}{\partial z} \right|_{z=z_{wg}^{(2)}}, h_{\rho,q}^{(2)} \right\rangle +$$

$$+ \sum_{c=1}^{N_f^{(h)}} c_c^{(h)} \left\langle -\frac{jm}{m^2 - k^2\rho^2} \left(\left. \frac{\partial u_c^{(h)}}{\partial \rho} \right|_{z=z_{wg}^{(2)}} + u_c^{(h)} \right), h_{\rho,q}^{(2)} \right\rangle$$

$$\left\langle \widehat{H}_\varphi^{(2)}, h_{\varphi,q}^{(2)} \right\rangle = \sum_{c=1}^{N_f^{(h)}} c_c^{(h)} \left\langle \left. u_c^{(h)} \right|_{z=z_{wg}^{(2)}}, h_{\varphi,q}^{(2)} \right\rangle .$$

So, the following matrix elements are defined:

$$\begin{cases} (\mathbf{C}^{(h,2)})_{qc} = \left\langle \left. u_c^{(h)} \right|_{z=z_{wg}^{(2)}}, h_{\varphi,q}^{(2)} \right\rangle \\[2mm] (\mathbf{H}^{(h,2)})_{qc} = \left\langle \left. \frac{1}{m^2 - k^2\rho^2} \left(\frac{\partial u_c^{(h)}}{\partial \rho} + u_c^{(h)} \right) \right|_{z=z_{wg}^{(2)}}, h_{\rho,q}^{(2)} \right\rangle \\[2mm] (\mathbf{K}^{(e,2)})_{qc} = \left\langle \left. \frac{\rho^2}{m^2 - k^2\rho^2} \frac{\partial u_c^{(e)}}{\partial z} \right|_{z=z_{wg}^{(2)}}, h_{\rho,q}^{(2)} \right\rangle , \end{cases}$$

and then the projection term of the equation in matrix form is written as:

$$\left[\mathbf{C}^{(h,2)} - jm\mathbf{H}^{(h,2)} \right] \mathbf{c}^{(h)} + jkY\mathbf{K}^{(e,2)}\mathbf{c}^{(e)}.$$

Definition of the projection matrix

The matrix $\mathbf{T}$ is defined as:

$$\mathbf{T} = \begin{bmatrix} \mathbf{C}^{(e,1)} - jm\mathbf{H}^{(e,1)} & -jkZ\mathbf{K}^{(h,1)} \\[3mm] jkY\mathbf{K}^{(e,1)} & \mathbf{C}^{(h,1)} - jm\mathbf{H}^{(h,1)} \\[3mm] \mathbf{C}^{(e,2)} - jm\mathbf{H}^{(e,2)} & -jkZ\mathbf{K}^{(h,2)} \\[3mm] jkY\mathbf{K}^{(e,2)} & \mathbf{C}^{(h,2)} - jm\mathbf{H}^{(h,2)} \end{bmatrix}$$

D.2.3   Formulation of the internal BVP: $m = 0$, TM_z case

In the TM_z problem of the $m = 0$ case, (D.8) and (D.10) simplify as:

$$\begin{aligned} E_\rho &= \frac{j}{kY} \frac{\partial H_\varphi}{\partial z} \\ E_z &= -\frac{j}{kY\rho} \frac{\partial(\rho H_\varphi)}{\partial \rho} = -\frac{j}{kY\rho} H_\varphi - \frac{j}{kY} \frac{\partial H_\varphi}{\partial \rho}. \end{aligned} \tag{D.15}$$

Then, (D.3) is cast in weak form by projecting it on test functions defined as $w_r^{(h)} = \rho^2 v_r^{(h)}$. This eliminates the singularity of the field components (D.15) in $\rho = 0$. Then, the Stokes theorem is applied to integrate the resulting equation by parts:

$$-\mathrm{j}kZ \iint_\Sigma H_\varphi w_r^{(h)*} \, \mathrm{d}z \, \mathrm{d}\rho + \iint_\Sigma \left[E_\rho \frac{\partial w_r^{(h)*}}{\partial z} - E_z \frac{\partial w_r^{(h)*}}{\partial \rho} \right] \mathrm{d}z \, \mathrm{d}\rho = \oint_\gamma (\mathbf{E}_t^{(\varphi)} w_r^{(h)*}) \cdot \mathrm{d}\mathbf{s}$$

$$(\mathrm{LHS})_r^{(h)} = (\mathrm{RHS})_r^{(h)}.$$

Now, (D.15) are substituted in the left-hand side of this equation, leading to:

$$(\mathrm{LHS})_r^{(h)} = -\mathrm{j}kZ \iint_\Sigma H_\varphi w_r^{(h)*} \, \mathrm{d}z \, \mathrm{d}\rho +$$

$$- \frac{1}{\mathrm{j}kY} \iint_\Sigma \frac{\partial H_\varphi}{\partial z} \frac{\partial w_r^{(h)*}}{\partial z} \, \mathrm{d}z \, \mathrm{d}\rho +$$

$$- \frac{1}{\mathrm{j}kY} \iint_\Sigma \left[\frac{1}{\rho} H_\varphi + \frac{\partial H_\varphi}{\partial \rho} \right] \frac{\partial w_r^{(h)*}}{\partial \rho} \, \mathrm{d}z \, \mathrm{d}\rho.$$

It should be noted that the integrand functions have a pole in $\rho = 0$; with this choice of the test functions, this singularity is removed; indeed:

$$w_r^{(h)} = \rho^2 v_r^{(h)}$$
$$\frac{\partial w_r^{(h)}}{\partial z} = \rho^2 \frac{\partial v_r^{(h)}}{\partial z}$$
$$\frac{\partial w_r^{(h)}}{\partial \rho} = \rho^2 \frac{\partial v_r^{(h)}}{\partial \rho} + 2\rho v_r^{(h)}.$$

This is now substituted in the previous equation, leading to:

$$(\mathrm{LHS})_r^{(h)} = -\mathrm{j}kZ \iint_\Sigma H_\varphi v_r^{(h)*} \rho^2 \, \mathrm{d}z \, \mathrm{d}\rho +$$

$$- \frac{1}{\mathrm{j}kY} \iint_\Sigma \frac{\partial H_\varphi}{\partial z} \frac{\partial v_r^{(h)*}}{\partial z} \rho^2 \, \mathrm{d}z \, \mathrm{d}\rho +$$

$$- \frac{1}{\mathrm{j}kY} \iint_\Sigma \left[H_\varphi + \rho \frac{\partial H_\varphi}{\partial \rho} \right] \left[\rho \frac{\partial v_r^{(h)*}}{\partial \rho} + 2 v_r^{(h)*} \right] \mathrm{d}z \, \mathrm{d}\rho.$$

Then, by substituting the expansion (D.14), this equation becomes:

$$(\text{LHS})_r^{(\text{h})} = \sum_{c=0}^{N_{\text{f}}^{(\text{h})}} c_c^{(\text{h})} \left\{ -\mathrm{j}kZ \iint_{\Sigma} H_\varphi v_r^{(\text{h})*} \rho^2 \, \mathrm{d}z \, \mathrm{d}\rho + \right.$$

$$- \frac{1}{\mathrm{j}kY} \iint_{\Sigma} \frac{\partial H_\varphi}{\partial z} \frac{\partial v_r^{(\text{h})*}}{\partial z} \rho^2 \, \mathrm{d}z \, \mathrm{d}\rho +$$

$$\left. - \frac{1}{\mathrm{j}kY} \iint_{\Sigma} \left[H_\varphi + \rho \frac{\partial H_\varphi}{\partial \rho} \right] \left[\rho \frac{\partial v_r^{(\text{h})*}}{\partial \rho} + 2v_r^{(\text{h})*} \right] \mathrm{d}z \, \mathrm{d}\rho \right\},$$

which is compactly written as:

$$(\text{LHS})^{(\text{h})} = \mathbf{A}^{(\text{h,h})} \mathbf{c}^{(\text{h})},$$

where:

$$\mathbf{A}^{(\text{h,h})} = -\mathrm{j}kZ\mathbf{M}^{(\text{h},0)} - \frac{1}{\mathrm{j}kY}\mathbf{K}^{(\text{h},0)},$$

and:

$$\mathbf{M}^{(\text{h},0)} = \iint_{\Sigma} u_c^{(\text{h})} v_r^{(\text{h})*} \rho^2 \, \mathrm{d}z \, \mathrm{d}\rho$$

$$\mathbf{K}^{(\text{h},0)} = \iint_{\Sigma} \frac{\partial u_c^{(\text{h})}}{\partial z} \frac{\partial v_r^{(\text{h})*}}{\partial z} \rho^2 \, \mathrm{d}z \, \mathrm{d}\rho + \iint_{\Sigma} \left[u_c^{(\text{h})} + \rho \frac{\partial u_c^{(\text{h})}}{\partial \rho} \right] \left[\rho \frac{\partial v_r^{(\text{h})*}}{\partial \rho} + 2v_r^{(\text{h})*} \right] \mathrm{d}z \, \mathrm{d}\rho.$$

Formulation of the continuity equations

The continuity of the electric field is automatically satisfied by the choice of the magnetic current densities at the access ports, as discussed in Chapter 1; therefore, to complete the formulation of the problem the continuity of the tangent magnetic field has to be enforced. Since $\mathbf{H}_{\text{t}} = \widehat{\boldsymbol{\varphi}} H_\varphi$, the continuity condition that should be enforced is:

$$\left\langle \widehat{H}_\varphi^{(k)}, h_{\varphi,q}^{(k)} \right\rangle = \left\langle \widetilde{H}_\varphi^{(k)}, h_{\varphi,q}^{(k)} \right\rangle,$$

which is written explicitly as:

$$2\pi \int_0^{\rho_{\text{wg}}^{(k)}} \widehat{H}_\varphi^{(k)} h_{\varphi,q}^{(k)*} \rho \, \mathrm{d}\rho = 2\pi \sum_{c=0}^{N_{\text{f}}^{(\text{h})}} c_c^{(\text{h})} \int_0^{\rho_{\text{wg}}^{(k)}} \widetilde{H}_\varphi^{(k)} h_{\varphi,q}^{(k)*} \rho \, \mathrm{d}\rho,$$

so, the right-hand side of this condition is written as:

$$2\pi \sum_{c=0}^{N_{\text{f}}^{(\text{h})}} c_c^{(\text{h})} \int_0^{\rho_{\text{wg}}^{(k)}} u_c^{(\text{h})} h_{\varphi,q}^{(k)*} \rho \, \mathrm{d}\rho = \mathbf{C}^{(\text{h},k)} \mathbf{c}^{(\text{h})},$$

and so:

$$\mathbf{T}_k^{(\mathrm{h})} = \mathbf{C}^{(\mathrm{h},k)},$$

where:

$$(\mathbf{C}^{(\mathrm{h},k)})_{qc} = 2\pi \int_0^{\rho_{\mathrm{wg}}^{(k)}} u_c^{(\mathrm{h})} h_{\varphi,q}^{(k)*} \rho \,\mathrm{d}\rho.$$

D.2.4   Formulation of the internal BVP: $m = 0$, TE_z case

In the TE_z problem of the $m = 0$ case, (D.9) and (D.11) simplify as:

$$
\begin{aligned}
H_\rho &= -\frac{\mathrm{j}}{kZ}\frac{\partial E_\varphi}{\partial z} \\
H_z &= \frac{\mathrm{j}}{kZ\rho}\frac{\partial(\rho E_\varphi)}{\partial \rho} = \frac{\mathrm{j}}{kZ\rho}E_\varphi + \frac{\mathrm{j}}{kZ}\frac{\partial E_\varphi}{\partial \rho}.
\end{aligned}
\tag{D.16}
$$

Then, (D.6) is cast in weak form by projecting it on test functions defined as $w_r^{(\mathrm{e})} = \rho^2 v_r^{(\mathrm{e})}$. This eliminates the singularity of the field components (D.16) in $\rho = 0$. Then, the Stokes theorem is applied to integrate the resulting equation by parts:

$$\mathrm{j}kY \iint_\Sigma E_\varphi w_r^{(\mathrm{e})*} \,\mathrm{d}z \,\mathrm{d}\rho + \iint_\Sigma \left[H_\rho \frac{\partial w_r^{(\mathrm{e})*}}{\partial z} - H_z \frac{\partial w_r^{(\mathrm{e})*}}{\partial \rho} \right] \mathrm{d}z \,\mathrm{d}\rho = \oint_\gamma (\mathbf{H}_{\mathrm{t}}^{(\varphi)} w_r^{(\mathrm{e})*}) \cdot \mathrm{d}\mathbf{s}$$

$$(\mathrm{LHS})_r^{(\mathrm{e})} = (\mathrm{RHS})_r^{(\mathrm{e})}.$$

Now, (D.16) are substituted in the left-hand side of this equation, leading to:

$$
\begin{aligned}
(\mathrm{LHS})_r^{(\mathrm{e})} = {}& \mathrm{j}kY \iint_\Sigma E_\varphi w_r^{(\mathrm{e})*} \,\mathrm{d}z \,\mathrm{d}\rho + \\
& + \frac{1}{\mathrm{j}kZ} \iint_\Sigma \frac{\partial E_\varphi}{\partial z}\frac{\partial w_r^{(\mathrm{e})*}}{\partial z} \,\mathrm{d}z \,\mathrm{d}\rho + \\
& + \frac{1}{\mathrm{j}kZ} \iint_\Sigma \left[\frac{1}{\rho}E_\varphi + \frac{\partial E_\varphi}{\partial \rho}\right] \frac{\partial w_r^{(\mathrm{e})*}}{\partial \rho} \,\mathrm{d}z \,\mathrm{d}\rho.
\end{aligned}
$$

It should be noted that the integrand functions have a pole in $\rho = 0$; with this choice of the test functions, this singularity is removed; indeed:

$$
\begin{aligned}
w_r^{(\mathrm{e})} &= \rho^2 v_r^{(\mathrm{e})} \\
\frac{\partial w_r^{(\mathrm{e})}}{\partial z} &= \rho^2 \frac{\partial v_r^{(\mathrm{e})}}{\partial z} \\
\frac{\partial w_r^{(\mathrm{e})}}{\partial \rho} &= \rho^2 \frac{\partial v_r^{(\mathrm{e})}}{\partial \rho} + 2\rho v_r^{(\mathrm{e})}.
\end{aligned}
$$

This is now substituted in the previous equation, leading to:

$$(\text{LHS})_r^{(\text{e})} = \text{j}kY \iint_{\Sigma} E_{\varphi} v_r^{(\text{e})*} \rho^2 \, \text{d}z \, \text{d}\rho +$$

$$+ \frac{1}{\text{j}kZ} \iint_{\Sigma} \frac{\partial E_{\varphi}}{\partial z} \frac{\partial v_r^{(\text{e})*}}{\partial z} \rho^2 \, \text{d}z \, \text{d}\rho +$$

$$+ \frac{1}{\text{j}kZ} \iint_{\Sigma} \left[E_{\varphi} + \rho \frac{\partial E_{\varphi}}{\partial \rho} \right] \left[\rho \frac{\partial v_r^{(\text{e})*}}{\partial \rho} + 2 v_r^{(\text{e})*} \right] \, \text{d}z \, \text{d}\rho.$$

Then, by substituting the expansion (D.14), this equation becomes:

$$(\text{LHS})_r^{(\text{e})} = \sum_{c=0}^{N_{\text{f}}^{(\text{e})}} c_c^{(\text{e})} \left\{ \text{j}kY \iint_{\Sigma} E_{\varphi} v_r^{(\text{e})*} \rho^2 \, \text{d}z \, \text{d}\rho + \right.$$

$$+ \frac{1}{\text{j}kZ} \iint_{\Sigma} \frac{\partial E_{\varphi}}{\partial z} \frac{\partial v_r^{(\text{e})*}}{\partial z} \rho^2 \, \text{d}z \, \text{d}\rho +$$

$$\left. + \frac{1}{\text{j}kZ} \iint_{\Sigma} \left[E_{\varphi} + \rho \frac{\partial E_{\varphi}}{\partial \rho} \right] \left[\rho \frac{\partial v_r^{(\text{e})*}}{\partial \rho} + 2 v_r^{(\text{e})*} \right] \, \text{d}z \, \text{d}\rho \right\},$$

which is compactly written as:

$$(\text{LHS})^{(\text{e})} = \mathbf{A}^{(\text{e},\text{e})} \, \mathbf{c}^{(\text{e})},$$

where:

$$\mathbf{A}^{(\text{h},\text{h})} = \text{j}kY \mathbf{M}^{(\text{e},0)} + \frac{1}{\text{j}kZ} \mathbf{K}^{(\text{e},0)},$$

and:

$$\mathbf{M}^{(\text{e},0)} = \iint_{\Sigma} u_c^{(\text{e})} v_r^{(\text{e})*} \rho^2 \, \text{d}z \, \text{d}\rho$$

$$\mathbf{K}^{(\text{e},0)} = \iint_{\Sigma} \frac{\partial u_c^{(\text{e})}}{\partial z} \frac{\partial v_r^{(\text{e})*}}{\partial z} \rho^2 \, \text{d}z \, \text{d}\rho + \iint_{\Sigma} \left[u_c^{(\text{e})} + \rho \frac{\partial u_c^{(\text{e})}}{\partial \rho} \right] \left[\rho \frac{\partial v_r^{(\text{e})*}}{\partial \rho} + 2 v_r^{(\text{e})*} \right] \, \text{d}z \, \text{d}\rho.$$

Formulation of the continuity equations

The continuity of the magnetic field is automatically satisfied by the choice of the electric current densities at the access ports, as discussed in Chapter 1; therefore, to complete the formulation of the problem the continuity of the tangent magnetic field has to be enforced. Since $\mathbf{E}_{\text{t}} = \widehat{\boldsymbol{\varphi}} E_{\varphi}$, the continuity condition that should be enforced is:

$$\left\langle \widehat{E}_\varphi^{(k)}, e_{\varphi,q}^{(k)} \right\rangle = \left\langle \widetilde{E}_\varphi^{(k)}, e_{\varphi,q}^{(k)} \right\rangle,$$

which is written explicitly as:

$$2\pi \int_0^{\rho_{\mathrm{wg}}^{(k)}} \widehat{E}_\varphi^{(k)} e_{\varphi,q}^{(k)*} \rho \, \mathrm{d}\rho = 2\pi \sum_{c=0}^{N_{\mathrm{f}}^{(e)}} c_c^{(e)} \int_0^{\rho_{\mathrm{wg}}^{(k)}} \widetilde{E}_\varphi^{(k)} e_{\varphi,q}^{(k)*} \rho \, \mathrm{d}\rho,$$

so, the right-hand side of this condition is written as:

$$2\pi \sum_{c=0}^{N_{\mathrm{f}}^{(e)}} c_c^{(e)} \int_0^{\rho_{\mathrm{wg}}^{(k)}} u_c^{(e)} e_{\varphi,q}^{(k)*} \rho \, \mathrm{d}\rho = \mathbf{C}^{(e,k)} \, \mathbf{c}^{(e)},$$

and so:

$$\mathbf{T}_k^{(e)} = \mathbf{C}^{(e,k)},$$

where:

$$(\mathbf{C}^{(e,k)})_{qc} = 2\pi \int_0^{\rho_{\mathrm{wg}}^{(k)}} u_c^{(e)} e_{\varphi,q}^{(k)*} \rho \, \mathrm{d}\rho.$$

D.3 Singularity-subtraction scheme

The double integrals involved in the formulation of the MEM described in Chapter 4 have the following form:

$$I = \int_0^1 \int_0^1 \frac{g(u,v)}{m - k\rho(u,v)} \, \mathrm{d}u \, \mathrm{d}v, \tag{D.17}$$

where $g(u,v)$ is a regular function in $(u,v) \in [0,1] \times [0,1]$. The singularity $\rho_{\mathrm{p}} = m/k$ in the spatial domain is mapped into a line of poles $v_{\mathrm{p}}(u)$ in the parent domain. Focusing on the bilinear mapping case, which is used to transform the unit square into a generic trapezoid with straight edges, the expression of $v_{\mathrm{p}}(u)$ is readily found, starting from the expressions of Appendix A.1:

$$\rho(u,v) = E + Fu + Gv + Huv. \tag{D.18}$$

If $\rho = \rho_{\mathrm{p}}$, $v = v_{\mathrm{p}}(u)$, and:

$$\rho_{\mathrm{p}} = E + Fu + Gv_{\mathrm{p}}(u) + Huv_{\mathrm{p}}(u),$$

then, by inverting this expression, the following result is obtained:

$$v_{\mathrm{p}}(u) = \frac{\rho_{\mathrm{p}} - E - Fu}{G + Hu}. \tag{D.19}$$

The integral in (D.17) is singular if $v_{\mathrm{p}}(u)$ intersects the interval $v \in [0, 1]$. In this case, a singularity-subtraction scheme is applied:

$$
\begin{aligned}
I &= \int_0^1 \int_0^1 \frac{g(u, v)}{m - k\rho(u, v)} \, \mathrm{d}u \, \mathrm{d}v = \\
&= \underbrace{\int_0^1 \int_0^1 \frac{g(u, v) - g(u, v_{\mathrm{p}}(u))}{m - k\rho(u, v)} \, \mathrm{d}u \, \mathrm{d}v}_{I_{\mathrm{diff}}} + \underbrace{\int_0^1 \int_0^1 \frac{g(u, v_{\mathrm{p}}(u))}{m - k\rho(u, v)} \, \mathrm{d}u \, \mathrm{d}v}_{I_{\mathrm{sing}}}. \tag{D.20}
\end{aligned}
$$

The integrand function of I_{diff} is continuous, since the numerator equals zero for $v = v_{\mathrm{p}}(u)$, and the integral is evaluated by means of the Gauss-Legendre quadrature rule. For what concerns I_{sing}, an analytical-numerical quadrature scheme is used to evaluate it efficiently.

D.3.1 Integral calculation: infinitesimal losses limit

The integral I_{sing} is properly interpreted as its limit for infinitesimal losses; therefore, by considering a complex dielectric permittivity:

$$\varepsilon_{\mathrm{r}} = \varepsilon_{\mathrm{r}}' - \mathrm{j}\varepsilon_{\mathrm{r}}'', \qquad \varepsilon_{\mathrm{r}}', \varepsilon_{\mathrm{r}}'' > 0, \qquad \varepsilon_{\mathrm{r}}', \varepsilon_{\mathrm{r}}'' \in \mathbb{R}.$$

Then:

$$k = \omega\sqrt{\mu_0\varepsilon_0}\sqrt{\varepsilon_{\mathrm{r}}} = k' - \mathrm{j}k'', \quad k', k'' > 0.$$

Now I_{sing} is manipulated, leading to

$$
\begin{aligned}
I_{\mathrm{sing}} &= \int_0^1 \int_0^1 \frac{g(u, v_{\mathrm{p}}(u))}{m - k\rho(u, v)} \, \mathrm{d}u \, \mathrm{d}v = \\
&= \int_0^1 g(u, v_{\mathrm{p}}(u)) \left[\int_0^1 \frac{1}{m - k\rho(u, v)} \, \mathrm{d}v \right] \mathrm{d}u = \\
&= \int_0^1 g(u, v_{\mathrm{p}}(u)) I_v(u) \mathrm{d}u.
\end{aligned}
$$

Then, focusing on the internal integral:

$$
\begin{aligned}
I_v(u) &= \int_0^1 \frac{1}{m - k\rho(u, v)} \, \mathrm{d}v = -\frac{1}{k(G + Hu)} \int_0^1 \frac{1}{v - \frac{\frac{m}{k} - E - Fu}{G + Hu}} \, \mathrm{d}v = \\
&= -\frac{1}{k(G + Hu)} \int_0^1 \frac{1}{v - v_{\mathrm{p}}(u)} \, \mathrm{d}v
\end{aligned}
$$

Since $k = k' - jk''$, then:

$$\frac{m}{k} = \rho_{\mathrm{p}} = \rho_{\mathrm{p}}' + j\rho_{\mathrm{p}}'', \qquad \rho_{\mathrm{p}}', \rho_{\mathrm{p}}' > 0,$$

knowing that:

$$v_{\mathrm{p}}(u) = \frac{\frac{m}{k} - E - Fu}{G + Hu},$$

where every quantity is real exception made for k, it is possible to identify the real and imaginary parts of $v_{\mathrm{p}}(u)$:

$$v_{\mathrm{p}}(u) = v_{\mathrm{p}}'(u) + jv_{\mathrm{p}}''(u).$$

Here,

$$
\begin{aligned}
v_{\mathrm{p}}'(u) = \mathbb{Re}\left\{v_{\mathrm{p}}(u)\right\} = \mathbb{Re}\left\{\frac{\frac{m}{k} - E - Fu}{G + Hu}\right\} = \\
= \frac{1}{G + Hu}\mathbb{Re}\left\{\frac{m}{k} - E - Fu\right\} = \\
= \frac{1}{G + Hu}\left[\mathbb{Re}\left\{\frac{m}{k}\right\} - E - Fu\right],
\end{aligned}
$$

where:

$$\frac{m}{k} = \frac{mk^*}{|k|^2} = \frac{m}{|k|^2}\left[k' + jk''\right],$$

so:

$$v_{\mathrm{p}}'(u) = \frac{1}{G + Hu}\left[\frac{m}{|k|^2}k' - E - Fu\right].$$

Then, with similar steps:

$$v_{\mathrm{p}}''(u) = \mathbb{Im}\left\{v_{\mathrm{p}}(u)\right\} = \mathbb{Im}\left\{\frac{\frac{m}{k} - E - Fu}{G + Hu}\right\} = \frac{1}{G + Hu}\frac{m}{|k|^2}k''.$$

So, by using these definitions:

$$
I_v(u) = \frac{1}{k(G+Hu)} \int_0^1 \frac{1}{v - v_{\mathrm{p}}(u)} \, \mathrm{d}v =
$$

$$
= -\frac{1}{k(G+Hu)} \int_0^1 \frac{1}{v - v_{\mathrm{p}}'(u) - \mathrm{j}v_{\mathrm{p}}''(u)} \, \mathrm{d}v =
$$

$$
= -\frac{1}{k(G+Hu)} \left[\int_0^1 \frac{v - v_{\mathrm{p}}'(u)}{(v - v_{\mathrm{p}}'(u))^2 + (v_{\mathrm{p}}''(u))^2} \, \mathrm{d}v + \right.
$$

$$
\left. + \mathrm{j}v_{\mathrm{p}}''(u) \int_0^1 \frac{\mathrm{d}v}{(v - v_{\mathrm{p}}'(u))^2 + (v_{\mathrm{p}}''(u))^2} \right] =
$$

$$
= -\frac{1}{k(G+Hu)} \left[\frac{1}{2} \int_0^1 \frac{2(v - v_{\mathrm{p}}'(u))}{(v - v_{\mathrm{p}}'(u))^2 + (v_{\mathrm{p}}''(u))^2} \, \mathrm{d}v + \right.
$$

$$
\left. + \mathrm{j}\frac{1}{v_{\mathrm{p}}''(u)} \int_0^1 \frac{\mathrm{d}v}{1 + \left(\frac{v - v_{\mathrm{p}}'(u)}{v_{\mathrm{p}}''(u)} \right)^2} \right] =
$$

$$
= -\frac{1}{k(G+Hu)} \left[\frac{1}{2} \ln \left| \frac{\left(1 - v_{\mathrm{p}}'(u)\right)^2 + (v_{\mathrm{p}}''(u))^2}{\left(v_{\mathrm{p}}'(u)\right)^2 + (v_{\mathrm{p}}''(u))^2} \right| + \right.
$$

$$
\left. + \mathrm{j} \arctan \left(\frac{v - v_{\mathrm{p}}'(u)}{v_{\mathrm{p}}''(u)} \right) \Big|_0^1 \right] =
$$

$$
= -\frac{1}{k(G+Hu)} \left[\frac{1}{2} \ln \left| \frac{\left(1 - v_{\mathrm{p}}'(u)\right)^2 + (v_{\mathrm{p}}''(u))^2}{\left(v_{\mathrm{p}}'(u)\right)^2 + (v_{\mathrm{p}}''(u))^2} \right| + \right.
$$

$$
\left. + \mathrm{j} \left(\arctan \left(\frac{1 - v_{\mathrm{p}}'(u)}{v_{\mathrm{p}}''(u)} \right) + \arctan \left(\frac{v_{\mathrm{p}}'(u)}{v_{\mathrm{p}}''(u)} \right) \right) \right].
$$

Some observations:

- The imaginary part of $I_v(u)$ is regular; indeed, it is given by the sum of two inverse tangent functions (that are smooth functions); the worse case occurs for infinitesimal losses, which means $v_{\mathrm{p}}''(u) \to 0$; in this case, the sum of the inverse tangents degenerates into the characteristic function of the domain. However, even if regularity is reduced, the imaginary part remains bounded.

- The real part is more critical, since, for $v_{\mathrm{p}}''(u) \to 0$, there are two discontinuities: u_0 such that $v_{\mathrm{p}}'(u_0) = 0$, and u_1 such that $v_{\mathrm{p}}'(u_1) = 1$. This means that the presence of losses regularizes the logarithm, and so the integral.

Finally, let us study the behavior of the imaginary part for infinitesimal losses. We proved that, for $\varepsilon_{\mathrm{r}}'' \to 0$, $v_{\mathrm{p}}''(u) \to 0^+$, since $\rho_{\mathrm{p}}'' > 0$, as we have proved previously. So:

$$1 - v_{\mathrm{p}}'(u) > 0 \implies \arctan\left(\frac{1 - v_{\mathrm{p}}'(u)}{0^+}\right) \to \frac{\pi}{2}$$

$$v_{\mathrm{p}}'(u) > 0 \implies \arctan\left(\frac{v_{\mathrm{p}}'(u)}{0^+}\right) \to \frac{\pi}{2}.$$

So:

$$\mathbb{Im}\left\{I_v(u)\right\} \to -\frac{1}{k(G + Hu)}\pi.$$

If the singular line intersects the domain, the integral has an imaginary part even if the integrand functions are real. This is reasonable, since π can be interpreted as half of the residual of the integrand function. In other words, this interpretation of the integrals coincides with their evaluation with the residuals theorem.

D.3.2 Bilinear mapping case 1: trapezoids with bases parallel to z

The case $F = 0$ and $F + H = 0$ in (D.19) is now considered. In this situation the horizontal singular line is mapped into a horizontal singular line, as in Fig. D.1 since:

$$v_{\mathrm{p}}(u) = \frac{\rho_{\mathrm{p}} - E}{G},$$

therefore, the line of poles is constant with respect to u. If the singular line is inside
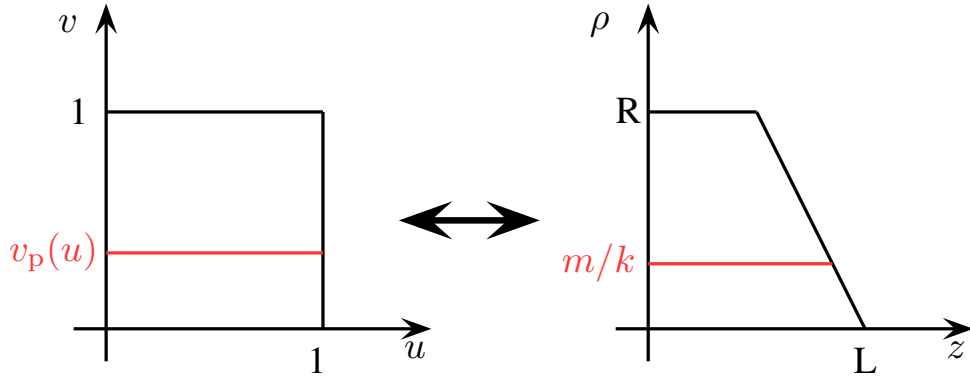
Figure D.1: Sketch of the parent domain (left) and of the spatial domain in the case $F = 0$, $F + H = 0$ of the bilinear mapping.

the $[0, 1] \times [0, 1]$ interval, the following integration scheme is applied to the singular part:

$$I_{\text{sing}} = \int_0^1 \int_0^1 \frac{g(u, v_{\text{p}}(u))}{m - k\rho(u, v)} \, du \, dv = -\frac{1}{kG} \int_0^1 g(u, v_{\text{p}}(u)) \int_0^1 \frac{1}{v - \frac{\rho_{\text{p}} - E}{G}} \, dv \, du =$$

$$= -\frac{1}{kG} \int_0^1 g(u, v_{\text{p}}(u)) \left[\ln \left| \frac{1 - v_{\text{p}}}{v_{\text{p}}} \right| + j\pi \right].$$

The logarithm does not introduce any singularity, so this integral can be calculated by means of a Gauss-Legendre quadrature rule.

D.3.3   Bilinear mapping case 2: trapezoids non-parallel bases

If in (D.19) $F + H = 0$ and $F \neq 0$, as sketched in Fig. D.2, two situations can occur:
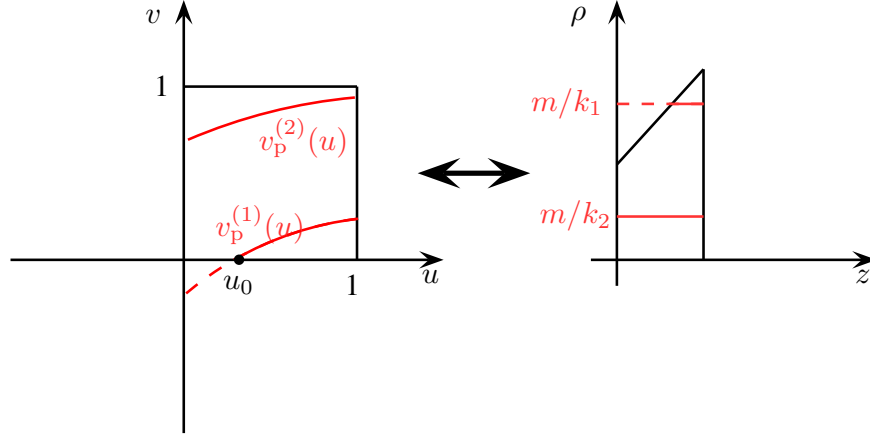
Figure D.2: Sketch of the parent domain (left) and of the spatial domain in the case $F \neq 0$, $F + H = 0$ of the bilinear mapping. The red lines identify two examples of pole lines for two different frequencies; the dashed parts of the red lines are associated to the parts of integrals outside of the spatial domain, which have to be properly treated.

- the singular line intersects a vertical side and an oblique side, as for $k = k_1$;

- the singular line intersects only the two vertical sides, as for $k = k_2$.

These case should be tackled separately; indeed, since $u \in [0, 1]$, if the singular line intersects only the vertical sides, it is entirely contained in the unit v interval. On the other hand, if the horizontal line intersects the oblique side in the natural domain, there is a point u_0 such that $v_{\text{p}}(u_0) = 0$, since, for $0 < u < u_0$, $v_{\text{p}}(u) \notin [0, 1]$. The two cases are now discussed.

Two vertical sides

If $\nexists \ u_0 \ : \ v_{\mathrm{p}}(u_0) = 0$, *i.e.*, the two vertical sides case, the quadrature scheme is quite similar to the integration case 1; in this situation:

$$I_{\mathrm{sing}} = \int_0^1 \int_0^1 \frac{g(u, v_{\mathrm{p}}(u))}{m - k\rho(u, v)} \, \mathrm{d}u \, \mathrm{d}v = -\frac{1}{k} \int_0^1 \frac{g(u, v_{\mathrm{p}}(u))}{G + Hu} \int_0^1 \frac{1}{v - \frac{\frac{m}{k} - E - Fu}{G + Hu}} \, \mathrm{d}v \, \mathrm{d}u =$$

$$= -\frac{1}{k} \int_0^1 \frac{g(u, v_{\mathrm{p}}(u))}{G + Hu} \left[\ln \left| \frac{1 - v_{\mathrm{p}}(u)}{v_{\mathrm{p}}(u)} \right| + \mathrm{j}\pi \right] \mathrm{d}u.$$

In this case the logarithm introduces no singularity, therefore this integral can be calculated once again with a Gauss-Legendre quadrature rule.

Intersection of the oblique side

If the oblique side is intersected by the singular line in the natural domain, $\exists \ u_0 \in [0, 1] \ : \ v_{\mathrm{p}}(u_0) = 0$. Since the mapping is injective, $v_{\mathrm{p}}(u)$ is a monotonic function, so the zero is unique and $v_{\mathrm{p}}(u) < 0$, for $u \in [0, u_0]$. This generates several problems, which are here reported:

- In $u = u_0$ the integrand function has an integrable singularity; this slows down the convergence of the integral, and therefore the Gauss-Legendre rule is not very effective.

- For $u < u_0$, the integral is not singular; therefore, the imaginary part of the integral equals zero, as it has been proved in the introduction. This introduces also a discontinuity of the imaginary part of the integrand function for $u = u_0$, which slows down the convergence of the Gauss-Legendre quadrature rule.

- As expansion and test functions Chebyshev polynomials are used (as described in Section 1.3 and A.1); for $u < u_0$, these polynomials are evaluated in values of $v < 0$; since there is a mapping $y = 2v - 1$ from the argument of the Chebyshev polynomials y and v, for $u_0 < 0$, $y < -1$; in this case, the Chebyshev polynomials explode, and their evaluation is not performed correctly.

These three critical points can be tackled by developing an ad-hoc quadrature scheme for this situation. In this case, it is convenient to start from the initial integral:

$$I = \int_0^1 \int_0^1 \frac{g(u, v)}{m - k\rho(u, v)} \, \mathrm{d}u \, \mathrm{d}v.$$

Given $\overline{u} = K_{\mathrm{th}} u_0$, where K_{th} is a defined threshold, $0 < K_{\mathrm{th}} < 1$ (in the practical case, $K_{\mathrm{th}} = 0.9$), it is possible to exploit the linearity property of the outer integral and to rewrite it as:

$$I = \int_0^{\overline{u}} \int_0^1 \frac{g(u,v)}{m - k\rho(u,v)} \, \mathrm{d}u \, \mathrm{d}v + \int_{\overline{u}}^1 \int_0^1 \frac{g(u,v)}{m - k\rho(u,v)} \, \mathrm{d}u \, \mathrm{d}v = I_1 + I_2.$$

The integral I_1 is regular, so it is possible to evaluate it with the Gauss-Legendre quadrature rule. The integral I_2 is treated with a singularity subtraction scheme:

$$I_2 = \int_{\overline{u}}^1 \int_0^1 \frac{g(u,v)}{m - k\rho(u,v)} \, \mathrm{d}u \, \mathrm{d}v =$$

$$= \underbrace{\int_{\overline{u}}^1 \int_0^1 \frac{g(u,v) - g(u,v_{\mathrm{p}}(u))}{m - k\rho(u,v)} \, \mathrm{d}u \, \mathrm{d}v}_{I_{2,\mathrm{diff}}} + \underbrace{\int_{\overline{u}}^1 \int_0^1 \frac{g(u,v_{\mathrm{p}}(u))}{m - k\rho(u,v)} \, \mathrm{d}u \, \mathrm{d}v}_{I_{2,\mathrm{sing}}}.$$

The integrand of $I_{2,\mathrm{diff}}$ is regular and its integral can be calculated with the usual Gauss-Legendre quadrature rule; instead, further manipulations should be applied to $I_{2,\mathrm{sing}}$.

$$I_{2,\mathrm{sing}} = \int_{\overline{u}}^1 \int_0^1 \frac{g(u,v_{\mathrm{p}}(u))}{m - k\rho(u,v)} \, \mathrm{d}u \, \mathrm{d}v = -\frac{1}{k} \int_{\overline{u}}^1 \frac{g(u,v_{\mathrm{p}}(u))}{G + Hu} \int_0^1 \frac{1}{v - \frac{\frac{m}{k} - E - Fu}{G + Hu}} \, \mathrm{d}v \, \mathrm{d}u =$$

$$= -\mathrm{j} \frac{\pi}{k} \int_{u_0}^1 \frac{g(u,v_{\mathrm{p}}(u))}{G + Hu} \, \mathrm{d}u - \frac{1}{k} \int_{\overline{u}}^1 \frac{g(u,v_{\mathrm{p}}(u))}{G + Hu} \ln \left| \frac{G + Hu - \frac{m}{k} + E + Fu}{\frac{m}{k} - E - Fu} \right| \, \mathrm{d}u =$$

$$= I_{2\mathrm{i},\mathrm{sing}} + I_{2\mathrm{r},\mathrm{sing}}.$$

The imaginary part integral is conveniently calculated from u_0 to 1, since the integrand function is multiplied times the domain characteristic function (given by the limit of the inverse tangents) equals zero in the $[\overline{u}, u_0]$ interval; by this way, $I_{2\mathrm{i},\mathrm{sing}}$ is regular. For what concerns $I_{2\mathrm{r},\mathrm{sing}}$, the following simplification is performed, exploiting the fact that $H + F = 0$ but $F \neq 0$:

$$I_{2\mathrm{r},\mathrm{sing}} = \int_{\overline{u}}^1 \frac{g(u,v_{\mathrm{p}}(u))}{G + Hu} \ln \left| \frac{G + Hu - \frac{m}{k} + E + Fu}{\frac{m}{k} - E - Fu} \right| \, \mathrm{d}u =$$

$$= -\frac{1}{k_0} \int_{\overline{u}}^1 \frac{g(u,v_{\mathrm{p}}(u))}{G + Hu} \left[\ln \left| \frac{E + G - \frac{m}{k_0}}{F} \right| - \log \left| u + \frac{E - \frac{m}{k_0}}{F} \right| \right] \, \mathrm{d}u =$$

$$= \underbrace{-\frac{1}{k_0} \int_{\overline{u}}^1 \frac{g(u,v_{\mathrm{p}}(u))}{G + Hu} \ln \left| \frac{E + G - \frac{m}{k_0}}{F} \right| \, \mathrm{d}u}_{I_{3\mathrm{b},\mathrm{sing}}} + \underbrace{\frac{1}{k_0} \int_{\overline{u}}^1 \frac{g(u,v_{\mathrm{p}}(u))}{G + Hu} \log |u - u_0| \, \mathrm{d}u}_{I_{3\mathrm{c},\mathrm{sing}}}.$$

The logarithm in $I_{3\mathrm{b},\mathrm{sing}}$ has no singularity; on the other hand, $I_{3\mathrm{c},\mathrm{sing}}$ still exhibits a singularity for $u = u_0$, which can be addressed by means of an ad-hoc quadrature scheme. The first step consists of dividing the integral in two contributions: one

for u smaller than u_0, one from u going from u_0 to the end of the domain. So, it is possible to remove the absolute value sign, writing:

$$I_{3c,sing} = \underbrace{\frac{1}{k_0} \int_{\bar{u}}^{u_0} \frac{g(u, v_p(u))}{G + Hu} \log(u_0 - u) \, du}_{I_{3c_1,sing}} + \underbrace{\frac{1}{k_0} \int_{u_0}^{1} \frac{g(u, v_p(u))}{G + Hu} \log(u - u_0) \, du}_{I_{3c_2,sing}}.$$

Now, focusing on the first integral, and the following change of variables is applied:

$$u_0 - u = e^{-x} \implies x = -\ln(u_0 - u),$$

so:

$$du = e^{-x} \, dx.$$

The integration bounds become:

- for $u = \bar{u}$, $x = -\ln(u_0 - \bar{u})$;

- for $u = u_0$, $x \to +\infty$.

So, the integral is transformed into:

$$\int_{\bar{u}}^{u_0} \frac{g(u, v_p(u))}{G + Hu} \log(u_0 - u) \, du \implies \int_{-\ln(u_0-\bar{u})}^{+\infty} \frac{g(u_0 - e^{-x}, v_p(u_0 - e^{-x}))}{G + H(u_0 - e^{-x})} (-x) e^{-x} \, dx.$$

Then, a second integration variable change is applied:

$$y = x + \ln(u_0 - \bar{u}) \implies x \quad dx = dy.$$

So:

- for $x = -\ln(u_0 - \bar{u})$, $y = 0$

- for $x \to +\infty$, $y \to +\infty$.

Finally:

$$\int_{-\ln(u_0-\bar{u})}^{+\infty} \frac{g(u_0 - e^{-x}, v_p(u_0 - e^{-x}))}{G + H(u_0 - e^{-x})} (-x) e^{-x} \, dx \implies$$

$$\implies I_{3c_1,sing} = \int_{0}^{+\infty} \frac{g(u_0 - e^{-y+\ln(u_0-\bar{u})}, v_p(u_0 - e^{-y+\ln(u_0-\bar{u})}))}{G + H(u_0 - e^{-y+\ln(u_0-\bar{u})})} (-y + \ln(u_0 - \bar{u})) e^{-y} \, dy.$$

This integral is calculated by means of a Gauss-Laguerre quadrature rule; therefore, these operations transformed an integral with an integrand exhibiting a logarithmic singularity, calculated in a bounded domain, to a regular integral to be calculated in an unbounded domain. A similar procedure is now applied to the second integral:

$$\int_{u_0}^{1} \frac{g(u, v_{\mathrm{p}}(u))}{G + Hu} \ln(u - u_0) \, \mathrm{d}u.$$

In this case, the change of variables is:

$$u - u_0 = \mathrm{e}^{-x} \implies x = -\ln(u - u_0),$$

so:

$$\mathrm{d}u = -\mathrm{e}^{-x} \, \mathrm{d}x.$$

The integration bounds are transformed as follows:

- $u = u_0 \implies x \to +\infty$;

- $u = 1 \implies x = -\log(1 - u_0)$

so:

$$\int_{u_0}^{1} \frac{g(u, v_{\mathrm{p}}(u))}{G + Hu} \ln(u - u_0) \, \mathrm{d}u \implies -\int_{+\infty}^{-\log(1-u_0)} \frac{g(u_0 + \mathrm{e}^{-x}, v_{\mathrm{p}}(u_0 + \mathrm{e}^{-x}))}{G + H(u_0 + \mathrm{e}^{-x})} (x) \mathrm{e}^{-x} \, \mathrm{d}x.$$

Finally, a second change of variables is applied:

$$y = x + \ln(1 - u_0),$$

so, the integral becomes:

$$I_{3c_2,\mathrm{sing}} = \int_{0}^{+\infty} \frac{g(u_0 + \mathrm{e}^{-y+\ln(1-u_0)}, v_{\mathrm{p}}(u_0 + \mathrm{e}^{-y+\ln(1-u_0)}))}{G + H(u_0 + \mathrm{e}^{-y+\ln(u_0-\overline{u})})} (-y + \ln(1 - u_0)) \mathrm{e}^{-y} \, \mathrm{d}y.$$

D.3.4   Bilinear mapping case 3: trapezoids non-parallel bases

Now, the $F + H \neq 0$, $F = 0$ case sketched in Fig. D.3 is studied. This case is quite similar to the previous one, and it will be solved using similar ideas. Recalling (D.19), under these hypotheses, the following expression of the line of poles is found:

$$v_{\mathrm{p}}(u) = \frac{\frac{m}{k_0} - E}{G + Hu}.$$
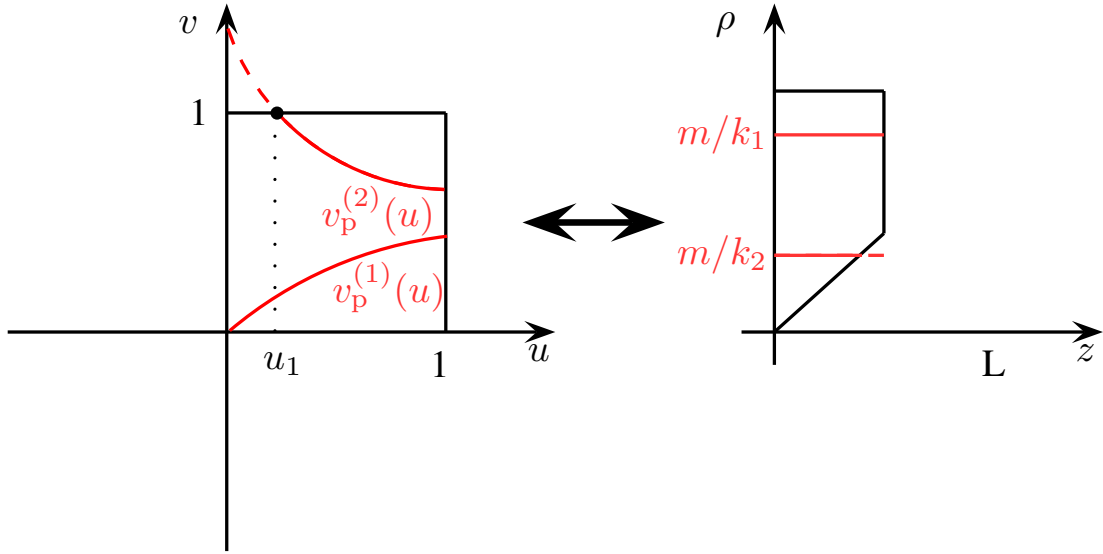
Figure D.3: Sketch of the parent domain (left) and of the spatial domain in the case $F = 0$, $F + H \neq 0$ of the bilinear mapping. The red lines identify two examples of pole lines for two different frequencies; the dashed parts of the red lines are associated to the parts of integrals outside of the spatial domain, which have to be properly treated.

The numerator of this function is not a function of u and therefore it can not equal zero; on the other hand, it is possible that the expression equals one; indeed:

$$1 = \frac{\rho_p - E}{G + Hu} \implies u_1 = \frac{\rho_p - E - G}{H}.$$

In this case the function $v_p(u)$ is monotonically descending, therefore it is still possible to define $\bar{u} < u_1$ and to divide the integrals in two contributions, just like in the previous case. Once again, this leads to the definition of very similar expressions. The first differences arise when defining of the sub-integrals $I_{2r,sing}$, according to the notation of the previous section; therefore, the calculations will start from this point:

$$
\begin{aligned}
I_{\mathrm{2r,sing}} &= -\frac{1}{k_0} \int_{\underline{u}}^{1} \frac{g(u, v_{\mathrm{p}}(u))}{G + Hu} \ln \left| \frac{G + Hu - \rho_{\mathrm{p}} + E + Fu}{\rho_{\mathrm{p}} - E - Fu} \right| \mathrm{d}u = \\
&= -\frac{1}{k_0} \int_{\underline{u}}^{1} \frac{g(u, v_{\mathrm{p}}(u))}{G + Hu} \ln \left| \frac{\frac{H(u - \rho_{\mathrm{p}} - E - G)}{H}}{\rho_{\mathrm{p}} - E} \right| \mathrm{d}u = \\
&= -\frac{1}{k_0} \int_{\underline{u}}^{1} \frac{g(u, v_{\mathrm{p}}(u))}{G + Hu} \left[\ln \left| u - \frac{\rho_{\mathrm{p}} - E - G}{H} \right| - \ln \left| \frac{\rho_{\mathrm{p}} - E}{H} \right| \right] \mathrm{d}u = \\
&= \underbrace{-\frac{1}{k_0} \int_{\underline{u}}^{1} \frac{g(u, v_{\mathrm{p}}(u))}{G + Hu} \ln \left| \frac{\rho_{\mathrm{p}} - E}{H} \right| \mathrm{d}u}_{I_{\mathrm{3b,sing}}} \underbrace{- \frac{1}{k_0} \int_{\underline{u}}^{1} \ln |u - u_1| \, \mathrm{d}u}_{I_{\mathrm{3c,sing}}}
\end{aligned}
$$

The integrand of $I_{\mathrm{3b,sing}}$ is regular and its integral can be evaluated by Gauss-Legendre; the remaining integral has the same form of $I_{\mathrm{3c,sing}}$ for the previous case, therefore it can be evaluated using a quadrature scheme equal to the previous case.

D.4 Evaluation of the mode conversion efficiency

In this section the algorithm used to evaluate the conversion efficiency from the TE_{11} mode to the balanced hybrid HE_{11} mode is described. This parameter has been used in Section 4.3 to describe choked mode converter performance, starting from the GSM evaluated with the MEM.

The expressions of the hybrid balanced modes are found in [37] and [43] are reported in the following.

- For HE_{1n} modes:

$$
\begin{aligned}
E_x(\rho, \varphi) &= e_{0,n}(\rho) \\
E_y(\rho, \varphi) &= 0;
\end{aligned}
$$

  as a matter of fact, one of the properties of the HE_{1n} modes is their linear polarization.

- For EH_{1n} modes:

$$
\begin{aligned}
E_x(\rho, \varphi) &= e_{2,n}(\rho) \cos(2\varphi) \\
E_y(\rho, \varphi) &= e_{2,n}(\rho) \sin(2\varphi).
\end{aligned}
$$

In these equations, a is the radius of the waveguide, $k'_{\mathrm{t},n} = \chi_{0n}/a$, where χ_{0n} is the n-th zero of the 0-order Bessel function of first kind, and the function $e_{\nu,n}(\rho)$ is defined as:

$$e_{\nu,n}(\rho) = \frac{\sqrt{2Z_0}}{a\sqrt{\pi}} \frac{J_\nu(k'_{t,n}\rho)}{J'_0(k'_{t,n}a)}.$$

It is useful to convert the components in cylindrical coordinates, by using the following change of basis:

$$E_\rho = E_x \cos\varphi + E_y \sin\varphi$$
$$E_\varphi = -E_x \sin\varphi + E_y \cos\varphi.$$

- For HE_{1n} modes:

$$E_\rho(\rho,\varphi) = e_{0,n}(\rho)\cos\varphi$$
$$E_z(\rho,\varphi) = -e_{0,n}(\rho)\sin\varphi.$$

- For EH_{1n} modes:

$$E_\rho(\rho,\varphi) = e_{2,n}(\rho)\left[\cos 2\varphi\cos\varphi + \sin 2\varphi\sin\varphi\right] = e_{2,n}(\rho)\cos\varphi$$
$$E_z(\rho,\varphi) = e_{2,n}(\rho)\left[-\cos 2\varphi\sin\varphi + \sin 2\varphi\cos\varphi\right] = e_{2,n}(\rho)\sin\varphi.$$

These expressions are now used to evaluate the projection matrices.

Projection of HE_{1n} modes on HE_{1n} modes

The following calculation is now performed:

$$\left\langle \mathbf{e}_n^{(HE)}, \mathbf{e}_m^{(HE)} \right\rangle = \int_0^{2\pi}\int_0^a \left[e_{0,n}\cos\varphi e_{0,m}\cos\varphi + e_{0,n}\sin\varphi e_{0,m}\sin\varphi\right]\rho\,\mathrm{d}\rho\,\mathrm{d}\varphi =$$
$$= \int_0^a e_{0,n}e_{0,m}\rho\,\mathrm{d}\rho \int_0^{2\pi}\left[\cos^2\varphi + \sin^2\varphi\right]\,\mathrm{d}\varphi =$$
$$= 2\pi\int_0^a e_{0,n}e_{0,m}\rho\,\mathrm{d}\rho =$$
$$= C_{mn}\delta_{mn},$$

where C_{mn} depends on the normalization constant of the hybrid modes.

Projection of EH_{1n} modes on EH_{1n} modes

The following calculation is now performed:

$$\left\langle \mathbf{e}_n^{(\mathrm{EH})}, \mathbf{e}_m^{(\mathrm{EH})} \right\rangle = \int_0^{2\pi} \int_0^a \left[e_{2,n} \cos\varphi e_{2,m} \cos\varphi + e_{2,n} \sin\varphi e_{2,m} \sin\varphi \right] \rho \, \mathrm{d}\rho \, \mathrm{d}\varphi =$$

$$= \int_0^a e_{2,n} e_{2,m} \rho \, \mathrm{d}\rho \int_0^{2\pi} \left[\cos^2\varphi + \sin^2\varphi \right] \mathrm{d}\varphi =$$

$$= 2\pi \int_0^a e_{2,n} e_{2,m} \rho \, \mathrm{d}\rho.$$

It is remarked that, in this case, the mode functions are not orthonormal, therefore the integral should be calculated explicitly.

Projection of EH_{1n} modes on HE_{1n} modes and of HE_{1n} modes on EH_{1n} modes

The following calculation is now performed:

$$\left\langle \mathbf{e}_n^{(\mathrm{HE})}, \mathbf{e}_m^{(\mathrm{EH})} \right\rangle = \int_0^{2\pi} \int_0^a \left[e_{0,n} \cos\varphi e_{2,m} \cos\varphi - e_{0,n} \sin\varphi e_{2,m} \sin\varphi \right] \rho \, \mathrm{d}\rho \, \mathrm{d}\varphi =$$

$$= \int_0^a e_{0,n} e_{2,m} \rho \, \mathrm{d}\rho \int_0^{2\pi} \left[\cos^2\varphi - \sin^2\varphi \right] \mathrm{d}\varphi =$$

$$= 0 = \left\langle \mathbf{e}_n^{(\mathrm{EH})}, \mathbf{e}_m^{(\mathrm{HE})} \right\rangle.$$

Definition of the mode projection matrix

The following projection matrix $\mathbf{T}$ is defined:

$$\mathbf{T} = \left[\begin{array}{c|c} (\mathrm{HE} \to \mathrm{HE}) & \mathbf{0} \\ \hline \mathbf{0} & (\mathrm{EH} \to \mathrm{EH}) \end{array} \right]$$

Definition of the known terms projection vector

The electromagnetic field $\mathbf{E}(\rho, \varphi, z)$ is represented in terms of circularly polarized circular waveguide modes:

$$\mathbf{E}(\rho, \varphi, z) = \left[\widehat{\boldsymbol{\rho}} e_\rho + \widehat{\boldsymbol{\varphi}} e_\varphi \right] \mathrm{e}^{+\mathrm{j}m\varphi},$$

therefore:

$$\left\langle \mathbf{E}, \mathbf{e}_m^{(\text{HE})} \right\rangle = \int_0^{2\pi} \int_0^a \left[e_\rho \mathrm{e}^{+\mathrm{j}m\varphi} e_{0,n} \cos \varphi - e_\varphi \mathrm{e}^{+\mathrm{j}m\varphi} e_{0,n} \sin \varphi \right] \rho \, \mathrm{d}\rho \, \mathrm{d}\varphi =$$

$$= \int_0^{2\pi} \mathrm{e}^{+\mathrm{j}m\varphi} \cos \varphi \, \mathrm{d}\varphi \int_0^a e_\rho e_{0,n} \rho \, \mathrm{d}\rho - \int_0^{2\pi} \mathrm{e}^{+\mathrm{j}m\varphi} \sin \varphi \, \mathrm{d}\varphi \int_0^a e_\rho e_{0,n} \rho \, \mathrm{d}\rho.$$

Then, for what concerns the EH modes:

$$\left\langle \mathbf{E}, \mathbf{e}_m^{(\text{EH})} \right\rangle = \int_0^{2\pi} \int_0^a \left[e_\rho \mathrm{e}^{+\mathrm{j}m\varphi} e_{2,n} \cos \varphi + e_\varphi \mathrm{e}^{+\mathrm{j}m\varphi} e_{2,n} \sin \varphi \right] \rho \, \mathrm{d}\rho \, \mathrm{d}\varphi =$$

$$= \int_0^{2\pi} \mathrm{e}^{+\mathrm{j}m\varphi} \cos \varphi \, \mathrm{d}\varphi \int_0^a e_\rho e_{2,n} \rho \, \mathrm{d}\rho + \int_0^{2\pi} \mathrm{e}^{+\mathrm{j}m\varphi} \sin \varphi \, \mathrm{d}\varphi \int_0^a e_\rho e_{2,n} \rho \, \mathrm{d}\rho.$$

Evaluation of the conversion efficiency

The conversion efficiency η_{conv} is now calculated. Given $\mathbf{e}$ the vector of mode functions defined as:

$$\mathbf{e} = \begin{bmatrix} \mathbf{e}_1^{(\text{HE})} \\ \mathbf{e}_2^{(\text{HE})} \\ \vdots \\ \mathbf{e}_{N_{\text{modes}}/2}^{(\text{HE})} \\ \mathbf{e}_1^{(\text{EH})} \\ \mathbf{e}_2^{(\text{EH})} \\ \vdots \\ \mathbf{e}_{N_{\text{modes}}/2}^{(\text{EH})} \end{bmatrix},$$

the expression of the electromagnetic field in a transversal section of the structure $\mathbf{E}(\rho, \varphi)$ is represented by using the hybrid mode basis:

$$\mathbf{E}(\rho, \varphi) = \sum_{n=1}^{N_{\text{modes}}} c_n \mathbf{e}_n \mathrm{e}^{\mathrm{j}m\varphi},$$

where c_n are unknown coefficients. To obtain their expression, both members are projected on the same modes $\mathbf{e}_m$:

$$\langle \mathbf{E}, \mathbf{e}_m \rangle = \sum_{n=0}^{N_{\text{modes}}} c_n \langle \mathbf{e}_n, \mathbf{e}_m \rangle,$$

but:

$$\langle \mathbf{e}_n, \mathbf{e}_m \rangle = (\mathbf{T})_{mn}.$$

Therefore, given

$$\mathbf{b}_m = \langle \mathbf{E}, \mathbf{e}_m \rangle,$$

the following system is obtained:

$$\mathbf{b} = \mathbf{T}\,\mathbf{c}.$$

So:

$$\mathbf{c} = \mathbf{M}^{-1}\,\mathbf{b}.$$

The vector $\mathbf{c}$ contains the projection coefficients; therefore, the following quantity is defined:

$$\eta_{\mathrm{conv}} = \sqrt{\frac{|c_1|^2}{\sum_{n=1}^{N_{\mathrm{modes}}} |c_n|^2}},$$

which is the ratio of the power of the coefficient c_1, related to the HE_{11} mode, to the sum of the powers of all the modes.

Results and comments

The algorithm discussed above has been applied to the choked mode converter described in [37], [38]. Since the parameter η_{conv} is strictly related to the cross-polar pattern of the structure, in Fig. D.4 η_{conv} a comparison of the two parameters has been reported. The cross-polar component has been obtained by applying the equivalence theorem at the aperture and by filling with PEC all the space around it [34]. The radiated field distribution has been used to obtain these radiation patterns; the plot has been build by taking the maximum of the pattern in the $0° \div 60°$ angular range, for $\varphi = 45$.
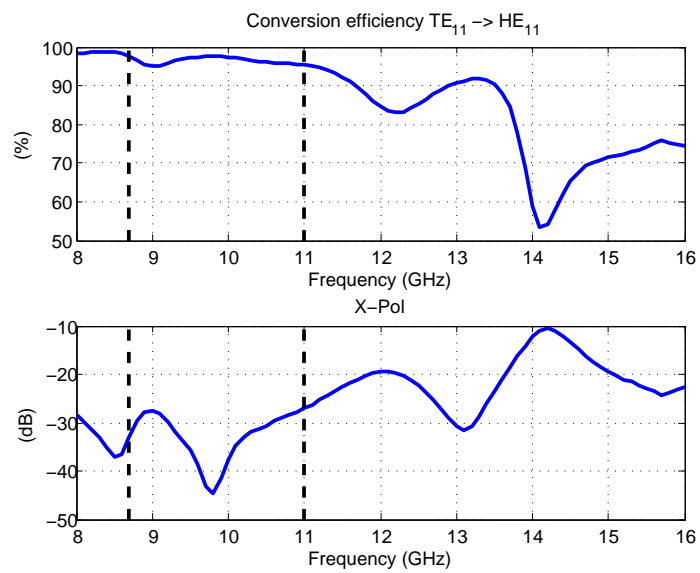
Figure D.4: Top: TE$_{11}$ →HE$_{11}$ conversion efficiency $\eta_{\mathrm{conv}}(f)$. Bottom: maximum of the cross-polar versus frequency.

Appendix of "A boundary-integral method for lens antennas"

E.1 Dyadic Green's function representation of the electromagnetic field

In this Appendix an integral representation of the electromagnetic field in a homogeneous medium based on the dyadic Green's function concept is recalled. The curl Maxwell's equation in the space-frequency domain are:

$$\begin{cases} \nabla \times \mathbf{H}(\mathbf{r}, \omega) = \mathrm{j}\omega\varepsilon\mathbf{E}(\mathbf{r}, \omega) + \mathbf{J}(\mathbf{r}, \omega) \\ \nabla \times \mathbf{E}(\mathbf{r}, \omega) = -\mathrm{j}\omega\mu\mathbf{H}(\mathbf{r}, \omega) - \mathbf{M}(\mathbf{r}, \omega). \end{cases} \tag{E.1}$$

The Green's function is derived in the spectral domain. Let $\mathbf{A}(\mathbf{r}, \omega)$ be a generic vector in the space-frequency domain; from now on, the frequency dependence is considered implicit ($\mathbf{A}(\mathbf{r}) = \mathbf{A}(\mathbf{r}, \omega)$). This vector can be written in a generic coordinate system as follows:

$$\mathbf{A}(\mathbf{r}) = \sum_{i=1}^{3} A_i(\mathbf{r})\widehat{\mathbf{u}}_i.$$

The triple Fourier transform $\mathcal{F}_3$ is used to map the i-th component of this vector from the space domain $\mathbf{r}$ to the spectral domain $\mathbf{k}$:

$$\mathcal{F}_3\left\{A_i(\mathbf{r})\right\} = \widetilde{A_i}(\mathbf{k}) = \int_{\mathbb{R}^3} A_i(\mathbf{r})\mathrm{e}^{\mathrm{j}\mathbf{k}\cdot\mathbf{r}} \, \mathrm{d}\mathbf{r}.$$

Similarly, it is possible to define the inverse triple Fourier operator, which allow us to return, from the spectral space $\mathbf{k}$ to the natural spatial domain $\mathbf{r}$, as follows:

$$\mathcal{F}_3^{-1}\left\{\widetilde{A_i}(\mathbf{k})\right\} = A_i(\mathbf{r}) = \int_{\mathbb{R}^3} \widetilde{A_i}(\mathbf{k})\mathrm{e}^{-\mathrm{j}\mathbf{k}\cdot\mathbf{r}}\,\mathrm{d}\mathbf{k}.$$

The derivation property of the Fourier transform is generalized, leading to:

$$\mathcal{F}_3\left\{\nabla A\right\} = -\mathrm{j}\mathbf{k}\widetilde{A}$$
$$\mathcal{F}_3\left\{\nabla\cdot\mathbf{A}\right\} = -\mathrm{j}\mathbf{k}\cdot\widetilde{\mathbf{A}}$$
$$\mathcal{F}_3\left\{\nabla\times\mathbf{A}\right\} = -\mathrm{j}\mathbf{k}\times\widetilde{\mathbf{A}},$$

where:

$$\widetilde{\mathbf{A}} = \sum_{i=1}^{3}\widetilde{A_i}(\mathbf{k})\widehat{\mathbf{k}}_i,$$

and each $\widehat{\mathbf{k}}_i$ is a unit vector for the coordinate system chosen to represent an element of the spectral domain. This is used to write the Maxwell's equations (E.1) in the spectral domain:

$$\begin{cases} -\mathrm{j}\mathbf{k}\times\widetilde{\mathbf{H}} = \mathrm{j}\omega\varepsilon\widetilde{\mathbf{E}} + \widetilde{\mathbf{J}} \\ -\mathrm{j}\mathbf{k}\times\widetilde{\mathbf{E}} = -\mathrm{j}\omega\mu\widetilde{\mathbf{H}} - \widetilde{\mathbf{M}}. \end{cases} \qquad (\text{E.2})$$

These two equations are now written in dyadic form. Let $\widetilde{\mathbf{I}}$ be the identity dyadic in the spectral domain; it is possible to write the vector $\widetilde{\mathbf{H}}$ as:

$$\widetilde{\mathbf{H}} = \widetilde{\mathbf{I}}\cdot\widetilde{\mathbf{H}},$$

therefore:

$$\mathbf{k}\times\widetilde{\mathbf{H}} = \mathbf{k}\times(\widetilde{\mathbf{I}}\cdot\widetilde{\mathbf{H}}) = (\mathbf{k}\times\widetilde{\mathbf{I}})\cdot\widetilde{\mathbf{H}} \triangleq \boldsymbol{\mathcal{D}}\cdot\widetilde{\mathbf{H}},$$

where $\boldsymbol{\mathcal{D}}$ is the dyadic defining the transformation:

$$\boldsymbol{\mathcal{D}}\cdot\widetilde{\mathbf{H}} \mapsto \mathbf{k}\times\widetilde{\mathbf{H}}$$

Now, it is possible to apply this "trick" to the Maxwell's equations by isolating the current densities and by rearranging (E.2) as follows:

$$-\mathrm{j}\omega\varepsilon\widetilde{\mathbf{E}} - \mathrm{j}\mathbf{k}\times\widetilde{\mathbf{H}} = \widetilde{\mathbf{J}}$$
$$\mathrm{j}\mathbf{k}\times\widetilde{\mathbf{E}} - \mathrm{j}\omega\mu\widetilde{\mathbf{H}} = \widetilde{\mathbf{M}}.$$

Then, by applying the "dyadics trick" and by collecting everything in matrix form, the following equation is written:

$$\mathcal{L} \cdot \begin{bmatrix} \widetilde{\mathbf{E}} \\ \widetilde{\mathbf{H}} \end{bmatrix} = \begin{bmatrix} \widetilde{\mathbf{J}} \\ \widetilde{\mathbf{M}} \end{bmatrix},$$

where the dyadic $\mathcal{L}$, which is multiplied by means of a dot product to the field vector, is defined as:

$$\mathcal{L} \triangleq \begin{bmatrix} -\mathrm{j}\omega\varepsilon\widetilde{\mathbf{I}} & -\mathrm{j}\mathbf{k} \times \widetilde{\mathbf{I}} \\ \mathrm{j}\mathbf{k} \times \mathbf{I} & -\mathrm{j}\omega\mu\widetilde{\mathbf{I}} \end{bmatrix}.$$

To sum up, at the left-hand side the dyadic linear operator $\mathcal{L}$ is applied to $\widetilde{\mathbf{E}}$ and $\widetilde{\mathbf{H}}$; this equals the electric and magnetic current densities. Since the objective is the derivation of a representation of the electromagnetic field radiate by the current densities, the dyadic operator $\mathcal{L}$ should be inverted, leading to an expression like:

$$\begin{bmatrix} \widetilde{\mathbf{E}} \\ \widetilde{\mathbf{H}} \end{bmatrix} = \widetilde{\mathcal{G}} \cdot \begin{bmatrix} \widetilde{\mathbf{J}} \\ \widetilde{\mathbf{M}} \end{bmatrix},$$

where:

$$\widetilde{\mathcal{G}} = \widetilde{\mathcal{L}}^{-1}.$$

Therefore, let $\widetilde{\mathcal{I}}$ be defined as:

$$\widetilde{\mathcal{I}} = \begin{bmatrix} \widetilde{\mathbf{I}} & \mathbf{0} \\ \mathbf{0} & \widetilde{\mathbf{I}} \end{bmatrix},$$

then, since $\widetilde{\mathcal{G}}$ is the inverse of $\widetilde{\mathcal{L}}$, the following condition is required:

$$\widetilde{\mathcal{L}} \cdot \widetilde{\mathcal{G}} = \widetilde{\mathcal{I}}.$$

This last equation is now written explicitly as follows, expanding the definition of $\widetilde{\mathcal{G}}$:

$$\begin{bmatrix} -\mathrm{j}\omega\varepsilon\widetilde{\mathbf{I}} & -\mathrm{j}\mathbf{k} \times \widetilde{\mathbf{I}} \\ \mathrm{j}\mathbf{k} \times \widetilde{\mathbf{I}} & -\mathrm{j}\omega\mu\widetilde{\mathbf{I}} \end{bmatrix} \begin{bmatrix} \widetilde{\mathbf{G}}^{(\mathrm{e,j})} & \widetilde{\mathbf{G}}^{(\mathrm{e,m})} \\ \widetilde{\mathbf{G}}^{(\mathrm{h,j})} & \widetilde{\mathbf{G}}^{(\mathrm{h,m})} \end{bmatrix} = \begin{bmatrix} \widetilde{\mathbf{I}} & \mathbf{0} \\ \mathbf{0} & \widetilde{\mathbf{I}} \end{bmatrix}, \qquad \text{(E.3)}$$

where:

- the dyadic $\widetilde{\mathbf{G}}^{(e,j)}$ acts on an electric current density $\widetilde{\mathbf{J}}$ and it produces an electric field contribution; for this reason, it can be thought as a **transimpedance**: its input is related to a current, while its output is dimensionally related to a voltage;

- the dyadic $\widetilde{\mathbf{G}}^{(e,m)}$ acts on a magnetic current density $\widetilde{\mathbf{M}}$ and it produces an electric field contribution; it can be dimensionally thought as a **voltage amplification/attenuation**, since both its input and output are related to voltages;

- the dyadic $\widetilde{\mathbf{G}}^{(h,j)}$ acts on an electric current density $\widetilde{\mathbf{J}}$ and it produces a magnetic field contribution; it can be dimensionally thought as a **current amplification/attenuation**, since both its input and output are related to currents;

- the dyadic $\widetilde{\mathbf{G}}^{(h,m)}$ acts on a magnetic current density $\widetilde{\mathbf{M}}$ and it produces a magnetic field contribution; for this reason, it can be thought as a **transadmittance**: its input is related to a voltage, while its output is dimensionally related to a current.

Derivation of the transimpedance Green's function

Equation (E.3) is now written as:

$$\begin{cases} -\mathrm{j}\omega\varepsilon\widetilde{\mathbf{G}}^{(e,j)} - \mathrm{j}\mathbf{k} \times \widetilde{\mathbf{G}}^{(h,j)} = \widetilde{\mathbf{I}} \\ \mathrm{j}\mathbf{k} \times \widetilde{\mathbf{G}}^{(e,j)} - \mathrm{j}\omega\mu\widetilde{\mathbf{G}}^{(h,j)} = \mathbf{0} \end{cases} \tag{E.4}$$

$$\begin{cases} -\mathrm{j}\omega\varepsilon\widetilde{\mathbf{G}}^{(e,m)} - \mathrm{j}\mathbf{k} \times \widetilde{\mathbf{G}}^{(h,m)} = \mathbf{0} \\ \mathrm{j}\mathbf{k} \times \widetilde{\mathbf{G}}^{(e,m)} - \mathrm{j}\omega\mu\widetilde{\mathbf{G}}^{(h,m)} = \widetilde{\mathbf{I}}. \end{cases} \tag{E.5}$$

Starting from the second equation of (E.4), the following expression is found:

$$\widetilde{\mathbf{G}}^{(h,j)} = \frac{1}{\mathrm{j}\omega\mu}\left(\mathrm{j}\mathbf{k} \times \widetilde{\mathbf{G}}^{(e,j)}\right); \tag{E.6}$$

this is substituted in the first equation of (E.4), leading to:

$$-\mathrm{j}\omega\varepsilon\widetilde{\mathbf{G}}^{(e,j)} - \mathrm{j}\mathbf{k} \times \frac{1}{\mathrm{j}\omega\mu}\left(\mathrm{j}\mathbf{k} \times \widetilde{\mathbf{G}}^{(e,j)}\right) = \widetilde{\mathbf{I}}.$$

Now, after some manipulations:

$$(-\mathrm{j}\omega\varepsilon)(\mathrm{j}\omega\mu)\widetilde{\mathbf{G}}^{(e,j)} - (\mathrm{j}\mathbf{k}) \times (\mathrm{j}\mathbf{k}) \times \widetilde{\mathbf{G}}^{(e,j)} = \mathrm{j}\omega\mu\widetilde{\mathbf{I}},$$

which becomes:

$$\left[\omega^2\varepsilon\mu\widetilde{\mathbf{I}} + \mathbf{k}\times(\mathbf{k}\times\widetilde{\mathbf{I}})\right]\cdot\widetilde{\mathbf{G}}^{(\mathrm{e,j})} = \mathrm{j}\omega\mu\widetilde{\mathbf{I}}.$$

Let $\mathbf{A}$, $\mathbf{B}$ be two vectors and let $\mathbf{C}$ be a dyadic; the, the following relationship holds:

$$\mathbf{A}\times\mathbf{B}\times\mathbf{C} = (\mathbf{A}\cdot\mathbf{C})\mathbf{B} - (\mathbf{A}\cdot\mathbf{B})\mathbf{C}.$$

By considering $\mathbf{A} = \mathbf{B} = \mathbf{k}$, $\mathbf{C} = \widetilde{\mathbf{I}}$, the following equation is found:

$$\mathbf{k}\times(\mathbf{k}\times\widetilde{\mathbf{I}}) = (\mathbf{k}\cdot\widetilde{\mathbf{I}})\mathbf{k} - (\mathbf{k}\cdot\mathbf{k})\widetilde{\mathbf{I}} = \mathbf{k}\,\mathbf{k} - k^2\widetilde{\mathbf{I}},$$

where:

$$k^2 \triangleq \mathbf{k}\cdot\mathbf{k}.$$

So, this can be substituted in our equation, obtaining:

$$\left[\omega^2\varepsilon\mu\widetilde{\mathbf{I}} + \mathbf{k}\,\mathbf{k} - k^2\widetilde{\mathbf{I}}\right]\cdot\widetilde{\mathbf{G}}^{(\mathrm{e,j})} = \mathrm{j}\omega\mu\widetilde{\mathbf{I}}.$$

Let $\mathbf{k}$ be written in the following coordinate system:

$$\mathbf{k} = k\widehat{\mathbf{k}} + \alpha\widehat{\boldsymbol{\alpha}} + \beta\widehat{\boldsymbol{\beta}},$$

then, a generic dyadic $\widetilde{\mathbf{D}}$ can be written in this coordinate system as:

$$\widetilde{\mathbf{D}} = \begin{bmatrix} a & b & c \\ d & f & g \\ h & l & m \end{bmatrix} = a\widehat{\mathbf{k}}\widehat{\mathbf{k}} + b\widehat{\mathbf{k}}\widehat{\boldsymbol{\alpha}} + c\widehat{\mathbf{k}}\widehat{\boldsymbol{\beta}} + d\widehat{\boldsymbol{\alpha}}\widehat{\mathbf{k}} + f\widehat{\boldsymbol{\alpha}}\widehat{\boldsymbol{\alpha}} + g\widehat{\boldsymbol{\alpha}}\widehat{\boldsymbol{\beta}} + h\widehat{\boldsymbol{\beta}}\widehat{\mathbf{k}} + l\widehat{\boldsymbol{\beta}}\widehat{\boldsymbol{\alpha}} + m\widehat{\boldsymbol{\beta}}\widehat{\boldsymbol{\beta}}.$$

This general case allow us to say that the identical dyadic can be written in this coordinate system as:

$$\widetilde{\mathbf{I}} = \begin{bmatrix} 1 & 0 & 0 \\ 0 & 1 & 0 \\ 0 & 0 & 1 \end{bmatrix} = \widehat{\mathbf{k}}\widehat{\mathbf{k}} + \widehat{\boldsymbol{\alpha}}\widehat{\boldsymbol{\alpha}} + \widehat{\boldsymbol{\beta}}\widehat{\boldsymbol{\beta}}.$$

This expression is substituted in the equation written before, obtaining:

$$\left[\omega^2\varepsilon\mu\widetilde{\mathbf{I}} + \mathbf{k}\,\mathbf{k} - k^2(\widehat{\mathbf{k}}\widehat{\mathbf{k}} + \widehat{\boldsymbol{\alpha}}\widehat{\boldsymbol{\alpha}} + \widehat{\boldsymbol{\beta}}\widehat{\boldsymbol{\beta}})\right] =$$
$$= \omega^2\varepsilon\mu\widehat{\mathbf{k}}\widehat{\mathbf{k}} + (\omega^2\varepsilon\mu - k^2)(\widehat{\boldsymbol{\alpha}}\widehat{\boldsymbol{\alpha}} + \widehat{\boldsymbol{\beta}}\widehat{\boldsymbol{\beta}}) =$$
$$= \begin{bmatrix} \omega^2\varepsilon\mu & 0 & 0 \\ 0 & \omega^2\varepsilon\mu - k^2 & 0 \\ 0 & 0 & \omega^2\varepsilon\mu - k^2 \end{bmatrix},$$

where, in the last step, the expression was simply re-written in matrix form. This is used to prove that:

$$\begin{bmatrix} \omega^2\varepsilon\mu & 0 & 0 \\ 0 & \omega^2\varepsilon\mu - k^2 & 0 \\ 0 & 0 & \omega^2\varepsilon\mu - k^2 \end{bmatrix} \cdot \widetilde{\mathbf{G}}^{(e,j)} = j\omega\mu\widetilde{\mathbf{I}}.$$

Finally, it is possible to write:

$$\widetilde{\mathbf{G}}^{(e,j)} = j\omega\mu \left(\begin{bmatrix} \omega^2\varepsilon\mu & 0 & 0 \\ 0 & \omega^2\varepsilon\mu - k^2 & 0 \\ 0 & 0 & \omega^2\varepsilon\mu - k^2 \end{bmatrix} \right)^{-1} \cdot \widetilde{\mathbf{I}}.$$

The inversion of this matrix is straightforward, since it is diagonal:

$$\widetilde{\mathbf{G}}^{(e,j)} = -j\omega\mu \begin{bmatrix} \dfrac{1}{\omega^2\varepsilon\mu} & 0 & 0 \\ 0 & \dfrac{1}{\omega^2\varepsilon\mu - k^2} & 0 \\ 0 & 0 & \dfrac{1}{\omega^2\varepsilon\mu - k^2} \end{bmatrix} \cdot \widetilde{\mathbf{I}}.$$

Let $\widetilde{\mathbf{G}}$ be:

$$\widetilde{\mathbf{G}} = -\widetilde{\mathbf{G}}^{(e,j)} = j\omega\mu \begin{bmatrix} \dfrac{1}{\omega^2\varepsilon\mu} & 0 & 0 \\ 0 & \dfrac{1}{\omega^2\varepsilon\mu - k^2} & 0 \\ 0 & 0 & \dfrac{1}{\omega^2\varepsilon\mu - k^2} \end{bmatrix} =$$

$$= -\frac{1}{\omega^2\varepsilon\mu}\widehat{\mathbf{k}\mathbf{k}} - \frac{1}{\omega^2\varepsilon\mu - k^2}\left(\widehat{\boldsymbol{\alpha}}\widehat{\boldsymbol{\alpha}} + \widehat{\boldsymbol{\beta}}\widehat{\boldsymbol{\beta}} \right);$$

therefore, we found that:

$$\widetilde{\mathbf{G}}^{(e,j)} = -j\omega\mu\widetilde{\mathbf{G}}(\mathbf{k}). \tag{E.7}$$

The dyadic $\widetilde{\mathbf{G}}$ is rewritten as:

$$\widetilde{\mathbf{G}}(\mathbf{k}) = -\frac{1}{\omega^2\varepsilon\mu}\widehat{\mathbf{k}\mathbf{k}} - \frac{1}{\omega^2\varepsilon\mu - k^2}\left(\widehat{\boldsymbol{\alpha}}\widehat{\boldsymbol{\alpha}} + \widehat{\boldsymbol{\beta}}\widehat{\boldsymbol{\beta}} \right) =$$

$$= -\frac{1}{\omega^2\varepsilon\mu}\widehat{\mathbf{k}\mathbf{k}} + \frac{1}{\omega^2\varepsilon\mu - k^2}\widehat{\mathbf{k}\mathbf{k}} - \frac{1}{\omega^2\varepsilon\mu - k^2}\widetilde{\mathbf{I}};$$

now, let $\widetilde{g}(\mathbf{k})$ be:

$$\widetilde{g}(\mathbf{k}) \triangleq \frac{1}{k^2 - \omega^2 \varepsilon \mu} = \widetilde{g}(k),$$

indeed, $\widetilde{g}$ does not depend on the entire $\mathbf{k}$ vector, but only on its first component, which is the one along the direction of the unit vector $\widehat{\mathbf{k}}$. So:

$$\begin{aligned}
\widetilde{\mathbf{G}}(\mathbf{k}) &= \frac{1}{k^2 - \omega^2 \varepsilon \mu} \widetilde{\mathbf{I}} + \left(\frac{1}{\omega^2 \varepsilon \mu - k^2} - \frac{1}{\omega^2 \varepsilon \mu} \right) \widehat{\mathbf{k}\mathbf{k}} = \\
&= \frac{1}{k^2 - \omega^2 \varepsilon \mu} \widetilde{\mathbf{I}} + \frac{1}{k^2 - \omega^2 \varepsilon \mu} \left(-1 - \frac{k^2 - \omega^2 \varepsilon \mu}{\omega^2 \varepsilon \mu} \right) \widehat{\mathbf{k}\mathbf{k}} = \\
&= \frac{1}{k^2 - \omega^2 \varepsilon \mu} \widetilde{\mathbf{I}} - \frac{1}{k^2 - \omega^2 \varepsilon \mu} \frac{k^2}{\omega^2 \varepsilon \mu} \widehat{\mathbf{k}\mathbf{k}} = \\
&= \frac{1}{k^2 - \omega^2 \varepsilon \mu} \widetilde{\mathbf{I}} + \frac{(-\mathrm{j}k\widehat{\mathbf{k}})(\mathrm{j}k\widehat{\mathbf{k}})}{k^2 - \omega^2 \varepsilon \mu}.
\end{aligned}$$

This becomes, grouping $\mathbf{k} = k\widehat{\mathbf{k}}$ and substituting $\widetilde{g}(k)$:

$$\widetilde{\mathbf{G}}(\mathbf{k}) = \left[\widetilde{\mathbf{I}} + \frac{(-\mathrm{j}\mathbf{k})(-\mathrm{j}\mathbf{k})}{\omega^2 \varepsilon \mu} \right] \widetilde{g}(k) \tag{E.8}$$

Then, by applying $\mathcal{F}_3^{-1}$, the following expression is obtained:

$$\mathbf{G}(\mathbf{r}) \triangleq \mathcal{F}_3^{-1} \left\{ \widetilde{\mathbf{G}(\mathbf{k})} \right\} = \left[\mathbf{I} + \frac{\nabla \nabla}{\omega^2 \varepsilon \mu} \right] g(r),$$

where $g(r)$ is the so-called scalar Green's function, which equals

$$g(\mathbf{r}) \triangleq \mathcal{F}_3^{-1} \left\{ \widetilde{g}(k) \right\} = \frac{\mathrm{e}^{-\mathrm{j}k_0 r}}{4\pi r} = g(r). \tag{E.9}$$

This expression depends only on r, which is the radial coordinate of a spherical coordinate system in the spatial domain; in other words, the scalar Green's function depends only on the distance from the origin of the coordinate system, not on the direction. The term k_0 has been implicitly defined as:

$$k_0 \triangleq \omega \sqrt{\varepsilon_0 \mu_0};$$

this definition can be extended for a homogeneous medium with different dielectric constant or magnetic permeability. Recalling the definition of the spectral domain transimpedance Green's function (E.7), it is immediately possible to define the spatial domain transimpedance Green's function as:

$$\mathbf{G}^{(\mathrm{e,j})}(\mathbf{r}) \triangleq \mathcal{F}_3^{-1} \left\{ \widetilde{\mathbf{G}}^{(\mathrm{e,j})}(\mathbf{k}) \right\} = -\mathrm{j}\omega\mu \mathbf{G}(\mathbf{r}).$$

Derivation of the voltage-voltage Green's function

From (E.6),

$$\widetilde{\mathbf{G}}^{(\mathrm{h,j})}(\mathbf{k}) = \frac{1}{\mathrm{j}\omega\mu}\left(\mathrm{j}\mathbf{k} \times \widetilde{\mathbf{G}}^{(\mathrm{e,j})}(\mathbf{k})\right),$$

so, by applying (E.7):

$$\widetilde{\mathbf{G}}^{(\mathrm{h,j})}(\mathbf{k}) = -\mathrm{j}\mathbf{k} \times \widetilde{\mathbf{G}}(\mathbf{k}), \tag{E.10}$$

which is transformed in the spatial domain, the following expression is obtained:

$$\mathbf{G}^{(\mathrm{h,j})}(\mathbf{r}) \triangleq \mathcal{F}_3^{-1}\left\{\widetilde{\mathbf{G}}^{(\mathrm{h,j})}(\mathbf{k})\right\} = \nabla \times \mathbf{G}(\mathbf{r}). \tag{E.11}$$

Expressions of the remaining Green's functions and duality notes

The remaining Green's functions are calculated as follows: starting from the first equation of (E.5), $\widetilde{\mathbf{G}}^{(\mathrm{e,m})}$ is derived, and substituted in the second equation; then, with very similar manipulations, for the spectral domain, the following expressions are obtained:

$$\widetilde{\mathbf{G}}^{(\mathrm{h,m})}(\mathbf{k}) = -\mathrm{j}\omega\varepsilon\widetilde{\mathbf{G}}(\mathbf{k}) \tag{E.12}$$

$$\widetilde{\mathbf{G}}^{(\mathrm{e,m})}(\mathbf{k}) = \mathrm{j}\mathbf{k} \times \widetilde{\mathbf{G}}(\mathbf{k}). \tag{E.13}$$

By applying the inverse triple Fourier transform to the expressions (E.12) and (E.13), the following spatial domain expressions are obtained:

$$\mathbf{G}^{(\mathrm{h,m})}(\mathbf{r}) = -\mathrm{j}\omega\varepsilon\mathbf{G}(\mathbf{r}) \tag{E.14}$$

$$\mathbf{G}^{(\mathrm{e,m})}(\mathbf{r}) = -\nabla \times \mathbf{G}(\mathbf{r}). \tag{E.15}$$

E.1.1 Electric Field and Magnetic Field integral expressions

From the previous sections, the following expressions were obtained:

$$\begin{cases} \widetilde{\mathbf{E}}(\mathbf{k}) = \widetilde{\mathbf{G}}^{(\mathrm{e,j})}(\mathbf{k}) \cdot \widetilde{\mathbf{J}}(\mathbf{k}) + \widetilde{\mathbf{G}}^{(\mathrm{e,m})}(\mathbf{k}) \cdot \widetilde{\mathbf{M}}(\mathbf{k}) \\ \widetilde{\mathbf{H}}(\mathbf{k}) = \widetilde{\mathbf{G}}^{(\mathrm{h,j})}(\mathbf{k}) \cdot \widetilde{\mathbf{J}}(\mathbf{k}) + \widetilde{\mathbf{G}}^{(\mathrm{h,m})}(\mathbf{k}) \cdot \widetilde{\mathbf{M}}(\mathbf{k}). \end{cases} \tag{E.16}$$

From these equations it is possible to derive the expressions of the electric and magnetic field in the space domain by applying the inverse triple Fourier transform to each component of $\widetilde{\mathbf{E}}$ and $\widetilde{\mathbf{H}}$. The result is:

$$\begin{cases} \mathbf{E}(\mathbf{r}) = \mathbf{G}^{(\mathrm{e,j})}(\mathbf{r}) \overset{*}{\cdot} \mathbf{J}(\mathbf{r}) + \mathbf{G}^{(\mathrm{e,m})}(\mathbf{r}) \overset{*}{\cdot} \mathbf{M}(\mathbf{r}) \\ \mathbf{H}(\mathbf{r}) = \mathbf{G}^{(\mathrm{h,j})}(\mathbf{r}) \overset{*}{\cdot} \mathbf{J}(\mathbf{r}) + \mathbf{G}^{(\mathrm{h,m})}(\mathbf{r}) \overset{*}{\cdot} \mathbf{M}(\mathbf{r}), \end{cases} \tag{E.17}$$

where the symbol $\overset{*}{\cdot}$ denotes the convolution by means of the scalar product; given the dyadic $\boldsymbol{\mathcal{D}}(\mathbf{r})$ and the vector $\mathbf{A}$, in carthesian coordinates, this is:

$$\boldsymbol{\mathcal{D}}(\mathbf{r}) \overset{*}{\cdot} \mathbf{A}(\mathbf{r}) = \int_{\mathbb{R}^3} \boldsymbol{\mathcal{D}}(\mathbf{r} - \mathbf{r}') \cdot \mathbf{A}(\mathbf{r}') \, \mathrm{d}\,\mathbf{r}' =$$

$$= \iiint_{\mathbb{R}^3} \boldsymbol{\mathcal{D}}(x - x', y - y', z - z') \cdot \mathbf{A}(x', y', z') \, \mathrm{d}x' \, \mathrm{d}y' \, \mathrm{d}z'$$

E.1.2 Mixed-Potential Integral Equations

Electric current density contributions

In the previous section the expressions of the electric and magnetic fields based on the dyadic Green's function formalism were derived for the homogeneous space. In this section an alternative formulation, based on the definition of potential functions, will be derived.

All the operators involved in these formulations are linear; therefore, let $\mathbf{M} = 0$, initially; by this way, only electric currents can produce the electromagnetic field. In a second step, the dual hypothesis will be assumed to complete the formulation; then, superposition will be applied. Recalling the expressions (E.16) and (E.8), the electric field in the spectral domain is written as:

$$\widetilde{\mathbf{E}}(\mathbf{k}) = \widetilde{\mathbf{G}}^{(\mathrm{e,j})}(\mathbf{k}) \cdot \widetilde{\mathbf{J}}(\mathbf{k}) = -\mathrm{j}\omega\mu\widetilde{\mathbf{G}}(\mathbf{k}) \cdot \widetilde{\mathbf{J}}(\mathbf{k}) =$$

$$= -\mathrm{j}\omega\mu \left[\widetilde{\mathbf{I}} + \frac{(-\mathrm{j}\mathbf{k})(-\mathrm{j}\mathbf{k})}{\omega^2\varepsilon\mu} \right] \widetilde{g}(k) \cdot \widetilde{\mathbf{J}}(\mathbf{k}) =$$

$$= -\mathrm{j}\omega\mu\widetilde{g}(\mathbf{k})\widetilde{\mathbf{J}}(\mathbf{k}) - \mathrm{j}\omega\mu\frac{1}{\omega^2\varepsilon\mu}(-\mathrm{j}\mathbf{k})(-\mathrm{j}\mathbf{k}) \cdot \widetilde{\mathbf{J}}(\mathbf{k})\widetilde{g}(k).$$

The continuity equations are reported in the following:

$$\begin{cases} \nabla \cdot \mathbf{J} + \mathrm{j}\omega q_{\mathrm{e}} = 0 \\ \nabla \cdot \mathbf{M} + \mathrm{j}\omega q_{\mathrm{m}} = 0, \end{cases}$$

where q_{e}, q_{m} are the charge densities. These equations are re-written in the spectral domain:

$$\begin{cases} -\mathrm{j}\mathbf{k} \cdot \widetilde{\mathbf{J}} + \mathrm{j}\omega\widetilde{q}_{\mathrm{e}} = 0 \\ -\mathrm{j}\mathbf{k} \cdot \widetilde{\mathbf{M}} + \mathrm{j}\omega\widetilde{q}_{\mathrm{m}} = 0. \end{cases}$$

By substituting the first continuity condition in the spectral domain in the expression derived above,

$$\mathbf{k} \cdot \widetilde{\mathbf{J}} = \omega \widetilde{q}_{\mathrm{e}},$$

so:

$$\widetilde{\mathbf{E}}(\mathbf{k}) = -\mathrm{j}\omega\mu\widetilde{g}(k)\widetilde{\mathbf{J}}(\mathbf{k}) - \frac{1}{\varepsilon}(-\mathrm{j}\mathbf{k})\widetilde{g}(k)\widetilde{q}_{\mathrm{e}}(\mathbf{k}).$$

The inverse triple Fourier transform of these expressions is:

$$\mathbf{E}(\mathbf{r}) = -\mathrm{j}\omega\mu \int_{\mathbb{R}^3} g(r - r')\mathbf{J}(\mathbf{r}')\,\mathrm{d}\mathbf{r}' - \frac{1}{\varepsilon}\nabla\left[\int_{\mathbb{R}^3} g(r - r')q_{\mathrm{e}}(\mathbf{r}')\,\mathrm{d}\mathbf{r}'\right].$$

The integrand have two variables, but the integration is performed only with respect to $\mathbf{r}'$; therefore, the output function will be dependent on $\mathbf{r}$. The following quantities are defined:

$$\mathbf{A}(\mathbf{r}) = \mu \int_{\mathbb{R}^3} g(r - r')\mathbf{J}(\mathbf{r}')\,\mathrm{d}\mathbf{r}' \tag{E.18}$$

$$\Phi(\mathbf{r}) = \frac{1}{\varepsilon}\left[\int_{\mathbb{R}^3} g(r - r')q_{\mathrm{e}}(\mathbf{r}')\,\mathrm{d}\mathbf{r}'\right], \tag{E.19}$$

where $\mathbf{A}(\mathbf{r})$ and $\Phi(\mathbf{r})$ are the vector and scalar potentials. Therefore, $\mathbf{E}(\mathbf{r})$ is expressed with the mixed-potential integral formula as follows:

$$\mathbf{E}(\mathbf{r}) = -\mathrm{j}\omega\mathbf{A}(\mathbf{r}) - \nabla\Phi(\mathbf{r}). \tag{E.20}$$

The ∇ operator applied to the scalar potential Φ acts on the natural domain $\mathbf{r}$, not on the integration variable $\mathbf{r}'$; therefore, it can be taken in the integral sign, if necessary.

Physical interpretation of the potentials

The MPIE can be derived in another way, considering the following Maxwell's equations in absence of magnetic sources:

$$\begin{cases} \nabla \times \mathbf{E}(\mathbf{r}) = -\mathrm{j}\omega\mu\mathbf{H}(\mathbf{r}) \\ \nabla \times \mathbf{H}(\mathbf{r}) = \mathrm{j}\omega\varepsilon\mathbf{E}(\mathbf{r}) + \mathbf{J}(\mathbf{r}) \\ \nabla \cdot (\mu\mathbf{H}(\mathbf{r})) = 0 \\ \nabla \cdot (\varepsilon\mathbf{E}(\mathbf{r})) = q_{\mathrm{e}}(\mathbf{r}). \end{cases}$$

Since:

$$\nabla \cdot (\mu \mathbf{H}(\mathbf{r})) = 0,$$

the field $\mu \mathbf{H}$ is solenoidal; mathematically, this means that $\mu \mathbf{H}$ can be written as the curl of another vector, which is the vector potential; so:

$$\mu \mathbf{H}(\mathbf{r}) = \nabla \times \mathbf{A}(\mathbf{r}),$$

or:

$$\mathbf{H}(\mathbf{r}) = \frac{1}{\mu} \nabla \times \mathbf{A}(\mathbf{r}).$$

Now, this is substituted in the curl of the electric field, leading to:

$$\nabla \times \mathbf{E}(\mathbf{r}) = -\mathrm{j}\omega \nabla \times \mathbf{A}(\mathbf{r}),$$

so, by using the linearity of the curl operator:

$$\nabla \times (\mathbf{E}(\mathbf{r}) + \mathrm{j}\omega \mathbf{A}(\mathbf{r})) = 0.$$

Since the curl of this vector equals zero, it is irrotational; therefore, it can be written as the gradient of a scalar potential Φ:

$$\mathbf{E}(\mathbf{r}) + \mathrm{j}\omega \mathbf{A}(\mathbf{r}) = -\nabla \Phi(\mathbf{r}),$$

so:

$$\mathbf{E}(\mathbf{r}) = -\mathrm{j}\omega \mathbf{A}(\mathbf{r}) - \nabla \Phi(\mathbf{r}),$$

which is exactly the same formula that was found manipulating the Green's function formulation. These calculations provide $\mathbf{A}(\mathbf{r})$ and $\Phi(\mathbf{r})$ with a physical interpretation: $\mathbf{A}$ is the vector such that its curl provides the magnetic induction $\mathbf{B}(\mathbf{r}) = \mu \mathbf{H}(\mathbf{r})$; $\Phi(\mathbf{r})$ is the scalar potential, and its gradient equals the electric field, plus the vector potential contribution. Moreover, in the electrostatic case, *i.e.*, $\omega \to 0$,

$$\mathbf{E}(\mathbf{r}) = -\nabla \Phi(\mathbf{r}).$$

In this case, $\Phi(\mathbf{r})$ is also called the static potential of the problem. By working on the magnetic field integral equation expressed, it is known from (E.16), (E.10) and (E.8) that:

$$\widetilde{\mathbf{H}}(\mathbf{k}) = \widetilde{\mathbf{G}}^{(\mathrm{h,j})}(\mathbf{k}) \cdot \widetilde{\mathbf{J}}(\mathbf{k}) = -\mathrm{j}\mathbf{k} \times \widetilde{\mathbf{G}}(\mathbf{k}) =$$

$$= -\mathrm{j}\mathbf{k} \times \left[\widetilde{\mathbf{I}} + \frac{(-\mathrm{j}\mathbf{k})(-\mathrm{j}\mathbf{k})}{\omega^2 \varepsilon \mu} \right] \widetilde{g}(k) \cdot \widetilde{\mathbf{J}}(\mathbf{k}).$$

The second term of the sum equals zero; indeed:

$$-\mathrm{j}\mathbf{k} \times [(-\mathrm{j}\mathbf{k})(-\mathrm{j}\mathbf{k})] = [(-\mathrm{j}\mathbf{k}) \times (-\mathrm{j}\mathbf{k})] \, (-\mathrm{j}\mathbf{k}) = 0.$$

So:

$$\widetilde{\mathbf{H}}(\mathbf{k}) = -\mathrm{j}\mathbf{k}\widetilde{g}(k) \times \widetilde{\mathbf{J}}(\mathbf{k}).$$

This can be re-transformed in the natural domain, obtaining:

$$\mathbf{H}(\mathbf{r}) = \nabla g(r) \overset{*}{\times} \mathbf{J}(\mathbf{r}) = \int_{\mathbb{R}^3} [\nabla g(r - r')] \times \mathbf{J}(\mathbf{r}') \, \mathrm{d}\mathbf{r}', \tag{E.21}$$

where the symbol $\overset{*}{\times}$ denotes a convolution integral by means of a vector product.

The previous result is not surprising; indeed, it was proved that:

$$\mathbf{H}(\mathbf{r}) = \frac{1}{\mu}\nabla \times \mathbf{A}(\mathbf{r}),$$

so, it was simply possible to use this formula to write the MFIE as a function of potentials; now, the result has been found by another way.

The electric field generated by an electric current density has two contributions: one given by the vector potential $\mathbf{A}(\mathbf{r})$, and one given by the scalar potential $\Phi(\mathbf{r})$. In this case the scalar potential does not provide any contribution.

Magnetic scalar and vector potentials $\Psi(\mathbf{r})$ and $\mathbf{F}(\mathbf{r})$ can be defined as well as the electric ones; the steps aimed at deriving these quantities are very similar to the ones used for the electric quantities. The starting point are the following Maxwell's equations (with only magnetic current contributions):

$$\begin{cases} \nabla \times \mathbf{E}(\mathbf{r}) = -\mathrm{j}\omega\mu\mathbf{H}(\mathbf{r}) - \mathbf{M}(\mathbf{r}) \\ \nabla \times \mathbf{H}(\mathbf{r}) = \mathrm{j}\omega\varepsilon\mathbf{E}(\mathbf{r}) \\ \nabla \cdot (\mu\mathbf{H}(\mathbf{r})) = -q_{\mathrm{m}}(\mathbf{r}) \\ \nabla \cdot (\varepsilon\mathbf{E}(\mathbf{r})) = 0. \end{cases}$$

Helmholtz equations for the potentials

Considering the following Maxwell's equations,

$$\begin{cases} \nabla \times \mathbf{E}(\mathbf{r}) = -\mathrm{j}\omega\mu\mathbf{H}(\mathbf{r}) \\ \nabla \times \mathbf{H}(\mathbf{r}) = \mathrm{j}\omega\varepsilon\mathbf{E}(\mathbf{r}) + \mathbf{J}(\mathbf{r}) \\ \nabla \cdot (\mu\mathbf{H}(\mathbf{r})) = 0 \\ \nabla \cdot (\varepsilon\mathbf{E}(\mathbf{r})) = q_{\mathrm{e}}(\mathbf{r}), \end{cases}$$

it has been found that the scalar potential $\Phi(\mathbf{r})$ has been defined as the scalar function satisfying the following property:

$$\mathbf{E}(\mathbf{r}) + \mathrm{j}\omega\mathbf{A}(\mathbf{r}) = -\nabla\Phi(\mathbf{r}),$$

and:

$$\mathbf{H}(\mathbf{r}) = \frac{1}{\mu}\nabla \times \mathbf{A}(\mathbf{r}).$$

It is possible to use the remaining Maxwell's equations to obtain additional results concerning the potentials; indeed, from the curl of the magnetic field,

$$\nabla \times \mathbf{H}(\mathbf{r}) = \nabla \times \nabla \times \mathbf{A}(\mathbf{r}) = \mathrm{j}\omega\varepsilon\mathbf{E}(\mathbf{r}) + \mathbf{J}(\mathbf{r}),$$

but:

$$\nabla \times \nabla \times \mathbf{A}(\mathbf{r}) = \nabla\nabla \cdot \mathbf{A}(\mathbf{r}) - \nabla^2\mathbf{A}(\mathbf{r}).$$

So, by re-writing $\mathbf{E}(\mathbf{r})$ using the expression dependent on the potentials, we have:

$$\nabla\nabla \cdot \mathbf{A}(\mathbf{r}) - \nabla^2\mathbf{A}(\mathbf{r}) = \mathrm{j}\omega\mu\varepsilon(-\mathrm{j}\omega\mathbf{A}(\mathbf{r}) + \nabla\Phi(\mathbf{r})) + \mu\mathbf{J}(\mathbf{r}).$$

Now, let $k_0 = \omega\sqrt{\varepsilon\mu}$; then:

$$\nabla\nabla \cdot \mathbf{A}(\mathbf{r}) = \nabla^2\mathbf{A}(\mathbf{r}) + k_0^2\mathbf{A}(\mathbf{r}) - \mathrm{j}\omega\varepsilon\mu\nabla\Phi(\mathbf{r}) + \mu\mathbf{J}(\mathbf{r}),$$

which can be re-written as:

$$\nabla^2\mathbf{A}(\mathbf{r}) + k^2\mathbf{A}(\mathbf{r}) = -\mu\mathbf{J}(\mathbf{r}) + \nabla\left(\nabla \cdot \mathbf{A}(\mathbf{r}) + \mathrm{j}\omega\varepsilon\mu\Phi(\mathbf{r})\right).$$

This is a Helmholtz equation, less than the gradient term at the right-hand side. From the divergence of the electric displacement the next equation follows:

$$\nabla \cdot (\varepsilon\mathbf{E}(\mathbf{r})) = q_{\mathrm{e}}(\mathbf{r}),$$

which becomes, by substituting the expression of the electric field as function of the potentials:

$$\nabla \cdot [\varepsilon(-\mathrm{j}\omega \mathbf{A}(\mathbf{r}) - \nabla \Phi(\mathbf{r}))] = q_{\mathrm{e}}(\mathbf{r}),$$

so:

$$-\nabla \cdot (\mathrm{j}\omega \mathbf{A}(\mathbf{r})) - \nabla \cdot \nabla \Phi(\mathbf{r}) = \frac{q_{\mathrm{e}}(\mathbf{r})}{\varepsilon},$$

and:

$$\nabla^2 \Phi(\mathbf{r}) = -\mathrm{j}\omega \nabla \cdot \mathbf{A}(\mathbf{r}) - \frac{q_{\mathrm{e}}(\mathbf{r})}{\varepsilon}.$$

Now, by adding $k_0^2 \Phi(\mathbf{r})$ at both the sides:

$$\nabla^2 \Phi(\mathbf{r}) + k_0^2 \Phi(\mathbf{r}) = -\frac{q_{\mathrm{e}}(\mathbf{r})}{\varepsilon} - \mathrm{j}\omega \nabla \cdot \mathbf{A}(\mathbf{r}) + k_0^2 \Phi(\mathbf{r}),$$

which, re-arranging some terms, is:

$$\nabla^2 \Phi(\mathbf{r}) + k_0^2 \Phi(\mathbf{r}) = -\frac{q_{\mathrm{e}}(\mathbf{r})}{\varepsilon} - \mathrm{j}\omega \left(\nabla \cdot \mathbf{A}(\mathbf{r}) + \mathrm{j}\omega\varepsilon\mu\Phi(\mathbf{r}) \right).$$

Also this equation is similar to the Helmholtz one; moreover, it is observed that the two equations are coupled, since there is a common term χ, which involves both the vector potential and the scalar potential:

$$\chi = \nabla \cdot \mathbf{A}(\mathbf{r}) + \mathrm{j}\omega\mu\Phi(\mathbf{r}).$$

If $\chi = 0$, the two equations are independent. The quantities $\mathbf{A}(\mathbf{r})$ and $\Phi(\mathbf{r})$ are not defined in an unique way; indeed, if:

$$\mathbf{A}'(\mathbf{r}) = \mathbf{A}(\mathbf{r}) + \nabla\psi(\mathbf{r}),$$

where ψ is a generic scalar function,

$$\nabla \times \mathbf{A}'(\mathbf{r}) = \nabla \times \mathbf{A}(\mathbf{r}) + \nabla \times \nabla\psi(\mathbf{r}) = \nabla \times \mathbf{A}(\mathbf{r}).$$

In fact, the second term is zero, due to the property of the gradient of being an irrotational field. So, it is possible to force $\chi = 0$; this choice is called Lorentz gauge, which is a transformation that maintains invariant the result. With this choice, the differential equations become:

$$\nabla^2 \mathbf{A}(\mathbf{r}) + k_0^2 \mathbf{A}(\mathbf{r}) = -\mu \mathbf{J}(\mathbf{r})$$

$$\nabla^2 \Phi(\mathbf{r}) + k_0^2 \Phi(\mathbf{r}) = -\frac{q_{\mathrm{e}}(\mathbf{r})}{\varepsilon}.$$

These are a vector and a scalar Helmholtz equations.

It is possible to observe that both $\Phi(\mathbf{r})$ and $g(r)$ are satisfying the Helmholtz equation; indeed, starting from the triple Fourier transform of (E.9), the following expression is obtained:

$$\widetilde{g}(k) = \frac{1}{k^2 - \omega^2 \varepsilon \mu},$$

which becomes, after an inversion:

$$-\left[(-\mathrm{j}\mathbf{k}) \cdot (-\mathrm{j}\mathbf{k}) + \omega^2 \varepsilon \mu\right] \widetilde{g}(k) = 1,$$

which is, in the spatial domain (applying the inverse triple Fourier transform to each side):

$$\nabla^2 g(r) + k_0^2 g(r) = \delta(\mathbf{r}).$$

This is the same Helmholtz equation previously defined. This show why $g(r)$ is called scalar Green's function: it actually is a Green's function, of the scalar Helmholtz equation. A final observation: using the Lorentz gauge, it is possible to obtain $\mathbf{E}(\mathbf{r})$ as a function of the vector potential $\mathbf{A}(\mathbf{r})$ only; indeed:

$$\nabla \left(\nabla \cdot \mathbf{A}(\mathbf{r}) + \mathrm{j}\omega\mu\varepsilon\Phi(\mathbf{r})\right) = 0,$$

so:

$$\nabla^2 \mathbf{A}(\mathbf{r}) + \mathrm{j}\omega\mu\varepsilon\nabla\Phi(\mathbf{r}) = 0,$$

which means that it is possible to derive $\nabla\Phi(\mathbf{r})$ as:

$$\nabla\Phi(\mathbf{r}) = -\frac{1}{\mathrm{j}\omega\mu\varepsilon}\nabla\nabla \cdot \mathbf{A}(\mathbf{r}).$$

This can be substituted in the expression of $\mathbf{E}(\mathbf{r})$:

$$\mathbf{E}(\mathbf{r}) = -\mathrm{j}\omega\mathbf{A}(\mathbf{r}) - \nabla\Phi(\mathbf{r}) = -\mathrm{j}\omega\mathbf{A}(\mathbf{r}) + \frac{1}{\mathrm{j}\omega\varepsilon\mu}\nabla\nabla \cdot \mathbf{A}(\mathbf{r}).$$

This means that, instead of using the expressions that have been found using the Green's function formalism applied to the Maxwell's equations, it is possible to derive the expression of the vector potential for a given source, and then apply this formula in order to derive the electric field. By applying the duality theorem described in the following sections, it is possible to obtain the very same results also for the magnetic scalar and vector potentials.

Magnetic current density contributions

The following duality theorem holds:

$$\mathbf{A} \longleftrightarrow \mathbf{F}$$
$$-\mu \longleftrightarrow \varepsilon$$
$$-q_{\mathrm{e}} \longleftrightarrow q_{\mathrm{m}}$$
$$-\mathbf{J} \longleftrightarrow \mathbf{M}$$
$$\mathbf{E} \longleftrightarrow \mathbf{H},$$

where $\mathbf{F}$ is defined in such a way that:

$$\nabla \times \mathbf{F} = -\varepsilon \mathbf{E}(\mathbf{r}).$$

Starting from the formalism of Green's functions, the following MPIE formulation can be derived:

$$\mathbf{H}(\mathbf{r}) = -\mathrm{j}\omega \mathbf{F}(\mathbf{r}) - \nabla \Psi(\mathbf{r}), \qquad (E.22)$$

where $\Psi(\mathbf{r})$ is the magnetic scalar potential, dual to $\Phi(\mathbf{r})$:

$$\nabla \Psi(\mathbf{r}) = \mathrm{j}\omega \mathbf{F}(\mathbf{r}). \qquad (E.23)$$

The vector and scalar potential related to magnetic current density contributions are defined as:

$$\mathbf{F}(\mathbf{r}) = \varepsilon \int_{\mathbb{R}^3} g(r - r') \mathbf{M}(\mathbf{r}') \, \mathrm{d}\mathbf{r}' \qquad (E.24)$$

$$\Psi(\mathbf{r}) = \frac{1}{\mu} \left[\int_{\mathbb{R}^3} g(r - r') q_{\mathrm{m}}(\mathbf{r}') \, \mathrm{d}\mathbf{r}' \right]. \qquad (E.25)$$

Final expressions of the mixed-potential integral equations

In this subsection, the MPIE expressions are summarized. The contributions related to the electric vector and scalar potentials, and the ones related to the magnetic vector and scalar potentials were derived separately; however, since the Maxwell equations are linear, it is possible to add these two contributions, applying the effect superposition:

$$\mathbf{E}(\mathbf{r}) = \mathbf{E}^{(\mathrm{j})}(\mathbf{r}) + \mathbf{E}^{(\mathrm{m})}(\mathbf{r})$$
$$\mathbf{H}(\mathbf{r}) = \mathbf{H}^{(\mathrm{j})}(\mathbf{r}) + \mathbf{H}^{(\mathrm{m})}(\mathbf{r}),$$

where:

$$\mathbf{E}(\mathbf{r})^{(\mathrm{j})} = -\mathrm{j}\omega\mathbf{A}(\mathbf{r}) - \nabla\Phi(\mathbf{r})$$

$$\mathbf{H}(\mathbf{r})^{(\mathrm{j})} = \frac{1}{\mu}\nabla \times \mathbf{A}(\mathbf{r})$$

$$\mathbf{H}(\mathbf{r})^{(\mathrm{m})} = -\mathrm{j}\omega\mathbf{F}(\mathbf{r}) - \nabla\Psi(\mathbf{r})$$

$$\mathbf{E}(\mathbf{r})^{(\mathrm{m})} = -\frac{1}{\varepsilon}\nabla \times \mathbf{F}(\mathbf{r}).$$

Therefore, substituting these four expressions in the previous two,

$$\mathbf{E}(\mathbf{r}) = -\mathrm{j}\omega\mathbf{A}(\mathbf{r}) - \nabla\Phi(\mathbf{r}) - \frac{1}{\varepsilon}\nabla \times \mathbf{F}(\mathbf{r})$$

$$\mathbf{H}(\mathbf{r}) = \frac{1}{\mu}\nabla \times \mathbf{A}(\mathbf{r}) - \mathrm{j}\omega\mathbf{F}(\mathbf{r}) - \nabla\Psi(\mathbf{r}).$$

To obtain the actual integral equations, it is finally possible to substitute the expressions of the potentials (E.18), (E.19), (E.24) and (E.25):

$$\mathbf{E}(\mathbf{r}) = -\mathrm{j}\omega\mu\int_{\mathbb{R}^3} g(r - r')\mathbf{J}(\mathbf{r}')\,\mathrm{d}\mathbf{r}' - \frac{1}{\varepsilon}\nabla\int_{\mathbb{R}^3} g(r - r')q_{\mathrm{e}}(\mathbf{r}')\,\mathrm{d}\mathbf{r}' +$$

$$-\int_{\mathbb{R}^3}[\nabla g(r - r')] \times \mathbf{M}(\mathbf{r}')\,\mathrm{d}\mathbf{r}'$$

$$\mathbf{H}(\mathbf{r}) = \int_{\mathbb{R}^3}[\nabla g(r - r')] \times \mathbf{J}(\mathbf{r}')\,\mathrm{d}\mathbf{r}' - \mathrm{j}\omega\varepsilon\int_{\mathbb{R}^3} g(r - r')\mathbf{M}(\mathbf{r}')\,\mathrm{d}\mathbf{r}' +$$

$$-\frac{1}{\mu}\nabla\int_{\mathbb{R}^3} g(r - r')q_{\mathrm{m}}(\mathbf{r}')\,\mathrm{d}\mathbf{r}',$$

where the terms $\mathbf{E}^{(\mathrm{m})}(\mathbf{r})$ and $\mathbf{H}^{(\mathrm{m})}(\mathbf{r})$ were found by duality. These equations have four unknowns: the electric/magnetic current densities, and the electric/magnetic charge densities. However, these two groups of unknown are related by the continuity equations; therefore, since:

$$q_{\mathrm{e}}(\mathbf{r}) = -\frac{1}{\mathrm{j}\omega}\nabla \cdot \mathbf{J}(\mathbf{r})$$

$$q_{\mathrm{m}}(\mathbf{r}) = -\frac{1}{\mathrm{j}\omega}\nabla \cdot \mathbf{M}(\mathbf{r}),$$

it is possible to write the final expressions of the MPIE as:

$$\mathbf{E}(\mathbf{r}) = -\,\mathrm{j}\omega\mu \int_{\mathbb{R}^3} g(r - r')\mathbf{J}(\mathbf{r}')\,\mathrm{d}\mathbf{r}' + \frac{1}{\mathrm{j}\omega\varepsilon}\nabla \int_{\mathbb{R}^3} g(r - r')\nabla \cdot \mathbf{J}(\mathbf{r}')\,\mathrm{d}\mathbf{r}' +$$

$$-\int_{\mathbb{R}^3} [\nabla g(r - r')] \times \mathbf{M}(\mathbf{r}')\,\mathrm{d}\mathbf{r}' \qquad (\text{E.26})$$

$$\mathbf{H}(\mathbf{r}) = \int_{\mathbb{R}^3} [\nabla g(r - r')] \times \mathbf{J}(\mathbf{r}')\,\mathrm{d}\mathbf{r}' - \mathrm{j}\omega\varepsilon \int_{\mathbb{R}^3} g(r - r')\mathbf{M}(\mathbf{r}')\,\mathrm{d}\mathbf{r}' +$$

$$\frac{1}{\mathrm{j}\omega\mu}\nabla \int_{\mathbb{R}^3} g(r - r')\nabla \cdot \mathbf{M}(\mathbf{r}')\,\mathrm{d}\mathbf{r}'. \qquad (\text{E.27})$$

The magnetic field equation can be found from the first one by duality and vice-versa.

E.1.3 Summary of the results derived in the previous sections

In this section the most significant results derived in the previous sections will be resumed.

Spectral domain Green's functions

$$\begin{cases} \widetilde{\mathbf{E}}(\mathbf{k}) = \widetilde{\mathbf{G}}^{(\mathrm{e,j})}(\mathbf{k}) \cdot \widetilde{\mathbf{J}}(\mathbf{k}) + \widetilde{\mathbf{G}}^{(\mathrm{e,m})}(\mathbf{k}) \cdot \widetilde{\mathbf{M}}(\mathbf{k}) \\ \widetilde{\mathbf{H}}(\mathbf{k}) = \widetilde{\mathbf{G}}^{(\mathrm{h,j})}(\mathbf{k}) \cdot \widetilde{\mathbf{J}}(\mathbf{k}) + \widetilde{\mathbf{G}}^{(\mathrm{h,m})}(\mathbf{k}) \cdot \widetilde{\mathbf{M}}(\mathbf{k}), \end{cases} \qquad (\text{E.28})$$

where:

$$\mathbf{G}^{(\mathrm{e,j})}(\mathbf{r}) = -\mathrm{j}\omega\mu\mathbf{G}(\mathbf{r})$$
$$\widetilde{\mathbf{G}}^{(\mathrm{h,j})}(\mathbf{k}) = -\mathrm{j}\mathbf{k} \times \widetilde{\mathbf{G}}(\mathbf{k})$$
$$\widetilde{\mathbf{G}}^{(\mathrm{h,m})}(\mathbf{k}) = -\mathrm{j}\omega\varepsilon\widetilde{\mathbf{G}}(\mathbf{k})$$
$$\widetilde{\mathbf{G}}^{(\mathrm{e,m})}(\mathbf{k}) = \mathrm{j}\mathbf{k} \times \widetilde{\mathbf{G}}(\mathbf{k}),$$

where:

$$\widetilde{\mathbf{G}}(\mathbf{k}) = \left[\widetilde{\mathbf{I}} + \frac{(-\mathrm{j}\mathbf{k})(-\mathrm{j}\mathbf{k})}{\omega^2\varepsilon\mu}\right]\widetilde{g}(k),$$

and:

$$\widetilde{g}(\mathbf{k}) \triangleq \frac{1}{k^2 - \omega^2\varepsilon\mu} = \widetilde{g}(k).$$

Electric and magnetic field integral equations

These are the EFIE and MFIE equations found using the Green's function formalism.

$$\begin{cases} \mathbf{E}(\mathbf{r}) = \mathbf{G}^{(\mathrm{e,j})}(\mathbf{r}) \overset{*}{\cdot} \mathbf{J}(\mathbf{r}) + \mathbf{G}^{(\mathrm{e,m})}(\mathbf{r}) \overset{*}{\cdot} \mathbf{M}(\mathbf{r}) \\ \mathbf{H}(\mathbf{r}) = \mathbf{G}^{(\mathrm{h,j})}(\mathbf{r}) \overset{*}{\cdot} \mathbf{J}(\mathbf{r}) + \mathbf{G}^{(\mathrm{h,m})}(\mathbf{r}) \overset{*}{\cdot} \mathbf{M}(\mathbf{r}), \end{cases} \tag{E.29}$$

where:

$$\mathbf{G}^{(\mathrm{e,j})}(\mathbf{r}) - \mathrm{j}\omega\mu\mathbf{G}(\mathbf{r})$$
$$\mathbf{G}^{(\mathrm{h,m})}(\mathbf{r}) = -\mathrm{j}\omega\varepsilon\mathbf{G}(\mathbf{r})$$
$$\mathbf{G}^{(\mathrm{h,j})}(\mathbf{r}) = \nabla \times \mathbf{G}(\mathbf{r})$$
$$\mathbf{G}^{(\mathrm{e,m})}(\mathbf{r}) = -\nabla \times \mathbf{G}(\mathbf{r}),$$

where:

$$\mathbf{G}(\mathbf{r}) \triangleq \mathcal{F}_3^{-1}\left\{\widetilde{\mathbf{G}(\mathbf{k})}\right\} = \left[\mathbf{I} + \frac{\nabla\nabla}{\omega^2\varepsilon\mu}\right] g(r),$$

where:

$$g(\mathbf{r}) \triangleq \mathcal{F}_3^{-1}\left\{\widetilde{g}(k)\right\} = \frac{\mathrm{e}^{-\mathrm{j}k_0 r}}{4\pi r} = g(r),$$

and:

$$k_0 \triangleq \omega\sqrt{\varepsilon_0\mu_0}.$$

These expressions have been elaborated, in order to relate them to the MPIE; the most significant results about these equations can be found in (E.26), (E.27). These equations are the starting point for the formulation of integral equations.

E.1.4 Dyadic Green's function in spherical coordinates

Explicit calculation of the Green's function in spherical coordinates

The expression of the dyadic $\mathbf{G}$ is:

$$\mathbf{G}(\mathbf{r}) = \left[\mathbf{I} + \frac{\nabla\nabla}{k^2}\right] g(r), \tag{E.30}$$

where $g(r)$ is the scalar Green's function for the homogeneous space:

$$g(r) = \frac{\mathrm{e}^{-\mathrm{j}kr}}{4\pi r}, \tag{E.31}$$

and k is the homogeneous space wavenumber:

$$k = \omega\sqrt{\varepsilon\mu}. \tag{E.32}$$

In order to proceed with the explicit calculation of the dyadic Green's function in the spherical coordinate system it is possible to define the vector $\mathbf{A}$ as the gradient of g:

$$\mathbf{A} = \nabla g,$$

then it is possible to define the dyadic $\mathbf{B}$ as the gradient of the vector $\mathbf{A}$:

$$\mathbf{B} = \nabla\mathbf{A}.$$

The components (ξ_1, ξ_2, ξ_3) used to describe the position of a point in the space have to be referred to the spherical coordinates system; therefore:

$$(\xi_1, \xi_2, \xi_3) \triangleq (r, \vartheta, \varphi)$$

so:

$$\mathbf{A} = \hat{u}_1 \frac{\partial g}{\partial \xi_1} = \widehat{\mathbf{r}} \frac{\mathrm{d}g}{\mathrm{d}r}.$$

Then:

$$\mathbf{B} = \nabla\mathbf{A} = \sum_{i=1}^{3} \hat{u}_i \frac{1}{h_i} \frac{\partial}{\partial \xi_i} \left(\widehat{\mathbf{r}} \frac{\partial g}{\partial r} \right).$$

The Leibnitz rule is applied, leading to:

$$\frac{\partial}{\partial \xi_i} \left(\widehat{\mathbf{r}} \frac{\mathrm{d}g}{\mathrm{d}r} \right) = \widehat{\mathbf{r}} \frac{\partial}{\partial \xi_i} \left(\frac{\mathrm{d}g}{\mathrm{d}r} \right) + \frac{\mathrm{d}g}{\mathrm{d}r} \frac{\partial \widehat{\mathbf{r}}}{\partial \xi_i},$$

so, recalling that, for the spherical coordinates system, $h_1 = 1$, $h_2 = r$, $h_3 = r\sin\vartheta$:

$$\begin{aligned}
\mathbf{B} = \nabla\mathbf{A} = {}& \widehat{\mathbf{r}} \left[\frac{\mathrm{d}g}{\mathrm{d}r} \frac{\partial \widehat{\mathbf{r}}}{\partial r} + \frac{\partial}{\partial r} \left(\frac{\mathrm{d}g}{\mathrm{d}r} \right) \widehat{\mathbf{r}} \right] + \\
& + \frac{\widehat{\boldsymbol{\vartheta}}}{r} \left[\frac{\mathrm{d}g}{\mathrm{d}r} \frac{\partial \widehat{\mathbf{r}}}{\partial \vartheta} + \widehat{\mathbf{r}} \frac{\partial}{\partial \vartheta} \left(\frac{\mathrm{d}g}{\mathrm{d}r} \right) \right] + \\
& + \frac{\widehat{\boldsymbol{\varphi}}}{r\sin\vartheta} \left[\frac{\mathrm{d}g}{\mathrm{d}r} \frac{\partial \widehat{\mathbf{r}}}{\partial \varphi} + \widehat{\mathbf{r}} \frac{\partial}{\partial \varphi} \left(\frac{\mathrm{d}g}{\mathrm{d}r} \right) \right].
\end{aligned}$$

Now, recalling that:

$$\widehat{\mathbf{r}} = \widehat{\mathbf{x}}\sin\vartheta\cos\varphi + \widehat{\mathbf{y}}\sin\vartheta\sin\varphi + \widehat{\mathbf{z}}\cos\vartheta,$$

it is apparent that:

$$\frac{\partial \widehat{\mathbf{r}}}{\partial r} = 0.$$

Indeed, $\widehat{\mathbf{r}}$ does not depend on r. Moreover,

$$\frac{\partial \widehat{\mathbf{r}}}{\partial \vartheta} = \widehat{\mathbf{x}} \cos \vartheta \cos \varphi + \widehat{\mathbf{y}} \cos \vartheta \sin \varphi - \widehat{\mathbf{z}} \sin \vartheta,$$

and:

$$\frac{\partial \widehat{\mathbf{r}}}{\partial \varphi} = -\widehat{\mathbf{x}} \sin \vartheta \sin \varphi + \widehat{\mathbf{y}} \sin \vartheta \cos \varphi.$$

But, since

$$\widehat{\boldsymbol{\vartheta}} = \widehat{\mathbf{x}} \cos \vartheta \cos \varphi + \widehat{\mathbf{y}} \cos \vartheta \sin \varphi - \widehat{\mathbf{z}} \sin \vartheta,$$

and

$$\widehat{\boldsymbol{\varphi}} = -\widehat{\mathbf{x}} \sin \varphi + \widehat{\mathbf{y}} \cos \varphi,$$

we have:

$$\frac{\partial \widehat{\mathbf{r}}}{\partial r} = 0$$
$$\frac{\partial \widehat{\mathbf{r}}}{\partial \vartheta} = \widehat{\boldsymbol{\vartheta}}$$
$$\frac{\partial \widehat{\mathbf{r}}}{\partial \varphi} = \widehat{\boldsymbol{\varphi}} \sin \vartheta.$$

Before substituting this in the expression of the operator $\mathbf{B}$, it is still necessary to calculate the expression of the derivative of the scalar Green's function with respect to r:

$$\frac{\mathrm{d} g}{\mathrm{d} r} = \frac{\mathrm{d}}{\mathrm{d} r} \left[\frac{1}{4\pi r} \mathrm{e}^{-\mathrm{j} k r} \right] = -\left[\mathrm{j} k + \frac{1}{r} \right] g(r).$$

Since this term depends neither on φ nor on ϑ, the next expression is obtained:

$$\frac{\partial}{\partial \vartheta} \frac{\mathrm{d} g}{\mathrm{d} r} = \frac{\partial}{\partial \varphi} \frac{\mathrm{d} g}{\mathrm{d} r} = 0,$$

and, for what concern r:

$$\frac{\mathrm{d}}{\mathrm{d}r}\frac{\mathrm{d}g}{\mathrm{d}r} = -\frac{\mathrm{d}}{\mathrm{d}r}\left\{\left[\mathrm{j}k + \frac{1}{r}\right]g(r)\right\} =$$

$$= -\left[0 - \frac{1}{r^2}\right]g(r) + \left[\mathrm{j}k + \frac{1}{r}\right]g(r)\left[\mathrm{j}k + \frac{1}{r}\right] =$$

$$= \left[\frac{1}{r^2} - k^2 + \frac{1}{r^2} + 2\mathrm{j}\frac{k}{r}\right]g(r) =$$

$$= \left[-k^2 + \frac{2\mathrm{j}k}{r} + \frac{2}{r^2}\right]g(r).$$

Now, these expressions are substituted in $\mathbf{B}$:

$$\mathbf{B} = \widehat{\mathbf{r}}\left[0 + g(r)\left(-k^2 + \frac{2\mathrm{j}k}{r} + \frac{2}{r^2}\right)\widehat{\mathbf{r}}\right] +$$

$$+ \frac{\widehat{\boldsymbol{\vartheta}}}{r}\left[-\left(\mathrm{j}k + \frac{1}{r}\right)g(r)\widehat{\boldsymbol{\vartheta}} + 0\right] +$$

$$+ \frac{\widehat{\boldsymbol{\varphi}}}{r\sin\vartheta}\left[-\left(\mathrm{j}k + \frac{1}{r}\right)\widehat{\boldsymbol{\varphi}}\sin\vartheta g(r) + 0\right].$$

So, by sorting all these terms and substituting them in $\mathbf{G}$, it is possible to find, recalling that $\mathbf{I} = \widehat{\mathbf{r}}\widehat{\mathbf{r}} + \widehat{\boldsymbol{\vartheta}}\widehat{\boldsymbol{\vartheta}} + \widehat{\boldsymbol{\varphi}}\widehat{\boldsymbol{\varphi}}$:

$$\mathbf{G}(\mathbf{r}) = \left[\mathbf{I} + \frac{\nabla\nabla}{k^2}\right]g(r) =$$

$$= \left[(\widehat{\mathbf{r}}\widehat{\mathbf{r}} + \widehat{\boldsymbol{\vartheta}}\widehat{\boldsymbol{\vartheta}} + \widehat{\boldsymbol{\varphi}}\widehat{\boldsymbol{\varphi}}) + \widehat{\mathbf{r}}\widehat{\mathbf{r}}\left(-k^2 + \frac{2\mathrm{j}k}{r} + \frac{2}{r^2}\right)\frac{1}{k^2} + \right.$$

$$\left. + \widehat{\boldsymbol{\vartheta}}\widehat{\boldsymbol{\vartheta}}\left(-\frac{1}{k^2 r}\left(\mathrm{j}k + \frac{1}{r}\right)\right) + \widehat{\boldsymbol{\varphi}}\widehat{\boldsymbol{\varphi}}\left(-\frac{1}{k^2 r}\left(\mathrm{j}k + \frac{1}{r}\right)\right)\right]g(r) =$$

$$= \left[\left(\frac{2\mathrm{j}}{kr} + \frac{2}{k^2 r^2}\right)\widehat{\mathbf{r}}\widehat{\mathbf{r}} + \left(1 - \frac{\mathrm{j}}{kr} - \frac{1}{k^2 r^2}\right)\widehat{\boldsymbol{\vartheta}}\widehat{\boldsymbol{\vartheta}} + \left(1 - \frac{\mathrm{j}}{kr} - \frac{1}{k^2 r^2}\right)\widehat{\boldsymbol{\varphi}}\widehat{\boldsymbol{\varphi}}\right]g(r).$$

This is a dyadic, and so it can be written compactly in matrix form, considering $\widehat{\mathbf{r}}$ equivalent to an index equal to 1, $\widehat{\boldsymbol{\vartheta}}$ equivalent to an index equal to 2, $\widehat{\boldsymbol{\varphi}}$ equivalent to an index equal to 3; let us define:

$$A(kr) \triangleq \frac{2\mathrm{j}}{kr} + \frac{2}{k^2 r^2} \tag{E.33}$$

$$B(kr) \triangleq 1 - \frac{A(kr)}{2}, \tag{E.34}$$

so, this becomes:

$$\mathbf{G}(\mathbf{r}) = \begin{bmatrix} A(kr) & 0 & 0 \\ 0 & B(kr) & 0 \\ 0 & 0 & B(kr) \end{bmatrix} g(r). \qquad (\text{E.35})$$

A similar procedure is applied to the term $\nabla \times \mathbf{G}(\mathbf{r})$. The first step is to recall:

$$\nabla \times \mathbf{G}(\mathbf{r}) = \nabla g(r) \times \mathbf{I}.$$

Moreover, we have already shown that:

$$\nabla g = -\left[\mathrm{j}k - \frac{1}{k}\right]\widehat{\mathbf{r}} = \mathrm{j}k\widehat{\mathbf{r}}\left[\frac{\mathrm{j}}{kr} - 1\right] g(r).$$

So, by defining the term $C(kr)$ as:

$$C(kr) \triangleq 1 - \frac{\mathrm{j}}{kr}, \qquad (\text{E.36})$$

since

$$\mathbf{I} = \widehat{\mathbf{r}}\widehat{\mathbf{r}} + \widehat{\boldsymbol{\vartheta}}\widehat{\boldsymbol{\vartheta}} + \widehat{\boldsymbol{\varphi}}\widehat{\boldsymbol{\varphi}},$$

it is possible to calculate $\widehat{\mathbf{r}} \times \mathbf{I}$ as:

$$\widehat{\mathbf{r}} \times \mathbf{I} = \widehat{\mathbf{r}} \times \left[\widehat{\mathbf{r}}\widehat{\mathbf{r}} + \widehat{\boldsymbol{\vartheta}}\widehat{\boldsymbol{\vartheta}} + \widehat{\boldsymbol{\varphi}}\widehat{\boldsymbol{\varphi}}\right] = \widehat{\mathbf{r}}\widehat{\mathbf{r}} + \widehat{\mathbf{r}} \times \widehat{\boldsymbol{\vartheta}}\widehat{\boldsymbol{\vartheta}} + \widehat{\mathbf{r}} \times \widehat{\boldsymbol{\varphi}}\widehat{\boldsymbol{\varphi}} = 0 + \widehat{\boldsymbol{\varphi}}\widehat{\boldsymbol{\vartheta}} - \widehat{\boldsymbol{\vartheta}}\widehat{\boldsymbol{\varphi}},$$

because $\widehat{\mathbf{r}} \times \widehat{\mathbf{r}} = 0$, $\widehat{\mathbf{r}} \times \widehat{\boldsymbol{\vartheta}} = \widehat{\boldsymbol{\varphi}}$, $\widehat{\mathbf{r}} \times \widehat{\boldsymbol{\varphi}} = -\widehat{\boldsymbol{\vartheta}}$; so, it is possible to define the dyadic $\mathbf{G}'$ as:

$$\mathbf{G}'(\mathbf{r}) = \nabla g \times \mathbf{I} = -\mathrm{j}k \begin{bmatrix} 0 & 0 & 0 \\ 0 & 0 & -C(kr) \\ 0 & C(kr) & 0 \end{bmatrix} g(r). \qquad (\text{E.37})$$

Resume of all previous results

In the previous section several results have been proven.

$$\mathbf{G}^{(\mathrm{e,j})}(\mathbf{r}) = -\mathrm{j}\omega\mu\mathbf{G}(\mathbf{r})$$
$$\mathbf{G}^{(\mathrm{e,m})}(\mathbf{r}) = -\nabla \times \mathbf{G}(\mathbf{r})$$
$$\mathbf{G}^{(\mathrm{h,j})}(\mathbf{r}) = \nabla \times \mathbf{G}(\mathbf{r})$$
$$\mathbf{G}^{(\mathrm{h,m})}(\mathbf{r}) = -\mathrm{j}\omega\varepsilon\mathbf{G}(\mathbf{r}),$$

where:

$$\mathbf{G}(\mathbf{r}) = \begin{bmatrix} A(kr) & 0 & 0 \\ 0 & B(kr) & 0 \\ 0 & 0 & B(kr) \end{bmatrix} g(r),$$

and:

$$\mathbf{G}'(\mathbf{r}) = \nabla \times \mathbf{G}(\mathbf{r}) = \nabla g \times \mathbf{I} = -\mathrm{j}k \begin{bmatrix} 0 & 0 & 0 \\ 0 & 0 & -C(kr) \\ 0 & C(kr) & 0 \end{bmatrix} g(r),$$

where:

$$A(kr) = \frac{2\mathrm{j}}{kr} + \frac{2}{k^2 r^2}$$

$$B(kr) = 1 - \frac{A(kr)}{2}$$

$$C(kr) = 1 - \frac{\mathrm{j}}{kr}.$$

Transformation of coordinates

Given a generic vector $\mathbf{A}(\mathbf{r})$, this can be written in cartesian coordinates, as well in spherical coordinates:

$$\mathbf{A}(\mathbf{r}) = A_x \widehat{\mathbf{x}} + A_y \widehat{\mathbf{y}} + A_z \widehat{\mathbf{z}} = A_r \widehat{\mathbf{r}} + A_\vartheta \widehat{\boldsymbol{\vartheta}} + A_\varphi \widehat{\boldsymbol{\varphi}}. \tag{E.38}$$

These expressions are now written as row-column products:

$$\mathbf{A}(\mathbf{r}) = \begin{bmatrix} \widehat{\mathbf{x}} & \widehat{\mathbf{y}} & \widehat{\mathbf{z}} \end{bmatrix} \begin{bmatrix} A_x \\ A_y \\ A_z \end{bmatrix} = \begin{bmatrix} \widehat{\mathbf{r}} & \widehat{\boldsymbol{\vartheta}} & \widehat{\boldsymbol{\varphi}} \end{bmatrix} \begin{bmatrix} A_r \\ A_\vartheta \\ A_\varphi \end{bmatrix}.$$

The objective of this section is to transform the vector components from one coordinate system into another, and then to extend this procedure to dyadics.

By inspection, the following expressions are written:

$$\widehat{\mathbf{x}} = \widehat{\mathbf{r}} \sin \vartheta \cos \varphi + \widehat{\boldsymbol{\vartheta}} \cos \vartheta \cos \varphi - \widehat{\boldsymbol{\varphi}} \sin \varphi$$

$$\widehat{\mathbf{y}} = \widehat{\mathbf{r}} \sin \vartheta \sin \varphi + \widehat{\boldsymbol{\vartheta}} \cos \vartheta \sin \varphi + \widehat{\boldsymbol{\varphi}} \cos \varphi$$

$$\widehat{\mathbf{z}} = \widehat{\mathbf{r}} \cos \vartheta - \widehat{\boldsymbol{\vartheta}} \sin \vartheta.$$

Similarly:

$$\widehat{\mathbf{r}} = \widehat{\mathbf{x}} \sin \vartheta \cos \varphi + \widehat{\mathbf{y}} \cos \vartheta \cos \varphi - \widehat{\mathbf{z}} \sin \varphi$$

$$\widehat{\boldsymbol{\vartheta}} = \widehat{\mathbf{x}} \sin \vartheta \sin \varphi + \widehat{\mathbf{y}} \cos \vartheta \sin \varphi + \widehat{\mathbf{z}} \cos \varphi$$

$$\widehat{\boldsymbol{\varphi}} = \widehat{\mathbf{x}} \cos \vartheta - \widehat{\mathbf{y}} \sin \vartheta.$$

The last three equations can be written in matrix form:

$$\begin{bmatrix} \widehat{\mathbf{r}} & \widehat{\boldsymbol{\vartheta}} & \widehat{\boldsymbol{\varphi}} \end{bmatrix} = \begin{bmatrix} \widehat{\mathbf{x}} & \widehat{\mathbf{y}} & \widehat{\mathbf{z}} \end{bmatrix} \begin{bmatrix} \sin \vartheta \cos \varphi & \cos \vartheta \cos \varphi & -\sin \varphi \\ \sin \vartheta \sin \varphi & \cos \vartheta \sin \varphi & \cos \varphi \\ \cos \vartheta & -\sin \vartheta & 0 \end{bmatrix}. \tag{E.39}$$

Now, it is possible to define the change-of-coordinates matrix $\mathbf{P}$ as:

$$\mathbf{P} \triangleq \begin{bmatrix} \sin \vartheta \cos \varphi & \cos \vartheta \cos \varphi & -\sin \varphi \\ \sin \vartheta \sin \varphi & \cos \vartheta \sin \varphi & \cos \varphi \\ \cos \vartheta & -\sin \vartheta & 0 \end{bmatrix}, \tag{E.40}$$

and so:

$$\begin{bmatrix} \widehat{\mathbf{r}} & \widehat{\boldsymbol{\vartheta}} & \widehat{\boldsymbol{\varphi}} \end{bmatrix} = \begin{bmatrix} \widehat{\mathbf{x}} & \widehat{\mathbf{y}} & \widehat{\mathbf{z}} \end{bmatrix} \mathbf{P}.$$

Then, by recalling a previous equation:

$$\begin{bmatrix} \widehat{\mathbf{x}} & \widehat{\mathbf{y}} & \widehat{\mathbf{z}} \end{bmatrix} \begin{bmatrix} A_x \\ A_y \\ A_z \end{bmatrix} = \begin{bmatrix} \widehat{\mathbf{r}} & \widehat{\boldsymbol{\vartheta}} & \widehat{\boldsymbol{\varphi}} \end{bmatrix} \begin{bmatrix} A_r \\ A_\vartheta \\ A_\varphi \end{bmatrix} = \begin{bmatrix} \widehat{\mathbf{x}} & \widehat{\mathbf{y}} & \widehat{\mathbf{z}} \end{bmatrix} \mathbf{P} \begin{bmatrix} A_r \\ A_\vartheta \\ A_\varphi \end{bmatrix},$$

since in both terms there is the row vector with $\widehat{\mathbf{x}}, \widehat{\mathbf{y}}$ and $\widehat{\mathbf{z}}$,

$$\begin{bmatrix} A_x \\ A_y \\ A_z \end{bmatrix} = \mathbf{P} \begin{bmatrix} A_r \\ A_\vartheta \\ A_\varphi \end{bmatrix}. \tag{E.41}$$

Since

$$\mathbf{P}^{-1} = \mathbf{P}^{\mathrm{T}},$$

where T denotes the transposition of the matrix, it is possible to write also the inverse transformation:

$$\begin{bmatrix} A_r \\ A_\vartheta \\ A_\varphi \end{bmatrix} = \mathbf{P}^{\mathrm{T}} \begin{bmatrix} A_x \\ A_y \\ A_z \end{bmatrix}. \tag{E.42}$$

Now, it has been shown how to transform the components of vectors from one coordinate system to another, focusing on the spherical-to-cartesian case.

Transformation of dyadics

The rule derived in the previous subsection will be applied to dyadics. A dyadic is defined as:

$$\mathbf{D} = \mathbf{A}\,\mathbf{B}.$$

So, in spherical coordinates:

$$\mathbf{D}^{(\text{spherical})} = \begin{bmatrix} A_r B_r & A_r B_\vartheta & A_r B_\varphi \\ A_\vartheta B_r & A_\vartheta B_\vartheta & A_\vartheta B_\varphi \\ A_\varphi B_r & A_\varphi B_\vartheta & A_\varphi B_\varphi \end{bmatrix},$$

or, in cartesian coordinates:

$$\mathbf{D}^{(\text{cartesian})} = \begin{bmatrix} A_x B_x & A_x B_y & A_x B_z \\ A_y B_x & A_y B_y & A_y B_z \\ A_z B_x & A_z B_y & A_z B_z \end{bmatrix}.$$

This last dyadic can be written as:

$$\begin{bmatrix} A_x B_x & A_x B_y & A_x B_z \\ A_y B_x & A_y B_y & A_y B_z \\ A_z B_x & A_z B_y & A_z B_z \end{bmatrix} = \begin{bmatrix} A_x \\ A_y \\ A_z \end{bmatrix} \left(\begin{bmatrix} B_x \\ B_y \\ B_z \end{bmatrix} \right)^{\mathrm{T}},$$

so, by applying the transformation above,

$$\begin{bmatrix} A_x \\ A_y \\ A_z \end{bmatrix} \left(\begin{bmatrix} B_x \\ B_y \\ B_z \end{bmatrix} \right)^{\mathrm{T}} = \left(\mathbf{P} \begin{bmatrix} A_r \\ A_\vartheta \\ A_\varphi \end{bmatrix} \right) \left(\mathbf{P} \begin{bmatrix} B_r \\ B_\vartheta \\ B_\varphi \end{bmatrix} \right)^{\mathrm{T}} = \mathbf{P} \left(\begin{bmatrix} A_r \\ A_\vartheta \\ A_\varphi \end{bmatrix} \begin{bmatrix} B_r & B_\vartheta & B_\varphi \end{bmatrix} \right) \mathbf{P}^{\mathrm{T}} =$$

$$= \mathbf{P} \begin{bmatrix} A_r B_r & A_r B_\vartheta & A_r B_\varphi \\ A_\vartheta B_r & A_\vartheta B_\vartheta & A_\vartheta B_\varphi \\ A_\varphi B_r & A_\varphi B_\vartheta & A_\varphi B_\varphi \end{bmatrix} \mathbf{P}^{\mathrm{T}}.$$

So:

$$\mathbf{D}^{(\text{cartesian})} = \mathbf{P}\,\mathbf{D}^{(\text{spherical})}\mathbf{P}^{\mathrm{T}}.$$

It is useful to calculate explicitly the components of $\mathbf{D}^{(\text{cartesian})}$ with the $\mathbf{P}$ defined in the section above. By using a symbolic calculator, it is possible to obtain, starting from the $\mathbf{D} = \mathbf{G}$ case:

$$\mathbf{D} = \begin{bmatrix} D_{rr} & 0 & 0 \\ 0 & D_{\vartheta\vartheta} & 0 \\ 0 & 0 & D_{\varphi\varphi} \end{bmatrix}.$$

$$D_{xx} = D_{rr}\cos^2\varphi\sin^2\vartheta + D_{\vartheta\vartheta}\cos^2\varphi\cos^2\vartheta + D_{\varphi\varphi}\sin^2\varphi$$

$$D_{xy} = -\cos\varphi\sin\varphi\left(D_{\varphi\varphi} - D_{\vartheta\vartheta}\cos^2\vartheta - D_{rr}\sin^2\vartheta\right) = D_{yx}$$

$$D_{xz} = \cos\varphi\cos\vartheta\sin\vartheta\left(D_{rr} - D_{\vartheta\vartheta}\right)$$

$$D_{yy} = D_{\varphi\varphi}\cos^2\varphi + G_{\vartheta\vartheta}\cos^2\vartheta\sin^2\varphi + D_{rr}\sin^2\varphi\sin^2\vartheta$$

$$D_{yz} = \cos\vartheta\sin\varphi\sin\vartheta\left(D_{rr} - D_{\vartheta\vartheta}\right) = D_{zy}$$

$$D_{zz} = D_{rr}\cos^2\vartheta + D_{\vartheta\vartheta}\sin^2\vartheta$$

Moreover, the other useful case, for $\mathbf{D}' = \nabla \times \mathbf{G}'$:

$$\mathbf{D}' = \begin{bmatrix} 0 & 0 & 0 \\ 0 & 0 & D'_{\vartheta\varphi} \\ 0 & D'_{\varphi\vartheta} & 0 \end{bmatrix},$$

where:

$$D'_{xx} = -\frac{1}{2}\sin(2\varphi)\cos\vartheta\left(D'_{\varphi\vartheta} + D'_{\vartheta\varphi}\right)$$

$$D'_{xy} = -\cos\vartheta\left(G'_{\varphi\vartheta}\sin^2\varphi - D'_{\vartheta\varphi}\cos^2\varphi\right)$$

$$D'_{xz} = D'_{\varphi\vartheta}\sin\varphi\sin\vartheta$$

$$D'_{yx} = -\cos\vartheta\left(-D'_{\varphi\vartheta}\cos^2\varphi + D'_{\vartheta\varphi}\sin^2\varphi\right)$$

$$D'_{yy} = \frac{1}{2}\sin(2\varphi)\cos\vartheta\left(D'_{\varphi\vartheta} + G'_{\vartheta\varphi}\right)$$

$$D'_{yz} = -D'_{\varphi\vartheta}\cos\varphi\sin\vartheta$$

$$D'_{zx} = D'_{\vartheta\varphi}\sin\varphi\sin\vartheta$$

$$D'_{zy} = -D'_{\vartheta\varphi}\cos\varphi\sin\vartheta$$

$$D'_{zz} = 0.$$

These calculations have been performed using the following MATLAB script:

```
clear
close all
clc


%-- This script calculates explicitly G and Gprime in the cartesian
```

```
%    coordinate system; this can be used to calculate efficiently
%    (vector implementation) the components of the dyadic Green's function.
%
%    This script is "specialized" in order to consider the (complete) free
%    space dyadic Green's function; so, Grt=0; Grp=0; Gtr=0; Gtp=0; Gpr=0;
%    Gpt=0; however, by removing the constraint, this script can be
%    generalized, leading to much more complex expressions.
%
%    Grr=G_{r,r}; Grt=G_{r,theta}; Grp=G_{r,phi} (and so on)

syms Grr Grt Grp Gtr Gtt Gtp Gpr Gpt Gpp
syms Gprr Gprt Gprp Gptr Gptt Gptp Gppr Gppt Gppp %-- Gprime components
syms theta phi

P=[
    sin(theta).*cos(phi),cos(theta).*cos(phi),-sin(phi) ;
    sin(theta).*sin(phi),cos(theta).*sin(phi),cos(phi)  ;
    cos(theta),-sin(theta),0
  ]


%-- G calculations

Grt=0; Grp=0; Gtr=0; Gtp=0; Gpr=0; Gpt=0;

Gspherical=[Grr Grt Grp;
            Gtr Gtt Gtp;
            Gpr Gpt Gpp
           ]

Gcartesian=P*Gspherical*P.';

Gxx=simple(Gcartesian(1,1))
Gxy=simple(Gcartesian(1,2))
Gxz=simple(Gcartesian(1,3))
Gyx=simple(Gcartesian(2,1))
Gyy=simple(Gcartesian(2,2))
Gyz=simple(Gcartesian(2,3))
Gzx=simple(Gcartesian(3,1))
```

```
Gzy=simple(Gcartesian(3,2))
Gzz=simple(Gcartesian(3,3))


%-- Gp calculations
Gprr=0; Gprt=0; Gprp=0; Gptr=0; Gptt=0; Gppr=0; Gppp=0;


Gpspherical=[Gprr Gprt Gprp;
             Gptr Gptt Gptp;
             Gppr Gppt Gppp
            ]


Gpcartesian=P*Gpspherical*P.';


Gpxx=simple(Gpcartesian(1,1))
Gpxy=simple(Gpcartesian(1,2))
Gpxz=simple(Gpcartesian(1,3))
Gpyx=simple(Gpcartesian(2,1))
Gpyy=simple(Gpcartesian(2,2))
Gpyz=simple(Gpcartesian(2,3))
Gpzx=simple(Gpcartesian(3,1))
Gpzy=simple(Gpcartesian(3,2))
Gpzz=simple(Gpcartesian(3,3))
```

E.1.5   Dyadic Green's function in cartesian coordinates

In this section the Green's function of the homogeneous space will be calculated directly in cartesian coordinates, by evaluating explicitly the derivatives that arise from the operators involved. Once again it is useful to recall (E.30):

$$\mathbf{G}(\mathbf{r}) = \left[\mathbf{I} + \frac{\nabla\nabla}{k^2} \right] g(r),$$

where r is the euclidean norm of the vector $\mathbf{r}$; in cartesian coordinates, it can be written as:

$$r = ||\mathbf{r}|| = \sqrt{x^2 + y^2 + z^2}.$$

So:

$$g(r) = g(x, y, z) = \frac{\mathrm{e}^{-\mathrm{j}kr\sqrt{x^2+y^2+z^2}}}{4\pi\sqrt{x^2 + y^2 + z^2}}. \tag{E.43}$$

Let ϕ be a scalar field; then, $\nabla\nabla\phi$ can be written as:

$$\nabla\phi = \widehat{\mathbf{x}}\frac{\partial\phi}{\partial x} + \widehat{\mathbf{y}}\frac{\partial\phi}{\partial y} + \widehat{\mathbf{z}}\frac{\partial\phi}{\partial z},$$

and so:

$$\nabla\nabla\phi = \widehat{\mathbf{x}}\frac{\partial}{\partial x}\left(\widehat{\mathbf{x}}\frac{\partial\phi}{\partial x} + \widehat{\mathbf{y}}\frac{\partial\phi}{\partial y} + \widehat{\mathbf{z}}\frac{\partial\phi}{\partial z}\right) +$$
$$+ \widehat{\mathbf{y}}\frac{\partial}{\partial y}\left(\widehat{\mathbf{x}}\frac{\partial\phi}{\partial x} + \widehat{\mathbf{y}}\frac{\partial\phi}{\partial y} + \widehat{\mathbf{z}}\frac{\partial\phi}{\partial z}\right) +$$
$$+ \widehat{\mathbf{z}}\frac{\partial}{\partial z}\left(\widehat{\mathbf{x}}\frac{\partial\phi}{\partial x} + \widehat{\mathbf{y}}\frac{\partial\phi}{\partial y} + \widehat{\mathbf{z}}\frac{\partial\phi}{\partial z}\right).$$

Now, it is possible to define a dyadic by expanding these products:

$$= \widehat{\mathbf{x}}\widehat{\mathbf{x}}\frac{\partial^2\phi}{\partial x^2} + \widehat{\mathbf{x}}\widehat{\mathbf{y}}\frac{\partial^2\phi}{\partial x\partial y} + \widehat{\mathbf{x}}\widehat{\mathbf{z}}\frac{\partial^2\phi}{\partial x\partial z} +$$
$$+ \widehat{\mathbf{y}}\widehat{\mathbf{x}}\frac{\partial^2\phi}{\partial y\partial x} + \widehat{\mathbf{y}}\widehat{\mathbf{y}}\frac{\partial^2\phi}{\partial y^2} + \widehat{\mathbf{y}}\widehat{\mathbf{z}}\frac{\partial^2\phi}{\partial y\partial z} +$$
$$+ \widehat{\mathbf{z}}\widehat{\mathbf{x}}\frac{\partial^2\phi}{\partial z\partial x} + \widehat{\mathbf{z}}\widehat{\mathbf{y}}\frac{\partial^2\phi}{\partial z\partial y} + \widehat{\mathbf{z}}\widehat{\mathbf{z}}\frac{\partial^2\phi}{\partial z^2},$$

which can be written in matrix form, as follows:

$$= \begin{bmatrix} \dfrac{\partial^2}{\partial x^2} & \dfrac{\partial^2}{\partial x\partial y} & \dfrac{\partial^2}{\partial x\partial z} \\[2mm] \dfrac{\partial^2}{\partial y\partial x} & \dfrac{\partial^2}{\partial y^2} & \dfrac{\partial^2}{\partial y\partial z} \\[2mm] \dfrac{\partial^2}{\partial z\partial x} & \dfrac{\partial^2}{\partial z\partial y} & \dfrac{\partial^2}{\partial z^2} \end{bmatrix}\phi.$$

This dyadic is used to represent the $\mathbf{G}(\mathbf{r})$ dyadic; indeed, by substituting in the previous expression, the following equation is found:

$$\mathbf{G}(x,y,z) = \begin{bmatrix} 1 + \dfrac{1}{k^2}\dfrac{\partial^2}{\partial x^2} & \dfrac{1}{k^2}\dfrac{\partial^2}{\partial x\partial y} & \dfrac{1}{k^2}\dfrac{\partial^2}{\partial x\partial z} \\[2mm] \dfrac{1}{k^2}\dfrac{\partial^2}{\partial y\partial x} & 1 + \dfrac{1}{k^2}\dfrac{\partial^2}{\partial y^2} & \dfrac{1}{k^2}\dfrac{\partial^2}{\partial y\partial z} \\[2mm] \dfrac{1}{k^2}\dfrac{\partial^2}{\partial z\partial x} & \dfrac{1}{k^2}\dfrac{\partial^2}{\partial z\partial y} & 1 + \dfrac{1}{k^2}\dfrac{\partial^2}{\partial z^2} \end{bmatrix} g(x,y,z) =$$

$$= \frac{1}{k^2}\begin{bmatrix} k^2 + \dfrac{\partial^2}{\partial x^2} & \dfrac{\partial^2}{\partial x\partial y} & \dfrac{\partial^2}{\partial x\partial z} \\[2mm] \dfrac{\partial^2}{\partial y\partial x} & k^2 + \dfrac{\partial^2}{\partial y^2} & \dfrac{\partial^2}{\partial y\partial z} \\[2mm] \dfrac{\partial^2}{\partial z\partial x} & \dfrac{\partial^2}{\partial z\partial y} & k^2 + \dfrac{\partial^2}{\partial z^2} \end{bmatrix} g(x,y,z). \qquad (E.44)$$

Now, it is necessary to calculate the Green's function contributions relative to $\nabla \times \mathbf{G}(\mathbf{r})$. Let us consider the $\nabla \times \mathbf{G}(\mathbf{r}) = \nabla g(r) \times \mathbf{I}$ operator applied to a generic vector $\mathbf{A}(\mathbf{r})$:

$$\mathbf{H}(\mathbf{r}) = \nabla g(r) \overset{*}{\times} \mathbf{A}(\mathbf{r}).$$

The objective is to obtain a dyadic that has to be multiplicated scalarly by $\mathbf{A}$. So:

$$\nabla g(r) \overset{*}{\times} \mathbf{A}(\mathbf{r}) = \left[\widehat{\mathbf{x}} \frac{\partial g}{\partial x} + \widehat{\mathbf{y}} \frac{\partial g}{\partial y} + \widehat{\mathbf{z}} \frac{\partial g}{\partial z} \right] \times [A_x \widehat{\mathbf{x}} + A_y \widehat{\mathbf{y}} + A_z \widehat{\mathbf{z}}] =$$

$$= \widehat{\mathbf{x}} \times \widehat{\mathbf{x}} \left(\frac{\partial g}{\partial x} A_x \right) + \widehat{\mathbf{x}} \times \widehat{\mathbf{y}} \left(\frac{\partial g}{\partial x} A_y \right) + \widehat{\mathbf{x}} \times \widehat{\mathbf{z}} \left(\frac{\partial g}{\partial x} A_z \right) +$$

$$+ \widehat{\mathbf{y}} \times \widehat{\mathbf{x}} \left(\frac{\partial g}{\partial y} A_x \right) + \widehat{\mathbf{y}} \times \widehat{\mathbf{y}} \left(\frac{\partial g}{\partial y} A_y \right) + \widehat{\mathbf{y}} \times \widehat{\mathbf{z}} \left(\frac{\partial g}{\partial y} A_z \right) +$$

$$+ \widehat{\mathbf{z}} \times \widehat{\mathbf{x}} \left(\frac{\partial g}{\partial z} A_x \right) + \widehat{\mathbf{z}} \times \widehat{\mathbf{y}} \left(\frac{\partial g}{\partial z} A_y \right) + \widehat{\mathbf{z}} \times \widehat{\mathbf{z}} \left(\frac{\partial g}{\partial z} A_z \right) =$$

$$= \widehat{\mathbf{z}} \frac{\partial g}{\partial x} A_y - \widehat{\mathbf{y}} \frac{\partial g}{\partial x} A_z - \widehat{\mathbf{z}} \frac{\partial g}{\partial y} A_x + \widehat{\mathbf{x}} \frac{\partial g}{\partial y} A_z + \widehat{\mathbf{y}} \frac{\partial g}{\partial z} A_x - \widehat{\mathbf{x}} \frac{\partial g}{\partial z} A_y =$$

$$= \left[\frac{\partial g}{\partial x} \widehat{\mathbf{z}\mathbf{y}} - \frac{\partial g}{\partial x} \widehat{\mathbf{y}\mathbf{z}} - \frac{\partial g}{\partial y} \widehat{\mathbf{z}\mathbf{x}} + \frac{\partial g}{\partial y} \widehat{\mathbf{x}\mathbf{z}} + \frac{\partial g}{\partial z} \widehat{\mathbf{y}\mathbf{x}} - \frac{\partial g}{\partial z} \widehat{\mathbf{x}\mathbf{y}} \right] \cdot$$

$$[A_x \widehat{\mathbf{x}} + A_y \widehat{\mathbf{y}} + A_z \widehat{\mathbf{z}}] =$$

$$= \begin{bmatrix} 0 & -\dfrac{\partial}{\partial z} & \dfrac{\partial}{\partial y} \\ \dfrac{\partial}{\partial z} & 0 & -\dfrac{\partial}{\partial x} \\ -\dfrac{\partial}{\partial y} & \dfrac{\partial}{\partial x} & 0 \end{bmatrix} g \begin{bmatrix} A_x \\ A_y \\ A_z \end{bmatrix}. \tag{E.45}$$

Explicit calculation of the terms of the dyadic Green's function in cartesian coordinates

The expression of the dyadic Green's function of the homogeneous space is derived. Starting from:

$$g(x, y, z) = \frac{e^{-jkr\sqrt{x^2+y^2+z^2}}}{4\pi\sqrt{x^2+y^2+z^2}},$$

it is possible to calculate the partial derivative with respect to the variable x:

$$\frac{\partial g}{\partial x} = \frac{\partial}{\partial x} \left(e^{-jkr\sqrt{x^2+y^2+z^2}} \right) \frac{1}{4\pi\sqrt{x^2+y^2+z^2}} + \frac{e^{-jkr\sqrt{x^2+y^2+z^2}}}{4\pi} \left(\frac{1}{\sqrt{x^2+y^2+z^2}} \right).$$

For Leibnitz's rule

$$\frac{\mathrm{d}}{\mathrm{d}x}\mathrm{e}^{f(x)} = f'(x)\mathrm{e}^{f(x)},$$

follows

$$\frac{\partial g}{\partial x} = \frac{1}{4\pi\sqrt{x^2 + y^2 + z^2}}\mathrm{e}^{-\mathrm{j}k\sqrt{x^2+y^2+z^2}}\left(-\mathrm{j}k\frac{1}{2}\frac{2x}{\sqrt{x^2 + y^2 + z^2}}\right) +$$

$$-\frac{1}{2}2x\frac{\mathrm{e}^{-\mathrm{j}k\sqrt{x^2+y^2+z^2}}}{4\pi\left(\sqrt{x^2 + y^2 + z^2}\right)^3} =$$

$$= -x\left(\mathrm{j}k\frac{1}{\sqrt{x^2 + y^2 + z^2}} + \frac{1}{x^2 + y^2 + z^2}\right)g(x,y,z).$$

It is defined a function $f_x(x,y,z)$ as:

$$f_x(x,y,z) \triangleq -x\left(\mathrm{j}k\frac{1}{\sqrt{x^2 + y^2 + z^2}} + \frac{1}{x^2 + y^2 + z^2}\right), \tag{E.46}$$

so,

$$\frac{\partial g}{\partial x} = f_x(x,y,z)g(x,y,z). \tag{E.47}$$

Since the scalar Green's function has almost the same dependence on x, y and z, it is straightforward to prove that:

$$\frac{\partial g}{\partial y} = f_y(x,y,z)g(x,y,z)$$
$$\frac{\partial g}{\partial z} = f_z(x,y,z)g(x,y,z), \tag{E.48}$$

where:

$$f_y(x,y,z) \triangleq -y\left(\mathrm{j}k\frac{1}{\sqrt{x^2 + y^2 + z^2}} + \frac{1}{x^2 + y^2 + z^2}\right)$$
$$f_z(x,y,z) \triangleq -z\left(\mathrm{j}k\frac{1}{\sqrt{x^2 + y^2 + z^2}} + \frac{1}{x^2 + y^2 + z^2}\right). \tag{E.49}$$

With these terms, the $\mathbf{G}' = \nabla \times \mathbf{G}$ dyadic terms are known. For what concerns the $\mathbf{G}$ matrix, it is still needed to calculate the second derivatives. So:

$$\frac{\partial^2 g}{\partial x^2} = \frac{\partial}{\partial x}\left(\frac{\partial g}{\partial x}\right) = \frac{\partial}{\partial x}(f_x g) = \frac{\partial f_x}{\partial x}g + f_x\frac{\partial g}{\partial x}, \tag{E.50}$$

where:

$$\frac{\partial f_x}{\partial x} = -\mathrm{j}k\frac{1}{\sqrt{x^2 + y^2 + z^2}} - \frac{1}{x^2 + y^2 + z^2} + \mathrm{j}kx\frac{1}{2}\frac{2x}{(x^2 + y^2 + z^2)^{\frac{3}{2}}} + \frac{2x^2}{(x^2 + y^2 + z^2)^2} =$$

$$= \frac{1}{x}f_x(x, y, z) + \frac{\mathrm{j}kx^2}{(x^2 + y^2 + z^2)^{\frac{3}{2}}} + \frac{2x^2}{(x^2 + y^2 + z^2)^2}. \tag{E.51}$$

By exploiting once again the dependence of the formula on the variables, it can be written that:

$$\frac{\partial f_y}{\partial y} = \frac{1}{y}f_y(x, y, z) + \frac{\mathrm{j}ky^2}{(x^2 + y^2 + z^2)^{\frac{3}{2}}} + \frac{2y^2}{(x^2 + y^2 + z^2)^2}$$

$$\frac{\partial f_z}{\partial z} = \frac{1}{z}f_z(x, y, z) + \frac{\mathrm{j}kz^2}{(x^2 + y^2 + z^2)^{\frac{3}{2}}} + \frac{2z^2}{(x^2 + y^2 + z^2)^2}. \tag{E.52}$$

For what concerns the mixed derivatives, it is possible to calculate, for instance:

$$\frac{\partial^2 g}{\partial y \partial x} = \frac{\partial}{\partial y}\left(\frac{\partial g}{\partial x}\right) = \frac{\partial}{\partial y}(f_x g) = \frac{\partial f_x}{\partial y}g + f_x\frac{\partial g}{\partial y} = \frac{\partial f_x}{\partial y}g + f_x f_y g, \tag{E.53}$$

where:

$$\frac{\partial f_x}{\partial y} = -x\left(-\frac{1}{2}\mathrm{j}k\frac{2y}{(x^2 + y^2 + z^2)^{\frac{3}{2}}} - \frac{2xy}{(x^2 + y^2 + z^2)^2}\right) =$$

$$= xy\left(\frac{\mathrm{j}k}{(x^2 + y^2 + z^2)^{\frac{3}{2}}} + \frac{2}{(x^2 + y^2 + z^2)^2}\right). \tag{E.54}$$

It is apparent that:

$$\frac{\partial f_x}{\partial y} = \frac{\partial f_y}{\partial x}. \tag{E.55}$$

Moreover, by using symmetries,

$$\frac{\partial f_z}{\partial x} = zx\left(\frac{\mathrm{j}k}{(x^2 + y^2 + z^2)^{\frac{3}{2}}} + \frac{2}{(x^2 + y^2 + z^2)^2}\right)$$

$$\frac{\partial f_z}{\partial y} = zy\left(\frac{\mathrm{j}k}{(x^2 + y^2 + z^2)^{\frac{3}{2}}} + \frac{2}{(x^2 + y^2 + z^2)^2}\right). \tag{E.56}$$

With this, the entire expression of the dyadic Green's function in cartesian coordinates has been derived.

Final remarks about the MoM

The expressions of the integrand functions relative to the radiation integrals have been written in an explicit form. However, it should be remarked that the end of all this formulation is to write an explicit formulation for the radiation of the currents found by means of a method of moments. The following expression is recalled:

$$\mathbf{E}(x,y,z) = \mathbf{G}^{(e,j)}(x,y,z) \overset{*}{:} \mathbf{J}(x,y,z) + \mathbf{G}^{(e,m)}(x,y,z) \overset{*}{:} \mathbf{M}(x,y,z)$$

$$\mathbf{H}(x,y,z) = \mathbf{G}^{(h,j)}(x,y,z) \overset{*}{:} \mathbf{J}(x,y,z) + \mathbf{G}^{(h,m)}(x,y,z) \overset{*}{:} \mathbf{M}(x,y,z),$$

where:

$$\mathbf{G}^{(e,j)}(x,y,z) \overset{*}{:} \mathbf{J}(x,y,z) = \int_{\mathbb{R}^3} \mathbf{G}^{(e,j)}(x-x', y-y', z-z') \cdot \mathbf{J}(x',y',z') \, \mathrm{d}x' \, \mathrm{d}y' \, \mathrm{d}z'$$

$$\mathbf{G}^{(e,m)}(x,y,z) \overset{*}{:} \mathbf{M}(x,y,z) = \int_{\mathbb{R}^3} \mathbf{G}^{(e,m)}(x-x', y-y', z-z') \cdot \mathbf{M}(x',y',z') \, \mathrm{d}x' \, \mathrm{d}y' \, \mathrm{d}z'.$$

The same notation can be applied to the magnetic field. In the method of moments, the unknown is represented as a linear combination of known functions:

$$\mathbf{J}(x,y,z) = \sum_{n=1}^{N_{\text{fun}}} J_n \mathbf{f}_n(x,y,z)$$

$$\mathbf{M}(x,y,z) = \sum_{n=1}^{N_{\text{fun}}} M_n \mathbf{f}_n(x,y,z),$$

where in this formulation the same functions (RWG) have been used as expansion functions for both the unknowns. The integrals should be calculated keeping into account these expansions, therefore as:

$$\mathbf{G}^{(e,j)}(x,y,z) \overset{*}{:} \mathbf{J}(x,y,z) = \sum_{n=1}^{N_{\text{fun}}} J_n \int_{\mathcal{D}'_n} \mathbf{G}^{(e,j)}(x-x', y-y', z-z') \cdot \mathbf{f}_n(x',y',z') \, \mathrm{d}x' \, \mathrm{d}y' \, \mathrm{d}z'$$

$$\mathbf{G}^{(e,m)}(x,y,z) \overset{*}{:} \mathbf{M}(x,y,z) = \sum_{n=1}^{N_{\text{fun}}} M_n \int_{\mathcal{D}'_n} \mathbf{G}^{(e,m)}(x-x', y-y', z-z') \cdot \mathbf{f}_n(x',y',z') \, \mathrm{d}x' \, \mathrm{d}y' \, \mathrm{d}z'.$$

These integrals are calculated on the source domain only, therefore only on the domain of the n-th basis function, $\mathcal{D}'_n$. The results are functions varying in the observation domain. The strategy for the evaluation of these integrals is: for each point (x,y,z) in which the electric field of the antenna should be calculated, the entire sum of integrals has to be calculated; so, for each point, it is necessary to calculate $4N_{\text{fun}}$ integrals (N_{fun} per each dyadic Green's function).

E.1.6 Dyadic Green's function of the hemispace in presence of a PEC ground plane

In this section the Green's function of a hemi-space in presence of a PEC ground plane parallel to the xy plane and placed at $z = 0$ will be derived. This will be done by applying the image theorem, which will be discussed and proved, and by modifying the dyadic Green's function of the homogeneous space.

Image theorem

Let $\mathbf{E}', \mathbf{H}'$ be the electric and magnetic fields generated by some current densities $\mathbf{J}'$ and $\mathbf{M}'$; these quantities are defined only in the upper half-space, so for $z \geq 0$. Then, let $\mathbf{E}''$, $\mathbf{H}''$, $\mathbf{J}''$ and $\mathbf{M}''$ be the fields obtained by applying a reflection transformation with respect to the $z = 0$ plane; then, the fields $\mathbf{E}$ and $\mathbf{H}$, defined as:

$$\begin{aligned}
\mathbf{E} &= \mathbf{E}' + \mathbf{E}'' \\
\mathbf{H} &= \mathbf{H}' + \mathbf{H}''
\end{aligned} \tag{E.57}$$

are the electromagnetic fields in every point of the space, generated by the currents $\mathbf{J}'$, $\mathbf{M}'$ keeping into account the effect of the PEC ground plane placed in $z = 0$.

Proof of the image theorem

This proof is based on geometrical considerations, and the fact that the PEC surface is a plane is a very strict condition for the application of the theorem. A cartesian orthogonal system (x', y', z') for the fields in the upper half-plane is defined. Since $\mathbf{E}'$ and $\mathbf{H}'$ satisfy Maxwell's equations,

$$\begin{cases}
\dfrac{\partial E_z'}{\partial y'} - \dfrac{\partial E_y'}{\partial z'} = -\mathrm{j}\omega\mu H_x' - M_x' \\[2mm]
-\dfrac{\partial E_x'}{\partial z'} + \dfrac{\partial E_z'}{\partial x'} = -\mathrm{j}\omega\mu H_y' - M_y' \\[2mm]
\dfrac{\partial E_x'}{\partial y'} - \dfrac{\partial E_y'}{\partial x'} = -\mathrm{j}\omega\mu H_z' - M_z' \\[2mm]
\dfrac{\partial H_z'}{\partial y'} - \dfrac{\partial H_y'}{\partial z'} = \mathrm{j}\omega\varepsilon E_x' + J_x' \\[2mm]
-\dfrac{\partial H_x'}{\partial z'} + \dfrac{\partial H_z'}{\partial x'} = \mathrm{j}\omega\varepsilon E_y' + J_y' \\[2mm]
\dfrac{\partial H_x'}{\partial y'} - \dfrac{\partial H_y'}{\partial x'} = \mathrm{j}\omega\varepsilon E_z' + J_z'.
\end{cases} \tag{E.58}$$

The reflection with respect to the $z = 0$ plane is now applied to these equations:

$$
\begin{aligned}
x'' &= x' \\
y'' &= y' \\
z'' &= -z'
\end{aligned}
\tag{E.59}
$$

This transformation is applied to the differential operators in Maxwell's equations; by doing this, it is possible to obtain, just grouping properly some $-$ signs:

$$
\begin{cases}
\dfrac{\partial E'_z}{\partial y'} + \dfrac{\partial E'_y}{\partial(-z')} = -\mathrm{j}\omega\mu H'_x - M'_x \\[2mm]
\dfrac{\partial E'_x}{\partial(-z')} + \dfrac{\partial E'_z}{\partial x'} = -\mathrm{j}\omega\mu H'_y - M'_y \\[2mm]
\dfrac{\partial E'_x}{\partial y'} - \dfrac{\partial E'_y}{\partial x'} = -\mathrm{j}\omega\mu H'_z - M'_z \\[2mm]
\dfrac{\partial H'_z}{\partial y'} + \dfrac{\partial H'_y}{\partial(-z')} = \mathrm{j}\omega\varepsilon E'_x + J'_x \\[2mm]
\dfrac{\partial H'_x}{\partial(-z')} + \dfrac{\partial H'_z}{\partial x'} = \mathrm{j}\omega\varepsilon E'_y + J'_y \\[2mm]
\dfrac{\partial H'_x}{\partial y'} - \dfrac{\partial H'_y}{\partial x'} = \mathrm{j}\omega\varepsilon E'_z + J'_z,
\end{cases}
$$

then, according to (E.59):

$$
\begin{cases}
\dfrac{\partial E'_z}{\partial y''} + \dfrac{\partial E'_y}{\partial z''} = -\mathrm{j}\omega\mu H'_x - M'_x \\[2mm]
\dfrac{\partial E'_x}{\partial z''} + \dfrac{\partial E'_z}{\partial x''} = -\mathrm{j}\omega\mu H'_y - M'_y \\[2mm]
\dfrac{\partial E'_x}{\partial y''} - \dfrac{\partial E'_y}{\partial x''} = -\mathrm{j}\omega\mu H'_z - M'_z \\[2mm]
\dfrac{\partial H'_z}{\partial y''} + \dfrac{\partial H'_y}{\partial z''} = \mathrm{j}\omega\varepsilon E'_x + J'_x \\[2mm]
\dfrac{\partial H'_x}{\partial z''} + \dfrac{\partial H'_z}{\partial x''} = \mathrm{j}\omega\varepsilon E'_y + J'_y \\[2mm]
\dfrac{\partial H'_x}{\partial y''} - \dfrac{\partial H'_y}{\partial x''} = \mathrm{j}\omega\varepsilon E'_z + J'_z.
\end{cases}
$$

These six equations are no longer Maxwell's equations; however, the components have not been transformed yet. The transformations of the components should be performed min such away to obtain equations in the form of (E.58). For example, it is necessary to put a $-$ sign in front of E'_y in the first equation, in order to restore the correct sign; the same thing on E'_x from the second equation, and so on. In other words, it is necessary to perform the following step:

$$
\begin{cases}
\dfrac{\partial E_z'}{\partial y''} - \dfrac{\partial (-E_y')}{\partial z''} = -j\omega\mu H_x' - M_x' \\[2mm]
-\dfrac{\partial (-E_x')}{\partial z''} + \dfrac{\partial E_z'}{\partial x''} = -j\omega\mu H_y' - M_y' \\[2mm]
-\dfrac{\partial (-E_x')}{\partial y''} + \dfrac{\partial (-E_y')}{\partial x''} = +j\omega\mu(-H_z') + (-M_z') \\[2mm]
-\dfrac{\partial (-H_z')}{\partial y''} + \dfrac{\partial H_y'}{\partial z''} = -j\omega\varepsilon(-E_x') - (-J_x') \\[2mm]
\dfrac{\partial H_x'}{\partial z''} - \dfrac{\partial (-H_z')}{\partial x''} = -j\omega\varepsilon(-E_y') - (-J_y') \\[2mm]
\dfrac{\partial H_x'}{\partial y''} - \dfrac{\partial H_y'}{\partial x''} = j\omega\varepsilon E_z' + J_z'.
\end{cases}
$$

By applying the following transformations of the components:

$$
\begin{aligned}
& E_x'' = -E_x' && E_y'' = -E_y' && E_z'' = E_z' \\
& H_x'' = H_x' && H_y'' = H_y' && H_z'' = -H_z' \\
& J_x'' = -J_x' && J_y'' = -J_y' && J_z'' = J_z' \\
& M_x'' = M_x' && M_y'' = M_y' && M_z'' = -M_z',
\end{aligned}
\tag{E.60}
$$

the last equations written become, applying this substitutions:

$$
\begin{cases}
\dfrac{\partial E_z''}{\partial y''} - \dfrac{\partial E_y''}{\partial z''} = -j\omega\mu H_x'' - M_x'' \\[2mm]
-\dfrac{\partial E_x''}{\partial z''} + \dfrac{\partial E_z''}{\partial x''} = -j\omega\mu H_y'' - M_y'' \\[2mm]
\dfrac{\partial E_x''}{\partial y''} - \dfrac{\partial E_y''}{\partial x''} = -j\omega\mu H_z'' - M_z'' \\[2mm]
\dfrac{\partial H_z''}{\partial y''} - \dfrac{\partial H_y''}{\partial z''} = j\omega\varepsilon E_x'' + J_x'' \\[2mm]
-\dfrac{\partial H_x''}{\partial z''} + \dfrac{\partial H_z''}{\partial x''} = j\omega\varepsilon E_y'' + J_y'' \\[2mm]
\dfrac{\partial H_x''}{\partial y''} - \dfrac{\partial H_y''}{\partial x''} = j\omega\varepsilon E_z'' + J_z'',
\end{cases}
$$

which are Maxwell's equations. Therefore, $\mathbf{E}''$ and $\mathbf{H}''$, defined according to this idea, are a maxwellian field. Now, it is possible to define $\mathbf{E}$ and $\mathbf{H}$ as:

$$\mathbf{E}(x', y', z') = \begin{bmatrix} E'_x(x', y', z') + E''_x(x'', y'', z'') \\ E'_y(x', y', z') + E''_y(x'', y'', z'') \\ E'_z(x', y', z') + E''_z(x'', y'', z'') \end{bmatrix} = \begin{bmatrix} E'_x(x', y', z') - E'_x(x', y', -z') \\ E'_y(x', y', z') - E'_y(x', y', -z') \\ E'_z(x', y', z') + E'_z(x', y', -z') \end{bmatrix}$$

$$\mathbf{H}(x', y', z') = \begin{bmatrix} H'_x(x', y', z') + H''_x(x'', y'', z'') \\ H'_y(x', y', z') + H''_y(x'', y'', z'') \\ H'_z(x', y', z') + H''_z(x'', y'', z'') \end{bmatrix} = \begin{bmatrix} H'_x(x', y', z') + H'_x(x', y', -z') \\ H'_y(x', y', z') + H'_y(x', y', -z') \\ H'_z(x', y', z') - H'_z(x', y', -z') \end{bmatrix}.$$

$$(E.61)$$

This notation is used to specify that the electric and the magnetic field in a point (x', y', z'), have two contributions: one from the current densities $\mathbf{J}'$ defined in the upper hemispace, one from the images $\mathbf{J}''$ in the lower hemispace; the same applies to $\mathbf{M}'$ and $\mathbf{M}''$. The $\mathbf{J}''$ and $\mathbf{M}''$ contributions are evaluated in $(x', y', -z')$.

It is straightforward to prove the connection between these geometrical considerations and the presence of a PEC ground plane in $z = 0$; indeed, it is possible to observe that $\mathbf{E}$ and $\mathbf{H}$ are satisfying the PEC boundary condition on $z = 0$:

$$\mathbf{E}(x', y', 0) = \begin{bmatrix} E'_x(x', y', 0) - E'_x(x', y', 0) \\ E'_y(x', y', 0) - E'_y(x', y', 0) \\ E'_z(x', y', 0) + E''_z(x', y', 0) \end{bmatrix} = \begin{bmatrix} 0 \\ 0 \\ 2E'_z(x', y', 0) \end{bmatrix}$$

$$\mathbf{H}(x', y', 0) = \begin{bmatrix} H'_x(x', y', 0) + H'_x(x', y', 0) \\ H'_y(x', y', 0) + H'_y(x', y', 0) \\ H'_z(x', y', 0) - H'_z(x', y', 0) \end{bmatrix} = \begin{bmatrix} 2H'_x(x', y', 0) \\ 2H'_y(x', y', 0) \\ 0 \end{bmatrix}.$$

The tangent components of the electric field are zero and the z component of the magnetic field are zero: this is the PEC boundary condition. So, $\mathbf{E}$ and $\mathbf{H}$, defined accordingly to the previous discussion, are the electric and magnetic fields radiated by currents in presence of a PEC ground plane.

The proof that has been proposed can be used also for the derivation of the transformations of the vector components in order to obtain a PMC boundary condition. Indeed, by using the same coordinate transformations, but, instead of (E.60), the following set of component transformations:

$$\begin{aligned} E''_x &= E'_x & E''_y &= E'_y & E''_z &= -E'_z \\ H''_x &= -H'_x & H''_y &= -H'_y & H''_z &= H'_z \\ J''_x &= J'_x & J''_y &= J'_y & J''_z &= -J'_z \\ M''_x &= -M'_x & M''_y &= -M'_y & M''_z &= M'_z \end{aligned}$$

$$(E.62)$$

the image theorem for a PMC ground plane is obtained.

Green's function for a PEC ground plane

The expression of the electric and magnetic fields are:

$$\begin{aligned}
\mathbf{E}(x,y,z) &= \mathbf{G}^{(\mathrm{e,j})}(x,y,z) \overset{*}{:} \mathbf{J}(x,y,z) + \mathbf{G}^{(\mathrm{e,m})}(x,y,z) \overset{*}{:} \mathbf{M}(x,y,z) = \\
&\triangleq \mathbf{E}^{(\mathrm{j})}(x,y,z) + \mathbf{E}^{(\mathrm{m})}(x,y,z) \\
\mathbf{H}(x,y,z) &= \mathbf{G}^{(\mathrm{h,j})}(x,y,z) \overset{*}{:} \mathbf{J}(x,y,z) + \mathbf{G}^{(\mathrm{h,m})}(x,y,z) \overset{*}{:} \mathbf{M}(x,y,z) = \\
&\triangleq \mathbf{H}^{(\mathrm{j})}(x,y,z) + \mathbf{H}^{(\mathrm{m})}(x,y,z),
\end{aligned} \tag{E.63}$$

where $\mathbf{E}^{(\mathrm{j})}$, $\mathbf{H}^{(\mathrm{j})}$ are the electric and magnetic field contributions generated by electric current densities and $\mathbf{E}^{(\mathrm{m})}$, $\mathbf{H}^{(\mathrm{m})}$ are generated by magnetic current densities,

$$\begin{aligned}
\mathbf{E}^{(\mathrm{j})}(x,y,z) &= \mathbf{G}^{(\mathrm{e,j})}(x,y,z) \overset{*}{:} \mathbf{J}(x,y,z) \\
\mathbf{E}^{(\mathrm{m})}(x,y,z) &= \mathbf{G}^{(\mathrm{e,m})}(x,y,z) \overset{*}{:} \mathbf{M}(x,y,z) \\
\mathbf{H}^{(\mathrm{j})}(x,y,z) &= \mathbf{G}^{(\mathrm{h,j})}(x,y,z) \overset{*}{:} \mathbf{J}(x,y,z) \\
\mathbf{H}^{(\mathrm{m})}(x,y,z) &= \mathbf{G}^{(\mathrm{h,m})}(x,y,z) \overset{*}{:} \mathbf{M}(x,y,z),
\end{aligned} \tag{E.64}$$

where:

$$\begin{aligned}
\mathbf{G}^{(\mathrm{e,j})}(x,y,z) &- \mathrm{j}\omega\mu\mathbf{G}(x,y,z) \\
\mathbf{G}^{(\mathrm{h,m})}(x,y,z) &= -\mathrm{j}\omega\varepsilon\mathbf{G}(x,y,z) \\
\mathbf{G}^{(\mathrm{h,j})}(x,y,z) &= \nabla \times \mathbf{G}(x,y,z) \\
\mathbf{G}^{(\mathrm{e,m})}(x,y,z) &= -\nabla \times \mathbf{G}(x,y,z),
\end{aligned}$$

and:

$$\mathbf{G}(x,y,z) = \frac{1}{k^2}\begin{bmatrix} k^2 + \dfrac{\partial^2}{\partial x^2} & \dfrac{\partial^2}{\partial x \partial y} & \dfrac{\partial^2}{\partial x \partial z} \\[2ex] \dfrac{\partial^2}{\partial y \partial x} & k^2 + \dfrac{\partial^2}{\partial y^2} & \dfrac{\partial^2}{\partial y \partial z} \\[2ex] \dfrac{\partial^2}{\partial z \partial x} & \dfrac{\partial^2}{\partial z \partial y} & k^2 + \dfrac{\partial^2}{\partial z^2} \end{bmatrix} g(x,y,z)$$

$$\nabla \times \mathbf{G}(x,y,z) = \begin{bmatrix} 0 & -\dfrac{\partial}{\partial z} & \dfrac{\partial}{\partial y} \\[2ex] \dfrac{\partial}{\partial z} & 0 & -\dfrac{\partial}{\partial x} \\[2ex] -\dfrac{\partial}{\partial y} & \dfrac{\partial}{\partial x} & 0 \end{bmatrix}.$$

Now, to find the expressions of the dyadic Green's function that keeps into account the radiation contributions by a ground plane, it is recalled that the total electric field has two contributions: the physical and image ones:

$$\mathbf{E}^{(j,\text{GND})}(x,y,z) = \mathbf{E}^{(j,\text{physical})}(x,y,z) + \mathbf{E}^{(j,\text{image})}(x,y,-z) =$$

$$= \mathbf{G}^{(e,j)}(x,y,z) \overset{*}{:} \mathbf{J}^{(\text{physical})}(x,y,z) + \mathbf{G}^{(e,j)}(x,y,-z) \overset{*}{:} \mathbf{J}^{(\text{image})}(x,y,-z)$$

$$\mathbf{E}^{(m,\text{GND})}(x,y,z) = \mathbf{E}^{(m,\text{physical})}(x,y,z) + \mathbf{E}^{(m,\text{image})}(x,y,-z) =$$

$$= \mathbf{G}^{(e,m)}(x,y,z) \overset{*}{:} \mathbf{M}^{(\text{physical})}(x,y,z) + \mathbf{G}^{(e,m)}(x,y,-z) \overset{*}{:} \mathbf{M}^{(\text{image})}(x,y,-z)$$

$$\mathbf{H}^{(j,\text{GND})}(x,y,z) = \mathbf{H}^{(j,\text{physical})}(x,y,z) + \mathbf{H}^{(j,\text{image})}(x,y,-z) =$$

$$= \mathbf{G}^{(h,j)}(x,y,z) \overset{*}{:} \mathbf{J}^{(\text{physical})}(x,y,z) + \mathbf{G}^{(h,j)}(x,y,-z) \overset{*}{:} \mathbf{J}^{(\text{image})}(x,y,-z)$$

$$\mathbf{H}^{(m,\text{GND})}(x,y,z) = \mathbf{H}^{(m,\text{physical})}(x,y,z) + \mathbf{H}^{(m,\text{image})}(x,y,-z) =$$

$$= \mathbf{G}^{(h,m)}(x,y,z) \overset{*}{:} \mathbf{M}^{(\text{physical})}(x,y,z) + \mathbf{G}^{(h,m)}(x,y,-z) \overset{*}{:} \mathbf{M}^{(\text{image})}(x,y,-z).$$

The image theorem is used to "remove" the ground plane, introducing, instead of it, the image current densities. Therefore, the space in which all these currents, physical and fictional, have to radiate, is homogeneous. So, for each contribution, the homogeneous space Green's function is used to evaluate the radiation contributions. To understand how the presence of the ground plane modifies the dyadic Green's function, it is useful for instance to consider the following product:

$$\mathbf{G}(x,y,-z) \overset{*}{:} \mathbf{J}^{(\text{image})}(x,y,-z) =$$

$$\begin{bmatrix} k^2 + \dfrac{\partial^2}{\partial x^2} & \dfrac{\partial^2}{\partial x \partial y} & \dfrac{\partial^2}{\partial x \partial z} \\ \dfrac{\partial^2}{\partial y \partial x} & k^2 + \dfrac{\partial^2}{\partial y^2} & \dfrac{\partial^2}{\partial y \partial z} \\ \dfrac{\partial^2}{\partial z \partial x} & \dfrac{\partial^2}{\partial z \partial y} & k^2 + \dfrac{\partial^2}{\partial z^2} \end{bmatrix} g(x,y,z) \begin{bmatrix} -J_x(x,y,-z) \\ -J_y(x,y,-z) \\ J_z(x,y,-z) \end{bmatrix} =$$

$$= \begin{bmatrix} k^2 + \dfrac{\partial^2}{\partial x^2} & \dfrac{\partial^2}{\partial x \partial y} & \dfrac{\partial^2}{\partial x \partial z} \\ \dfrac{\partial^2}{\partial y \partial x} & k^2 + \dfrac{\partial^2}{\partial y^2} & \dfrac{\partial^2}{\partial y \partial z} \\ \dfrac{\partial^2}{\partial z \partial x} & \dfrac{\partial^2}{\partial z \partial y} & k^2 + \dfrac{\partial^2}{\partial z^2} \end{bmatrix} \begin{bmatrix} -1 & 0 & 0 \\ 0 & -1 & 0 \\ 0 & 0 & 1 \end{bmatrix} g(x,y,z) \begin{bmatrix} J_x(x,y,-z) \\ J_y(x,y,-z) \\ J_z(x,y,-z) \end{bmatrix}.$$

To obtain a single dyadic Green's function, the terms $\mathbf{G}$ and $\nabla \times \mathbf{G}$ are now modified. Let $\mathbf{D}$ be:

$$\mathbf{D} \triangleq \begin{bmatrix} -1 & 0 & 0 \\ 0 & -1 & 0 \\ 0 & 0 & 1 \end{bmatrix}.$$

So, it is possible to calculate the dyadic $\mathbf{G}$ that keeps into account the effect of the ground plane as:

$$\mathbf{G}^{\mathrm{GND}}(x, y, z) = \mathbf{G}(x, y, z) + \mathbf{G}(x, y, -z)\mathbf{D};$$

the same applies to $\nabla \times \mathbf{G}$:

$$\nabla \times \mathbf{G}^{(\mathrm{GND})}(x, y, z) = \nabla \times \mathbf{G}(x, y, z) + \nabla \times \mathbf{G}(x, y, -z)\mathbf{D}.$$

Therefore, the following quantities are defined:

$$\mathbf{G}^{(\mathrm{e,j,GND})}(x, y, z) - \mathrm{j}\omega\mu\mathbf{G}^{(\mathrm{GND})}(x, y, z)$$
$$\mathbf{G}^{(\mathrm{h,m,GND})}(x, y, z) = -\mathrm{j}\omega\varepsilon\mathbf{G}^{(\mathrm{GND})}(x, y, z)$$
$$\mathbf{G}^{(\mathrm{h,j,GND})}(x, y, z) = \nabla \times \mathbf{G}^{(\mathrm{GND})}(x, y, z)$$
$$\mathbf{G}^{(\mathrm{e,m,GND})}(x, y, z) = -\nabla \times \mathbf{G}^{(\mathrm{GND})}(x, y, z),$$

and, finally:

$$\mathbf{E}^{(\mathrm{GND})}(x, y, z) = \mathbf{G}^{(\mathrm{e,j,GND})}(x, y, z) \overset{*}{:} \mathbf{J}(x, y, z) + \mathbf{G}^{(\mathrm{e,m,GND})}(x, y, z) \overset{*}{:} \mathbf{M}(x, y, z)$$
$$\mathbf{H}^{(\mathrm{GND})}(x, y, z) = \mathbf{G}^{(\mathrm{h,j,GND})}(x, y, z) \overset{*}{:} \mathbf{J}(x, y, z) + \mathbf{G}^{(\mathrm{h,m,GND})}(x, y, z) \overset{*}{:} \mathbf{M}(x, y, z).$$
$$(\mathrm{E}.65)$$

E.2 Green's functions of stratified structures

E.2.1 Spectral Green's functions representations

In the previous sections the homogeneous space Green's function has been derived by transforming the wave equations into the spectral domain by means of the triple Fourier transform, by applying some manipulation and finally by returning in the spatial domain by applying the inverse operator; this approach is very convenient for the homogeneous space problem.

This procedure can not be applied to more complex geometries, such as stratified structures; considering a cartesian coordinate system, they have homogeneous media in the x and y directions, whereas ε_{r} changes abruptly along z; dielectric slabs are an example of these structures. In these situations, Maxwell's equations are transversalized with respect to z, and a double Fourier transform is applied to the transverse components; then, the calculation of the spectral domain Green's function is reduced to the calculation of voltage and currents on transmission lines. By this way, the two spectral domain variables k_x and k_y are defined; let:

$$k_{\mathrm{t}}^2 = k_x^2 + k_y^2,$$
$$(\mathrm{E}.66)$$

and:

$$k_{zi}^2 = k_i^2 - k_t^2, \tag{E.67}$$

where:

$$k_i = \omega\sqrt{\varepsilon_i\varepsilon_0\mu_0}, \tag{E.68}$$

and ε_i is the dielectric constant of the i-th stratification. The wavevector component k_{zi} is the propagation constant of the transmission line in the i-th stratification. The characteristic impedances of the transmission lines relative to the TE and TM polarizations are:

$$Z_{\infty i}^{\text{TE}} = Z_i\frac{k_i}{k_{zi}} \qquad Z_{\infty i}^{\text{TM}} = Z_i\frac{k_{zi}}{k_i}, \tag{E.69}$$

where:

$$Z_i = \frac{1}{\sqrt{\varepsilon_i}}\sqrt{\frac{\mu_0}{\epsilon_0}}. \tag{E.70}$$

In the following the expressions of the dyadic Green's functions in the spectral domain are reported [73], [74]:

- Electric field generated by an electric current density:

$$
\begin{aligned}
\widetilde{\mathbf{G}}^{(\text{e,j})}(k_x, k_y, z) = & \\
\begin{bmatrix}
-\dfrac{k_x^2 V_j^{\text{TM}} + k_y^2 V_j^{\text{TE}}}{k_t^2} & \dfrac{(V_j^{\text{TE}} - V_j^{\text{TM}})k_x k_y}{k_t^2} & Z\dfrac{k_x}{k}V_m^{\text{TM}} \\[3mm]
\dfrac{(V_j^{\text{TE}} - V_j^{\text{TM}})k_x k_y}{k_t^2} & -\dfrac{k_x^2 V_j^{\text{TE}} + k_y^2 V_j^{\text{TM}}}{k_t^2} & Z\dfrac{k_y}{k}V_m^{\text{TM}} \\[3mm]
Z\dfrac{k_x}{k}I_j^{\text{TM}} & Z\dfrac{k_y}{k}I_j^{\text{TM}} & -\dfrac{Z}{k}\left(Z\dfrac{k_t^2}{k}I_m^{\text{TM}} - \text{j}\delta(z)\right)
\end{bmatrix}.
\end{aligned}
\tag{E.71}
$$

- Magnetic field generated by an electric current density:

$$
\widetilde{\mathbf{G}}^{(\mathrm{h,j})}(k_x, k_y, z) = \begin{bmatrix} \dfrac{(I_\mathrm{j}^\mathrm{TM} - I_\mathrm{j}^\mathrm{TE})k_x k_y}{k_\mathrm{t}^2} & \dfrac{k_x^2 I_\mathrm{j}^\mathrm{TE} + k_y^2 I_\mathrm{j}^\mathrm{TM}}{k_\mathrm{t}^2} & -Z\dfrac{k_y}{k} I_\mathrm{m}^\mathrm{TM} \\[4mm] -\dfrac{k_x^2 I_\mathrm{j}^\mathrm{TM} + k_y^2 I_\mathrm{j}^\mathrm{TE}}{k_\mathrm{t}^2} & \dfrac{(I_\mathrm{j}^\mathrm{TE} - I_\mathrm{j}^\mathrm{TM})k_x k_y}{k_\mathrm{t}^2} & Z\dfrac{k_x}{k} I_\mathrm{m}^\mathrm{TM} \\[4mm] \dfrac{k_y}{kZ} V_\mathrm{j}^\mathrm{TE} & -\dfrac{k_x}{kZ} V_\mathrm{j}^\mathrm{TE} & 0 \end{bmatrix}.
$$
$$(\mathrm{E.72})$$

- Electric field generated by a magnetic current density:

$$
\widetilde{\mathbf{G}}^{(\mathrm{e,m})}(k_x, k_y, z) = \begin{bmatrix} \dfrac{(V_\mathrm{m}^\mathrm{TM} - V_\mathrm{m}^\mathrm{TE})k_x k_y}{k_\mathrm{t}^2} & -\dfrac{k_x^2 V_\mathrm{m}^\mathrm{TM} + k_y^2 V_\mathrm{m}^\mathrm{TE}}{k_\mathrm{t}^2} & \dfrac{k_y}{kZ} V_\mathrm{j}^\mathrm{TE} \\[4mm] \dfrac{k_x^2 V_\mathrm{m}^\mathrm{TE} + k_y^2 V_\mathrm{m}^\mathrm{TM}}{k_\mathrm{t}^2} & \dfrac{(V_\mathrm{m}^\mathrm{TE} - V_\mathrm{m}^\mathrm{TM})k_x k_y}{k_\mathrm{t}^2} & -\dfrac{k_x}{kZ} V_\mathrm{j}^\mathrm{TE} \\[4mm] -Z\dfrac{k_y}{k} I_\mathrm{m}^\mathrm{TM} & Z\dfrac{k_x}{k} I_\mathrm{m}^\mathrm{TM} & 0 \end{bmatrix}.
$$
$$(\mathrm{E.73})$$

- Magnetic field generated by a magnetic current density:

$$
\widetilde{\mathbf{G}}^{(\mathrm{h,m})}(k_x, k_y, z) =
$$
$$
\begin{bmatrix} -\dfrac{k_x^2 I_\mathrm{m}^\mathrm{TE} + k_y^2 I_\mathrm{m}^\mathrm{TM}}{k_\mathrm{t}^2} & \dfrac{(I_\mathrm{m}^\mathrm{TM} - I_\mathrm{m}^\mathrm{TE})k_x k_y}{k_\mathrm{t}^2} & \dfrac{k_x}{kZ} I_\mathrm{j}^\mathrm{TE} \\[4mm] \dfrac{(I_\mathrm{m}^\mathrm{TM} - I_\mathrm{m}^\mathrm{TE})k_x k_y}{k_\mathrm{t}^2} & -\dfrac{k_x^2 I_\mathrm{m}^\mathrm{TM} + k_y^2 I_\mathrm{m}^\mathrm{TE}}{k_\mathrm{t}^2} & \dfrac{k_y}{kZ} I_\mathrm{j}^\mathrm{TE} \\[4mm] \dfrac{k_x}{kZ} V_\mathrm{m}^\mathrm{TM} & \dfrac{k_y}{kZ} V_\mathrm{m}^\mathrm{TM} & -\dfrac{1}{kZ}\left(\dfrac{k_\mathrm{t}^2}{kZ} B_\mathrm{j}^\mathrm{TE} - \mathrm{j}\delta(z)\right) \end{bmatrix}. \quad (\mathrm{E.74})
$$

The term V_j is the voltage evaluated in $z = z_\mathrm{obs}$ due to the current generator that models the electric current density $\mathbf{J}$; similarly, V_m is generated by the voltage source modeling the magnetic current density $\mathbf{M}$. The term I_j is the current generated by the electric current density $\mathbf{J}$, whereas I_m is the current generated by the magnetic current density $\mathbf{M}$.
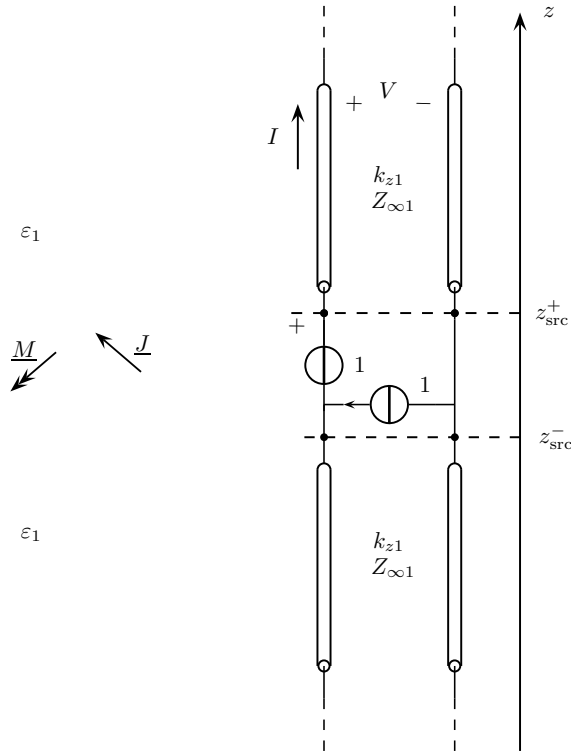
Figure E.1: Homogeneous space equivalent transmission line.
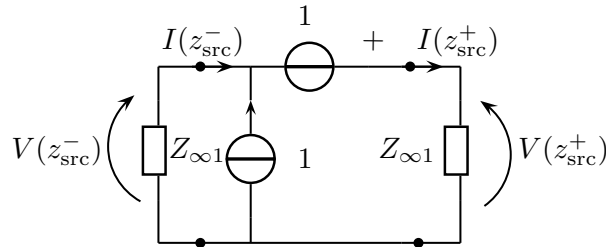
Figure E.2: Homogeneous space equivalent circuit at $z = z_{\mathrm{src}}$.

E.2.2   Examples of calculations

In this section the voltages and currents for some stratified structures are calculated. These expressions can be substituted in (E.71) to (E.74) to obtain the explicit expressions of the spectral domain dyadic Green's functions.

Homogeneous space case

The first example is given by the homogeneous space, as sketched in Fig. E.1: an electric and a magnetic current densities, placed at $z = z_{\mathrm{src}}$, which radiate in free space. The right part of Fig. E.1 reports the equivalent circuit of this scenario. The Thévenin equivalent circuits seen from the source generators at $z = z_{\mathrm{src}}$ are the

two characteristic impedances $Z_{\infty 1}$, as shown in Fig. E.2.

Let z_{obs} the point in which the Green's function has to be evaluated; it is possible to study separately the effects of the two generators by superposition, defining:

$$V(z_{\mathrm{obs}}) = V_{\mathrm{j}}(z_{\mathrm{obs}}) + V_{\mathrm{m}}(z_{\mathrm{obs}}).$$

For what concerns currents:

$$I(z_{\mathrm{obs}}) = I_{\mathrm{j}}(z_{\mathrm{obs}}) + I_{\mathrm{m}}(z_{\mathrm{obs}}).$$

The contributions for this case are:

$$I_{\mathrm{j}}(z_{\mathrm{src}}^{+}) = \frac{1}{2}, \qquad V_{\mathrm{j}}(z_{\mathrm{src}}^{+}) = \frac{1}{2}Z_{\infty 1} \tag{E.75}$$

$$I_{\mathrm{j}}(z_{\mathrm{src}}^{-}) = -\frac{1}{2}, \qquad V_{\mathrm{j}}(z_{\mathrm{src}}^{-}) = \frac{1}{2}Z_{\infty 1}. \tag{E.76}$$

Indeed, the electric current density corresponds to a magnetic field discontinuity; for this reason, the current generator, related to the magnetic field in z_{src}, are different; on the other hand the voltage generators, related to the electric field, are equal. Instead, for what concern the magnetic current densities, dual considerations can be performed:

$$V_{\mathrm{m}}(z_{\mathrm{src}}^{+}) = \frac{1}{2}, \qquad I_{\mathrm{m}}(z_{\mathrm{src}}^{+}) = \frac{1}{2Z_{\infty 1}} \tag{E.77}$$

$$V_{\mathrm{m}}(z_{\mathrm{src}}^{-}) = -\frac{1}{2}, \qquad I_{\mathrm{m}}(z_{\mathrm{src}}^{-}) = \frac{1}{2Z_{\infty 1}}. \tag{E.78}$$

The next step is the calculation of the voltage in a generic point z_{obs}:

$$\frac{V_{\mathrm{j}}(z_{\mathrm{obs}})}{V_{\mathrm{m}}(z_{\mathrm{obs}})} = \frac{V_{\mathrm{j}}(z_{\mathrm{src}}^{\pm})}{V_{\mathrm{m}}(z_{\mathrm{src}}^{\pm})} \mathrm{e}^{-\mathrm{j}k_{z1}|z_{\mathrm{obs}} - z_{\mathrm{sc}}|}. \tag{E.79}$$

Then, to calculate currents, it is possible to divide voltage by $Z(z_{\mathrm{obs}})$; since in this case the transmission lines are infinitely long,

$$Z(z_{\mathrm{zobs}}) = Z_{\infty 1}.$$

The circuit calculations are always the same for both polarizations; the difference between the TE and TM cases lies in the different characteristic impedances.

Homogeneous half-plane with PEC plane

The second case is summarized in Fig. E.3: for $z > 0$ the space is filled with dielectric ε_1, whereas at $z = 0$ there is a PEC ground plane.
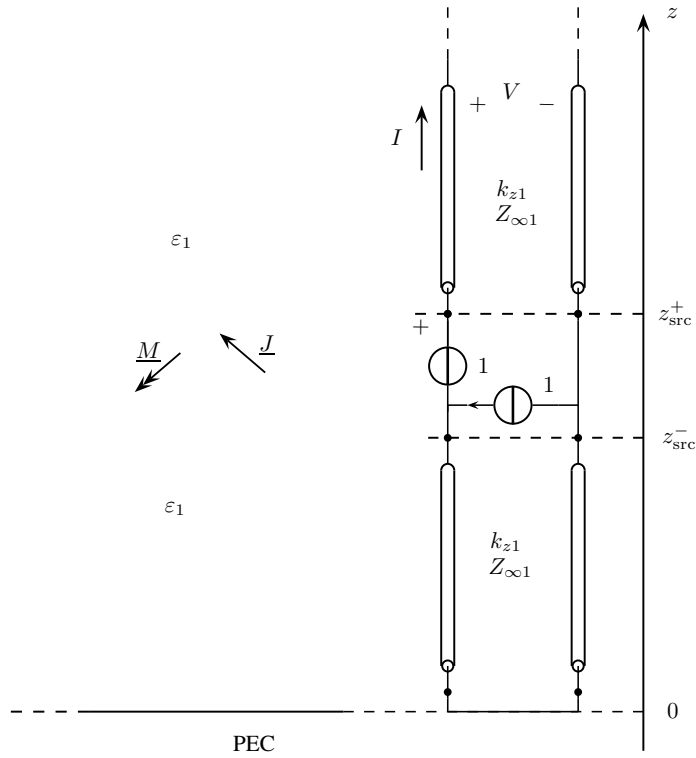
Figure E.3: Equivalent transmission line of the homogeneous space with PEC ground plane at $z = 0$.
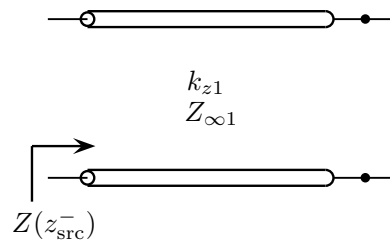

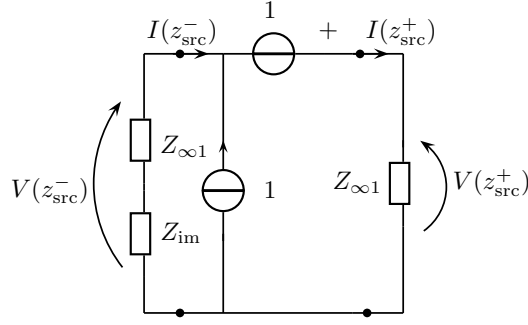Figure E.4: Circuit for the evaluation of the input impedance.

Figure E.5: Equivalent circuit at $z = z_{\text{src}}$ of the half-homogeneous space + PEC ground plane.

$z_{\text{obs}} < z_{\text{src}}$ case

The first step is the calculation of the Thévenin equivalent; for z_{src}^+, this is equal to the previous case; instead, for z_{src}^-:

$$\Gamma_{\text{B}^-} = -1; \qquad \Gamma_{\text{A}^+} = -e^{-j2k_{z1}l_{\text{AB}}} = -e^{-j2k_{z1}z_{\text{src}}},$$

so:

$$Z(z_{\text{src}}^-) = Z_{\infty 1}\frac{1 + \Gamma_{\text{A}^+}}{1 - \Gamma_{\text{A}^+}} = Z_{\infty 1}\frac{1 - e^{-j2k_{z1}z_{\text{src}}}}{1 + e^{-j2k_{z1}z_{\text{src}}}}.$$

It is possible to identify two contributions: the direct one, which equals the homogeneous space one, and the one reflected by the short circuit; to this aim, it is convenient to write the input impedance as the sum of two contributions:

$$Z(z_{\text{src}}^-) = Z_{\infty 1}\frac{1 - e^{-j2k_{z1}z_{\text{src}}}}{1 + e^{-j2k_{z1}z_{\text{src}}}} = Z_{\infty 1} - 2Z_{\infty 1}\frac{e^{-j2k_{z1}z_{\text{src}}}}{1 + e^{-j2k_{z1}z_{\text{src}}}} \triangleq Z_{\infty 1} + Z_{\text{im}}. \quad \text{(E.80)}$$

This leads to the definition of the equivalent circuit of Fig. E.5. It is possible to compute $V_{\text{m}}(z_{\text{src}}^-)$ as:

$$V_{\text{m}}(z_{\text{src}}^-) = -\frac{Z_{\infty 1} + Z_{\text{im}}}{Z_{\infty 1} + Z_{\infty 1} + Z_{\text{im}}}.$$

Now, by manipulating this expression to isolate the homogeneous space contribution from the one coming from the reflecting short circuit:

$$V_{\text{m}}(z_{\text{src}}^-) = -\frac{Z_{\infty 1} + Z_{\text{im}}}{2Z_{\infty 1} + Z_{\text{im}}} = -\frac{1}{2}\frac{2Z_{\infty 1} + 2Z_{\text{im}}}{2Z_{\infty 1} + Z_{\text{im}}} = -\frac{1}{2} - \frac{1}{2}\frac{Z_{\text{im}}}{2Z_{\infty 1} + Z_{\text{im}}}. \quad \text{(E.81)}$$

Now, by considering the contribution that arise from the electric current density:

$$I_{\mathrm{j}}(z_{\mathrm{src}}^-) = -\frac{Z_{\infty 1}}{2Z_{\infty 1} + Z_{\mathrm{im}}} = -\frac{1}{2}\frac{2Z_{\infty 1}}{2Z_{\infty 1} + Z_{\mathrm{im}}} = -\frac{1}{2}\frac{2Z_{\infty 1} + Z_{\mathrm{im}} - Z_{\mathrm{im}}}{2Z_{\infty 1} + Z_{\mathrm{im}}} =$$
$$= -\frac{1}{2} + \frac{1}{2}\frac{Z_{\mathrm{im}}}{2Z_{\infty 1} + Z_{\mathrm{im}}}, \tag{E.82}$$

so:

$$V_{\mathrm{j}}(z_{\mathrm{src}}^-) = \left[-\frac{1}{2} + \frac{1}{2}\frac{Z_{\mathrm{im}}}{2Z_{\infty 1} + Z_{\mathrm{im}}}\right][Z_{\infty 1} + Z_{\mathrm{im}}]. \tag{E.83}$$

Then:

$$\frac{V_{\mathrm{j}}(z_{\mathrm{obs}})}{V_{\mathrm{m}}(z_{\mathrm{obs}})} = \frac{V_{\mathrm{j}}^+(z_{\mathrm{obs}})}{V_{\mathrm{m}}^+(z_{\mathrm{obs}})}[1 + \Gamma(z_{\mathrm{obs}})] = \frac{V_{\mathrm{j}}^+(z_{\mathrm{src}})}{V_{\mathrm{m}}^+(z_{\mathrm{src}})}\mathrm{e}^{-\mathrm{j}k_{z1}|z_{\mathrm{obs}} - z_{\mathrm{src}}|}[1 + \Gamma(z_{\mathrm{obs}})] =$$
$$\frac{V_{\mathrm{j}}(z_{\mathrm{src}})}{V_{\mathrm{m}}(z_{\mathrm{src}})}\frac{1 + \Gamma(z_{\mathrm{obs}})}{1 + \Gamma(z_{\mathrm{src}-})}\mathrm{e}^{-\mathrm{j}k_{z1}|z_{\mathrm{obs}} - z_{\mathrm{src}}|},$$

where:

$$\Gamma(z_{\mathrm{obs}}) = -\mathrm{e}^{-\mathrm{j}2k_{z1}z_{\mathrm{obs}}},$$

and:

$$\Gamma(z_{\mathrm{src}}^-) = -\mathrm{e}^{-\mathrm{j}2k_{z1}z_{\mathrm{src}}}.$$

Finally, it is possible to calculate the current by dividing the voltage times $Z(z_{\mathrm{obs}})$; in this case this is not equal to the characteristic impedance, since the line is loaded on the reflecting element; therefore:

$$Z(z_{\mathrm{obs}}) = \frac{1 + \Gamma(z_{\mathrm{obs}})}{1 - \Gamma(z_{\mathrm{obs}})},$$

and:

$$\frac{I_{\mathrm{j}}(z_{\mathrm{obs}})}{I_{\mathrm{m}}(z_{\mathrm{obs}})} = \frac{1}{Z(z_{\mathrm{obs}})}\frac{V_{\mathrm{j}}(z_{\mathrm{obs}})}{V_{\mathrm{m}}(z_{\mathrm{obs}})}.$$

$z_{\mathrm{obs}} > z_{\mathrm{src}}$ **case**

Once again, it is necessary to compute the voltage at $z = z_{\mathrm{src}}^+$:

$$V_{\mathrm{m}}(z_{\mathrm{src}}^+) = \frac{Z_{\infty 1}}{2Z_{\infty 1} + Z_{\mathrm{im}}} = \frac{1}{2} - \frac{1}{2}\frac{Z_{\mathrm{im}}}{2Z_{\infty 1} + Z_{\mathrm{im}}}, \tag{E.84}$$
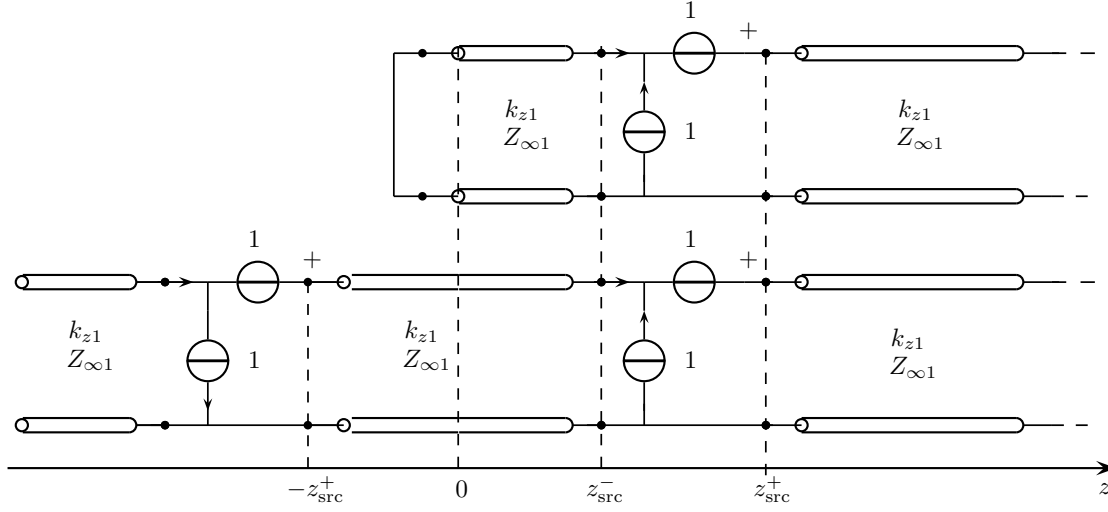
and:

Figure E.6: Circuit before (top) and after (bottom) the application of the image theorem.

$$I_j(z_{\text{src}}^+) = \frac{Z_{\infty 1} + Z_{\text{im}}}{2Z_{\infty 1} + Z_{\text{im}}} = \frac{1}{2} + \frac{1}{2}\frac{Z_{\text{im}}}{2Z_{\infty 1} + Z_{\text{im}}}, \tag{E.85}$$

which leads to:

$$V_j(z_{\text{src}}^+) = Z_{\infty 1}\left[\frac{1}{2} + \frac{1}{2}\frac{Z_{\text{im}}}{2Z_{\infty 1} + Z_{\text{im}}}\right]. \tag{E.86}$$

Then, since for $z_{\text{obs}} > z_{\text{src}}$ there is an infinitely-long transmission line, no reflection is occurring, and:

$$\frac{V_j(z_{\text{obs}})}{V_m(z_{\text{obs}})} = \frac{V_j^+(z_{\text{obs}})}{V_m^+(z_{\text{obs}})} = \frac{V_j^+(z_{\text{src}})}{V_m^+(z_{\text{src}})}e^{-jk_{z1}|z_{\text{obs}}-z_{\text{src}}|} = \frac{V_j(z_{\text{src}})}{V_m(z_{\text{src}})}e^{-jk_{z1}|z_{\text{obs}}-z_{\text{src}}|},$$

and, in this case, $Z(z_{\text{obs}}) = Z_{\infty 1}$.

Homogeneous half-plane with PEC plane: image theorem

In this section an alternative derivation of the previous results is proposed; this procedure is based on the application of the image theorem to the transmission line. It is straightforward to prove that the two circuits represented in Fig. E.6 are equivalent; indeed, by adding the voltage contributions coming from the image and from the original sources at $z = 0$, it is possible to observe that in this point voltage equals zero.

In Fig. E.7 the two equivalent circuits at $z = -z_{\text{src}}$ and at $z = z_{\text{src}}$ are reported, where the image current generator has opposite sign; the contributions coming from
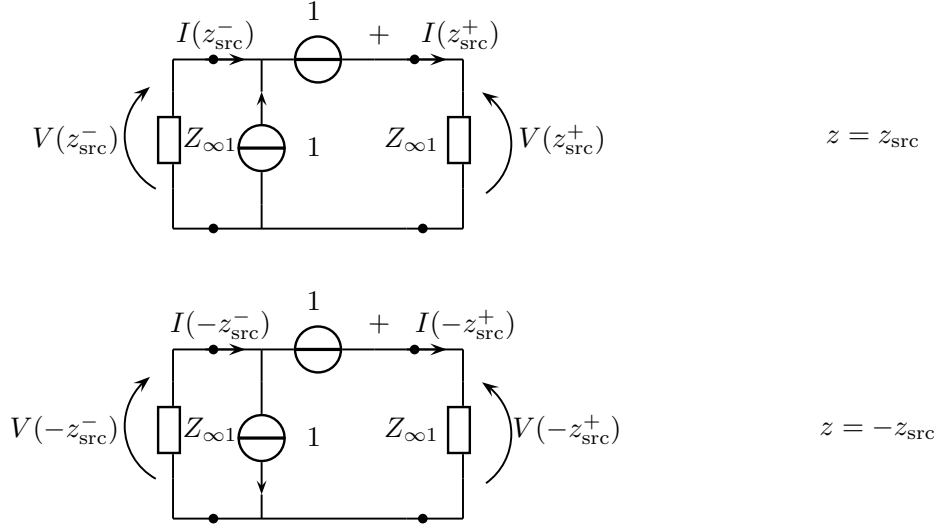
Figure E.7: Equivalent Thévenin circuits at $z = z_{\text{src}}$ and at $z = -z_{\text{src}}$.

the left sources are identified by the superscript "i" (image), whereas the ones coming from the right sources by "d" (direct). For the left part, only the contributions that go towards z are useful, because this circuit is equivalent to the previous one only for $z > 0$; for the $z < 0$ part of the circuit:

$$V_{\text{m}}^{(\text{i})}(-z_{\text{src}}^{+}) = \frac{1}{2}$$

$$I_{\text{j}}^{(\text{i})}(-z_{\text{src}}^{+}) = -\frac{1}{2} \implies V_{\text{j}}^{(\text{i})}(-z_{\text{src}}^{+}) = -\frac{1}{2}Z_{\infty 1}.$$

Instead, for the right circuit, it is equal to the homogeneous space case, here recalled:

$$I_{\text{j}}^{(\text{d})}(z_{\text{src}}^{+}) = \frac{1}{2}, \qquad V_{\text{j}}^{(\text{d})}(z_{\text{src}}^{+}) = \frac{1}{2}Z_{\infty 1}$$

$$I_{\text{j}}^{(\text{d})}(z_{\text{src}}^{-}) = -\frac{1}{2}, \qquad V_{\text{j}}^{(\text{d})}(z_{\text{src}}^{-}) = \frac{1}{2}Z_{\infty 1}$$

$$V_{\text{m}}^{(\text{d})}(z_{\text{src}}^{+}) = \frac{1}{2}, \qquad I_{\text{m}}^{(\text{d})}(z_{\text{src}}^{+}) = \frac{1}{2Z_{\infty 1}}$$

$$V_{\text{m}}^{(\text{d})}(z_{\text{src}}^{-}) = -\frac{1}{2}, \qquad I_{\text{m}}^{(\text{d})}(z_{\text{src}}^{-}) = \frac{1}{2Z_{\infty 1}}.$$

In both cases, the sources are radiating in free-space, so no reflections are occurring:

$$\begin{matrix} V_{\text{j}}(z_{\text{obs}}) \\ V_{\text{m}}(z_{\text{obs}}) \end{matrix} = \begin{matrix} V_{\text{j}}^{(\text{d})}(z_{\text{src}}^{\pm}) \\ V_{\text{m}}^{(\text{d})}(z_{\text{src}}^{\pm}) \end{matrix} e^{-jk_{z1}|z_{\text{obs}} - z_{\text{src}}|} + \begin{matrix} V_{\text{j}}^{(\text{i})}(-z_{\text{src}}^{+}) \\ V_{\text{m}}^{(\text{i})}(-z_{\text{src}}^{+}) \end{matrix} e^{-jk_{z1}(z_{\text{obs}} + z_{\text{src}})}.$$

On each point, $Z(z_{\text{obs}}) = Z_{\infty 1}$.
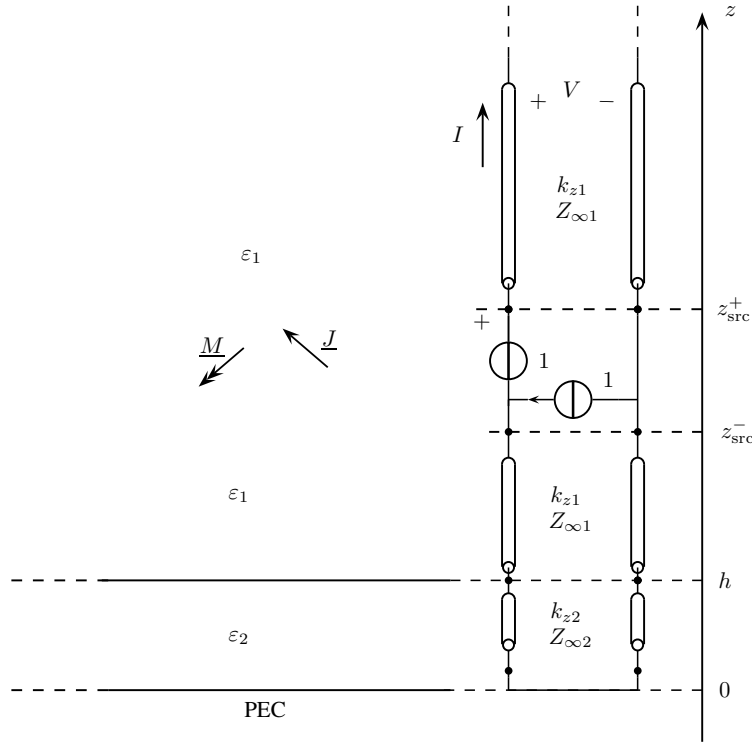
Figure E.8: Equivalent transmission line for the dielectric slab.

Dielectric slab with ground plane

In this section the formulation of the spectral domain Green's function of a dielectric slab backed by a ground plane of Fig. E.8 will be derived. The ground plane is located at $z = 0$ and the dielectric discontinuity is in $z = h$. Since this problem is useful to model a slot printed on a ground plane, it is interesting to compute the magnetic field on the ground plane, and the electric and magnetic field in a generic point of the region filled with dielectric ε_1, so for $z > h$.

Case 1: $z_{\mathrm{src}} = 0$

In this situation it is necessary to solve the circuit in Fig. E.9 with a voltage generator in $z = 0$. The input impedance seen from $z = 0$ is calculated by solving the circuit in Fig. E.10; the first step is the calculation of the reflection coefficient at the dielectric discontinuity:

$$\Gamma_{\mathrm{C}-} = \frac{Z_{\infty 1} - Z_{\infty 2}}{Z_{\infty 1} + Z_{\infty 2}} \triangleq \Gamma_{21}.$$

This reflection coefficient is now propagated to $z = 0^+$, so:

$$\Gamma_{\mathrm{B}+} = \Gamma_{\mathrm{C}-}\mathrm{e}^{-\mathrm{j}2k_{z2}h}.$$

Figure E.9: Equivalent transmission line for the dielectric slab: scenario of $z_{\mathrm{src}} = 0$.

Figure E.10: Circuit to be solved for the evaluation of the input impedance seen from the ground plane.

Then:

$$
Z_{\text{in}} = \frac{1 + \Gamma_{\text{B}^+}}{1 - \Gamma_{\text{B}^+}} Z_{\infty 1} = \frac{1 + \dfrac{Z_{\infty 1} - Z_{\infty 2}}{Z_{\infty 1} + Z_{\infty 2}} \text{e}^{-\text{j}2k_{z2}h}}{1 - \dfrac{Z_{\infty 1} - Z_{\infty 2}}{Z_{\infty 1} + Z_{\infty 2}} \text{e}^{-\text{j}2k_{z2}h}} =
$$
$$
= \frac{Z_{\infty 1} + Z_{\infty 2} + (Z_{\infty 1} - Z_{\infty 2}) \, \text{e}^{-\text{j}2k_{z2}h}}{Z_{\infty 1} + Z_{\infty 2} - (Z_{\infty 1} - Z_{\infty 2}) \, \text{e}^{-\text{j}2k_{z2}h}}. \tag{E.87}
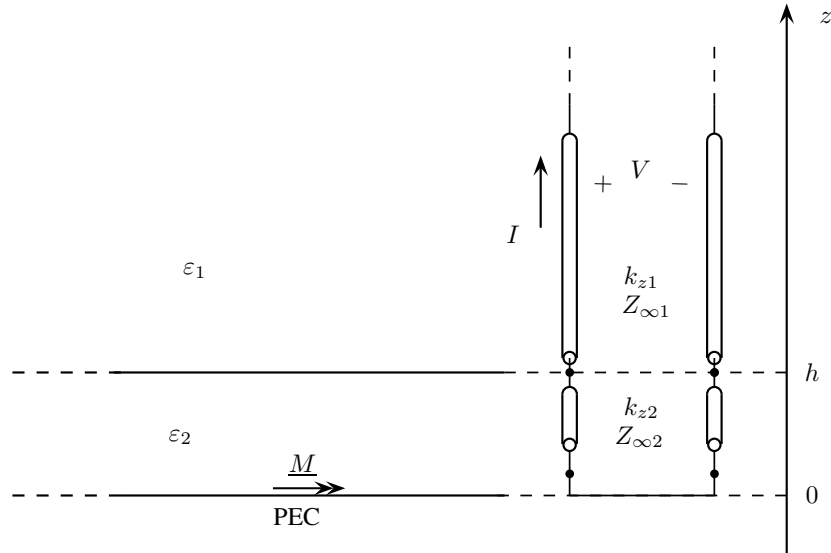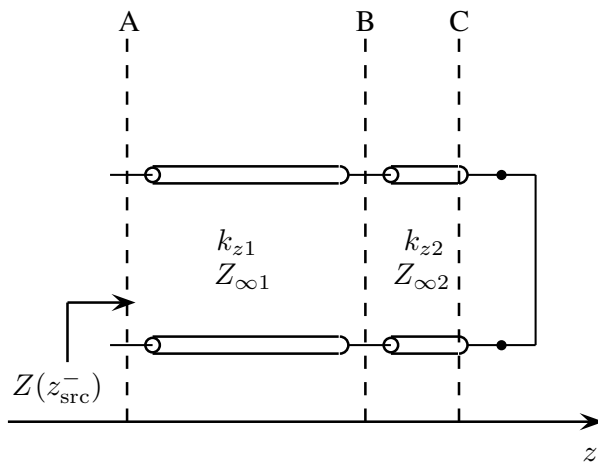$$

If $z_{\text{obs}} = z_{\text{src}} = 0$, the calculation is complete; instead, if $z_{\text{obs}} > h$:

$$
V(z_{\text{obs}}) = V^+(z_{\text{obs}}) = V^+(h^+)\text{e}^{-\text{j}k_{z1}(z_{\text{obs}}-h)} = V(h^+)\text{e}^{-\text{j}k_{z1}(z_{\text{obs}}-h)} =
$$
$$
= V^+(h^-) \left[1 + \Gamma_{\text{C}^-}\right] \text{e}^{-\text{j}k_{z1}(z_{\text{obs}}-h)} =
$$
$$
= V^+(0^+) \left[1 + \Gamma_{\text{C}^-}\right] \text{e}^{-\text{j}k_{z1}(z_{\text{obs}}-h)}\text{e}^{-\text{j}k_{z2}h} =
$$
$$
= V(0)\frac{1 + \Gamma_{\text{C}^-}}{1 + \Gamma_{\text{B}^+}}\text{e}^{-\text{j}k_{z1}z_{\text{obs}}}\text{e}^{-\text{j}(k_{z2}-k_{z1})h}, \tag{E.88}
$$

where $V(0) = 1$, since it equals the voltage of the voltage generator that models the presence of a magnetic current density at $z = 0$.

Case 2: $z_{\text{src}} > 0$

Input impedance

Observing from $z = z_{\text{src}}$ to the right, there is an unbounded region filled with dielectric ε_1; therefore, the impedance seen from right is $Z_{\infty 1}$. In order to evaluate the impedance observed looking from $z = z_{\text{src}}$ to the left, it is necessary to solve the circuit of Fig. E.11. There are three relevant sections: A, B, C; $l_{\text{AB}} = z_{\text{src}} - h$, $l_{\text{BC}} = h$. Since this transmission line is loaded on a short circuit,

$$
\Gamma_{\text{C}^-} = -1 \qquad \Longrightarrow \Gamma_{\text{B}^+} = -\text{e}^{-\text{j}2k_{z2}l_{\text{BC}}}.
$$

It is known that, in order to obtain the normalized impedance from the reflection coefficient,

$$
\zeta_{\text{B}^+} = \frac{1 + \Gamma_{\text{B}^+}}{1 - \Gamma_{\text{B}^+}} = \frac{1 - \text{e}^{-\text{j}2k_{z2}l_{\text{BC}}}}{1 + \text{e}^{-\text{j}2k_{z2}l_{\text{BC}}}},
$$

so, to solve the impedance discontinuity,

$$
\zeta_{\text{B}^-} = \frac{Z_{\infty 2}}{Z_{\infty 1}}\zeta_{\text{B}^+} = \frac{Z_{\infty 2}}{Z_{\infty 1}}\frac{1 - \text{e}^{-\text{j}2k_{z2}l_{\text{BC}}}}{1 + \text{e}^{-\text{j}2k_{z2}l_{\text{BC}}}}.
$$

Then, from here:

$$
\Gamma_{\mathrm{B}^-} = \frac{\zeta_{\mathrm{B}^-} - 1}{\zeta_{\mathrm{B}^-} + 1} =
$$

$$
= \frac{\dfrac{Z_{\infty 2}}{Z_{\infty 1}}\dfrac{1 - \mathrm{e}^{-\mathrm{j}2k_{z2}l_{\mathrm{BC}}}}{1 + \mathrm{e}^{-\mathrm{j}2k_{z2}l_{\mathrm{BC}}}} - 1}{\dfrac{Z_{\infty 2}}{Z_{\infty 1}}\dfrac{1 - \mathrm{e}^{-\mathrm{j}2k_{z2}l_{\mathrm{BC}}}}{1 + \mathrm{e}^{-\mathrm{j}2k_{z2}l_{\mathrm{BC}}}} + 1} = \frac{Z_{\infty 2}\left[1 - \mathrm{e}^{-\mathrm{j}2k_{z2}l_{\mathrm{BC}}}\right] - Z_{\infty 1}\left[1 + \mathrm{e}^{-\mathrm{j}2k_{z2}l_{\mathrm{BC}}}\right]}{Z_{\infty 2}\left[1 - \mathrm{e}^{-\mathrm{j}2k_{z2}l_{\mathrm{BC}}}\right] + Z_{\infty 1}\left[1 + \mathrm{e}^{-\mathrm{j}2k_{z2}l_{\mathrm{BC}}}\right]} =
$$

$$
= \frac{Z_{\infty 2} - Z_{\infty 1} + \mathrm{e}^{-\mathrm{j}2k_{z2}l_{\mathrm{BC}}}\left[-Z_{\infty 2} - Z_{\infty 1}\right]}{Z_{\infty 2} + Z_{\infty 1} + \mathrm{e}^{-\mathrm{j}2k_{z2}l_{\mathrm{BC}}}\left[-Z_{\infty 2} + Z_{\infty 1}\right]} =
$$

$$
= \frac{\dfrac{Z_{\infty 2} - Z_{\infty 1}}{Z_{\infty 2} + Z_{\infty 1}} - \mathrm{e}^{-\mathrm{j}2k_{z2}l_{\mathrm{BC}}}}{1 - \dfrac{Z_{\infty 2} - Z_{\infty 1}}{Z_{\infty 2} + Z_{\infty 1}}\mathrm{e}^{-\mathrm{j}2k_{z2}l_{\mathrm{BC}}}}.
$$

Let Γ_{21} be:

$$
\Gamma_{21} \triangleq \frac{Z_{\infty 2} - Z_{\infty 1}}{Z_{\infty 2} + Z_{\infty 1}},
$$

so, this becomes:

$$
\Gamma_{\mathrm{B}^-} = \frac{\Gamma_{21} - \mathrm{e}^{-\mathrm{j}2k_{z2}l_{\mathrm{BC}}}}{1 - \Gamma_{21}\mathrm{e}^{-\mathrm{j}2k_{z2}l_{\mathrm{BC}}}}.
$$

Now, it is possible to propagate this coefficient up to the section A^+, obtaining:

$$
\Gamma_{\mathrm{A}^+} = \Gamma_{\mathrm{B}^-}\mathrm{e}^{-\mathrm{j}2k_{z1}l_{\mathrm{AB}}},
$$

and then, finally:

$$
Z(z_{\mathrm{src}}) = Z_{\infty 1}\frac{1 + \Gamma_{\mathrm{A}^+}}{1 - \Gamma_{\mathrm{A}^+}} =
$$

$$
= Z_{\infty 1}\frac{1 + \dfrac{\Gamma_{21} - \mathrm{e}^{-\mathrm{j}2k_{z2}l_{\mathrm{BC}}}}{1 - \Gamma_{21}\mathrm{e}^{-\mathrm{j}2k_{z2}l_{\mathrm{BC}}}}\mathrm{e}^{-\mathrm{j}2k_{z1}l_{\mathrm{AB}}}}{1 - \dfrac{\Gamma_{21} - \mathrm{e}^{-\mathrm{j}2k_{z2}l_{\mathrm{BC}}}}{1 - \Gamma_{21}\mathrm{e}^{-\mathrm{j}2k_{z2}l_{\mathrm{BC}}}}\mathrm{e}^{-\mathrm{j}2k_{z1}l_{\mathrm{AB}}}} =
$$

$$
= Z_{\infty 1}\frac{1 - \Gamma_{21}\mathrm{e}^{-\mathrm{j}2k_{z2}l_{\mathrm{BC}}} + \left[\Gamma_{21} - \mathrm{e}^{-\mathrm{j}2k_{z2}l_{\mathrm{BC}}}\right]\mathrm{e}^{-\mathrm{j}2k_{z1}l_{\mathrm{AB}}}}{1 - \Gamma_{21}\mathrm{e}^{-\mathrm{j}2k_{z2}l_{\mathrm{BC}}} - \left[\Gamma_{21} - \mathrm{e}^{-\mathrm{j}2k_{z2}l_{\mathrm{BC}}}\right]\mathrm{e}^{-\mathrm{j}2k_{z1}l_{\mathrm{AB}}}} =
$$

$$
= Z_{\infty 1} + \frac{2Z_{\infty 1}\left[\Gamma_{21} - \mathrm{e}^{-\mathrm{j}2k_{z2}l_{\mathrm{BC}}}\right]\mathrm{e}^{-\mathrm{j}2k_{z1}l_{\mathrm{AB}}}}{1 - \Gamma_{21}\mathrm{e}^{-\mathrm{j}2k_{z2}l_{\mathrm{BC}}} - \left[\Gamma_{21} - \mathrm{e}^{-\mathrm{j}2k_{z2}l_{\mathrm{BC}}}\right]\mathrm{e}^{-\mathrm{j}2k_{z1}l_{\mathrm{AB}}}}. \tag{E.89}
$$

In the last expression the input impedance has been divided into two parts: the one seen from z_{src} looking from left, $Z_{\infty 1}$, plus another term. It should be observed that, if $\varepsilon_2 = \varepsilon_1$, the latter term equals zero; indeed, in this case, the slab is actually a

homogeneous space. This can be interpreted as a free space contribution, plus the dielectric discontinuity one. Let us define Z_{im} as:

$$Z_{\mathrm{im}} \triangleq \frac{2Z_{\infty 1}\left[\Gamma_{21} - \mathrm{e}^{-\mathrm{j}2k_{z2}l_{\mathrm{BC}}}\right]\mathrm{e}^{-\mathrm{j}2k_{z1}l_{\mathrm{AB}}}}{1 - \Gamma_{21}\mathrm{e}^{-\mathrm{j}2k_{z2}l_{\mathrm{BC}}} - \left[\Gamma_{21} - \mathrm{e}^{-\mathrm{j}2k_{z2}l_{\mathrm{BC}}}\right]\mathrm{e}^{-\mathrm{j}2k_{z1}l_{\mathrm{AB}}}}. \tag{E.90}$$

It can be observed that in the case of no dielectric contrast, *i.e.*, $\varepsilon_1 = \varepsilon_1$, we have $\Gamma_{21} = 0$, and this expression degenerates to (E.80):

$$Z_{\mathrm{im}} = -2Z_{\infty 1}\frac{\mathrm{e}^{-\mathrm{j}2k_{z1}(l_{\mathrm{AB}}+l_{\mathrm{BC}})}}{1 + \mathrm{e}^{-\mathrm{j}2k_{z1}(l_{\mathrm{AB}}+l_{\mathrm{BC}})}},$$

so, $Z_{\mathrm{im}} + Z_{\infty 1}$ equals the input impedance of a transmission line with parameters k_{z1}, $Z_{\infty 1}$ long $l_{\mathrm{AB}} + l_{\mathrm{BC}}$ and closed on a short circuit. If $h = 0$, $l_{\mathrm{AB}} = z_{\mathrm{src}}$, while $l_{\mathrm{BC}} = 0$, and we obtain the same expression of the $\Gamma_{21} = 0$ case.

$z_{\mathrm{src}} > z_{\mathrm{obs}}$ **case**

If $z_{\mathrm{src}} > z_{\mathrm{obs}}$, it is possible to use (E.81) and (E.83) to write the expressions of voltage at $z = z_{\mathrm{src}}^-$:

$$V_{\mathrm{m}}(z_{\mathrm{src}}^-) = -\frac{1}{2} - \frac{1}{2}\frac{Z_{\mathrm{im}}}{2Z_{\infty 1} + Z_{\mathrm{im}}}$$

$$V_{\mathrm{j}}(z_{\mathrm{src}}^-) = \left[-\frac{1}{2} + \frac{1}{2}\frac{Z_{\mathrm{im}}}{2Z_{\infty 1} + Z_{\mathrm{im}}}\right][Z_{\infty 1} + Z_{\mathrm{im}}].$$

The following quantities are defined:

$$V(z_{\mathrm{src}}^-) = V_{\mathrm{m}}(z_{\mathrm{src}}^-) + V_{\mathrm{j}}(z_{\mathrm{src}}^-)$$

$$V(z_{\mathrm{obs}}) = V_{\mathrm{m}}(z_{\mathrm{obs}}) + V_{\mathrm{j}}(z_{\mathrm{obs}}).$$

Now, the voltage in $z = z_{\mathrm{obs}}$ between the sections A and B is calculated:

$$V(z_{\mathrm{obs}}) = V^+(z_{\mathrm{obs}})\left[1 + \Gamma(z_{\mathrm{obs}})\right] = V^+(z_{\mathrm{src}})\mathrm{e}^{-\mathrm{j}k_{z1}|z_{\mathrm{src}}-z_{\mathrm{obs}}|}\left[1 + \Gamma(z_{\mathrm{obs}})\right] =$$

$$= V(z_{\mathrm{src}}^-)\frac{1 + \Gamma(z_{\mathrm{obs}})}{1 + \Gamma(z_{\mathrm{src}})}\mathrm{e}^{-\mathrm{j}k_{z1}|z_{\mathrm{src}}-z_{\mathrm{obs}}|} =$$

$$= V(z_{\mathrm{src}}^-)\frac{1 + \Gamma(z_{\mathrm{obs}}) + \Gamma(z_{\mathrm{src}}) - \Gamma(z_{\mathrm{src}})}{1 + \Gamma(z_{\mathrm{src}})}\mathrm{e}^{-\mathrm{j}k_{z1}|z_{\mathrm{src}}-z_{\mathrm{obs}}|} =$$

$$= V(z_{\mathrm{src}}^-)\left[1 + \frac{\Gamma(z_{\mathrm{obs}}) - \Gamma(z_{\mathrm{src}})}{1 + \Gamma(z_{\mathrm{src}})}\right]\mathrm{e}^{-\mathrm{j}k_{z1}|z_{\mathrm{src}}-z_{\mathrm{obs}}|},$$

where:

$$\Gamma(z_{\text{obs}}) = \Gamma_{\text{B}-}e^{-\text{J}2k_{z1}(z_{\text{obs}}-h)} \qquad \Gamma(z_{\text{src}}) = \Gamma_{\text{B}-}e^{-\text{J}2k_{z1}(z_{\text{src}}-h)}.$$

Several complications arise for the analysis of this structure. Indeed, in this case, $G_{xy} \neq G_{yx}$, owing to the presence of the slab. Moreover, if no slab is present, it is possible to distinguish the image and direct contributions, to calculate the direct ones with the well known methods, and the images with efficient calculations (for instance, by means of asymptotic evaluations). Instead, in this case the direct contribution can not be propagated in the homogeneous space. In order to prove this statement, now $V_{\text{m}}(z_{\text{obs}})$ will be explicitly calculated:

$$V_{\text{m}}(z_{\text{obs}}) = \left[-\frac{1}{2} - \frac{1}{2}\frac{Z_{\text{im}}}{2Z_{\infty1} + Z_{\text{im}}} \right] \left[1 + \frac{\Gamma(z_{\text{obs}}) - \Gamma(z_{\text{src}})}{1 + \Gamma(z_{\text{src}})} \right] e^{-jk_{z1}|z_{\text{src}}-z_{\text{obs}}|} =$$

$$= -\frac{1}{2}e^{-jk_{z1}|z_{\text{src}}-z_{\text{obs}}|} +$$

$$- \frac{1}{2}e^{-jk_{z1}|z_{\text{src}}-z_{\text{obs}}|} \left[\frac{\Gamma(z_{\text{obs}}) - \Gamma(z_{\text{src}})}{1 + \Gamma(z_{\text{src}})} + \right.$$

$$\left. + \frac{Z_{\text{im}}}{2Z_{\infty1} + Z_{\text{im}}} \frac{\Gamma(z_{\text{obs}}) - \Gamma(z_{\text{src}})}{1 + \Gamma(z_{\text{src}})} + \frac{Z_{\text{im}}}{2Z_{\infty1} + Z_{\text{im}}} \right].$$

The first term is a homogeneous-space contribution, so it can be calculated using the routines based on the spatial homogeneous space Green's function. Instead, the second contribution comes from the presence of the slab and of the ground plane. In other words, there are two direct contributions, and two image contributions; moreover, the second direct contribution can not be calculated directly in the spatial domain, because of the voltage/current divider, which has no closed-form inverse Fourier transform (Z_{im} is a function of the geometry). It is possible to define $Z(z_{\text{obs}})$ as the impedance seen in $z = z_{\text{obs}}$; therefore, it can be calculated as:

$$Z(z_{\text{obs}}) = \frac{1 + \Gamma(z_{\text{obs}})}{1 - \Gamma(z_{\text{obs}})}.$$

It should be remarked that these complications arise from the presence of the dielectric slab; indeed, if there is no air gap, it is possible to compute the image contribution by applying the image theorem to the transmission line, and by considering only the generator located in $-z_{\text{src}}$; in this case it is not possible to isolate the free-space part simply by ignoring the generators located at z_{src}, owing to the presence the slab; this can be seen studying the impedance seen from this generator, which has a contribution coming from the dielectric discontinuity.

$z_{\text{src}} < z_{\text{obs}}$ **case**

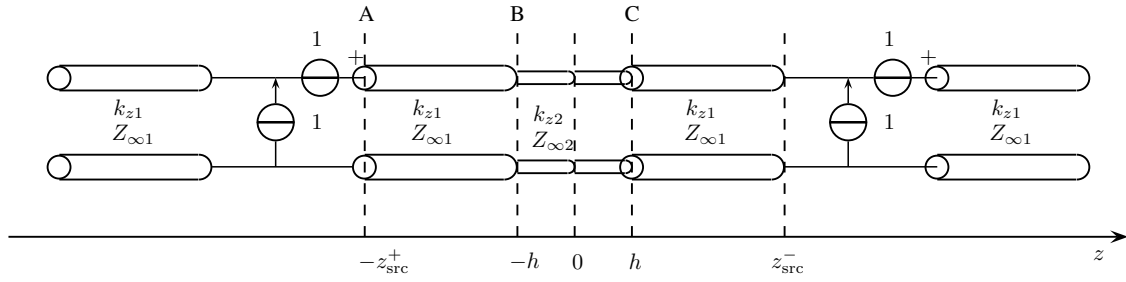If $z_{\text{src}} < z_{\text{obs}}$, it is possible to use (E.84) and (E.86):

Figure E.11: Equivalent transmission line of the slab backed by ground plane, after the application of the image theorem.

$$V_{\mathrm{m}}(z_{\mathrm{src}}^+) = \frac{1}{2} - \frac{1}{2}\frac{Z_{\mathrm{im}}}{2Z_{\infty 1} + Z_{\mathrm{im}}}$$

$$V_{\mathrm{j}}(z_{\mathrm{src}}^+) = Z_{\infty 1}\left[\frac{1}{2} + \frac{1}{2}\frac{Z_{\mathrm{im}}}{2Z_{\infty 1} + Z_{\mathrm{im}}}\right].$$

Then, let $V(z_{\mathrm{src}}^+)$ be:

$$V(z_{\mathrm{src}}^+) = V_{\mathrm{m}}(z_{\mathrm{src}}^+) + V_{\mathrm{j}}(z_{\mathrm{src}}^+),$$

and, by recalling that:

$$V(z_{\mathrm{obs}}) = V_{\mathrm{m}}(z_{\mathrm{obs}}) + V_{\mathrm{j}}(z_{\mathrm{obs}}),$$

follows

$$V(z_{\mathrm{obs}}) = V^+(z_{\mathrm{obs}}) = V^+(z_{\mathrm{src}})\mathrm{e}^{-\mathrm{j}k_{z1}|z_{\mathrm{obs}} - z_{\mathrm{src}}|} = V(z_{\mathrm{src}})\mathrm{e}^{-\mathrm{j}k_{z1}|z_{\mathrm{obs}} - z_{\mathrm{src}}|}.$$

Indeed, since the transmission line is semi-infinitely long, only progressive waves are present. In this situation, $Z(z_{\mathrm{obs}}) = Z_{\infty 1}$.

Dielectric slab with ground plane: application of the image theorem

The scenario of Fig. E.7 can be studied also by applying the image theorem; this leads to the circuit in Fig. E.11. It is possible to obtain the Thévenin equivalent circuits in Fig. E.12. The impedance Z_{im} is the same in the two circuits. Now, its expression will be calculated explicitly.

$$\Gamma_{\mathrm{C}^-} = \frac{Z_{\infty 1} - Z_{\infty 2}}{Z_{\infty 1} + Z_{\infty 2}},$$
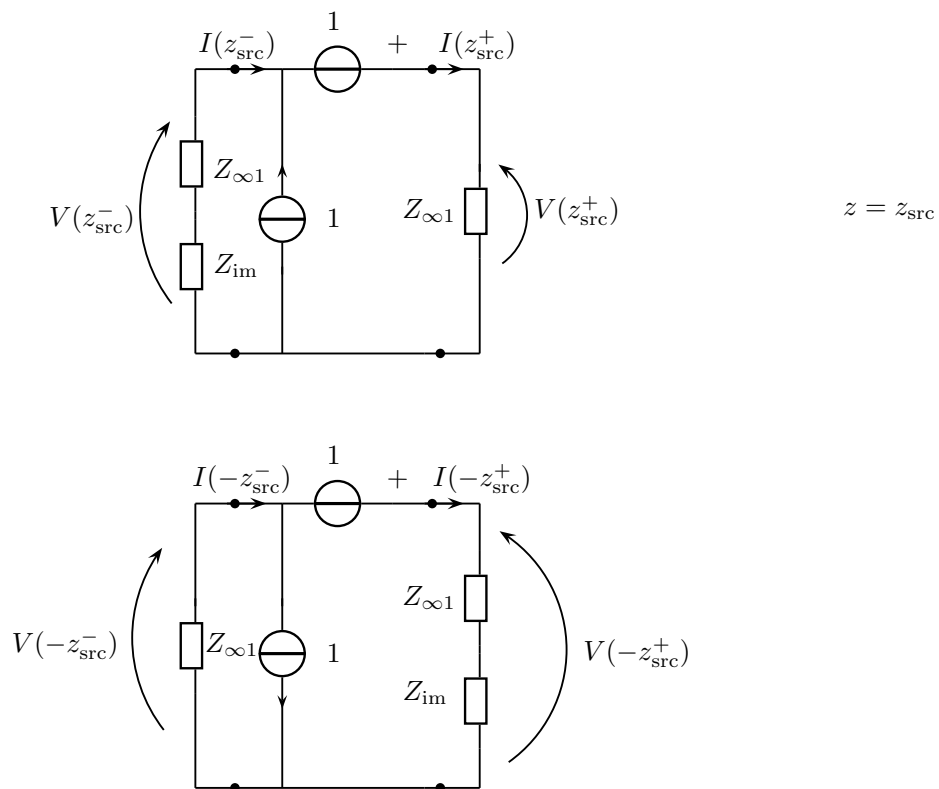
so:

Figure E.12: Equivalent transmission line of the slab backed by ground plane, after the application of the image theorem.

$$\Gamma_{\mathrm{B+}} = \Gamma_{\mathrm{C-}}\mathrm{e}^{-\mathrm{j}2k_{z2}(2h)}.$$

Then, the reflection coefficient after the discontinuity is:

$$\Gamma_{\mathrm{B-}} = \frac{\Gamma_{12} + \Gamma_{\mathrm{B+}}}{1 + \Gamma_{12}\Gamma_{\mathrm{B+}}},$$

where:

$$\Gamma_{12} = \frac{Z_{\infty 2} - Z_{\infty 1}}{Z_{\infty 2} + Z_{\infty 1}}.$$

Then:

$$\Gamma_{\mathrm{A+}} = \Gamma_{\mathrm{B-}}\mathrm{e}^{-\mathrm{j}2k_{z1}(z_{\mathrm{src}}-h)},$$

and, finally:

$$Z_{\mathrm{in}} = \frac{1 + \Gamma_{\mathrm{A+}}}{1 - \Gamma_{\mathrm{A+}}}Z_{\infty 1} = Z_{\infty 1}1 - 2Z_{\infty 1}\frac{\Gamma_{\mathrm{A+}}}{1 - \Gamma_{\mathrm{A+}}} \triangleq Z_{\infty 1} + Z_{\mathrm{im}}.$$

Then, if $z_{\mathrm{obs}} > h$, it is possible to write the expression of the voltage in this point as a function of the image generators as:

$$
\begin{aligned}
V(z_{\mathrm{obs}}) = V^+(z_{\mathrm{obs}}) &= V^+(h^+)\mathrm{e}^{-\mathrm{j}k_{z1}(z_{\mathrm{obs}}-h)} = V(h)\mathrm{e}^{-\mathrm{j}k_{z1}(z_{\mathrm{obs}}-h)} = \\
&= V^+(h^-)\left[1 + \Gamma_{\mathrm{C-}}\right]\mathrm{e}^{-\mathrm{j}k_{z1}(z_{\mathrm{obs}}-h)} = V^+(-h^+)\mathrm{e}^{-\mathrm{j}k_{z2}(2h)}\mathrm{e}^{-\mathrm{j}k_{z1}(z_{\mathrm{obs}}-h)}\left[1 + \Gamma_{\mathrm{C-}}\right] = \\
&= V^+(-h^-)\frac{1 + \Gamma_{\mathrm{B-}}}{1 + \Gamma_{\mathrm{B+}}}\mathrm{e}^{-\mathrm{j}k_{z2}(2h)}\mathrm{e}^{-\mathrm{j}k_{z1}(z_{\mathrm{obs}}-h)}\left[1 + \Gamma_{\mathrm{C-}}\right] = \\
&= V^+(-z_{\mathrm{src}}^+)\mathrm{e}^{-\mathrm{j}k_{z1}(z_{\mathrm{src}}-h)}\frac{1 + \Gamma_{\mathrm{B-}}}{1 + \Gamma_{\mathrm{B+}}}\mathrm{e}^{-\mathrm{j}k_{z2}(2h)}\mathrm{e}^{-\mathrm{j}k_{z1}(z_{\mathrm{obs}}-h)}\left[1 + \Gamma_{\mathrm{C-}}\right] = \\
&= V(-z_{\mathrm{src}}^+)\frac{1 + \Gamma_{\mathrm{C-}}}{1 + \Gamma_{\mathrm{A+}}}\frac{1 + \Gamma_{\mathrm{B-}}}{1 + \Gamma_{\mathrm{B+}}}\mathrm{e}^{-\mathrm{j}k_{z1}(z_{\mathrm{obs}}-h)}\mathrm{e}^{-\mathrm{j}k_{z1}(z_{\mathrm{src}}-h)}\mathrm{e}^{-\mathrm{j}k_{z2}(2h)},
\end{aligned}
$$

where:

$$V(-z_{\mathrm{src}}^+) = V_{\mathrm{m}}(-z_{\mathrm{src}}^+) + V_{\mathrm{j}}(-z_{\mathrm{src}}^+),$$

and:

$$V_{\mathrm{m}}(-z_{\mathrm{src}}^+) = \frac{Z_{\infty 1} + Z_{\mathrm{im}}}{2Z_{\infty 1} + Z_{\mathrm{im}}}$$

$$V_{\mathrm{j}}(-z_{\mathrm{src}}^+) = -\frac{Z_{\infty 1}}{2Z_{\infty 1} + Z_{\mathrm{im}}}\left[Z_{\infty 1} + Z_{\mathrm{im}}\right].$$

E.3 Method of moments - slot problem

The details of the MoM aimed at solving the slot problem are now reported. The unknown of the integral equation is $\mathbf{M}^{(\mathrm{s})}$; therefore, it is represented as a sum of known functions defined on $\Sigma_c^{(\mathrm{s})} \subset \Sigma^{(\mathrm{s})}$, weighted by unknown coefficients:

$$\mathbf{M}^{(\mathrm{s})}(x, y) = \sum_{c=1}^{N_{\mathrm{fun}}^{(\mathrm{s})}} x_c^{(\mathrm{s})} \mathbf{M}_c(x, y);$$

where the basis functions are defined in the following subsection. Recalling (5.3):

$$\sum_{n=1}^{N_{\mathrm{fun}}^{(\mathrm{s})}} x_n^{(\mathrm{s})} \iint_{\Sigma_n^{(\mathrm{s})}} \mathbf{G}(x, x', y, y') \cdot \mathbf{M}_n^{(\mathrm{s})}(x', y') \, \mathrm{d}x' \mathrm{d}y' = \mathbf{H}^{(\mathrm{inc})},$$

where $\mathbf{G}(x, x', y, y')$ is defined as

$$\mathbf{G}(x, x', y, y') = \mathbf{G}^{(0)}(x, x', y, y') + \mathbf{G}^{(1)}(x, x', y, y').$$

Since each of these Green's functions describe the k-th equivalent sub-problem, their contributions are non-vanishing for $z \geq 0$ ($\mathbf{G}^{(1)}$) or for $z \leq 0$ ($\mathbf{G}^{(0)}$). The last integral equation is finally discretized by testing it on the functions $\{\mathbf{M}_m\}$, leading to:

$$\sum_{n=1}^{N_{\mathrm{fun}}^{(\mathrm{s})}} x_n^{(\mathrm{s})} \iint_{\Sigma_m^{(\mathrm{s})}} \mathbf{M}_m(x, y) \cdot \iint_{\Sigma_n^{(\mathrm{s})}} \mathbf{G}(x, x', y, y') \cdot \mathbf{M}_n^{(\mathrm{s})}(x', y') \, \mathrm{d}x' \mathrm{d}y' =$$
$$= \iint_{\Sigma_m^{(\mathrm{s})}} \mathbf{M}_m(x, y) \cdot \mathbf{H}^{(\mathrm{inc})} \, \mathrm{d}x \, \mathrm{d}y.$$

Now, by focusing on the left-hand side term, the Green's function can be written as its inverse Fourier transform:

$$\mathbf{G}(x, x', y, y') = \frac{1}{4\pi^2} \iint_{\mathbb{R}^2} \widetilde{\mathbf{G}}(k_x, k_y) \mathrm{e}^{-\mathrm{j}k_x(x-x')} \mathrm{e}^{-\mathrm{j}k_y(y-y')} \, \mathrm{d}k_x \, \mathrm{d}k_y.$$

This is substituted in the left-hand side integral, leading to:

$$\frac{1}{4\pi^2} \iint_{\Sigma_m^{(\mathrm{s})}} \mathbf{M}_m(x, y) \cdot \iint_{\Sigma_n^{(\mathrm{s})}} \iint_{\mathbb{R}^2} \widetilde{\mathbf{G}}(k_x, k_y) \mathrm{e}^{-\mathrm{j}k_x(x-x')} \mathrm{e}^{-\mathrm{j}k_y(y-y')} \, \mathrm{d}k_x \, \mathrm{d}k_y \cdot$$
$$\cdot \mathbf{M}_n^{(\mathrm{s})}(x', y') \, \mathrm{d}x' \mathrm{d}y'.$$

After some internal re-arrangements, this becomes:

$$\iint_{\Sigma_m^{(\mathrm{s})}} \mathbf{M}_m(x,y)\mathrm{e}^{-\mathrm{j}k_x x}\mathrm{e}^{-\mathrm{j}k_y y}\mathrm{d}x\mathrm{d}y\cdot$$

$$\cdot \iint_{\mathbb{R}^2} \widetilde{\mathbf{G}}(k_x,k_y)\cdot \iint_{\Sigma_n^{(\mathrm{s})}} \mathrm{e}^{\mathrm{j}k_x x'}\mathrm{e}^{\mathrm{j}k_y y'}\cdot \mathbf{M}_n^{(\mathrm{s})}(x',y')\mathrm{d}x'\mathrm{d}y'\mathrm{d}k_x\,\mathrm{d}k_y.$$

But:

$$\widetilde{\mathbf{M}}_m^{(\mathrm{s})}(-k_x,-k_y) = \iint_{\Sigma_m^{(\mathrm{s})}} \mathbf{M}_m(x,y)\mathrm{e}^{-\mathrm{j}k_x x}\mathrm{e}^{-\mathrm{j}k_y y}\mathrm{d}x\mathrm{d}y$$

$$\widetilde{\mathbf{M}}_n^{(\mathrm{s})}(k_x,k_y) = \iint_{\Sigma_n^{(\mathrm{s})}} \mathbf{M}_n(x',y')\mathrm{e}^{\mathrm{j}k_x x}\mathrm{e}^{\mathrm{j}k_y y}\mathrm{d}x\mathrm{d}y,$$

and the integral equation becomes:

$$\sum_{n=1}^{N_{\mathrm{fun}}^{(\mathrm{s})}} x_n^{(\mathrm{s})} \iint_{\mathbb{R}^2} \widetilde{\mathbf{M}}_m^{(\mathrm{s})}(-k_x,-k_y)\cdot \widetilde{\mathbf{G}}(k_x,k_y)\cdot \widetilde{\mathbf{M}}_n^{(\mathrm{s})}(k_x,k_y)\,\mathrm{d}k_x\,\mathrm{d}k_y =$$

$$= \iint_{\Sigma_m^{(\mathrm{s})}} \mathbf{M}_m(x,y)\cdot \mathbf{H}^{(\mathrm{inc})}\,\mathrm{d}x\,\mathrm{d}y.$$

E.3.1 Basis functions

The following basis functions are defined:

$$\mathbf{M}_n(x,y) = \widehat{\mathbf{x}}\,f_n(x)\,g(y),$$

where $g(y)$ is an entire domain function, so it is not depending on n; two possible choices are now presented; let w be the width of the slot; then:

- edge-singular functions:

$$g^{(\mathrm{es})}(y) = \begin{cases} -\dfrac{2}{\pi w}\dfrac{1}{\sqrt{1-\left(\frac{2y}{w}\right)^2}}, & -\dfrac{w}{2}\le y\le \dfrac{w}{2} \\[4mm] 0, & \text{otherwise}. \end{cases}$$

It is possible to calculate the Fourier transform of this function as:

$$\mathcal{F}\left\{g^{(\mathrm{es})}(y)\right\} = -J_0\left(\frac{w}{2}k_y\right).$$

This function is interesting because it models the behavior of the slot at the edges; however, this is more complicated to be integrated.

- rect functions:

$$g(y) = \begin{cases} \frac{1}{w} & -\frac{w}{2} \leq y \leq \frac{w}{2} \\ 0, & \text{otherwise .} \end{cases}$$

It can be shown that:

$$\mathcal{F}\{g(y)\} = \frac{\sin\left(\frac{w}{2}k_y\right)}{\frac{w}{2}k_y}.$$

The second function will be used to represent the y dependence of the unknowns. For what concerns the x dependence on the unknown, piece-wise linear functions (PWL) are used; given N_{fun} the number of basis functions used to represent the unknown, the interval along x has to be divided in $N_{\text{fun}} + 2$ points, and then the N_{fun} intern points are considered; these points c_n are the centers of the PWL functions. So:

$$f_n(x) = \begin{cases} \frac{2}{a_{\text{BF}}}\left[\frac{a_{\text{BF}}}{2} - |x - c_n|\right], & c_n - \frac{a_{\text{BF}}}{2} \leq x \leq c_n + \frac{a_{\text{BF}}}{2} \\ 0, & \text{otherwise ,} \end{cases}$$

where $a_{\text{BF}} = c_2 - c_1$. It can be shown that:

$$\mathcal{F}\{f_n(x)\} = \int_{c_n - \frac{a_{\text{BF}}}{2}}^{c_n + \frac{a_{\text{BF}}}{2}} f_n(x) e^{jk_x x}\, dx = \frac{a_{\text{BF}}}{2}\frac{\sin^2\left(\frac{a_{\text{BF}}}{4}k_x\right)}{\left(\frac{a_{\text{BF}}}{4}k_x\right)^2}e^{jc_n k_x}.$$

To sum up (in the interval where the function is not equal to zero):

$$\mathbf{M}_n(x, y) = \widehat{\mathbf{x}}\, f_n(x)\, g(y) = \frac{2}{a_{\text{BF}}}\left[\frac{a_{\text{BF}}}{2} - |x - c_n|\right]\frac{1}{w},$$

and:

$$\widetilde{\mathbf{M}}_n(k_x, k_y) = \frac{a_{\text{BF}}}{2}\frac{\sin^2\left(\frac{a_{\text{BF}}}{4}k_x\right)}{\left(\frac{a_{\text{BF}}}{4}k_x\right)^2}e^{jc_n k_x}\frac{\sin\left(\frac{w}{2}k_y\right)}{\frac{w}{2}k_y}.$$

E.4   Method of moments - lens problem

The expression of electric field relative to the j-th problem is written according to the MPIE formulation:

$$\mathbf{E}_t^{(j)} = -j\omega\mu_0\int_{\mathcal{D}'} g_j(\mathbf{r} - \mathbf{r}')\mathbf{J}(\mathbf{r}')\, d\mathbf{r}' + \frac{1}{j\omega\varepsilon_0\varepsilon_j}\nabla\int_{\mathcal{D}'} g_j(\mathbf{r} - \mathbf{r}')\nabla \cdot \mathbf{J}(\mathbf{r}')\, d\mathbf{r}' +$$

$$- \int_{\mathcal{D}'}[\nabla g_j(\mathbf{r} - \mathbf{r}')] \times \mathbf{M}(\mathbf{r}')\, d\mathbf{r}'.$$
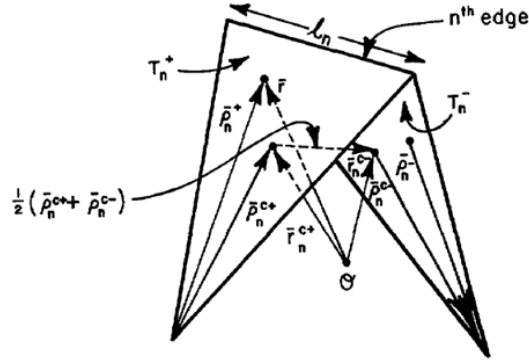
Figure E.13: Triangle pair and geometrical parameters associated with interior edge.

Here, $\mathcal{D}'$ is the source domain. Then:

$$g_j(\mathbf{r} - \mathbf{r}') = \frac{\mathrm{e}^{-\mathrm{j}k_j||\mathbf{r}-\mathbf{r}'||_2}}{4\pi\,||\mathbf{r}-\mathbf{r}'||_2}$$

$$k_j = \omega\sqrt{\mu_0\varepsilon_0\varepsilon_j} = k_0\sqrt{\varepsilon_j}. \tag{E.91}$$

Here only the direct contribution is accounted for; for what concerns the effect of the ground plane, the ground plane Green's function is used instead of the homogeneous one; its expression is derived in Appendix E.1.6. The unknowns of the problem $\mathbf{J}$ and $\mathbf{M}$ are represented as a linear combination of div-conforming functions $\{\mathbf{f}_n\}$; RWG basis functions are used as basis functions [53]:

$$\mathbf{f}_n(\mathbf{r}) = \begin{cases} \dfrac{l_n}{2A_n^+}\boldsymbol{\rho}_n^+, & \text{if } \mathbf{r} \in T_n^+ \\[2mm] \dfrac{l_n}{2A_n^-}\boldsymbol{\rho}_n^-, & \text{if } \mathbf{r} \in T_n^- \\[2mm] \underline{0} & \text{otherwise,} \end{cases} \tag{E.92}$$

where all the terms used in this definition are reported in Fig. E.13. The same set of functions is used for both the unknowns. So:

$$\mathbf{J}(\mathbf{r}) \simeq \sum_{c=1}^{N_{\mathrm{fun}}} x_c^{(\mathrm{j})}\mathbf{f}_c(\mathbf{r})$$

$$\mathbf{M}(\mathbf{r}) \simeq \sum_{c=1}^{N_{\mathrm{fun}}} x_c^{(\mathrm{m})}\mathbf{f}_c(\mathbf{r}). \tag{E.93}$$

These expressions can be substituted in the previous equation, obtaining:

$$\mathbf{E}_{\mathrm{t}}^{(j)} \simeq \sum_{c=1}^{N_{\mathrm{fun}}} x_c^{(\mathrm{j})} \left\{ -\mathrm{j}\omega\mu_0 \int_{\mathcal{D}'_c} g_j(\mathbf{r} - \mathbf{r}')\mathbf{f}_c(\mathbf{r}')\,\mathrm{d}\mathbf{r}' + \frac{1}{\mathrm{j}\omega\varepsilon_0\varepsilon_j}\nabla \int_{\mathcal{D}'_c} g_j(\mathbf{r} - \mathbf{r}')\nabla \cdot \mathbf{f}_c(\mathbf{r}')\,\mathrm{d}\mathbf{r}' \right\} +$$

$$- \sum_{c=1}^{N_{\mathrm{fun}}} x_c^{(\mathrm{m})} \int_{\mathcal{D}'_c} [\nabla g_j(\mathbf{r} - \mathbf{r}')] \times \mathbf{f}_c(\mathbf{r}')\,\mathrm{d}\mathbf{r}',$$

where $\mathcal{D}'_n$ is the support of the n-th expansion function used to represent the problem.

In order to complete the formulation of the method of moments for the electric field equation terms it is necessary to test these contributions on a set of functions $\mathbf{g}_r(\mathbf{r})$. Let us consider the following inner product definition:

$$\langle \mathbf{A}(\mathbf{r}), \mathbf{B}(\mathbf{r}) \rangle = \int_{\Sigma} \mathbf{A}(\mathbf{r}) \cdot \mathbf{B}(\mathbf{r})\,\mathrm{d}\mathbf{r} \tag{E.94}$$

(no conjugation operation is applied, since testing functions are assumed to be real). Then, for what concerns the electric field equation, let us consider:

$$\mathbf{g}_r(\mathbf{r}) = \mathbf{f}_r(\mathbf{r}),$$

meaning that the Galerkin form of the weighted residuals method is applied. Then, by exploiting linearity:

$$\left\langle \mathbf{E}_{\mathrm{t}}^{(j)}, \mathbf{f}_r(\mathbf{r}) \right\rangle = \sum_{c=1}^{N_{\mathrm{fun}}} x_c^{(\mathrm{j})} \left\{ -\mathrm{j}\omega\mu_0 \int_{\mathcal{D}_r} \mathbf{f}_r(\mathbf{r}) \cdot \int_{\mathcal{D}'_c} g_j(\mathbf{r} - \mathbf{r}')\mathbf{f}_c(\mathbf{r}')\,\mathrm{d}\mathbf{r}'\,\mathrm{d}\mathbf{r} + \right.$$

$$\left. + \frac{1}{\mathrm{j}\omega\varepsilon_0\varepsilon_j} \int_{\mathcal{D}_r} \mathbf{f}_r \cdot \nabla \int_{\mathcal{D}'_c} g_j(\mathbf{r} - \mathbf{r}')\nabla \cdot \mathbf{f}_c(\mathbf{r}')\,\mathrm{d}\mathbf{r}\,\mathrm{d}\mathbf{r}' \right\} +$$

$$- \sum_{c=1}^{N_{\mathrm{fun}}} x_c^{(\mathrm{m})} \int_{\mathcal{D}_r} \mathbf{f}_r(\mathbf{r}) \cdot \int_{\mathcal{D}'_c} [\nabla g_j(\mathbf{r} - \mathbf{r}')] \times \mathbf{f}_c(\mathbf{r}')\,\mathrm{d}\mathbf{r}'\,\mathrm{d}\mathbf{r} \quad \forall r = 1...N_{\mathrm{fun}}.$$
$$\tag{E.95}$$

The second integral (the one relative to the gradient of the scalar potential) is re-written in a different way, shifting the derivative operator to the test functions; let us prove this.

$$\int_{\mathcal{D}_r} \mathbf{f}_r(\mathbf{r}) \cdot \nabla\Phi(\mathbf{r})\,\mathrm{d}\mathbf{r} = \int_{\mathcal{D}_r} [\nabla \cdot (\Phi(\mathbf{r})\mathbf{f}_r(\mathbf{r})) - \Phi(\mathbf{r})\nabla \cdot \mathbf{f}_r(\mathbf{r})]\,\mathrm{d}\mathbf{r} =$$

$$= \int_{\mathcal{D}_r} \nabla \cdot (\Phi(\mathbf{r})\mathbf{f}_r(\mathbf{r}))\,\mathrm{d}\mathbf{r} - \int_{\mathcal{D}_r} \Phi(\mathbf{r})\nabla \cdot \mathbf{f}_r(\mathbf{r})\,\mathrm{d}\mathbf{r},$$

where the divergence version of the Leibnitz rule has been applied. Then, it is possible to apply the Ostrogradsky's theorem to the first integral:

$$\int_{\mathcal{D}_r} \nabla \cdot (\Phi(\mathbf{r})\mathbf{f}_r(\mathbf{r})) \, \mathrm{d}\mathbf{r} = \int_{\gamma \mathcal{D}_r} \widehat{\mathbf{n}}(\mathbf{r}) \cdot (\Phi(\mathbf{r})\mathbf{f}_r(\mathbf{r})) \, \mathrm{d}\mathbf{s}.$$

It is possible to prove that the boundary term equals zero; indeed, RWG basis functions have no normal components, exception made for the edge on which it is defined; however, in that edge, the boundary terms are neutralized due to the continuity property of the normal component to this edge, so no contributions should be counted. Therefore:

$$\int_{\mathcal{D}_r} \mathbf{f}_r(\mathbf{r}) \cdot \nabla \Phi(\mathbf{r}) \, \mathrm{d}\mathbf{r} = -\int_{\mathcal{D}_r} \Phi(\mathbf{r})\nabla \cdot \mathbf{f}_r(\mathbf{r}) \, \mathrm{d}\mathbf{r}.$$

Now, (E.94) can be re-written compactly, defining the following matrix elements:

$$(\mathbf{D}^{(j)})_{rc} = \mathrm{j}\omega\mu_0 \int_{\mathcal{D}_r} \mathbf{f}_r(\mathbf{r}) \cdot \int_{\mathcal{D}_c'} g_j(\mathbf{r} - \mathbf{r}')\mathbf{f}_c(\mathbf{r}') \, \mathrm{d}\mathbf{r}' \, \mathrm{d}\mathbf{r} +$$

$$+ \frac{1}{\mathrm{j}\omega\varepsilon_0\varepsilon_j} \int_{\mathcal{D}_r} \nabla \cdot \mathbf{f}_r(\mathbf{r}) \int_{\mathcal{D}_c'} g_j(\mathbf{r} - \mathbf{r}')\nabla \cdot \mathbf{f}_c(\mathbf{r}') \, \mathrm{d}\mathbf{r}' \mathrm{d}\mathbf{r} \qquad (\text{E.96})$$

$$(\mathbf{K}^{(j)})_{rc} = \int_{\mathcal{D}_r} \mathbf{f}_r(\mathbf{r}) \cdot \int_{\mathcal{D}_c'} [\nabla g_j(\mathbf{r} - \mathbf{r}')] \times \mathbf{f}_c(\mathbf{r}') \, \mathrm{d}\mathbf{r}' \, \mathrm{d}\mathbf{r}. \qquad (\text{E.97})$$

An observation on $(\mathbf{K}^{(j)})_{rc}$: assuming that $\mathcal{D}_r$ and $\mathcal{D}_c'$ lie on the same plane, this integral equals zero. To prove this, let us calculate the gradient of the scalar Green's function, calculated with respect to the source variable $\mathbf{r}'$; since it is defined in spherical coordinates, it is easier to perform this calculation in this reference system.

In spherical coordinates, the gradient of a scalar function that depends only on the r coordinate (just like in this case) $f = f(r)$ equals:

$$\nabla f = \widehat{\mathbf{r}}\frac{\partial f}{\partial r}, m$$

therefore, by applying the Leibnitz rule and the fact that we differentiate in $\mathrm{d}\mathbf{r}'$, we write:

$$\frac{\partial g_j}{\partial r'}\widehat{\mathbf{R}} = \left[-(-\mathrm{j}k_j)\frac{\mathrm{e}^{-\mathrm{j}k_j(r-r')}}{4\pi(r-r')} - \left(-\frac{\mathrm{e}^{-\mathrm{j}k_j(r-r')}}{4\pi(r-r')^2}\right)\right]\widehat{\mathbf{r}} = \left[\mathrm{j}k_j + \frac{1}{r-r'}\right]g_j(r-r')\widehat{\mathbf{R}}.$$
$$(\text{E.98})$$

If $\mathcal{D}_c'$ is on the same plane of $\mathcal{D}_r$, then $\widehat{\mathbf{r}}$, defined as:

$$\widehat{\mathbf{R}} = \frac{\mathbf{r} - \mathbf{r}'}{||\mathbf{r} - \mathbf{r}'||},$$

lies on the plane of $\mathcal{D}'_c$ and $\mathcal{D}_r$. This observation will be briefly useful; now, let us perform some manipulation on the integral; the first point is that $\mathbf{f}_m(\mathbf{r})$ is brought inside the inner integral, since the inner integral is in $\mathbf{r}'$ and so $\mathbf{f}_m(\mathbf{r})$ is constant with respect to it; so:

$$(\mathbf{K}^{(j)})_{rc} = \int_{\mathcal{D}_r} \mathbf{f}_r(\mathbf{r}) \cdot \int_{\mathcal{D}'_c} [\nabla g_j(\mathbf{r} - \mathbf{r}')] \times \mathbf{f}_c(\mathbf{r}')\, \mathrm{d}\mathbf{r}'\, \mathrm{d}\mathbf{r} =$$
$$\int_{\mathcal{D}_r} \int_{\mathcal{D}'_c} \mathbf{f}_r(\mathbf{r}) \cdot [\nabla g_j(\mathbf{r} - \mathbf{r}')] \times \mathbf{f}_c(\mathbf{r}')\, \mathrm{d}\mathbf{r}'\, \mathrm{d}\mathbf{r}.$$

Then, it is possible to use the property of the triple product as follows:

$$\int_{\mathcal{D}_r} \mathbf{f}_r(\mathbf{r}) \cdot \int_{\mathcal{D}'_c} [\nabla g_j(\mathbf{r} - \mathbf{r}')] \times \mathbf{f}_c(\mathbf{r}')\, \mathrm{d}\mathbf{r}'\, \mathrm{d}\mathbf{r} =$$
$$\int_{\mathcal{D}_r} \int_{\mathcal{D}'_c} [\nabla g_j(\mathbf{r} - \mathbf{r}')] \cdot \mathbf{f}_c(\mathbf{r}') \times \mathbf{f}_r(\mathbf{r})\, \mathrm{d}\mathbf{r}'\, \mathrm{d}\mathbf{r} = 0,$$

indeed, ∇g_j is parallel to $\widehat{\mathbf{R}}$, which is a vector belonging to the same plane of $\mathbf{f}_m(\mathbf{r})$ and $\mathbf{f}_n(\mathbf{r}')$; since all these functions are in the same plane, and since $\mathbf{f}_r(\mathbf{r}) \times \mathbf{f}_c(\mathbf{r}')$ is a vector orthogonal to the plane where the two functions lie, then the projection of ∇g_j of it equals zero. Finally, using the definitions (E.96) - (E.98), it is possible to rewrite (E.95) as:

$$\left\langle \mathbf{E}_\mathrm{t}^{(j)}, \mathbf{f}_r(\mathbf{r}) \right\rangle = \sum_{c=1}^{N_\mathrm{fun}} x_c^{(\mathrm{j})} (\mathbf{D}^{(j)})_{rc} - \sum_{c=1}^{N_\mathrm{fun}} x_c^{(\mathrm{m})} (\mathbf{K}^{(j)})_{rc}, \tag{E.99}$$

where the number of test functions have been chosen in order to obtain a square matrix. Similar considerations will be applied to the magnetic field contributions. According to the MPIE formulation,

$$\mathbf{H}_\mathrm{t}^{(j)} = - \mathrm{j}\omega\varepsilon_0\varepsilon_j \int_{\mathcal{D}'} g_j(\mathbf{r} - \mathbf{r}')\mathbf{M}(\mathbf{r}')\, \mathrm{d}\mathbf{r}' + \frac{1}{\mathrm{j}\omega\mu_0}\nabla \int_{\mathcal{D}'} g_j(\mathbf{r} - \mathbf{r}')\nabla \cdot \mathbf{M}(\mathbf{r}')\, \mathrm{d}\mathbf{r}' +$$
$$+ \int_{\mathcal{D}'} [\nabla g_j(\mathbf{r} - \mathbf{r}')] \times \mathbf{J}(\mathbf{r}')\, \mathrm{d}\mathbf{r}'.$$

By applying the expansions (E.93) to the previous equation, it becomes:

$$\mathbf{H}_\mathrm{t}^{(j)} \simeq \sum_{c=1}^{N_\mathrm{fun}} x_c^{(\mathrm{m})} \left\{ -\mathrm{j}\omega\varepsilon_0\varepsilon_j \int_{\mathcal{D}'_n} g_j(\mathbf{r} - \mathbf{r}')\mathbf{f}_c(\mathbf{r}')\, \mathrm{d}\mathbf{r}' + \frac{1}{\mathrm{j}\omega\mu_0}\nabla \int_{\mathcal{D}'_c} g_j(\mathbf{r} - \mathbf{r}')\nabla \cdot \mathbf{f}_c(\mathbf{r}')\, \mathrm{d}\mathbf{r}' \right\} +$$
$$+ \sum_{c=1}^{N_\mathrm{fun}} x_c^{(\mathrm{j})} \int_{\mathcal{D}'_c} [\nabla g_j(\mathbf{r} - \mathbf{r}')] \times \mathbf{f}_c(\mathbf{r}')\, \mathrm{d}\mathbf{r}'.$$

This equation should now be tested on a set of functions $\{\mathbf{g}_r\}$; also in this case RWG functions have been used for the calculation of the moments:

$$\mathbf{g}_r(\mathbf{r}) = \mathbf{f}_r(\mathbf{r}).$$

By applying the testing procedure, the following equation can be found:

$$
\left\langle \mathbf{H}_{\mathrm{t}}^{(j)}, \mathbf{f}_r(\mathbf{r}) \right\rangle = \sum_{c=1}^{N_{\mathrm{fun}}} x_c^{(\mathrm{m})} \left\{ -\mathrm{j}\omega\varepsilon_0\varepsilon_j \int_{\mathcal{D}_r} \mathbf{f}_r(\mathbf{r}) \cdot \int_{\mathcal{D}_c'} g_j(\mathbf{r} - \mathbf{r}')\mathbf{f}_c(\mathbf{r}')\,\mathrm{d}\mathbf{r}'\,\mathrm{d}\mathbf{r} + \right.
$$
$$
\left. + \frac{1}{\mathrm{j}\omega\mu_0} \int_{\mathcal{D}_r} \mathbf{f}_r \cdot \nabla \int_{\mathcal{D}_c'} g_j(\mathbf{r} - \mathbf{r}')\nabla \cdot \mathbf{f}_c(\mathbf{r}')\,\mathrm{d}\mathbf{r}\,\mathrm{d}\mathbf{r}' \right\} +
$$
$$
+ \sum_{c=1}^{N_{\mathrm{fun}}} x_c^{(j)} \int_{\mathcal{D}_r} \mathbf{f}_r(\mathbf{r}) \cdot \int_{\mathcal{D}_c'} [\nabla g_j(\mathbf{r} - \mathbf{r}')] \times \mathbf{f}_c(\mathbf{r}')\,\mathrm{d}\mathbf{r}'\,\mathrm{d}\mathbf{r}. \qquad (\mathrm{E}.100)
$$

It is possible to recognize that these terms are very similar to the previous one, exception made for the multiplying constants; however, it is possible to see that:

$$\mathrm{j}\omega\mu_0 = \mathrm{j}\omega\varepsilon_0\varepsilon_j \frac{\mu_0}{\varepsilon_0\varepsilon_j}.$$

So, by defining Z_j as the homogeneous space impedance of the medium characterized by $(\mu_0, \varepsilon_0\varepsilon_j)$ as:

$$Z_j = \sqrt{\frac{\mu_0}{\varepsilon_0\varepsilon_j}},$$

it is possible to write the matrix equation relative to the MFIE contribution of this formulation in function of the previously computed terms:

$$
\left\langle \mathbf{H}_{\mathrm{t}}^{(j)}, \mathbf{f}_r(\mathbf{r}) \right\rangle = \frac{1}{Z_j^2} \sum_{c=1}^{N_{\mathrm{fun}}} x_c^{(\mathrm{m})} (\mathbf{D}^{(j)})_{rc} + \sum_{c=1}^{N_{\mathrm{fun}}} x_c^{(j)} (\mathbf{K}^{(j)})_{rc}. \qquad (\mathrm{E}.101)
$$

Bibliography

[1] D. Gottlieb and S. A. Orszag, "Numerical analysis of spectral methods: theory and applications," *Society for Industrial and Applied Mathematics,* Philadelphia, Pennsylvania, 1977.

[2] C. Canuto, M. Y. Hussaini, A. Quarteroni, and T. A. Zang, "Spectral methods: evolution to complex geometries and applications to fluid dynamics," *Springer-Verlag,* Berlin, Germany, 2007.

[3] C. Canuto, M. Y. Hussaini, A. Quarteroni, and T. A. Zang, "Spectral methods in fluid dynamics," *Springer-Verlag,* Berlin, Germany, 1988.

[4] C. Canuto, M. Y. Hussaini, A. Quarteroni, and T. A. Zang, "Spectral methods: fundamentals in single domains," *Springer-Verlag,* Berlin, Germany, 2006.

[5] U. Lee, "Spectral element method in structural dynamics," *John Wiley & Sons (Asia),* Singapore, 2009.

[6] J. H. Lee, T. Xiao, and Q. H. Liu, "A 3-D spectral-element method using mixed-order curl conforming vector basis functions for electromagnetics fields," *IEEE Trans. Microw. Theory Techn.,* vol. 54, no. 1, pp. 437-444, Jan. 2006.

[7] Y. Liu, J. H. Lee, T. Xiao, and Q. H. Liu, "A spectral-element time-domain solution of Maxwell's equations," *Microw. Opt. Technol. Lett.,* vol. 48, no. 4, pp. 673-680, Feb. 2006.

[8] J. H. Lee and Q. H. Liu, "A 3-D spectral-element time-domain method for electromagnetic simulation," *IEEE Trans. Microw. Theory Techn.,* vol. 55, no. 5, pp. 983-991, May 2007.

[9] O. A. Peverini, G. Addamo, G. Virone, R. Tascone, and R. Orta, "A spectral-element method for the analysis of 2-D waveguide devices with sharp edges

and irregular shapes," *IEEE Trans. Microw. Theory Techn.*, vol. 59, no. 7, pp. 1685-1695, July 2011.

[10] L. B. Felsen and N. Marcuvitz, "Radiation and scattering of waves," *John Wiley & Sons,* Jan. 1994.

[11] J. Meixner, "The behavior of electromagnetic fields at edges," *IEEE Trans. Antennas Propag.,* vol. 20, no. 4, pp. 442-446, July 1972.

[12] P. P. Silvester and R. L. Ferrari, "Finite elements for electrical engineers," *Cambridge University Press,* Cambridge, 1996.

[13] V. N. Kanellopoulos and J. P. Webb, "A complete *E*-plane analysis of waveguide junctions using the finite element method," *IEEE Trans. Microw. Theory Tech.,* vol. 38, no. 3, pp. 290-295, Mar. 1990.

[14] C. K. Aanandan, P. Debernardi, R. Orta, R. Tascone, and D. Trinchero, "Problem-matched basis functions for moment method analysis - an application to reflection gratings," *IEEE Trans. Antennas Propag.,* vol. 48, no. 1, pp. 35-40, Jan. 2000.

[15] G. Pelosi, A. Cocchi, and A. Monorchio, "A hybrid FEM-based procedure for the scattering from photonic crystals illuminated by a gaussian beam," *IEEE Trans. Antennas Propag.,* vol. 48, no. 6, pp. 973-980, June 2000.

[16] G. Pelosi, A. Freni, and R. Coccioli, "Hybrid technique for analysing scattering from periodic structures," *IEE Proc-H,* vol. 140, no. 2, pp. 65-70, Apr. 1993.

[17] M. Yokota and M. Sesay, "Two-dimensional scattering of a plane wave from a periodic array of dielectric cylinders with arbitrary shape," *J. Opt. Soc. Am. A,* vol. 25, no. 7, pp. 1691-1696, July 2008.

[18] H. Toyama and K. Yasumoto, "Electromagnetic scattering from periodic arrays of composite circular cylinder with internal cylindrical scatterers," *PIER,* vol. 52, pp. 321-333, 2005.

[19] R. Orta, P. Savi, and R. Tascone, "Numerical Green's function technique for the analysis of screens perforated by multiply connected apertures," *IEEE Trans. Antennas Propag.,* vol. 44, no. 6, pp. 765-776, June 1996.

[20] A. Coves, B. Gimeno, J. Gil, M. V. Andrés, A. A. S. Blas, and V. E. Boria, "Full-wave analysis of dielectric frequency-selective surfaces using a vectorial modal method," *IEEE Trans. Antennas Propag.,* vol. 52, no. 8, pp. 2091-2099, Aug. 2004.

[21] G. Conciauro, M. Guglielmi, and R. Sorrentino, "Advanced modal analysis," *John Wiley & Sons,* New York, USA, 1999.

[22] M. Bozzi, S. Germani, L. Minelli, L. Perregrini, and P. de Maagt, "Efficient calculation of the dispersion diagram of planar electromagnetic band-gap structures by the MoM/BI-RME method," *IEEE Trans. Antennas Propag.,* vol. 53, no. 1, pp. 29-35, Jan. 2005.

[23] F. Xu, K. Wu, and W. Hong, "Finite-difference time-domain modeling of periodic guided-wave structures and its application to the analysis of substrate integrated nonradiative dielectric waveguide," *IEEE Trans. Microw. Theory Techn.,* vol. 55, no. 12, pp. 2502-2511, Dec 2007.

[24] A. Tibaldi, R. Orta, O. A. Peverini, G. Addamo, G. Virone, and R. Tascone, "A mortar-element method for the analysis of periodic structures," *ICEAA 2013,* pp. 117-120, Sept. 2013.

[25] A. Tibaldi, R. Orta, O. A. Peverini, R. Tascone, G. Addamo, and G. Virone, "Analysis of diffraction gratings by the mortar-element method," *Numerical Electromagnetic Modeling and Optimization (NEMO), 2014,* 14-16 May 2014.

[26] A. Tibaldi, R. Orta, O. A. Peverini, G. Addamo, G. Virone, and R. Tascone, "Skew incidence plane-wave scattering from 2-D dielectric periodic structures: analysis by the mortar-element method," *IEEE Trans. Microw. Theory Techn.,* vol. 63, no. 1, pp. 11-19, Jan. 2015.

[27] CST Microwave Studio. Comput. Technol. Simulation, Darmstadt, Germany, 2014 [Online]. Available: www.cst.com, (free download of software not available).

[28] S. A. Kemme, "Microoptics and nanooptics fabrication," *CRC Press,* Boca Raton, Florida, 2010.

[29] http://refractiveindex.info.

[30] R. Orta, S. Bastonero, and R. Tascone, "Numerical analysis of surface relief gratings," *Diffractive Optics and Optical Microsystems, S. Martellucci and A. Chester Eds.,* pp. 47-56, New York, USA, 1997.

[31] S. Bastonero, O. A. Peverini, R. Orta, and R. Tascone, "Anisotropic surface relief diffraction gratings under arbitrary plane wave incidence," *Opt. Quant. Electron.,* vol. 32, no. 6-8, pp. 1013-1025, 2000.

[32] S. K. Rao, "Design and analysis of multiple-beam reflector antennas," *IEEE Antennas Propag. Mag.,* vol. 41, no. 4, pp. 53-59, Sep. 1999.

[33] L. Zappelli, "On the definition of the generalized scattering matrix of a lossless radial line," *IEEE Trans. Microw. Theory Techn.,* vol. 52, no. 6, pp. 1654-1662, June 2004.

[34] G. Addamo, O. A. Peverini, G. Virone, R. Tascone, and R. Orta, "Model-order reduction technique for the efficient analysis of complex waveguide structures - an application to the design of corrugated horns," *IEEE Antennas Wireless Propag. Lett.,* vol.8, pp. 1039-1042, 2009.

[35] A. K. Bhattacharyya, "Multimode moment method formulation for waveguide discontinuities," *IEEE Trans. Microw. Theory Techn.,* vol. 42, no. 8, pp. 1567-1571 Aug. 1994.

[36] K. K. Chan and S. K. Rao, "Design of high efficiency circular horn feeds for multibeam reflector applications," *IEEE Trans. Antennas Propag.,* vol. 56, no. 1, pp. 253-258, Jan. 2008.

[37] J. Teniente Vallinas, "Modern corrugated horn antennas," Ph. D. Thesis, Universidad Pública de Navarra, Pamplona, Spain, July 2003.

[38] J. Teniente Vallinas, D. Goñi, R. Gonzalo, and C. del-Río, "Choked gaussian antenna: extremely low sidelobe compact antenna design," *IEEE Antennas Wireless Propag. Lett.,* vol. 1, no. 1, pp. 200-202, 2002.

[39] J. Teniente Vallinas, R. Gonzalo, and C. del-Río, "Reply to "Comments on 'Choked gaussian antenna: extremely low sidelobe compact antenna design' "," *IEEE Antennas Wireless Propag. Lett.,* vol. 2, no. 1, pp. 364-366, 2003.

[40] M. A. Morgan and K. K. Mei, "Finite-element computation of scattering by inhomogeneous penetrable bodies of revolution," *IEEE Trans. Antennas Propag.,* vol. 27, no. 2, pp. 202-214, Mar. 1979.

[41] J. M. Gil, J. Monge, J. Rubio, and J. Zapata, "A CAD-oriented method to analyze and design radiating structures based on bodies of revolution by using finite elements and generalized scattering matrix," *IEEE Trans. Antennas Propag.,* vol. 54, no. 3, pp. 899-907, Mar. 2006.

[42] A. Tibaldi, G. Addamo, O. A. Peverini, R. Orta, G. Virone, and R. Tascone, "Analysis of Axisymmetric Waveguide Components by a Multi-Domain Spectral Method," *IEEE Trans. Microw. Theory Techn.,* vol. 63, no. 1, pp. 115-124, Jan. 2015.

[43] P. J. B. Clarricoats and A. D. Olver, "Corrugated horns for microwave antennas," *IEE electromagnetic waves series*, vol. 18, London, 1984.

[44] A. Neto and S. Maci, "Green's function of an infinite slot printed between two homogeneous dielectrics - Part I: magnetic currents," *IEEE Trans. Antennas Propag.,* vol. 51, no. 7, pp. 1572-1581, July 2003.

[45] S. Maci and A. Neto, "Green's function of an infinite slot printed between two homogeneous dielectrics - Part II: uniform asymptotic solution," *IEEE Trans. Antennas Propag.,* vol. 52, no. 3, pp. 666-676, Mar. 2004.

[46] D. F. Filipovic, S. S. Gearhart, and G. M. Rebeiz, "Double-slot antennas on extended hemispherical and elliptical silicon dielectric lenses," *IEEE Trans. Microw. Theory Techn.,* vol. 41, no. 10, pp. 1738-1749, Oct. 1993.

[47] A. Neto, S. Bruni, G. Gerini, and M. Sabbadini, "The leaky lens: a broad-band fixed-beam leaky-wave antenna," *IEEE Trans. Antennas Propag.,* vol. 53, no. 10, pp. 3240-3246, Oct. 2005.

[48] A. Neto, "UWB, non dispersive radiation from the planarly fed leaky lens antenna - Part I: theory and design," *IEEE Trans. Antennas Propag.,* vol. 58, no. 7, pp. 2238-2247, July 2010.

[49] A. Neto, S. Monni, and F. Nennie, "UWB, non dispersive radiation from the planarly fed leaky lens antenna - Part II: demonstrators and measurements," *IEEE Trans. Antennas Propag.,* vol. 58, no. 7, pp. 2248-2258, July 2010.

[50] A. Neto, N. Llombart, J. J. A. Baselmans, A. Baryshev, and S. J. C. Yates, "Demonstration of the leaky lens antenna at submillimeter wavelengths," *IEEE Trans. THz Sci. Technol.,* vol. 4, no. 1, pp. 26-32, Jan. 2014.

[51] A. Neto, P. de Maagt, and S. Maci, "Optimized basis functions for slot antennas excited by coplanar waveguides," *IEEE Trans. Antennas Propag.,* vol. 51, no. 7, pp. 1638-1646, July 2003.

[52] J. R. Mautz and R. F. Harrington, "Electromagnetic scattering from a homogeneous body of revolution," *Department of Electrical and Computer Engineering,* TR-77-10, Syracuse, New York, Nov. 1977.

[53] S. M. Rao, D. Wilton, and A. W. Glisson, "Electromagnetic scattering by surfaces of arbitrary shape," *IEEE Trans. Antennas Propag.,* vol. 30, no. 3, pp. 409-418, May 1982.

[54] D. R. Wilton, S. M. Rao, A. W. Glisson, D. H. Schaubert, O. Al-Bundak, and C. M. Butler, "Potential integrals for uniform and linear source distributions on polygonal and polyhedral domains," *IEEE Trans. Antennas Propag.,* vol. 32, no. 3, pp. 276-281, Mar. 1984.

[55] R. D. Graglia, "On the numerical integration of the linear shape functions times the 3-D Green's function or its gradient on a plane triangle," *IEEE Trans. Antennas Propag.,* vol. 41, no. 10, pp.1448-1455, Oct. 1993.

[56] D. A. Dunavant, "High degree efficient symmetrical gaussian quadrature rules for the triangle," *International journal for numerical methods in engineering,* vol. 21, no. 1, pp. 1129-1148, 1985.

[57] P. Arcioni, M. Bressan, and L. Perregrini, "On the evaluation of the double surface integrals arising in the application of the boundary integral method to 3-D problems," *IEEE Trans. Microw. Theory Techn.,* vol. 45, no. 3, pp.436-439, Mar. 1997.

[58] I. Hänninen, M. Taskinen, and J. Sarvas, "Singularity subtraction integral formulae for surface integral equations with RWG, rooftop and hybrid basis functions," *PIER,* vol. 63, pp. 243-278, 2006.

[59] A. W. Gunst and M. J. Bentum, "The LOFAR phased array telescope system," *IEEE International Symposium on Phased Array Systems,* pp. 632-639, Waltham, Oct. 2010.

[60] S. W. Ellingson, T. E. Clarke, A. Cohen, J. Craig, N. E. Kassim, Y. Pihlstrom, L. J. Rickard, and G. B. Taylor, "The Long Wavelength Array," *Proc. IEEE,* vol. 97, no. 8, pp. 1421-1430, Aug. 2009.

[61] C. J. Lonsdale, R. J. Cappallo *et al.*, "The Murchison widefield array: design overview," *Proc. IEEE,* vol. 97, no. 8, pp. 1497-1506, Aug. 2009.

[62] R. Mittra, "Square Kilometer Array - A unique instrument for exploring the mysteries of the universe using the Square Kilometer Array," *AEMC,* pp. 1-6, Dec. 2009.

[63] J. G. bij de Vaate *et alii*, "Low Frequency Aperture Array Developments for Phase 1 SKA," *General Assembly and Scientific Symposium, 2011 XXXth URSI*, pp. 1-4, Istanbul, Aug. 2011.

[64] M. Murgia, G. Bianchi, P. Bolli, G. Comoretto, D. Dallacasa, M. Z. Farooqui, F. Gaudiomonte, L. Gregorini, F. Govoni, K. H. Mack, M. Massardi, M. Mattana, M. Melis, J. Monari, L.

Mureddu, G. Naldi, F. Paonessa, F. Perini, A. Poddighe, I. Porceddu, I. Prandoni, G. Pupillo, M. Schiaffino, F. Schillirò, G. Serra, A. Tibaldi, T. Venturi, G. Virone and A. Zanichelli, "Sardinia Aperture Array Demonstrator," *SPIE*, Montreal, June 2014.

[65] G. Virone, G. Addamo, O. A. Peverini and R. Tascone, "Broadband Array Element for the SKA Low-Frequency Aperture Array," *ICEAA,* pp. 560-561, Sept. 2011.

[66] G. Virone, R. Sarkis, C. Craeye, G. Addamo, and O. A. Peverini, "Gridded Vivaldi Antenna Feed System for the Northern Cross Radio Telescope," *IEEE Trans. Antennas Propag.,* vol. 59, no. 6, pp. 1963-1971, June 2011.

[67] A. Tibaldi, G. Virone, F. Perini, J. Monari, M. Z. Farooqui, M. Lumia, O. A. Peverini, G. Addamo, and R. Tascone and R. Orta, "Design considerations for a low-frequency Vivaldi array element," *PIERS,* Stockholm, Aug. 2013.

[68] J. Monari, F. Perini, M. Schiaffino, G. Bianchi, A. Mattana, G. Naldi, G. Pupillo, G. Tartarini, S. Rusticelli, G. Virone, A. Tibaldi, R. Tascone, O. A. Peverini, G. Addamo, P. Debernardi, A. M. Lingua , M. Piras, A. Cina, P. Maschio, and H. Bendea, "Aperture array for low frequency: the Vivaldi solution," *ICEAA,* Torino, Sept. 2013.

[69] P. Bolli, F. Perini, S. Montebugnoli, G. Pelosi, and S. Poppi, "Basic Element for Square Kilometer Array Training (BEST): Evaluation of the Antenna Noise Temperature," *IEEE Antennas Propag. Maga.,* vol. 50, no.2, pp.58-65, Apr. 2008.

[70] G. Virone, A. M. Lingua, M. Piras, A. Cina, F. Perini, J. Monari, F. Paonessa, O. A. Peverini, G. Addamo, and R. Tascone, "Antenna pattern verification system based on a micro unmanned aerial vehicle (UAV)," *IEEE Antennas Wireless Propag. Lett.,* vol. 13, pp. 169-172, Feb. 2014.

[71] G. Virone, F. Paonessa, A. Tibaldi, M.Z. Farooqui, G. Addamo, O.A. Peverini, R. Tascone, P. Bolli, A. Mattana, J. Monari, G. Naldi, F. Perini, G. Pupillo, M. Schiaffino, A. M. Lingua, M. Piras, P. Maschio, I. Aicardi, I.H. Bende and A. Cina, "UAV-based radiation pattern verification for a small low-frequency array," *IEEE-APS,* pp. 995-996, Memphis, July 2014.

[72] F. Canavero, I. Montrosset, and R. Orta, "Linee di trasmissione," *Levrotto & Bella,* Torino, 1990.

[73] G. Lovat, "Fenomeni di leakage in strutture planari dielettriche, stampate e metamateriali," Ph. D. Thesis, Università "La Sapienza", Roma, 2005.

[74] D. Cavallo, "Connected array antennas," Ph. D. Thesis, Technische Universiteit Eindhoven, Eindhoven, 2011.